advanced building skins

Proceedings of the International Conference
on Building Envelope Design and Technology
23-24 April 2015 I Graz I Austria

Oliver Englhardt
Editor

Advanced Building Skins
Proceedings of the International Conference on Building Envelope Design and Technology
23-24 April 2015 | Graz | Austria

Institute of Building Construction
Graz University of Technology

http://baukonstruktion.tugraz.at/
http://buildingskins.tugraz.at/

The conference was kindly supported by:

Imprint

Editor

Oliver Englhardt, Prof. Dr., Graz University of Technology

Layout / Cover

Matej Banozic, Graz University of Technology

Institute of Building Construction
Graz University of Technology
Lessingstrasse 25/III | 8010 | Graz | Austria
http://baukonstruktion.tugraz.at/

www.ub.tugraz.at/Verlag

e-book ISBN 978-3-85125-397-9
DOI 10.3217/978-3-85125-397-9

Editorial

In every architectural period the facade was most important for the expression and appearance of a building. Facades characterize the different architectural periods - they characterize our cities. But we are under the impression, we perceive, that cities - the buildings we live in and we live with - are becoming almost identical. Are we moving towards global uniformity? If we reflect on our fundamental expectations and demands on our built environment I am not necessarily convinced that this is the case. There are different needs almost everywhere. It’s not only about the appearance, the esthetics. If we have a more detailed look, it’s much more about the functional equipment and this causes the complexity of building enclosures. There is, in fact, a strong diversity.

Nowadays half of the 7 billion and in the nearby future 75 percent of the worlds population of then about 9 billion is expected to be concentrated in cities. The city will be the principal habitat of mankind. Cities are characterized by variability. Outside and inside a building, everything is non-steady, everything is changing continually. Buildings will be confronted with diverse external influences, with impacts, boundary conditions and their temporal changes, - with alterations of different kinds. In addition, we will be challenged to use buildings - and that means the building enclosure - as power plants, as energy converters. Active and adaptive, changeable constructions are the next big step in the conception of buildings - and even more in the conception and design of building enclosures. The facade will have a profound impact on the ecological balance of our habitat, the human condition and the quality of our life. And they will make up a substantial proportion in the building construction and operating costs. That is why facades - and their design - matter!

After our conference in 2012 it is now the second time I am organizing this international platform at the Graz University of Technology. This Conference again focuses on the enormous diversity of façade architecture, on new production processes and on the vast amount of new materials broadening the design base for extraordinary building envelopes.
With this international conference we will bring them together: creative and innovative professionals and researchers at the forefront of skin design to discuss tasks and issues in research, design and man-ufacturing of high-performance façades and building envelopes.

The articles assembled in this publication are showing new perspectives on, and an enhanced insight into, developments and research in design and engineering for tomorrow’s advanced building skins. All papers are peer reviewed doubly before publication by the international scientific committee. I would like to thank the members of the scientific committee and I would in particular like to thank all the authors who have enriched this publication with their revealing and extraordinary contributions!

Best regards,

Oliver Englhardt

Table of Content

ADAPTIVE FACADES

STRUCTURAL GLASS

REFURBISHMENT

FUNCTIONAL GLASS

MEMBRANES

MATERIALS

adaptive façades

Latest Developments in Building Skins A new holistic Approach

Winfried Heusler, Prof. Dr.-Ing.
Schüco International KG, Germany, www.schueco.com

Summary

The building skin is mainly relevant for the building`s fitness for purpose and durability, as well as for protecting people and property. The acceptance of new concepts for building skins is closely linked to the quality of comfort, as well as the wellbeing of people. As an important part of a new holistic approach the principle of convergence within modular façade units enables designers, producers and maintenance companies to achieve more sustainable solutions. In combination with advanced computational methods and a seamless digital process chain the new approach not only eliminates the unnecessary and useless consumption of energy, material, time and money in design, construction, operation and maintenance but also guarantees consistent quality and peace of mind.

Keywords: Façade, adaptive, convergence, modular system, parametric design.

1 Introduction

Before the advent of the 20th century, buildings and the building process were shaped by local social systems, living arrangements and modes of working on the one hand, and by locally available materials and construction methods on the other. During the 20th century, with globalization progressing apace, local traditions increasingly took a back seat. In the late 1980s, a somewhat diverging tendency could be observed in central Europe where it became of more and more significance that façades don't just have to "look good". More than that the building skin is mainly relevant for the building`s fitness for purpose and durability, as well as for protecting people and property. The acceptance of advanced concepts is closely linked to the quality of comfort, as well as the wellbeing of people. Daniels [1] pointed out that façades are the key for indoor comfort and operational expenditures. They are not only responsible for the cost related to the operation of the building's mechanical systems but can determine whether, or to what degree, a building needs such systems in the first place. Technological advances have been an integral part of human development throughout history. In the last twenty years the introduction of the Internet provided the medium for distributed communication and collaboration on a scale unimaginable before. Along with rapid advances in miniaturization, speed, power and mobility the physical world and the virtual world – or cyber-space – had been merging within the last five years. Many of the new technologies have quickly penetrated into activities in the daily life of ordinary people. In the near future cyber-physical systems will contribute to safety, efficiency, comfort and human health. Based on the Internet and cognitive computing technology systems for remote monitoring of autonomous production systems are under development for manufacturing, logistics and transportation.

2 Thirty years of practical experience

In the last thirty years many buildings with innovative building skins have been built as "prototypes". Since that time a lot of practical findings have emerged, that should be considered in future product development as well as in the process of planning, building and operating building skins. Many of the innovative products available today are not yet in reliable quality and cost-effective in the processes of prefabrication, workshop assembly, on-site installation and putting into operation. Furthermore, it is often difficult, especially under site conditions, to integrate them with other building components in order to create an effective overall system. The relevant standards and regulations for façade technology, electrics, heating, ventilation and air conditioning – if indeed they are available for such a special case – are also not always observed. An analysis of completed building projects also reveals weaknesses in the planning phase. For example, the client's specific requirements are often not discussed thoroughly enough or clarified unequivocally at an early stage. Many planners are not familiar enough with the relevant exterior and interior building conditions, or the full possibilities of innovative products. This is especially so with projects in unfamiliar climates. There will however always be clients and architects who are interested only in the short term. During the planning stage and when the contract is awarded, they are much more concerned with investment costs than the quality of construction and the later operational and maintenance costs. In addition, financial reasons mean that project planners and companies responsible for completing the project frequently do not implement the original objectives in a consistent fashion. Another finding was that users and control equipment did not operate the components of the building skin and building technology in the way that was assumed during planning. For example, the use of natural light to improve room lighting will only save energy if artificial lighting is switched off or dimmed. Other difficulties were caused by individual components failing to remain in working order, maintenance-free or even maintenance-friendly in the long term, especially when damaged components could not be quickly replaced with compatible parts. Problems can occur with geometrically and technically complex buildings, especially if there are insufficient funds or there is a lack of appreciation of the amount of maintenance required. No wonder therefore that the need for repairs is increasing. After all, if you never have your car serviced, soon or later you are bound to find yourself facing a large repair bill. Another phenomenon frequently observed is that cleaning and maintenance work is not carried out and, when the usage of individual rooms is subsequently changed, the rooms were not fitted out to their original high standard. In building projects that integrate all trades, it has sometimes proven difficult to establish who is responsible for warranties and defects once the building is in use.

3 Efficient fabrication, assembly and installation of building skins

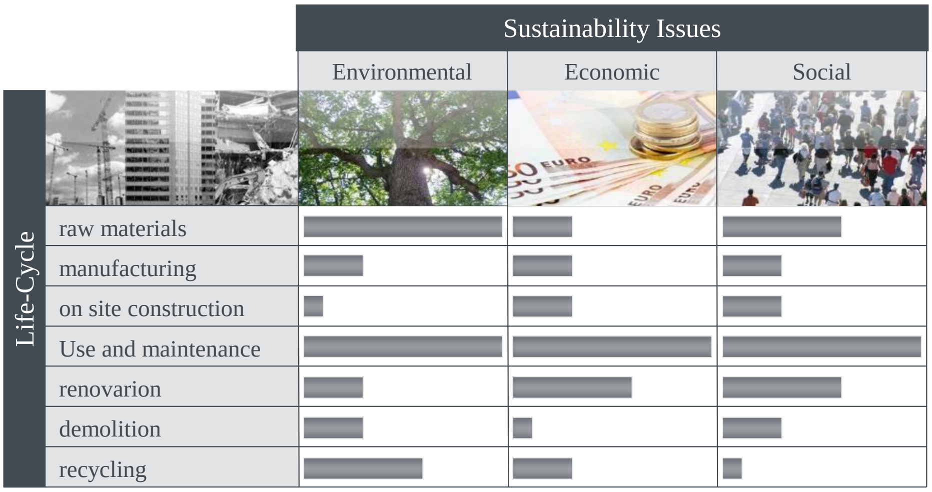

Figure 1: Aspects of sustainability in the life-cycle of buildings and building skins (Source: Schueco Int. KG).

A first step to a sustainable building (figure 1) is to optimize the efficiency of the fabrication-, assembly- and installation-process of building skins. From a construction perspective, there are two basic types of external walls: load-bearing external walls and curtain walls which are not load-bearing. Furthermore external walls can be constructed with a single layer or multiple layers. The structural and physical properties of single layer (monolithic) external walls are limited by the material used and its thickness. The material used must therefore meet multi-functional requirements. By way of contrast, with multi-layer façades, the materials of the individual layers can be optimized with regard to the function that each performs. In terms of their construction, external walls can be distinguished according to whether individual components or pre-assembled modules are delivered to site. Assembly of individual components is very common with curtain walling (stick-systems). Assembly on site is time-consuming and dependent on the weather plus scaffolding is also required. By way of contrast, unitized façades are manufactured and assembled at the factory. Such modules comprise enclosed frames of windows, ribbon windows or façades including glass, panel, metal sheet and insulation, in extreme cases with natural stone and solar shading, sensors and motors. The major advantage of unitized façades in contrast to stick-systems, is the high degree of automation and accuracy possible under controlled factory conditions. The result is reliable quality assurance that ensures high standards. The modules are transported in their entirety to site and fitted to consoles which were previously attached to and adjusted on the building`s structure. This design requires greater use of materials and more work in the factory not to mention experienced construction engineers. Design errors cannot be easily corrected with additional manual work on site. Unitized façades always require more planning and a corresponding amount of pre-planning and this may also need to be taken into account when projects are awarded.

If a design is not suitably in tune with the practicalities of construction, considerable additional costs can arise. This can be avoided, whilst still observing technical and design limitations, if buildings are planned and constructed as far as possible on task-specific standards (system technology), project-specific standards (platform strategy) are only applied where necessary, and working with no standards at all should be avoided as far as possible. This will also considerably reduce the problems named in chapter two. System technology is a principle that helps promote simple, cost-effective and error-free construction. This principle involves standardizing building components for different task-specific requirements in construction series and modular systems with identical parts, and harmonizing the interface between the components in terms of their dimensions and geometries.

In the development process, the individual system components of the building skin are optimized from the point of view of the environment, functionality, fabrication, assembly and design, as are the interfaces between components and between the façade and the adjacent structures (building skin and interior fittings). As there are fewer different construction types and parts, the project is less complex. In addition, components and modules that are commercially and industrially (pre)fabricated as standard products are less complex than custom designed products. Thus the cost of planning, fabrication and assembly is lowered, while quality is increased. The benefits resulting from the high repetition factor and the simple, secure system solutions also mean lower training requirements for the employees of window and façade construction companies – whether engineers or skilled manual workers. In addition, the documentation and software prepared for the products can be reused many times over in future projects. For example, window and façade builders can access time-saving software and databases containing an extensive range of compatible products.

The more extensive and well thought-out the system and the more intelligently the planners and designers use it in adapting the design to fit the project specific requirements, the greater the chance of combining the system components to meet technical and design requirements in an efficient and individual way. Project-specific constructions are developed on a system basis (platform strategy). This also applies to large projects involving a high degree of repetition, for which the task-specific system is not necessarily the most economical. If the components relevant to the function are then used from the system, the key benefits of the system are retained. The proven underlying technology is thus secure and cost-effective and, when applied in projects, reduces development times while maintaining plenty of design scope for the architect.

4 Functional optimization of building skins

The second step to a sustainable building (figure 1) is to optimize the energy-efficiency of a building across its entire life span. With advanced building skins it is possible to even out long term differences between outside climatic influences and interior comfort conditions independent of the season. Short term variations within the climatic situation (for instance between day- to nighttime) can be dampened and smoothed out as well. The better the quality of thermal insulation of a building skin, the more important is a focus on thermal loss due to ventilation or infiltration. The overarching goal must be that uncontrolled ventilation due to gaps in the construction needs to be avoided. More than this sub-optimal operational procedures not only cause an enormous increase in operating cost but also result in non-acceptable interior comfort conditions. The optimization of energy use should not stop at the reduction of thermal losses. Transparent and translucent surfaces of the façade collect thermal gains as well. In the case of buildings with high internal loads and large glass surfaces, solar radiation causes overheating if no additional measures are considered. External shading systems reduce the solar radiation and the resulting thermal gains noticeable. Daylight systems, on the other hand, have the role of evenly distributing the entering daylight within a room and optimizing the daylight quality. De-centralized mechanical ventilation components built into the building skin can be equipped with regenerative heat exchangers, which work for example with phase-change-materials (PCM). They will be capable of balancing diurnal temperature fluctuations. If the capability to store thermal energy is great and, additionally, the local climate possesses the advantage of diurnal temperature swings even during heating periods, mechanical cooling systems may become obsolete.

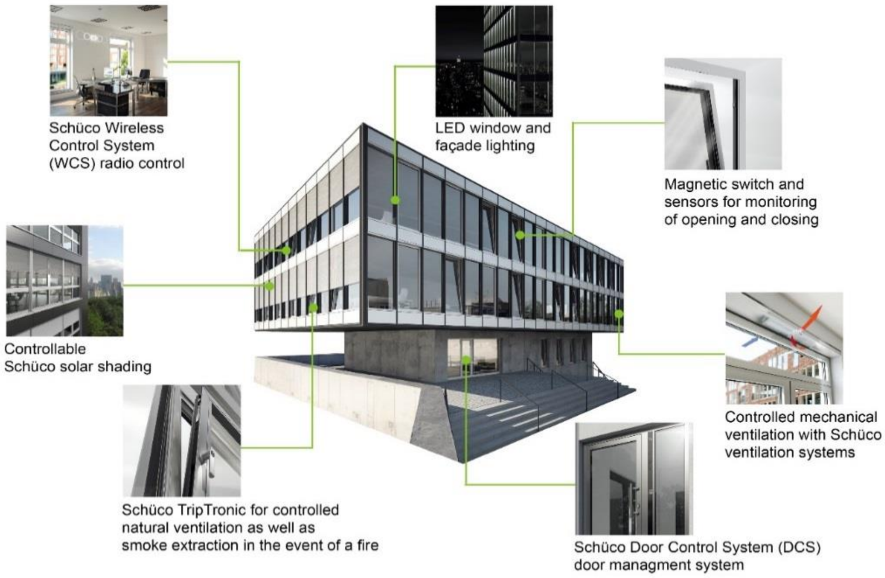

Figure 2: Integration of electric, electronic and mechatronic components into the building skin to improve energy efficiency and safety as well as comfort and human health (Schueco International KG).

A key factor in sustainability is having a building structure that is suitable for its location and its use, in conjunction with an appropriate building skin. Three trends can currently be observed: passive, active and cognitive building concepts [2]. In a passive building concept passive façade components seal off the interior from external factors as far as possible. Contemporary building technology ensures a comfortable interior environment. Conversely, in active building concepts dynamic façade components respond specifically to changing internal and external conditions. The aim here is to minimize the use of mechanical systems, especially by means of natural ventilation, passive use of solar energy and daylight. Researchers have worked on the development of materials that may control the flux of light, energy, ventilation, and sound in a self-controlling fashion. One such research goal is the invention of glass types that are controllable or self-adaptable. An additional goal has been the development of electrically operated ventilation flaps in façades connected to a building management system (BMS). They allow for the accelerated and increased nighttime cooling of internal thermal storage masses within a building. It is important to point out that the knowledge of users and/or operators of buildings, an aspect we may call “Operational Competence” becomes of increasing significance. The most innovative building concept will inadvertently fail if it only performs in theory. It shows that purely passive building concepts are only advantageous when compared to active concepts if the location, the height or the use of the building excludes natural ventilation, as well as solar energy and use of daylight for at least two-thirds of the year.

In many moderate climatic zones, optimum energy efficiency is provided by cognitive building concepts. Their façade and mechanical-system components with dynamically adjustable functions are connected to each other through an intelligent building automation system. Adaptive components of the building skin are capable of reacting to non-continuous, changing external and internal conditions that are in many instances predictable and can be calculated, such as the case with annual or diurnal swings in meteorological conditions (i.e., solar altitude angle) or the times of a building's operation. However, non-predictable weather and operational aspects - such as variations in cloudiness and spontaneous presence of users - should be included by means of appropriate sensors or via the Internet through the weather forecast.

Energy efficiency can also be increased if a designer widens the "systemic boundaries". For example the space between neighboring building parts may be designed as a large buffer zone, resulting in an atrium or mall-type space. Such buffer zones may be equipped with natural or mechanical systems to provide a general thermal environment ranging in air temperature between 15 and 30 °C annually, independent of external weather conditions. To achieve this goal with the least amount of energy, visual light transmission, solar heat gain, and the degree of natural ventilation through the building skin must be controlled by a building-management system. The internal surfaces of such spaces, their roofs and façades, on the other hand, are relatively simple and do not require any particular attention in regards to wind loads or driving rain. Such a "climate hull" therefore increases also the usability of the enclosed building. In an ideal scenario, the user will be enabled to control the components of the internal façades individually, without negative effects on energy consumption. Important nevertheless is the quality of the inner surfaces of the buffer zones with regard to sound absorption and thermal storage capacity.

If a building is optimized with regard to its energy efficiency, it is recommended that renewable energy sources be considered to compensate for the remaining energy consumption. In the case of building skins, mainly two available active-solar energy sources are to be considered: electric and thermal. The direct use of solar radiation for space heating and warm water consumption can be achieved with various available systems which work according to various principles, such as air or water collectors or heat absorbers with heat pumps. Their performance can be increased with the addition of thermal storage systems. Especially for the building type of an office building, the generation of cooling energy with the help of thermal heat collectors (absorption chillers/cooling) is of big interest. The principle is simple: in case of the greatest cooling demand, the sun will provide the greatest heat gain for cooling. This, of course, is an elegant balance between „supply and demand". Building-integrated photovoltaic systems (BIPVs) today have long passed the experimental phase. Currently, BIPV is available for façades and roofs for fixed and movable solar shading systems. In the meantime, the problems of proper cable routing and electric connectors are solved in detail, and excellent systems are available.

5 Cyber-physical systems for adaptive building skins

Cognitive buildings with adaptive building skins are the answer to the current architecture`s desire for optimum comfort, energy efficiency, safety and security. As a result of innovative solutions for this kind of concepts we are facing a large variety of mechanical, electric and electronic components as well as new materials within building skins. Different trades` competences are necessary for the successful solution of this cross-disciplinary challenge. For that reason in other industries "convergence" - the merging of trades as well as the blurring of existing lines, within which enterprises used to position themselves – has been on the rise for more than ten years. In the current façade industry the principle of convergence represents the next evolutionary step towards value-added solutions for the building`s life cycle. By designing building skins modularly with integrated and scalable functional groups for each of the different trades, even complex project specific solutions can be planned and executed more efficiently and with a higher quality. The basis for this advanced concept is a flexible cooperation between the functional groups through optimized interfaces. Modular systems - with standardized functional principles and carry-over parts across several series, system-specific construction characteristics as well as typical joining details and connection technologies - are favorable for that purpose. More than that interoperable components lead to easier integration efforts.

Cyber-physical systems (CPS) represent the next evolutionary step for cognitive building concepts. Within Cyber-physical systems computational components (i.e. hardware and software) are interacting with physical components (i.e. machines and devices). They are part of a globally networked future world, in which products, equipment and objects interact with embedded hardware and software beyond the limits of single applications. With the help of sensors, these systems process data from the physical world and make it available for network-based services, which in turn can have a direct effect on processes in the physical world using actuators [3]. The computational and physical processes are tightly interconnected and coordinated to work together effectively, often with humans in the loop. They are enabling a new generation of cognitive buildings that offer increased effectiveness, and productivity while increasing performance and reliability. The potential of CPS to change every aspect of life is enormous. They will shift the reliance on human decision making into new, more strategic aspects and will increasingly rely on operationalizing human knowledge through computational intelligence [4]. The basis is a high-confidence computing system that can interact appropriately with humans and the physical world in dynamic environments and under unforeseen conditions. Cognitive technologies and cyber-physical systems will have an influence on architecture, the building industry and the built environment. The research project 'KogniHome' [5] has been launched to develop a networked home that supports the health, quality of life and safety of families, people living alone and senior citizens. In the project the question of how 'intelligent' and 'trustworthy' technical systems can be realized to help people in their everyday lives is addressed. One of the interesting research challenges is the objective that the future home needs to learn from its user and be able to adjust to new demands and phases of life. The aim is that inhabitants be able to communicate with the networked apartments with everyday language and gestures. The apartment will, amongst other means, communicate with its inhabitants in the form of an avatar – a digital person [5]. But in the end we have to remember the fact that building techniques and methods are to be tailored to the people for whom the building is intended rather than matching the tenants to the newest possible techniques and methods.

6 Formal and communicative aspects of building skins

We as engineers are accustomed to arguing technical aspects. Nevertheless the architectural integration of technical components into the building skin plays a major role in modern architecture. At this point the "theory of product language" offers interesting perspectives. In the mid-1970s Gros [6] made a distinction between the practical functions (the user`s perspective) of a product on the one hand, and the formal and communicative aspects, the so-called product language functions on the other (figure 3).

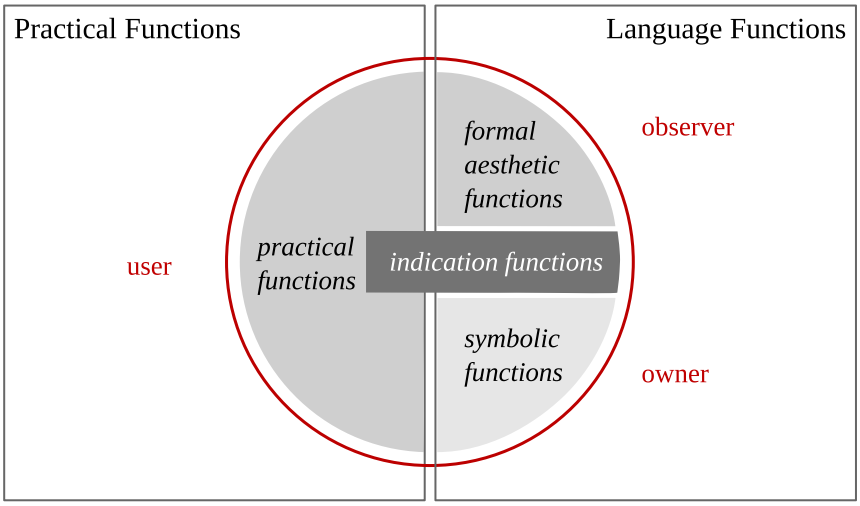

Figure 3: The Offenbach Theory of Product Language [6] (figure by Schueco International KG).

Formal aesthetic functions distinguish two antagonistic principles: order versus complexity, and reduction of stimuli versus richness of stimuli in terms of shapes, color, texture and material for instance (the observer`s perspective). Indication functions visualize and explain the various practical functions of a product and how it should be used (the user`s perspective). Thus, they play an important role concerning recognition, usability and self-explanation of products. Symbolic functions are associated with objects in the imagination of the recipient or user, depending on the particular context. They refer to conceptions and associations that come to a person`s mind while contemplating an object: for example, societal, socio-cultural, historical, technological, economic and ecological aspects (the owner`s perspective). Accordingly products as well as architecture are bearers of meaning, beside their utilitarian functions. In the end façades might be projection surfaces for meaning and the architect as the façade designer could act as the “story-teller”. And a successful story might even become a myth [7].

7 Parametric design

An important step to achieving a functional optimization of building skins and an architecturally successful integration of their components is the parametric design approach. It takes into consideration form and function of the building skin. Clients and users of buildings are only truly satisfied with their building skin when the project-specific requirements and conditions have been properly clarified, the planners are aware of the relevant technical possibilities and have thoroughly evaluated their effectiveness, and the project planners and companies performing the work have properly implemented the defined objectives. It is, however, crucial to remember that it is cheaper to make alterations at the beginning of the planning process, and that the costs increase as the planning activities progress. Making changes at the construction stage comes at a high price. Therefor the team considers several possible solutions that meet the specific conditions and requirements defined in the specifications as soon as possible in the design process.

Figure 4: Opaque and transparent building skins with complex geometry (“Schueco Parametric Concept” at trade fair Bau Munich 2013) (Source: Schueco International KG).

The idea is to work out the best solution from each perspective and different design viewpoints. It is important to identify which part will strongly affect the end result, which one cannot easily be altered later, and what therefore must be decided straightaway at each stage of the planning process. The answer is a design approach, using parametric methods. It`s ultimate principle is the use of variables and algorithms to generate alternative concepts with a hierarchy of physical, mathematical and geometric relations. It serves the automated parameter-based generation of architectural elements that change their properties [8]. The optimized design can be easily controlled and elements can be automatically drawn and eventually produced. It is the shift from using CAD software as a drafting tool, to an efficient design tool. An important point is not to focus on improving individual components, but to optimize the overall performance of the building structure, building envelope, interior walls, floors, ceilings, storage mass, technical fixtures and fittings, and building management technology. The actual challenge is to decouple the costs of the building skin (material and fabrication) from it`s functional (especially in regard to air- and water-tightness) and design quality (three-dimensionally curved appearance).

8 The Building Excellence Approach

Nowadays the complexity in the design process is not only geometrical; it also refers to a number of factors like energy efficiency, material efficiency and optimized functions. Our Building Excellence Concepts (figure 5) are designed to think outside the box. We are trying to find advanced concepts for cognitive buildings, that suit the local climate and specific purpose, using the appropriate building automation technology and choosing control strategies that fit the purpose of the building. A first step to achieving a functional optimization of façades and an architecturally successful integration of their components is a holistic design approach. It takes into consideration form and function of the building skin as well as aspects of production, installation, maintenance and demolition. By designing building skins modularly with integrated and scalable functional groups for each of the different trades, even complex project specific solutions can be planned and executed more efficiently and with a higher quality. The basis for this advanced concept is a flexible cooperation between the functional groups through optimized interfaces. Modular systems - with standardized functional principles and carry-over parts across several series, system-specific construction characteristics as well as typical joining details and connection technologies - are favorable for that purpose. More than that interoperable components lead to easier integration efforts.

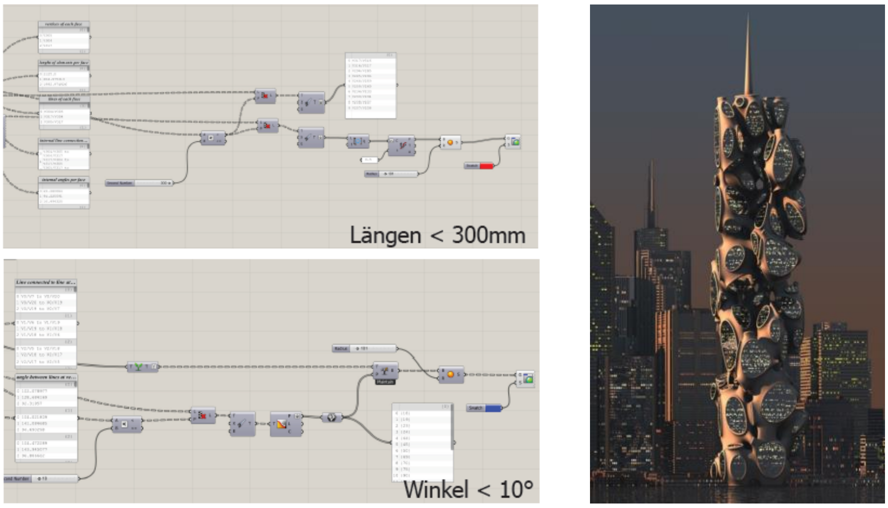

Figure 5: Building Excellence Concepts, the basis for long term research on advanced methods of façade design and construction (Source: P. Guenther & W.Schulz / Schueco International KG).

Our new holistic process, the Building Excellence Approach, is based on the principles of BIM. It takes into account environmental, economic and social aspects (Figure 1) and uses the latest digital technologies to consider the relevant needs of people across the entire lifecycle of the building. The comprehensive process runs from design, planning to construction, through operation and maintenance, updating and upgrading, up to demolition with possible reuse or recycling of building components and materials. It not only eliminates the unnecessary and useless consumption of energy, material, time and money but also guarantees consistent quality and peace of mind. It considers the ecological aspects of sustainability including the protection of the natural environment and the care for resources. For a long time, only a focus on “initial cost” commanded the economic thinking in the building industry. In our advanced process, however, a careful optimization of investment costs and the resulting operational expenses is the norm. In addition, social and cultural aspects of sustainability gain importance, such as in the exterior appearance of buildings, but more importantly the way the building is being used and the spatial quality it provides to the user. At least in office and administrative buildings, the importance of a comfortable temperature, fresh air, the use of daylight and acoustic comfort will grow in the future as the public becomes increasingly aware that they have a direct impact on performance and absenteeism.

In our Building Excellence Approach we are using an advanced parametric method for the holistic and detailed step-by-step analysis and optimization with respect to the following factors: cost-efficiency (investment, operating and maintenance costs), energy requirements (heating, cooling, ventilating, lighting etc.), environmental impact, room comfort (thermal, visual, acoustic etc.), ease of use/operation, cost and ease of maintenance, as well as the flexibility to change use and upgrade facilities. The level of priority given to the various planning criteria depends on whose point of view is being considered mostly. For example, the investor will primarily be interested in cost efficiency, meeting deadlines, and staying on budget. Clients and investors who think in the long term are more likely to focus on the needs of the future operator or tenant (operating costs, image, flexibility and so on) and the eventual user of the building (comfort, security). We found out in our previous team-discussions that since our social systems, tastes and the way we live and work seem to change with increasing speed, the flexibility of buildings is bound to become more significant. This is particularly true if we consider that for a building to be cost-effective in the long term, vacancy periods must be short and the costs of building maintenance, conversion (e.g. if a new user has different requirements) and renovation (e.g. addition of new energy-saving or improved comfort features) are low. Cost-effective buildings are those that need only be equipped to meet current requirements, and then as those requirements change, can be altered quickly, easily and causing as little disruption as possible.

In combination with advanced rendering and visualization tools the Building Excellence Approach allows designers to quickly explore a much larger solution space through virtual functional and visual mock-ups, as well as rapid prototyping models (figure 6). It helps to predict the final outcome more accurately and permits to take realization concerns into account at an earlier stage. It is the up to date basis for a fruitful and dynamic cross-disciplinary optimization process between architects and engineers. To achieve the best possible results, it is important to consider complete systems whose components interact with each other. Concentration on individual parts is only admissible, if they do not have a significant impact on other building components. Thus the purpose is to consider the building as a whole, including all the trades involved and all interfaces between geometrically or functionally connected modules.

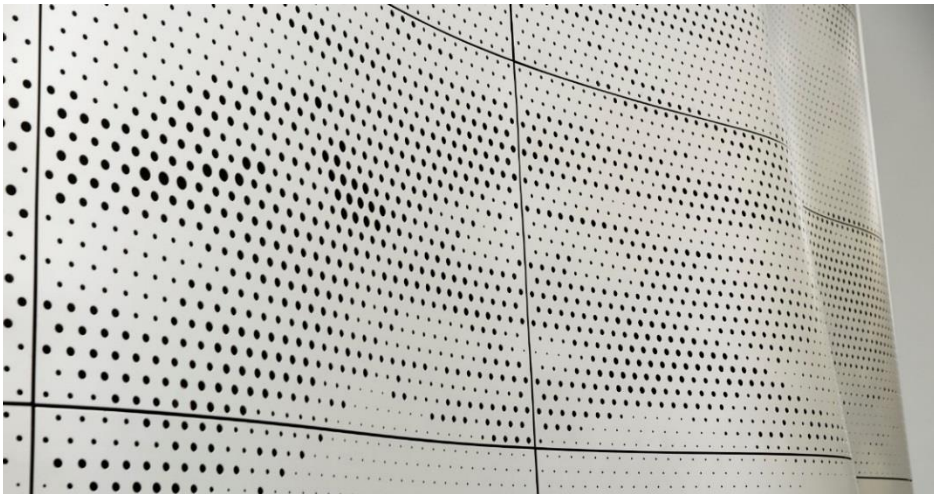

Figure 6: Opaque and semitransparent building skins with complex geometry (“Schueco Design Cover Concept” at trade fair Bau Munich 2015) (Source: Schueco International KG).

For façade planners and builders our Building Excellence Approach also deals with the optimization of fabrication, assembly and installation, by means of merging digital and physical methods. The starting point of our approach is the fact that the first three industrial revolutions came about as a result of mechanization, electricity and IT. In the future the introduction of the Internet of Things and Services into the building environment will be part of the fourth industrial revolution. In the manufacturing environment cyber-physical systems comprise smart machines, storage systems and production facilities capable of autonomously exchanging information, triggering actions and controlling each other independently [9]. This is one of the reasons, why my vision starts with the assumption, that the future of the façade business is based on the continuous digitalization of the process chain – cradle-to-cradle - connecting architects and engineers as well as main contractors, system suppliers, façade and maintenance companies with their specific activities spread all over the world. CPS-based (on site?) factories for components of the building skin will be directly connected to the design office and allow individual design requirements to be met. They enable last-minute changes and deliver the ability to respond flexibly to disruptions and failures on site, measured through 3D-scanning equipment. Thus parametric design and construction in combination with CPS-based construction methods will be the perfect basis for a fruitful and dynamic cross-disciplinary optimization process between architects, engineers and manufacturers. Smart components of the building skin will be uniquely identifiable. More than that they may be located at all times and know their own history, current status and alternative routes to achieving their target state throughout their lifetime from production through maintenance, functional updating and upgrading up to and including reuse or recycling. Machines, site and maintenance equipment as well as CBS-components of buildings will autonomously control their maintenance and repair strategy depending on the degree of "workload".

In the end it can be advantageous to build, operate and maintain the whole building twice: First of all virtually (by means of augmented reality) and finally in reality. Within the real construction and operation process every step can be compared between the virtual model and the reality (for instance through mobile 3D-scanning methods in combination with RFID tags and image recognition technology). Smart assistance systems (e.g. cyber glasses) release workers and maintenance staff from extensive and sophisticated product manuals and from having to perform routine tasks, enabling them to focus on creative, value-added activities. All of that will only be possible in the real world if common standards are being developed. The journey towards CPS-based building concepts with cognitive building skins will be an evolutionary process. At the same time it will radically transform architects`, engineers` and workers' job and competence profiles. It is therefore necessary to implement appropriate training strategies and to organize work in a way that fosters learning [9]. Thus in combination with advanced computational methods and a seamless digital process chain the new holistic approach in design, construction, operation and maintenance not only eliminates the unnecessary and useless consumption of energy, material, time and money but also guarantees consistent quality and peace of mind.

9 References

[1] Daniels, K.: *The Technology of Ecological Building – Basic Principles and Measures, and Ideas*; Birkhäuser Verlag Basel – Boston – Berlin (1995).

[2] Heusler W.: *Bewegung in der Gebäudehülle? Gegenüberstellung passiver und aktiver Konzepte*; in: Hrsg. Weller B., Tasche S.: Glasbau 2013: Ernst & Sohn Verlag Berlin (2013).

[3] acatech (Ed.): *Cyber-Physical Systems* **-** *Driving force for innovation in mobility, health, energy and production* (acatech POSITION PAPER), Munich 2011. http://www.acatech.de/fileadmin/user_upload/Baumstruktur_nach_Website/Acatech/root/de/Publikationen/Stellungnahmen/acatech_POSITION_CPS_Englisch_WEB.pdf.

[4] N.N.: *Strategic R&D Opportunities for 21st Century Cyber-Physical Systems – Connecting computer and information systems with the physical world*. Report of the Steering Committee for foundation in Innovation for Cyber Physical Systems, USA (January 2013). http://www.nist.gov/el/upload/12-Cyber-Physical-Systems020113_final.pdf.

[5] Ritter H.: *KogniHome – An intelligent apartment for life*; Bielefeld University – Cluster of Excellence Cognitive Interaction Technology (CITEC); 19 Aug. 2014. http://ekvv.uni-bielefeld.de/blog/uninews/entry/an_intelligent_apartment_for_life.

[6] Gros, J.: *Sinnliche Funktionen im Design, in: form, Zeitschrift für Gestaltung*, 1st series No. 74, 2nd series No. 75 (1976).

[7] Spath, C.; Foerg B.G.: *Storytelling & Marketing; Echomedia*, Vienna (2006).

[8] Heusler, W.: *Cyber-physical systems for cognitive building skins*; Proceedings 9th Advanced Building Conference, Oct. 2014, Brixen / Italy (2014).

[9] Kagermann H, Wahlster W, Helbig J.: *Recommendations for implementing the strategic initiative INDUSTRIE 4.0.* Technical report, acatech – National Academy of Science and Engineering. http://www.acatech.de/fileadmin/user_upload/Baumstruktur_nach_Website/Acatech/root/de/Material_fuer_Sonderseiten/Industrie_4.0/Final_report_Industrie.

Proceedings of the International Conference on Building Envelope Design and Technology, Graz
Advanced Building Skins 2015

Concepts for an environmental-reactive, interactive architectural design.

Bernhard Sommer, Dipl.-Ing.
University of Applied Arts, Vienna, Austria, bernhard.sommer@uni-ak.ac.at

Galo Moncayo, Mag. arch.
University of Applied Arts, Vienna, Austria, galo.moncayo@uni-ak.ac.at

Ulrich Pont, Dr. Dipl.-Ing.
Vienna University of Technology, Austria, ulrich.pont@tuwien.ac.at

Summary

As climate and society change, customizing buildings towards specific usage patterns and local weather conditions that might be obsolete within a few years, does not seem to be the smartest approach to building design. The paper shows results from a design research towards interactive, adaptive building envelopes combining an aesthetic celebration of change with energeticaly sustainable design strategies. Finally, it presents prototypes that combine the idea of interaction with the production of biomass, shifting the idea of architecture from being a shelter to being a habitat.

Keywords: Design Research, Interactivity, Responsive Architecture, Performative Architecture, Kinetic Architecture

1 Introduction

The present contribution reviews a set of architectural design studies that have been developed under implementation of adaptive and kinetic structures. The conceptual ideas behind the different design approaches are different, but all designs share the idea of interaction between the environment, the user and the building skin. While architectural theory and history show many examples of conceptual approaches toward moving, changeable or interactive buildings few realizations have been made, and even fewer approaches toward sustainability in these adaptive structures were conducted. As an example the Heliotrop House in Freiburg by Architect Rolf Disch can be mentioned. Also concepts of interactive architecture, as defined by Oosterhuis and his Hyperbody research institution have been – until now - rarely realized.

1.1 Task

The design concepts in this study pursue the task to develope performative, interactive architectural concepts while following the necessity of highly energy-efficient building skins. Each project follows a procedural design process influenced by inspirations from natural (for instance) but also antropogenic (for instance japanese origami paper folding techniques) origin, and links these inspirations with thoughts for energetic, ecologic and environmental architecture. This procedural workflow in design led to five innovative concepts of different scales. These concepts were not only analyzed toward their potential realization, indeed they were constructed as scaled models, that could react to environmental influences from outside or user inputs. These models use single-board microcontrollers and small electrical actuators to change their envelopes. The present paper introduces the ideas and concepts of the designs, illustrates the realization of the scaled and fully operable models, and analyzes the potentials (and potential problems) of full-scale realizations. The projects were documented from the viewpoint of building physics and energy design. All projects were created in the department of energy design at the University of Applied Arts in Vienna, and were shown in an architectural performance in the Museum of Applied Arts Vienna (MAK).

1.2 State of the art

Traditional approaches toward energy efficient and ecological friendly buildings address optimization of the building materials and systems of a given building envelope. Geometrical changes of the building morphology happen during design and optimization processes, however, few designs stay convertible once they are built, and even less offer short-term flexibility during operation. If so, then the flexibility normally applies to automatically operated window and door openings, radiation sensitive shading devices and adaptable HVAC-Systems. Very few approaches consider the transformation of the overall building shape, be it an Euclidian operation (such as rotation) or an Non-Euclidian transformations, such as NURBS-based skewing, squeezing and distortion.

- A well-known example for Euclidian movement of a building skin as a whole is the **Heliotrop House** in Freiburg by Architect Rolf Disch, [1] illustrated in Figure 1. This highly-insulated building was constructed in 1994, and features a centralized plan, where the envelope can be rotated around its vertical central axis to pursue the sun position for maximizing solar gains.
- A less known example for the rotation of a whole building (not only the skin) is the **Rotating Aluminium House** in Snow Creek, Palms Springs, erected by aerospace engineer Floyd D'Angelo, depicted in Figure 2. This project is for its time especially mentionable, as "*In order to rotate the home […] D'Angelo adapted a device from his product company that was made to open and close aluminum loovers. Originally, D'Angelo powered the mechanical equipment through a photovoltaic cell on the roof which powered the system's rotation arc*." [2] When the one of the authors visited the place, the power supply was a Diesel engine. It was only set into motion for presenting it to the visitors, but was not in use properl anymore.
- Further well known examples of Euclidian transformation of building geometry include Hoberman Associates, who realized an Euclidian **transforming curtain** as a stage installation at the Salt Lake City Olympics Medals Plaza in 2002 [3], Figure 3,
- as well as the infrastructure building of the **Falkirk wheel**, completed in 2001, designed by Nicoll Rusell Studios, Figure 4, [4].

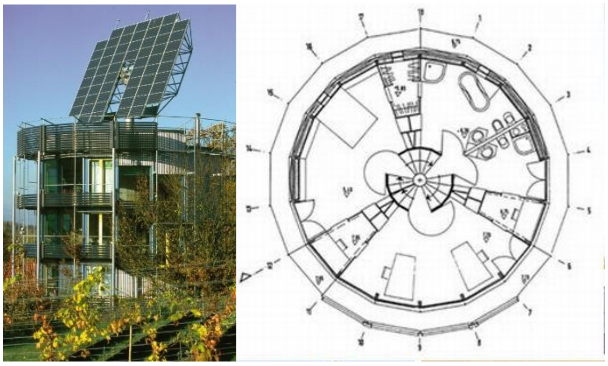

Figure 1: Heliotrop House. Rolf Disch (pictures: www.rolfdisch.de (left) and www.ecofriend.com (right).

Figure 2. D'Angelo House, Snow Creek, Palms Spring. A rotating structure for minimizing the solar impact (picture courtesy of B.Sommer).

Figure 3. Hoberman Arch, Salt Lake City, different transformations (pictures: S.R. Edupuganti 2013).

Figure 4: Falkirk Wheel, Nicoll Rusell Studio,(pictures: (https://www.youtube.com/watch?v=n61KUGDWz2A&feature=kp)

There are fewer examples of non-Euclidian geometry transformations, some examples have been chronologically listed below:

- Frei Otto's **Inflatable Marquee** 1979 [5]; This study of Frei Otto shows a growing and diving changeable pneumatic construction;
- **Dynamat**, Simon Conolly and Mark Fisher 1971 [6]; This project' structure is as well based on a pneumatic principles showing two layers of inflatable cushions, thus allowing for a fully controlled transformation of non-curved into single- and doublecurved forms. With this principle both synclastic and anticlastic forms can be realized.
- The **Hyposurface projects** of the dECOi architects [7]: These projects resemble interactively reacting, physically moving screens, based on indivually controlled pistons;
- Michael Fox's **Flock Wall** working out with fishing lines and reels to change form [8];
- The **Kiefer-Technik Showroom** by Giselbrecht and partner ZT [9] is one of the few realized full scale application of a controllable three-dimensional surface close to the afore-mentioned hyposurface projects, implemented as a shading device.
- The concepts of **interactive architecture**, as defined by Oosterhuis [10] and his Hyperbody research institution have been – until now - rarely realized. The design principles of Hyperbody do not clearly tackle the question of energy performance as a first prerequisite, but easily could be adapted for this purposes.

Most of the concepts of the Non-Euclidean projects targeted interactive design strategies in the first place. It is remarkable that Non Euclidean geometries seem to be an intrinsic approach when it comes to the realization of interactive architecture.

In this paper, five design studies are presented and reviewed, which combined interactive transformation of building envelopes, similar to the above mentioned, with energy performance considerations. These five designs are presented and discussed in the subsequent sections.

2 MAK NITE Lab - Ecological Ballet

With „Ecological Ballet" five student teams of the Department of Energy Design, University of Applied Arts Vienna, presented their prototypical projects on sustainable design. Since early 2013, the Department of Energy Design aims to develop interactive concepts for sustainable architecture under the title "Energy Design Adaptive Strategies". First results of this new approach have been presented to the public for the first time with an architecture performance at the MAK NITE Lab, a platform for experiments and experimental designs of Vienna´s Museum of Applied Arts / Contemporary Art curated by Marlies Wirth.
The students have taken up the challenge to re-conceptualize architectural elements, such as the building skin and structure trying to find new ways to react to varying climate conditions and to changing social developments.

2.1 Floral Skin

This approach (Students: M. Lichtenwagner and C. Yönetim) was based on an Origami pattern, and features an adaptive building envelope, capable of changing the volume to surface ratio (compactness). Additionally, parts of the skin are capable of being rotated towards the sun-position for optimal usage of insolation with Photovoltaics. As shown in Figure 5, he structure features 4 different surface types:

- black surfaces resemble solar collectors with a high degree of solar absorption to produce heat;
- grey surfaces symbolize Photovoltaic panels for generation of electrical power;
- blue surfaces symbolize transparent parts of the building envelope;
- white surfaces are opaque with a high degree of reflection.

The expanded structure is optimized for winter season and resembles a closed air tight building skin. The collapsed structure on the one hand totally folds away the black absorbing areas and reduces transparent surfaces, while keeping the highly-reflecting as shading devices in place. The PV-cells are in this mode better protected against overheating, thus will show a higher efficiency. On the other hand, through collapsing the skin is opened for natural ventilation. Figure 6 shows the manipulation of the model (influencing the photosensors on the surface), while Figure 7 illustrates the folding process of the skin.

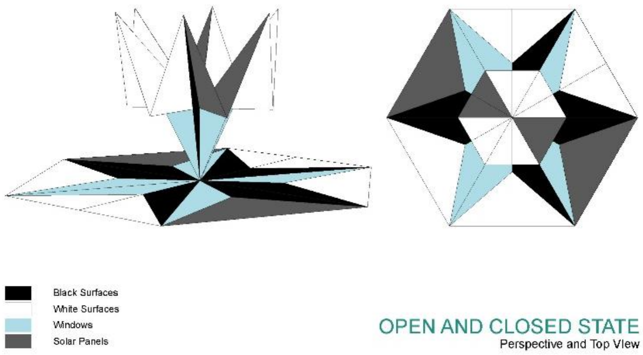

Figure 5: Design principle of Floral Skin. (picture courtesy of M.Lichtenwagner and C.Yönetim)

Figure 6: Floral Skin in winter mode (left) and summer mode (right). (picture courtesy MAK/K.Wißkirchen)

Figure 7: Folding process of Floral Skin. (Picture courtesy G.Moncayo)

2.2 Breathe

With this design (Students: M. Urschler, R. Portillo) the building skin actively supports the ventilation of the interior space. It features a mode for the cooling and a mode for the heating season.
A folding structure allows the building skin to be expanded in summer (increased volume) and decreased in winter times (smaller volume) to reduce the area of the skin as well as the amount of preconditioned air for ventilation and thus the heating demand. The underlying principle influences the characteristic length of the object, optimizing it for the prevailing season.
Independent of the season and state of compression, the structure is capable of “breathing”, which means peristaltic movements of the skin itself to force ventilation. The realization as a model was done via an origami-like folded paper structure. It was actuated by three rotational electric motors influenced by lighting levels in the area of the three entrances of the building model. The control scheme forces pre-warmed air from sun-exposed areas into the interior in the heating period, while in cooling period it funnels cool air from shaded areas into the building. Figure 8 illustrates the applied construction, while Figure 9 shows a visitor manipulating the shading sensor.

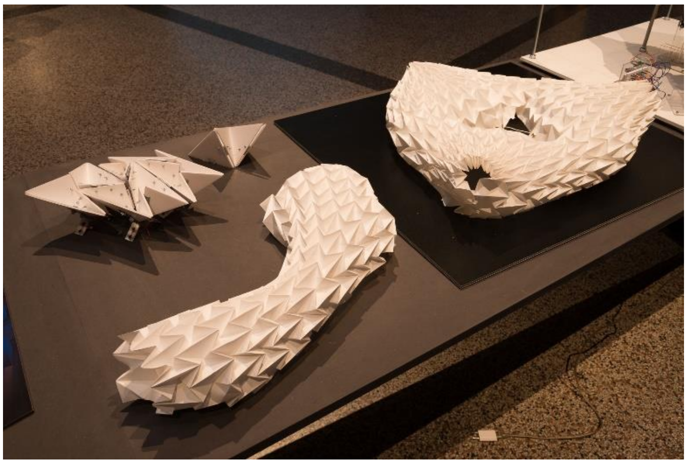

Figure 8: Breathe (picture courtesy MAK/K.Wißkirchen).

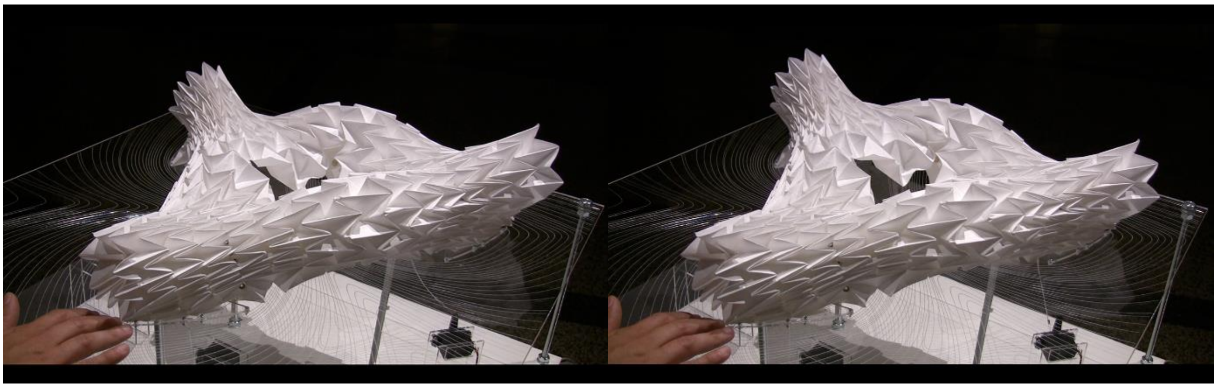

Figure 9: A visitor ineracting with Breathe. (Picture courtesy G.Moncayo)

2.3 Kaleidoskin

This project (Students: B. Chompff and C. Wunderlich) is about the use of passive energy resources such as solar gains and natural ventilation - customized for an individual person and just in time. The skin performs according to user requirements and preferences during occupancy. For instance, during occupancy a maximum of daylight penetration could be set as a user defined target. Whenever no user is present within a certain distance, the performance goal of the structure is to maintain a constant indoor climate, e.g. by shading or ventilation. The building skin is designed to remember user preferences and towards learning and adjusting its behavior to specific users. The project was realized as a technical 1:1 mock-up. The interaction with users is driven by proximity sensors, so that the façade fragment follows the visitors according to seasonal and individual preferences. The double layered skin driven by rotational actuators creates an infinite number of patterns and gradients between different degrees of transparency on the one hand, and different permeability for ventilation on the other hand. Figures 10 and 11 show the principle design of Kaleidoskin, while Figures 12 and 13 show the surfaces and proximity sensor and the transformation process.

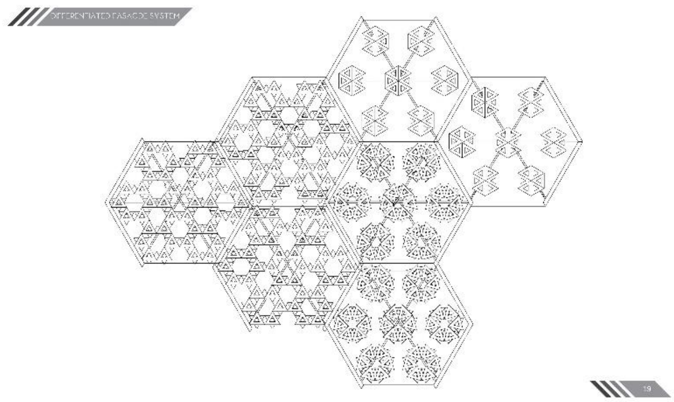

Figure 10: Design sketch of Kaleidoskin. Courtesy of B. Chompff and C. Wunderlich

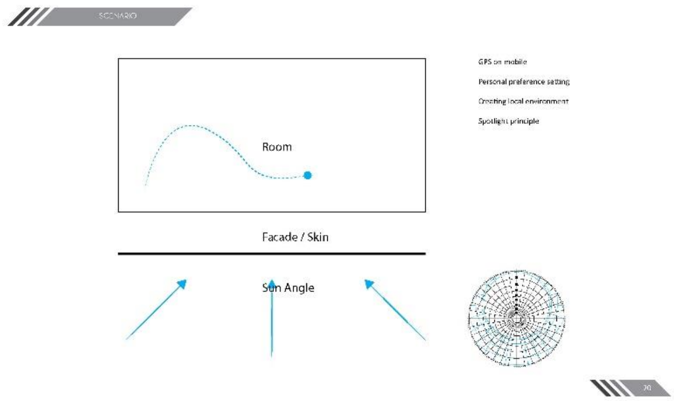

Figure 11: Interaction Scheme of Kaleidoskin. Courtesy of B. Chompff and C. Wunderlich

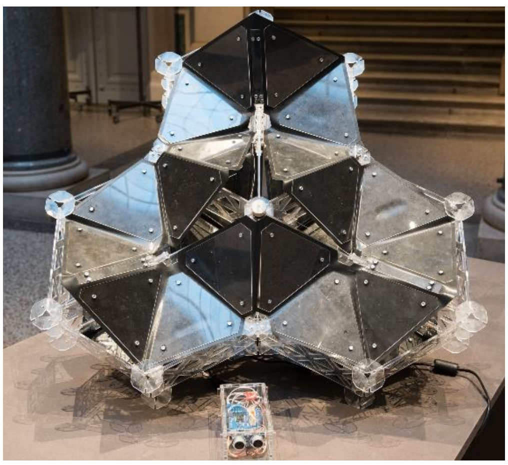

Figure 12: the different layers surfaces and the proximity sensor. Picture courtesy MAK/K. Wißkirchen

Figure 13: Transformation of the Mock Up. Picture courtesy of G.Moncalo

2.4 Jelly

This design of a pavillon (Students: D. Prost, K. Sitzmann) features an elegant kinematic form changing mechanism inspired by Theo Jansen. It lifts a curtain-like skin in wintertime to allow a maximum of solar gains, while in summer it lifts the skin only where it is shaded to avoid overheating inside. Therefore, a sophisticated control scheme for the envelope was designed. This includes a set of sensing devices, measuring the temperature inside and outside of the structure, as well as the solar radiation via pyranometers on different grid points on the surface. In the heating period (desired temperature inside > outside), Jelly opens the curved envelope to the points of maximum solar incidence, while in the cooling period (desired temperature inside < temperature outside) it allows for ventilation openings, where the solar incidence is at a minimum - see Figure 14. This setup allows for a real-time interactive adaption of the building skin to the indoor and outdoor climate, not only considering the sun inclination, but also cloud cover and seasonal changes. In the scaled model, this advanced control scheme has not been realized 1:1, as the model was constructed for a display in a museum (no outside climate impact): The impact of the environment was replaced by the audience, which would shade light sensors thus triggering the transformation process of the pavillion´s skeleton. Figure 17 shows visitors deliberately amplifying the effect of shading on the model, while Figure 18 illustrates the transformation process.
The challenge of bringing the designs' complex movement patterns into reality was solved with a kinetic system driven by just one single rotational actuator. The structure allows for more than just a repetitive movement pattern, as the rotational movement in the xy-plane has been combined with a translation in the z-axis (compare Figures 15 and 16).

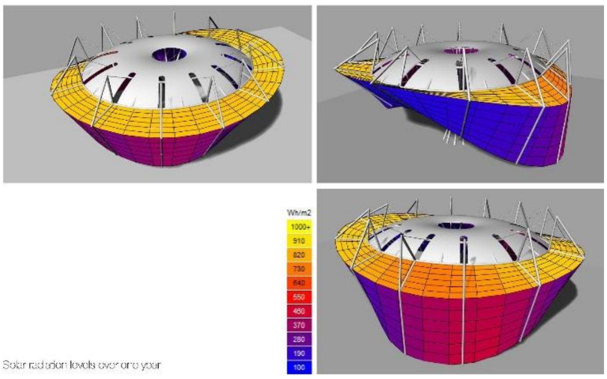

Figure 14: Summer behaviour. Courtesy of D.Prost and K.Sitzmann

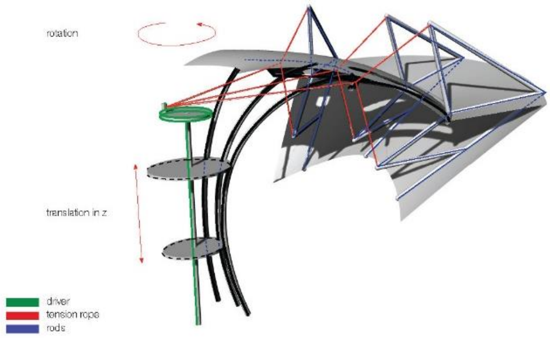

Figure 15: Transformation principles. Courtesy of D.Prost and K.Sitzmann

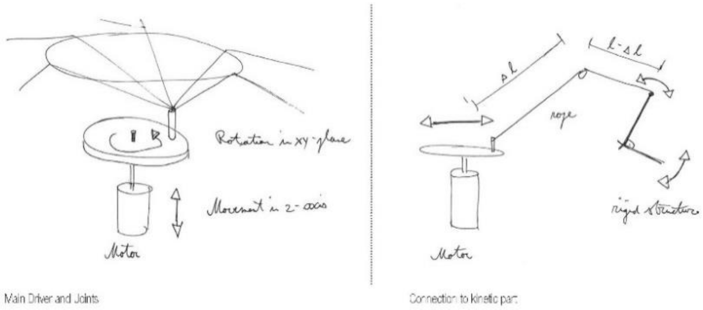

Figure 16: Transformation principles. Sketches courtesy of D.Prost and K.Sitzmann

Figure 17: Visitor interaction. Picture courtesy MAK/K. Wißkirchen

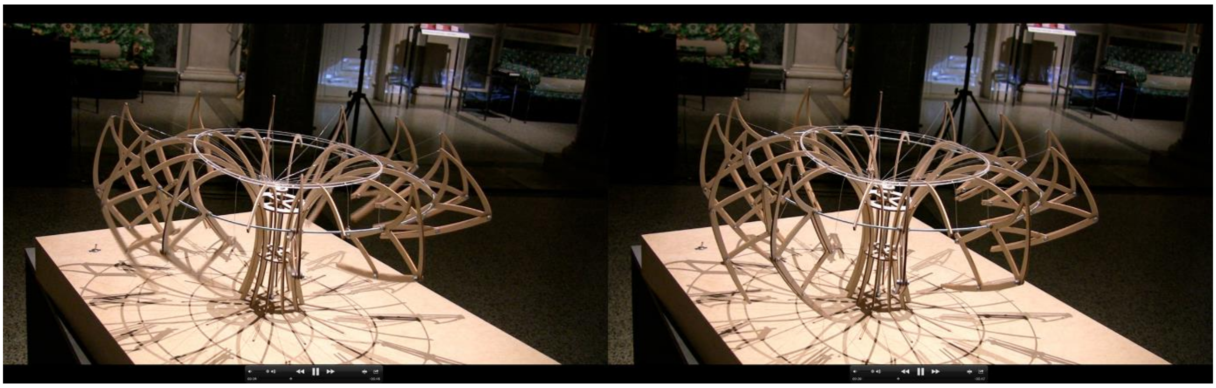

Figure 18: Transformation of the pavillion. Picture courtesy G.Moncayo

2.5 Dancing with the winds

This design project was originally intended for the local micro-climate of the city of Hong Kong, and uses (prevailing) wind speed and direction as an actuator for change of the form of a high-rise. Mild and slow winds are used for chilling the building, thus the building turns its broad side to the wind, while strong winds make the building show its narrow sides to reduce wind pressure stress on the façade elements and the overall structure. If outside conditions are fine for wind chilling and natural ventilation the building enlarges its surfaces toward the wind direction, thus using windward and leeward effects to control pressure differences for cross ventilation (Figure 19). A realization of this concept would need a sensing grid (wind speed, temperature, humidity) on the façade of such a structure as well as indoor climate monitoring. That way the shape of the tower can precisely respond to different microclimatic states on the facade. In the exhibiton, the scaled model interacted with the visitors through insufflation. If the airflow is slow, the modell enlarges the surface towards the direction of the prevailing winds, if the airflow is strong the building minimizing the surface towards the prevailing wind direction. Figure 20 shows the transformation of the tower model.

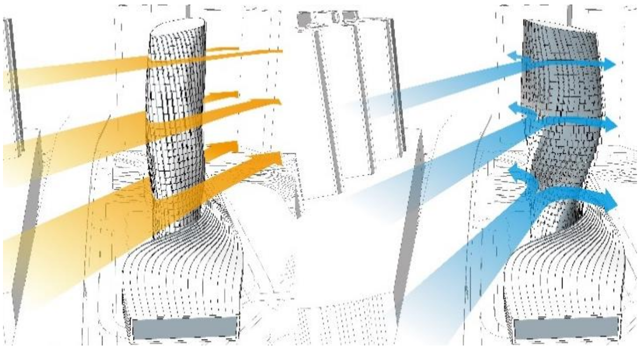

Figure 19: Different pressure and temperature situations minimizes (right) or maximizes (left) the skin area towards the wind direction. Courtesy of P.Reinsberg and X.Wan.

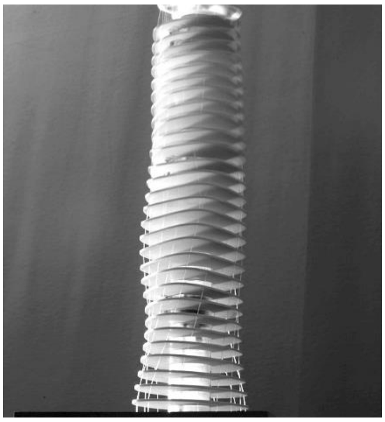

Figure 20: Tower while transforming. Picture courtesy of R. Zettl

3 Sol Seduction - A Phyto-Solar Ball-Room

The projects of the Ecologic Ballet have been presented and discussed at the 10th European Conference on Product & Process Modelling in September 2014 [11]. One conclusion was that future work should address the realization of such concepts in 1:1 mock-ups. With SolSeduction a few mock-ups could be realized and were presented in an exhibition in November 2014 at the Heiligenkreuzer Hof in Vienna. The conceptual approach and task was deepened for this follow-up seminar.

The idea of buildings producing more energy as they need is widely discussed and projects are being realized, usually under the label "Plus-Energie-Gebäude". However, this concept is probelmatic, if seen as a fundamental solution for the energy demand of buildings: North of the tropical and sub-tropical zones, where most developed countries are located and the total energy demand is highest, the production of solar electrical energy is more or less limited to the summer period, where demand e.g. for lighting is much higher in the winter season [12]. One alternative and further developement could be the production of biomass as a way of chemically storing energy and transforming it to electricity and heat just in time, when needed. The biomass production could be integrated in the building skin. A building with an algae bioreactor facade has first been developed to realization by the Austrian architecture office *Splitterwerk* in cooperation with *Arup* [13]. Taking up this approach, we want to re-think the architectural environment towards a symbiotic habitat. The role of energy thus is not seen as a question of supply, but as one parameter among others that shapes the environment. A habitat, in our definition, relies on the physical, chemical and social interaction of different elements and organisms. Full-scale spatial prototypes, as elements of such a habitat, have been developed focussing on these interfaces between climate, people and other organisms, such as plankton and algae.
The prototypes were presented in the above mentioned exhibition. Each prototype was equipped with different sensors to enable them to interact with visitors and the physical conditions on site, re-acting and adapting in real-time.

3.1 Luminiscent.Tracings.

(Students: A. Chantanakajornfung, M. Hanshans, N. Polo, A. Staskevits) This habitat provides an artificial day zone and an artificial night zone. Bioluminiscent organisms - *pyrocystis lunula* - help to orient in the darkness and accompany the visitors in the night zone. According to movement of the visitors, transparent cushions will vibrate, triggering the necessary turbulences to make the plankton glow. The movement is traced by a kinect sensor. As the plankton needs a more or less precise 12 hour rythm of day and night, there are two different populations, that change sides after 12 hours. The change is driven by a mechanical clock, that slowly lowers respectively raises the two elements, so that the fluid with the plankton can flow freely to the other zone.

Figure 21: Luminiscent.Tracings. Picture courtesy of Alek Kawka

3.2 Oxy.Clmn.

(Students: A. Chantanakajornfung, M. Hanshans, N. Polo, A. Staskevits) From a column, pools of algae - *chlorella vulgaris* - spread towards the ceiling. The algae consume the CO_2 that the visitors exhale giving back oxygen to the exhibition space. They actively take in the air around them, just as they would breathe. If there are more visitors in the space around them, their breathing activity decreases, as they will get enough CO2 anyway. That way, efforts of pumping air into their system can be reduced. The organism add to an ornamental cladding and contribute an air, clean and rich on oxygen, to the exhibition space. A dozen of light sensors orchestrate the interaction between visitors and algae.

Figure 22: Oxy.Clmn. Picture courtesy of Alek Kawka

3.3 .

(Student: C. Anich, D. Rhomberg) This project is an instrument that is ruled by a slime mould. Four satellite stations distributed in the exhibition space around the slime moulds center house loudspeakers and kinect proximity sensors. The activity of the sensor is visualized by a blue glowing light. The slime mould lives in a habitat, trying to reach nutrition, yet, avoiding light. LEDs in the mould habitat glow according to the activity and distribution of the people in the room. The activity is fed into a synthesizer, creating an ambient electronic sound. The slime mould can conduct electricity and is connected with the synthesizer. As it changes its growth pattern due to the LEDs, it changes the music.

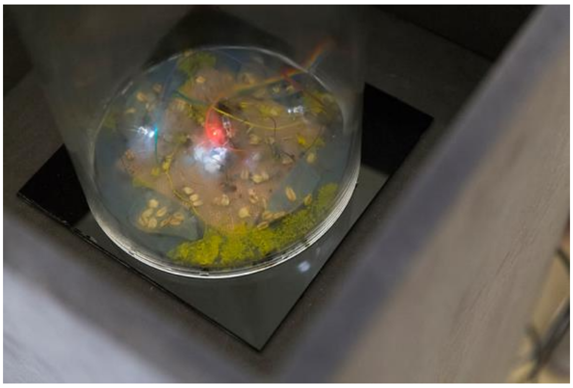

Figure 23: Drone.Synthesis. Picture courtesy of Alek Kawka

4 Conclusion

A wide variety of design options and new aesthetic experiences can be obtain by taking up new sustainable technical strategies. This potential lies completely open and architects should learn to use these new strategies as design drivers. From the present work, most promising seems the project Oxy.Clmn., as the algae significantly reproduced after two weeks of exhibition, although the exhibition room was not very well lit and although the exhibition took place in November. Compared with the realized *The Algae House*, from *Splitterwerk / Arup*, the project shows at least two steps forward: it combines the production of biomass with the cleaning of the indoor air and the algae does not need to be heated in winter.

5 Acknowledgements

The projects were made possible by extra funding from the Rektor of the University of Applied Arts Vienna, Gerald Bast. The developement of the prototypes was accompanied by visiting critics Claudia Pasquero and Marco Poletto from UCL Bartlett / ecoLogicStudio.

6 References

[1] Disch. 1994. *Heliotrop*. http://www.rolfdisch.de/
[2] D'Angelo 1963. *D'Angelo House*. http://la.curbed.com/archives/2012/11/deserts_rotating_dangelo_house_hits_the_market_for_279k.php
[3] Edupuganti S.R. 2014. *Dynamic Shading: An Analysis.* Master-Thesis. University of Wahsington. Supervisors: B.R. Johnson, R. Corser.
[4] *Falkirk Wheel*. 2014. http://www.thefalkirkwheel.co.uk/about-the-wheel-/design-and-engineering
[5] Otto, F., *Pneu und Knochen,* Institut für Leichte Flächentragwerke, IL35, Stuttgart 1989
[6] Häuplik S., Sommer B., and Aguzzi M. 2007. *Inflatable Technologies – From Dream to Reality*, in: 58th International Astronautical Congress 2007, India Hyderabad, Paper number IAC-07-C2.2.08
[7] *dECOi*. 2014 www.hyposurface
[8] Fox M. 2009. Flockwall: *A Full-Scale Spatial Environemnt with Discrete Collaborative Modules*; available from: http://cumincad.architexturez.net/system/files/pdf/acadia09_90.content.pdf (accessed April 2014)
[9] Giselbrecht und Partner ZT. 2014, http://www.giselbrecht.at/
[10] Oosterhuis K. (ed): *Hyperbody – the first decade of interactive architecture*, JapSamBooks, Rotterdam 2013
[11] B. Sommer, G. Moncayo, and U. Pont: *Ecological ballet – a design research towards environmental-reactive, adaptive architectural design*, in: eWork and eBusiness in Architecture, Engineering and Construction. Aug 2014, pp. 215 -220
[12] Leibundgut, H.: *LowEx building design: für eine ZeroEmission Architecture*, vdf Hochschulverlag AG, 2011, pp. 56-58
[13] Blaschitz , M., Wurm, J. , Hemmrich E., Arup , Splitterwerk: *Das Algenhaus / The Algae House*, Niggli Verlag, Zürich, 2014

An open source method for prototyping kinematic building components

Christoph Müller, Univ.Lektor Dipl.-Ing. BSc
Vienna University of Technology, Austria, mail@mueller-christoph.com, www.mueller-christoph.com

Summary

Virtual, as well as physical prototypes, enhance the design-process by pointing out problems and potentials in early design stages. Furthermore, they communicate the concepts to contractors and clients. But when building prototypes for kinematic architecture, moveable parts – especially computer controlled moving parts – are often a challenge to architects. This paper describes an explicit method for an easy and cost-efficient way to handle this challenge. It is focusing especially on conceptual and design-relevant needs from an architect's point of view.

Keywords: Interactive architecture, kinematic components, open source, design-methods, prototyping

1 Impulse

During my ongoing doctoral research at UT Vienna, a prototype controlled by 48 servos was created. Even if I am interested in computer graphics, mechanics and robotics beside to architecture, it was hard to be up to this task. A lot of knowledge from other disciplines is needed. Even if the information is accessible, it is hard to read and understand as a member from neighboring fields. The idea of this paper is to give an overview of one possible method done with open source software. It is between theory and practice and extended with the possibility to download all examples at my homepage. Instead of starting by zero, those who want to build their own prototypes can modify these reference models.

2 Method

2.1 Virtual and physical prototyping

In order to develop kinematic architecture, the interaction between analog and digital form-finding-methods is a key point. In most cases there is no hierarchical order of handmade sketches rather than modelling with a PC. It consists much more in a constant change of methods, leading to different points of view, on a complicated topic. Both approaches deliver different kinds of information to precise the design process. Focusing on this topic: Virtual prototypes, especially parametric ones, provide the possibility to work on the logic of shapes and simulate physical behavior cost efficiently. Physical prototypes on the other hand, inform about the scale, the proportions as well as the robust dimensioning of components. There is no chronological order either. Nevertheless, this paper starts out with the digital part.

2.2 Software

Classical CAD-Software used by architects is designed to draw static models. But when it comes to developing moving parts, they lack the fitting tools. Especially the missing possibilities to simulate connections between parts.

In this case, we have to watch out for better solutions. The animation-movie-industry already deals with the topic of moveable models in computer graphics for a long time. Game developers are also into the interaction and the control of geometry in virtual space. This is the reason why tools from this industries could also be fitting environments for prototyping kinematic building-parts in architecture. For example: There are tools which allow to setup up different joints between single components. If one part is moving, others will follow automatically. A lot of mathematics, as for instance the calculation of inverse kinematics, is done invisibly in the background. Rather than tipping numbers to drive a motor, a setup of turning sliders, as well as brushing weights and moving attractors are preferable methods. Not only because it is more comfortable. They provide a real-time feedback of the influence on the shape when changing a value. Geometrical consequences can be concluded.

From the side of the software, we can split the entire task of prototyping kinematic building components into three sections:

- Design and modeling of geometry
- Setup and simulation of kinematic constraints
- Connecting to the model and controlling it

Right now, there is no tool which would allow all these steps at once satisfyingly. Tools specialized in a few single steps are more powerful. However, especially the first steps rely on each other. The constraints between geometry is heavily influencing the shape and defines design rules as well as vice versa. A fast interaction between chosen tools is important. This paper discuses a combination of tools and their connection among each other.

The used tool in this method is the DCC-program called Blender 3D. The most important reason is, that a lot of colleagues in the field of architecture already use it for visualizing their CAD-models. Furthermore, it is open-source, which in this case means that it is free to use. By the way: One big advantage of most open source is also the wide community which can give feedback really quickly.

Of course it is possible to draw static parts with classical CAD and just export it into DCC. But the mentioned need of fast interaction between the modelling and simulating section could be done in one program. The goal is to shorten the “pipeline” between modelling, simulating, evaluating and updating the geometry with new knowledge.

2.3 Connection from bottom up

Newton’s third axiom actio-reactio tells us that every action is forcing a reaction. But who has got the power and how is just driven? This part is not about mechanics. It is about the possibility that a motor in a physical prototype not necessarily has to be the initial action in its virtual clone. Let’s discuss this with the help of an example.

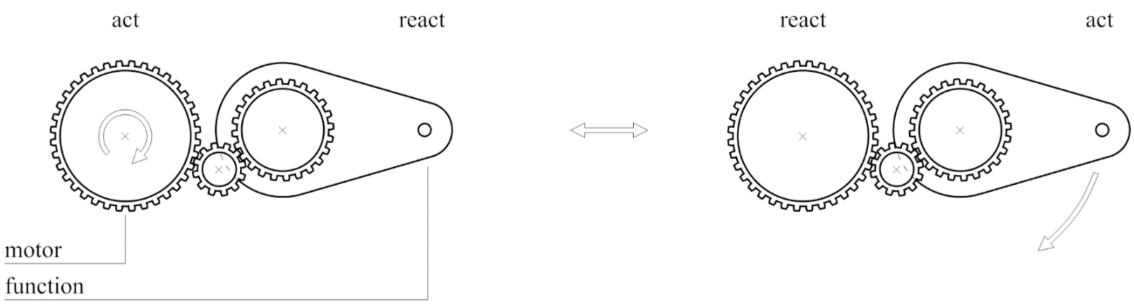

Figure 1: Example for translating rotary motion

The above figure shows a simple gear. To setup up such connections we need to transfer a rotation from one object to another. Therefore we can use the Copy-Rotation. The question is: Which is affecting the other? Let’s say, in the physical prototype, that the first wheel is the motor that rotates the second one. The second Wheel is transferring to the third wheel, which is representing a function in this case. Of course we can clone this relation to our virtual model. What we would get is actually the same information as in the physical model. But we are not interested in how far the motor is spinning, rather than how the last gear-wheel in the row has to be driven. So let's turn it around. In the virtual space the third gear-wheel is going to be the source transferring via the second one finally to the motor. With the principle of reverting this chain we can explore the behavior of more complex prototypes.

Excursion: In general we can differentiate between two principal types of motion: Rotary and linear movement. Every movement can finally be split up into this to basic motions as well as a combination of both [1]. Furthermore a rotary movement can be transferred to a linear as is discussed in the next example.

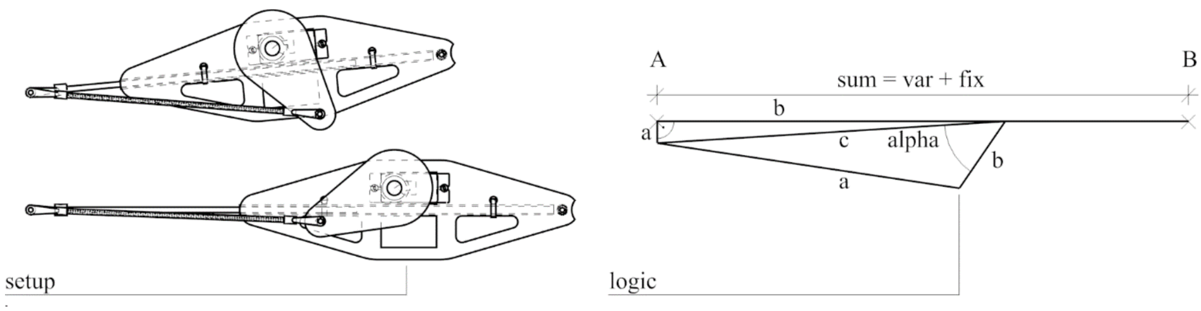

Figure 2: Example for translating rotary to linear motion

What are the other goals in virtual prototyping? This transfer from rotary to linear movement exists out of several single parts. We could think of controlling this whole setup via two points and mount each single part in a way it can automatically follow.

If point B is moving, the object origin of the support should move to the same position in real-time. To do so, we can setup a Copy Location for the support. At the same time, its tip should always aim to the opposite Point A. To achieve this, we setup a Track To and call Point A as target. For the steering, the same method works vice versa.

The next step is making the motor stick to the support. We could just join them, but it is a good chance to show a connection via child and parent. In this case the motor is child of its parent support. In opposition to Copy Location, the Child-Parent-Connection allows to transfer the whole location and rotation in relation to the parent object.

The last step is to setup a connection with the rods. Therefore we could use an armature of two bones whit an Inverse Kinematic setup, between the origin of the motor and the two points. This allows us to make the two rods child of each in order to follow them. (Please take a look at the downloadable example)

Instead of using a visual setup to connect the parts, we can use math only. This part describes the calculation of the distance via Theorem of Pythagoras [2] and Law of Cosines [2].

$$\text{var} = \sqrt{(xB - xA)^2 + (yB - yA)^2 + (zB - zA)^2} - fix$$

$$alpha = \arccos\left(\frac{c^2 + b^2 - c^2}{2bc}\right)$$

We should also note that beside math, every single tool within Blender 3D can also be accessed via scripting. For a more complex geometry this is quite useful. If changes are made during the design process, the script can be executed again with different parameters. Furthermore, it allows more than one person to work on the project at once. (To find out more you can check out the examples in the download section)

2.4 Connection from top down

When setting up connections between components, it is important to think about the wanted relation between the single part and the overall system. Do we want to control a system from the movement of its single parts, or do we want to get information on how single parts should move in order to achieve a change of the overall system?

Contemporary architecture is dealing with the idea of fields [3]. Gradient transition between different areas is topic as well. For example facades with a lot of single elements that can react to different situations. Controlling each motor separately would be time consuming or even not possible. Therefore, we need to setup control mechanisms that allow to drive more motors simultaneously by overall rules.

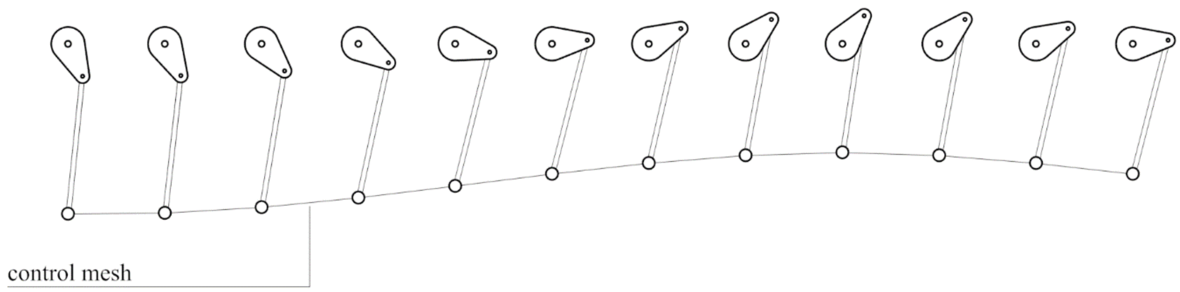

Figure 3: Control mesh

As discussed above, it is handy to mount components to points for efficient control. One step further we can connect these points to fields in the form of a control mesh. This mesh can be easily deformed with proportional editing or Laplacian Deform, to control a field of single components.

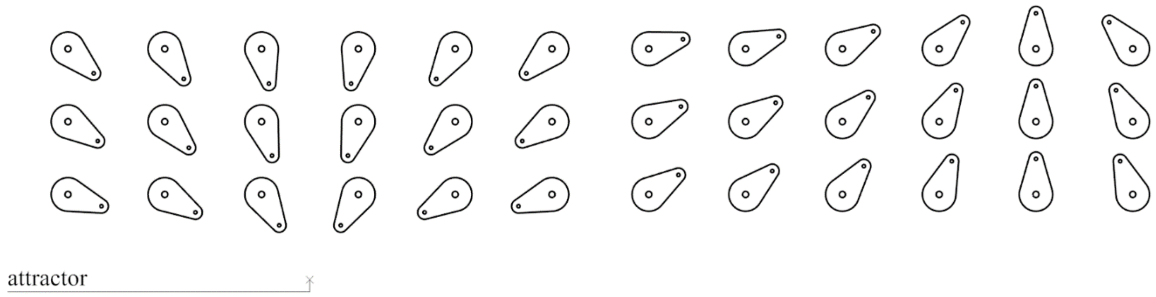

Figure 4: Attractors

Another possible method to do so is the use of Attractors. In the shown example, Empties are used as targets for each of the components. When moving one Empty, components react as field on them. Not only the angle, also the distance and other parameters could be used as input.

2.5 Control

An easy way to affect this top down principle of controlling geometry is the Shape Key System. It allows to save different alterations of the same shape. Furthermore it is possible to blend this shape between one another. Doing so, the geometry can change smoothly from one condition to another. But how can we control a prototype interactively?

Blender 3D offers two different engines. The first one is Blender Render, the usual interface to create and manipulate geometry. This engine is used by default and therefore a familiar way to change for example a mesh. If a prototype is connected to this mesh, such as explained before, the user is controlling the physical prototype just like he is used to change the shape of a mesh. Therefore it is a simple and easy solution to use in the first stage.

The second engine is Blender Game. As the name suggests, it is used to develop and run computer games. It provides setup to connect to Joystick, Mouse and Keyboard via the Logic Editor. Controlling a virtual character would be a common task. So of course we can also use this engine to control a prototype in virtual space and cloning its motion to the physical model. Simple node setups allow to setup an input in order to manipulate any property of the 3D-Modell.

Furthermore this engine provides a simple export method to create a standalone application. This is handy in order to easily design one's own graphical user interfaces. It also allows to use technology developed for real-time rendering of computer games in order to visualize material properties and light. Especially when communicating with customers, this is an important part. For non-architects, a geometry is much more readable, with material and lightened – even if it's only in a sketchy way. In this case, digital and analog models are completing each other. The digital Model is providing information on material as well as information on the logic and more like mention before. The analog one is giving impression on scale and more.

Last but not least, one should mention that a prototype can also be entirely controlled by its own. You will find additional information later on.

2.6 Simulation of other physics

Before getting into the hardware part of the paper, on more topic should be considered. Until now, we have only discussed methods to clone for example a mechanical motor to the virtual space. Furthermore, tools from movie and gaming industry, just like Blender 3D, do have the possibility to simulate physical phenomena like cloth and so on. They do not deliver a precise physical calculation rather than just quickly imitate their behavior. For architecture this is a fast method to have visual feedback on a concept working for example with membranes and much more.

2.7 Connection to hardware

We have already discussed various methods to simulate the motion of a motor in virtual space. We also found methods to evaluate the angle a motor has to turn. One missing component is the connection between computer and motor. This gap is filled with a microcontroller like in this case an Arduino derivate called Dagu Red Back Spider. This controller is connected via USB and can be accessed via the Serial Port. Each servo is then connected to one pin at the controller.

The common approach now is sending a data package consisting of two numbers: The pin, which is going to be accessed and the angle in which it should move. To achieve a smooth motion of the servo and to control its speed, we are sending this information constantly.

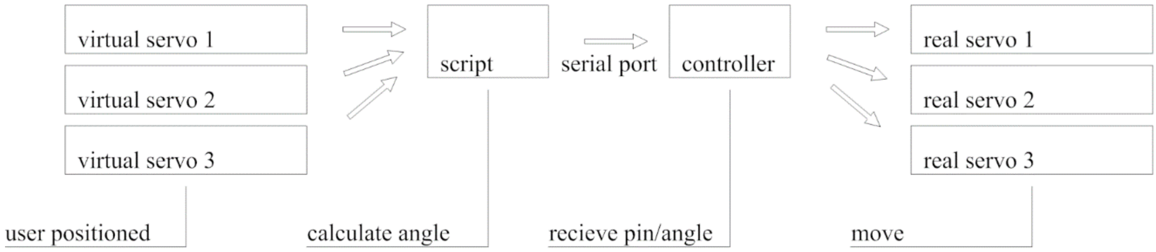

Figure 5: Schema

In order to make the controller able to handle this information we have to program it in advance. There is a detailed instruction available at Arduinos homepage. To control more than one servo you will find instruction from the manual of Dagu Red Back Spider.

When programming the controller this way, it is able to work on its own. It would be also possible to drive the physical prototype entirely without PC. The shown method is focusing on more complicated calculations which cannot be done on the controller. Furthermore we can setup the whole connection between parts with visual feedback.

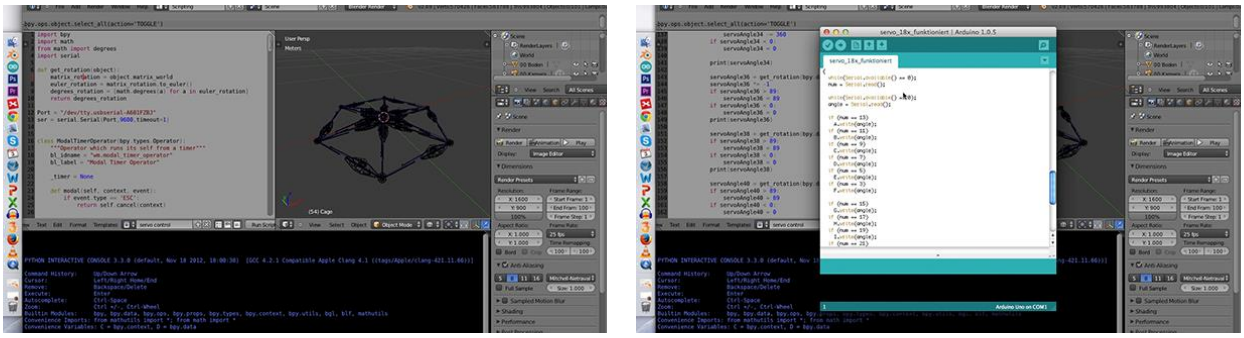

Figure 6: prototype

The pictures above finally show a virtual prototype and the panel of Arduino. This setup allows to simulate the motion of the physical clone in advance. Finally the motion can be transferred to the physical clone in order to make it move.

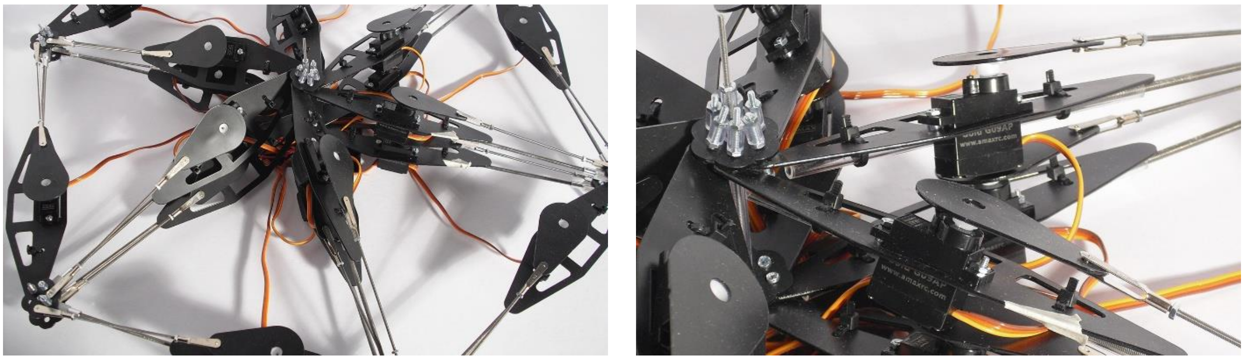

Figure 7: physical clone

3 Conclusion

Interaction and Sharing is a keyword in the whole process of prototyping kinematic building components. Beside the verbatim interaction and sharing of information between software and hardware, the interaction and sharing between disciplines like informatics, mathematics, electronics, engineering, architecture and much more is necessary. To push the development in kinematic architecture forward, the idea of open source should be considered.

4 Acknowledgements

The present paper is part of an ongoing doctoral research under the direction of Manfred Berthold and Margit Gföhler at Vienna University of Technology. The focus of the research is the creation a self-organizing kinematic surface working as interactive building skin.

5 References

[1] Schumacher, M., Schaeffer O., Vogt M-M.: *MOVE: Architektur in Bewegung - Dynamische Komponenten und Bauteile,* Birkhäuser Verlag AB, Basel, 2010.

[2] Papula, L.: *Mathematische Formelsammlung für Ingenieure und Naturwissenschaftler,* Vieweg + Teubner, Wiesbaden, 2009.

[3] Allen, S.: *From object to field,* in: AD Profile 127 (Architecture after Geometry) Architectural Design vol.67 no.5/6 May/June (1997) issue 9, pp. 24-31.

Proceedings of the International Conference on Building Envelope Design and Technology, Graz
Advanced Building Skins 2015

Schüco Parametric System Uniqueness in Series

Andreas Fuchs, Prof.
FAT LAB, Germany, afuchs@fat-lab.de

Stefan Peters, Prof. Dr.-Ing.
Graz University of Technology,
Austria, stefan.peters@engelsmannpeters.at

Oliver Hans, Dipl.-Ing. M.Sc.
Schüco, Germany, ohans@schueco.com

Jörg Möhring, Dr.-Ing.
Schüco, Germany, jmoehring@schueco.com

Summary

Today's parametric design tools allow for geometric variation throughout architectural projects, permitting the designer to manipulate i.e. an entire façade while controlling each element individually. The technical implementation of constructions developed parametrically is generally complex and demanding. Architects, engineers and fabricators are confronted with challenges of geometry, structural design, complicated detailing and varying software interfaces during design and production. With the Schüco Parametric System these problems have been addressed by developing a tested aluminium façade system based on a set of variable geometries that are parametrically adaptable and supported by a secure digital process chain as well as embedded structural analyses and the mass customization of certain components.

Keywords: Parametric modelling, digital process, BIM, mass customization.

1 Introduction

For over two decades and following a century of efficient, functional and often orthogonal architecture, we have experienced the extensive search for ever more complex building geometries and expressive architectural forms. This development is shaped by a wide variety of motives which, from our point of view, could hardly be more different. In some projects it appears important to architects and clients to set themselves apart from the "formal" standard. At the same time designers declare solar radiation, shading and optimum lighting of the rooms to be "design parameters" and thus shape both the building form and the building envelope. Example projects, such as the C10 high-rise of Darmstadt University of Applied Sciences (German Façade Prize 2013 [1]) by Staab Architects and the Oxford Street Project in London by Future Systems show prismatic façades despite a different approach in the design process. If the objective in Darmstadt was clearly the fusion of design with solar shading functionality, then the project by Future Systems shines in its optical brilliance and inimitability. Both however are still shaped by the rhythmical repetition of the same units. If you were to implement such strategies on free-form architecture, there would be an almost infinite number of different unit geometries. Façade technology today therefore faces key challenges:

- Curtain-wall technology, now over 100 years old, is not a system that offers a strategic solution here. The classic glass curtain wall was developed against the backdrop of serial production for flat surfaces and is based on the addition of industrial, identical, mainly right-angled modules.
- Due to the progress and dissemination of modern parametric 3D planning tools in connection with Building Information Modelling (BIM), the aforementioned design strategies can be represented

visually and geometrically, and in many respects successfully. However, this means that the standard market components must be forced into the desired form, which often makes each individual component a prototype.

1.1 Systematic approach

The desire for "free forms" requires "free construction products" in the sense of systems that can be manipulated parametrically. The fact that expensive individual solutions had to be used to implement nearly all the existing free-form designs of recent years is counterproductive and at odds with the creative will of the architects. To resolve this, SCHÜCO and FAT LAB began a joint research project entitled "Parametric Concept" in 2012, the objective of which was to develop a façade system to enable geometric freedom in both the individual façade unit and the entire system. The constructive structural processing during prototyping and product development was carried out by ENGELSMANN PETERS engineering. After the initial prototypes for BAU 2013 in Munich, the *PARAMETRIC SYSTEM* could be presented to visitors at BAU 2015 (Fig. 1). The systems concept still applies here and has a regulatory function. However, thanks to the large number of possible combinations and geometric manipulation, the formal designs are almost limitless. A distinction must be drawn at façade level between local and global manipulation:

- Local manipulation can be understood as the geometric differentiation of the individual façade unit. In this way, for example, deliberately turning transparent surfaces away from the sun can considerably reduce solar heat gain. Conversely, the generation of energy can be improved by the targeted alignment of PV surfaces. Key here is that a SINGLE repetitive geometry is not the aim; instead, EVERY unit can be designed in accordance with its position and function.
- We refer to the application on building structures which are not right-angled and extruded as global manipulation. Through the coupling of units, covering double fold surfaces with rhombic or diamond-shaped units becomes possible. The unit connectors take on the task of "flexible" joints.

The

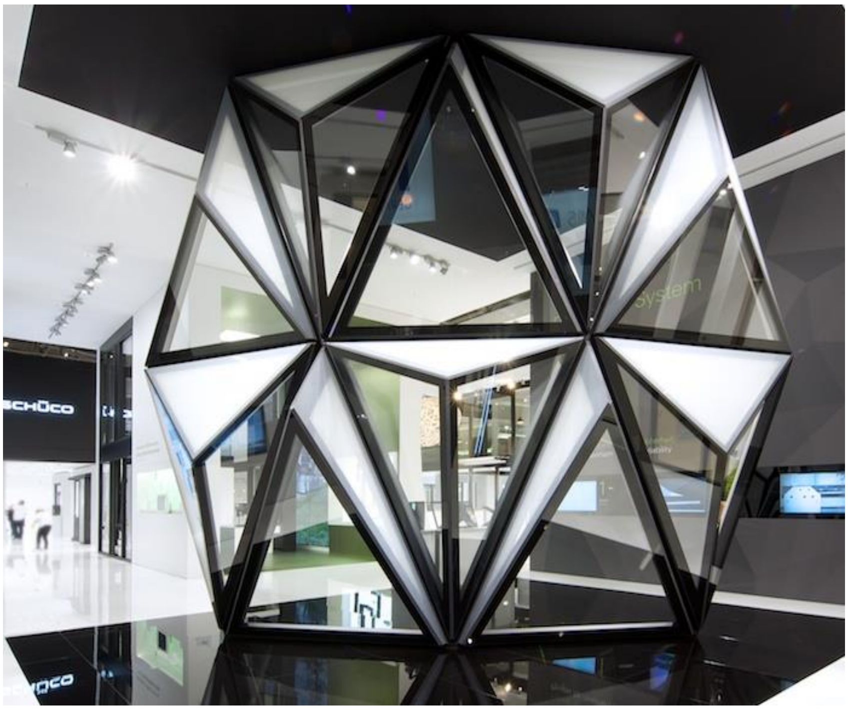

Figure 1: Presentation of the Schüco Parametric System at BAU 2015

choice of profile geometry is an essential element of the system concept which is understood as a strategy for the solution of a diverse range of tasks. The round tube geometry and nodes using inserted and therefore invisible corner cleats are at the core of the "Parametric System". The selected geometries and intersections of individual transparent, translucent or opaque surfaces permit the angle within each individual unit to be determined almost

completely at will. The infill units are bonded to an aluminium frame and installed onto an internal adapter frame, creating the thermal seal of the building as a structural glazing façade.
The cutting-edge Parametric System exhibit for BAU 2015 plays with the overall and individual unit geometries as well as unit depths. The local distinction between transparent and translucent glass units as well as the global flection of the entire surface suggest the future possibilities for façade design.

2 System structure

There are two notable innovations concerning the load-bearing structure of the façade:

- the parametric optimisation of the load-bearing structure
- the bonding of the insulating glass.

The modules of the Parametric System consist of a load-bearing aluminium unit frame which is fixed to the building structure at selective points and connects the modules structurally. Atop the unit frame is an aluminium tubular frame which, within the bounds of the module dimensions, geometrically defines and bears a three-dimensional, folded surface consisting of several panes of i.e. insulating glass (Fig. 2). To achieve structural rigidity, the aluminium tubes are connected using welded steel nodes with multiple arms. The node arms are inserted into the aluminium tubes with a plastic adapter, form-fitted with metal adhesive and are force-fitted securely. Panes of insulating glass securely connect the fields of the three-dimensional frames constructed in this way. These panes of insulating glazing can be attached to the tubular frame using screws thanks to an adapter profile on the tubes and a frame bonded to the glass with two-component silicone. The panes are blocked to bear the dead load (Fig. 3).

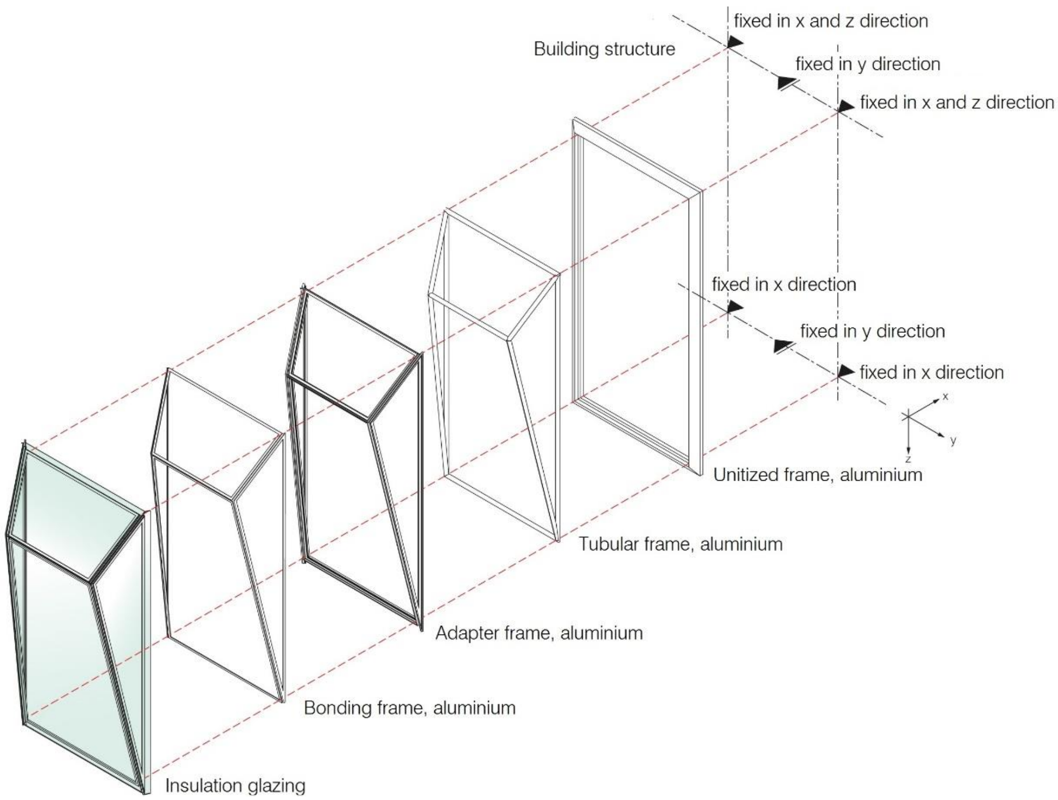

Figure 2: Modular construction and structural system of the Schüco Parametric System

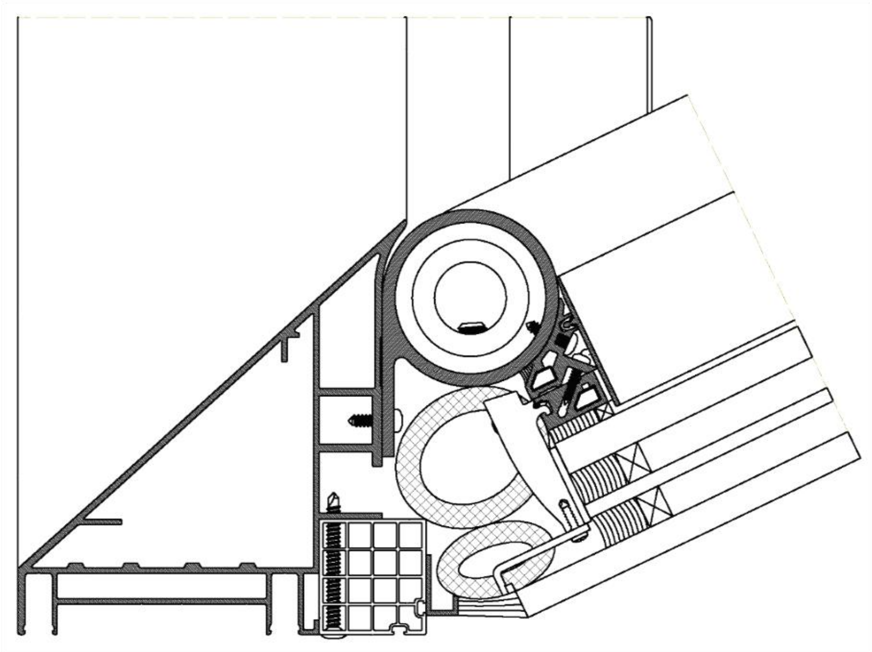

Figure 3: Construction detail of the Schüco Parametric System.

3 Digital process chain

The design and implementation of geometrically complex façade systems generally requires improved coordination and planning by everyone involved. Coordinated interfaces in the process chain are essential to ensuring the continuity of the geometries and reference points [2] [3]. The faultless transfer of model information from one planning stage or software tool to the next has to be ensured. The repeated checking, adjusting and creation of drawings would otherwise drastically increase the time required for design. Ultimately, and of no lesser importance, the implementation requires highly detailed and robust information to ensure the precise machining, reliable creation and subsequent installation of the components [4].
The Schüco Parametric System offers diverse ways to design façades geometrically. To ensure the simple, reliable and fast design and implementation of this potential diversity, in addition to the profile system, a continuous, closed software process has been developed from the first design stages through to fabrication. The use of a façade system rather than an individual solution is of benefit here as system rules and components can be used as a basis on which to build. Individual planning steps can thus be supported, automated and the complexity of the design process reduced through dedicated software components. The depth of information is adjusted in accordance to the planning stage in a Building Information Modelling (BIM) process.

3.1 Draft

Two plug-ins are available for the design and form finding process which can be embedded into the Grasshopper [5] and Revit [6] CAD environments respectively. A library of intelligent base modules with intrinsic system conditions thus facilitates the draft design and negates the necessity to know the rules underlying the system. The modules can undergo additional parametric modelling through the use of further external software components. Developers therefore have diverse ways to generate and optimise shapes at their disposal. A systematic plausibility check inside the plug-ins ensures feasibility, whilst departing from the limits of the system remains possible. Special constructions beyond the system limits can therefore also be generated and subsequently implemented as a project solution. The models are simplified at this first level of design and do not contain all of the system components to prevent slowing the design process.

3.2 Detailing

The planning process is automated through the creation of detailed parametric detail models of the basic modules. The entire structure required are added to the designed geometries upon import into the Autodesk Inventor [7] software. An internal rule set forms the basis for generating the system and special components required, as well as their dimensions, processing and position. The plausibility of the models is tested again at this stage. Editing the detailed models, so that alterations and adjustments are ensured, remains possible.

3.3 Implementation

The detailed model allows components and system profiles to be ordered directly via SchüCal, the manufacturer's own software. The contractors do not have to carry out own planning work. This is particularly significant in reference to the required stepped glazing and the system nodes (Fig. 4). Latter are manufactured as system articles on the basis of the geometry transferred while ordering in a mass-customisation process. When generating the detailed model they are also clearly marked to ensure their correct assignment and position in the units. The data for the precise computer-aided manufacturing is also stored here and allows the machining to be performed directly on a 5-axis processing centre, i.e. the Schüco DC500.

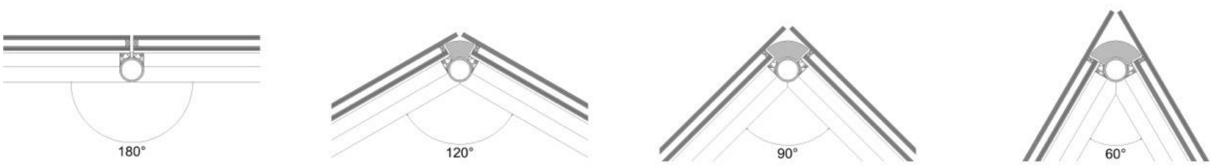

Figure 4: The length of the stepped glazing is dependent on the angles of the design geometry

Throughout the continuous software process, all the data constantly remains in a single geometric model (Fig. 5), which everyone involved in the project phase can access at the required level. Here, the possibilities for parameterisation are not only used in the first design phase but also in particular during detailing. Compared to conventional design, the process of implementation is therefore accelerated considerably and system reliability is also the idea behind the software process.

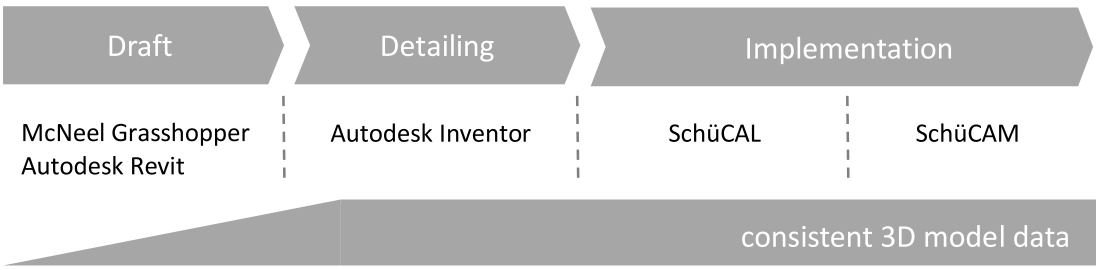

Figure 5: Process steps and accompanying software chain of the Schüco Parametric System

4 Static system optimisation

The fundamental challenge in the development and in particular the optimisation of material use of the load-bearing structure consisted in the geometric freedom of the system. With 11 different static module geometry types as the starting point, an almost infinite number of geometric variations can be created through the flexible variation of the internal tubular frame nodes in the X, Y and Z axes. This naturally raises the question concerning which of the geometries is the least favourable in respect of the loads on the bars, nodes and connectors and which of the geometries should be used for the dimensioning of the components. The effects on the load-bearing structure of the façade include dead, wind, snow and temperature loads as well as live loads if the bottom of a structure is angled outwards. An approximate approach or a simplified estimate will not suffice here to ensure

a structure that is really cost-efficient. A parametric model was therefore created and used for the structural design. This makes it possible to create any number of geometric variations to cover all areas of application. All these variations are then calculated automatically for the significant load combinations and pre-dimensioned via a programmed interface to a finite-element program. This makes it possible to precisely define geometric areas of application depending on the cross section dimensions sought and material strengths as well as to subsequently store them in a configuration tool.
The safety concept of the Parametric System envisages calculating the load-bearing capacity of the tubular frame. The stiffening effect of the bonded panes of insulating glass is initially not taken into account in the proof of the ultimate limit state. In contrast, the stiffening effect of the bonded panes of glass is taken into consideration for the serviceability limit state. The interaction between the effects of the supporting structure and the panes is recorded using a highly detailed finite-element model, taking into account the stiffness of the bonding joints, which ultimately also allows the load on the bonded joints to be recorded. On the basis of such calculated estimates and accompanying tests, the number of areas of application of load-bearing silicone bonds has increased dramatically over the past few years. Glazing in the overhead area could therefore be supported and fixed exclusively using a bonded joint for the exhibit at the BAU 2015 trade fair on the basis of a precisely specified test and monitoring concept. The lack of any supports and retaining clips was approved by granting consent in individual cases.

5 Conclusion

Modern digital planning and fabrication technologies open new paths for architectural expression, though also require the planning process and construction method to be rethought. In conjunction with the possibilities for reliably simulating and parametrically depicting complex relations, these new technologies provide important stimuli for overcoming the challenges of our time. The digital revolution certainly has the potential to help occasion another evolutionary leap in construction comparable to the development away from solid structures and towards skeleton structures, which not only embodied a new construction method but also fundamentally altered and shaped the architecture of the last century. Elementary research projects require close cooperation and a willingness to re-think existing approaches. This ensures constant technological development through innovative products and processes. The authors view the great interest and positive responses at BAU 2013 and BAU 2015 as the vindication of their endeavours to develop innovative solutions to future challenges.

6 References

[1] FVHF, “Deutscher Fassadenpreis 2013 für vorgehängte hinterlüftete Fassaden (VHF),” FVHF – Fachverband Baustoffe und Bauteile für vorgehängte hinterlüftete Fassaden e.V., Berlin, Berlin, 2013.

[2] Azhar, S., “Building Information Modeling (BIM): Trends, Benefits, Risks, and Challenges for the AEC Industry,” vol. 11, no. 3, p. 241–252, 2011.

[3] K. Vollmers, Twist&Build creating non-orthogonal architecture, 010 Publishers, 2001.

[4] B. Kolarevic, “Architecture in the Digital Age – Design and Manufacturing.,” Oxford, Taylor & Francis, 2003.

[5] “Grasshopper 3D v1.0,” Robert McNeel & Associates, 2014.

[6] “Revit 2015,” Autodesk, 2014.

[7] “Inventor 2015,” Autodesk, 2014.

Intelligent Building Envelopes: Design and Applications

Yara Masri, PhD Candidate
University of Southern California, USA, ymasri@usc.edu

Summary

This paper presents intelligent building envelopes as the future direction for high-performance sustainable façades. The paper reviews some of the definitions in current literature and proposes a working definition for intelligent envelopes. A discussion of design methods leads to a proposed dynamic design approach, supported by an expert survey that provides insight into the effectiveness of the design method in practice. The paper concludes with analysis of the survey and recommendations for the integration of intelligence in sustainable façades.

Keywords: Intelligent building envelopes, adaptive façades, building skins, automated buildings, responsive envelopes, design methods

1 Introduction

Energy has been a recurring theme in the design of the 'wall'; whether a tent, heavy masonry, concrete walls, or a glass house, the wall has acted as shelter from the outside environment, as means to maintain desired temperatures within. In design and construction, the building envelope has gone through a shift in both its physical systems and its aesthetic value.

Although the debate of the relationship between mechanical environmental systems and building design was explored as early as the 1920s, the increased awareness of the effect of buildings on energy consumption grew in the 1960s with the concept of 'bioclimatic architecture' [27] and especially in the 1970s following the energy crisis. However, fully developed ideas on sustainable building and envelope design did not emerge until the 1990s [35,15] with prominent projects of Foster, Otto, Rogers, and Piano [21,18].

Buildings account for over 40% of the total energy consumption [1,3,33], to which the building envelope significantly contributes, through the demand on building services such as the control of the internal ventilation and thermal environment [35]. Energy savings can be achieved by simple alterations in the façade alone. In an experimental model presented at the *Eighth International IBPSA Conference* in the Netherlands in 2003, a typical glass office façade was redesigned and simulated. The investigators found that simply using roller blinds and high-efficiency glazing resulted in a 40% decrease in heating energy cost [19].

The building envelope, being the first barrier against extreme environmental conditions, serves as a 'level of control' between the indoor/outdoor environments, occupant needs, and economic concerns [31]. A façade that offers dynamic variability to the different requirements of the building is the eventual fruition of the energy theme in design. The technology for achieving the comprehensive design for intelligent envelopes is already in the market, and growing at a rapid pace, based on the industry acquisition of smart materials and control systems in the past few years [25]. Figure 1 shows projections of the savings in energy through applying current available technologies.

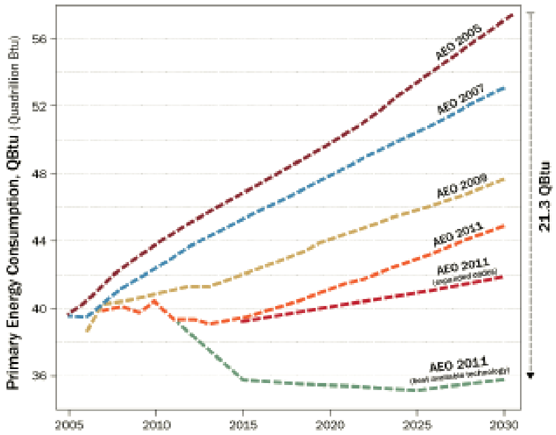

Figure 1 US Residential and Commercial Energy Consumption, Projections from 2005 to 2030 (Architecture 2030: EIA AEO Data 2005, 2007, 2009, 2011)

2 The Intelligent Facade

2.1 The Active Façade

The term 'intelligent', when applied to a façade, has to indicate the responsive ability of the façade to change according to environmental conditions [13]. In tall office buildings, occupancy levels are not constant throughout the day, the requirements of ventilation and lighting, for example, are not the same when the building is occupied and nearly absent when it is empty. The changes in occupancy levels, climate, and time require the need for variations of response—a more dynamic one. This dynamic response requires that the building should 'know' the changes that happen inside and outside, 'decide' on the most efficient solution to provide the comfortable environment for the occupants, and 'respond' according to that decision [4,10,11,35].

The conventional façade would now change into an active and transitional climatic control for the interior space. The ability for the façade to change has been mainly operated by an occupant (i.e. opening windows, adjusting blinds). The intelligent façade, in contrast, should be able to change itself through 'instinctive autonomic adjustment' [35]. The intelligent skin is therefore a composition of elements, which acts as a barrier to the outside environment, yet is able to respond to the climatic changes, through automatic reconfiguration of its systems.

Because occupants' needs and climatic conditions are changing variables [31], the high-performance façade, as a static element, cannot address these conditions and bring about the maximum benefit of high-performance design. The envelope should have the capacity to adapt to different conditions and respond to these changes; it becomes 'intelligent'. The intelligent building envelope transcends the traditional function of an enclosure and becomes an *active controller* between the internal and external conditions to maintain indoor comfort and reduce energy consumption. The following section provides a basis for establishing a definition of intelligent building envelopes that facilitates the design of the intelligent façade.

2.2 Definitions

Although the literature on intelligent envelopes is still lacking, there is no shortage of definitions for intelligent buildings and intelligent façades. A precise definition has been difficult to pinpoint [34], as each author emphasizes certain factors over others. For example, system-based definitions connote the technological aspects used in the building systems, such as automation, control systems, communications, and networking [23,34]. Such system-based definitions were especially prevalent in the early stages of applying intelligence and automation to buildings. Other definitions necessitate that the intelligence is either related to cost-benefit through work productivity and flexibility in spaces, or to occupant interaction with automated systems and intelligent-system response to personal preferences [12,34,36]. See Table 1. However, it is crucial to define the intelligent envelope based on its environmental performance, and, as mentioned earlier, the ability of the building to 'know', 'decide', and 'respond'.

Table 1: Summary of Definitions Classification for Intelligence in Buildings

Systems/Technical-based	Integration of various systems to manage resources Focus on technological aspects Allow computer configuration changes in offices Modification of algorithms in building management system	Leifer 1988, Wong et al. 2008, Atkin 1989, Atkin and Brooks 2009
Performance-based	Performance re-adjustment based on internal/external changes in conditions Algorithm modification based on unexpected environmental data Reports on building's energy consumption and occupant interaction Based on feedback loops	Wigginton and Harris 2002, Selkowitz 2001, Elkadi 2012, Masri 2015
Occupant-based	Adapts to human comfort 'standards' Allows for human override User interaction with system	Wang 2009, Clements-Croome 2011
Cost-based	Maximize investment and operating Life-cycle approach Maximize workplace productivity and reduce cost	Smith 2002, Wong and So 2002

A definition based on performance of both a sustainable *and* an intelligent façade will have to incorporate performance criteria, such as:

- Sun Protection
- Daylight control and active shading
- Active air control and ventilation
- Optimized tradeoffs
- Renewable energy
- Indoor air quality control
- Passive design strategies
- Reports on performance criteria
- Self-adjustment of systems based on feedback loops

The definition of the intelligent building envelope is: *a dynamic filter composed of one or more active systems that have the ability to sense environmental conditions, actuate an appropriate response to the condition—based on a predicted environmental pattern—or a modified response based on performance feedback, all within the main objective of providing increased comfort while consuming energy more efficiently.* The intelligent envelope is in a state of constant change based on its actuated response. It also employs passive design solutions for high-performance envelopes while adjusting active features with varying indoor and outdoor environmental conditions. The active façade is controlled by a main building management system (BMS), which stores the data required for a predictable active response. The BMS modifies the control algorithms based on performance data reports, finds contradictions and synergies in the performance, and predicts future response criteria and operating strategies for anticipated conditions. The intelligent envelope also allows the occupant to override the system based on personal preferences, on condition that the override does not jeopardize the overall building performance [25]. See Figure 2.

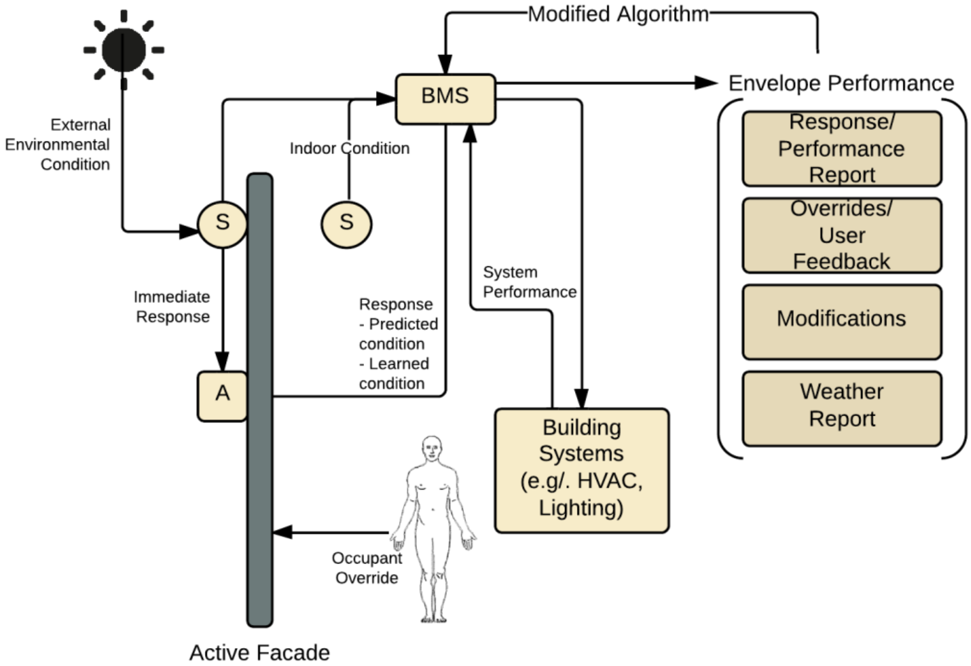

Figure 2 Intelligent Envelope Schematic Design (S: sensor, A: Actuator), [Masri 2015]

3 Approach to Designing an Intelligent Envelope

3.1 Design Methods

Architecture is a discipline with changing methodologies and processes. The digital environment—including BIM, modeling software, generative systems and algorithms—added a new dimension to the field that is different from the traditional way of thinking, exploring new tools and approaches to collaboration [24,20].

The design process itself has many aspects. This paper identifies various parameters in the design of intelligent façades: environmental, economic, post-occupancy, cultural, and programmatic parameters. The designer has the responsibility to improve the standard of living for the occupants—what Fuller called “converting the high technical potential to account through design”—to increase user-benefit, while consuming minimal energy and materials [17,37,26]. The designer chooses to emphasize a particular parameter, feature, or aspect in the design. The preference, in turn, becomes the main design goal for façade performance. With architectural composition, for example, the expression through which the architecture can be understood emerges from a prevailing emphasis in the design [22], as we see in some structural aesthetic expression in façades.

The early attempts to ‘scientize’ the research of design methods, whether by arranging the design problem into patterns with interactions between requirements [2] or testing rational methods of science into design [7,32], were too simplistic for more complex design situations, especially when considering intelligent envelope design. Such linear models may be attractive because they have a logical sequence and a well-defined understanding of problem *and* solution [8]. Linear models in design methods, however, cannot apply to the design of intelligent façades. There is no clear definition of problem-to-solution sequence in the process of the design, as environmental parameters, which must be integrated in the design of a sustainable façade, have what can be described as 'conflicting values'—a term used by Rittel [29] to describe 'wicked problems' as "problems which are ill-formulated, where the information is confusing, where there are many clients and decision makers with conflicting values, and where the ramifications in the whole system are thoroughly confusing" [9].

Furthermore, the relationship between architectural knowledge and design methods—the theoretical basis—must be considered with regards to new technologies. Practice-driven theories "demand a process of redefinition of the intellectual and cultural framework of architecture, as well as the theoretical foundations" [28]. Cognitive models of design [Rowe, 28] and 'designerly ways of knowing' [14] indicate knowledge in the design process, which, in turn, implies that there might be a cognitive, knowledge-based aspect to the design process. This knowledge-based design demands 'theoretical framework and didactic principles' for the new age of digital design [28]; but these theories are not applicable to the field of digital design let alone parametric, environmental, automated, and active—which is far from any form of static design knowledge.

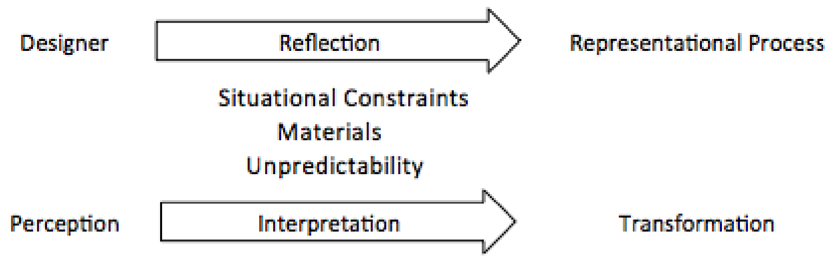

Figure 3 Design Process, Schön

Previous design theories focused on the process of exploration and 'reflection in action' (Figure 3), where situational backtalk is part of a creative process; design becomes a 'reflective conversation with the materials of the situation' [30]. This suggests that the representations are not only projections of the intention of the designer, but they are also the product of the designer's intentions—a goal that has been pre-defined. The 'situational feedback' is the interplay between the designer, situational constraints, and materials. This method still implies a certain level of linearity, which has been the conventional way of design thinking. Communicating with the design team is crucial, and the performance-indicators and results need to be analyzed and compared through mechanisms of performance-based comparisons [5]. The fact that the variables can be conflicting and result in more complex outcomes, leads one to think about the design process as a non-linear, multi-faceted, multi-objective integrative design approach—a 'wicked problem' perhaps.

3.2 Expert Survey

This paper proposes a non-linear expert-feedback-based method to analyze parameters in intelligent façade design. The expert-feedback was gathered through a survey study conducted for the author's dissertation research [25]. Design leaders and major contributors to the research on intelligent façades provided their opinion on different aspects in the pre-design, design development, and construction phases of the façade. The study focused on the environmental parameters in regards to intelligence in façades, and the interaction of the design team with the concept development, tools, and recommendations. The study revolves around five main categories, from which different sub-categories (Table 2) are investigated:

- Design Goals
- Activities during different stages of the design on the intelligent façade
- Data sources for the design of the façade
- Design solutions and tools
- Post-occupancy systems modifications

Table 2 Categories of Survey on Intelligent Façade Design (Masri 2015)

Design Goals	Operational energy performance Embodied energy Carbon reduction Durability (facade system and subsystem service life definition) Waste (reuse, recycling, and control of construction debris)	Resilience Health and comfort Adaptability (consideration for accommodation of changing use) Acoustic performance (STC or OITC specification) Security (blast resistance, forced entry, etc.)
Design Activities	Whole-building energy modeling Durability planning (incl. design standard or maintenance cycle plan) Daylighting design Interior or exterior glare analysis Façade systems commissioning plan	ZNE-ready (zero net energy ready) facade system design LCA or LCCA Acoustic Analysis Indoor air quality management planning Thermal comfort modeling Post occupancy evaluation (POE)
Data Sources	Indoor lighting Daylighting Sun path Solar heat gain Indoor glare measurement Outside glare reflecting from building to street or surrounding Occupancy	Outside temperature Indoor temperature Human interaction with system Metered energy consumption of the façade system System's self-regulatory indicators Overall energy consumption Post-occupancy data
Design solutions	Automated shades Automated interior lighting Automated HVAC systems Smart materials in the façade glazing (e.g. piezo-electric, photochromic, electrochromic, nano-insulation, liquid crystal, smart films, etc.) Smart materials in the shading device Automated window/façade cleaning and maintenance systems	Motion/ Occupancy sensors Automated security features Environmental/ chemical hazards automated systems On-site energy generation (e.g. PV solar generation, solar thermal, wind turbines, heat ground sources, etc) Occupant override based on personal condition preference (thermal, lighting, ventilation)
Post-occupancy systems modifications	HVAC and/or mechanical systems Lighting systems were upgraded or replaced Occupancy sensors	Daylighting controls A building management system (or energy management system) On-site energy generation incorporated (e.g. PV solar generation)

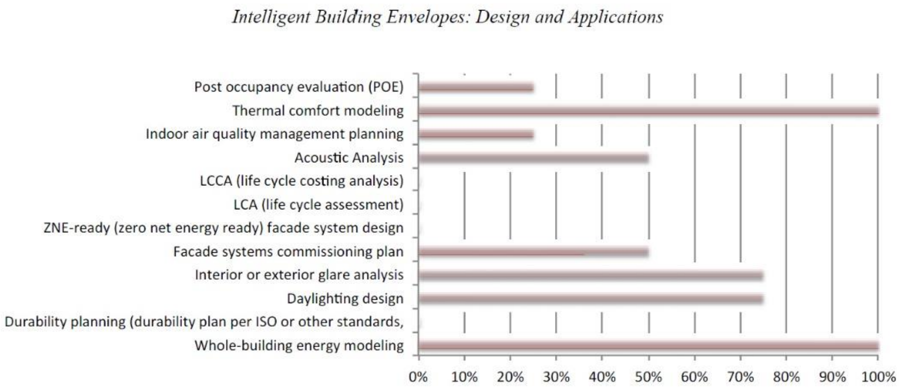

Figure 4 Study Result Example: Activities Included in the Design of The Intelligent Façade

3.3 The Design Approach

As already established, conventional methods and applications are not able to address the ever-changing dynamic activities of the intelligent façade. The 'interactive space is both intelligent and kinetic, and adapts within context of human and environmental interaction' [16], thus requiring a new method and approach to design. The method proposed follows the path of a performance-based façade design, with *performance* as an initial step towards the design method. In an attempt to understand the decision-making process in regards to improving energy performance, and the application of the survey study, the author examined previous study-based design methods. One study [6] conducted surveys for pre-design, sketch, and detail phases of the design process, in order to systemize the design process and modeling. Austin et al. [6] codified design process, thereby identifying different modeling methodology and subsequently forming a dependency structure matrix analysis in order to have inputs in project design programs. Figure 5 explains the Integrated Definition (IDEF) technique, where intra-disciplinary, cross-disciplinary, and external source inputs are integrated.

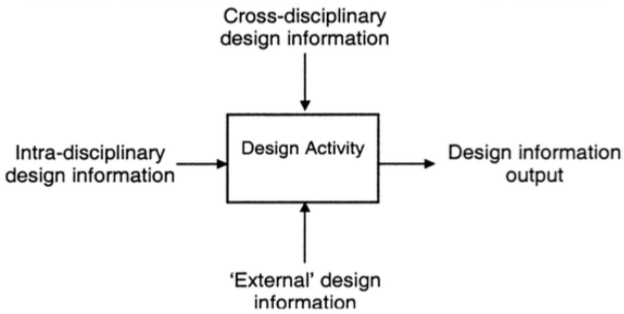

Figure 5 Modified IDEF Notation (Austin et al. 1999)

Similarly, and following the logic of a 'wicked problem', the conventional linear design process must change from the conceptual stage (Figure 6), where the intelligent features are discussed early on with the design team, experts, and stakeholders. The determination of a solution is no longer a viable method, as there are conflicting 'solutions', which will jeopardize the overall performance. The design follows the basic principles:

- Performance is the end objective
- Design is a process of 'framing and reframing'
- New possibilities not selection of alternatives
- Mapping between function and parameter
- No single alternative is available
- Dominant feature will be the first selected

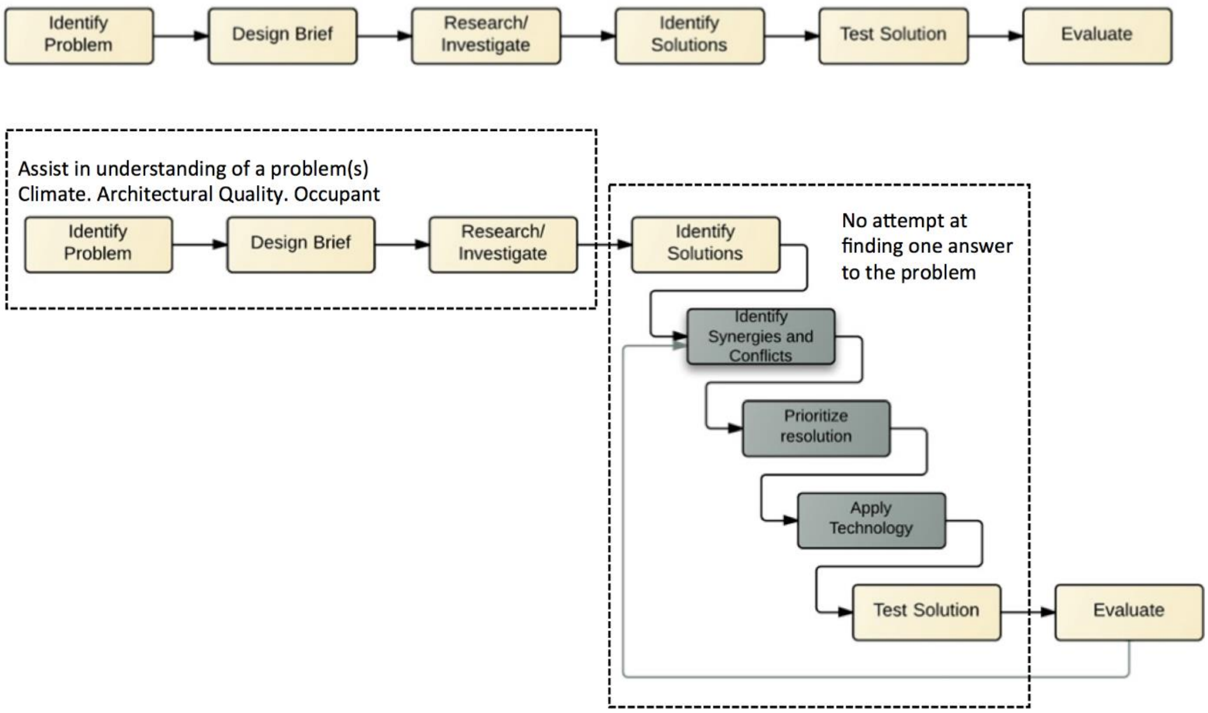

Figure 6, Traditional Design Process compared with Proposed Design Approach (Masri 2015)

4 Conclusion

In the expert survey, designers provide insight into challenges they faced while integrating the intelligent features in the building façade. The majority of the participants explained the trouble of finding a team of specialists who were familiar with the technology of automated façades. Also, the integration of the materials and systems' suppliers was a difficult task during the design phase of the façade. Other main issues were that the process to educate a client, the engineer, and the contractor was time consuming and expensive. In addition, there is insufficient analysis software for intelligent façade modeling, and the accuracy of simulation tools is under debate [25].

In summary, the challenges in the practice of designing an intelligent façade are:

- Scarcity of literature and guidebooks on the topic in general
- Poor integration with material/ system suppliers
- Fragmented approach to design between stakeholders
- Lack of familiarity with automation, smart materials, complex systems at the time of the project
- Difficulty assembling the team of specialists
- Hesitancy in seeking new technologies for design solutions
- Late decision-making for integrating automation in the design process

The design process cannot stay as a linear method. The cross-disciplinarity of parameters becomes a labyrinth of information, and defining a single alternative solution is obsolete. Furthermore, the data feedback feature in an intelligent façade adds to the complexity of alternatives and solutions. Instead, the approach proposed in this paper treats the design method as a 'continuous reframing process'; the designer follows performance objectives without ruling out synergies with other parameters, which create a truly intelligent façade that is both active and adaptive.

Designers are confronted with maximizing the potential for architectural façades, namely reducing energy consumption and increasing comfort levels indoors. The approach towards designing a façade needs to change in order to address the new requirements for a more active-dynamic evolution in technology and sustainability objectives. Intelligent façades emerge as a response to the sustainable design challenges as the concept of the intelligent building envelope offers this dynamic variability; and the need for more research in the field, whether in literature or tools, is crucial.

5 Acknowledgements

The author wishes to thank Professor Douglas Noble for his continuing support during the dissertation project, of which this paper is a distillation. Additional thanks go to colleagues Andrea Martinez and Mic Patterson at the University of Southern California for the inspiration behind the survey study, as well as to the experts and design leaders who participated in it. The author has been fortunate to have enthusiastic supporters at the TU-Berlin and TU-Munich, who were generous with their time and facilities. She is also grateful to Prof. Derek Clements-Croome for his motivation and advice.

6 References

[1] "2030 Palette: Design and Planning Strategies for the Next Building Environment, Today." 2011. Architecture 2030. Accessed November 9, 2012. http://architecture2030.org/the_problem/buildings_problem_why.
[2] Alexander, Christopher. 1964. *Notes on the Synthesis of Form*. Harvard University Press.
[3] "Annual Energy Review, 2011." 2012. *U.S Department of Energy: Energy Information Administration*. Accessed April 2. http://www.eia.doe.gov/totalenergy/data/annual/index.cfm#consumption.
[4] Atkin, Brian. 1989. *Intelligent Buildings: Applications of IT and Building Automation to High Technology Construction Projects*. Halsted Pr.
[5] Augenbroe, Godfried. 2004. "Developments in Interoperatbility." In *Advanced Building Simulation*, by Ali Malkawi and Godfried Augenbroe. Taylor & Francis.
[6] Austin, Simon, Andrew Baldwin, Baizhan Li, and Paul Waskett. 1999. "Analytical Design Planning Technique: A Model of the Detailed Building Design Process." *Design Studies* 20 (3): 279–96. doi:10.1016/S0142-694X(98)00038-6.
[7] Broadbent, G., and A. Ward, eds. 1969. *Design Methods in Architecture*. London: Lund Humphries.
[8] Buchanan, Richard. 1992. "Wicked Problems in Design Thinking." *Design Issues*, 5–21.
[9] Churchman, C. West. 1967. "Guest Editorial: Wicked Problems." *Management Science* 14 (4): B141–42. doi:10.2307/2628678.
[10] Clements-Croome, Derek. 1997. "What Do We Mean by Intelligent Buildings?" *Automation in Construction* 6 (5-6): 395–400. doi:10.1016/S0926-5805(97)00018-6.
[11] ———. 2004. *Intelligent Buildings: Design, Management and Operation*. Thomas Telford.
[12] ———. 2011. "Sustainable Intelligent Buildings for People: A Review." *Intelligent Buildings International* 3 (2): 67.
[13] Compagno, Andrea. 2002. *Intelligente Glasfassaden / Intelligent Glass Façades: Material, Anwendung, Gestaltung / Material, Practice, Design*. 5., rev. u. aktual. Aufl. Birkhäuser Basel.
[14] Cross, Nigel. 2001. "Designerly Ways of Knowing: Design Discipline versus Design Science." *Design Issues, MIT* 17 (3): 49–55.
[15] Elkadi, Hisham. 2012. *Cultures of Glass Architecture*. Ashgate.
[16] Fox, Michael, and Miles Kemp. 2009. *Interactive Architecture*. New York: Princeton Architectural Press.
[17] Fuller, Richard Buckminster. 2001. *Your Private Sky: Discourse*. Springer Science & Business Media.
[18] Hawkes, Dean, and Wayne Forster. 2002. *Energy Efficient Buildings: Architecture, Engineering, and Environment*. W. W. Norton & Company.
[19] Jansen, S.C., R.M.J Bokel, A.A.J.F van den Dobbelsteen, and M. van der Voorden. 2003. "An Energy-Saving Office Façade Adaptable to Outside Weather Conditions in the Netherlands." In *Building Simulation 2003*. Eindhoven, The Netherlands.
[20] Kensek, Karen, and Douglas Noble. 2014. *Building Information Modeling : BIM in Current and Future Practice*. Somerset, NJ, USA: Wiley. http://site.ebrary.com/lib/alltitles/docDetail.action?docID=10868214.
[21] Knaack, Ulrich. 2007. *Façades: Principles of Construction*. Basel: Birkhäuser.

[22] Kwok, Alison, and Walter Grondzik. 2011. *The Green Studio Handbook*. 2 edition. Amsterdam ; Boston: Routledge.
[23] Leifer, D. 1988. "Intelligent Buildings: A Definition." *Architecture Australia*, no. 77 (May): 100–102.
[24] Liu, Yu-Tung, and Chor-Kheng Lim. 2006. "New Tectonics: A Preliminary Framework Involving Classic and Digital Thinking." *Design Studies*, Digital Design Digital Design, 27 (3): 267–307. doi:10.1016/j.destud.2005.11.008.
[25] Masri, Yara. 2015. "Intelligent Building Envelopes: A Design Methodology." *Dissertation in Progress*. Los Angeles: University of Southern California.
[26] Nigan Bayazit. 2004. "Investigating Design: A Review of Forty Years of Design Research." *Design Issues, MIT* 20 (1): 16–29.
[27] Olgyay, Victor. 1963. *Design With Climate: Bioclimatic Approach to Architectural Regionalism*. First Edition edition. Princeton University Press.
[28] Oxman, Rivka. 2008. "Digital Architecture as a Challenge for Design Pedagogy: Theory, Knowledge, Models and Medium." *Design Studies* 29 (2): 99–120. doi:10.1016/j.destud.2007.12.003.
[29] Rittel, Horst. 1972. "On the Planning Crisis: Systems Analysis of the 'First and Second Generations.'" *Bedriftsokonomen*, no. 8: 390–96.
[30] Schon, Donald A. 1984. *The Reflective Practitioner: How Professionals Think In Action*. Basic Books.
[31] Selkowitz, Stephen E. 2001. "Integrating Advanced Façades into High Performance Buildings." In . Tampere, Finland: Lawrence Berkeley National Laboratory.
[32] Simon, Herbert A. 1996. *The Sciences of the Artificial, 3rd Edition*. MIT Press.
[33] UNEP-SBCI. 2009. *Buildings and Climate Change*. dti/1240/pa. Sustainable Buildings &Climate Initiative. United Nations Environment Programme. http://www.unep.org/sbci/pdfs/SBCI-BCCSummary.pdf.
[34] Wang, Shengwei. 2009. *Intelligent Buildings and Building Automation*. 1st ed. Spon Press.
[35] Wigginton, Michael, and Jude Harris. 2002. *Intelligent Skins*. Oxford: Butterworth-Heinemann.
[36] Wong, J. K. W., H. Li, and S. W. Wang. 2005. "Intelligent Building Research: A Review." *Automation in Construction* 14 (1): 143–59. doi:10.1016/j.autcon.2004.06.001.
[37] Zung, Thomas T. K. 2002. *Buckminster Fuller: Anthology for the New Millennium*. Macmillan.

Numerical Simulation of Energy Performance, and Construction of the Adaptive Solar Façade

Prageeth Jayathissa, Zoltan Nagy, Nicola Offeddu, Arno Schlueter
Architecture and Building Systems, Institute of Technology in Architecture, ETH Zürich, Switzerland, jayathissa@arch.ethz.ch, www.systems.arch.ethz.ch

Summary

In this paper we discuss the development of the Adaptive Solar Façade (ASF), which consists of an array of independently actuated CIGS solar panels. The ASF allows for precise control of solar insolation that reduces building energy demand. Furthermore it can generate electricity on site. A test simulation of the ASF mounted in front of a south facing office shows total energy reductions of 8.9%. The solar energy production of the ASF is higher than the energy demands of the office space behind. A life cycle analysis of grey energy and CO_2 shows an energy payback of 2.5 years and a CO_2 payback of 1.5 years. We describe two prototypes to demonstrate the application of the ASF. Further integration in real world test-bed scenarios will demonstrate the energy and emission saving potentials.

Keywords: Adaptive Solar Façade, Building Integrated Photovoltaics, Kinetic Architecture, Building Simulation, Life Cycle Analysis

1 Introduction

Buildings contribute to 40% of global primary energy consumption and 30% of CO_2 emissions [1]. The building envelope, acting as a buffer between the interior and exterior environment, is an important place to address this issue and reduce building energy consumption. The energy exchange mechanisms through the envelope can be used for the reduction of heating, cooling and lighting loads. Nowadays, this is done with passive methods such as shading [2][3], natural daylight distribution [4], heat dissipative construction [5], as well as active methods such as solar energy harvesting [6].

In this study we will be analysing an Adaptive Solar Façade (ASF), which combines the aforementioned mechanisms to minimise building energy demands. The ASF consists of an array of independently actuated panels shown in Figure 1. This enables the facade to respond to internal and external inputs as shown in Figure 2a-c. Figure 2d shows a mixed state where the ASF is blocking direct radiation, ensuring sufficient daylight distribution and generating electricity. We discuss methods to find the optimal configuration with respect to natural lighting, glare reduction, energy generation from photovoltaics, and solar irradiation to reduce heating and cooling loads. We use soft pneumatic actuators to increase the durability against environmental factors such as rain and mechanical stress due to wind. Beside the advantages in energy savings, dynamic systems are also opening new aesthetics for architectural design [7][8].

The paper is organized as follows. In Section 2, we run energy performance simulation of the adaptive solar façade. We obtain optimal configurations for each hour of the year to minimize heating, cooling, and lighting loads. In Section 3 we present the design and construction of our first two prototypes. Finally in Section 4 we conduct a carbon dioxide and energy life cycle analysis to determine the manufacturing pay back period of the ASF.

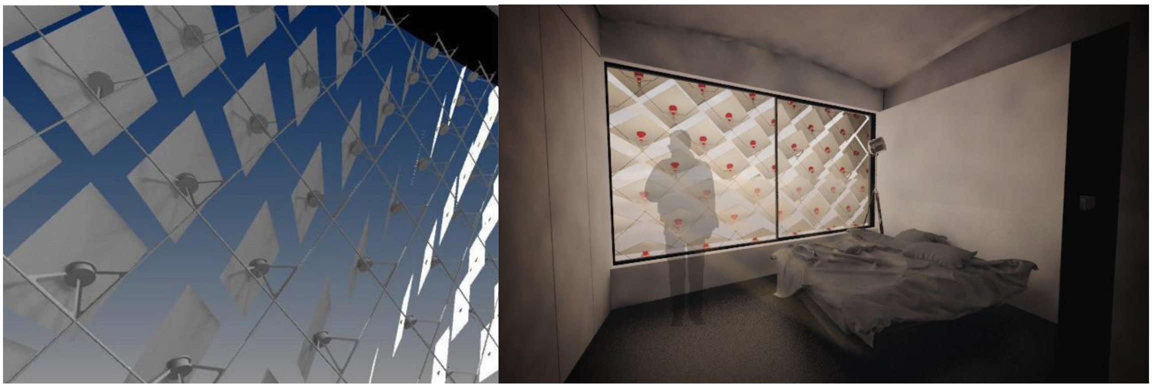

Figure 1: Inside view of an adaptive solar facade mounted on steel cables

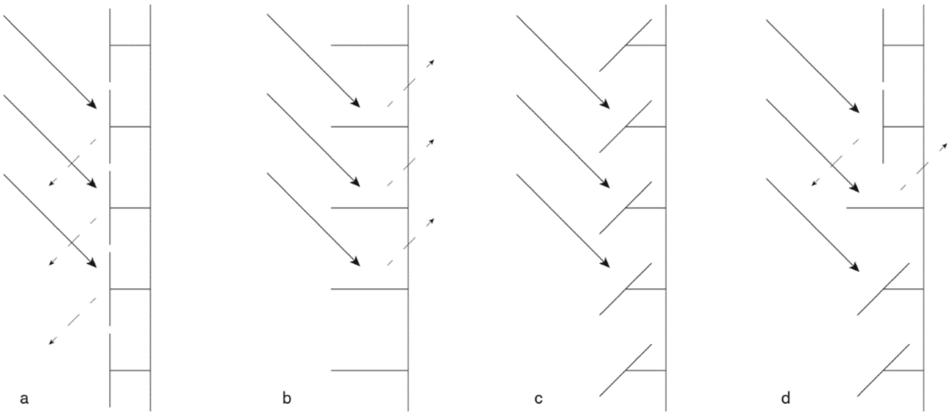

Figure 2: Various states of adaptive facade panels [9]

a) closed state, b) open state, c) solar tracking state, and d) mixed state. It is the flexibility of the mixed state that gives a system the ability to adapt to user desires

The ASF will ultimately be constructed in two living labs, the House of Natural Resources (HoNR, www.honr.ethz.ch), and the Hilo demonstration module at NEST (www.hilo.arch.ethz.ch). The simulations and prototypes will therefore incorporate case studies of these two living lab scenarios.

2 Numerical Simulations

2.1 Methodology

The simulation was conducted for a south facing office similar to the room in the House of Natural Resources (HoNR) building where the ASF will first be realized. The room, 7 meters in length, 4.9 meters wide, and 3.1 meters high was modeled using the Rhinoceros 3D CAD [10] package, shown in **Fehler! Verweisquelle konnte nicht gefunden werden.**. Grasshopper [11] was used to model the ASF, which consists of 400 mm square CIGS solar panels. The panels are grouped into three bands where each band can exist in a fully open (90°), fully closed (0°), and slanted (45°) state on a horizontal axis. On the vertical axis all the panels can move from 90° to -90° in steps of 15°. This results in 324 possible configurations of the modules.

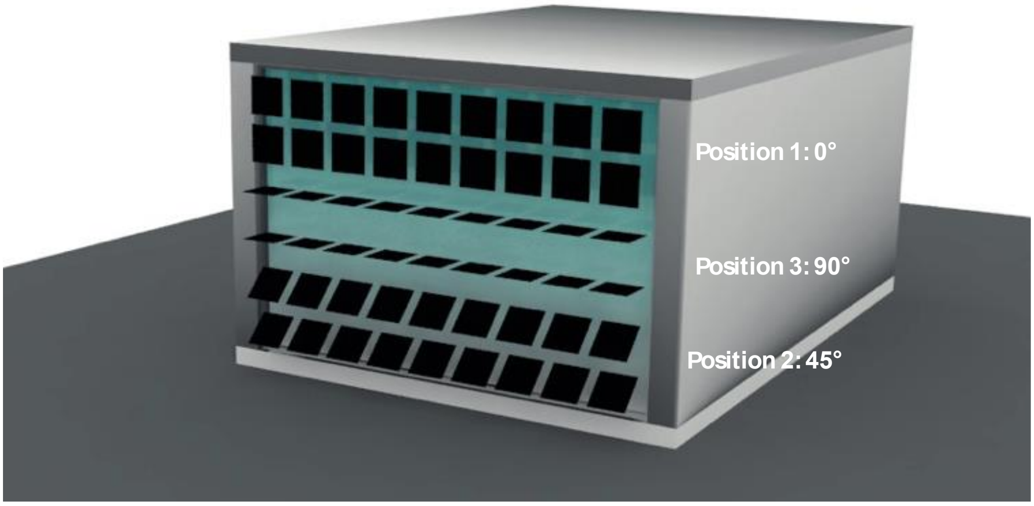

Figure 3: The studied room with the Adaptive Solar Facade attached. In this scenario the panels are at 0°on the vertical axis, and 0°, 90°, and 45° on the horizontal axis from top to bottom respectively. This creates a (1,3,2) configuration

Table 1: Simulation Parameters

Office Envelope:	Roof: Adiabatic Floor: Adiabatic Walls: Adiabatic Window: Double glazed LoE (ε=0.2), Glass 3mm/13mm Air
Thermal Set points	Heating set point: 22°C Cooling set point: 26°C
Lighting control	Lighting set point: 11.8W/m^2 Lighting control: 300lux threshhold
Occupancy	Office: weekdays from 8:00 – 18:00 People set point: 0.1people/m^2 Infiltration: 0.5 exchanges per hour
Adaptive Solar Facade	Solar reflectance: 0.5 Visible reflectance: 0.5
Weather File	Geneva, Switzerland (067000_IWEC)

Each of the 324 possible ASF configurations was imported into Energy Plus [12] through the DIVA [13] interface. A single zone thermal analysis was conducted on each possible configuration at hourly time steps. The results were then processed in MATLAB [14] to determine optimal configuration for each hour of the year. With the exception of the glazing, the office boundaries are not in contact with the external environment. As a result all surfaces except the glazing were considered adiabatic. A summary of simulation parameters can be found in Table1.

For the analysis of energy savings we focussed on two aspects. Firstly we look at the net energy demand for heating, cooling and lighting. We then convert this energy demand to the end electricity demand of the HoNR office based in Switzerland. We assume that the office temperature is regulated through a water based heating system using a heatpump. The heatpump has an approximate coefficient of performance (COP) of 5. The office is cooled using incoming district water, and the room is illuminated with LED lighting.

2.2 Optimum configurations of the Adaptive Solar Facade

The optimal orientations to minimise heating, cooling and lighting were analysed in MATLAB. Figure 4 and Figure 5 show the optimal configurations for minimising energy demands for each hour of the year for the horizontal and vertical axis of rotations respectively. The configurations are represented by a three number code. 1 represents the closed 0° position, 2 represents a 45° positions, and 3 is an open 90° position. The example shown in Figure 3 has a '132' representation. The different colours in Figure 4 represent one of the horizontal combinations.

We can see in the carpet plots on Figure 4 that the heating, cooling and lighting loads optimisation is dependent on the season and time of the day. In the afternoon hours of the warm summer months the 222 configuration (all rotated to 45° on the horizontal axis) is predominant, as shown in Figure 4a. Likewise the rotations along the vertical axis as shown in Figure 5a display a tendency to track the sun. In the morning hours it is orientated at 75° (east facing), enters the neutral position at midday and is orientated at -30° (west facing) in the evening. All these actions work together to provide maximum shading and thus reduce summer heat gains. In the afternoon of the cold winter months (Figure 4b) the panels are most commonly found in the 333 configuration (all open to 90°), with the vertical rotation also set to 90°. This allows for maximum solar insolation, and therefore a reduced heating demand. Lighting control appears only to be necessary during office hours in the morning and evening where the natural light is dim. An overall energy minimisation combining the heating, cooling and lighting demands produces a final optimised configuration for all hours of the year, shown in Figure 4d – Figure 5d. In this minimisation we see examples where the ASF finds optimal solutions for conflicting scenarios. For example, in the evening of the summer months the optimum configurations of the cooling and lighting demands overlap. This results in mixed state configurations such as 312, 322, 133, and 223 being optimal as they can reduce cooling loads and provide natural lighting.

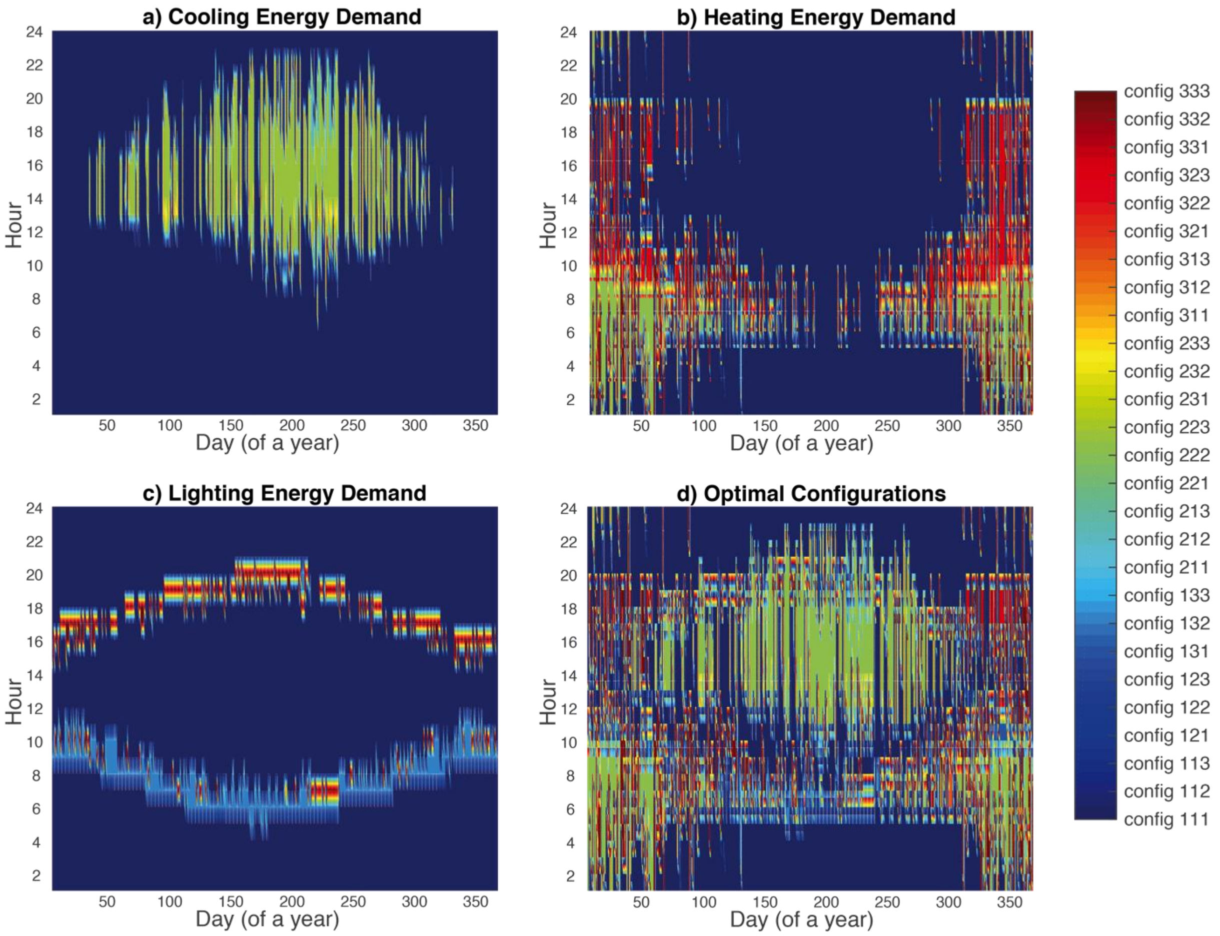

Figure 4: Configurations on the horizontal rotational axis minimising heat, cooling, lighting consumption. The graphs' horizontal axis is a standard year from January to December

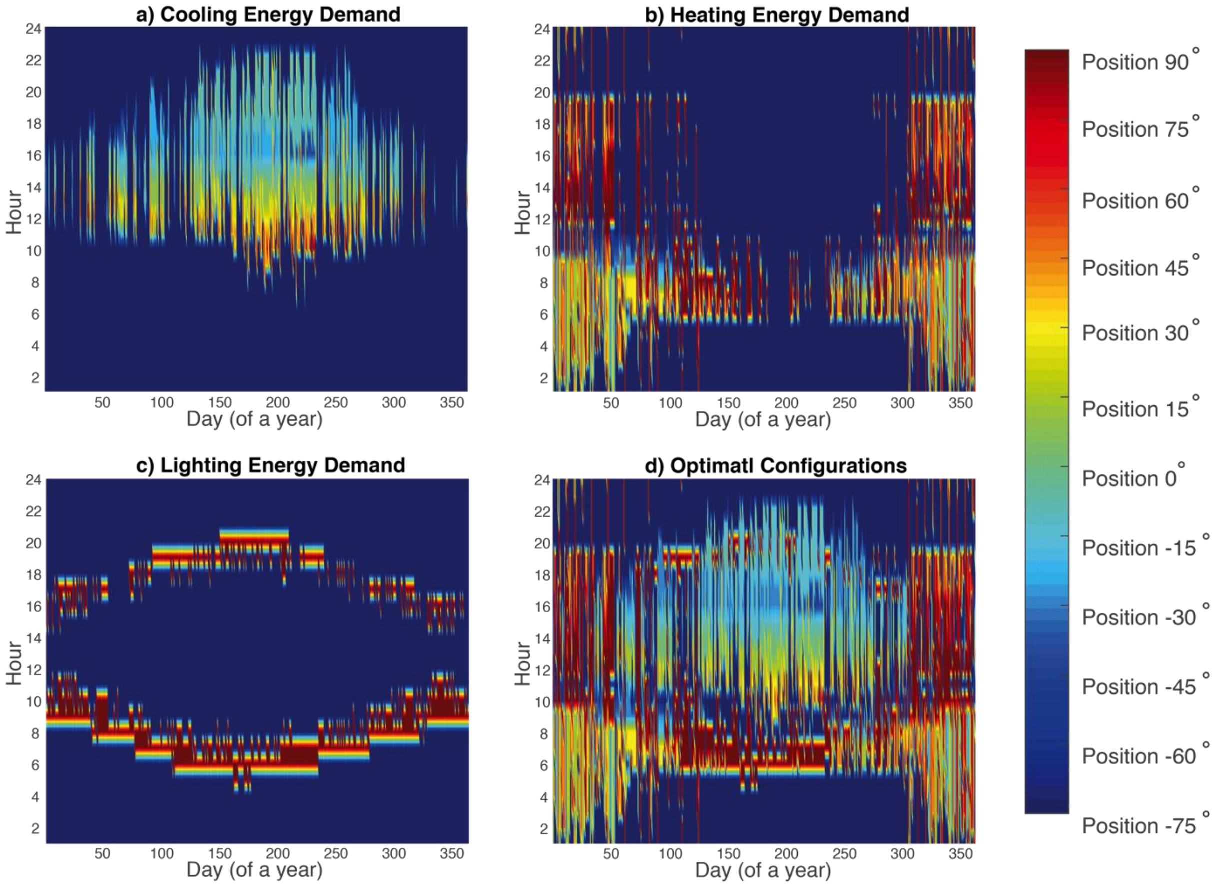

Figure 5: Orientations on the vertical axis that minimise cooling, heating and lighting demand

2.3 Energy Savings from the Adaptive Solar Façade

Using the setup described above we compare the energy consumption and savings of the ASF with two reference configurations: a standard louver system with blinds at 45°, and a case with no shading at all. The net energy demands comparing the three cases are summarised in Table 2. As we use the same simulation setup for all three façade configurations the relative changes are most important.

Having no shading system naturally has the lowest heating and lighting requirements, as all solar insolation is incident on the glazing. However the cooling requirements are very high. Fixed louvers at 45° have significantly lower cooling loads, but in turn have higher heating and lighting demands. Because of the ASFs independently actuated panels there is a potential to balance between the benefits of solar insolation for heating and lighting energy reduction, and drawbacks in terms of cooling energy consumption. We calculate total energy savings of 25% compared to louvers at 45°, and savings of 56% compared to a case with no facade shading.

To understand the final electricity consumption of our office case study, we converted the net energy demands to end use electricity. For this we assume a heat pump for heat generation with an approximated COP of 5. For cooling purposes, free cooling using cold water is assumed; therefore only pumping electricity is taken into account. The room is illuminated with approximately 113 Watts of LED lighting. Using this setup we can compare the annual electricity demands of the room relative to louvers at 45°, summarised in Table 3. In total the ASF shows reductions in office end electricity consumption by 8.9% compared to the fixed louvers at 45°. This corresponds to a CO_2 offset of 15.3kgCO_2-eq per year based on the EU grid mix.

The solar panels that will be used are high efficiency thin film CIGS solar panels. With the existing façade configurations we estimate a production of 580kWh of electricity per year. When combined with the energy savings of the ASF, this corresponds to an offset of 247kgCO_2-eq per year.

Table 2: Net energy demand of the office room

	No Shading System	Louvers at 45°	Adaptive Solar Facade	% Savings compared to No Shading	% Savings compared to Louvers at 45°
Heating (GJ)	4.64	5.29	4.70	-1%	11%
Lighting (GJ)	1.56	1.65	1.60	-3%	3%
Cooling (GJ)	13.5	4.53	2.39	82%	47%
Total (GJ)	19.7	11.5	8.69	56%	24%

Table 3: Total electricity demand of the office room

	Louvers at 45°	Adaptive Solar Facade	Savings (absolute)	Savings (%)
Heating COP5 (kWh)	301.2	267.4	33.0	11
LED Lighting (kWh)	124.9	121.1	3.78	22
Cooling Pump cost only (kWh)	4.17	3.24	0.9	3.0
Total (kWh)	430	391.8	38.4	8.9
kgCO2-eq (EU grid mix)	171.7	156.3	15.3	8.9

3 Prototypes

3.1 Proof of concept

The actuation of the panels requires a robust, cheap, waterproof, and reliable actuation system. As the main component that facilitates the dynamic behaviour of the façade we have created a soft pneumatic actuator to rotate the solar panels on two axis [15][16]. The soft pneumatic actuator bears the potential to be simpler, more robust and cost cost-effective compared to standard motor-operated actuators. This is because it contains no mechanical or electrical parts, and allows for physical flexibility when encountering wind loads.
The first prototype consisting of eight photovoltaic panels was constructed to test the functionality of the soft pneumatic actuators, see Figure 6. The actuators can rotate the photovoltaic panel in two degrees of freedom at an angle ±40°. The actuators are attached via aluminium and laser cut plexiglas (PMMA) cantilevers to a steel cable net support, see Figure 7.

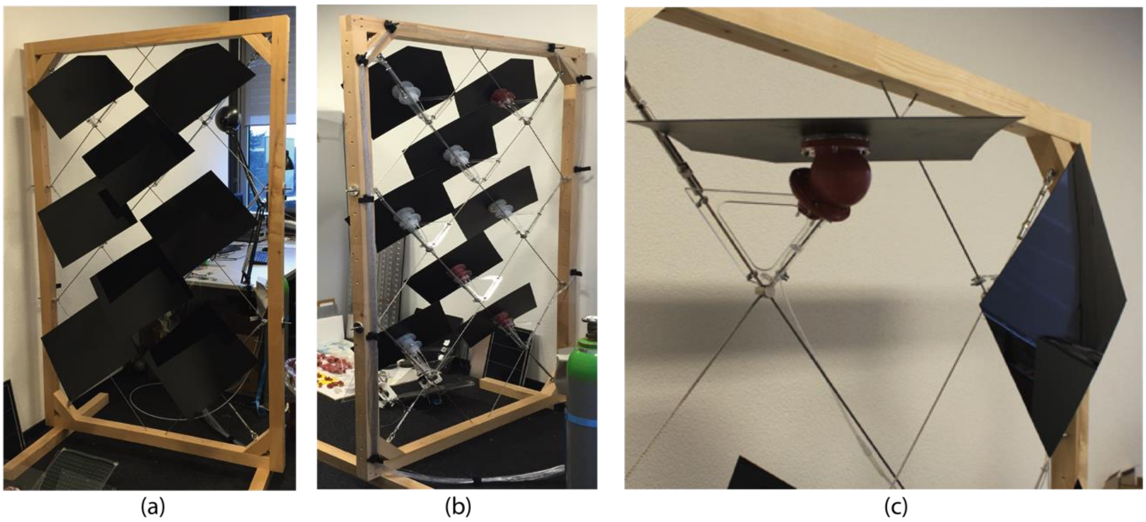

Figure 6: Proof of concept with 8 panels on a wooden frame. (a) Front view, (b) rear view exposing the actuators and cable net, (c) open and closed configurations

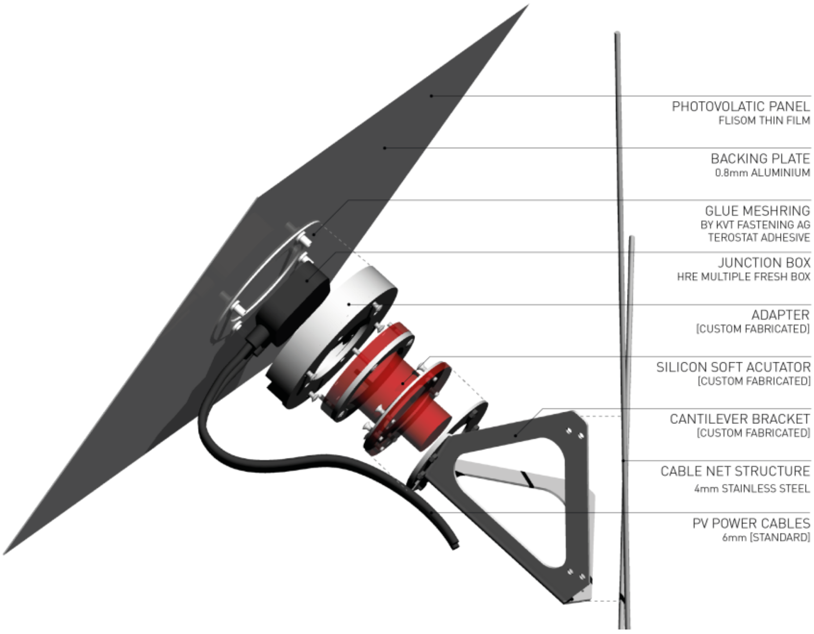

Figure 7: Exploded view of the actuator build up

3.2 Building Scale Prototype

The next iteration saw the production of a 1:1 scale prototype of the ASF which is going to be implemented in the HiLo building at NEST (www.hilo.arch.ethz.ch). A rendering and final prototype can be seen in Figure 8. A cable net structure with 4mm cables spanned on an aluminium frame was the simplest and least visually impairing structure to mount the actuated solar panels. Aluminium was chosen for this prototype due to its ease of manufacture. The final version however will use a steel frame to reduce grey emissions and overall size.

Figure 8: (left) Indoor rendering of the ASF, (right) Prototype with six panels and an aluminium frame. A photovoltaic panel will be mounted at each cable intersection.

4 Life Cycle Analysis

As shown in Section 2, the ASF can offset 247kg of CO_2 per year from electricity generation and energy savings. To complete the picture it is necessary to analyse the grey energy and CO_2 emissions for production over an approximated 20-year lifetime.

The ASF can be divided into four distinct components: the frame and cable net, CIGS solar panels, cantilevers, and pneumatic actuators, see Section 3. The grey emissions were calculated using the KBOB eco-bau IPB 2009/1:2014 [17], and the Eco-invent database [18]. Manufacturing data for the CIGS solar panels was obtained from Raugei et al [19]. The inventory of main inputs along with their total grey energy emissions and global warming potential is summarised in Table 4.

The analysis shows an energy pay back time of the façade with solar generation of 2.5 years. The facade will need to be in operation for 1.5 years to offset the greenhouse gas emissions released in manufacturing the ASF. This is less than half of the payback period of traditional silicon PV modules that have an energy payback period of 5.5 years [19].

Table 4: Grey energy emissions and life cycle CO2 analysis

	Inventory	MJ oil-eq	Kg CO2-eq
Cantilevers	Sheet Aluminium: 1.8kg Plexiglass: 1.26kg Electricity: 0.36MJ	311	19
CIGS Solar Panels	EVA: 5.04kg Sheet Aluminium: 12.42kg Copper: 13kg Electricity: 504MJ	3154	209
Actuators	Silicone: 9kg PMMA: 0.7kg	661	61
Steel Frame	Steel profile: 110kg	1463	84.7
Total		**5589**	**374**

5 Conclusion

In this paper we discussed the development of the Adaptive Solar Façade concept. Energy simulations provided first indicators of how such a modular system on a south-facing window can reduce office energy consumption for heating, cooling, and lighting. For our particular setup we achieved end electricity savings of 8.9%. Additionally, the ASF generates more electricity than the office room consumes through thin film CIGS solar panels, thus providing a surplus of renewable energy to be used for other applications in the building. An initial life cycle analysis of the global warming potential and grey energy emissions, based on the current knowledge on construction, shows an energy payback time of 2.5 years and a carbon dioxide payback time of 1.5 years. This is less than half the energy payback period of traditional silicon PV modules [19]. Through the construction of prototypes we have iteratively optimised the structural design to deal with external environmental conditions such as wind loading.

The next steps of this research will analyse the effects of the façade in different application scenarios and climates. If the façade were to be applied in a hot climate such as Singapore, then we should see even larger energy savings compared to the base case in a moderate climate such as Switzerland. The application of the facade in two real-world living labs will allow the validation of the simulation using measurements and, moreover, the conduction of thermal and lighting comfort analysis to complement the energy savings and renewable energy generation, respectively.

6 Acknowledgements

The authors would like to acknowledge the HiLo and HoNR project members. Supermanoeuvre (Sydney Australia) and the Professorship of Architecture and Structures (BRG, ETH Zürich) for their work in designing the HiLo building; and the Institute of Structural Engineering (IBK, ETH Zürich) for their work in designing the HoNR building. The authors would also like to thanks other key contributors to the ASF project: Bratislav Svetozarevic, Moritz Begle and Giovanni Bianchi. Funding from Climate-KIC through the Building Technologies Accelerator (BTA) Program is gratefully acknowledged.

Funding for the conduction of this research came from the Building Technologies Accelerator program of Climate-KIC.

7 References

[1] Huovila P.: *Buildings and climate change: status, challenges, and opportunities.* United Nations Environment Programme. Sustainable Consumption and Reduction Branch, Paris, France, 2007.
[2] Lenoir A., Cory S., Donn M. and Garde F.: *Optimisation methodology for the design of solar shading for thermal and visual comfort in tropical climates*. 13th Conference of International Building Performance Simulation Association, Chambery, France, 2013.
[3] Palmero-Marrero, Ana I., and Armando C. Oliveira. *Effect of louver shading devices on building energy requirements.* Applied Energy 87.6 (2010): 2040-2049.
[4] Almussaed A. and Almssad A.: *Natural lighting efficiency by means of sun-skylight-tubes*. International Journal of Engineering and Advanced Technology, ISSN: 2249-8958, Volume 3, Issue 3.
[5] Santamouris M., Synnefa A., Kolokotsa D., Dimitriou V. and Apostolakis K: *Passive cooling of the built environment – use of innovative reflective materials to fight heat islands and decrease cooling needs*. International Journal of Low-Carbon Technologies, Volume 3, Issue 2, 2008.
[6] Rizk J and Chaiko Y.: *Solar tracking system: More efficient use of solar*. World Academy of Science, Engineering and Technology, Volume 2, 2008.
[7] Fortmeyer R. and Linn C.: *Kinetic architecture: Designs for active envelopes.* Images Publishing, 2014
[8] Giselbrecht E. *Dynamic Facades*, Advanced Building Skins, Gratz, Austria, 2012
[9] Rossi D., Nagy Z. and Schlueter A.: *Adaptive distributed robotics for environmental performance, occupant comfort and architectural expression.* In: International Journal of Architectural Computing (2012), Volume 10.
[10] "Rhinoceros." *Rhinoceros*. Web. 27 Jan. 2015. <https://www.rhino3d.com/>.
[11] "Grasshopper." - *Algorithmic Modeling for Rhino*. Web. 27 Jan. 2015. <http://www.grasshopper3d.com/>.

[12] "EnergyPlus." *Building Technologies Office: Energy Simulation Software*. Web. 27 Jan. 2015. <http://apps1.eere.energy.gov/buildings/energyplus/>.
[13] "DIVA for Rhino." *DIVA for Rhino*. Web. 27 Jan. 2015. <http://diva4rhino.com/>.
[14] "MATLAB." *The Language of Technical Computing*. Web. 27 Jan. 2015. <http://www.mathworks.com/products/matlab/ >.
[15] Rossi D., Nagy Z. and Schlueter A.: *Soft robotics for architects.* In: Soft Robotics, Volume 1, No.2, pp. 157-153, 2014.
[16] Svetozarevic, B., Nagy, Z., Rossi, D., and Schlueter, A.: *Experimental Characterization of a 2-DOF Soft Robotic Platform for Architectural Applications*, Robotics: Science and Systems Conference, Workshop on Advances on Soft Robotics, UC Berkeley, California, 2014.
[17] KBOB-Eco Bau Katalogue: IBP 2009/1:2014 <http://www.eco-bau.ch/>.
[18] "Eco-Invent." *Home*. Web. 27 Jan. 2015. <http://www.ecoinvent.ch/>.
[19] Raugei, Marco, Silvia Bargigli, and Sergio Ulgiati: *Life cycle assessment and energy pay-back time of advanced photovoltaic modules: CdTe and CIS compared to poly-Si*. Energy 32.8 (2007) 1310-1318

Towards sustainable adaptive building skins with embedded hygromorphic responsiveness

Artem Holstov, PhD Candidate
School of Civil Engineering and Geosciences, Newcastle University, UK
artem.holstov@newcastle.ac.uk

Philip Morris, MArch Candidate
School of Architecture Planning and Landscape, Newcastle University, UK
philip.morris@newcastle.ac.uk

Graham Farmer, Prof., Head of Architecture
School of Architecture Planning and Landscape, Newcastle University, UK
graham.farmer@newcastle.ac.uk

Ben Bridgens, Dr., Lecturer in Structural Engineering
School of Civil Engineering and Geosciences, Newcastle University, UK
ben.bridgens@newcastle.ac.uk

Summary

The evolution of the shape, structure and behaviour of natural responsive systems, such as pine cones, is defined by the necessity to maximise the use of the inherent properties of available materials. This principle forms the basis for a new approach to adaptive architecture that goes beyond the current performance-oriented technological paradigm of sustainability and seeks to address a wider range of sustainable considerations by deploying materials with embedded responsive properties. This paper presents research into novel biomimetic hygromorphic (moisture-sensitive) materials that employ the natural responsiveness of wood to moisture, and argues that they provide opportunities for the design of simpler yet more versatile responsive building skins which are passively attuned to the variable rhythms of the internal and external environment. It provides an overview of the principles for the design and application of multi-functional hygromorphic façades and introduces analytical tools for optimising material selection and composite configuration.

Keywords: Hygromorphic materials; Passive climate-responsiveness; Sustainable adaptive facades; Wood hygroexpansion; Biomimetic architecture

1 Introduction

1.1 Improved Sustainability through Passive Climate-Responsiveness

The notion of sustainability in building design is commonly associated with reduced energy consumption and carbon footprint [1]. It is widely recognised that a substantial reduction in building energy use can be achieved through the application of passive design measures that allow increased exploitation of natural heating, cooling and light to maintain comfortable interior conditions for the longest time without the need for external energy inputs [2]. However, in most cases even buildings with a good passive design require the occasional use of active (i.e. energy-consuming) building systems to ameliorate the effects of the changeable external environment. Adaptive building skins that are able to adjust and optimise their properties depending on the ambient conditions can help address the challenges of continuously maintaining occupant comfort whilst reducing energy use [3]. Contemporary adaptive systems tend to rely on technologically-imposed intelligence [4] enabled by application and interaction of sophisticated mechanical and electronic sensors, control systems and actuators which results in a dependency on energy supply, high complexity and cost, and potential reliability and maintenance issues. This points to the need for further research into design approaches, materials and techniques that could combine the simplicity and low-cost of zero-energy bioclimatic design and the dynamic response of high-tech adaptive architecture. The inspiration for this 'hybrid' approach to adaptive architecture can be drawn from nature where elegance and functionality often coexist and the robustness and efficiency of responsive systems, such as conifer cones, is enabled by employment of the inherent properties of their constituent materials [5]. Application of materials with intrinsic sensitivity to climatic stimuli can therefore serve as an underpinning principle for development of simpler, yet more versatile adaptive building skins with passive embedded response. It is argued that these systems could provide designers with means of simultaneously addressing a range of multidimensional sustainability considerations [6,7] beyond energy efficiency.

1.2 From Pine Cones to Hygromorphic Materials

Production of many of the modern man-made smart materials, such as thermobimetals and shape memory alloys, is often complex, power-intensive and requires materials with limited availability which diminishes their applicability in large-scale building applications. For this reason, there is an increasing research interest in examples of natural responsive mechanisms that are architecturally scalable. One example of such mechanisms is the opening and closing of conifer cones (e.g. pine cones) (Figure 1).

Figure 1: Reversible moisture-driven opening and closing of pine cones.

The large seed-producing scales of the pine cones consist of two layers exhibiting different amounts of dimensional changes when exposed to moisture [8]. As a result, the scales bend outwards in dry conditions and close in humid or wet environment. A similar actuation mechanism is also observed in a number of other natural systems with reversible moisture-induced response, for example, wheat awns and orchid tree seedpods [9, 10]. Conifer cones retain their responsiveness over a large number of cycles as the mechanism operates passively and is performed by the tissues of the fallen cones, which are no longer alive [4]. The structure of the responsive scales of the pine cone can be replicated to produce low-tech low-cost artificial hygromorphic (moisture-sensitive) materials (a.k.a. hygromorphs) consisting of active wood layers and natural or synthetic passive layers (Figure 2).

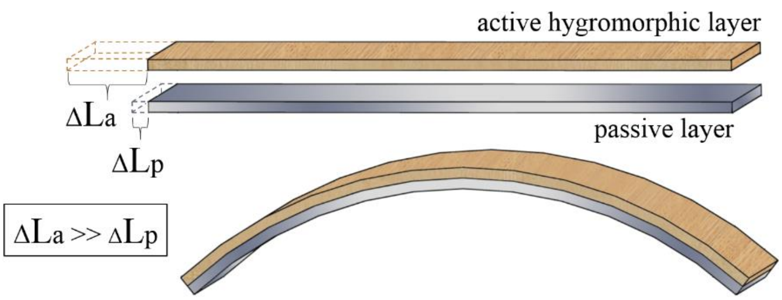

Figure 2: Principle of the response of hygromorphic composites based on differential hygroexpansion (i.e. shrinkage or swelling) of active and passive layers.

2 Guidance for Selection and Production of Hygromorphic Materials

2.1 Method for Assessment of Properties

It is considered that the following properties will affect the applicability of hygromorphic composites as a responsive building material:

- Responsiveness (the magnitude of shape changes)
- Reactivity (response time)
- Actuation capacity (force produced by the response)
- Structural resistance (ability to withstand applied loads without excessive deflection and irreversible damage)
- Durability (resistance to degradation)
- Sustainability (environmental impact, effects on people and economic considerations)
- Aesthetics and texture.

The behaviour and properties of bi-layer hygromorphic composites are determined by their configuration (i.e. the choice of material for each layer, their thicknesses, orientation and type of bond) and the initial production conditions. Considering a wide range of wood species and types and an even greater number of the materials potentially applicable for the passive layer, selection of optimal configurations and production methods is essential to enable improved applicability of the composites.

A combination of analytical tools and experimental data have been used to assess and compare the properties of a variety of possible configurations of hygromorphic materials. Owing to the similarity between the response mechanisms of bi-layer hygromorphs and thermo-bimetallic strips, Timoshenko's theory for bi-metal thermostats [8,11] has been used to predict curvature of the composites 'K' resulting from moisture-induced response. Timoshenko's equation has been modified to account for hygroscopic shrinkage of the layers by replacing the corresponding thermal expansion coefficients with coefficients of hygroexpansion (α), which can be assumed to be linear for simplicity [12], and temperature change with effective moisture content change (ΔMC') (i.e. the amount of moisture content change within the range of 0% to ~30%) (Equation 1):

$$K = \frac{1}{R} = \frac{\Delta\alpha \cdot f(m,n) \cdot \Delta MC'}{t_{total}} + \frac{1}{R_0} \quad (1)$$

where

$$f(m,n) = \frac{6(1+m)^2}{3(1+m)^2 + (1+m \cdot n)\left(m^2 + \frac{1}{m \cdot n}\right)}\ ;\ \Delta\alpha = \alpha_a - \alpha_p;\ m = \frac{t_p}{t_a}\ and\ n = \frac{E_p}{E_a} \quad (2)$$

and t = thickness of a layer, E = elastic modulus (stiffness), R = radius of curvature of the composite, and subscripts 'a' and 'p' denote the active and passive layers respectively.

2.2 Choice of Active Layer

Similar to the woody tissues of the scales of conifer cones, hygroexpansion of wood is a passive material capacity resulting from its hygroscopicity (i.e. continuous exchange of moisture with the surrounding environment through processes of adsorption and desorption) [13] and micro- and macro-structure, which are independent from biological cell activity. The ability to adsorb water is not unique to wood, however, unlike many other hygroscopic materials (e.g. paper and concrete), it is able to exhibit comparatively large dimensional changes resulting from variations in its moisture content (hygromorphy) and is characterised by good flexibility and low weight. This in combination with ubiquitous availability and low environmental impact of wood as a renewable natural material [14,15,16] make it well-suited for the use in the active layer of hygromorphic materials.

Water can be stored in wood in two different states - free water inside cell cavities and bound water in the cell walls. The effects of the presence of free water on dimensional changes are negligible; therefore, considering that the maximum amount of water that can be adsorbed into the cell walls corresponds to the moisture content (MC) of approximately 26-30% for most wood species, any significant hygroexpansion can only occur as a result of moisture content variations below the point of fibre saturation (MCf) [12,15]. In freshly-sawn timber (green wood) MC is always above MCf [14], thus only dried wood can exhibit hygroexpansion. Over time, unless exposed to liquid water or quickly changeable climate, wood comes to equilibrium with the surrounding environment (Equilibrium Moisture Content, EMC) and stops gaining or losing bound water [13]. The response of hygromorphic composites can be triggered by direct contact with moisture or changes in relative humidity (RH) and to a lesser degree, ambient temperature, which determine EMC of the active wood layer. It is also possible to calibrate or pre-programme the response of the materials through adjustment of the initial production MC of the active layer or the initial curvature of the composite.

Since wood is formed as a functional tissue of trees, its structure has evolved to provide the necessary support and resistance against axial and bending forces (from the weight of the tree and wind loading) and allow transport and storage of sap and carbohydrates within the tree. This explains anisotropy of many of its properties, including much greater strength and stiffness of wood along the grain than in each of the transverse directions [17]. The hygroexpansion of wood is significantly different in the three orthogonal directions – tangential (tan.), radial (rad.) and longitudinal (lon.). Its magnitude varies for different wood species, but maximum dimensional changes always occur along the growth rings, with around 40% smaller changes in the radial direction and at least an order of magnitude smaller hygroexpansion in the longitudinal direction [15,18] (Figure 3). Therefore, considering that the response of bi-layer hygromorphs is proportional to the difference between the dimensional changes of the two layers, configurations with higher responsiveness can be produced by selecting rotary or plain-cut veneer (or plain-sawn boards, depending on the required thickness) of wood species exhibiting high amount of movement (i.e. maximum tangential shrinkage/swelling above ~8%) for their active layers (Figure 4 & 5), for example, European beech/*Fagus sylvatica*. The largest curvature change of the composites will occur in the direction orthogonal to the grain direction of the active layer.

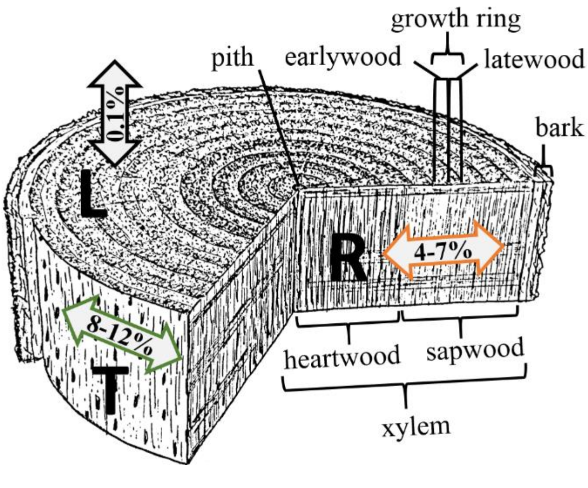

Figure 3: Section of a wood trunk showing approximate maximum hygroexpansion in each of the grain directions. Produced using information from [13,18].

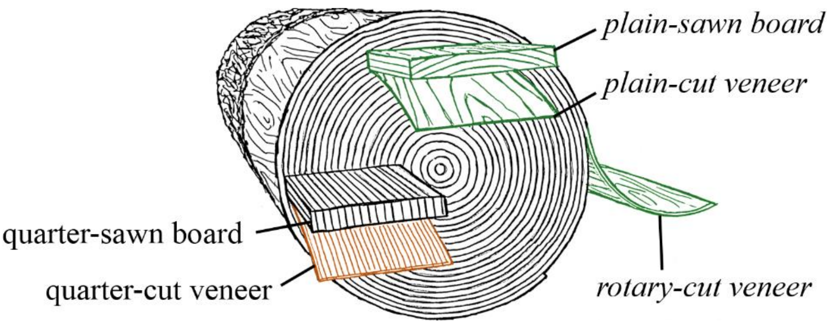

Figure 4: Types of lumber and veneer which should be used in the active layer to employ tangential (maximum) hygroexpansion (green/italics).

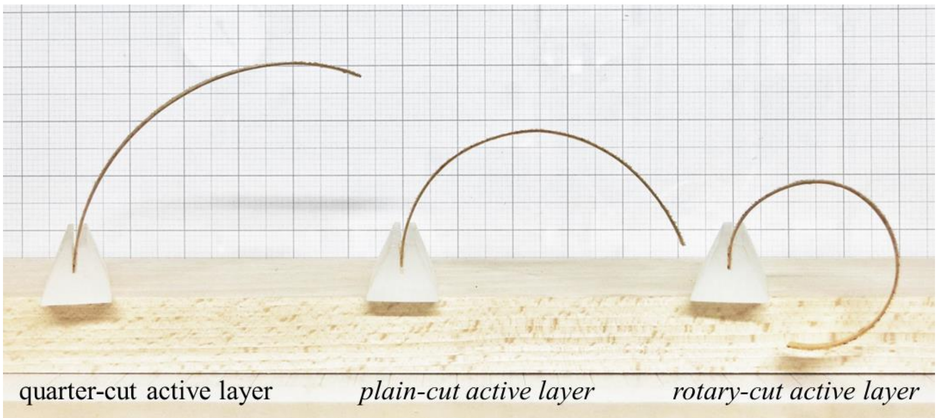

Figure 5: Hygromorphs with active layers of plain-cut and rotary-cut wood veneer are more responsive than those with quarter-cut veneer active layers. The figure shows the response of initially straight samples (at 45%RH and 22C^{o}) to wetting by sprayed water. With the exception of the type of veneer used for the active layer, the samples are identically configured and sized.

In addition to hygroexpansion, other properties to consider when selecting wood species suitable for the active layer include grain characteristics (i.e. the proportion and distribution of cells of different types and sizes) and durability. Even-grained wood with relatively small variation between the sizes and wall thicknesses of the cells in earlywood and latewood sections of growth-rings should be selected for improved consistency of properties of the composites with thin active layers. Whilst, even-grained softwood species are uncommon in temperate climates, a range diffuse-porous hardwoods are grown in Europe [14] (e.g. European maple/*Acer pseudoplatanus*). However, considering greater general availability and affordability of a variety of softwood species in Europe, it may be more economical to use softwood for the composites with thicker active layers (above ~1.5mm). It is important to note that some variability of properties of the active layer is inevitable (e.g. variations of around 15% from the nominal hygroexpansion can be expected in normal wood of the same species and type) as wood is a natural climate-dependent anisotropic material [15].

Regardless of the choice of species, wood is rarely susceptible to biological decay at MC below 20% [17]. Therefore the lifespan of the composites protected from direct contact with water and RH above 90% (e.g. indoor applications) will in most cases be determined by the rates of UV and mechanical degradation most affected by the thickness of the wood layer. Selection of wood species with good natural resistance to biodegradation (e.g. European cherry/*Prunus avium* and European larch/*Larix europaea*) can potentially improve the longevity of hygromorphs in applications that require the exposure or response to wet environment. Given the potential aesthetic value of adaptive building skins clad with the responsive materials, visual characteristics of different wood species such as colour and figure may also play a significant role in material selection depending on the proposed application.

2.3 Choice of Passive Layer

The passive layer is used to amplify the effects of movement of the active layer by providing a constraint to its planar hygroexpansion and forcing the composite to bend. This can be achieved through selection of materials with small hygroscopicity (i.e. small water absorption index) or low hygroexpansion. Considering that hygroexpansion of wood along the grain is negligible in comparison to the dimensional changes in each of the transverse directions, one of the possible configurations of the responsive composites can comprise of two identical layers of wood veneer aligned with their grain directions perpendicular (cross-grained veneer laminate). A smaller more 'acute' angle between the grain directions of the layers will result in a reduced response with the composite twisting as well as bending. An order of magnitude lower embodied energy of wood when compared to the majority of other potentially applicable passive layers, including synthetic polymers, fibreglass or carbon fibre [19], will benefit the environmental performance of cross-grained veneer laminates. One of the concerns associated with the use of wood veneer in the passive layer is that its dimensional changes will result in bi-directional differential expansion of the layers leading to reduced responsiveness and increased internal stresses in the responsive panels with similar width and length [20], especially if the thicknesses of the layers are equal.

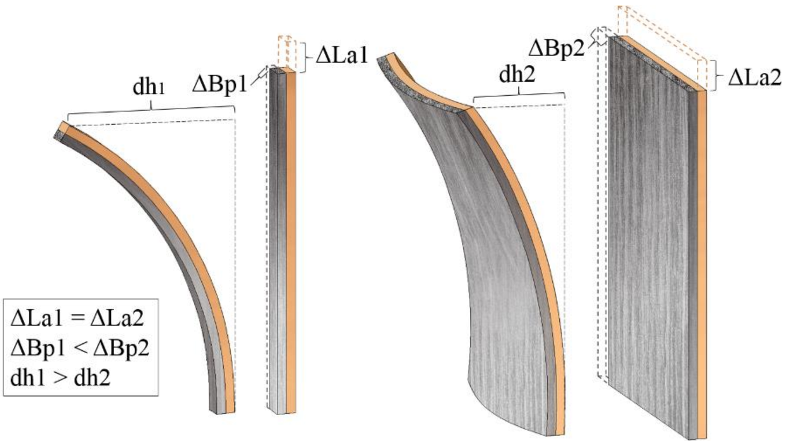

Figure 6: Bidirectional hygroexpansion of active and passive layers (ΔBp and ΔLa respectively) results in a tendency of wider responsive elements to develop double curvature leading to a reduced response.

A range of synthetic polymers, fibre-reinforced polymers (FRPs) and other non-hygroscopic materials can be used in the passive layer to ensure its dimensional stability. Many of these materials, such as Polyethylene Terephthalate (PET), which is widely used and recycled, are characterised by substantially greater overall durability, toughness and better resistance to UV degradation than wood [19] and can improve the longevity of the resulting semi-synthetic composites. It is essential that the selected passive layer is capable of undergoing repetitive bending without changing its properties (e.g. due to creep, fatigue or brittleness). Similarly, the bond between the layers has to be flexible enough to withstand bending of the composite without failure, but at the same time, be strong and stiff enough to transfer forces induced by hygroexpansion between the layers. This can be achieved through the use of water-resistant structural adhesives, such as epoxy resins and polyurethane, or through direct lamination of engineering fabrics (e.g. fiberglass) onto the wood layer. Considering that recycling of glued composites and synthetic FRPs is challenging [21], significant reduction in the environmental footprint of hygromorphs can be achieved if the passive layers are produced from natural fabrics (e.g. jute and flax) laminated with sustainable bio-resin alternatives to epoxy resins.

2.4 Optimal Layer Thicknesses

Equation 1 reveals that the responsiveness of bi-layer hygromorphic composites is linearly related to the value of the function f(m;n) (coefficient of curvature change, found using Equation 2). Firstly, since the function is only affected by the stiffness ratio of the layers 'n', not their individual stiffness, the use of both layers with increased stiffness can allow improved structural properties of the composites without compromising their responsiveness. Secondly, plotting f(m,n) for a wide range of possible stiffness ratios (Figure 7) shows that in each case maximum responsiveness (f(m,n)=1.5) can be achieved at a single thickness ratio 'm' (optimal thickness ratio). Hence, optimal thickness ratios can be plotted against the corresponding stiffness ratios of the layers (Figure 8).

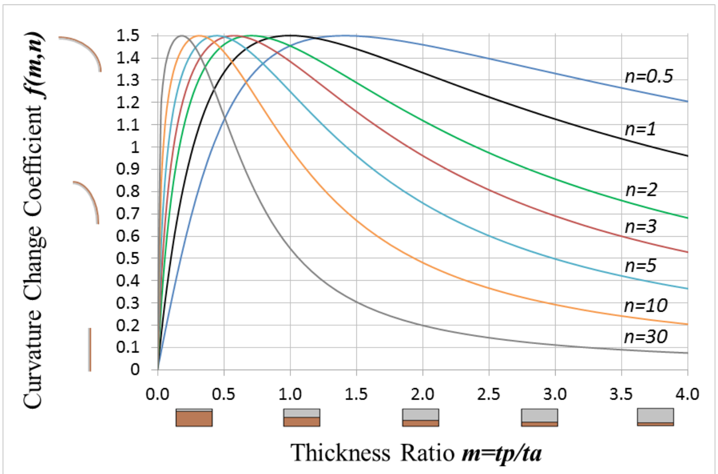

Figure 7: Curvature change coefficient f(m,n) as a function of thickness ratios 'm' for various stiffness ratios 'n'.

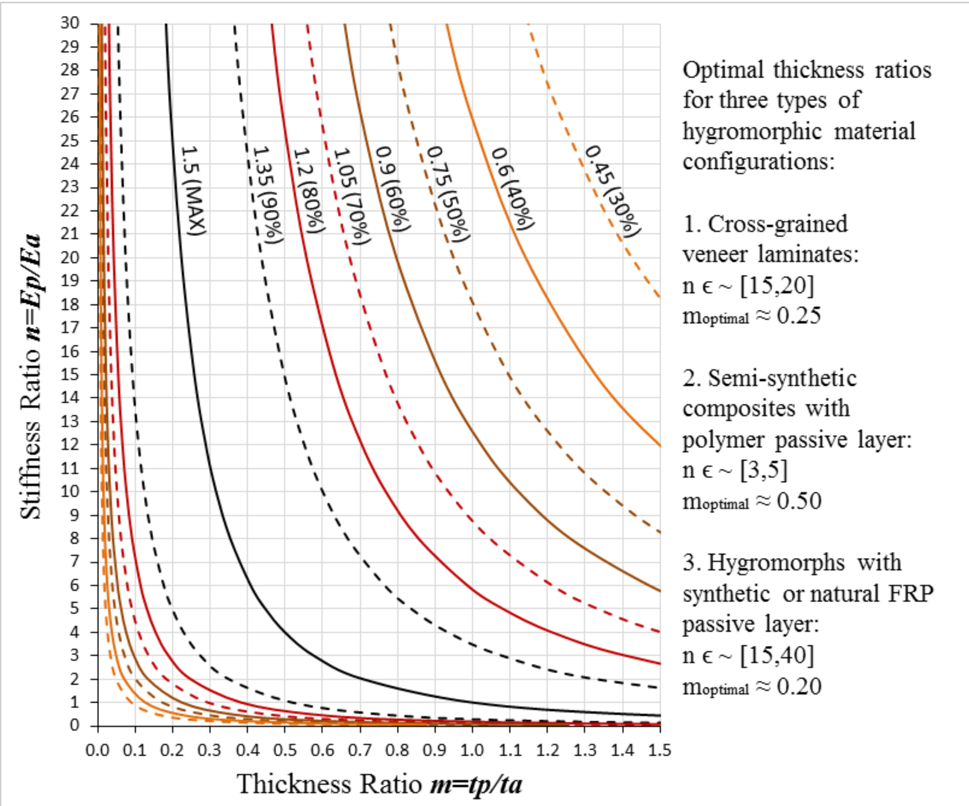

Figure 8: Combinations of thickness and stiffness ratios of the two layers allowing to achieve different levels of responsiveness, including the optimal combinations for any given overall thickness and hygromorphic properties of the layers (bold black line, f(m,n)=1.5).

As seen from Figure 8, selection of materials with equal stiffness requires the use of the layers with the same thickness in order to produce composites exhibiting maximum response. In other cases the peak value of f(m,n) can be achieved if larger stiffness of one layer is compensated by increased thickness of the other layer (and vice versa). In practice, the transverse stiffness of wood is usually much lower (~0.6GPa tangential and ~1.2GPa radial stiffness) [17] than that of most of the applicable passive layers meaning that a thinner passive layer has to be used for optimal responsiveness. Whilst, given the same total thickness and hygromorphic properties of the layers, composites with different optimal combinations of layer thickness and stiffness ratios should be equally responsive, structurally, the configurations with thinner (reduced 'm'), but stiffer (increased 'n') passive layers will have greater flexural rigidity than those with relatively thick but less stiff passive layers (Figure 9). Practically, this will benefit structural performance of the composites with thin laminated fibre-reinforced passive layers, which are characterised by high stiffness and strength (e.g. thicknesses in the range of 0.05mm to 0.5mm are achievable when laminating a single layer of fiberglass onto wood).

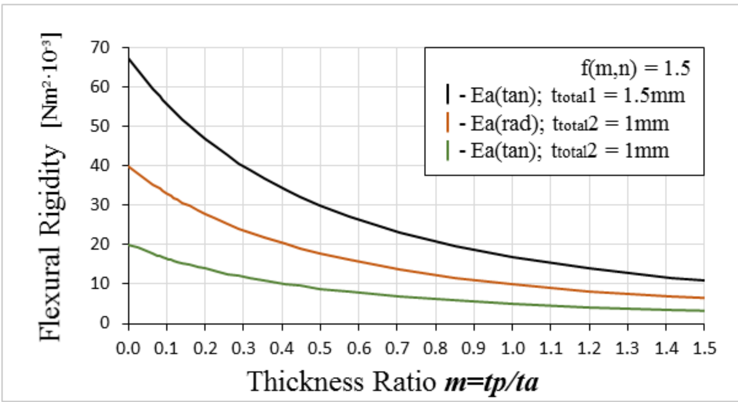

Figure 9: Flexural rigidity of bi-layer hygromorphs with various optimal combinations of layer thickness and stiffness ratios. Rectangular shape of responsive elements with an arbitrary 0.1m width has been assumed.

According to Equation 1, responsiveness is linearly related to the ratio between the difference in coefficients of hygroexpansion of the layers and the total thickness of the composite ($\Delta\alpha/t_{total}$). Owing to greater tangential hygroexpansion of wood, hygromorphs with active layers of rotary-cut veneer can achieve the same responsiveness as 1.5 thinner composites with quarter-cut veneer active layers and the same optimal thickness and stiffness ratios. As shown in Figure 9, despite radial stiffness of wood assumed to be twice larger than the tangential stiffness, the composites with rotary-cut active layers will exhibit around 40% greater flexural rigidity in comparison to the thinner hygromorphs with quarter-cut active layers. For any combination of layer types, selection of optimal thickness ratios can allow using thicker more durable composites while maintaining a good level of responsiveness (Figure 10). The thickness of the active layer is also the main factor affecting the response speed. Composites with comparatively thick active layers can be applied where the response to longer-term changes in the surrounding conditions is required (i.e. daily, monthly or even seasonal changes), whilst thinner composites can react rapidly to hourly changes of ambient humidity or sudden rain.

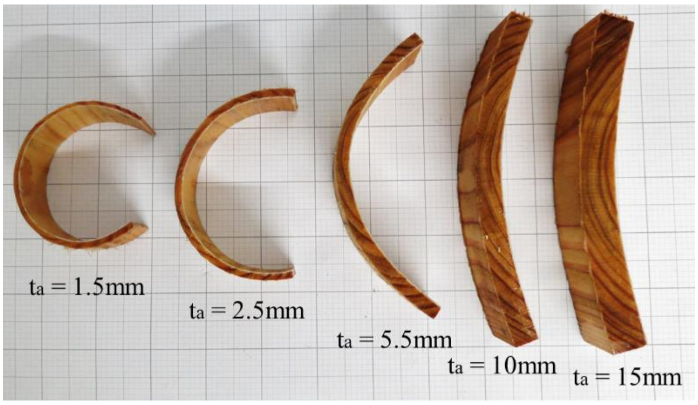

Figure 10: The response of initially straight (at 35% RH and 22C°) 150mm long samples of hygromorphic composites with different thicknesses (‘t_a’) of plain-sawn European larch (*Larix europaea*) active wood layers and thin 0.3mm laminated fiberglass layers to wetting by sprayed water. Considering a more than twentyfold difference between the stiffness of the layers, significant response of even the thickest samples is achieved thanks to a small thickness ratio ‘m’.

3 Potential Applications in Adaptive Building Skins

Recent research on hygromorphic materials has mainly been focused on testing of material responsiveness and demonstration of the dramatic aesthetic appeal of the technique through production of small-scale prototype structures with different shapes and arrangements of responsive elements. Several authors have speculated on the general categories of possible applications for hygromorphs as sensors or actuators [8] or in larger scale applications such as building envelopes and roofs of stadiums and semi-indoor spaces [22]. However, the wider challenges and opportunities of building integration and the potential functional and aesthetic applications of the materials in architecture are yet to be established.

Since the building envelope serves as a barrier between the internal conditioned and the external unconditioned space, it is argued that the use of responsive materials to enable its adaptive behaviour and employ it for control over the interior climate and occupant comfort is one of their most promising building applications. For example, a cladding system comprising of hygromorphic materials could fold or deploy when exposed to rain (or in advance, by responding to high relative humidity) creating a watertight shelter and managing water runoff (Figure 11). In large-scale fully conditioned buildings requiring more substantial weather sealing, the responsive composites could be used as an active component of the building systems controlling air movement and the exchange of heat and moist air between the indoor space and the outdoor environment through continuous passive adjustment of porosity. In arid climate regions, hygromorphic building systems could be configured to help maintain thermal comfort through enhanced natural ventilation in hot dry weather. Alternatively, the response of the materials to temperature could be triggered by evaporation (relative humidity changes) and condensation (adsorption of condensed water). Whilst hygromorphs are not photosensitive, hygromorphic systems could be designed to control illumination and prevent excessive solar gain and glare based on the assumption of a link between relative humidity and the amount of available daylight. Responsive elements preinstalled into retrofitted modular cladding or integrated as part of the windows could be preprogrammed to fold providing shading in dry sunny weather and open up in humid conditions when the sky is overcast to maximize the use of daylight.

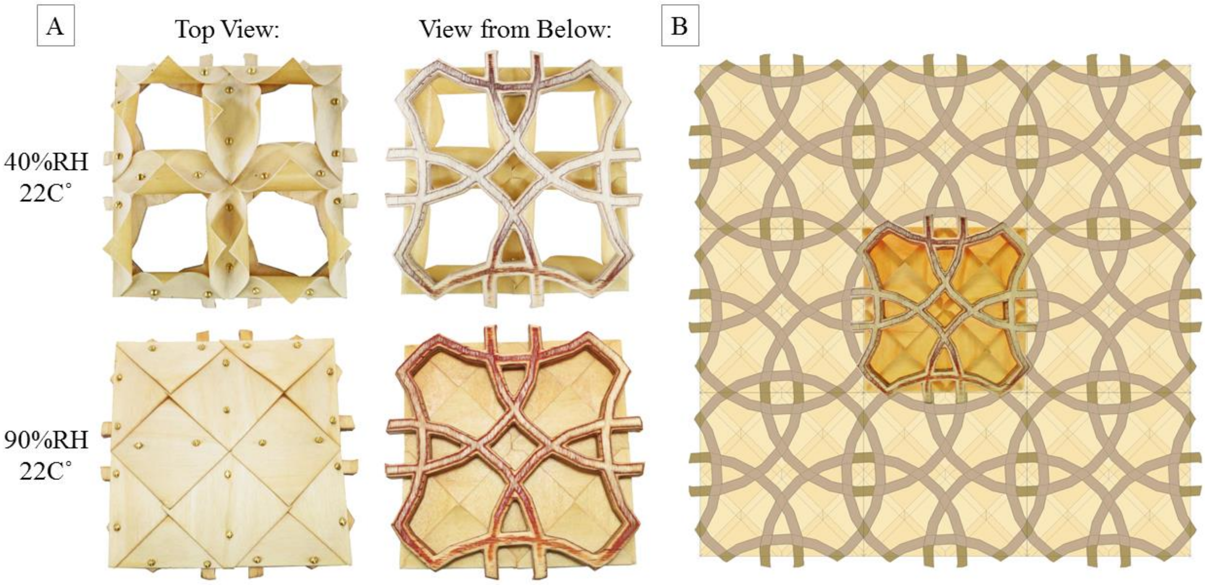

Figure 11: Response of a hygromorphic cladding module prototype to changes in ambient relative humidity (A) and the illustration of the understructure design achieved when several modules are assembled together (B).

The façade is often the defining element of the building in terms of its visual, tectonic and contextual expression. In this context, the possibility of responsive hygromorphic building skins that are in continuous formal interaction and synchronisation with their ambient environment provides opportunities for creation of unique architectural designs, vividly different from the static structures that typify the current architectural production. The dynamic behaviour of hygromorphic cladding elements and the inherent variability of their response would give buildings with responsive envelopes a rich texture reminiscent of that of natural organisms. Responsive cladding that is attuned to the natural rhythms of the external climate would provide a direct visual and formal reference to the ambient conditions of the climate positively contributing to the subjective enjoyment of the design and psychological occupant comfort. Beyond the functional and aesthetic applications, the integration of climatically responsive hygromorphs into buildings has the potential to address wider concerns about the technological intensity of modern buildings as well as helping to move beyond the focus on resource efficiency towards a more holistic view of environmental well-being. It is this possibility to simultaneously contribute towards climatic adaptability and environmental performance and the expressive potential of the technology that probably provides its most progressive and viable building-related future applications.

4 Conclusions and Recommendations for Future Research

Natural organisms with passive responsive capacities offer inspiration into the way sustainable building design can move away from the excessive reliance on complex and expensive mechanical control over internal building environments. The development and building integration of hygromorphic materials can facilitate creation of climatically adaptive architectures with materially embedded responsiveness enhancing occupant comfort and well-being and providing a spectacular visual expression and impact. Adjustment of the parameters of the composite build up allows optimization of hygromorphs' response size and time as well as other properties depending on the proposed application.

The future research could focus on three main themes running in parallel:

- the possibilities of improving the environmental performance and durability of the composites through the substitution of the synthetic passive layers with recycled or natural materials which have sufficiemt stiffness and strength to enable the use of thicker active layers

- design of responsive systems with enhanced adaptive properties and visual impact through employing a range of response mechanisms and arrangements of hygromorphic elements
- development of strategies for practical application of the technology.

5 Acknowledgements

We gratefully acknowledge financial support from the Engineering & Physical Science Research Council and from Newcastle University School of Architecture, Planning and Landscape. We would also like to thank Achim Menges, Steffen Reichert and Doris Kim Sung for providing the inspiration for this research.

6 References

[1] Banfill, P. and Peacock, A.: *Energy-efficient new housing–the UK reaches for sustainability*, in Building Research & Information 35 (2007) issue 4, pp. 426-436.
[2] Sadineni, S.B., Madala, S. and Boehm, R.F.: *Passive building energy savings: A review of building envelope components,* in: Renewable and Sustainable Energy Reviews 15 (2011) issue 8, pp. 3617-3631.
[3] Loonen, R.C.G.M., Trčka, M., Cóstola, D. and Hensen, J.L.M.: *Climate adaptive building shells: State-of-the-art and future challenges,* in: Renewable and Sustainable Energy Reviews 25 (2013), pp. 483-493.
[4] Menges, A. and Reichert, S.: *Material Capacity: Embedded Responsiveness*, in Architectural Design 82 (2012) issue 2, pp. 52-59.
[5] Pawlyn, M.: *Biomimicry in architecture*, Riba Publishing, London, 2011.
[6] Guy, S. and Farmer, G.: *Reinterpreting sustainable architecture: the place of technology,* in Journal of Architectural Education 54 (2001) issue 3, pp. 140-148.
[7] Holstov, A., Bridgens, B. and Farmer, G.: *Hygromorphic Materials for Sustainable Responsive Architecture* [article submitted to Construction and Building Materials journal and is under review], 2015.
[8] Reyssat, E. and Mahadevan, L.: *Hygromorphs: from pine cones to biomimetic bilayers,* in J R Soc Interface 6 (2009) issue 39, pp. 951-957.
[9] Fratzl, P. and Barth, F.G.: *Biomaterial systems for mechanosensing and actuation*, in Nature 462 (2009) issue 7272, pp. 442-448.
[10] Erb, R. M., Sander, J. S., Grisch, R., and Studart, A.R.: *Self-shaping composites with programmable bioinspired microstructures*, in Nature communications, 4 (2013), p. 1712.
[11] Timoshenko, S.: *Analysis of bi-metal thermostats,* in J. Opt. Soc. Am., 11 (1925) issue 3, pp. 233-255.
[12] Skaar, C.: *Wood-water relations*, Springer-Verlag, London, 1925.
[13] Hoadley, R.B.: *Understanding wood: a craftsman's guide to wood technology*, Taunton press, Newtown, 2000.
[14] United States Department of Agriculture (USDA): *Wood handbook: wood as an engineering material*, USDA–Forest Products Laboratory, Madison, 1999.
[15] Dinwoodie, J. M.: *Timber, its nature and behaviour*, Taylor & Francis, London, 2000.
[16] Wang, L., Toppinen, A. and Juslin, H.: *Use of wood in green building: a study of expert perspectives from the UK*, in Journal of Cleaner Production 65 (2014), pp. 350-361.
[17] Tsoumis, G.: *Science and technology of wood*: *Structure, properties, utilization,* Van Nostrand Reinhold, New York, 1991.
[18] Rijsdijk, J.F. and Laming, P.B.: *Physical and related properties of 145 timbers: information for practice,* Springer, Dordrecht, 1994.
[19] Granta 2013: *Granta CES Edupack Material Selector* [Material Property Database] http://www.grantadesign.com/products/ces/.
[20] Alben, S., Balakrisnan, B., and Smela, E.: *Edge effects determine the direction of bilayer bending,* in Nano letters 11 (2011) issue 6, pp. 2280-2285.
[21] Meira Castro, A., Ribeiro, M., Santos, J., Meixedo, J.P., Silva, F.J., Fiúza, A., Dinis, M. and Alvim, M.R.: *Sustainable waste recycling solution for the glass fibre reinforced polymer composite materials industry*, in Construction and Building Materials 45 (2013), pp. 87-94.
[22] Reichert, S., Menges, A., and Correa, D.,: *Meteorosensitive architecture: Biomimetic building skins based on materially embedded and hygroscopically enabled responsiveness,* in Computer-Aided Design (2014) (available at: http://dx.doi.org/10.1016/j.cad.2014.02.010).

Proceedings of the International Conference on Building Envelope Design and Technology, Graz
Advanced Building Skins 2015

The Al Bahr Towers: shading, the real envelope

Giorgio Buffoni MSc CEng MCIBSE IntPE(UK)
Arup, 13 Fitzroy Street, London W1T 4BQ, United Kingdom, giorgio.buffoni@arup.com

Konrad Xuereb BE&A,A&CE,MSc,MIStructE,MICE,CEng,ARB,EurIng
Arup, 13 Fitzroy Street, London W1T 4BQ, United Kingdom, konrad.xuereb@arup.com,
UCL, Gower Street, London WC1E 6BT, United Kingdom, konrad.xuereb.10@ucl.ac.uk

Summary

This paper presents the novel shading system that wraps the Al Bahr towers in Abu Dhabi. It describes how the system adapts to the solar radiation reaching the towers, how it controls solar gains and optimise daylight within the buildings. The paper elaborates on the challenges encountered in implementing the innovative shading system and the comprehensive tests carried out to mitigate the risks inherent in implementing the system in a large building project. It elaborates on sustainability credentials in relation to energy performance of the project. The paper describes how solar and daylighting performance are controlled by the Mashrabiya screen and the typology of the curtain wall lying behind it.

Keywords: Al Bahr Towers, Mashrabiya, Adaptive Shading System, Sustainability

1 Introduction

Located in the financial centre of Abu Dhabi, the award winning Al Bahr Towers consist of two quasi-identical, 150m tall buildings that embody an adaptive facade wrapping around the towers. The towers feature an innovative dynamic shading screen, the Mashrabiya, which enhances the sustainable criteria of the development by optimising the use of natural daylight whilst controlling solar gains.

Following an international design competition in 2008 the design bid submitted by London-based architect AHR, together with Arup as multidisciplinary engineering designer, was chosen as the winning entry by the client body. Arup was involved from the competition through to the construction stages, providing a full range of design services and specialist advice, ranging from the core disciplines of SMEP (structural, mechanical, electrical, public health) and Façade engineering to specialisms like environmental physics, fire, acoustics and advanced technology. Construction began in March 2009 and was completed in early 2013.

A key design driver was to develop a building envelope that was both efficient and iconic, related to Islamic architecture. The conceptual designs embodied a novel approach to reduce the effects of the high ambient temperatures and intense solar radiation that characterize the local environment. From the start, it was evident that the towers' cladding design and its thermal, solar and lighting performance would play a crucial role in the project's success. The idea adopted by the design team was radical yet simple – to control solar gains by introducing an external movable shading system instead of relying solely on the glass to filter the solar radiation. The team drew inspiration from the Mashrabiya, a form of shading screen that had been used for centuries in Islamic architecture to protect the building occupants from the intense sun whilst providing comfortable internal spaces and sustainable buildings in a harsh environment *[Fig.1]*. The challenge was to re-interpret this concept in a modern architectural language and to apply it to 150m high towers having complex geometries.

Fig.1 - Traditional shading screen used in vernacular Islamic architecture

2 Design – performance and materials

2.1 Objective

The design aspired to achieve a highly glazed building, allowing spectacular views from the inside whilst providing the best possible levels of internal visual and thermal comfort. The design approach sought was to adopt a glass system that was more transparent than those typically used for similarly glazed buildings in the region. This would result in key benefits, in particular enhanced daylighting within the building, reduced use of artificial lights and associated energy saving.

But how to keep the sun out?
A philosophical leap in the design process was to incorporate an adaptable shading system that attained the above benefits whilst controlling solar gains into the towers by filtering the direct solar radiation. Such a system would reduce the internal surface temperature of the framing and glass, and improve the working conditions and the thermal comfort by minimizing any radiative effect from a hot surface into a mechanically cooled environment. The solution was the innovative Mashrabiya adaptable shading devices which wrap the Al Bahr towers. In fact, the Mashrabiya became a key architectural theme in the towers' design, reflected also in the structural geometry and the interior design too.

2.2 Geometry

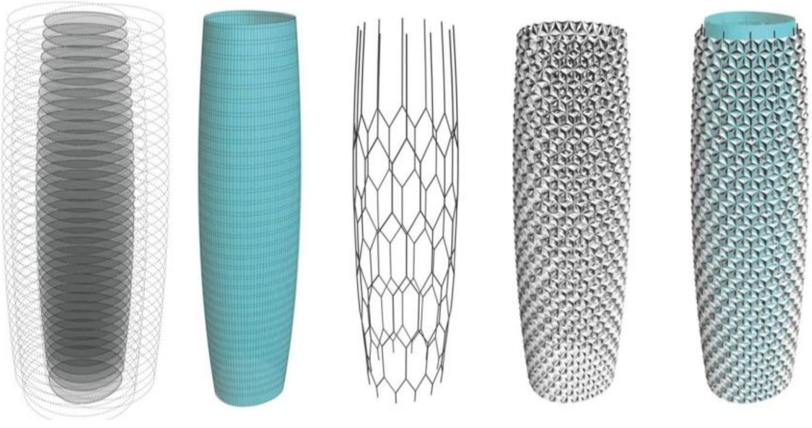

Fig.2 - Early 3D models of the primary structure, facade and shading system *(AHR)*

The complex elliptical shapes of the towers, both on plan and in section, necessitated a system that was more sophisticated than industry-standard louver systems *[Fig.2]*. A triangulated shading system, opening and closing according to the sun position, was thus conceived similar to a big 'umbrella'. This system created a pattern related to the local traditional geometric forms. Models and sketches were developed during the competition phase to investigate how the panels could operate, in particular the challenging interaction where an array of adjacent shading elements meet at the nodes *[Fig.3]*. The final result seven years later, after an intense research and development process, looks remarkably similar.

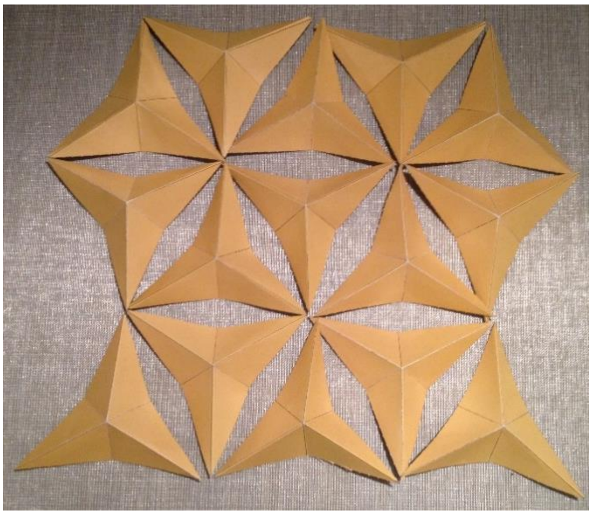

Fig.3 **-** Paper model, Mashrabiya panels grouped together *(Arup)*

2.3 Performance

The design team undertook extensive thermal modelling and 3D solar analysis of the effect that this unique active shading system would have on various zones of the towers at different times through the year. This process helped identify the required extent of the shading device and its regime of opening and closing. These studies also allowed the design team to derive the precise portion of the North facing facade where the shading was not required *[Fig.4]*.

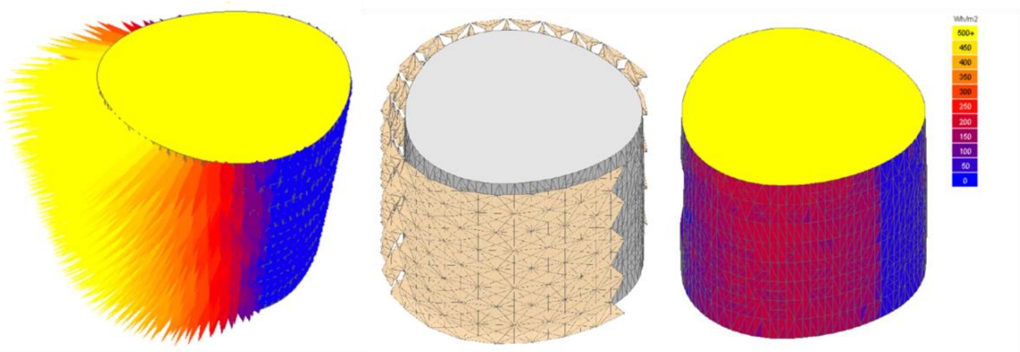

Summer, 9am – total solar radiation on the façade without Mashrabiya | Summer, 9am – view from the sun. 3D model with Mashrabiya | Summer, 9am – view from the sun. Solar radiation on the façade with the Mashrabiya

Fig.4 - 3D solar exposure analysis on the central portion of the tower *(Arup)*

The vision area within the tower floor plates consisted of floor to ceiling high double glazed units, with laminated inner and monolithic outer panes, both heat-strengthened. In an intense climate as Abu Dhabi, with maximum temperatures of around 45˚C and very high solar radiation levels year-round, the primary aim was to control the solar radiation. Conductive gains due to temperature difference are normally less of an issue. However, in heavily shaded buildings with reduced gains due to solar radiation, the conductive component becomes more and more relevant. For this reason particular attention was paid to enhance the thermal performance by specifying Argon filled double glazed units and introducing thermal breaks where the brackets supporting the Mashrabiya penetrate the thermal line *[Fig.5]*.

The building physics analyses were essential to define the right balance between solar control and light transmission performance of the glazing and shading components, and the effect of the combined systems. A clear glass with a high performance coating was selected, achieving a g-value (solar control) of 0.26 and a light transmission of 44%. Both values are significantly higher than any other similar building in the Middle East.

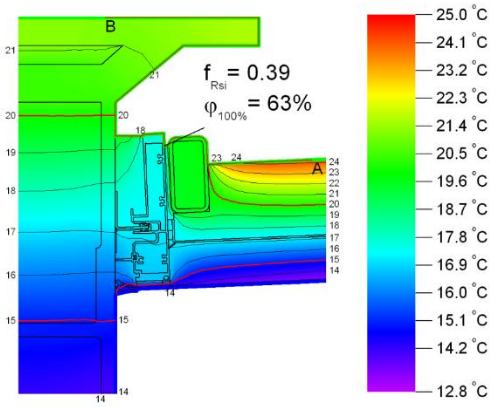

Fig.5 - Condensation and thermal bridge assessment of the Mashrabiya bracket in the spandrel area - horizontal section *(Yuanda)*

The crown, a vaulted observation level that tops each tower and offers spectacular views of the surroundings, was the subject of a separate 3D solar and thermal analysis. Additional measures were required to control the solar gains in these upper levels as architectural constraints did not allow the shading to extend to the very top of the building. The glass performance in this area was improved by applying ceramic fritting on face #2 of the double glazed unit with a variable pattern, according to the level of solar exposure *[Fig.6]*.

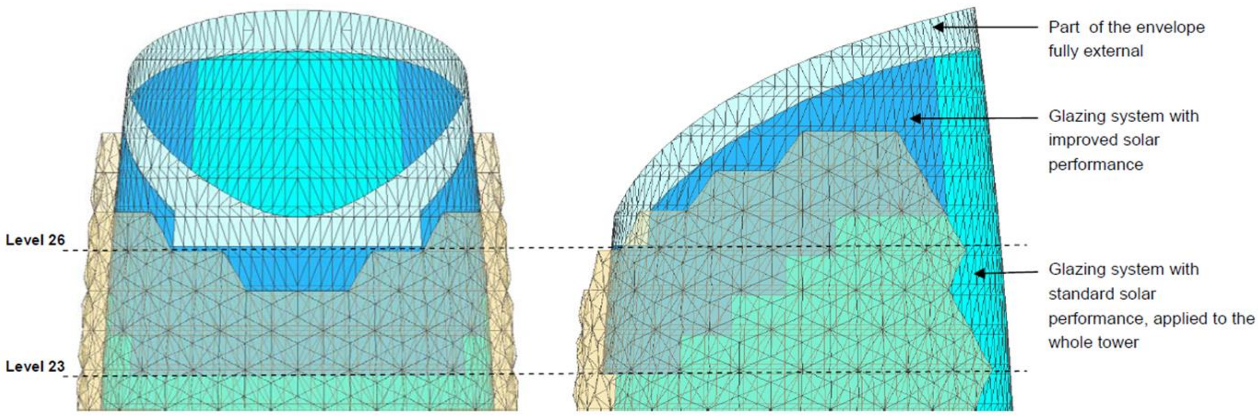

Fig.6 – Crown, showing the Mashrabiya extent and additional treatment to the glass *(Arup)*

2.4 Materials

The exceptional levels of transparency adopted for the towers and the resulting increased daylighting were made possible by a careful selection of the mesh material of the movable Mashrabiya shading system sitting in front of the façade. Different options were investigated to select the most appropriate fabric for the triangular panels, and PTFE-coated glass fibre mesh was identified as the most durable and best-performing solution. PTFE fiberglass coating is capable of withstanding high temperatures and it is a 'self-cleaning' fabric, which helps reducing cleaning and maintenance time. The final fabric presented an open area of 15% and a light transmission of 25% *[Fig.7]*.

Fig.7 **-** View from the inside through the PTFE fabric. The supporting frame is a combination of aluminium and duplex stainless steel, to withstand the aggressive marine environment *(AHR)*

3 Facade

The façade consists of a facetted unitised curtain wall system. The panels are typically 4200mm high and of variable width due to both the barrel shape of the towers on elevation and the floor plate that vary in dimension across the height of the towers.

The floor to ceiling vision area is 3100mm high and the resulting spandrel area is 1100mm high. The spandrel consists of two zones of 350mm high double glazed units and back insulation, with the cavity between the glass and insulation pressure equalized to the outside. The central portion of the spandrel is a 400mm high metal clad fascia. All the profiles are in aluminium, thermally broken and natural anodized. The glass is structural silicone bonded on 4 sides and the aluminum extrusions were designed to accommodate a small carrier frame in case of glass replacement. Mechanical restraints were introduced to carry the dead load of the double glazed units. An additional metal fascia is installed on the outside, running in front of the unitized panels, replicating the honeycomb geometry of the internal primary structure. These aluminium panels are fixed to the curtain wall with small brackets and can be easily removed to allow access to the panel joints in case of replacement.

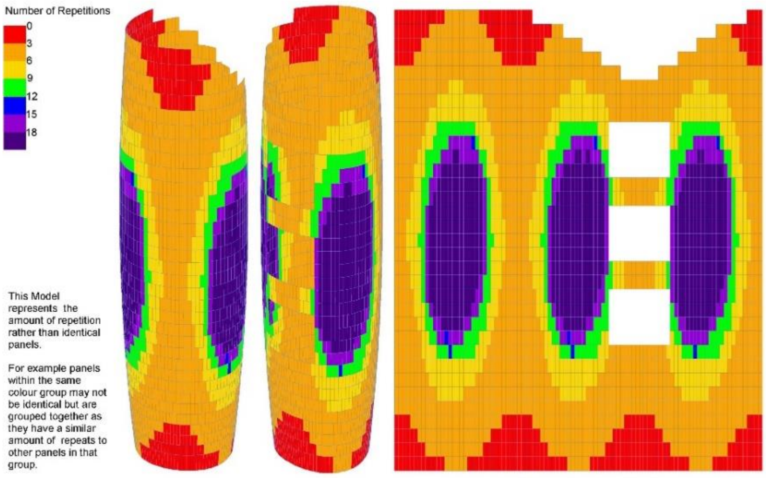

Fig.8 – Curtain wall panel repetition study allowing for a 10mm tolerance *(Arup)*

Simplifying the building geometry and achieving the architectural intent was an important step of the design process. The design and overall shape of the building were optimized to improve panel repetition, and to limit rectangularity deviation and warping. This approach helped reduce significantly the system's complexity and ultimately the costs *[Fig.8]*. A similar approach was carried out on the secondary structure of the shading panels, reviewing the length and relative angle between the Mashrabiya elements. The design process informed the geometric development of the façade and facilitated the detailing and installation of the system, reducing unnecessary complexity. This allowed the bidding contractors to grasp the challenging aspects of the façade and manage the associated risks accordingly.

The façade to floor plate ratio is different on every floor for half of the tower, and this required a high level of coordination between the Architect and Arup's Façade, Building Services and Structural teams through rigorous use of 3D design modelling. Another critical aspect of the façade design was the interface between the unitised curtain wall panels and the cantilever stainless steel arms supporting the Mashrabiya shading panels. A few options were explored during the design phase, modifying the design of the spandrel area and the position of the stack joint. The design option implemented in the tender package and developed further by the Façade Contractor consisted of a spandrel area shaped to allow the units to be installed around the bracket from both sides. Alternate panels – the bracket supporting the shading system occurs every four panels - accommodated this special arrangement *[Fig.9]*.

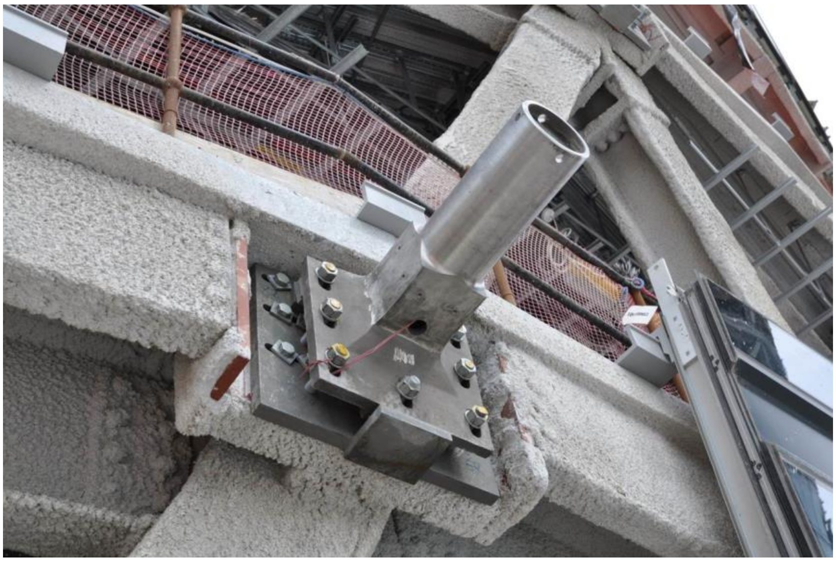

Fig.9 - Stub connection for Mashrabiya, bolted to ends of radial beams to house cantilever bracket *(Arup)*

The cleaning and replacement strategy for the façade panels is executed by a building maintenance unit (BMU) system supported by dedicated cranes located above the central cores at the towers roof levels. The BMU runs within the cavity between the curtain wall and the Mashrabiya shading system of each tower. The curtain wall framing was designed to accommodate local pins that provide lateral restraint to the BMU basket and keep it adjacent to the façade even where the envelope is leaning outward in the lower half of the towers. The BMU system also allows the basket to run outside the cavity for any maintenance and replacement required to the shading system on the external faces.

4 Mashrabiya: design process and testing

The most iconic element of the all building is clearly the movable shading, which wraps most of the envelope and modifies its shape, appearance and performance any time of the year, reflecting natural daily and seasonal rhythms *[Fig.10]*. The shading becomes the real envelope and defines the building, with form and function working in close harmony. This visually striking effect is the result of a thorough design process.

Hand sketches, paper models, small scale physical models and 3D digital models were the preliminary steps embarked on to refine the competition idea and to prove to the client body that the innovative concept was feasible. As the design progressed, it soon became evident that the interface between the Mashrabiya and the towers' superstructure presented a key challenge. Various structural arrangements were assessed in the early design stages, and the creative collaborative input from the various disciplines (including structure, façade, lighting and architecture) resulted in the Mashrabiya shading elements being conceived as unitised systems, cantilevering 2.8m from the primary structure. This solution allowed each element to be replaced without affecting the structural stability of the whole system. The cantilevering stainless steel arms were detailed to allow a neat connection where the tapered ends of six adjoining panels meet at each node.

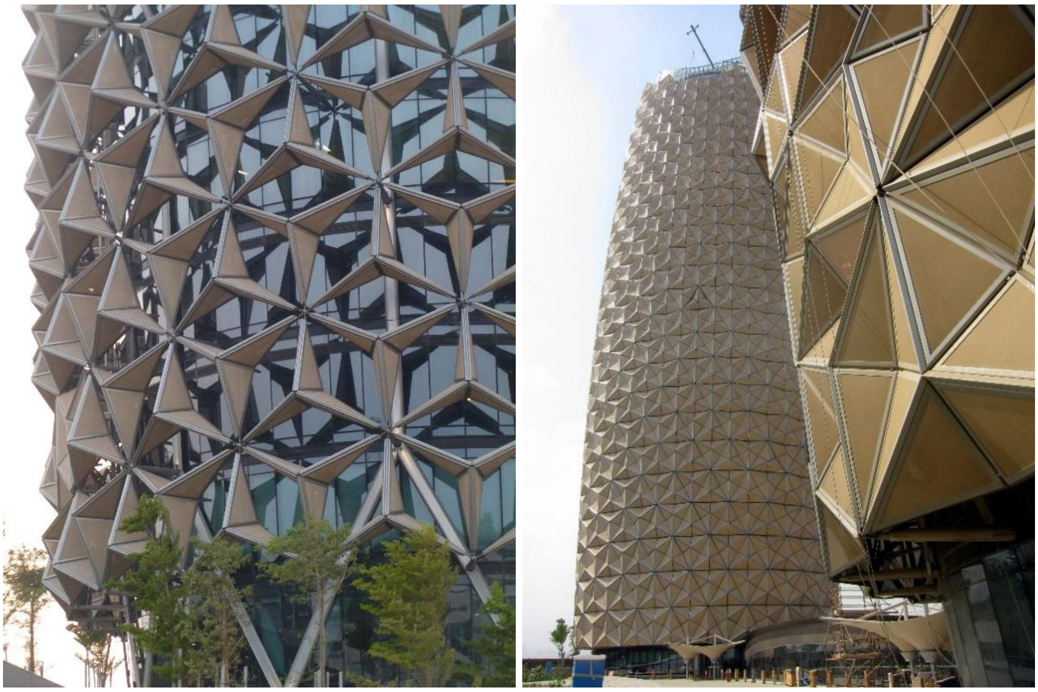

a. b.

Fig.10a&b - The geometry, perceived color and texture of the towers can vary in a few hours *(AHR)*

In total each tower has 1049 Mashrabiya panels, weighing about 600 kg each (1.5 tonnes with supporting steel brackets) *[Fig.11]*. No precedents of movable shading systems on this scale were available and Arup built on knowledge gained in other projects with movable elements. The design team's efforts were focused on de-risking the process, making sure that this unique and unconventional shading system was able to protect the building from the solar radiation and could also operate reliably in an aggressive environment.

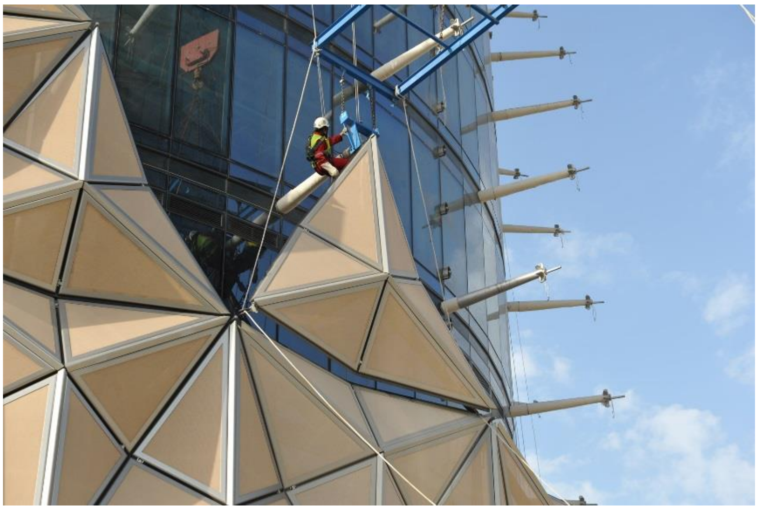

Fig.11 – Installation of the Mashrabiya panels. The shape of the building in plan and elevation led to 22 different variations in the panel geometries *(AHR)*

As part of the façade technical performance specifications, a thorough testing regime was specified in addition to the performance targets and materials requirements. A key milestone in the design process was the assembly of a fully functional 1:1 scale prototype by the façade contractor responsible for the post-tender design development phase. The design was then refined and tested in a wind tunnel facility and in a climatic chamber. More than 30,000 opening and closing cycles were simulated at different temperature conditions, varying from 24°C to 60°C, and at different levels of relative humidity. Sand and salted water were applied regularly throughout the testing process on all the critical joints to qualify that the required durability life of actuators, bearings and mechanisms were attained *[Fig.12]*.

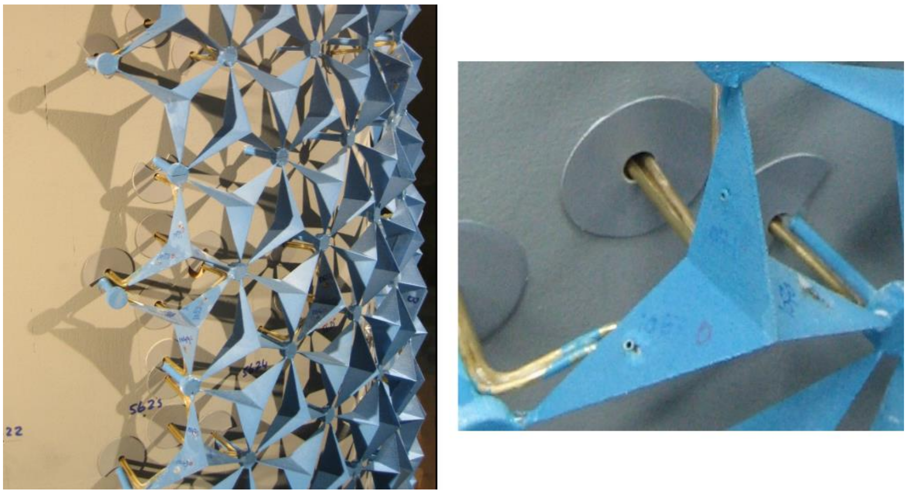

Fig.12 – Wind tunnel testing, 1:75 scale – pressure taps on open Mashrabiya panels *(Arup)*

The Mashrabiya panels cover 3 predefined positions – folded, intermediate, unfolded. The design allowed them to be re-programmed in any required configuration should this be deemed preferable in the future *[Fig.13]*. The Mashrabiya panels are grouped in sectors and are operated by a sun tracking software controlling the opening and closing sequence according to the sun's position. It is possible to override the system to control individual panels. The control system is linked to anemometers and solar radiation sensors at the top of the towers, to adjust the position in case of extreme wind speed or prolonged overcast conditions.

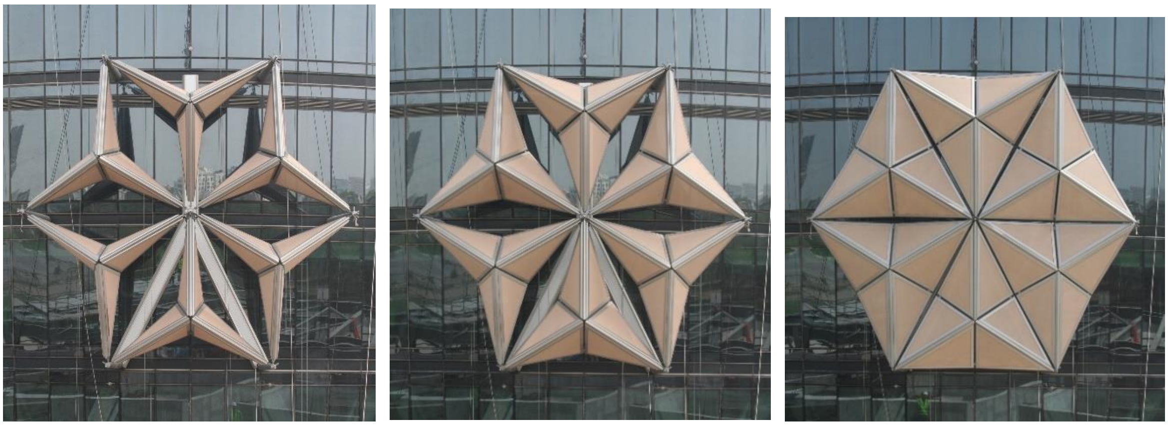

a. **b.** **c.**

Fig.13a,b&c - Mock-up Mashrabiya in situ – (a) folded configuration, (b) intermediate configuration*, and (c)* unfolded configuration *(Arup)*

5 Benefits of the shading system

The presence of a movable external shading helps to significantly reduce the solar radiation, only when and where it is needed. Assuming as a benchmark a glazed envelope achieving a g-value (solar control) of 0.20 and a light transmission of 25-30% - common figures in the region -, the combined shading and glazing systems adopted in the Al Bahr Towers reduces the solar gains by more than 50%, achieving a much higher level of light transmission.

A preliminary assessment carried out during the design phase showed how the external Mashrabiya helped reduce the capital cost of the cooling system by approximately 15%, achieving a 20% electricity load saving as a result of the smaller cooling plants. This strategy also played a major role in reducing the carbon footprint of the building, reducing the CO_2 emission by approximately 20% and helping it obtain a LEED (Leadership in Energy and Environmental Design) silver assessment. The external shading maximize the useful daylighting penetration *[Fig.14]*. It also reduces the amount of working hours when internal blinds need to be lowered to control any glare effect, significantly increasing the lighting energy savings in the process.

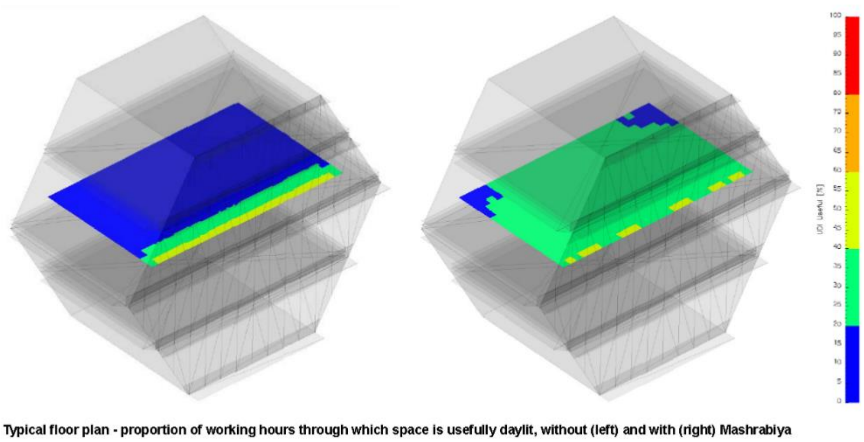

Fig.14 - proportion of working hours through which the space is usefully daylit *(Arup)*

6 Conclusion

An enlightened client body, an inspired architectural team and more than 300 Engineers across 14 different disciplines worked together delivering a truly integrated design to achieve a unique project with a novel shading system *[Fig.15]*. The team challenged conventional thinking and managed to turn a great intuition into reality, enabling a paradigm shift in the design of tall buildings and setting a benchmark to be followed for many years to come.

The project secured the 2012 Council for Tall Buildings & Urban Habitat's (CTBUH) Innovation Award, and it was listed amongst its 20 most Innovative Tall Buildings of the 21st Century. It featured in the November 2012 Time as one of the '25 best inventions of the year'. Al Bahr Towers also won the 2013 Society of Façade Engineering Award.

Fig.15 **-** View of the completed project form the East *(AHR)*

7 Project credits

Client: Abu Dhabi Investment Council, Abu Dhabi, United Arab Emirates.
Architect: AHR, London.
Multidisciplinary Engineering Designer: Arup, multiple offices (Façade, Structure, Building Services, Civil Engineering, Geotechnics, Lighting, Acoustics, Fire, Wind, Security, Traffic, Vertical Transportation, IT and Comm, Catering Consulting).
Façade A&M: Reef, London.
Architect and engineer of record: Diar Consult, Abu Dhabi, United Arab Emirates.
Cost Consultant: Abu Dhabi office of AECOM (formerly Davis Langdon).
Project manager: Mace, London.
Main Contractor: Al-Futtaim Carillion LLC, Abu Dhabi, United Arab Emirates.
Façade Contractor: Yuanda China Holdings Limited, Shenyang, China.

8 References

[1] Oborn P., Al Bahr Towers, The Abu Dhabi Investment Council Headquarters, Wiley, ISBN 978-1-119-97415-4, (2013).

[2] http://www.ctbuh.org/LinkClick.aspx?fileticket=JVPxRjG1wyY%3D&tabid=3359&language=en-GB

[3] http://techland.time.com/2012/11/01/best-inventions-of-the-year-2012/

[4] http://specificationonline.co.uk/news-article/5702/society-of-facade-engineering-al-bahr-towers-wins-first-facades-award

[5] http://www.building.hk/products/view.asp?id=1171

[6] Buffoni G., Xuereb K., et al., In the Shade: Al Bahr Towers, The Arup Bulletin (June 2013)

A high performing and multifunctional building skin with four different grades of transparency.

Aracil Mónica, M. Sc.
LEICHT structural engineering and specialist consulting GmbH, M.Aracil@LEICHTonline.com

Schöne Lutz, Dr. Ing.
LEICHT structural engineering and specialist consulting GmbH,
L.Schoenel@LEICHTonline.com

Weininger Florian, Dipl. Ing.
LEICHT structural engineering and specialist consulting GmbH,
F.Weininger@LEICHTonline.com

Summary

The new headquarters of the Swatch AG in Biel, Switzerland, is designed as a snake confronting the old and listed area of the Omega building, with its modernity and aggressiveness. The main challenges are to adopt the façade to the geometry of the outer surface, which is a NURBS surface, and to develop 4 different kinds of elements – transparent glass elements, translucent ETFE/PC-elements, façade-integrated PV elements, and rather simple "opaque" ones- which need to fulfill high climatic requirements and can be distributed in a free order.

Keywords: Elemented façade, cold bended glass, ETFE, polycarbonate, freeform, LEICHT

1 Introduction

Shigeru Ban, Pritzker Prize 2014, was awarded for the design of the Swatch Headquarters in Biel, Switzerland. In the same complex Shigeru Ban designs also a museum and a production building for Omega. The Swatch building is designed as a free formed shell in the shape of a snake that ends up at the top of the Omega museum, creating a covered plaza at the entrance of the Swatch Building.

The Swatch building includes the construction of 11000 square meter shell, composed by a primary timber structure, and a high performance façade, all under a high standard design concept. It becomes a challenge for a multidisciplinary international team composed by design and local architects, timber specialists, façade specialists, and an independent 3D modeling specialist.

The façade must adopt the geometry of the outer surface, which is a NURBS surface, and it must be able to have a free distribution of four main types of façade elements: Transparent glass elements, translucent ETFE/Polycarbonate elements, Photovoltaic elements, and rather simple Opaque elements.

Figure 1: Swatch Headquarters [1]

2 Design driving conditions

2.1 New generation shells

In the last years, timber structures became a new architecture language, which Shigeru Ban has proved as a very successful technique in previous projects like the Haesley Nine Bridges Golf Clubhouse, the Centre Pompidou-Metz, or the Tamedia office building, among many others which are still in Progress.

New generations of milling machines and advanced 3D modeling techniques allow architects and designers to create absolute free forms where limits are only given by the static requirements of the material. At the Swatch headquarters, there are 11000m of timber beams, which require more than 2000m³ of timber.

However, the most challenging part comes when this high-tech three dimensional structure must be covered. In cases like the center Pompidou in Metz by Shigeru Ban, the Crossrail Station in London by Normal Foster, or the Strasbourg Train Station by AREP, the only functional requirement was water and wind tightness, no thermal insulation requirements, what allows the utilization of a simple membrane, ETFE cushions, or even double curved simple glazing. All alternatives, with higher or lower cost impact, have a well known and practiced technology behind them.

This is not the case of the Swatch Headquarters (S1 from now on). The free form timber structure hosts in this case an office building with very demanding performances. This means that a part from having an energetically efficient façade, all kind of facilities like water pipes for heating and cooling panels, sprinkler pipes, electricity trays and dry air supply for the façade, must run along the timber beams.

Swatch watches are composed by 51 elements; all disposed in an optimized way in order to achieve the minimum thickness possible. This was the inspiration for the design intent of Shigeru Ban by including all facilities in one integrated and optimized shell. The specialists team coordination is the key to success in the technical development of such a shell, which approaches more and more the design of a perfectly running machine where every single screw must be carefully planned and coordinated.

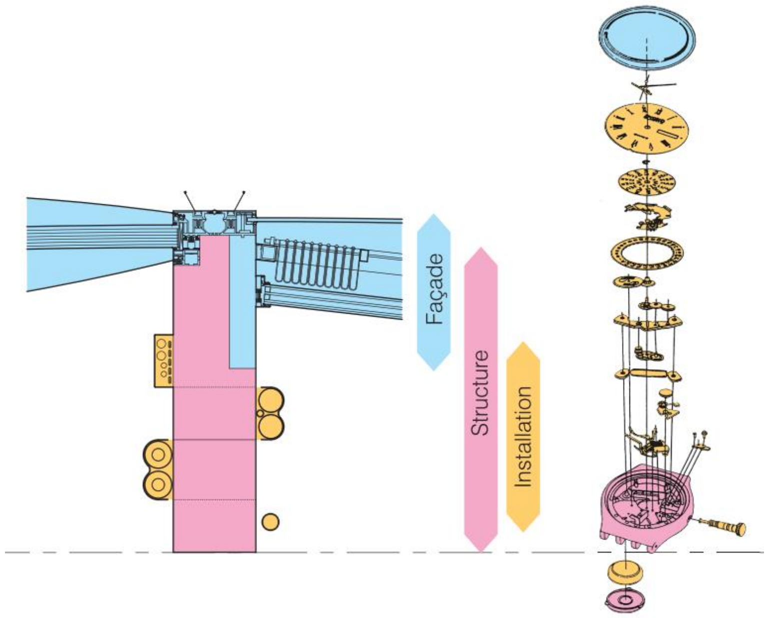

Figure 2: Integrated Shell. Source: Shigeru Ban Architects

Not only are the requirements high in terms of facilities and installations, but also in terms of energetic efficiency. After the studies run by the climatic engineers, very low U values for the different façade elements were fixed. Additionally, part of the elements must incorporate Photovoltaic panels.

Table 1: Required Ug value for the different types of elements

Façade element type	Total area [m²]	Quantity of elements [pc.]	Ug [W/m²K]
Solid	3435	859	0.20
Solid - PV	1920	448	0.20
Translucent	2755	750	0.40
Transparent	1990	474	0.60
Global	10100	2531	0.35

2.2 New generation facades

The challenge in the S1 façade is to develop an elemented façade which also works on the roof areas and, at the same time, follows the geometry of a doubly curved master surface. The technology for the development of free form facades is already well known; actually, many of the contemporary architecture pieces are based on the free form of their shell, as we can see in pieces from well-known architects like Frank Gehry, Zaha Hadid, or Shigeru Ban himself. On the other hand, the implementation of façade elements at roof areas is a new topic that is still to be studied and proved.

The design decisions are founded on the border conditions that the project provides:

<u>Doubly curved master surface</u>
The timber shell and the new milling technologies have the big advantage of being able to create a smooth outer surface. Therefore, it is a challenge for the façade to follow the provided surface and create a double curved and smooth shell.

Of course, some disadvantages come with this decision, like the need of having bended and torsioned façade profiles, or providing a double curved outer surface of the façade elements.

However, this is not only disadvantageous for the façade, timber provides enough stiffness and the perfect surface for cold bending the aluminum profiles on it, and, most importantly, no geometric collisions happen at the nodes. This allows us to use a quadrangular grid and avoids the need of providing a sub division on a triangulated grid, as would happen in case of building planar elements.

<u>Elemented facade/roof</u>
There was almost no other way of realizing the design provided by Shigeru Ban Architects. The design claimed for a high flexibility on the distribution of the different types of elements.

Additionally, the timber structure requires a fast mounting process in order to protect it from possible weather damages.

In any case, maximizing the production at the workshops will reduce tolerances and inaccuracies, what will ensure the performance and durability of the façade.

3 Transparency grades

The design efforts of a multidisciplinary team will allow meeting all previously described requirements; in the following chapter each element type will be described with its particular challenges and engineered solutions.

3.1 Transparency grade 1. Transparent elements

The transparent elements, or glass elements, are the ones with the highest degree of transparency with a 70% light transmittance requirement and a maximum energy transmission of g=0,5.

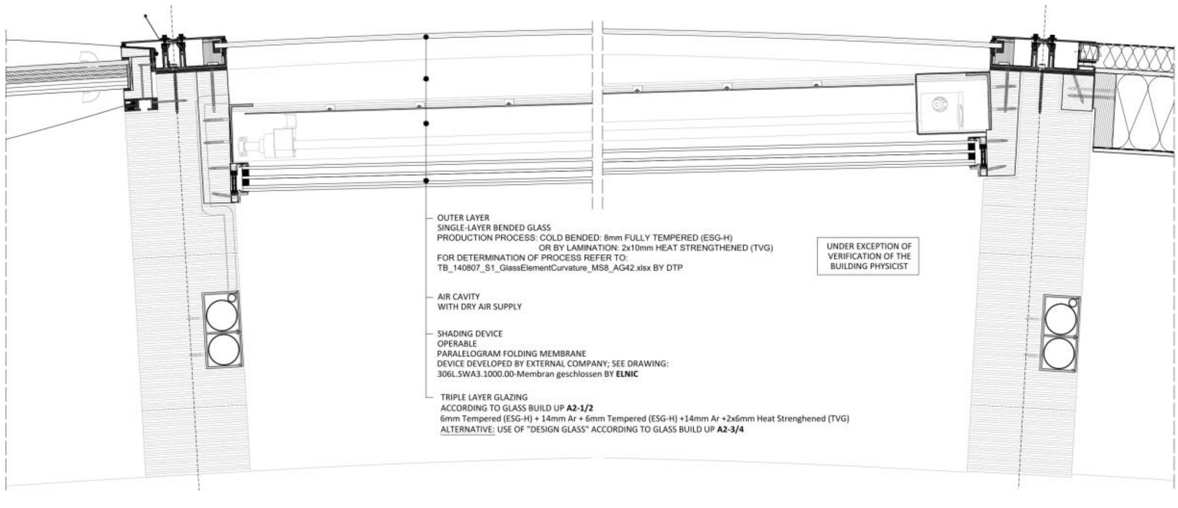

Figure 3: Transparent element

The element is conceived as a Closed Cavity Façade (CCF), which is a relatively new technology, but already built and proved by several façade contractors like GIG, Gartner, and as recently presented in the last BAU Fair in Munich, companies like WICONA already offer an standardized CCF system.

In within the decision of building a closed cavity façade we can talk about different topics that were critical points of discussions during the design process:

The outer cold bended glass pane

As described in the chapters before, the outer surface must follow the double curved master surface provided by the design architects and the timber engineers. Therefore, it became necessary to deal with double curved glass panes.

Many investigations about the available products in the market showed up that the cost of producing 474 warm bended glass panes with different radiuses and dimensions would make the costs rise exponentially.

For this reason, and taking advantage of the low bending radiuses (an average radius of 20 to 25 m), a simple cold bended fully tempered glass pane was proposed for the outer layer of the glass elements. Many Finite Element (FEM) Calculations and tests were carried out to ensure the feasibility of the construction.

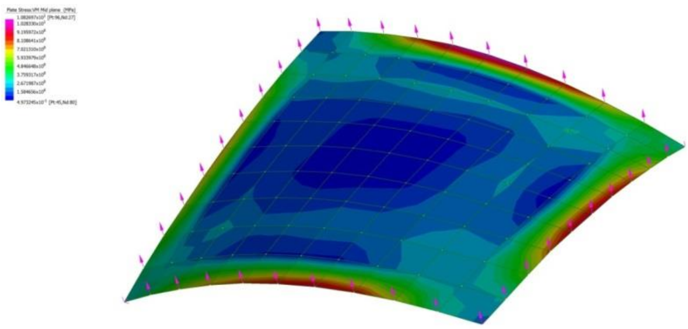

Figure 4: Glass cold bending FEM results - VM stresses in the middle plane of the plate

Figure 5: Glass cold bending test

The inner flat triple layer glazing

With no curvature issues anymore, the inner surface of the glass element is a simple triple layer glazing which will ensure that the element meets the thermal and energetic requirements.

Due to the geometric constraints, the cavity between the outer and inner layer has a variable height. The minimum height will be determined by the maximum height of the specially developed shading device.

<u>The shading device</u>
No standard product available nowadays is able to fit all requirements of the S1 facade. The elements are inclined on a range between 0 and 90º, and they are tilted on elevation. Additionally, the climatic engineers did not recommend fixed shading devices or rotatable lamellas, as it is necessary to have a fully operable shading device in order to achieve the values of light transmission necessary for the working places at the office building.

But not only are the geometric requirements a problem for the system, but also the closed cavity conditions, which are very harmful for any device: high temperatures and dry air. As a consequence, a specially developed shading device was planned by a machinery developer.

It consists on a folded membrane that closes and opens automatically controlled according to the weather conditions. The main challenge is to ensure that each of the elements that compose the device is fully operative with the closed cavity conditions.

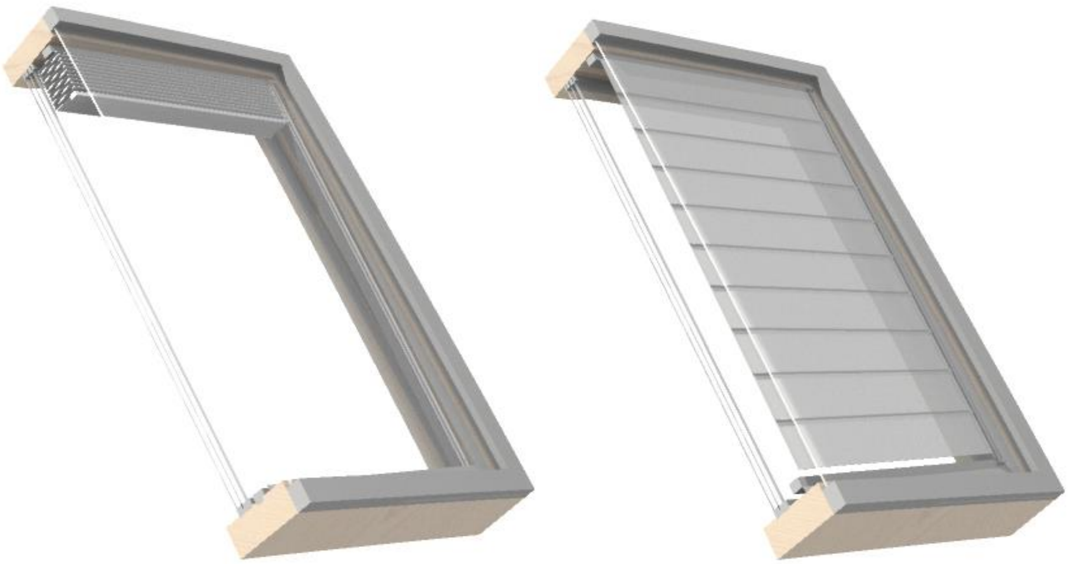

Figure 6: Shading device in opened and closed position

3.2 Transparency grade 2. Translucent elements

The translucent elements do not allow looking through them, but they bring diffuse light into the building with a 10% of light transmission and a maximum energy transmission of g=0,1.

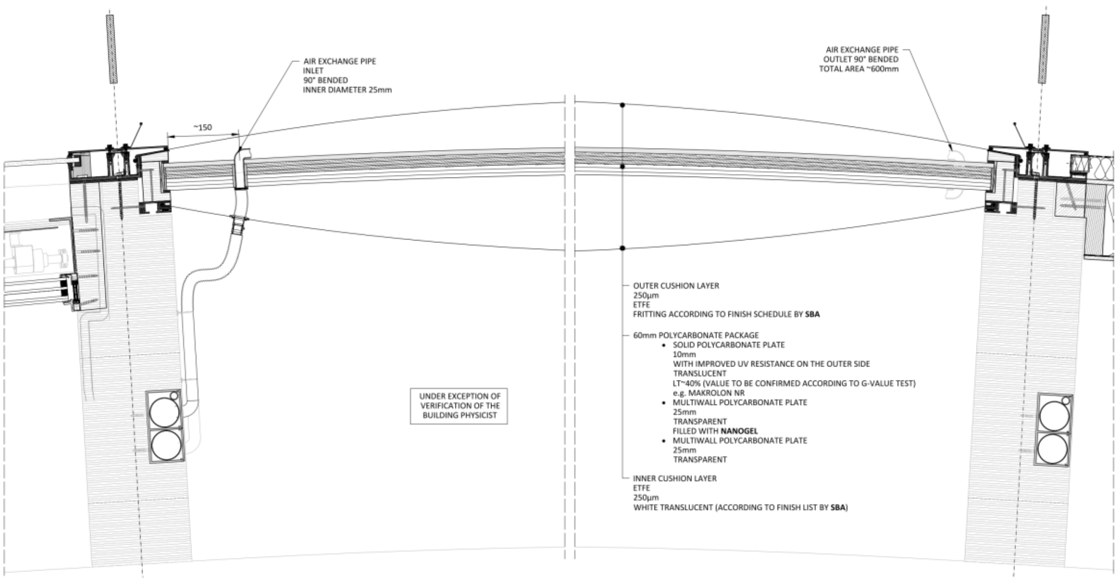

Figure 7: Translucent element

The Swatch Group aggregates several watch brands like *Omega* or *Tissot* within many others, the brand *Swatch* is the most fresh and young-public oriented, their watches are mainly fabricated with plastic colorful materials. The idea of fabricating a plastic façade was part of the project presented by Shigeru Ban Architects at the architectural competition. This idea is still remaining at the translucent elements, as they are fully composed by plastic materials.

The wish of building ETFE cushions in an office building was a problem because of its very poor thermal properties; a basic triple layer cushion cannot achieve more than an Ug=1,7W/m^{2}K, and the thermal bridge at the profiles is not a minor problem as well.

At the Swatch Headquarters, the ETFE cushion will be provided with an internal layer of multiwall polycarbonate panels filled with *Nanogel* and an additional 10mm solid polycarbonate plate, this will provide the thermal and acoustic insulation properties necessary to fulfill all specialists requirements.

Multiwall polycarbonate plates with *Nanogel* infill

The Nanogel infilled multiwall polycarbonate plates are a very interesting product by itself. The so called Nanogel is a product created by the laboratories Cabot, and until now they are the only producers of this material. Those particles have a high thermal resistance (λ=0.018W/mK) while being translucent and very light.

The multiwall polycarbonate plates will be cold bended to the given geometry as well, following the same concept as with the outer glass pane. FEM calculations were also carried out, and no static problems are foreseen within the given boundary geometries.

Solid polycarbonate plate

Even though the ETFE cushions have a substantially improved acoustic behavior in comparison with simple layer membrane constructions, the drum effect of the rain on the cushions is a non solved issue. Together with the very high demands of an office building, the acoustic behavior of the translucent elements became a major issue during the design of the S1 façade.

In several acoustic tests, the construction was proved to be too light; the addition of mass would improve its behavior. Therefore, a 10mm solid polycarbonate plate was implemented together with the polycarbonate package. The mass provided by the solid plate allowed the element to provide a proper acoustic insulation.

ETFE Cushion

The great advantage of the design for the S1 facade is the possibility to have a separated connection for each ETFE layer. It is important though to provide a thermally broken profile as well. This way the thermal bridge will be completely solved and the condensation around the profiles will be avoided.

3.3 Transparency grade 3. Opaque elements

The opaque elements are planned to be built as a traditional timber roof and connected to the façade system profile. The outer layer will be an FPO membrane.

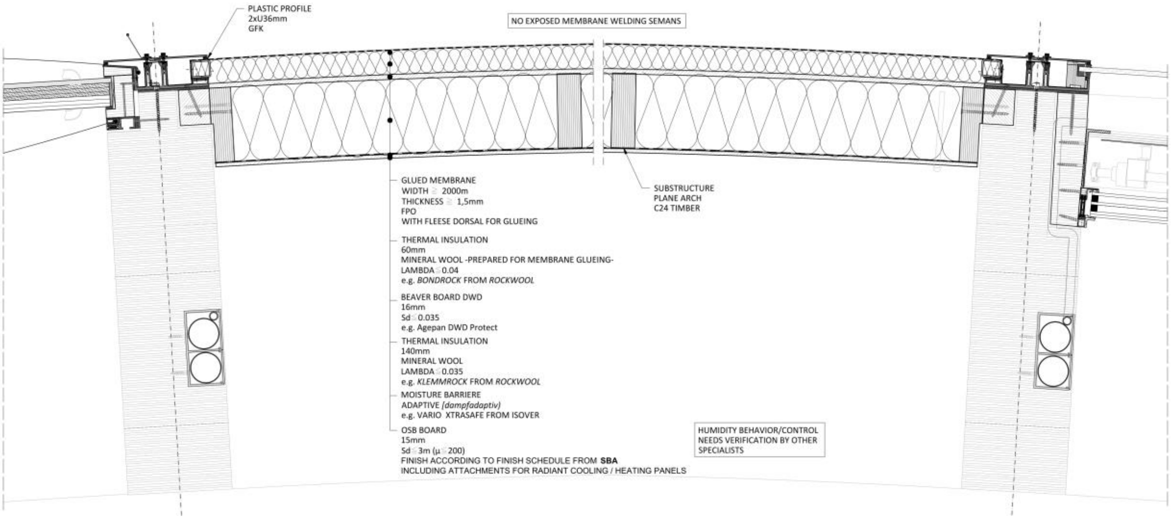

Figure 8: Opaque element

The main issue was to proof its proper hygrothermic behavior. For a proper functionality of a traditional timber roof, rear ventilation is necessary in order to enhance the evaporation of the condensed water that inevitably will pass through the vapor barrier. Rear ventilation of the outer layer is not possible in the S1 façade system profile; therefore, a layer of thermal insulation will be directly glued under the FPO membrane, lowering the temperature at the most outer surface of the façade buildup.

3.4 Transparency grade 4. Photovoltaic elements

Although the photovoltaic elements have no different transparency grade than the solid elements, they have an upgraded behavior; the production of green electricity.

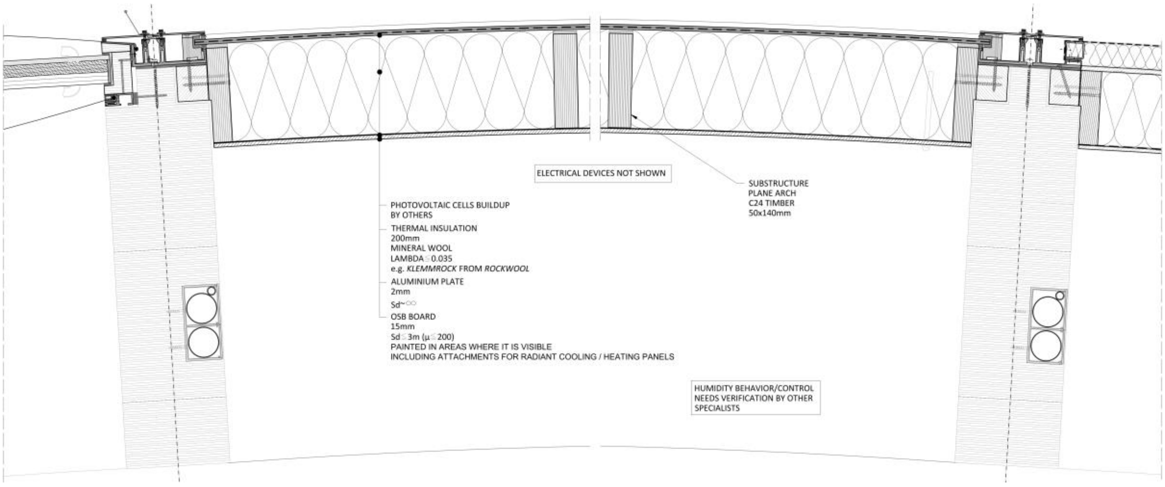

Figure 9: Photovoltaic element

The Photovoltaic panels will be implemented on the elements analogous to the outer glass pane and the opaque element together. An aluminum profile will host the photovoltaic panels, and an insulated opaque element will provide the required U values.

<u>Photovoltaic panel</u>
Great developments have improved the possibilities for architects and designers to implement photovoltaic panels into their designs. Supported by a photovoltaic specialist, the cells have been planned to be laminated between to glass layers. The complete package will be curved (only in one direction) and installed as a façade element.

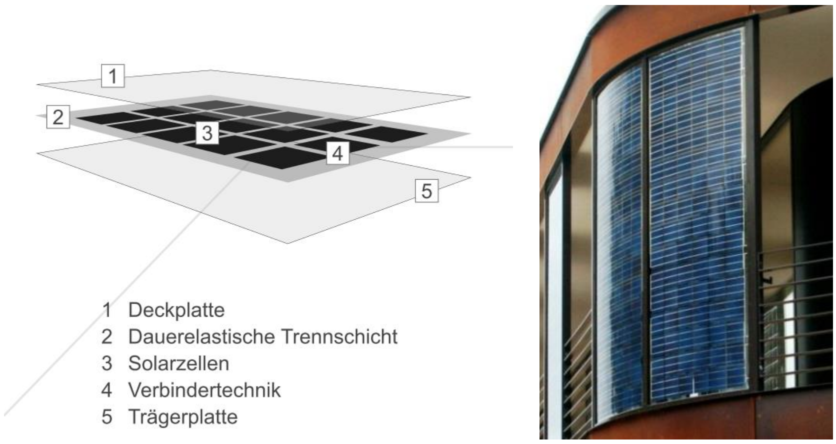

Figure 10: eFORM by Sunovation GmbH [2]

<u>Simple curvature</u>
The adaptation of simply curved glass panels onto the double curved geometry is possible in a high percentage of the façade elements. In most of them, the secondary curvature is minimal; the deviations that occur between a simple curved surface and the real double curved master surface of the building can be solved by the tolerances of the profiles.

<u>Moisture control</u>
Even though it seems to be a very similar construction to the solid element, its hygrotermic behavior is completely different. Meanwhile the FPO membrane allows drying up the occasional condensation under it; the glass panel will not allow the water go through.

Therefore, no humidity at all is allowed into the element. This would be a similar concept to the well known aluminum sandwich panels, composed by two aluminum sheets and internal insulation, they are tightened, and no moisture is allowed into the inner space.
In our design, an additional aluminum sheet is planned in the inner side of the element.

4 Conclusions

A lot of energy has been invested on the design of the façade for the Swatch Headquarters. It is full of intentions and innovations that are on the way of being realized.

This is de design provided to the construction companies in the tender. From this point on, the façade constructors will have to make their own proposal for the actual construction and make sure that it meets all requirements, and, at the same time it has to match with their working procedures and their own performance standards.

Nevertheless, the most challenging phase will come after the design is completed. The workshop planning will become a very complex task that will only be possible with a fully parameterized 3D model and a deep understanding of the geometric boundaries.

The inauguration of the building is foreseen for the end of 2016, until then, a big effort is to be done in order to ensure a high performance and excellent quality of the façade and turn this adventure into a great success.

5 References

[1] DETAIL ONLINE (03.02.2012). Shigeru Ban builds for Swatch [Blog post]. Retrieved from http://www.detail-online.com/daily/shigeru-ban-builds-for-swatch-2756/

[2] Sunovation Referenzen (04.02.2015). Solarstrom-Fassade mit gebogenen Glas-Glas Modulen. Retrieved from http://www.sunovation.de/166/

Proceedings of the International Conference on Building Envelope Design and Technology, Graz
Advanced Building Skins 2015

Hybrid Element Façade - Thermal Engineering and Related Structural Evaluation of a Solar Activated Integral Panel

Helmut Schober, Arch. Dipl.-Ing.
Institute of Building Construction, Graz University of Technology
helmut.schober@tugraz.at

Daniel Brandl, Dipl.-Ing.
Institute of Thermal Engineering, Graz University of Technology
daniel.brandl@tugraz.at

Manfred Zellinger, Dipl.-Ing. Dr.techn.
Institute of Building Construction, Graz University of Technology

Thomas Mach, Dipl.-Ing. Dr.techn.
Institute of Thermal Engineering, Graz University of Technology

Oliver Englhardt, Univ.-Prof. Dipl.-Ing. Dr.nat.techn.
Institute of Building Construction, Graz University of Technology

Summary

In the course of the research project “Sustainable Design Process and Integrated Building Envelopes“ (UNAB) the potential of solar activated sandwich panels, which simultaneously enable the thermal conditioning (heating and cooling) of the interior rooms is being analyzed. These features are achieved by forming the inner and outer steel sheets of the sandwich panel to pipes filled with a heat transfer fluid. In order to find a suitable construction a parameter study was performed using three-dimensional CFD and FEM models. In a first step the results regarding the fluid outlet temperature, the heat transfer efficiency and the thermal protection were compared. In the second step the positive static influence of the pipes, especially on normal stress within steel sheets and elastic deformation of the whole sandwich panel was evaluated.

Keywords: Sandwich Panel, Solar Activated Panel, Integrated Building Skin

1 Introduction

Common sandwich panels are able to meet multiple demands on modern façade constructions such as carrying the load, forming the thermal building envelope, influencing the architectural appearance, prefabrication and assembling. Using sandwich panels as envelope for residential and office building is not usual and therefore remains largely confined to industrial applications. The possibilities of sandwich panels for solar activation and simultaneously for influencing the visual appearance of the whole building because of their metallic surface are not being utilized. The objective of the research project “Sustainable Design Process and Integrated Building Envelopes“ (UNAB) is to evolve an optimized integration of functions and thus the construction of multifunctional components, considering the entire development, manufacturing and assembly process of façade elements. The focus is on the design and conception of energetically activated, integral, self-supporting, hybrid, opaque façade structures of metallic materials.

1.1 Flat-plate collectors

In traditional design of flat-plate collectors a coated absorber plate, which is usually made of copper (rarely aluminum), is connected with a tube register (also made of copper) filled with a heat transfer fluid. In this context, brazing and welding are conventional methods to ensure this connection. But the small contact area between the absorber plate and the pipe along the welding seam proves to be a disadvantage for the heat transport to the fluid causing significant heat losses (Figure 1).

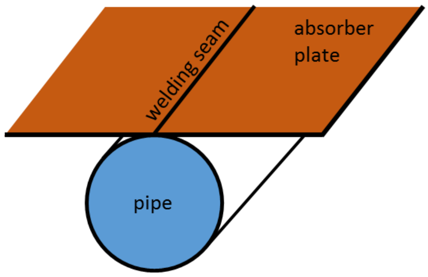

Figure 1: Conventional absorber plate with welded pipe.

Recent developments are based on direct flow absorbers, where the coated absorber plates and the fluid transporting pipes form a unity (Figure 2). This allows the heat transfer paths on the absorber plate are kept as short as possible. For this kind of absorbers production techniques from the automotive industry such as roll bonding are used.

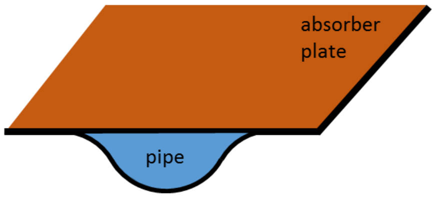

Figure 2: Direct flow absorber.

1.2 Solar activated sandwich panel

The idea now is to integrate the function of a thermal solar collector - especially a flat-plate collector - into a sandwich panel by using the inner and outer sheets as absorber plates. The exterior surface enables the thermal use of solar energy, while the interior surface ensures the thermal conditioning (heating and cooling) of the rooms. The insulator located between represents the thermal building envelope and should keep heat losses as low as possible (Figure 3).

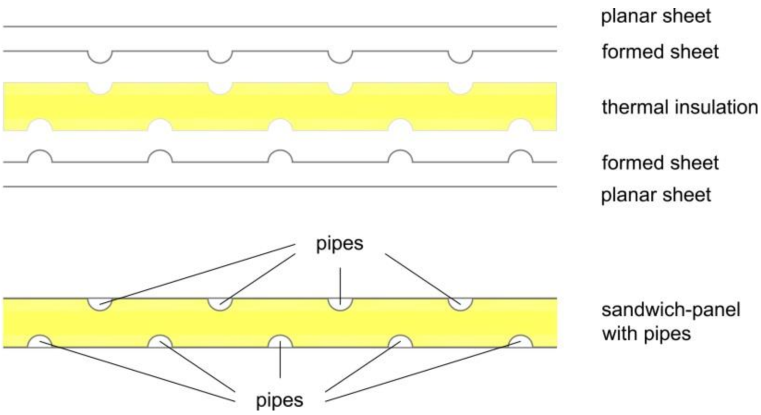

Figure 3: Solar activated sandwich panel (cross section).

One of the characteristics of sandwich panels is their ability to carry loads and - depending on the materials used and the cross-section values - to bridge large spans (for example the distance between floor slabs) without needing any substructure. To evaluate the thermal behavior of solar activated sandwich panels and to analyze the influence of their pipe equipped cross sections on mechanical properties the following studies were carried out.

2 Evaluation of the thermal behavior

A numerical model of the thermal activated sandwich panel was designed to evaluate the theoretically thermal performance for a variety of geometrical and operational parameters. The main objective was to find an initial selection of sandwich panel designs for future developments within the research project UNAB.
With the installed fluid pipes enough solar energy could be gathered to load a domestic hot fluid storage or for heating applications directly for the conditioning of the local room.

2.1 Numerical approach and boundary conditions

For the determination of the thermal behavior of the thermal activated sandwich panel three-dimensional CFD (Computational Fluid Dynamics) models were used. All simulations were performed with the software Fluent ANSYS [1]. With the help of this software it is possible to calculate the heat transfer effects inside the sandwich panel and between solid and fluid components. The k-ε turbulence model was selected for the numerical description of the fluid behavior in all simulations [2].

In the simulations the CFD model was simplified to a section of the sandwich panel façade element containing one single pipe (Figure 4).

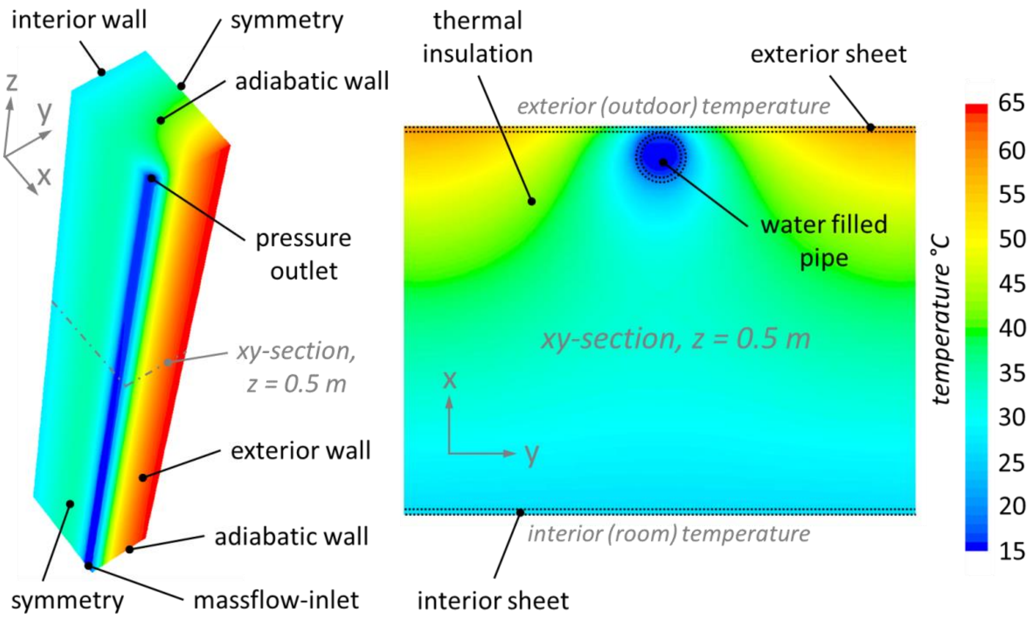

Figure 4: Three-dimensional thermal reference CFD model (RF) and a section through xy-surface with temperature contours at the middle of the panel´s height (z-length = 0.5 m) for summer conditions.

Two symmetries in the CFD model allow a theoretically multiplicity into a continuous façade. In the cross-comparison between the different variants the panel height was 1 m. Furthermore the thermal insulation had a thickness (x-length) of 150 mm, the thickness of the interior and exterior steel sheets as well as the integrated pipe were 0.8 mm in the thermal reference model (RF). The distance between the pipes (y-length) was 200 mm in the thermal reference model. A circular pipe with an inner diameter of 16 mm was integrated where the fluid could be heated by the solar radiation. Stainless steel was used for the sheets and the pipe whereas the thermal insulation was made of polyurethane.

All designed CFD models were performed at 'steady state', hot (summer) climate conditions where the highest solar radiation intensity occurred. The exterior temperature was 40 °C while the interior room temperature was 26 °C. A solar radiation of 1000 W/m² was assumed for the thermal evaluation of the thermal behavior at summer conditions, the solar absorptivity of the exterior sheet´s surface was assumed to 0.8. Furthermore a heat transfer coefficient of 25 W/m²K at the exterior and 5 W/m²K at the interior was used to consider the convective heat transfer at the façade´s interior and exterior surfaces. In the thermal reference model the fluid was introduced with a volume flow rate of 100 l/h and at a temperature of 15 °C.

2.2 Preliminary thermal evaluation

In the course of an initial thermal evaluation a various number of geometrical and operational scenarios of the thermal activated sandwich panel were conceived. The computed temperature contours of these scenarios (RF, SC0 - SC16) are shown in Figure 5.

- Shape of the fluid pipes, whereby all pipes had the same sectional area (SC0 = semicircular, SC1 = square and SC2 = equilateral triangle)
- Position of the fluid pipes (SC3 = centered, SC4 = outside)
- Size (radius) of the fluid pipes (SC5 = radius 12.5 mm)
- Sheet thickness and wall thickness of the pipes (SC7 = 1.6 mm, SC8 = 3.2 mm)
- Materials for pipes and sheets (SC10 = aluminum, SC10-1 = copper)
- Distance (y-length) between the pipes (SC11 = 100 mm, SC12 = 300 mm)
- Thickness (x-length) of the thermal insulation (SC13 = 75 mm, SC14 =225 mm)
- Volume flow rate of the fluid inside the pipes (SC15 = 200 l/h, SC16 = 300 l/h)

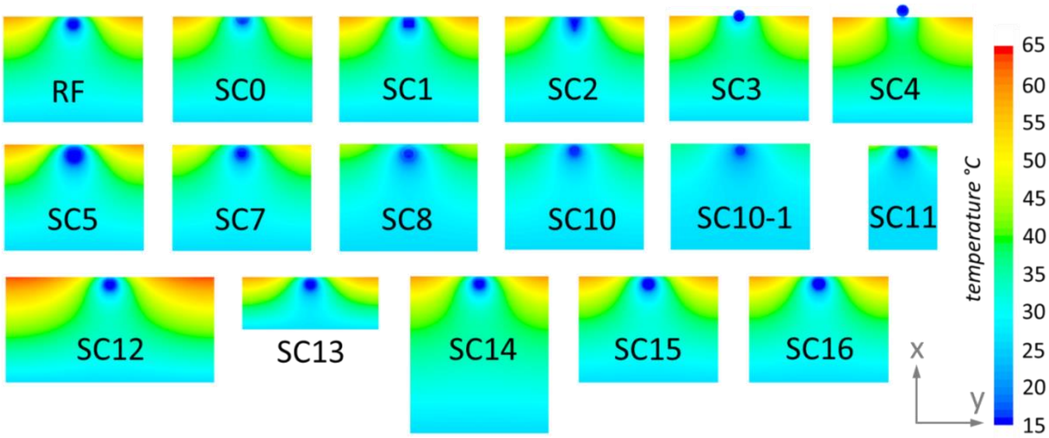

Figure 5: Comparison of the temperature contours between the RF scenario and the scenarios SC0 - SC16.

After evaluation of the thermal performance of the scenarios SZ0 - SZ16 further scenarios of the sandwich panel were developed.

- SC20: a rectangular pipe with an aspect ratio of 2/3 (x/y), 100 mm distance between the pipes and a sheet thickness of 1 mm.
- SC21: a semicircular pipe profile with a distance of 100 mm between the pipes and a sheet thickness of 1 mm.
- SC22: again a circular pipe (as shown in SC11) but with an additional weld to increase the thermal conductivity. Furthermore the sheet thickness was increased to 1mm.
- SC23: A wave profile, based on two sheets with a thickness of 1mm was designed with a distance between the pipes of 100 mm. The radius of the wave was 11.5 mm to achieve the same sectional area as in the RF scenario (Figure 6).
- SC23-1: same wave profile as used in SC23 but with a distance between the pipes of 200mm.
- SC23-2: again the wave profile from SC23 but the wave was formed by the outer sheet.

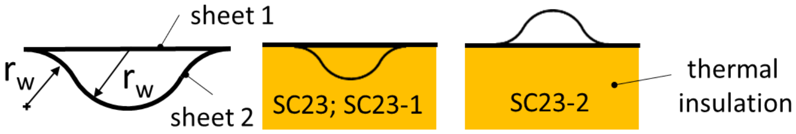

Figure 6: Schematic of the wave profile and the scenarios using this profile.

Finally 22 different scenarios (mentioned above) were compared regarding to fluid outlet temperature and heat transfer (heat flow) between the exterior heated surface and the fluid inside the pipes (Figure 7).

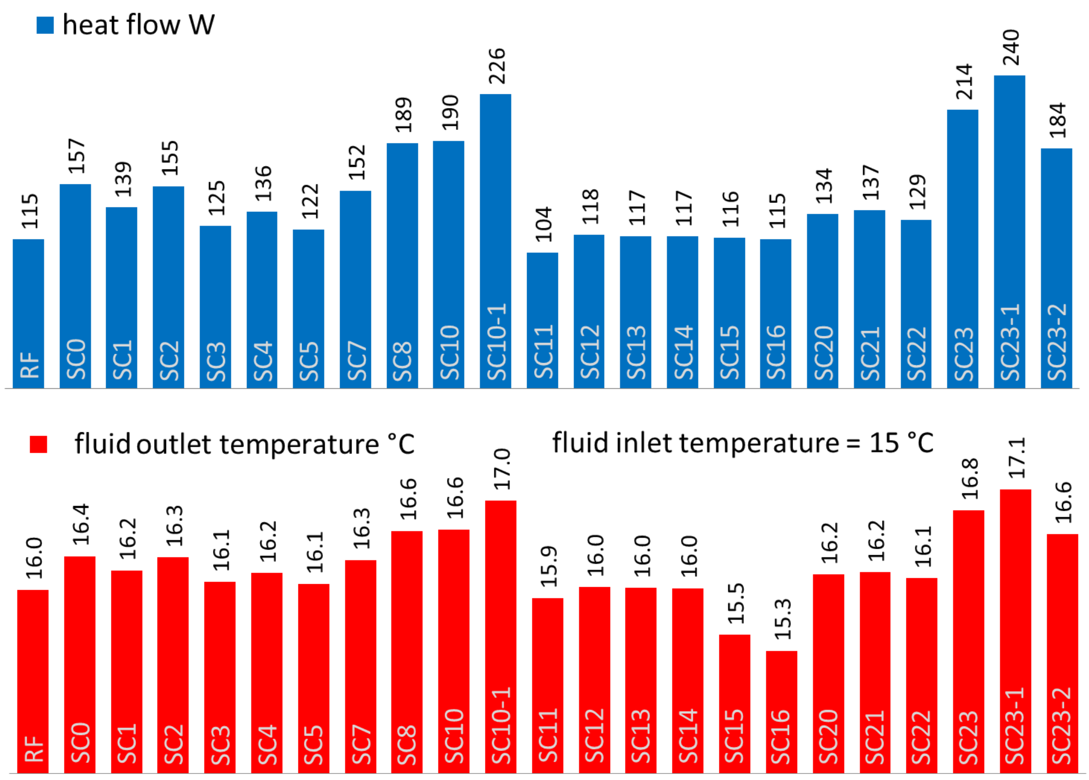

Figure 7: Comparison of the non-area-weighted heat flow of a single pipe and the fluid outlet temperature between the RF scenario and the different scenarios (RF, SC0 - SC23-2).

In the RF scenario the fluid outlet temperature was 16 °C and heat of 115 W was transferred from exterior into the fluid. Over a panel height of 1 m the fluid temperature could be increased by 1 °C in the reference scenario.
In the variations of the pipe´s shape (SC0 - SC2) the fluid outlet temperature was higher than in the reference scenario. The heat flux was improved due to the larger contact surface between the pipe and the exterior sheet.
Scenario SC3 and SC4, where the pipe positon was varied, showed a slightly higher heat flow than in the RF scenario. This could be explained by the direct contact of the fluid pipe with the exterior and the solar radiation. Due the higher heat losses to the exterior the enhancement of the fluid outlet temperature was only marginal.
Also the enlargement of the pipe´s diameter (SC5) showed only little improvement of the thermal performance compared to the RF scenario.
Integration of thicker steel sheets and pipes (SC7, SC8) into the sandwich panel led to an indeed improvement of the thermal performance but necessarily followed by an increase of self-weight.
Almost the highest impact in the improvement in the thermal performance was achieved by the exchange of the steel sheets of the pipe and the sheets by materials with higher thermal conductivity (SC10, SC10-1). But these materials are expensive and moreover have lower strength properties than steel, which has a negative impact on the structural behavior.
Generally a reduction of the distance between the pipes (SC11) in the sandwich panel had a negative influence on the thermal performance but allows the integration of more pipes at the same surface area. The enlargement of the pipe´s distance (SC12) did not result in any significant changes in thermal behavior.
Neither the reduction (SC13) nor enlargement (SC14) of the thickness of the thermal insulation obtained a significant difference in the thermal behavior compared to the RF scenario.
Increasing the fluid volume flow inside the pipes (SC15, SC16) led to a decreasing of outlet temperature whereas the heat flow was almost at the same level as in the RF scenario.

All additional designed scenarios showed higher fluid outlet temperature compared to the RF scenario. But the best thermal performance and the highest outlet temperatures were received for scenarios using the wave profile formed by the inner sheet of the exterior panel´s shell (SC23, SC23-1). For this reason, further investigations with the wave profile scenarios were made.

2.3 Investigation of the thermal behavior of sandwich panels using a wave profile

After the preliminary evaluation of a variety of scenarios (2.2) the wave profile chosen for further investigations on the thermal behavior and heat flow. For this investigation a sandwich panel with the wave profile was modelled over one as well as two stories with a story height of 3.5m. In the first step of this evaluation again a section of the façade containing one fluid pipe was observed. In all these simulations the wave profile´s radius was 11.5 mm, the volume flow was assumed to 50 l/h.

- SC30: 3.5 m panel height, 100 mm distance between pipes and a sheet thickness of 0.6mm
- SC31: 3.5 m panel height, 200 mm distance between pipes and a sheet thickness of 0.6mm
- SC32: 7.0 m panel height, 100 mm distance between pipes and a sheet thickness of 0.6mm
- SC33: 7.0 m panel height, 200 mm distance between pipes and a sheet thickness of 0.6mm
- SC34: 3.5 m panel height, 100 mm distance between pipes and a sheet thickness of 0.4mm
- SC35: 3.5 m panel height, 200 mm distance between pipes and a sheet thickness of 0.4mm
- SC36: 7.0 m panel height, 100 mm distance between pipes and a sheet thickness of 0.4mm
- SC37: 7.0 m panel height, 200 mm distance between pipes and a sheet thickness of 0.4mm

Figure 8 shows a comparison of the temperature contours to point out the differences in temperature distribution between a standard sandwich panel (without fluid pipes) and a panel with integrated wave profile pipes at two different distances between the pipes. The resulting contours show that the temperature inside the panel and especially at the exterior surface temperature strongly depends on the distance between the fluid pipes.

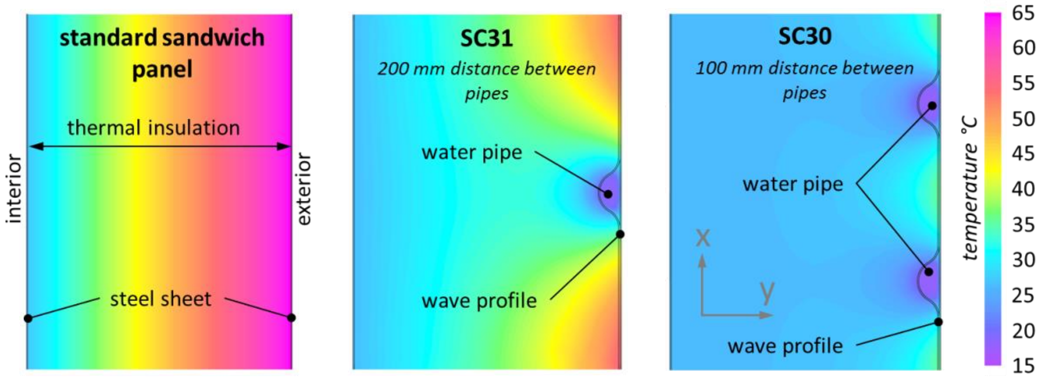

Figure 8: Comparison of the temperature contours between a standard sandwich panel and a thermal activated panel with integrated wave profile with different distance between the fluid pipes.

The calculated fluid outlet temperatures and the heat flows for the wave profile scenarios SC30 - SC37 are illustrated in Figure 9.

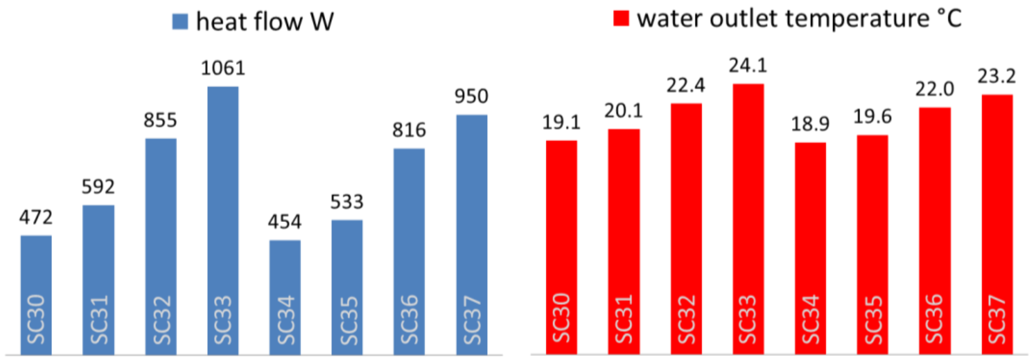

Figure 9: Comparison of the non-area-weighted heat flow of a single pipe and the fluid outlet temperature between the wave profile scenarios SC30 - SC37.

Because of the increased panel height, higher fluid outlet temperatures were received than in the simulations of the scenarios in chapter 2.2. But these temperatures were still too low for hot water supply applications in buildings. Therefor a comprehensive parameter analysis was made to find a scenario which can provide enough hot water at a suitable temperature level to load a hot water storage for example. Figure 10 illustrates the influence on the thermal performance by varying the volume flow (1), the distance between the pipes (2) as well as the pipe size (3).
With decreasing volume flow the fluid outlet temperature increased while the heat flow was reduced (diagram 1 in Figure 10). The changes of fluid outlet temperature and heat flow were negligible for volume flows above 200 l/h.
Fluid outlet temperature and heat flow were increasing when the distance between the pipes was increased (diagram 2 in Figure 10). This increase almost disappeared for a pipe distances of more than 200 mm. In diagram 3 in Figure 10 the influence of the pipe size on the fluid outlet temperature and the heat flow is illustrated at constant volume flow as well as constant velocity of the fluid inside the pipes. Only with the reduction of the volume flow for providing constant fluid velocities had a significant impact on the fluid outlet temperature in the simulations.

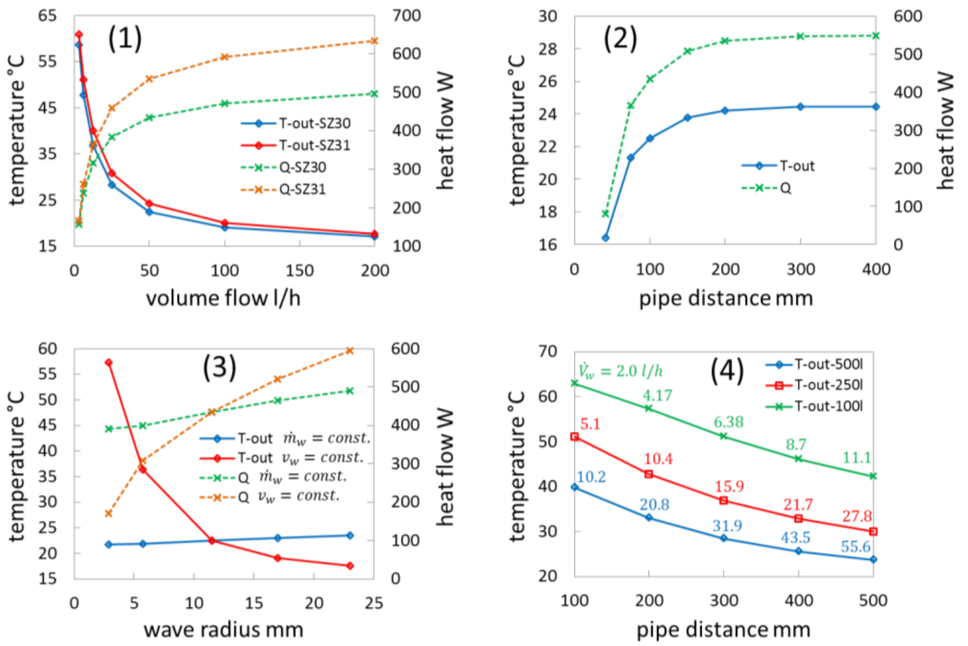

Figure 10: Temperature profiles and heat flow for (1) different volume flows, (2) different distances between the fluid pipes and (3) the variation of the pipe size (wave radius). (4) Comparison of the fluid outlet temperature for a (5 x 3.5 m) sandwich panel with integrated fluid pipes with different distances between the pipes.

In final investigation of this study the level of the fluid outlet temperature for a 5m wide and 3.5 m high sandwich panel and integrated (wave profile) pipes was observed. With the heated fluid a hot water storage (of 100 l, 250 l or 500 l) could be charged. Same boundary conditions as in chapter 2.1 were assumed at a charging duration of one hour. Due to the different distances between the integrated pipes the number of pipes was varying in the observed scenarios and consequently the volume flow had to be changed to provide the same quantity of fluid for the storage over an hour. The resulting temperature profiles of this for the moment very simplified calculations are illustrated in diagram 4 in Figure 10.

3 Influence on the mechanical properties

In order to quantify the influence of the formed cover sheets on the mechanical properties of sandwich panels, those cross-sectional shapes which have shown most promising thermal behavior were subjected to a static analysis. Using the CAE (Computer-Aided Engineering) software tool Abaqus [3] the principal stresses within formed sheets and the elastic deformations (especially the deflection in load direction) of the sandwich panels were calculated and compared to a standard panel with flat cover sheets.

3.1 Numerical approach and boundary conditions

For simulating the static behavior a three-dimensional FEM model using the following element types were generated: The insulating core was modelled as 3d continua with 20 nodes (solid element code C3D20) in contrast to the formed sheets, which were generated as 2d shell elements with 8 nodes and reduced integration (shell element code S8R). The mid-planes of the sheets are connected shear-resistant to the inner and outer surface of the insulating core with an eccentricity in extent of half the thickness of the sheets.

The assumptions made for the calculations in Abaqus [3] are listed below:

- Static model: one-way slab, span 3.5 m (supposed distance between floor slabs), width 0.5 m
- Boundary conditions: statically determinate with line supports at both ends of the panel
- Load: uniformly distributed surface load, 1 kN/m^2 perpendicular to the panel (wind pressure)
- Cross section: insulator thickness 150 mm, sheet thickness 0.8 mm
- Materials: The material data partly were determined according to Torsakul [4].
  Sheets: steel S275, density 7 850 kg/m^3, Young´s-Modulus: 21 000 kN/m^2, Poisson´s ratio: 0.3
  Insulator: polyurethane foam, density 40 kg/m^3, Young´s-Modulus: 1.4 kN/m^2, Poisson´s ratio: 0.3

According to the results of the thermal evaluation the mechanical behavior of the following cross sections was calculated (Figure 11). The center distance between axes of the pipes was reduced from 200 mm at cross section 2 (reference scenario, RF) to 100 mm at cross section 3 (wave model, SC30).

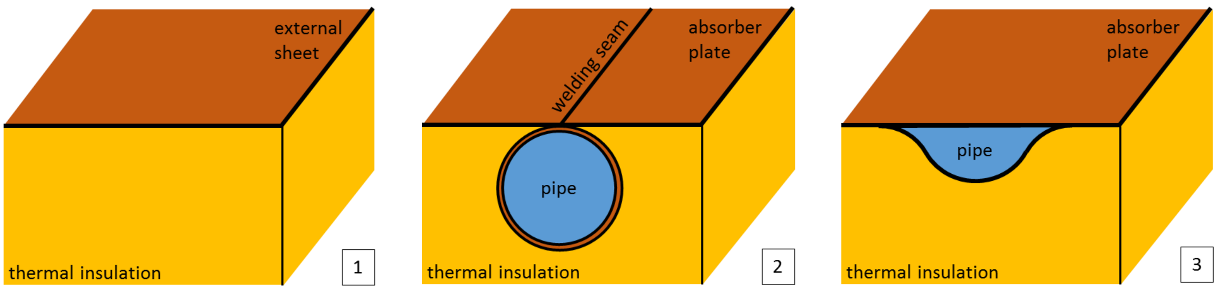

Figure 11: Analyzed cross sections: standard sandwich panel (1), reference scenario (2), wave model (3).

The results of calculations regarding the principal stresses within formed sheets in longitudinal direction and the elastic deformation in load direction of the sandwich panels are shown below (Figure 12 - 17):
Cross section 1 - standard sandwich panel

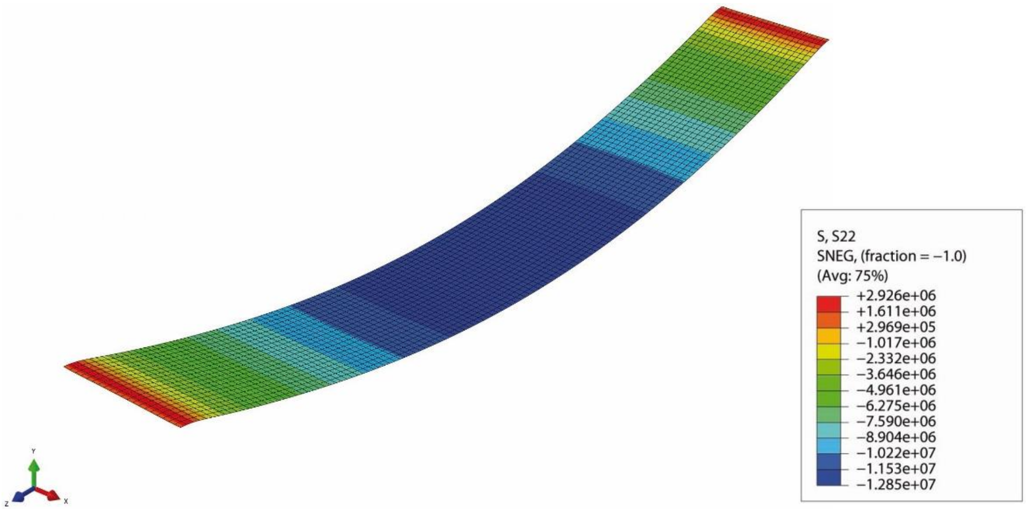

Figure 12: Cross section 1, principal stresses on the outer surface of the external sheet.

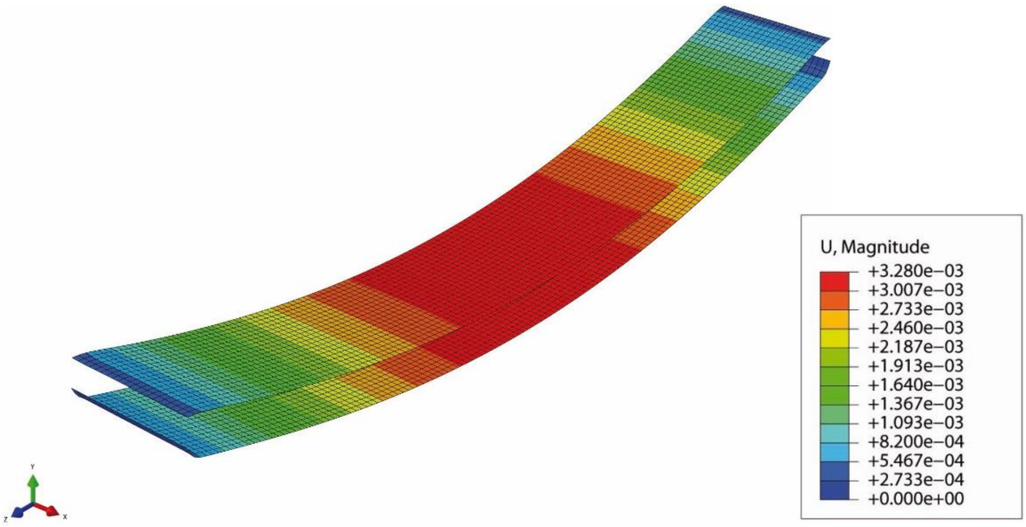

Figure 13: Cross section 1, elastic deformation.

Cross section 2 - reference scenario (RF)

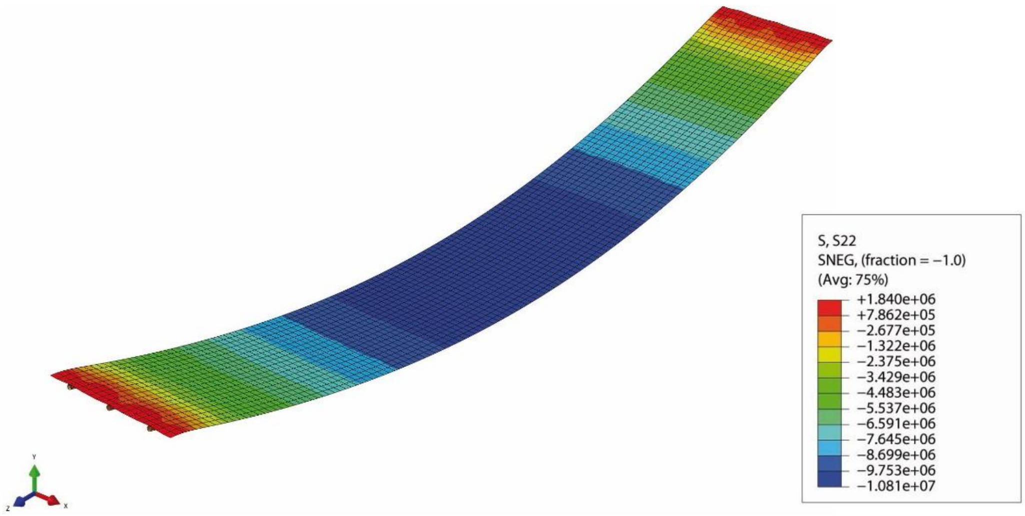

Figure 14: Cross section 2, principal stresses on the outer surface of the external sheet.

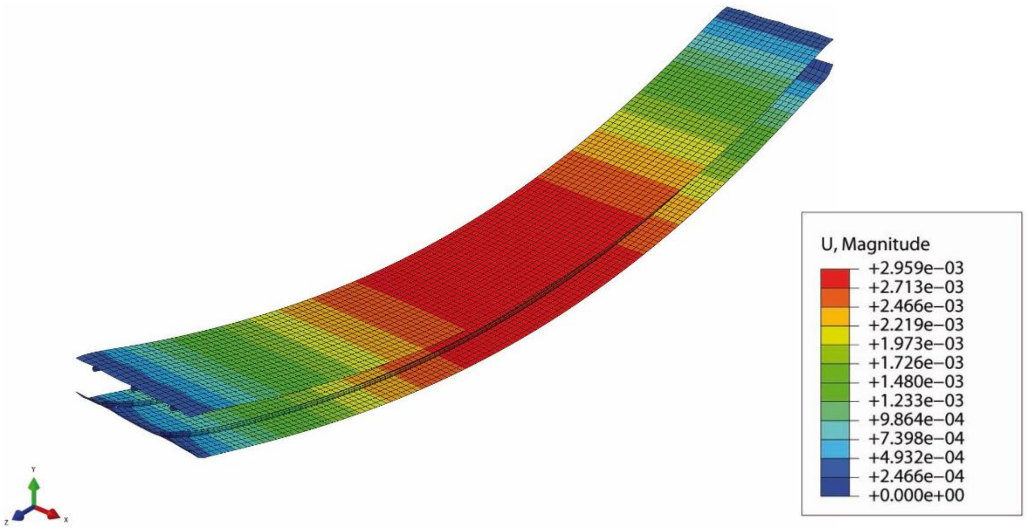

Figure 15: Cross section 2, elastic deformation.

Cross section 3 - wave model (SC30)

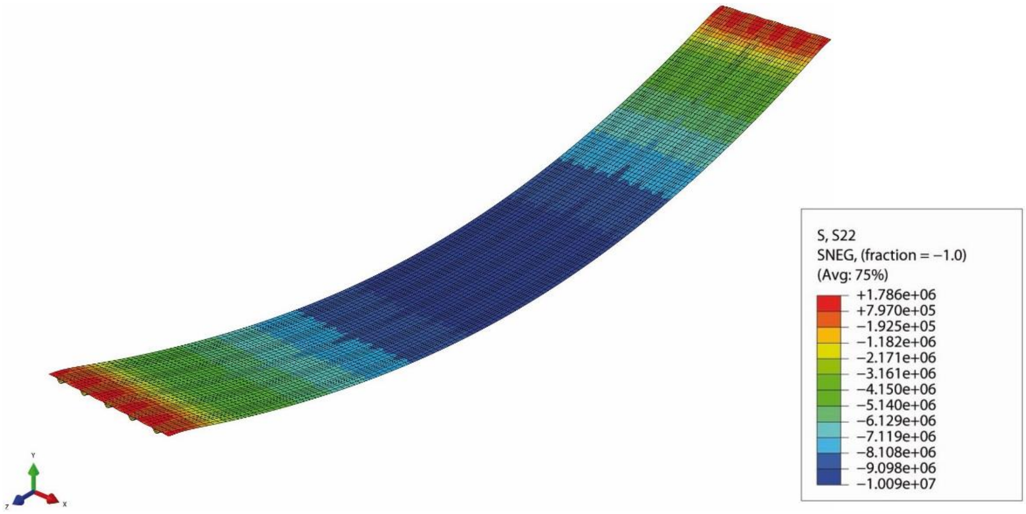

Figure 16: Cross section 3, principal stresses on the outer surface of the external sheet.

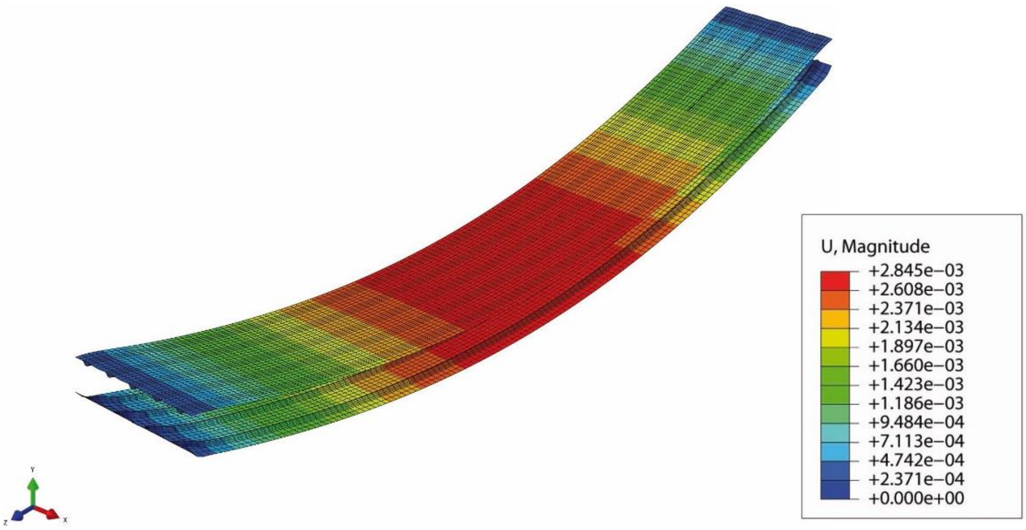

Figure 17: Cross section 3, elastic deformation.

The results of the static analysis in brief (Table 1):

Table 1: Summery of the calculated results.

Cross section	Self-weight (sheets) [kN]	Self-weight (sheets) [%]	Principal stress [kN/cm^2]	Principal stress [%]	Elastic deformation [mm]	Elastic deformation [%]
Standard panel (1)	0.220	100.00	±1.29	100.00	3.28	100.00
Reference scenario (2)	0.278	126.39	±1.08	84.12	2.96	90.21
Wave model (3)	0.314	142.68	±1.01	78.52	2.85	86.74

4 Conclusions and Outlook

For a various number of different scenarios for an activated sandwich panel the thermal performance could be determined (for hot climate conditions). The scenarios using a wave profile pipe showed the best thermal performance and were used in a comprehensive parameter analysis.

The influence of the volume flow, the pipe distance as well as the pipe size on the thermal behavior was determined. The volume flow, especially the velocity of the fluid inside the pipes showed the highest impact on the heat flow to the fluid. Also the pipe distance had a considerable impact on the fluid outlet temperature but not as high as for the variation of the volume flow. It could be concluded that the pipes should be positioned within a distance between 100 and 200 mm.

The analysis has shown that equipping a conventional sandwich panel with pipes for thermal activation has positive influences on static performance. Especially the center distance between axes of pipes influences the quantity of principal stresses and elastic deformation. In comparison to the standard sandwich panel the principal stress of the wave model can be reduced up to 21% and the elastic deformation decreases by 13%.

To increase the fluid outlet temperature a network of pipe channels for the exterior sheet should be observed following to the examples of heat exchangers, heaters or evaporators in refrigerators. Therefore the pipe routings have to be designed to further improve the static performance.

In conventional sandwich panels the thermal insulation is glued shear fixed to the sheets. One of the next steps is to realize the shear fixed joint without the glue, only by having mechanical connections.

A glass cover should be integrated as a further improvement of the thermal performance of the sandwich panel.

5 Acknowledgements

The analysis and results described are part of a current research project “UNAB - Sustainable design process & integrated façades” at Graz University of Technology, Austria. The authors would like to acknowledge all the participants of the UNAB project. A summary and a list with all the members can be found in TUGonline [5]. Finally, the authors are grateful to be financially supported by the Zukunftsfonds Steiermark.

Das Land Steiermark ZUKUNFTSFONDS STEIERMARK

6 References

[1] Ansys Inc., Ansys Fluent, Release 14.0, November 2011
[2] Ansys Inc., Ansys Fluent User‘s Guide, Release 14.0, November 2011
[3] Dassault Systèmes, Abaqus/CAE, Release 6.10-1, April 2010
[4] Torsakul, S.: Modellierung und Simulation eines Verbunds von Sandwichplatten zur Entwicklung einer mechanischen Verbindungstechnik. PhD-thesis, RWTH Aachen, 2007
[5] TUGonline, https://online.tugraz.at/tug_online/webnav.ini, April 2015

Proceedings of the International Conference on Building Envelope Design and Technology, Graz
Advanced Building Skins 2015

Timber-frame facade elements for hybrid construction

René Stein, Dipl.-Ing. project manager, Miriam Kleinhenz, Dipl.-Ing.,
Stefan Winter, Univ.-Prof. Dr.-Ing.
Technische Universität München, Chair for timber structures and buildung construction, Germany, r.stein@tum.de / www.hb.bgu.tum.de

Summary

In the interdisciplinary research project three chairs of TUM (Chair of Timber Structures and Buildung Construction, of Energy Efficient and Sustainable Design and Building and of Concrete and Masonry Structures) as well as Ift Rosenheim (Department of Building Acoustics) are working together. The symbiosis between timber-frame elements and solid structure is being developed considering the state-of-the-art with regard to all relevant aspects of structural design and building physics including heat, moisture, sound and fire protection. Additionally, the field of increasing emphasis, life cycle analysis and recyclability of materials used in construction is included by considering certain carbon footprint values etc.
The outcome is a construction catalogue for hybrid construction including standardized elements and details with technical and legal feasibility.

Keywords: Carbon Footprint, Construction catalogue, Recyclability, Reinforced concrete structures, Timber-frame façade elements

1 Introduction

In multi-storey buildings very efficient and well-proven structural work solutions are offered by reinforced concrete frame and bulkhead constructions, while non-load bearing external walls with high quality can be provided using prefabricated timber-frame facade elements. Nevertheless, in Germany such façade elements are rarely used in new reinforced concrete, steel or composite constructions.
Against the background of the significantly increased degree of industrialization of timber construction companies, a greater cooperation between the classical construction sector and timber construction companies should be expected in future.
Due to certain application technologies, prefabricated timber-frame elements allow delivering to the building site highly insulated elements including glazing and appliqued facade elements. Consequently, the time of building constructions can considerably be reduced in total.
The evaluation of different projects has shown that combining different construction methods offers a great potential for further industrialization and acceleration during construction processes in combination with an increase of quality standards and an improvement of working conditions. Knowledge gaps in the field of sound insulation, fire protection and deformation compatibility as well as the lack of information of consistent and coordinated construction details are considered and included in the project.
The execution of well-designed and defect-free constructions has an important part to play in influencing sustainability. In order to achieve the climate protection targets, the energy and resource efficiency of new buildings have to be improved during pre-fabrication and erection, including the essential part of the optimization of building skins.

Furthermore, comprehensive systematic descriptions of application possibilities are compiled, for example residential, office or school constructions. In case of residential and office buildings, the timber-frame facade elements can be used up to the limit of high-rise buildings (≤ eight storeys).

In parallel, experiences gained during the process of research-supporting projects (e.g. construction project "Städtischer Hartplatz" in Penzberg) give an insight of the practicability of hybrid constructions and provide helpful results for the elaboration of the construction catalogue.

2 Integrative planning process

During the entire construction process - including the design of the structure and the building progress - the basic, preliminary and conceptual planning phase imply the decisive phase. Here, problem-solving processes of pre-planning are already included and determine the following phases. During this decisive phase, costs, time and quality are essentially determined.

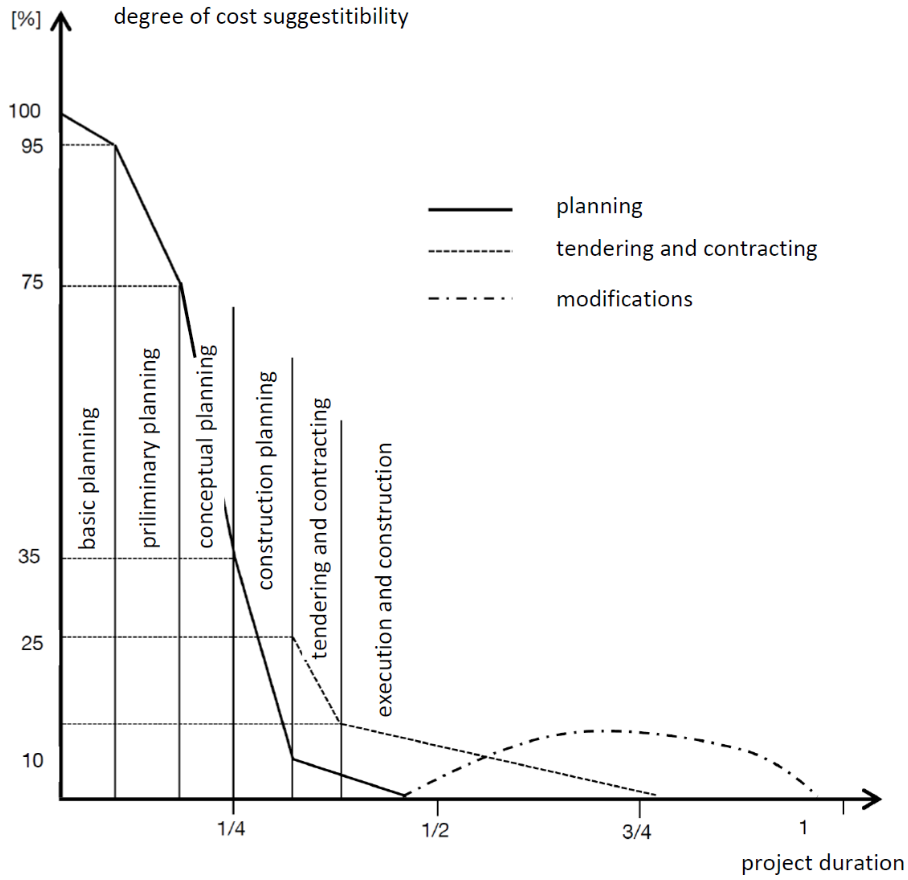

Figure 1: Dependence of cost sugesstibility in the construction phase,
taken from [1] in modified form

Economic and time constraints can only be complied, if the procedure of pre-fabrication and erection are also considered in the planning phase. Already in the early stages of a project, integrative and cooperative planning is indispensable for intensive networking between planning and construction processes. This networking is mirrored in the composition of the different chairs and by the support of the project related working group.

3 Identification of hybrid design

The load-bearing structure consists of reinforced concrete elements, e.g. in situ concrete, partly and fully prefabricated concrete elements as well as reasonable mixed structures. The design principles can be divided into skeleton and / or bulkhead structures.

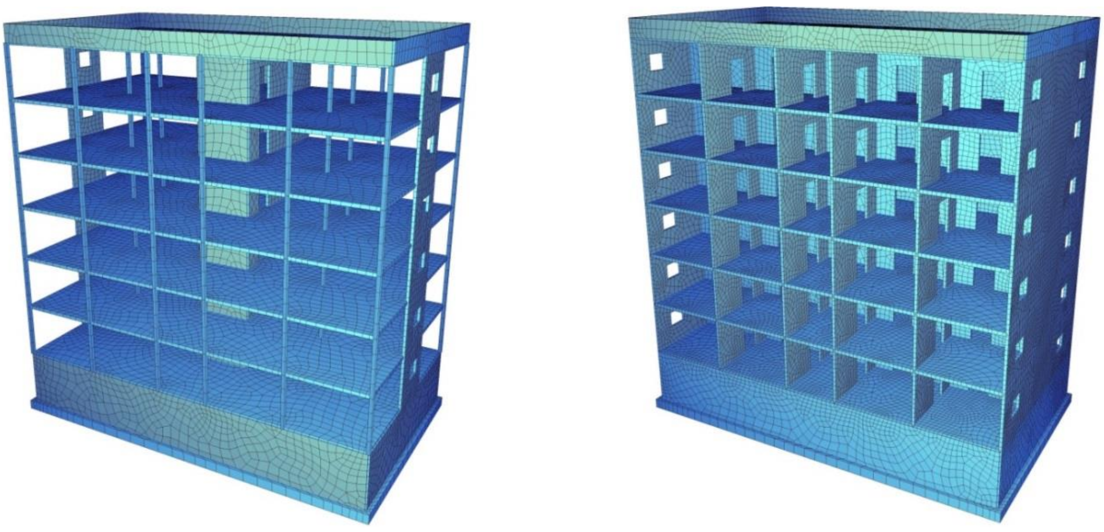

Figure 2: Examples for load-bearing structures in reinforced concrete, frame structure (left) and bulkhead structure (right)

The non-loadbearing timber-frame elements are fixed to the supporting concrete structure. For non-loadbearing exterior walls a fire resistance of 30 minutes is required in building class 4 and 5. With regard to fire protection, the timber-frame elements should be anchored in each storey. Otherwise the elements have to be classified as load-bearing elements including a fire resistance of 60 minutes in building class 4 and 90 minutes in building class 5. Figure 3 shows the position and fixing possibilities of timber-frame elements related to the concrete structure.

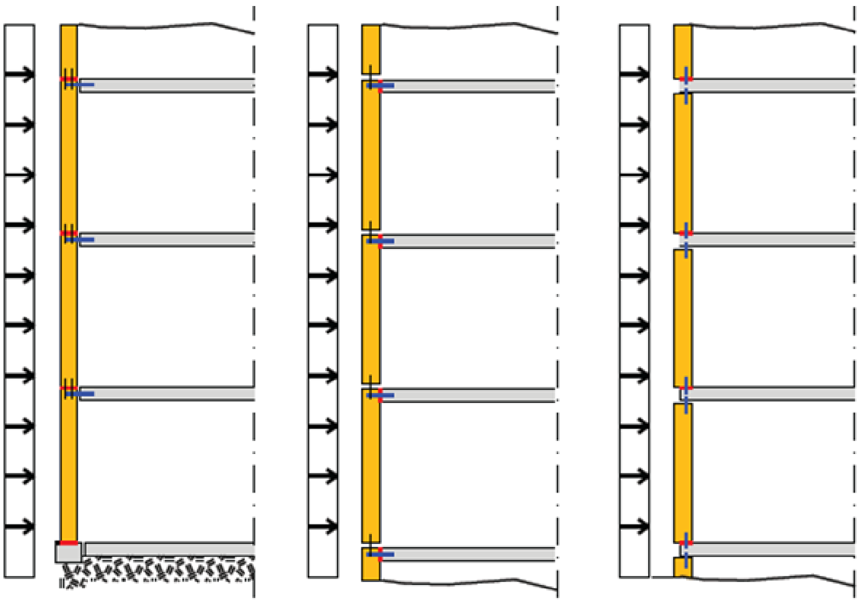

Figure 3: Principles of highly-insulated timber-frame elements related to reinforced concrete structures, outside supporting below (left) and on top (centre), partly or fully integrated (right)

Taking into account the aspect of the erection and a useful attachment of the prefabricated timber elements, only the exterior walls situated outside (case left) or integrated in the supporting concrete structure (case right) are further included in the construction catalogue.

4 Detailing of timber-frame facade elements

In combination with the load-bearing structure the following issues are to be solved:

a) Mechanical resistance and stability:

- Connections between reinforced concrete and timber-frame assemblies have to be designed most economically.
- In reinforced concrete structures, e.g. floor constructions with spans of 5,50 m to 7,00 m, not only short but also long-term deformations have to be taken into account. These deformations have a great influence on the connection between the timber and the concrete structures. Gaps between floor and exterior wall constructions have to fulfill the requirements related to long-term deformations as well as mounting tolerances.

b) Safety in case of fire:

- The spread of fire through ventilated facade systems, over joints between timber elements and concrete structure has to be prevented.

c) Energy economy and heat retention:

- For the defined connections a complete catalog of thermal bridges will be provided.

d) Protection against noise:

- Values of flanking transmission of structure-borne and impact sound will be measured in laboratory and building site including also constructions with increased noise protection.

e) Sustainable use of natural resources

- In the context of contract decision and certification systems the life cycle analysis (LCA) and recyclability of used assemblies becomes increasingly important. Therefore it is necessary to provide CO_2-equivalents etc. for the timber-frame assemblies.

Figure 4 shows for example the thermal bridge coefficient of a connection between reinforced concrete floor and external wall ($U = 0{,}15\ Wm^{-2}K^{-1}$).

BA7a	Anschluss Außenwand - Decke - Außenwand
Randbe-dingungen:	Randdämmstreifen mit WLS 040

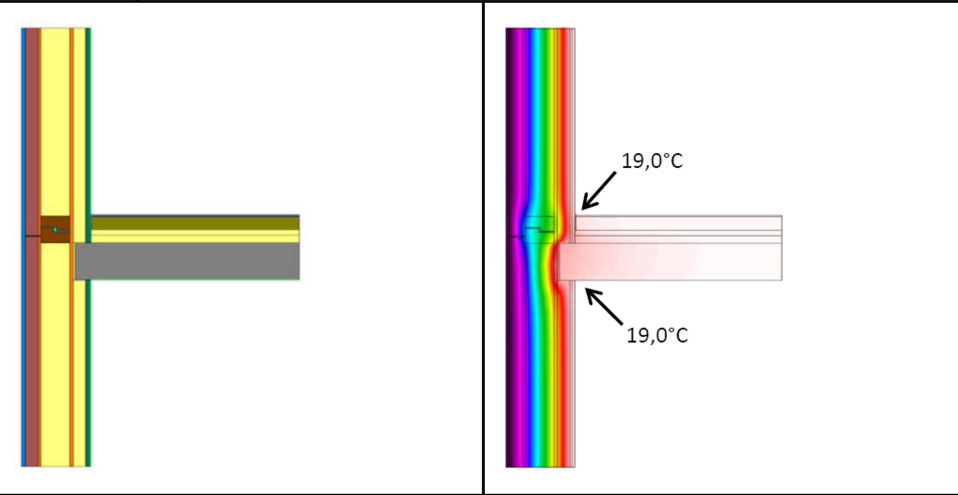

Wärmebrückenkoeffizient Ψe (außenmaßbezogen)	0,032 W/mK	f_{Rsi}	0,96 oben 0,96 unten

Figure 4: Connection of reinforced concrete floor with timber frame elements

Figure 5 shows the influence of thermal bridge coefficient of the same connection including a window.

BA7g	Anschluss Roka-Shadow - Decke - Außenwand
Randbe-dingungen:	Randdämmstreifen mit WLS 040, Außenmaßbezug auf Rohbaumaß des Fensters

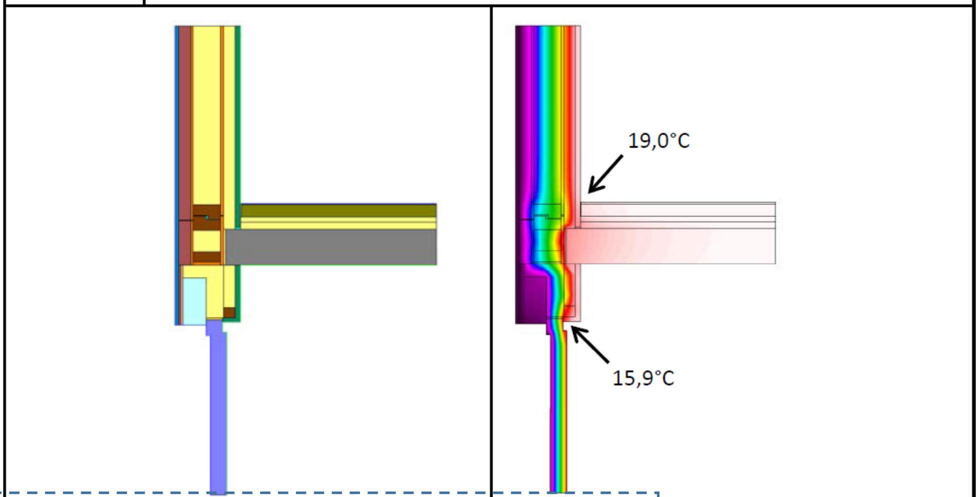

Wärmebrückenkoeffizient Ψe (außenmaßbezogen)	0,085 W/mK	f_{Rsi}	0,96 oben 0,84 unten

Figure 5: Connection of reinforced concrete slab with timber frame elements including a window

The details were developed in a workshop with the project-supporting working group. The range of thermal bridge coefficients will be specified in parametric studies.

5 Project-related example

The fact of the growing importance of environmental issues - particularly in the construction industry - is leading to an increased demand for sustainably constructed buildings and neighborhoods with investors, builders and users. Sustainable construction is also worthwhile in economic terms, because this is the major impulse for the development of a master plan. With the construction project "Städtischer Hartplatz" in Penzberg (Germany) initiated by Krämmel GmbH & Co. KG an innovative and sustainable residential development shall be created. The complex consists of ten terraced houses (basement + II + attic), three point houses (basement + II + attic) and two apartment buildings in row construction (basement + III + attic).
Primary objectives will be the improvement of ecological and economic conditions, recoverability and quality of the buildings. There will be different sustainable criteria taken into account, which generate the following additional benefit:

- High comfort
- High user acceptance
- Low operating, maintenance and repair costs
- Sustainable buildings
- Positive public perception
- Good marketing of the object
- High economic output

Figure 6: 3D-visualisation (planning alliance „Städtischer Hartplatz“:
Krämmel Bauplan GmbH und Lang Hugger Rampp GmbH)

The aim of the project "Städtischer Hartplatz" is the development of an integral overall concept by creating a residential neighbourhood in low-energy standard (KfW-efficiency 55 house standard according to Energieeinsparverordnung 2014) and by using ecological materials as well as low-tech solutions. For achieving these goals the following three components has to be considered:

- Grey energy
- Passive energy system

- Energy supply

The interdisciplinary team of the Technische Universität München on the one hand and the long-standing expertise of the construction company in project realization on the other hand can include the different topics with a wider range.

6 Acknowledgements

The authors would like to thank the Stiftung Bayerisches Baugewerbe for the financial support.

And grateful thanks to the project team:
- Technische Universität München:
Chair for Energy Efficient and Sustainable Design and Building, *Werner Lang, Univ.-Prof. Dr.-Ing.*
Research Associates: Christina Dotzler, Dipl.-Ing. M.Eng and Patricia Schneider, Dipl.-Ing. Architekt

Chair for masonry and timber structures, Germany, Oliver Fischer Univ.-Prof. Dr.-Ing.
Research Associate: Christof Volz, Dipl.-Ing.

- Ift Rosenheim, Department of Building Acoustics
Joachim Hessinger, Dr.

7 References

[1] Knaack, U., Chung-Klatte, S., Hasselbach, R.: *Systembau - Prinzipien und Konstruktion.* Birkhäuser Verlag, Basel, 2012.

Timber-glass composite Façade with integrated building systems

Vitalija Rosliakova, PhD candidate
Department of Structural Design and Timber Engineering, Vienna University of Technology, Karlsplatz 13/252.2 1040 Vienna, Austria, vitalija.ros@gmail.com

Summary

This paper relates to analysis of case studies in Vienna as a State of Art, which aim to define the properties and functions that the modern integrated facade must have and to investigate the potential of Timber-glass composite (TGC) for a advanced building envelope capable to integrate building systems and incorporating solar energy gains.

The understanding of market demand for a modern building envelope can clearly benefit investigation process and quality of architectural design by making development of a façade composite more efficient.

Keywords: Timber-glass, façade, building systems, solar energy

1 Introduction

The architectural needs for structures that are light in appearance, offering a high level of transparency but at the same time provide load-bearing properties challenge the development in façade industry.
Timber-glass composite (TGC) is an innovative hybrid structure that takes advantage of the high stiffness and strength of glass. Accordingly its post-breakage behavior increases in comparison with pure glass structures and it provides the possibility of using traditional timber joint techniques. [1] Within the research projects Holzforschung Austria (HFA) developed a patented structural system (HFA patent No 502470) – a circumferential adapter frame glued on all four edges of the glass (Figure 1). This interchangeable panel can be prefabricated at workshop and screwed to the load-bearing substructure on site [2], [3], [4]. Two different principles of mounting the glass pane have been developed: 1) using a continuous adhesive bound line along the perimeter of the glass pane and 2) using a combination of adhesive mount and stiffening blocks at corners, transferring the external load by contact with the edge of the glass (Figure 1) [3].

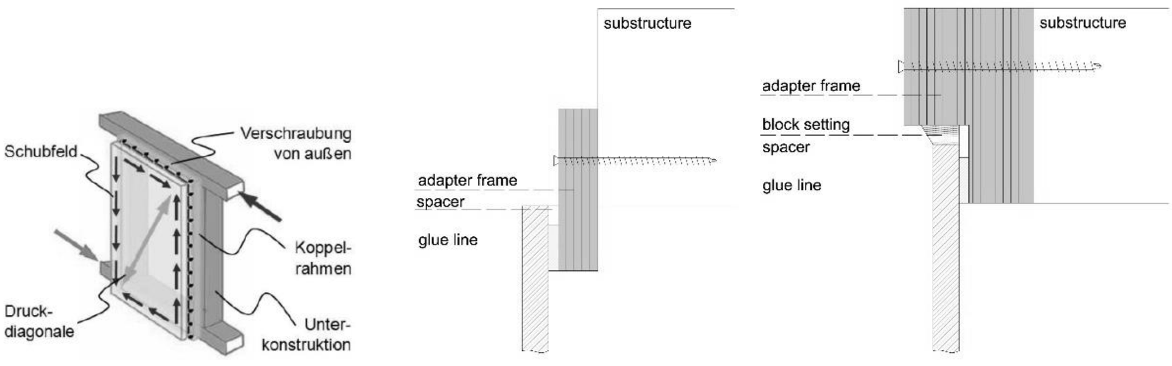

Figure 1: Basic principle of the TGC element for building stiffening (left) [3]. Detail of using a continuous adhesive bound line along the perimeter of the glass pane and Detail of using a combination of adhesive mount and stiffening blocks (right) [5].

This paper in a compressed way presents the analysis of case studies in Vienna as a State of Art, which aims to guide the development of TGC based facade. This study relates to study made within ongoing doctoral thesis“Resource efficiency and feasibility of Timber-glass composite (TGC) structure for High-performance building envelope” under supervision of o. Univ. Prof. DDI Wolfgang Winter at the Department of Structural Design and Timber Engineering, Vienna University of Technology (VUT).

2 Modern facade concepts

Modern façade concepts, known with different names, such as *Intelligent façades, Active façades, Advanced Integrated facades, etc.* are results of highly increased expectations for the building envelope performance ensuring the comfort condition inside the building. All these tendencies result the transformation of building skin into a complex system with high degree of automatisation and electrical control based on of cutting edge technologies.

Meantime building industry is as well forced to focus towards environmental sustainability which sets the goal for an energy efficient architecture, which consumes little to zero energy while maintaining high comfort level. This influences the emerging low-tech tendency, which seeks for simple solutions based on efficient use of local resources.

The understanding of market demand can benefit the investigation and development process as well as architectural design variety and quality.

The architectural tendencies forms basic functional expectation on a building envelope that can be classified to a protection function performed by building skin and building service that addresses to building systems. The building skin is an active boundary layer between outer and inner conditions that takes control of thermal insulation, illuminance, visual reference, glare protection, light redirection, sound insulation and wind attenuation. While building services provide solar screening, heat and energy gains, fresh air supply [6].

The study focuses towards glazed building envelopes, in which glass has a special role to play as takes over large area of the façade. The State of the Art market is offering a bright variety of glazing able to provide different properties as for example triple glazing and use of various coatings capable to ensure the comfort standards inside the building. Unfortunately, these influence an increased weight of the glass elements. The heavy glazing requires appropriate technologies to maintain its functionality and that forms an additional challenge designing with structural glass hybrid composites. TGC is compatible with various different glazing as long the inner glass panel is laminated safety glass.

The integration level of building systems depends on a facade typology whether it is a single-skinned or a double facade. Despite the differences in technical solution building systems can be defined as *Integrated* or *Stand alone* systems (Figure 3).

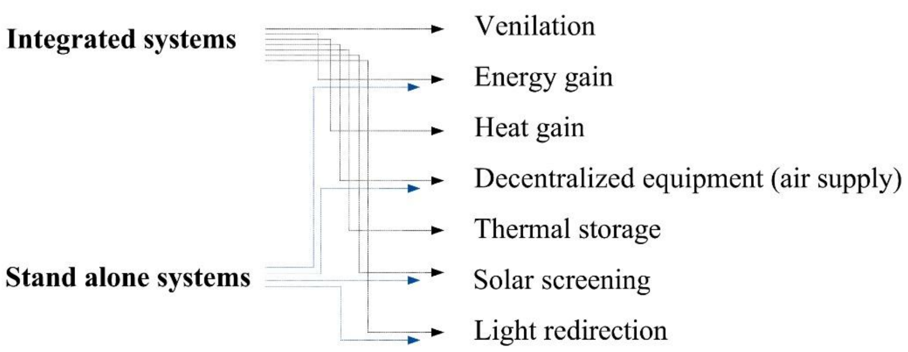

Figure 2: Integrated and Stand alone building systems

The TGC composite has a proper depth of the construction suitable for incorporation of such systems like solar screening, which is defined as composite-independent system. So that introduction of independent elements is not an issue. This analysis focused to define and investigate integrated technologies that could influence the development of TGC based façade construction.

Considering the low-tech character of composite the integration of ventilation is considered to be of a great interest. At the same time solar energy gain by building integrated PV is the most common and most economically efficient active energy strategy that has an increased been realized in various buildings. These two integration strategies were studied with the case study analysis and are presented in follow chapters.

3 Façade integrated ventilation

3.1 Case studies

Definition of reference project for analysis was defined within the lecture of *Wahlseminar Konstruktiver Glasbau*, 254.094 at Vienna University of Technology. The case study analysis incorporates results of student works together with the State of the Art of my doctoral thesis. Most recent buildings built in Vienna were chosen to be analyzed to define the latest tendencies in integration of building systems focusing on the technological as well as architectural aspects

Case study analysis clarified tree most common types of façade integrated ventilation, presented in the Tables 1.

Table 1: Case studies: ventilation

Types of façade integrated ventilation:		
Classical window opening	Horizontal air in- and outlets	Frame integrated ventilation
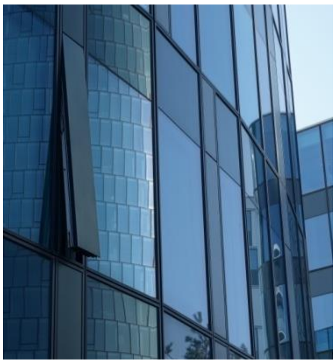 Source: author	 Source: author	 Source: author
Rundvier, Vienna	Erste Campus, Vienna	DC Tower, Vienna

The regular window opening is most common façade ventilation. This type of ventilation would not be applicable to TGC structure due to its specific construction that forms fixed structural layer. This layer plays stiffening role in bracing the building and preferred to be uninterrupted.

Horizontal air in- and outlets can be met either in single or in double-skinned facades. It provides the constant or regulated opening in the outer layer at the level of ceiling. It has a bright range of different technological solutions form a simple flap-alike construction to very sophisticated automated air mix technology. This type of ventilation is not seen inside but can be visually dominating in the architecture of the building.

The other type: frame integrated ventilation, mostly applied in high rise buildings, where due to the strong wind conditions regular window opening could be an inappropriate solution. It is light in appearance from inside of the building and can be unrecognizable in the exterior. Built-in within the elemental façade unit can be prefabricated ensuring the high technical quality and simplified application process (Figure 5).

Both horizontal air in- and outlets as well as frame integrated ventilation demonstrates the potential to be integrated into TGC structure.

Figure 3: Frame integrated ventilation, DC Tower, Vienna. Source: K. Kizilaslan, L.B. Toprak [7]

3.2 TGC façade with integrated ventilation

Within the resent ongoing investigation ITI has developed a new assembly of the composite (Figure 4). This development was carried out facing the challenges that reduced size of adapter frame meets within the purpose of caring out the force transmission between adapter frame and substructure. The principle of this assembly consists of connecting bracket mounted on the post and it is transferring the pressure forces of compression diagonal to the substructure [5].

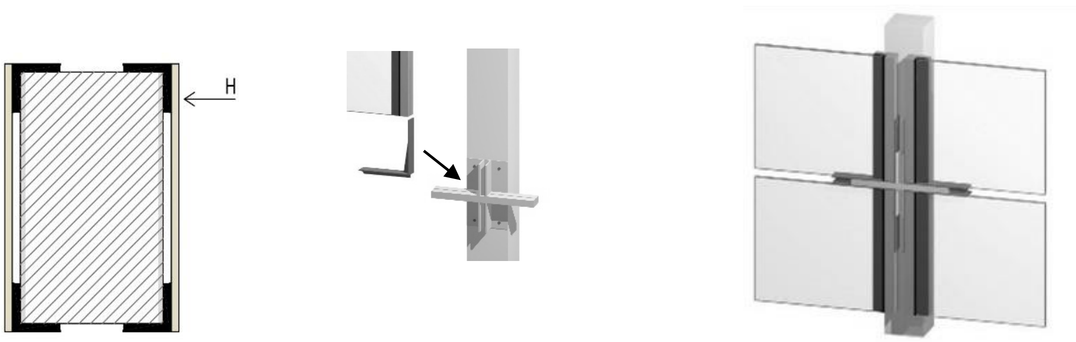

Figure 4: Detail developed adapter frame, ITI [4].

This principle allows the estimation that the horizontal elements of adapter frame could be eliminated. This provides a potential to use open space of former horizontal frame element for integration of constant or regulated ventilation. As well the horizontal element of the frame can be replaced by integrated more sophisticated technology for a supply air mix or pre-heating.

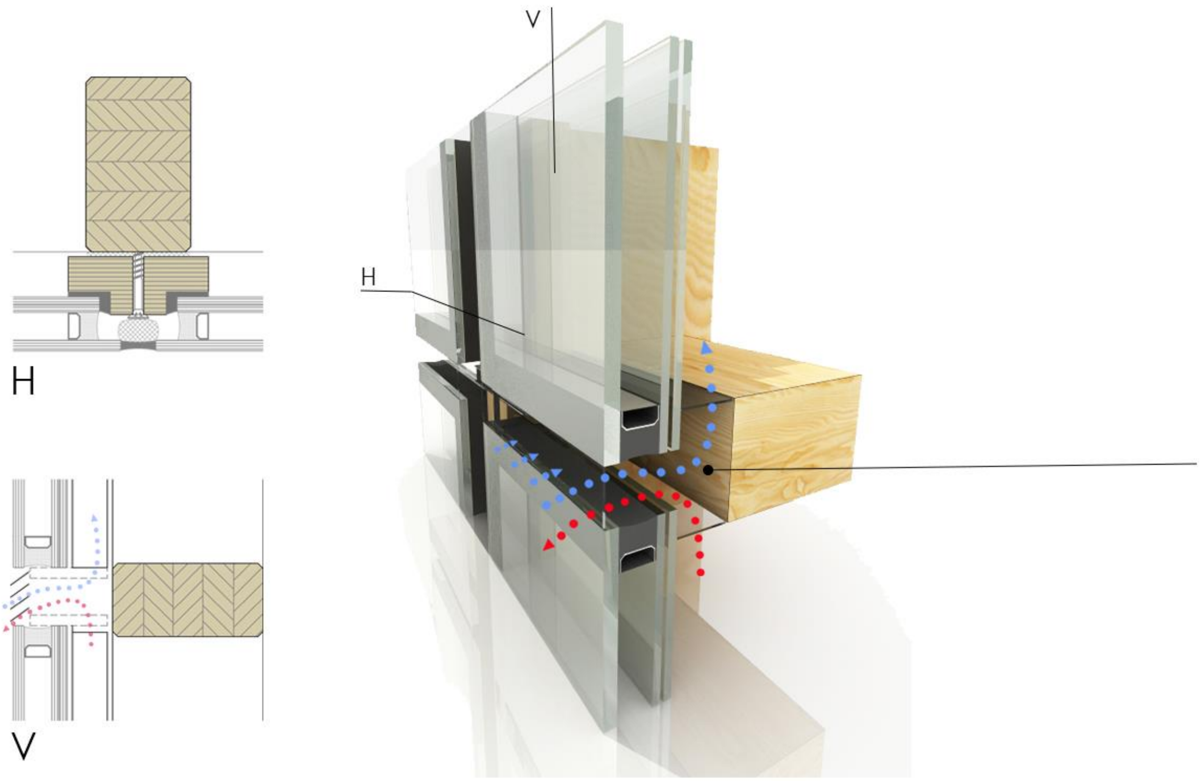

Figure 5: Potential of ventilation integration to TGC structure based façade.

Ventilation along the horizontal line could provide prevention of condensation formation. The detailed analysis of Pilot projects realized within previous research projects (Schatenbox: Holzforschung Austria, Vienna [8], 2011; Haas Haus: UniGlas, Vienna, 2014 [7]) had showed that the structure have faced condensate problems. The detailed development of ventilation integration must include thermal performance and building physics study due to prevent formation of thermal bridges and evaluate the potential to reduce condensate formation.

4 Solar energy gain

4.1 Case studies

As mentioned previously the building integrated PV (BIPV) is the most common and most economically efficient active energy strategy that has an increased popularity within design of new buildings as well as refurbishment of existing.

The recently realized refurbishment of TU Campus, Getreidemarkt, Vienna was chosen for the comprehensive study as it incorporates integration of different typology of BIPV and is the first energy-plus development of this dimensions. Two types of opaque panels as well as transparent laminated glass integrated PV were used (Table 2). The specific assembly, integration and installation of different technologies can be compared as well as their performance and influence for the architectural design.

Table 2: Building integrated PV.

BIPV, TU Campus, Vienna

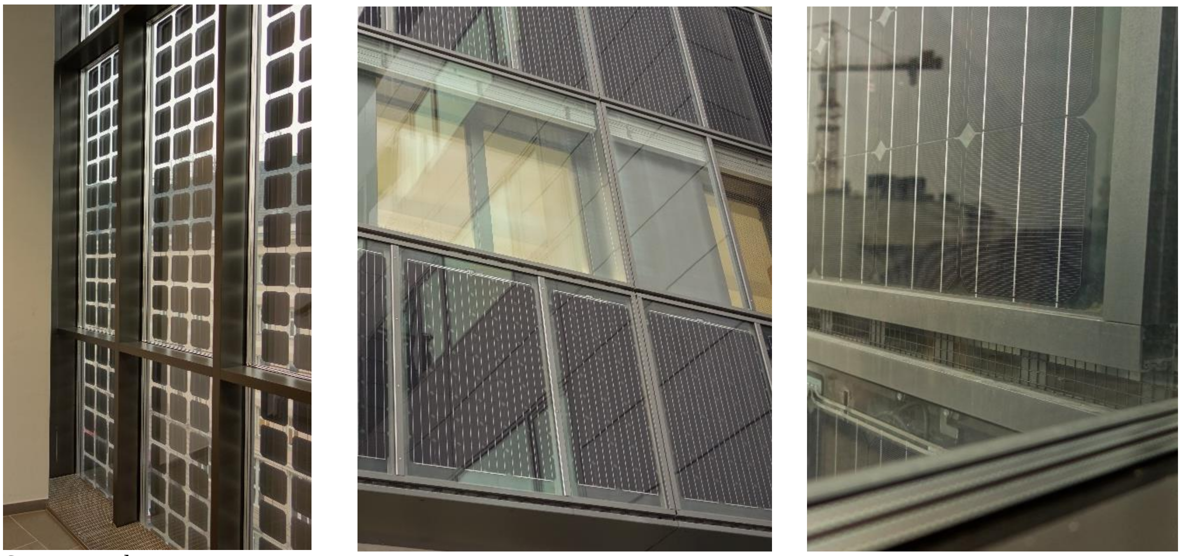

Source: author

4.2 TGC face with integrated PV

Laminated glass, which is a structural unit within the TGC composite, is used for structural as well as safety reasons. That provides the possibility to integrate PV in the same process of production.
In this respect Thin-film technology is of the great interest [9]. Being capable to offer different level of transparency and meanwhile performing as solar screening it is seen as having a high potential for a different type of the buildings.

On the other hand PV integration into a structural glass panel has to be investigated as the deformation and displacements that could appear in between the glass layers can influence both the efficiency of PV as well as structural performance of laminated glass.

3 types of BIPV Timber-glass facades were defined to be detailed designed and investigated within the doctoral thesis (Table 3). The investigation will focus on development of single-skinned and double-skinned facades with integrated building systems and thin-film PV technology. The development will focus to technical as well as architectural aesthetics aspects, efficient construction design and aesthetic of detailing.

Table 3: Potential of BIPV within Timber-glass building envelope

Single-skin facade	Double-skinned facade	
	PV integration: Cold facade	PV integration: Warm facade
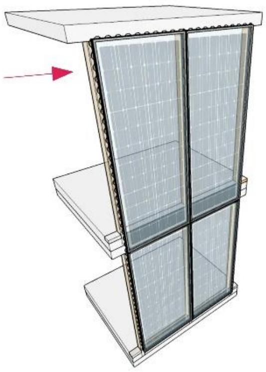	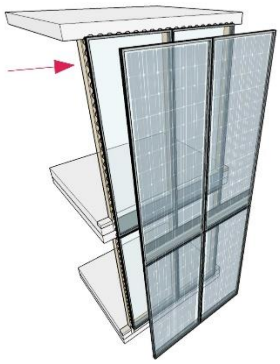	
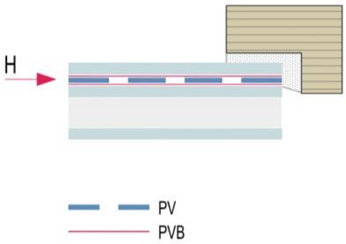	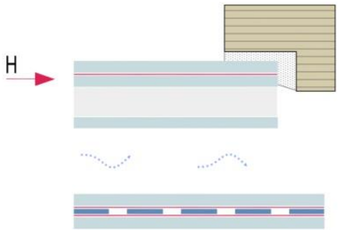	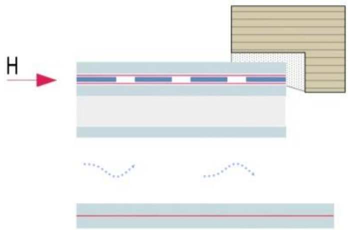
• The inner laminated glass pane is load bearing; • PV integration into load-bearing glass	• Inner layer: insulated glazing with load-bearing laminated glass • Outer layer: laminated safety glass • PV integration into outer layer of double facade	• Inner layer: insulated glazing with load-bearing laminated glass • PV integration into load-bearing glass • Outer layer: laminated safety glass

5 Outlook

The appearance of integrated technologies in the building skin creates a certain architectural language. Depending on a design of the building the visual representation of technology can evidence undesirable side effect that stands in contradiction to the sustainable goals it often refers for.

Besides that the wood based composite has a potential to provide an ecological alternative façade as the previous comparison study has showed that TGC has lower primary energy demand for its production and present much lower CO_2 emissions then conventional aluminum facade [11]; it provides a warm aesthetics of a natural material.

Defined potential for ventilation integration and building integrated PV into Timber-glass composite structure based façade will be detailed investigated within the doctoral thesis with the focus to functionality of different types of façade, aesthetics of detailing and thermal and building physics performance.

Considering the low-tech principle of composite with a potential for high performance, low-tech is seen as a goal concept for the Timber-glass based façade development.

The very early integration of design goals into development process can provide possibility to achieve high technical performance with desirable aesthetic quality. At the same time it poses a significant challenge especially designing with structural glass within hybrid structures. The issues of constructability, post-breakage behavior, maintenance and cost associated with replacement of elements must be considered. It's important to ensure that engineers and developers will not over-engineer the system in order to mitigate risk and the potential aesthetic quality will be taken into account. [10] In most cases, it is the detailing of assembly that will make or break the aesthetics of a design.

6 References

[1] Nicklisch F., Dorn M., Weller B., Serano E,; *Joint study on material properties of adhesives to be used in load-bearing timber composite elements*; ; in: Glass, Facade, Energy, at Engineered transparency, Düsseldorf, Germany, 2014; pp 271-280

[2] Hackspiel Ch., Fadai A.; *Timber-glass composite use as bracing system in wooden frame-houses*; in: Glass, Facade, Energy, at Engineered transparency, Düsseldorf, Germany, 2014, pp 281-290.

[1] Hochhauser W., Winter, W., Kreher, K.: Holz-Glas-Verbundkonstruktionen: State of the Art, Forschungsbericht, StudentischeArbeiten. Final report of the research project "*Holz-Glas-Verbundkonstruktionen: Berechnung und Bemessungskonzept*", Vienna, Vienna University of Technology, 2011.

[2] Hochhauser, W., Doctoral thesis: Ein Beitrag zur Berechnung und Bemessung von geklebten und geklotzten Holz-Glas-Verbunfscheiben, Vienna, Vienna University of Technology, 2011.

[3] Fadai, A., Winter, WJöbst R.A..: *Development of timber-glass composite for multi-storey facades,* in: Glass, Facade, Energy, at Engineered transparency, Düsseldorf, Germany, 2014, pp 301-210.

[4] Hausladen G., Saldanha M., Leidl P.: *Climate Skin. Building-skin Concepts that Can Do More with Less Energy*, Berlin, 2008.

[5] *Wahlseminar Konstruktiver Glasbau*, 254.094 at Vienna University of Technology, 2013

[6] Neubauer, G.: Doctoral thesis: *Entwicklung und Bemessung von statisch wirksamen Holz-Glas-Verbundkonstruktionen zum Einsatz im Fassadenbereich*, Vienna, Vienna University of Technology, 2011.

[7] Saleh Pascha K.: Wood-glass composite elements for Chilean building market, in: Glass, Facade, Energy, at Engineered transparency, Düsseldorf, Germany, 2014, pp 329-336

[8] Kooymans J.W.: *Engineered transparency in North America: The role of the engineer*; in: Glass, Facade, Energy, at Engineered transparency, Düsseldorf, Germany, 2014, pp 17-30

[9] Rosliakova V.: Architectural application and ecological impact studies of timber-glass composite structure, in: Glass, Facade, Energy, at Engineered transparency, Düsseldorf, Germany, 2014, pp 345-352

structural glass

Proceedings of the International Conference on Building Envelope Design and Technology, Graz
Advanced Building Skins 2015

Glass Building Skins: Presentation of the Research Project and Intermediary Findings

Vlad Alexandru Silvestru, Dipl.-Ing.
Institute of Building Construction, Graz University of Technology, Austria, silvestru@tugraz.at

Georg Helmut Erik Kolany, Dipl.-Ing.
Institute of Building Construction, Graz University of Technology, Austria, georg.kolany@tugraz.at

Oliver Englhardt, Univ.-Prof. Dipl.-Ing. Dr.nat.techn.
Institute of Building Construction, Graz University of Technology, Austria, englhardt@tugraz.at

Summary

Glass Building Skins is a research project running at Graz University of Technology in collaboration with the steel-glass-structures division of Waagner-Biro AG. The project focuses on transparent self-carrying building envelopes using the hybrid load-bearing behavior of glass-metal-structures. The main idea on which the project is based is the activation of the in-plane load bearing capacity of the glass panes, which are used only as infilling elements up to the present moment. In this paper an introduction of the research project along with the different work packages is given, the current state of the project is presented and an insight into first intermediary findings is provided. These first results deal with the mechanisms and the materials for transferring occurring loads between the metal frame and the glass pane in a single façade element. This paper is a report of the performed investigations and does not provide evaluated results.

Keywords: Transparent Facade, Structural Use of Glass, Structural Adhesive, Resin-based Grout, Plate Buckling

1 Introduction

Increasing requirements regarding the energetic and sustainable performance of building envelopes coupled with high geometrical complexity and the demand for maximal transparency lead to façade concepts, where the involved elements and materials are used at the highest possible level according to their properties. For building envelopes this can be translated in an increasing complexity during the processes of design, planning and production resulting both from requirements concerning building physics and performance as well as from optimized structural behavior.

An optimized structural behavior for glazed building envelopes is the main theme of the research project *Glass Building Skins*. The project, which runs over a timespan of three years and started in April 2013, focuses on transparent self-carrying building envelopes using the hybrid load-bearing behavior of glass-metal-structures. The Institute of Building Construction from Graz University of Technology collaborates with the steel-glass-structures division of Waagner-Biro AG and with the Laboratory for Structural Engineering from the same university to investigate an innovative structural concept for glazed facades. The glass panes, which are used in current envelopes as infilling elements and are considered only for bearing out-of-plane loads, are activated as well for in-plane loads by using the load-bearing capacity of the material glass. This step requires complex investigations of load-paths between the metal frame and the glass pane of one element as well as between several elements, selection of suitable materials for proper load-transfer as well as consideration of building physics related aspects.

Figure 1: Examples of transparent building skins with a potential structural use of the glazing: Cooperative Group Headquarters in Manchester (left) and Hofburg-Courtyard roofing in Vienna (right) [by courtesy of Waagner-Biro].

Figure 1 shows two examples of building envelopes, where the use of the glazing as a structural component could lead to achieving increased transparency and reduced material consumption for the frames. The methodology used in the research project to reach these goals includes theoretical, engineer-like analysis, numerical studies, experimental investigations and their comparative evaluation.

The funding of the research is covered by the Austrian Research Promotion Agency (FFG) and by Waagner-Biro Stahlbau AG.

2 Work packages and flowchart of the project

The aim of the investigations conducted in this research project is to provide a significant contribution for developing glass-metal structures with hybrid load-bearing behavior for building envelopes. The advantages of such structures are on one hand an increased transparency and on the other hand a decreased material consumption for the frames. According to the approved research proposal [1], the project is structured in six main work packages (WP) and each of them is subdivided in several sub-packages.

The six main work packages are listed and explained below. The relationship between them is shown in Figure 2 by a sequential arrangement.

- **WP 1: Actions and requirements:** The main loads acting on a transparent building envelope are investigated and the loads acting on a single element are determined. Additionally, the requirements for a transparent envelope resulting from the architectural concept, the structural design and especially the building physics are analyzed. These aspects serve as a basis for the investigations in the other work packages.

- **WP 2: Load transfer and assembling for a single element:** Existing load transfer types between the metal frame and the glass pane for loads acting in-plane and out-of-plane are analyzed. Numerical studies are performed for in-plane loads transferred by contact (setting blocks or resin-based grout) or by shear (adhesives). Adhesive connections are also investigated numerically for out-of-plane loads transferred by tension.

- **WP 3: Load-bearing behavior and load-bearing capacity of the glass pane:** First, research results for the buckling behavior of glass panes under different types of loading are analyzed. Afterwards, the influence of production imperfections, different glazing types (LSG, IGU) and glazing dimensions on the buckling behavior are investigated.

- **WP 4: Substructure and joining technology:** The influence of the frame stiffness on the load-bearing, stability and deformational behavior of a single element is investigated. Furthermore, details for the filigree frame profiles and the connection of several elements to each other are developed.

- **WP 5: Mechanical tests:** This work package contains all the mechanical tests which are performed within the research project. These are material-tests to determine the mechanical properties of the used load-transfer materials, connection-tests to investigate the behavior of the load-transfer materials under different loadings as well as multi-component-tests, which will illustrate the overall behavior of a single element with all its significant components.

- **WP 6: Behavior of several elements and design approach:** The findings of the performed detailed investigations are summed up and approaches for practical use are prepared. The behavior of envelope structures consisting of several elements is analyzed, possible simplifications for modelling are investigated and first concepts for a structural design are proposed.

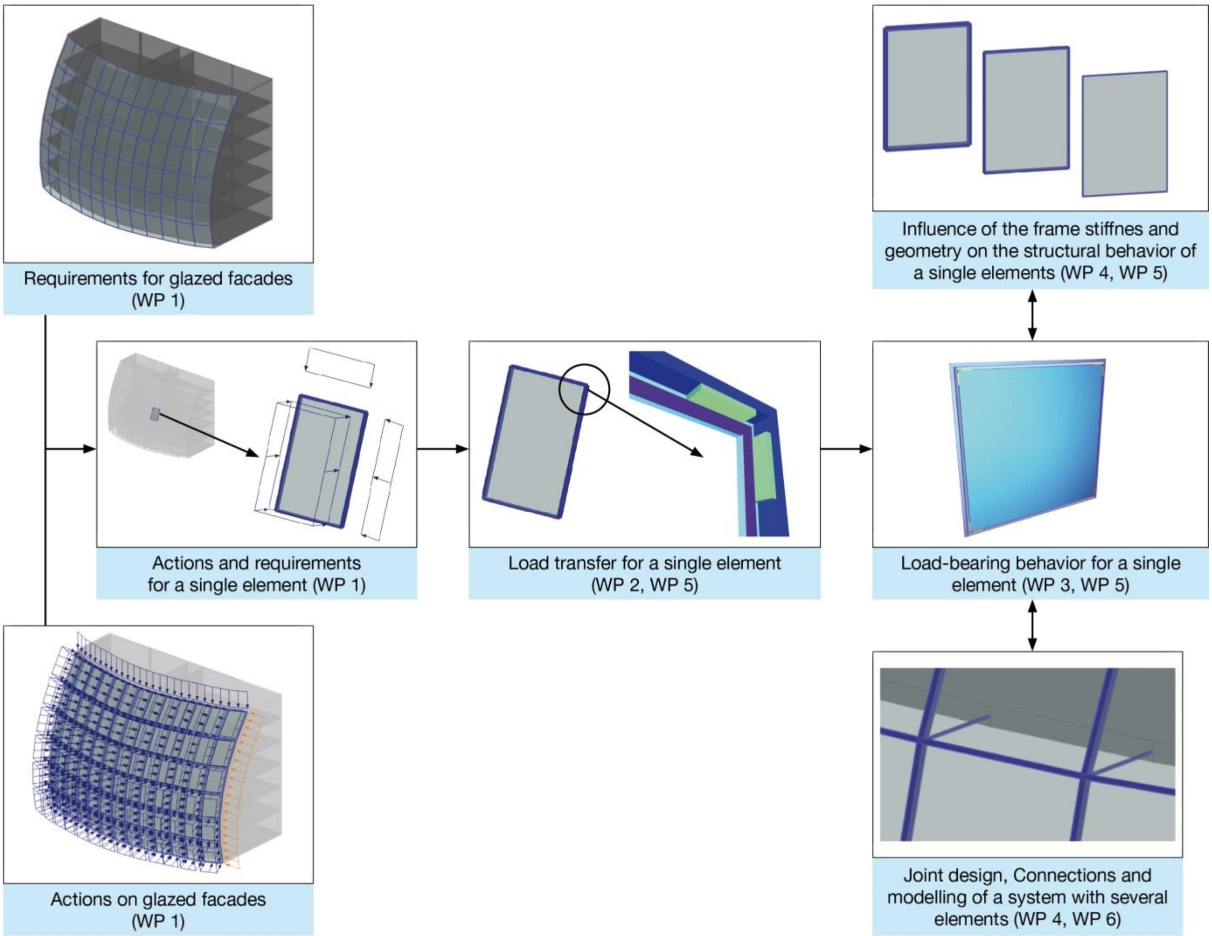

Figure 2: Flowchart of the project showing the different work packages and the relationship between them.

3 State of the art - existing related research results

The idea of activating the glass panes as bracing elements for transparent building envelopes has been mentioned in different research projects during the last decade. These projects focused either on the stability behavior of mostly square glass panes or on different materials which allow a reduction of occurring stress peaks at the glass pane supports. Although the investigations in the research project *Glass Building Skins* consider also building physics related aspects, the most significant state of the art findings are the two mentioned above.

Both for the stability behavior of a glass pane and for the properties of the load-transfer materials an important issue is the occurring loading. Therefore, Figure 3 shows for an exemplary façade the main possible loads resulting on a single element: out-of-plane wind suction or wind pressure and in-plane dead load of above lying elements, a diagonal stabilization load resulting from wind and thermal loads resulting from temperature differences and different thermal expansion coefficients of the materials.

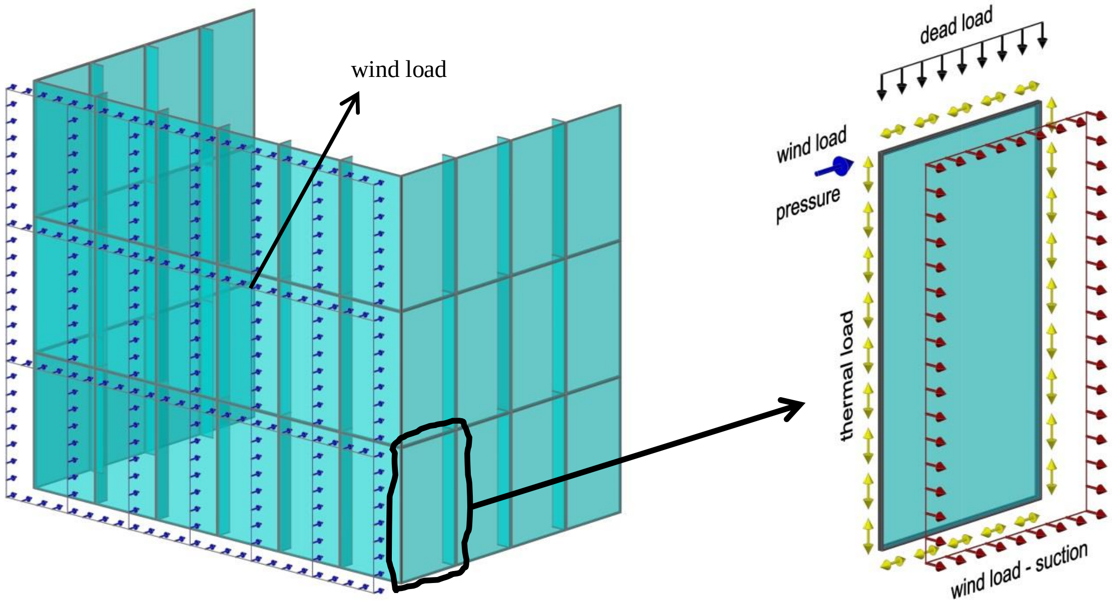

Figure 3: In-plane and out-of-plane loads which are considered in the research project.

3.1 Stability behavior of glass panes

Glass elements show usually a high slenderness. If they are used in a structural way, stability issues have to be considered during design. In the case of glass panes used in façades the stability problem which is occurring is plate buckling. Depending on the type of loading and on the boundary conditions different buckling shapes are formed. In Figure 4 the different loading possibilities are shown for a square glass element which is supported out-of-plane along all four edges.

Panes loaded only by compression have been investigated in [2] and [3]. In [3] the panes were either monolithic (4, 6 and 8 mm float glass or FTG) or laminated (2 x 4 mm HSG or 2 x 4 mm FTG) and had square (1.0 x 1.0 m) or rectangular (2.0 x 1.0 m) dimensions. The studies of the buckling and post-buckling behavior revealed the high load bearing capacity of glass panes and the occurrence of unexpected buckling shapes because of production imperfections.

The loading by shear of glass panes has been analyzed in [4] and [5] for square panes with an edge length between 1.0 m and 1.6 m. While in [5] only monolithic panes made of float glass have been tested, in [4] monolithic and laminated panes made of HSG as well as an IGU have been investigated.

These research projects focused on the behavior of the glass pane itself under the different loadings. In the project *Glass Building Skins* these findings will be extended for hybrid elements consisting of the glass pane and a surrounding filigree metal frame. Additionally, combined loads in-plane and out-of-plane for these elements will be investigated.

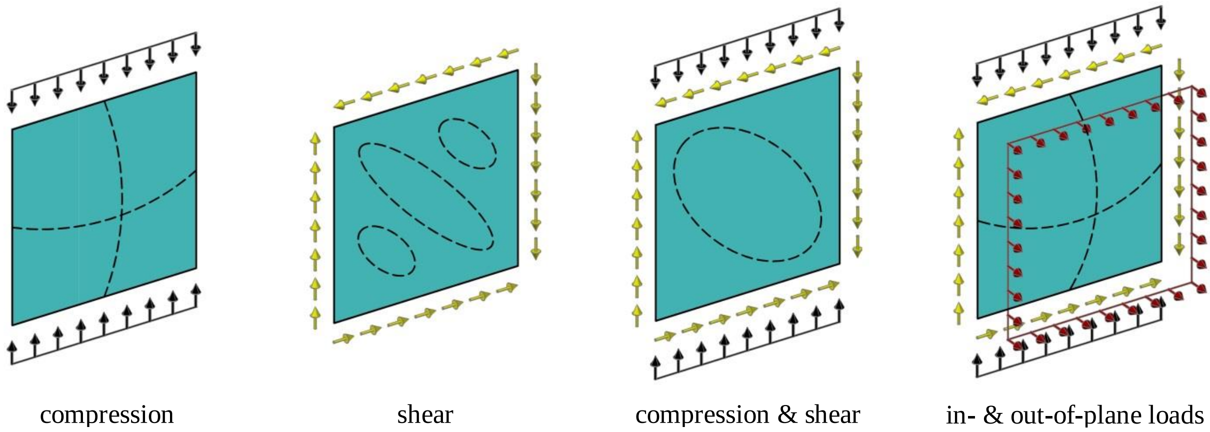

Figure 4: Different loading of glass panes in facades and their related buckling types.

3.2 Load transfer mechanisms

In the research projects mentioned in the previous subchapter different materials were used to support the glass panes in-plane. Englhardt [3] used setting blocks made of POM for applying the compression loads. Wellershoff [4] used both an injection grout to apply the diagonal loads at the corners of the glass pane as well as an adhesive to apply a shear loading circumferentially. Huveners [5] investigated different adhesive types and positions for applying a circumferential shear loading. These mechanisms are illustrated in Figure 5.

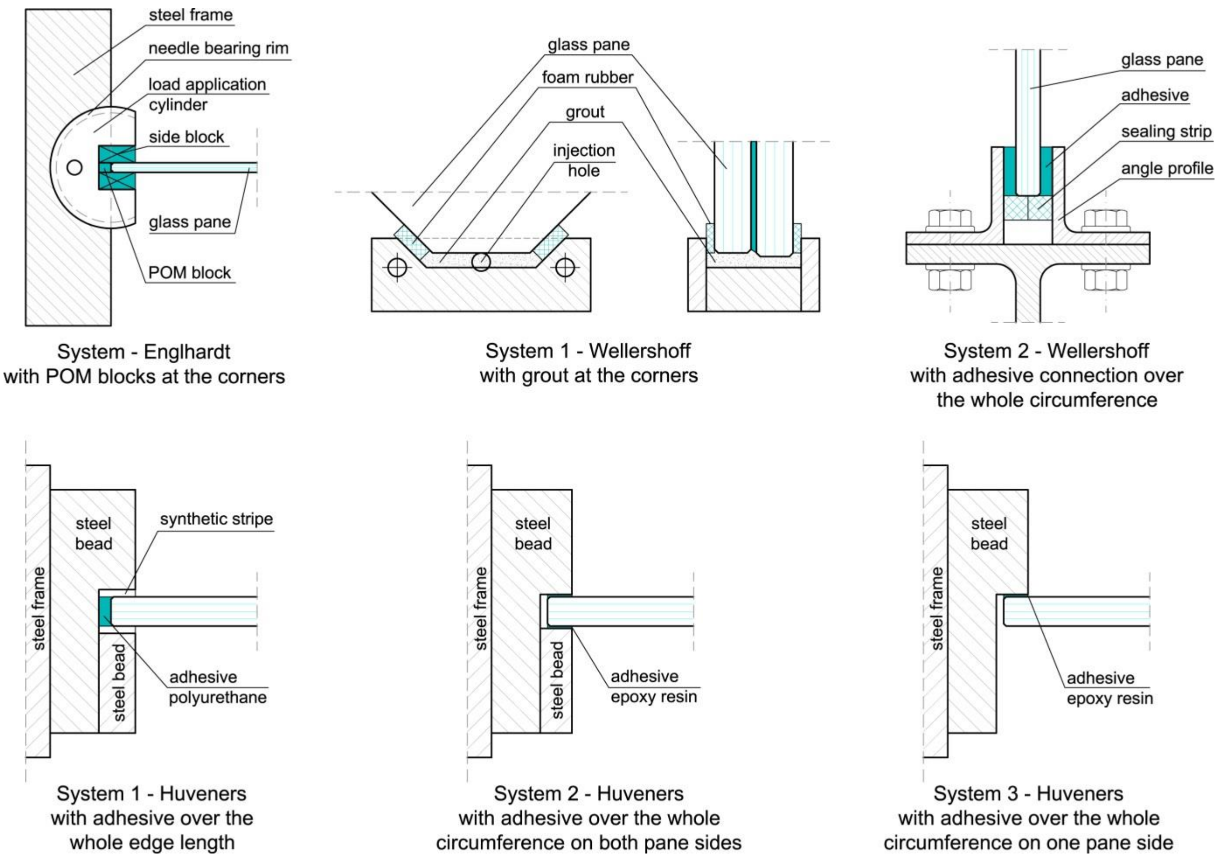

Figure 5: Different support type used for the buckling analysis of glass panes in [3], [4] and [5].

The investigated materials showed both advantages and disadvantages. For instance the setting blocks are suitable for applying high loads into the glass pane, but are not able to compensate edge offsets of laminated glass. Adhesive connections as in the system 2 investigated by Wellershoff as well as in the system 2 by Huveners show a good load-bearing and stability behavior of the glass panes. The disadvantage is adhesives showing high shear stiffness are not approved for the structural use because of durability and weathering issues.

In *Glass Building Skins*, the strengths and the weaknesses of existing load transfer systems and materials are evaluated and based on the results new materials are chosen and investigated or new systems are developed.

4 Current state of the project and intermediary findings

As usual for research projects of this size the labor time distribution between the work packages differs in reality compared to the approved proposal. The main reasons for this are findings during the progress of the project, which show the need for detailed investigations of certain aspects. In the case of *Glass Building Skins* these aspects were the properties of the considered load transfer materials and the behavior of these materials in connections under different loadings. Therefore, after completing the first work package and evaluating the findings, which serve as criteria for the material selection, the focus was pointed on bulk material properties and connections with these materials.

The materials selected for investigation can be divided into two main categories:

- Materials for load transfer by compression at the glass edge: In this category a resin-based grout and a thermoplastic (POM) have been chosen, both of which are already used in practice for applications with structurally used glass. Nevertheless, the existing material data is limited especially for multi-axial loading cases, where the material deformation is restrained in certain directions.

- Materials for load transfer by tension and/or shear at the glass edge or at the glass surface: This category includes adhesives with structural properties. For investigations within the project two structural silicones, which are approved for SSG facades, as well as an acrylate were selected. For the more flexible silicones there already exists certain knowledge, but there is still need for analysis regarding adhesion to different surface finishing of metal components and regarding combined loading. For the acrylate, which is able to reach higher shear stiffness, moisture sensitivity is an issue and investigations for a suitable material model are missing.

4.1 Investigations of bulk material properties

In a first step basic mechanical properties of the selected materials were determined by bulk material tests. The obtained results were used to verify existing data as well as to add missing parameters and serve as a basis for developing suitable material models.

For the resin-based grout short-term (Figure 6 left) and long-term (Figure 6 center) uniaxial compressive tests have been performed. The used test specimens were rectangular prisms with section dimensions of 10 x 10 mm and a height of 20 mm. In the short-term tests the short-term Young's modulus ($E_{mean} \approx 2500$ N/mm^2), the Poisson's ratio ($\mu_{mean} \approx 0.40$) and the compressive strength ($f_{c,mean} \approx 75$ N/mm^2) have been determined. The long-term tests were used to investigate the creeping and the resilience behavior. Afterwards, short-term tests have been performed on the long-term loaded specimens to determine the changing of the before mentioned values. Detailed information on the testing procedure and the results can be found in [6].

The mentioned thermoplastic has been investigated under compression loads in [7]. For both materials the 4-parameter Burger-model [8] can be used as a first approach.

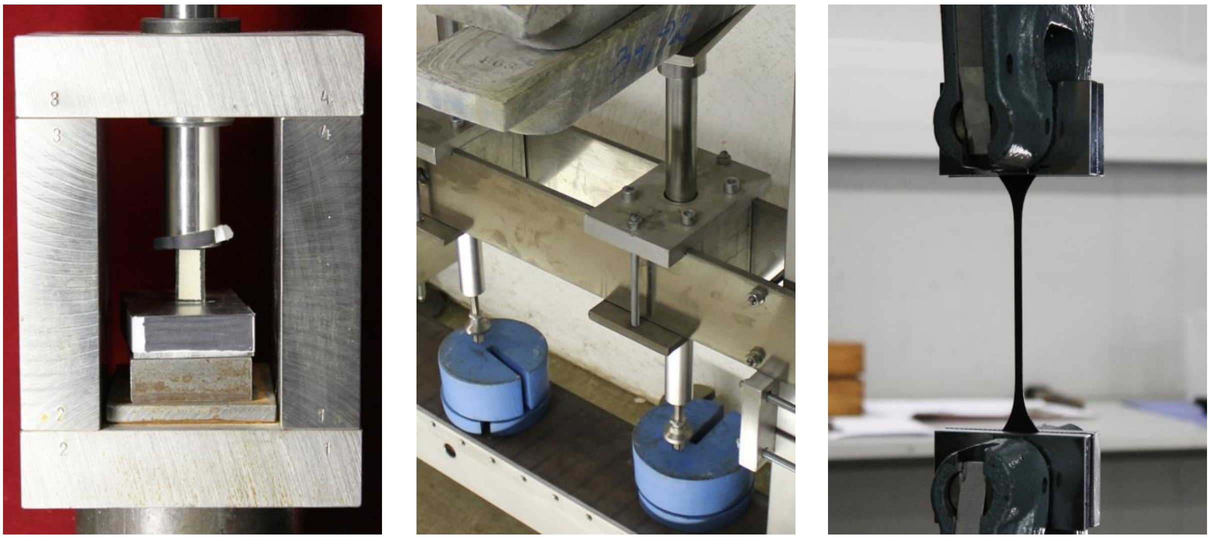

Figure 6: Short-term and long-term uniaxial compressive test on prisms made of a resin-based grout (left & center); uniaxial tensile test on dumbbell specimens made of silicone and acrylate adhesives (right).

For the selected adhesives most of the required properties are available either from technical data sheets or from the producers. Uniaxial tensile tests on dumbbell specimens of type 2 (see Figure 6 right) have been performed according to [9] with the aim to obtain an own data set for comparison with the existing data and as an input for material models used in numerical studies. The silicones showed tensile strength values of approx. 2.3-3.0 N/mm^2 and Young's moduli for low strains of about 1.5-2.1 N/mm^2. The tensile strength of the acrylate averaged approx. 10.0 N/mm^2 and the Young's modulus approx. 180 N/mm^2. Detailed information on the tests and the investigated material models can be found in [10]. For the silicones hyper-elastic models are suitable (Arruda-Boyce or Mooney-Rivlin), while for the acrylate a multi-linear model shows a good agreement.

4.2 Investigations on connections

In a next step experimental and numerical studies of the selected materials in connections between metal components and glass panes have been performed. The aim of these investigations is to verify the chosen material models as well as to analyze the performance of the materials in applications similar to the ones planned to occur in hybrid glass-metal elements for building envelopes.

Figure 7: Compressive test performed on contact connections between glass and steel with a resin-based grout and with a thermoplastic (left); shear test on adhesive connections between glass and stainless steel (right).

For the resin-based grout and the thermoplastic compressive tests, where the material deformation is restrained in the direction of the width, have been performed (see Figure 7 left). The grout and the thermoplastic have been fixed in a steel bracket, while a glass pane was pressed against them. Different dimensions of the load transfer material were investigated. For the glass pane both monolithic FTG and laminated safety glass made of FTG have been used in different thicknesses. Both, the grout and the thermoplastic, show plastic deformations at high loads. A detailed evaluation of the results is currently running.

The selected adhesives were tested in tension and shear for connections between stainless steel components and glass pane surfaces. The specimens tested in tension were single-lap joints, while the ones tested in shear were double-lap joints (see Figure 7 right). The reason for the double-lap is to avoid a rotation of the specimen during loading. The stainless steel showed a grinded surface finishing with a corn size P300. All the bonded surfaces were appropriately cleaned and the stainless steel surface has been also treated with a primer before applying the adhesives. Both silicones showed only cohesive failure under tension and under shear. In the case of the acrylate mixed cohesive-adhesive failure on the glass surface could be observed for some specimens tested under tension while for some specimens tested under shear adhesive failure occurred on some glass surfaces. The reason for this is still to be investigated. The evaluation of the reached strengths and stiffnesses as well as a comparison with numerical models is currently running.

5 Outlook

The research project *Glass Building Skins* aims to provide a significant contribution for an optimized structural use of the material glass in future transparent building envelopes. To achieve this goal three main aspects are considered to be essential: the materials and mechanisms used to transfer loads between the metal frame and the glass pane, the load-bearing and stability behavior of the elements consisting of a glass pane and a filigree metal frame and the joints and load transfer between several elements. The investigations performed until now within the project cover the first aspect and summarize the state of the art for the second aspect.

The next steps will be to finish the evaluation of the performed connection tests and with the obtained findings to proceed to the development of a hybrid glass-metal element for transparent building envelopes. This element will then be analyzed by numerical studies from a structural point of view. Also experimental tests on such elements under combined loading are planned. In a final step design concepts for the joints between several elements as well as approaches for a structural analysis of a single element and of several elements will be elaborated.

6 Acknowledgements

The authors would like to acknowledge the collaboration with the steel-glass-structures division of Waagner-Biro AG and with the Laboratory for Structural Engineering at Graz University of Technology on the research project *Glass Building Skins – Transparent self-carrying building skins with the application of the hybrid load-bearing behavior of glass-steel-structures*. The financial support for this research project is partly covered by the FFG (The Austrian Research Promotion Agency) and partly by Waagner-Biro Stahlbau AG. Sika Services AG, Dow Corning GmbH and Hilti Deutschland AG are gratefully acknowledged for the support with information and material for the test specimens.

7 References

[1] Englhardt, O.: *Glass Building Skins – Transparente selbsttragende Gebäudehüllen unter Einsatz der hybriden Verbundtragwirkung von Glas-Stahl-Konstruktionen*, FFG Bridge-programme, research proposal nr. 3262171, 2012.
[2] Luible, A.: *Stabilität von Tragelementen aus Glas*, PhD Thesis, EPFL Lausanne, 2004.
[3] Englhardt, O.: *Flächentragwerke aus Glas – Tragverhalten und Stabilität*, PhD Thesis, BOKU Vienna, 2007.
[4] Wellershoff, F.: *Nutzung der Verglasung zur Aussteifung von Gebäudehüllen*, PhD Thesis, RWTH Aachen, 2006.
[5] Huveners, E.M.P.: *Circumferentially Adhesive Bonded Glass Panes for Bracing Steel Frames in Facades*, PhD Thesis, Eindhoven University of Technology, 2009.
[6] Kolany, G.H.E., Silvestru, V.A., Englhardt, O.: *Long-term behavior of a synthetic resin mortar under compressive stress*, in: engineered transparency. International Conference at glasstec, pp. 221-230, Düsseldorf, 2014.
[7] Ebert, J.: *Einleitung hoher Lasten in Glaskanten – Ein Beitrag zum Einsatz von Kunststoffen als Klotzungsmaterial*, PhD Thesis, TU Dresden, 2014.
[8] Ehrenstein, G.W.: *Polymer-Werkstoffe*, 3rd Edition, Carl Hanser, Munich, 2011.
[9] ISO 37: *Rubber, vulcanized or thermoplastic – Determination of tensile stress-strain properties*, 2011.
[10] Silvestru, V.A., Kolany, G.H.E., Englhardt, O.: *Analyses on loads and adhesives for hybrid glass-steel façade structures*, in: engineered transparency. International Conference at glasstec, pp. 581-591, Düsseldorf, 2014.

Glazed Link, complex geometry stainless steel artwork supported by structural glass walls

Thomas Henriksen, M.Sc Eng CEng MIStructE
Waagner-Biro Stahlbau AG, Austria, thomas.henriksen@waagner-biro.at

Andreas Fritsch, Dipl.-Ing. Dr.
Waagner-Biro Stahlbau AG, Austria, andreas.fritsch@waagner-biro.at

Summary

For the Glazed Linked building in Manchester designed by UK-based Architect Ian Simpson, Waagner-Biro designed and built a glass building consisting of a freeform mirror polished stainless steel roof supported by 20 glass panels acting as the buildings walls. The glass panels provide both axial stiffness as well as lateral stiffness, and therefore work as primary structural elements. This paper explains the design methodology which was followed to get the complex structural system to work and implications on the manufacture of the laminated glass panels. The structural system for the glass walls are in general semi pinned columns. The glass panels are bonded in top and bottom to a stainless steel shoe which provides the building with its lateral stiffness. Considering the self-weight of the mirror polished stainless steel roof of 27 tons, supported by 7.5 m tall glass walls (at a total building height of 8 m), this glass structure is unique compared to other glass structures previously constructed. The foot print of the building linking the Central Library with the Town Hall Extension is approximately 120 m2, whereby both ends of the building consist of 6 curved glass panels, and straight glass panels are located in the middle part. The mirror polished stainless steel roof was lowered on the glass and the building was finalised in May 2014.

Keywords: Glass, Complex geometry, Artwork, laminated glass, mirror polished stainless steel

1 Introduction

The Glazed Link building, Library Walk in Manchester, UK is designed by UK-based Architect Ian Simpson. The building is meant to link the Manchester City Library and the Manchester City Town Hall together (see Figures 1-2). Waagner-Biro won the design and build competition in August 2012. The design work commenced in January 2013 and the installation on site started in October 2013, the last glass element was installed in May 2014 and the roof was lowered onto the glass. The building is scheduled to open in spring 2015. Glazed Link is considered to be a non-heated building, and thus the glass walls are single laminated glass panels. It consists of two elements, a mirror polished stainless steel roof which is supported by glass walls. The glass walls are the primary structural elements and carry the weight of the roof and the live loads applied to the roof.

Figure 1: Glazed link building when the last glass element was installed.

The original scheme of the Glazed Link building consisted of segmented glass walls with glass fins to prevent the segmented glass from buckling. During the design stage Waagner-Biro proposed to replace the segmented glass walls and glass fins with continuous glass walls. The latter allow for transferring the forces from the overturning moment due to wind to the foundations directly. Thereby, the continuous glass walls act as shear walls.

The Glazed Link building consists of 26 glazing elements. 20 of these elements are load bearing, whereas the remaining 6 glazing elements are positioned over the access doors in the front and back of the building and over side doors which access the Manchester City Library and the Manchester City Town Hall. The setting out of the building is shown in Figure 2.

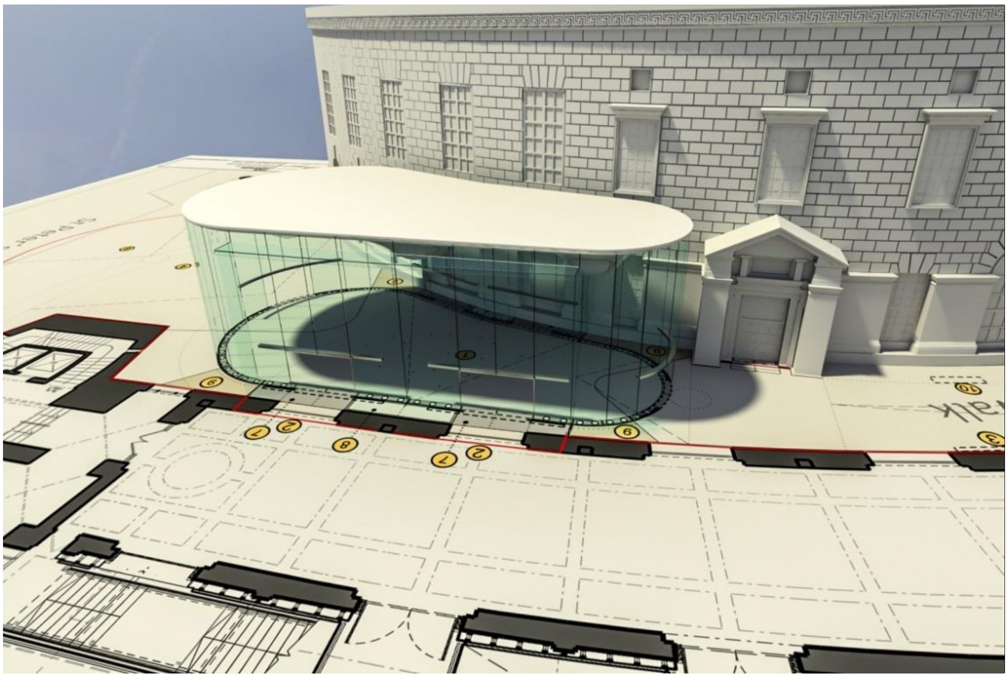

Figure 2: Perspective view of Glazed Link building.

The aim of the present paper is to analyse and evaluate which structural system is most suited to accommodate the applied live loads on the building. The paper discusses and concludes on the necessary tests to support the assumptions made for the chosen structural system, and recommends further testing to understand the load transfer in the connection details.

2 Glazed Link structural system

The structural system for the Glazed Link building is based on a similar structural system used on the work of Art "Your Rainbow Panorama" on the ARoS art museum in Aarhus, Denmark [1] [2]. On the ARoS project the glass is the only primary structural element supporting the roof. The roof is considered as a stiff plate which distributes the wind load and other horizontal forces in the roof plane to the glass walls parallel to the horizontal force. The glass walls work as shear walls and transfer the load from the roof plane to the substructure, thus providing lateral stability to the building. The glass walls of the Glazed Link building are also the only primary structural elements which support the roof.

For the Glazed Link building the appropriate structural system was evaluated amongst the design team because of the height of the panels being approximately 8 m which is significantly higher than the panels used on the ARoS building. At the same time, the glass on the Glazed Link building supports a mirror polished stainless steel roof with a weight of approximately 27 tons. The glass wall has to accommodate two main load conditions:

- Axial load from the weight of the steel roof
- The overturning moment from wind load on the building

The axial load in the glass panels from the weight of the roof is the most critical load. Since the roof steel structure is free formed shaped, it has a changing stiffness along its length giving different reactions to the glass panels. The calculated reaction forces from the steel roof are shown in Table 1. The maximum in-plane force in the flat panels was calculated to be 3,6 kN, based on a total load in the roof plane of 28,5kN, and the 28,5kN equally distributed between the 8 flat glass panes perpendicular to the main wind load direction.

Table 1: Vertical reaction forces in the glazing from the steel roof.

Pane	ST1	ST2	ST3	ST4	ST5	ST6	ST7	ST8	ST9	ST10
Max [kN]	39.3	29.1	**95.8**	74.9	33.8	43.9	44.1	22.9	82.0	88.2
Min [kN]	3.3	1.6	1.9	1.5	4.2	5.5	5.3	2.7	3.5	**0.1**

Pane	ST11	ST12	ST19	ST20	ST21	ST22	ST23	ST24	ST25	ST26
Max [kN]	31.3	32.1	48.4	27.9	32.6	28.0	53.3	28.7	31.9	36.9
Min [kN]	1.6	3.9	10.6	1.5	1.0	0.8	8.8	6.4	4.8	0.5

The temperature load combined with the dead load of the roof is the most critical load combination. The temperature load causes the end of the stainless steel roof to lift up, and it concentrates the dead load of the roof to the straight centre panels of the Glazed Link building. At the same time the centre panes also provide the main lateral stability of the building. From Table 1 it can be seen that the maximum downwards load is 95.8 kN. To transfer the dead load from the roof to the glass, from the glass to the steel shoe, and from the steel shoe to the concrete slab, three different support conditions were considered, see Figure 3:

(1). Two support points between roof and top of glass pane, and two support points between glass pane and steel shoe.
(2). One support point between roof and top of glass pane and two support points between glass pane and steel shoe.
(3). One support point between roof and top of glass pane and one support points between glass pane and steel shoe.

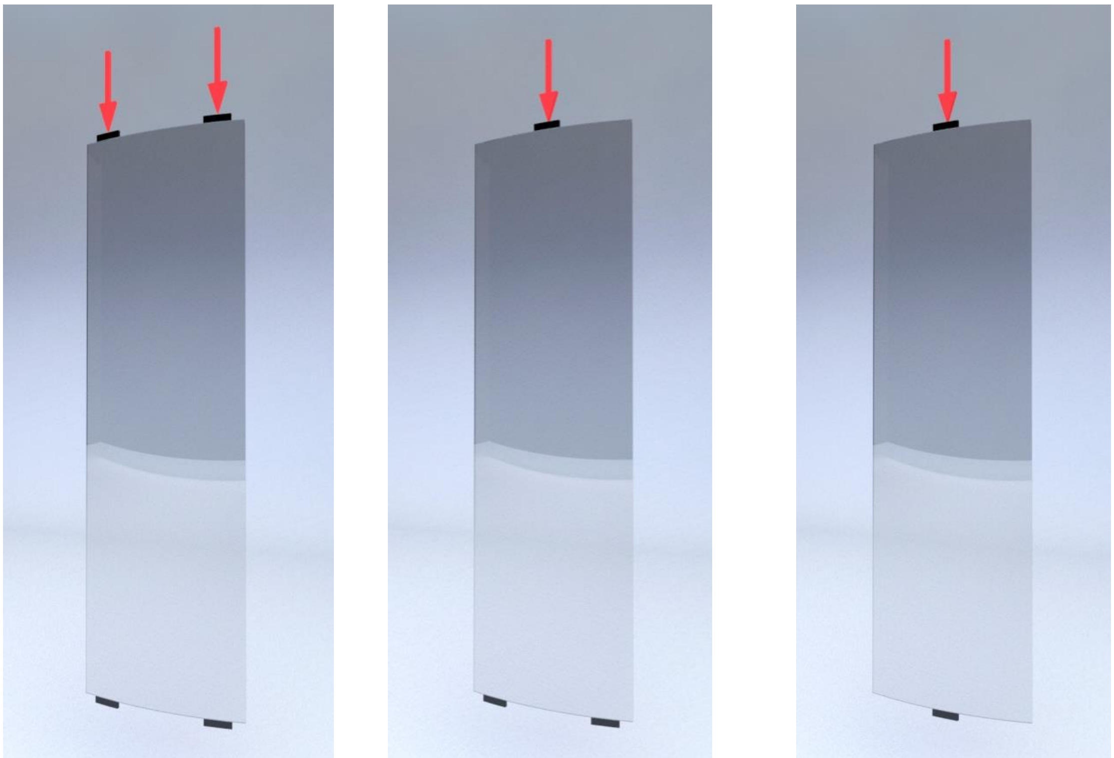

Figure 3: Support conditions for roof weight load transfer.

Options (1) and (2) do restrain the glass from moving and prevent the silicone in the steel shoe to be engaged. Therefore option (3) was implemented with the glass being supported centrally and the load applied centrally on top of the glass. For the lateral stability of the Glazed Link building two different solutions were considered.

1. A structural system with a mechanical fixing between the stainless steel shoes at top and bottom, and the glass
2. Bonded connection between the steel shoe and the glass, where the structural silicone would be used as bonding material.

The two systems for the lateral stability considered for the Glazed Link building are shown in Figure 4.

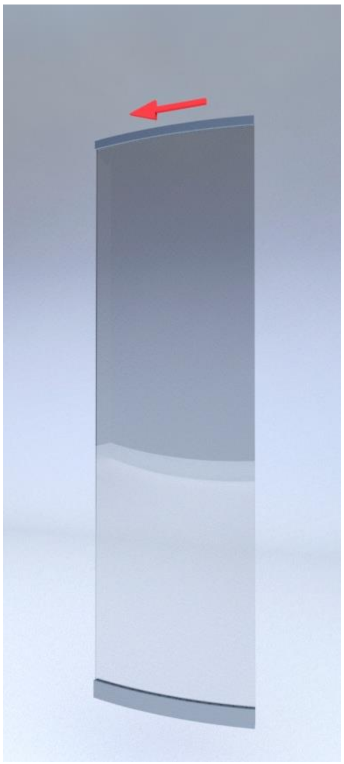


Figure 4: Structural systems for lateral stability

The two different systems providing lateral stability were described in the research work by Mocibob [4]. The mechanical fixed system is based on holes drilled in the glass, requires less maintenance and at the same time the load transfer from the building's overturning moment is determined. The mechanical fixing, however, is prone to stress concentrations in the glass which could exceed the ultimate stress level and cause breakage. The pros and cons of the mechanical fixing system are shown in Table 2.

Table 2: Pros and cons of the mechanical fixing system.

Pros	Cons
Determined force flow	Stress concentrations in glass
Little maintenance necessary	Bolt holes in glass
Long design life	

The bonded system (see Table 3) relies on the glass being bonded to the stainless steel shoe, and the stiffness of the system is determined by the stiffness of the bond. The glass is bonded to the stainless steel using a structural silicone. The bonded system acts as a spring under each glass panel and allows the horizontal forces in the roof plane to be transferred through the glass wall with the most stiffness. This allows the building to flex and the glass panels are not subjected to stress concentrations in bolt holes in the glass. The structural silicone used for the bonding between the glass and the stainless steel shoe has a more limited design life than the mechanical fixing, however the structural silicon has been in service for 25 years [5] and is considered as a durable material.

Table 3: Pros and cons of the bonded system.

Pros	Cons
Avoid stress concentrations in glass	Undetermined force flow
Allow building to flex	

To avoid stress concentrations in the glass from a mechanical fixing via bolt holes, the bonded system was chosen for the Glazed Link building. This required a detailed calculation of the connection between the glass and the stainless steel shoe, since the bonded connection has to accommodate the uplift force from the overturning moment combined with a potential uplift force from the roof structure. From Table 1, however, it can be seen that the minimum load from the roof structure is 0.5 kN. Therefore, the bonded connection only has to accommodate the load from the overturning moment.

3 Test of connection detail

The bonded connection between the glass and the stainless steel for the Glazed Link building required a significant height to be able to accommodate the calculated uplift force. The bottom steel shoe was designed to be semi-rigid, since a full rigid bottom connection is not possible with the silicone bonding. This combination had not been tested before. To confirm the bonding strength of the connection between the stainless steel and the glass, pull out test were performed. A test method was developed to resemble the bonded bottom steel shoe. The test sample consisted of a 770 mm x 330 mm and 15 mm thick glass plate, bonded to a stainless steel shoe, with a bonded area of 230 mm x 370 mm. The glass would then act as a beam and the stainless steel element was fixed to the pull out machine which applied the pull out force. The test setup as shown in Figure 5 was used to test the bonding strength between the glass and stainless steel.

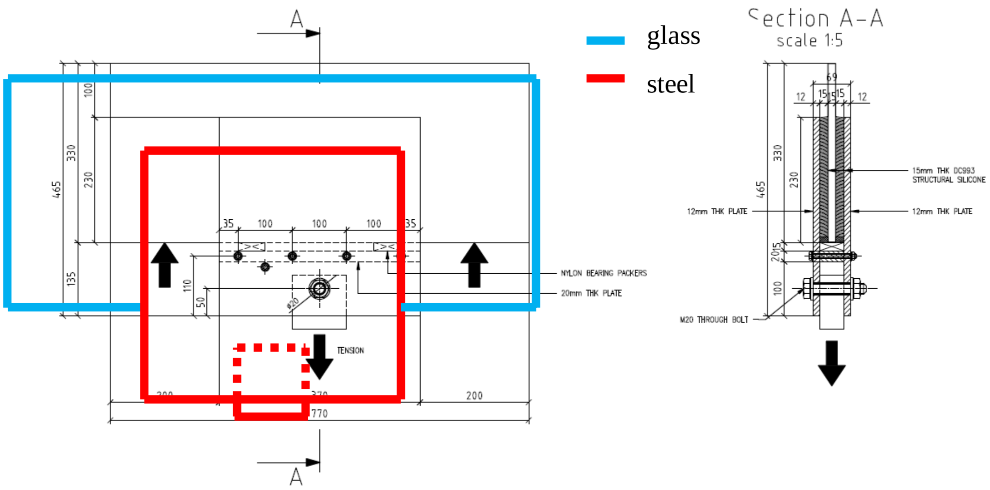

Figure 5: Setup for testing the bonding between the glass and the stainless steel

The test was carried out using three test specimens. The testing rate of the pull out was set to 5 mm/min corresponding to a quasi-static load. The structural silicone samples had been cured for 15 days before the test had commenced. The structural silicone used in the test was DC993.

DC993 is a two component silicone which cures relatively fast, however because of the large bonded area it would have an effect on the curing process of the silicone because the chemical processes in the silicone are slowed down due to the height of the stainless steel shoe. The tested sample after the pull out is shown in Figure 6.

Figure 6: Test sample after the approved test: the failure mode is cohesive.

The pull out forces was tested to maximum load of 141,5kN, all the test results gave a test stress above the allowable design stress (see Table 4) if a safety factor of 4 is applied according to ETAG002 [6]. The shore hardness of the test specimen was measured to Shore 25 at the edges and shore 15 in the middle. The shore hardness of fully cured DC993 is approximately 40 Shore. From the pictures it can be seen that the failure mode was cohesive, which indicates that the bond between the stainless steel and the structural silicon was sufficient. The 2 lines in the test sample were perforated tubes used to accelerate the curing process of the silicone. It was estimated that the sample would need 6 weeks to fully cure due to the height of the steel shoe. The test conclusion was positive, since there was a complete cohesive failure. As part of the test stainless steel with a different surface treatment was also tested, however the silicone had problems with adhesive failure and the surface treatment was rejected. As a consequence of the failed test with the lower surface treatment a test program was initiated with Graz University of Technology to investigate the influence of the surface treatment of the stainless steel with the structural silicone.

Table 4: Results from the pull out test.

	Sample 1	Sample 2	Sample 3
Pull out load	141,5 kN	114,4 kN	118,6 kN
Test speed	50 N/s	5 mm/min	5 mm/min
Material stress	0,83 MPa	0,67 MPa	0,70 MPa

4 Conclusion

In the paper, the Glazed Link building in Manchester, UK has been presented. The structural concept for glass as primary structural elements has been analysed in terms of the vertical load from the weight of the stainless steel roof and the horizontal load from the wind acting on the Glazed link building. It has been shown that the maximum vertical design load from the roof combined with the horizontal load from the wind can be accommodated by the glass walls. It has been shown how the loads are transferred from the roof plane through the glass down to the concrete slab. The structural system for the lateral stability was solved by engaging the structural silicone in the steel shoes. The bonding between the stainless steel shoe and the glass was tested and the test result showed that the bonding strength was higher than the required design stress. However from the test it was acknowledged that the curing time for a deep bonding height is significant higher than a normal structural bonding of 40 mm. For future reference, a lower bonding height is recommended or alternatively sufficient curing time is necessary before testing the samples. Additional tests will be carried out to further understand the relationship between the surface condition of the stainless steel and the structural silicon. For this reason, a test program has been initiated with Graz University of Technology in terms of the bonding between stainless steel and the glass. Results are expected in spring 2016.

5 Acknowledgements

Waagner-Biro would like to thank Laing O'Rourke, Ian Simpson Architects and Manchester City Council for the collaboration on this project. In addition, Waagner-Biro would like to thank EOC and John Colvin for their support.

6 References

[1] Henriksen, T.: *ARoS, Your Rainbow Panorama,* GPD 2009 – Glass Performance Days, Tampere, Finland, 2009.
[2] Henriksen, T.: *Engineers Construct Art*, in: Pottgieser, U., Strauss, H. (editors): *Product Development and Architecture*, Birkhäuser Verlag, Basel, 2013.
[3] Mocibob, D.: *Glass Panels under Shear Loading* **-** *Use of Glass Envelopes in Building Stabilization.* PhD thesis, École polytechnique fédérale de Lausanne, 2008.
[4] Carbary, L.: *A Review of the Durability and of Performance Silicone Structural Glazing Systems*. GPD 2007 – Glass Performance Days, Tampere, Finland, 2007.
[5] Haldimann, M., Luible, A. and Overend, M.: *Structural Use of Glass.* Zurich : IABSE, 2008.
[6] ETAG002 Part 1, Guideline for Europen Technical Approval for Structural Sealant Glazing Kits, EOTA, May 2012

Structural glass applications & design considerations

Timo Bühlmeier, Dipl.-Ing., Design Development Manager
Josef Gartner GmbH, Germany, timo.buehlmeier@josef-gartner.de,
www. josef-gartner.de

Summary

The use of structural glass elements like glass fins, glass columns and glass beams evolved to commonly used façade systems for highly transparent building enclosures and other structural systems.

Based on recent Josef Gartner projects like World Financial Center and Columbia Medical Center the general approach and design process regarding design development and technical challenges of structural glass elements will be shown. Furthermore the application of new connection technologies for glass fins will be discussed with the example of the ongoing project Square One Shopping Center.

The paper gives an overview about several structural glass projects of Josef Gartner and is an experience report how innovative & transparent structural glass applications can be realized with the currently available knowledge of research projects, engineering tools and project specific testing.

Keywords: structural glass elements, glass fins, glass beams, splice joints, bolted glass-glass connections

1 Introduction

The paper will discuss structural glass elements which are typically non-membrane elements and mainly multi-laminated glass elements highlighting their characteristics and the requirement for a design approach combining finite element analysis, analytical methods and project specific testing. In contrast, standard cases can be usually dimensioned by simplified procedures and related publications.

Furthermore, the constructability of long spanning structural glass elements will be shown on project examples. Due to limited available size of multi-laminated glass elements, it is required to join long spanning glass elements with connections of minimal visibility and in accordance with the architectural design intent at structurally appropriate locations. Exemplary different load bearing connections will be described, starting with traditional steel splice joints towards bolted glass-glass connections without any external steel bracket. Specialties of the different connection designs will be highlighted and test results discussed.

2 General design development

2.1 Producibility of large laminates

Glass fins and glass beams are usually designed as very slender structural glass elements causing limitations due to the production process. Already the tempering process of the glass limits the height/ depth ratio to reasonable values mostly below 20. As most structural glass elements consist of multi-laminated and tempered or heat strengthened glass elements, the available size of the autoclave is another important boundary condition defining the producible size of laminates. Most manufactures, with few exceptions, are limited to maximum lengths up to approximately 8000-9000mm. Additionally, the overall thickness of the laminate and its implications must be considered as the lamination process requires amongst others sufficient heating of the interlayers to ensure appropriate and permanent bonding of the single glass layers. In some cases it is architecturally intended to shape structural glass elements tapered according to their internal load distribution. These specific shapes require cutting respectively machining and therefore careful assessment of the glass supplier's production capabilities.

Due to the mostly limited available size of multi-laminated glass elements, it is required to join those long spanning glass elements with connections of minimal visibility and in accordance with the architectural design intent at structurally appropriate locations. The figures show typical options which can be applied:

- Splice joint with external steel connectors located at mid span of a single span beam/ fin
- Splice joint with external steel connectors located in the third sections of a single span beam
- Choice of a structural system allowing for splices in less stressed areas either with external steel connectors or via bolted glass-glass solutions

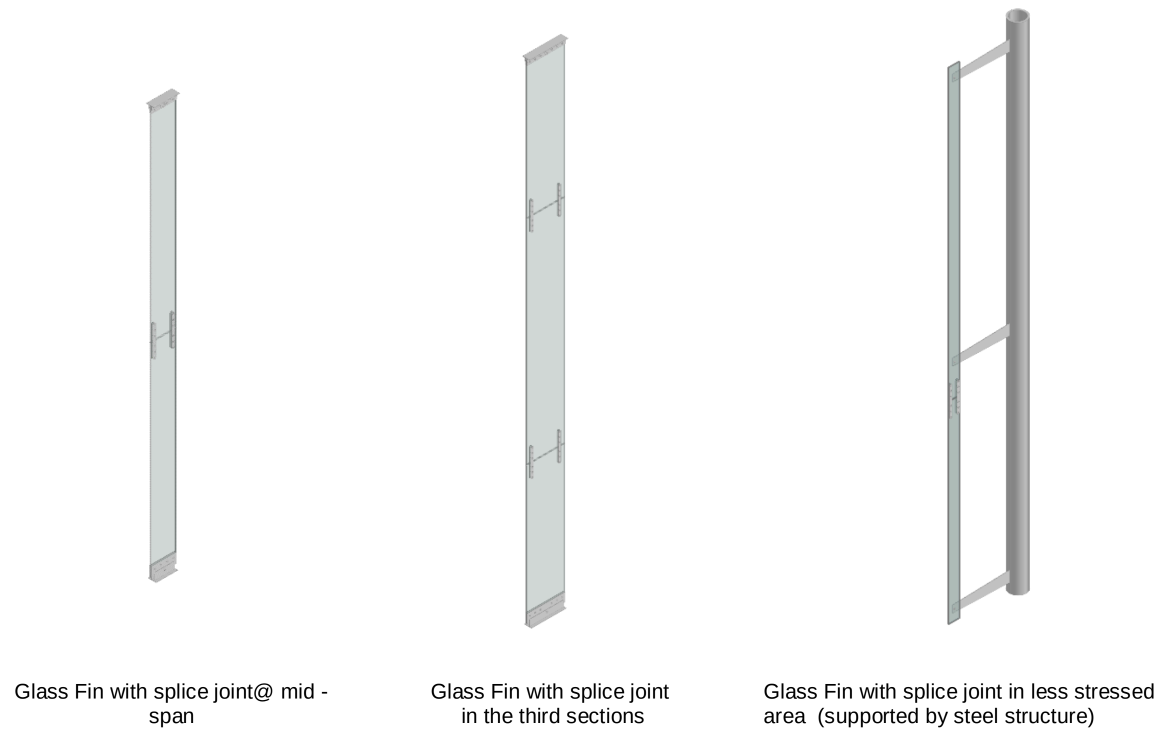

Figure 1: Various glass fin options

2.2 Specific design considerations

The design of structural glass elements like beams, fins and columns is mainly driven by stability issues (buckling, lateral torsional buckling), stress concentrations at connections and at glass edges as well as an appropriate consideration of the compound effect of the multi-laminated glass elements. Therefore the structural design of such advanced elements requires a good understanding of the material glass. Furthermore, it implies an approach based on scientific research and project-specific testing due to the absence of generally agreed design procedures respectively the lack of standards for such demanding structural glass applications.

Edge strength

Structural glass elements are typically non-membrane elements where the maximum tensile stresses occur frequently at the glass edges under in-plane loads compared to membrane elements like infill glass panels where maximum stresses are located within the glass surface under lateral loads. The edge strength is affected by the residual stress distribution at edges which is different from residual stress distribution away from edges. Additionally other parameters such as edge finishing, size of the element and the load duration have an impact on the edge strength '[1]'. The manufacturing process has an influence on number and shape of edge flaws. The size effect is important as the probability of larger flaws increases with the size of the element, the load duration has an impact on time dependent strength of glass '[1]'. Those issues should be considered in the design method of structural glass elements.

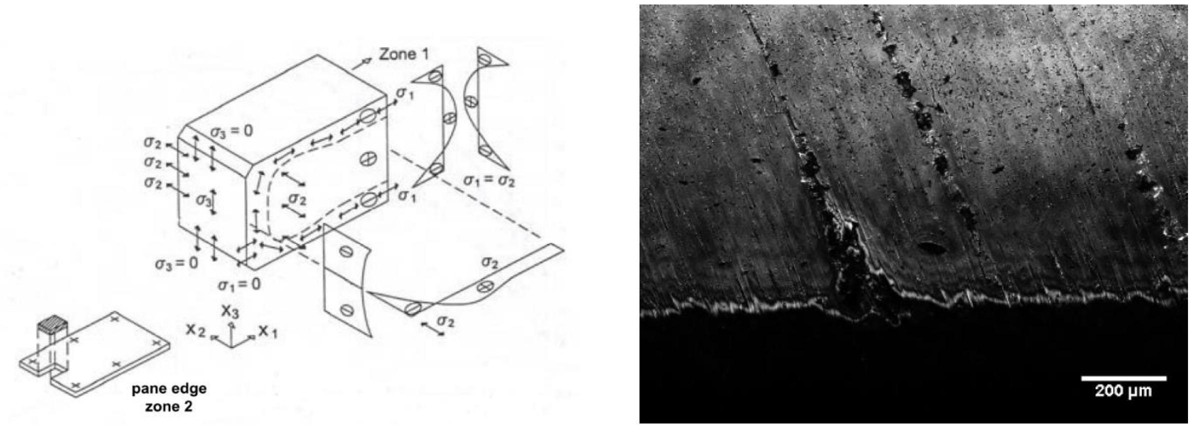

Figure 2: Residual stress distribution at edges [3] (left) and surface flaw polished edge [2] (right)

Conceptually, there are two general groups of design methods: European design methods, which are based on the design method of damage equivalent load and resistance (DELR), and North American design methods, which are based on the glass failure prediction model (GFPM) '[4]'. Currently applied standards do not address the edge strength under in-plane loads and do not provide verification formats. Only the European draft code prEN 13474-1:1999, Section 3.2.4. addresses this issue so far and allows to calculate the maximum principle stress of a glass beam (acc. DELR) '[4]'.

The above mentioned approaches are based on the Weibull distribution which has not been confirmed by experimental data yet (e.g. Fink (2000); Laufs 2000) '[4]'. Due to the lack of information regarding edge strength, the results of diverse scientific research can be used. The reduction ratio of the tensile strength at edges is compared to the tensile strength in the glass surface (away from the edge) up to approximately 67% for tempered glass and 75% for annealed glass '[6]'. It can be distinguished between straight edges and curved edges respectively holes. New approaches like 'Lindqvist [2]' show that the glass strength can be predicted based on edge flaws which seems promising for future approaches.

Stability

Due to the slenderness of most structural glass elements the load bearing capacity is limited in many cases by the stability criteria '[7]'. Fundamental research is available for column buckling, lateral torsional buckling and plate buckling (e.g. Luible, Holberndt, Englhardt, Wellershoff, etc.) '[8]' allowing the determination of critical buckling loads with analytical methods. The appropriate analytical method depends on the type of the stability problem and also on the system specific boundary conditions like glass built-up (monolithic or laminate) and support situation. For example a glass-beam with supported tension chord respectively compression chord produces different results compared to a system with unsupported chords as shown in the figure below.

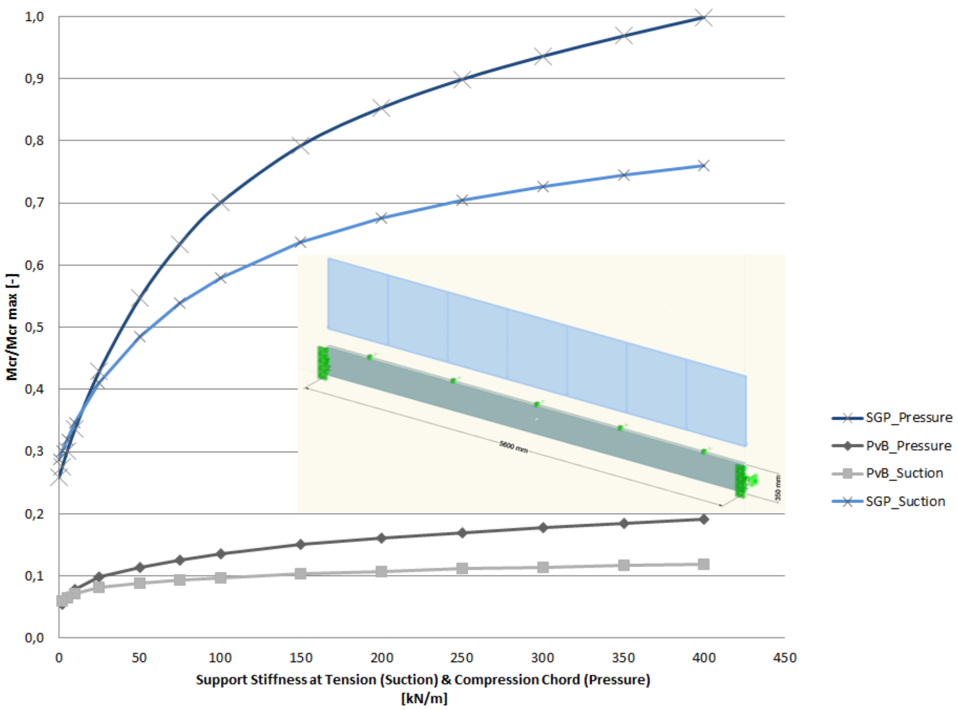

Figure 3: Critical buckling mode of a glass beam (length 5600mm; height 350mm; 4x10mm in dependence of the lateral support stiffness at the chord and the interlayer material (PVB and SGP)

In general, analytical models serve straight forward design of stability sensitive structural glass elements based on buckling curves. Nevertheless, it is often required to perform involved numerical analysis by finite element models to precisely consider any boundary condition of the system (e.g. support stiffness, glass built-up etc.). Under increasing loads those pre-deformed FE-models show non-linear deformations. Either the material strength will be achieved while increasing the load or the deformations will be too big and show an asymptotic approximation to the critical buckling loads.

Compound effect

Structural glass elements are typically laminates. The appropriate consideration of the compound effect is crucial for simplified analysis with an equivalent cross section. Exemplary the following formulas show the approach to determine the equivalent stiffness $EI_{z,eff}$ and GK_{eff} for a beam section consisting of a laminate with two glass layers according to the sandwich-theory '[9, 10]', as described by 'Luibil A. and Crisinel M. [5]'.

$$EI_{z,eff} = EI_s\left(\frac{\alpha\beta\pi^2+\alpha+1}{1+\pi^2\beta}\right) \qquad \alpha = \frac{I_1+I_2}{I_s};\ I_s = h\ (t_1 z_1^2 + t_2 z_2^2)\ ;\ \beta = \frac{t_{PVB}}{G_{PVB}\,h(z_1+z_2)^2}\cdot\frac{EI_s}{L^2}$$

$$GK_{eff} = GK_{glass1} + GK_{glass2} + GK_{compound}$$

$$GK_{comp} = GI_s\left(1-\frac{\tanh\frac{\lambda h}{2}}{\frac{\lambda h}{2}}\right)$$

$$I_s = 4\left(\frac{t_1+t_2}{2}+t_{PVB}\right)^2\frac{t_1 t_2}{t_1+t_2}h$$

$$\lambda = \sqrt{\frac{G_{PVB}}{G_{glass}}\cdot\frac{t_1+t_2}{t_{PVB}\cdot t_1 t_2}}$$

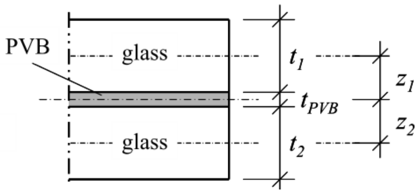

Figure 4: Built-up Laminate with two glass plies [5]

The determination of the equivalent stiffness for laminates with three glass layers is also available according to the sandwich-theory. The obtained $EI_{z,eff}$ and GK_{eff} can be incorporated in the analytical stability checks or being used for finite element models. Laminates consisting of more than two or three glass layers require alternate approaches (e.g. FEM Analysis).

Strength of bolted connections

A particularly useful and straight forward solution for the connection of brackets and splice joints of structural glass elements are bolted connections.

For the design of those connections, the before mentioned considerations regarding edge strength of glass must be considered. Additionally it must be highlighted that the contact mechanism of bolted connections is very complex and requires precise assumptions for the boundary conditions influencing the stress distribution at holes in glass elements. Available simplified design procedures to determine stresses around holes are provided within the literature for example by 'Techen [11]' or 'Baitinger [12]'. The analytical approaches are often associated with some drawbacks. In the proposal of 'Techen [11]', for example, the coefficient for pressure contact depends on test results and the edge distance of holes is neglected. The proposal provided by 'Baitinger [12]' considers a big variety of influencing parameters which leads to results on the safe side.

Due to the before mentioned issues, bolted project-specific testing is very useful and informative as it provides besides failure loads substantial knowledge about the glass failure mechanisms. Additionally, it is principally required to gain information about the load distribution and load paths within the connections.

3 Recent Josef Gartner examples

Columbia University Medical Center (CUMC), New York

The new state-of-the-art medical and graduate education building on the CUMC campus in the Washington Heights community of Northern Manhattan is currently under construction. The 14-story facility is designed by Diller Scofidio + Renfro, in collaboration with Gensler as executive architect.

The building façade consists of 1700m² highly transparent glass fin façade (Josef Gartner contract) and 4000 m² unitized curtain wall (contract Josef Gartner affiliated company Permasteelisa North America). The glass fins are typically hanging single spans between the floor levels. Some of the glass fins are multi-spans using the slabs as intermediate support. In areas with large spans where the slab edge is too far away a horizontal steel flat bar was introduced in the façade design to allow for homogeneous fin dimensions within the project. The design proves that glass fin-facades can be used with a curtain wall approach in large-scale and under challenging boundary conditions.

The distinctive geometry of the building with folded slabs creates multiple fin types regarding built-up, length and system depth. Typical glass built-ups are 3x10mm up to 3x15mm fully tempered glass with PVB Interlayer. Glass fin lengths are up to almost 9m and height/depth ratio up to nearly 20. The structural design of the glass fin façade is based on analytical approaches verified by finite element analysis. The sufficient strength of the bolted glass fin connections was verified based on test results.

Figure 5: Glass fin solution with intermediate steel flat bar (left), project rendering Columbia University Medical Center © Diller Scofidio + Renfro (right)

Entry Pavilion, World Financial Center/Brookfield Place, New York (USA)

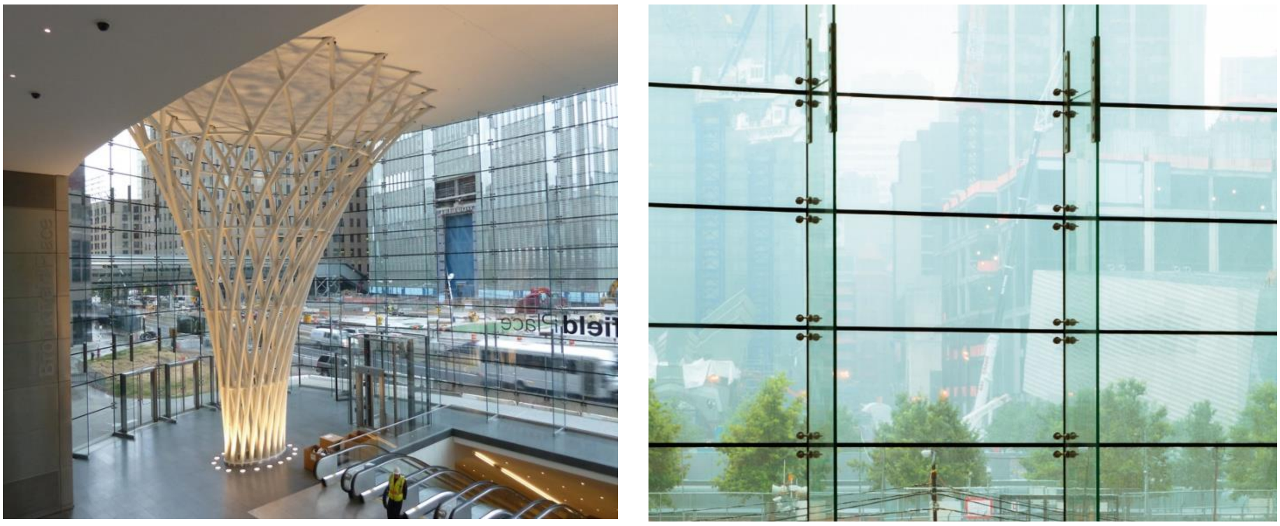

Figure 6: Internal views Entry Pavilion, World Financial Center © Karin Jobst

The new World Financial Center located at the corner West Street and Vesey Street in Lower Manhattan is entered through an almost 17 meter high glass pavilion designed by the Team of Pelli Clark Pelli Architects. The roof construction of the pavilion is supported by two filigree funnel-shaped mega columns. The glass fin façade is suspended from the roof level. The typical glass units are 3080 x 1350 mm large and point supported.

The 1250mm deep glass fins in a distance of 3100mm are made up of three pieces connected with stainless steel pins and brackets. The glass fins consist of three layers of fully tempered glass (3x12mm). Even though the splice joints of the glass fins are located approximately in the third sections of the span and not at mid span, the internal forces to be transferred are still design driving for the system depth (not lateral torsional buckling).

Designing the glass fins, the full variety of available approaches was used namely analytical approach, numerical approach and project-specific testing for the glass fin splice connections.

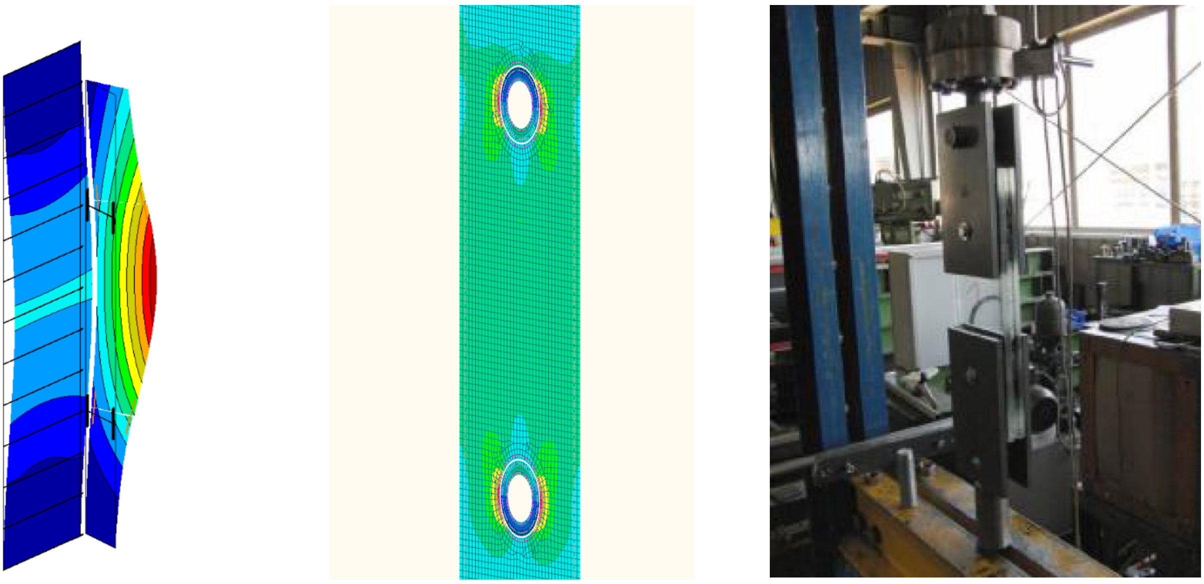

Figure 7: FEM investigation of buckling mode (left), analysis of local stresses at bolted connections (center), test assembly for bolted connections (right)

Square One Shopping Center, South Expansion Mississauga, Ontario (CA)

The new expansion of the Square One Shopping Center designed by MMC International Architects LTD. in collaboration with the engineering office Read Jones Christofferson is currently in the phase of detailed design. The rotunda building of the shopping center utilizes most prominently a highly minimalistic approach for the glass fin system.

Glass fins with a max. span of 7m are hung from the roof. The longest fin is 14m long with three joints and two intermediate supports. The dead load of the façades glazing panels is also suspended from the roof level via stainless steel hanger mullions. The splice joints of the glass fins are designed as half lap splice joints without any steel splices. This connection methodology could be realized by locating the splices close to the zero-position of the moment curve. Intermediate support brackets are designed as inserts to reduce visible steel elements in the façade. The fin built-up consists of six layers with 8 mm fully tempered glass. Even at locations with a reduced glass built-up, the stability of the system can be ensured in the case of the breakage of one lite.

Figure 8: Rendering Rotunda glass fin façade , Square One Shopping Center © Read Jones Christofferson (left); Rendering half lap splice joints glass fin © Read Jones Christofferson (right)

Here again project-specific testing was carried out to verify the numerical approach and to consider all characteristics of the half-lap splice joints like bushing and interlayer materials used between the laps of the single fin parts. The chosen test set-up follows the four point-bending test regime.

The test scenarios ultimate load test and post breakage test were investigated with the set-up shown in fig. 10. The failure loads, load-dependent displacements and modes of failure were recorded during testing. The samples were loaded with horizontal and vertical load in several load steps until failure.

On all specimens glass breakage occurred on the edge of the drilled holes of the glass. Always the most inner glass-layer of the triple laminate broke first and then the remaining layers broke. This issue is currently under further investigation as the first breakage would have been expected at the outermost glass layers. The modes of failure recorded during testing are shown on the following diagrams (see fig.9).

Post-breakage tests with one pre-damaged external respectively one pre-damaged internal layer showed ultimate loads in the same range as undamaged specimens did.

The load bearing capacity of the applied single-shear joints is very limited due the unfavorable load paths caused by the eccentricities of the connection. Therefore, the connection methodology should only be applied in minor loaded zones of the structural glass element.

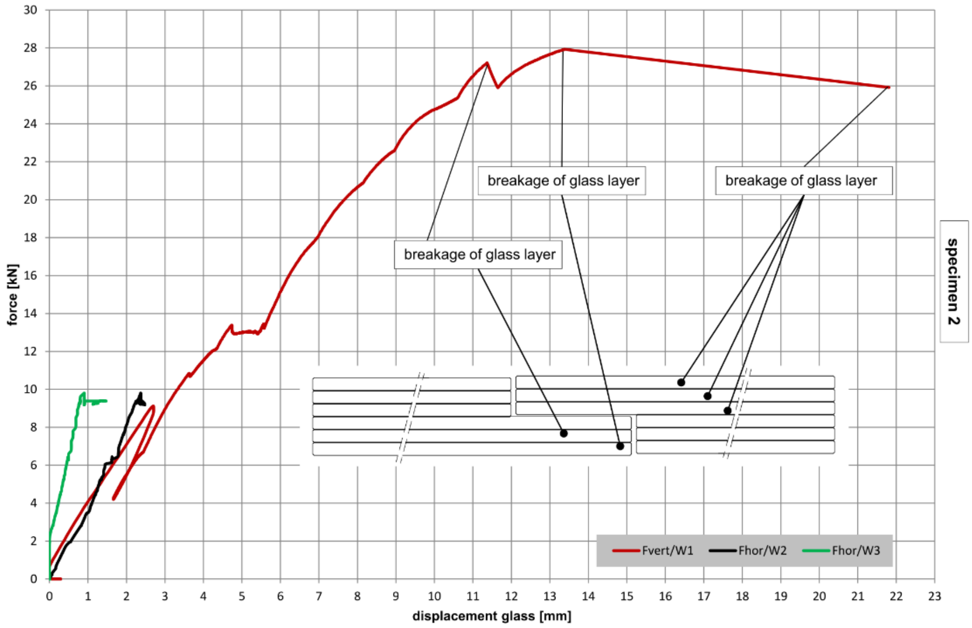

Figure 9: Load deformation diagram half lap splice joint

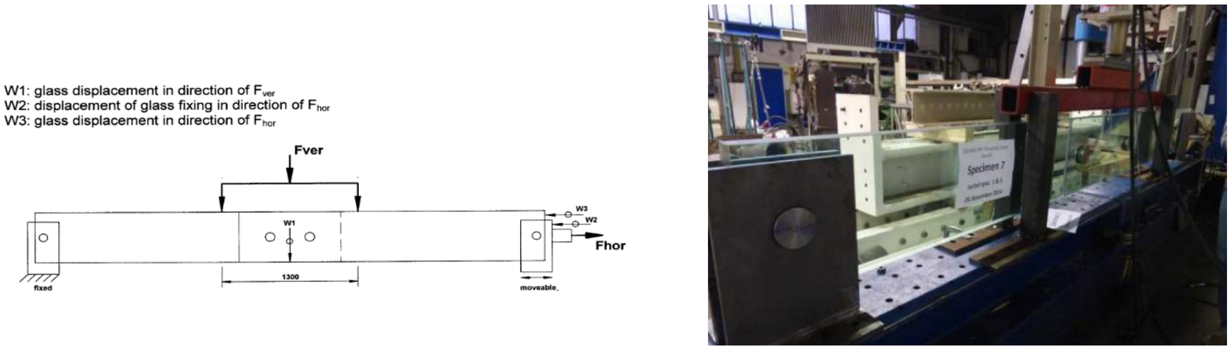

Figure 10: Test Set-up half lap splice joints (left) and test assembly overview (right)

4 Conclusion

The experience of recent Gartner projects shows the successful application of structural glass elements and the possibility to use glass as secondary element and in large scale. To care for the complexity of such structures, a fundamental in-depth knowledge of the material glass combined with a holistic design approach is required. The specific design considerations of these mostly slender elements show the need of a highly precise structural model taking into account various characteristics respectively boundary conditions. Nevertheless areas prone to high tensile stresses should be verified by project-specific testing. In general, a user friendly design method for structural glass elements considering the material specifics and quality should be implemented.

5 References

[1] Vandebroek M., Lindqvist M., Belis J., Louter C.: *Edge Strength of cut and polished glass beams*, Glass Performance Days, 17 -20 June, Tampere, Finnland, 2011.

[2] Lindqvist M.: *Structural Glass Strength Prediction Based on Edge Flaw Characterization;* These No 5627 EPFL Ėcole Polytechnique Federale de Lausanne, 22. February, Lausanne, Switzerland, 2013.

[3] Maniatis I.: *Numerical and Experimental Investigation on the Stress Distribution of Bolted Glass Connections under In-Plane Loads,* Thesis, TU München, Germany, 2006

[4] Haldimann M.: *Fracture Strength of Structural Glass Elements – Analytical and Numerical Modelling, Testing and Design*, These No 3671, EPFL, Lausanne, Switzerland, 2006.

[5] Luible A. and Crisinel M.: *Design of Glass Beams Subjected to Lateral Torsional Buckling;* IABSE Symposium 2006 "Responding to Tomorrows Challenges in Structural Engineering" 13-15 Sept., Budapest, Hungary, 2006.

[6] Weller B., Nicklisch F.; Thieme S., Weimar T.: *Glasbau-Praxis Konstruktion und Bemessung*; Bauwerk Verlag GmbH, 2010

[7] Pankratz P., Simmert R. , Hildebrand J.: *Stabilitätsanalysen im Konstruktiven Glasbau*, Glasbau 2014 Bernhard Weller, TU Dresden, Germany, 2014

[8] Haldimann M., Luible A., Overend A.: *Structural Use of Glass*, International Association for Bridge and Structural Engineering, Zürich, Switzerland, 2008

[9] Stamm, K.; Witte, H.: *Sandwichkonstruktionen – Berechnung, Fertigung, Ausführung,* Springer Verlag, 1974

[10] Zenkert, D.: *The Handbook of Sandwich Construction;* Engineering Materials Advisory Service Ltd., United Kindom, 1997

[11] Techen, H.: *Fügetechnik für den konstruktiven Glasbau,* Thesis, TU Darmstadt, Germany, 2006

[12] Baitinger, M.: *Zur Bemessung von SL-belasteten Anschlüssen im konstruktiven Glasbau,* Thesis, RWTH Aachen, Germany, 2009

Proceedings of the International Conference on Building Envelope Design and Technology, Graz
Advanced Building Skins 2015

Design nomograms for cable facades

Frank Wellershoff, Prof. Dr.-Ing.
HafenCity Universität Hamburg, Germany, frank.wellershoff@hcu-hamburg.de

Matthias Förch, Dipl.-Ing. (FH)
HafenCity Universität Hamburg, Germany, matthias.foerch@hcu-hamburg.de

Manuel Boensch, M.Sc.
HafenCity Universität Hamburg, Germany, manuel.boensch@hcu-hamburg.de

Summary

A cable façade is highly transparent and looks simple to design. High challenges arise if the large deflections under wind loads are regarded. High pre tension forces in the cables are required to decrease these wind deflections but they remain in critical high ranges so that the resulting warping in the glass panels are a limiting factor. Additionally the high pre tension forces must be bearable by the framing structure of the façade where the cables are connected.

The structural design of cable facades is driven by an iterative and complex computer model analysis to find the best solution for suitable cable pre tension and limited glass panes warping. Besides the computer modelling a theoretical analysis is possible. The results of these theoretical analysis can be illustrated in nomograms. These nomograms can be used for quick pre designing as well as for verification of computer models.

Keywords: façade, cable, glass, dimensioning, nomogram, force, deformation, warping

1 Introduction

Cable net facades belong to the most transparent façade types. Although it is obvious that a façade out of straight steel cables will have a maximum transparency, this façade type was first time build in 1993 for the atrium of the Munich Airport Hotel, designed by Helmut Jahn architects together with the engineers of Schlaich Bergermann und Partner. Cable net facades are so flexible that greatest challenges are related to the deformations under wind loads. Even with highest pre-tension in the cables these deformations are in ranges of L/100 to L/20. Additionally the pre-tension forces of the cables must be considered in the sub-structure to which the cables are connected.

The design of cable net facades is therefore driven by many parameters that are interacting. These parameters are: Cable length, cable diameter, cable young’s modulus, cable pre- stress, self weight of the cables and the glazing, wind loads, temperature changes, sub-structure deformations, and glass warping.

In this paper the theoretical background for structural design of pre-stressed cables is summarized and new developed design nomograms for cable net facades are shown. With these nomograms it is possible to analyze the interaction of the above mentioned parameters without complex computer tools in shortest time. The nomograms could be effectively used in pre-dimensioning phases as well as for verification of complex computer models.

2 Cable Net Facades

2.1 Surface types

Generally cable net facades can be class-divided by the curvature of the glass surface and the directions of the straight cables. The glass surface can be simple flat, or can be curved over one axis ore two axis. Obviously straight cables are possible in surfaces with one curvature if the cables are directed orthogonal to the curvature (e.g. in the longitudinal direction of a cylinder). But straight surface lines do also occur in specific double curved surfaces (diagonal directions in hyper shells with negative Gaussian curvature).

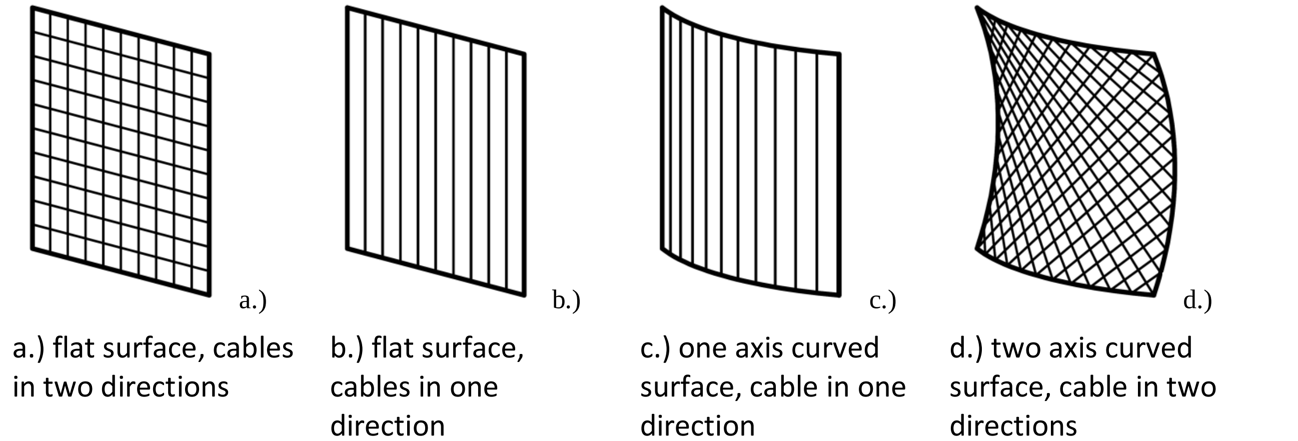

Figure 1. Overview of cable net façade geometries

2.2 Cable types

Basically there are many different types of cables available on the market. For cable façade application group B cables of Eurocode 3 are mostly used (see figure 2):

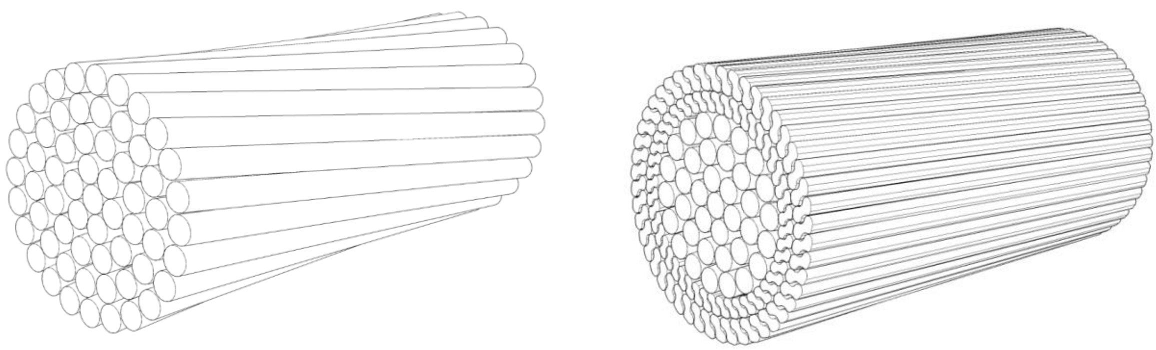

Figure 2. Spiral cable (left), full locked cable (right).

Cables consist of many single wires (single wire cross sections), which in sum generate a better redundancy and safety compared to monolithic cross sections. However, the main reason for choosing cables instead of monolithic cross sections is the advantage regarding production and transportation length.

Spiral cables consist of single wires, which are round and spiral shaped over the cable length. Full locked cables consist of a core with round wires, that is enclosed by layers of Z-shaped wires. Compared to spiral cables, full locked cables have a higher Young’s Modulus, a higher surface pressure- and corrosion resistance.

Both cable types are available in Galfan-coated or stainless steel quality, depending on the designated application. Spiral cables usually start with nominal diameters from 6 mm, full locked cables with 20 mm as minimum.

2.3 Cable end connections

There are two different principles for connecting cables to their end fittings. One way is to press the end fitting under high mechanical pressure onto the cable end by cold deformation. A second way is to connect the cable with the fitting by metal or resin socketing. More information about cable end fittings can be found in EN 13411. From structural point of view also two different systems for the connection of the fittings with the adjacent structure exist. The bolted connection, where the bolt axis is parallel to the cable axis (Fig. 3, left), has a certain bending stiffness, that could lead do cable damage due to the limitation of the cable end rotation. The connection where the bolt axis is perpendicular to the cable axis (Fig. 3, right) is rotational free about the bolt axis. The rotational friction between bolt and fitting should be checked under high tension loads.

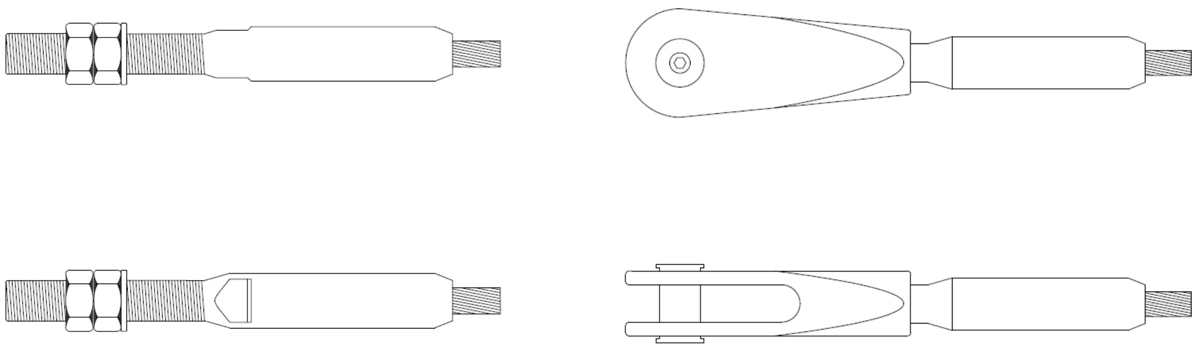

Figure 3. Typical cable end connector types for façade applications.

3 Calculation of cable systems

3.1 Theory

It is state of the art in engineering to work with idealized systems for the structural design. Depending on the structural system and task, there are different ways of analyzing beam-shaped structures. Theory I. Order calculations consider equilibrium in undeformed state. This approach is appropriate for structures with small deformations. Theory II. Order is a more rigorous approach considering equilibrium under deformed state with small but not negligible deflections. Bending moments due to normal forces are considered herein, which can be used for buckling analysis, but the superposition principle is not valid. Theory III. Order is necessary for the structural design, if membrane forces due to large deformations act in a structural system. Cable and membrane structures, as well as glass panels, are examples for typical Theory III. Order applications.

3.2 Computer based modeling

For structural calculations, cables are usually considered being capable to transfer tension forces only. Bending moments, compression and shear forces cannot be transferred by cable elements, which can be selected within many computer programs. Therefore only the longitudinal stiffness of the element (Young's Modulus multiplied by cross sectional area) is required. The longitudinal stiffness of cables is lower than the Young's Modulus of the base wire-material because of the stranding. Values are normally provided by technical approvals of cable systems. Despite the reduced Young's Modulus, the real cross sectional area has to be used for calculation, because it is considerable smaller than the nominal area defined by cable diameter. In this context care should be taken of possible program settings regarding material safety factors (γ_M), which can result in underestimation of maximum cable forces.
The number of cable elements over the entire cable length should be sufficiently defined in FEA software, because angle rotation is only possible at nodes and especially straight cables can only bear forces by large deformations or angle rotations respectively. Being not capable of bearing compression forces, cable elements are pre tensioned to compensate compression forces by reduction of tension forces. In case of compression force results within cable elements the number of iterations for finding convergence may be increased. When dealing

with large deformations analysis, it is sometimes difficult to find converged solutions. Loading the system in multiple load steps may be appropriate in this case, because equilibrium state is reached after each load step.

3.3 Design criteria for cable facades

There are three design criteria for cable facades, which have to be controlled:

- Maximum tension force
- Maximum deformation
- Maximum glass panel warping

The cables have to be designed, that the maximum allowable tension force is not exceeded. Restraint forces due to temperature changes or support movements have to be considered. The maximum deformation of cable facades is usually not design relevant, but has to be investigated anyhow to ensure, that no collisions between deformed cable façade and primary structure occurs. Maximum glass panel warping is a design criterion, which is often design relevant. A rectangular glass panel is defined by its 4 corner points in contrast to a plane, which is defined by 3 points. Glass panel warping appears especially in façade corners where 3 corners of the glass panel are fixed to the stiff façade surrounding structure and only the forth corner is attached to a cable. This forth corner will be displaced under wind loads.

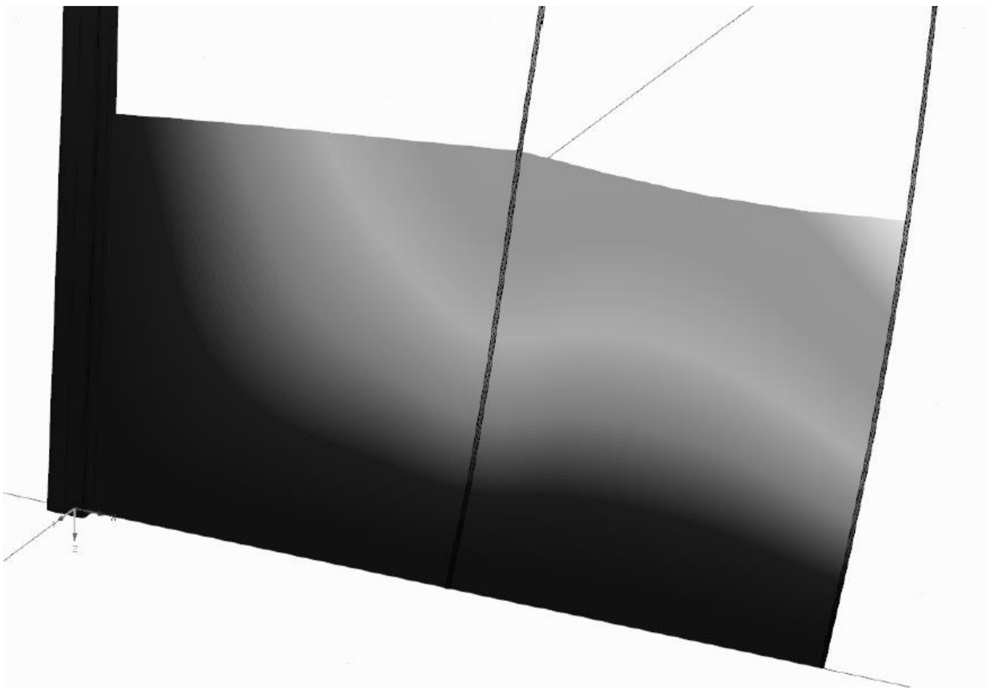

Figure 4. Glass panel warping in deformed cable façade corner (exaggerated deformation).

4 Design with Nomograms

4.1 Design equations

An indeterminate system is given by translational fixed cable end supports (see figure 5). The cable force can be calculated by consideration of the cable strain and force equilibrium conditions. Hence the cable force is nonlinear related to the perpendicular load q and the cable deformation.

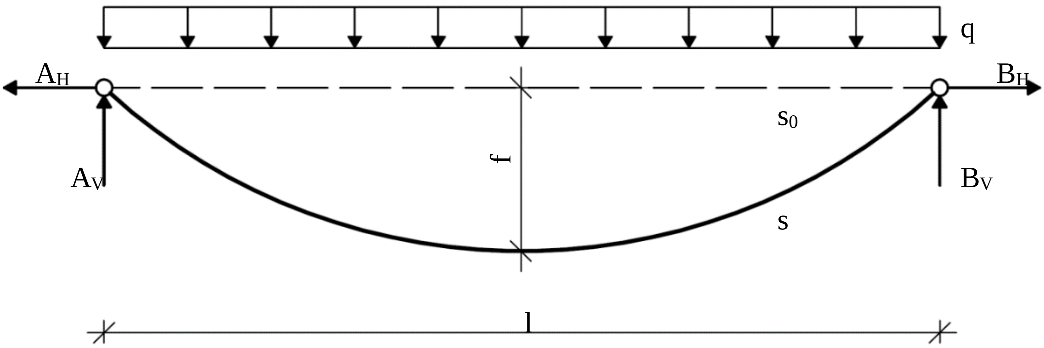

Figure 5. straight cable under orthogonal load

The length „s" of the deformed and stretched cable is defined by [1]:

$$s = s_0 + \Delta s + \Delta s_t \tag{1}$$

with:

s_0	length of the unstretched cable
Δs	cable elongation due to perpendicular load q
Δs_t	cable elongation due to temperature change Δt

For a uniform perpendicular load q the length „s" can approximately be described by [2]:

$$s = l\left[1 + \frac{8}{3}\left(\frac{f}{l}\right)^2\right] \tag{2}$$

A force equilibrium condition is given by:

$$f = \frac{ql^2}{8H} \tag{3}$$

The cable elongation Δs is given by the cable force and the longitudinal stiffness:

$$\Delta s = \frac{H \cdot s_0}{EA} \tag{4}$$

Equation (2) to (4) can be replaced into (1):

$$l\left[1 + \frac{g^2 \cdot l^2}{24 \cdot H^2}\right] = s_0(1 + \alpha_t \cdot \Delta t) + \frac{H \cdot s_0}{EA} \tag{5}$$

By transformation we get the "principle cable equation":

$$H^3 + H^2 EA\left[1 - \frac{l}{s_0} + \propto_t \cdot \Delta t\right] = \frac{EA \cdot q^2 \cdot l^3}{24 s_0} \tag{6}$$

1 [1], page 8-10
2 This approximation is sufficient for structural engineering purpose. [1], page 9

For a straight cable in unloaded condition ($l = s_0$) equation (6) simplifies to:

$$H^3 + H^2 EA\,(\propto_t \cdot \Delta t) = \frac{EA \cdot q^2 \cdot l^2}{24} \quad (7)$$

Temperature elongations can later be considered by support displacements. Therefor we can simplify equation (7) with $\Delta t = 0$ and get:

$$H^3 = \frac{EA \cdot q^2 \cdot l^2}{24} \quad (8)$$

<u>Pre tension:</u>

The relation of pre tension and cable force is defined by figure 6.

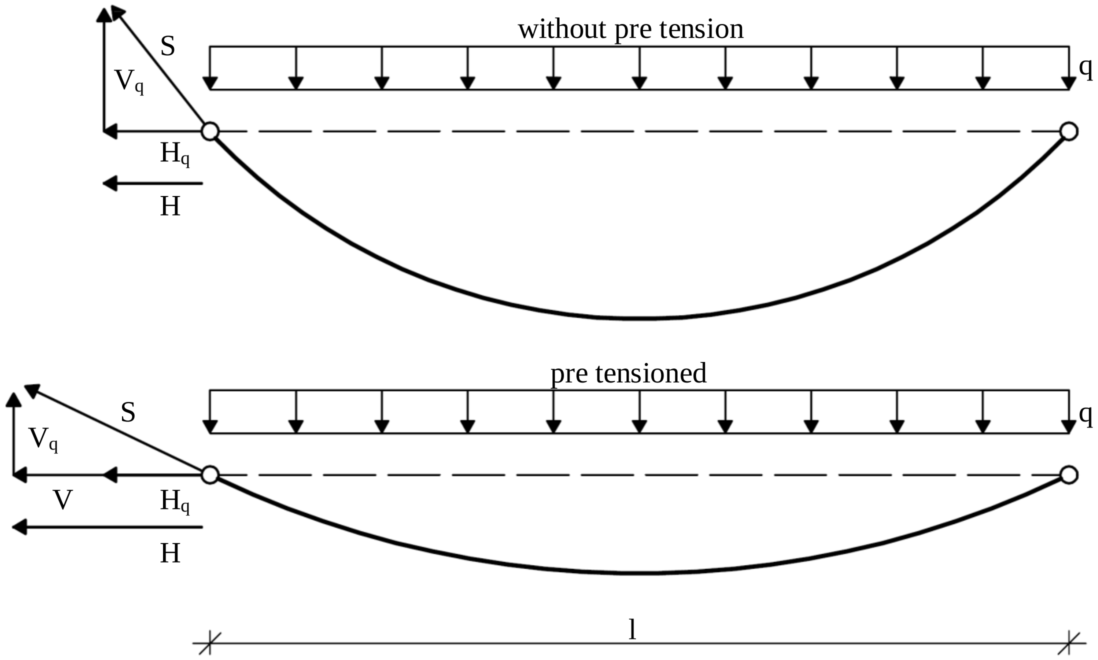

Figure 6. support forces for cables with and without pre tension

The support force V_q depends only on the perpendicular load q. The support force H depends on the load q and the pre tension force V. Thus the pre tension increases the cable force and decreases the deflection. The length of the cable changes under the load q and the pre tension force V by the value of Δs:

$$\Delta s = \frac{H_q \cdot s_0}{EA} = \frac{(H-V) \cdot s_0}{EA} \quad (9)$$

Analogue to equation 5 to 8 the “principle equation for a pre tensioned cable” can be determined to:

$$H^2(H - V) = \frac{EA \cdot q^2 \cdot l^2}{24} \quad (10)$$

Support displacements:
A support displacement Δl can be considered by an additional "elongation term":

$$H^2(H-V)+H^2EA\left[\frac{\Delta l}{l}\right]=\frac{EA\cdot q^2\cdot l^2}{24} \tag{11}$$

Support springs:
It must be controlled that a minimum pre tension force remains also under a shortening of the support distance by support displacements and a cable elongation under increasing temperature. This can be critical in short cables with low values of stretching under the pre tension force. In this case additional support springs may decrease the elongation stiffness and increase therefore the value of stretching. Some of the following nomograms consider therefore additional support springs with a stiffness of 20% of the cable stiffness itself.

$$C_{spring}=\frac{1}{5}\cdot C_{cable} \tag{12}$$

Hence the spring stiffness of the serial system of a spring plus a cable is:

$$C_{total}=\frac{1}{\frac{1}{C_{spring}}+\frac{1}{C_{cable}}}=\frac{1}{\frac{1}{EA/5\cdot l}+\frac{1}{EA/l}}=\frac{EA}{6\cdot l} \tag{13}$$

This corresponds to a modified elongation stiffness of the serial system with $EA/6$:

$$C\cdot l=EA_{mod}=\frac{EA}{6} \tag{14}$$

Deformation / Warping:
The cable deflection is related to the perpendicular load q, the cable force H, and the cable length l. The deflection in a distance x from the middle point of the cable can be derived from equilibrium relations:

$$f(x)=\frac{q}{2H}\,x^2-\frac{ql^2}{8H} \tag{15}$$

4.2 Nomogram Parameters

The nomograms cover a wide rage of potential cable facades concerning the values of the cable length, the cable diameter, the glass panel height, the pre tension force, and the orthogonal load. Whenever support springs are considered their spring stiffness is 20% of the cable stiffness (see equation 13). Changes in the cable length due to support displacements and temperature changes are covered by realistic values of $\Delta l=\pm l/1000$ respectively $\Delta l=+l/500$. Stainless steel cables and "Galfan" galvanized cables are considered with their specific Young's Modulus E_Q and typical available metallic cross sections A_m. All relevant values are given in each nomogram.

4 References

[1] Palkowski, S.: Statik der Seilkonstruktionen: Theorie und Zahlenbeispiele, Springer Verlag, 1990
[2] Sobek, W.: Beispiele für verglaste Vertikalseilfassaden, Stahlbau (73), S. 224-229, Ernst & Sohn, 2004

5 Nomograms

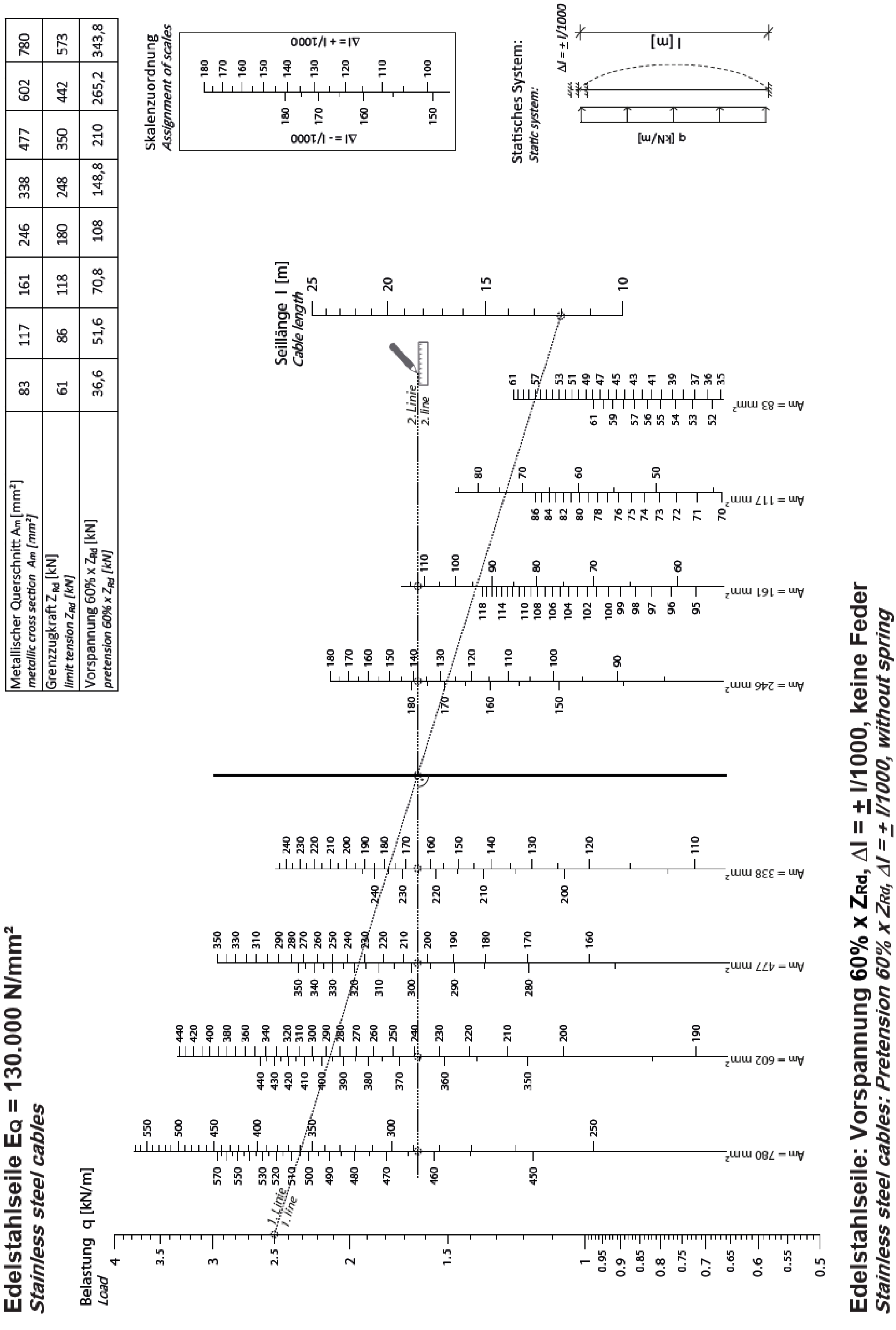

Metallischer Querschnitt A_m [mm²] *metallic cross section A_m [mm²]*	83	117	161	246	338	477	602	780
Grenzzugkraft Z_{Rd} [kN] *limit tension Z_{Rd} [kN]*	61	86	118	180	248	350	442	573
Vorspannung 60% x Z_{Rd} [kN] *pretension 60% x Z_{Rd} [kN]*	36,6	51,6	70,8	108	148,8	210	265,2	343,8

Edelstahlseile E_Q = 130.000 N/mm²
Stainless steel cables

Metallischer Querschnitt A_m [mm²] *metallic cross section A_m [mm²]*	83	117	161	246	338	477	602	780
Grenzzugkraft Z_{Rd} [kN] *limit tension Z_{Rd} [kN]*	61	86	118	180	248	350	442	573
Vorspannung 85% x Z_{Rd} [kN] *pretension 85% x Z_{Rd} [kN]*	51,9	73,1	100,3	153	210,8	297,5	375,7	487,1

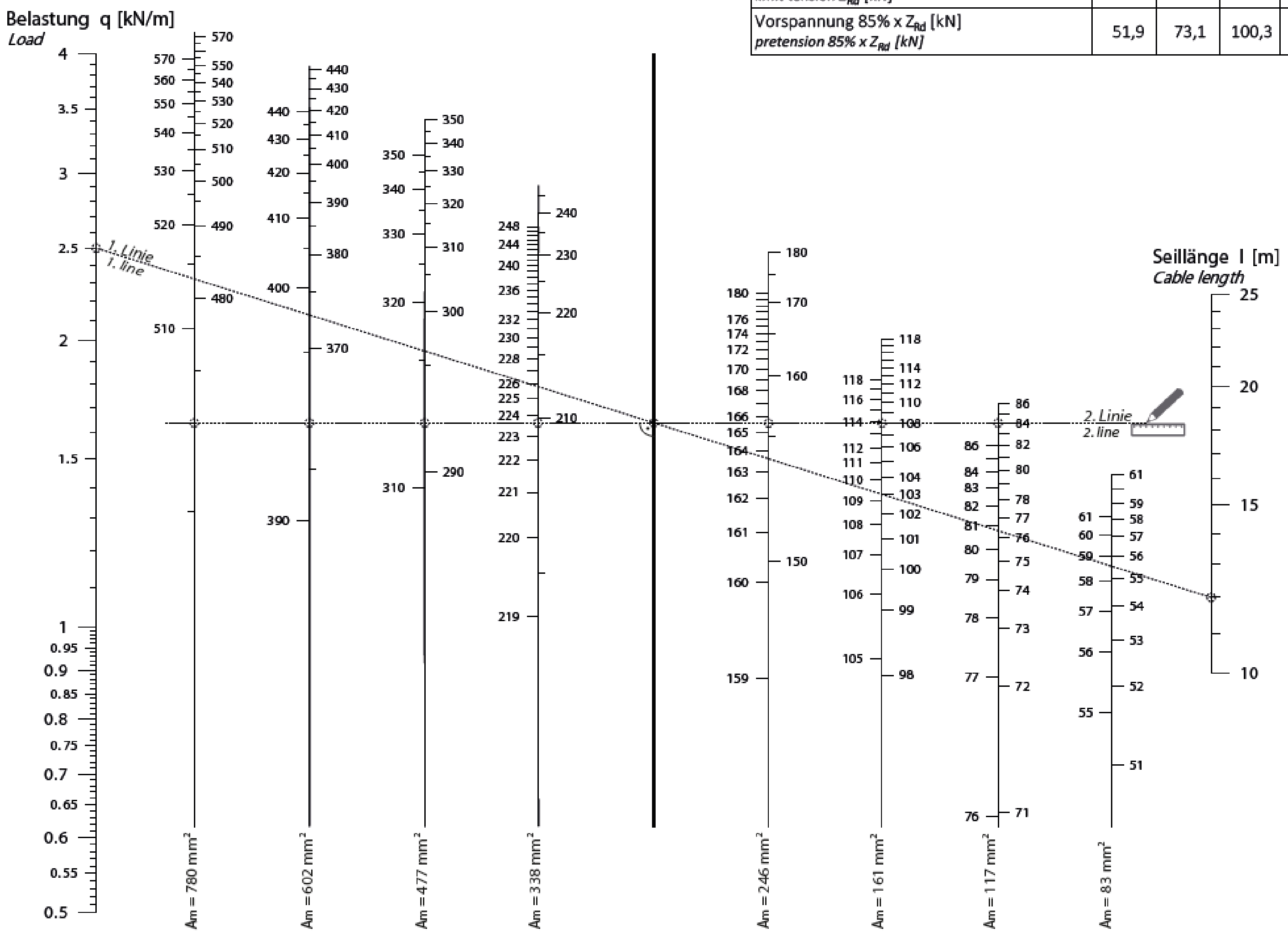

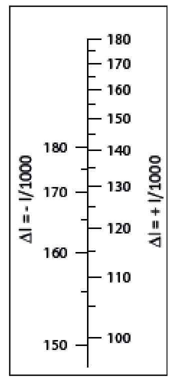

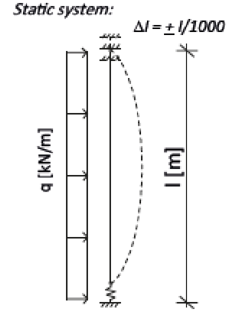

Edelstahlseile: Vorspannung 85% x Z_{Rd}, Δl = ± l/1000, mit Feder
Stainless steel cables: Pretension 85% x Z_{Rd}, Δl = ± l/1000, with spring

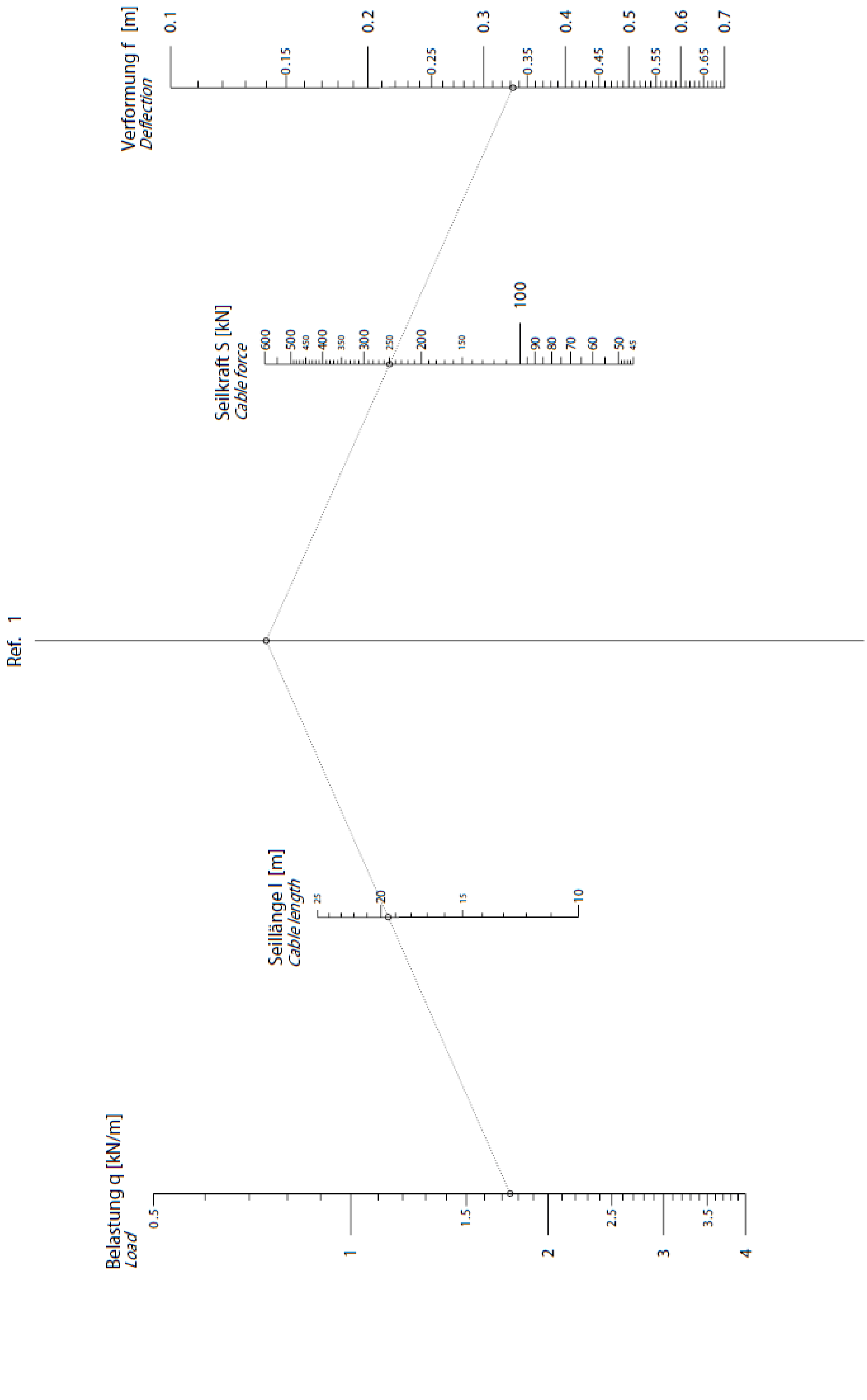

Nomogramm zur Ermittlung der maximalen Verformung
Nomogram to determine the maximum deflection

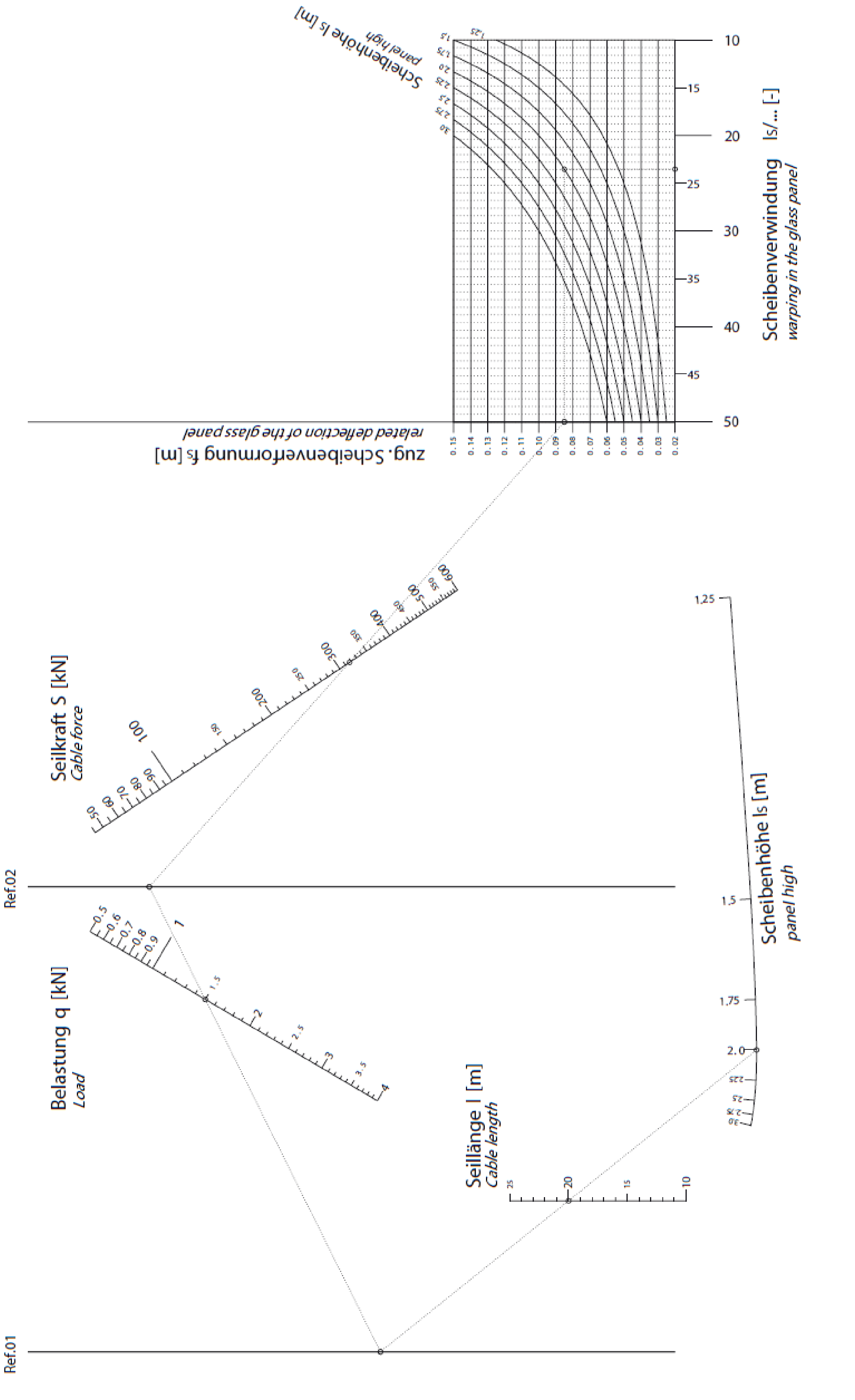

Nomogramm zur Ermittlung der Scheibenverwindung
Nomogram to determine the warping in the glass panel

Proceedings of the International Conference on Building Envelope Design and Technology, Graz
Advanced Building Skins 2015

Tottenham Court Road Station Upgrade – Structural Glass Plazas

Josef Ludwig, Dipl.-Ing. (FH)
P4E – passion for engineering, Germany, josef.ludwig@p4engineering.de
former
se-austria GmbH & Co. KG,MD, Austria

Summary

Tottenham Court Road (TCR) station is undergoing a major upgrade as part of London Underground's (LU) investment program. Part of the project encompasses the installation of two new iconic crystalline structures, intersected with a glazed plank installation, allowing increased access to the station demise. This paper will explain the concept and application for the use of structural glazing on the project.

The southern entrance (the larger volume) contains 8no primary frames, the northern entrance 6no frames, with geometry allowing an exciting dynamic fanned arrangement in plan and elevation. The load bearing frames are glass fins, which are combined with a newly developed technique involving titanium components laminated into the glass for an even greater transparency. By producing glass columns up to 14m long this contributes decisively to this maximum transparency. The complex geometry of the panes of glass calls for absolute precision: cross-sections and plan forms with multiple twists in addition to the diagonal lines of these glass structures result in numerous different angles and a corresponding number of different formats for the glass envelope. All of these bespoke and complex elements are used as structural components to finally reach the necessary structural integrity.

The installation of a structurally glazed plaza's allows a visual connection for the travelling public within the below-ground concourse to the above-ground urban landscape, improving visual orientation and aiding the way-finding strategy.

1 Introduction

Tottenham Court Road (TCR) station is currently going through a major upgrade as part of London Underground's (LU) investment program. Part of the Tottenham Court Road Station Upgrade (TCRSU) encompasses the installation of two new iconic crystalline structures, intersected with a glazed plank installation, allowing increased access to the station demise.

The original design of the structures was completed by Stanton Williams (RIBA Stage D Report completed in April 2007), with technical assistance provided by seele, as a competition submission to LU for the design of the new Centre Point Plaza area at TCR. The intent to add two sculptural glass prisms to this rich urban tapestry will create a stunning visual and public realm experience.

Figure 1: Artist impression of the glazed plaza entrances

The southern entrance (the larger volume) contains 8no primary frames, the northern entrance 6no frames, with geometry allowing an exciting dynamic fanned arrangement in plan and elevation. Maximum dimensions between members has been minimized ensuring that an obtrusive secondary support system, for the glazed panels in elevation, isn't required. In the roof a glass fin system provides secondary support to the roof glazing for residual strength conditions.

For both entrance structures at Tottenham Court Road Underground Station, we have transformed the initial architects' vision into a design in which materials and structure are minimized. The load bearing frames are glass fins, which are combined with a newly developed technique involving titanium components laminated into the glass for an even greater transparency. By producing glass columns up to 14m long this contributes decisively to this maximum transparency. Stainless steel sections finish off the frames internally and externally. The complex geometry of the panes of glass calls for absolute precision: cross-sections and plan forms with multiple twists in addition to the diagonal lines of these glass structures result in numerous different angles and a corresponding number of different formats for the glass envelope. All of these bespoke and complex elements are used as structural components to finally reach the necessary structural integrity.

The new prismatic entrances to the TCR station will form a visually imposing addition to the Centre Point Plaza landscape. The sheer size and nature of the structures in addition to the extensive use of geometrical complicated structural glazing make this quantum of works worthwhile of further dissemination.

2.1 The design concept

The TCRSU refurbishment includes reorganizing and upgrading station access and egress through the construction of new entrance structures, complementing the retention of an existing entrance. Two of these new entrance structures have been designed in glass, which places high demands on their construction. The structures could be described as irregular prismatic blocks with principal dimensions (south entrance) of approx. 14.5m high, 22m long and 11m wide.

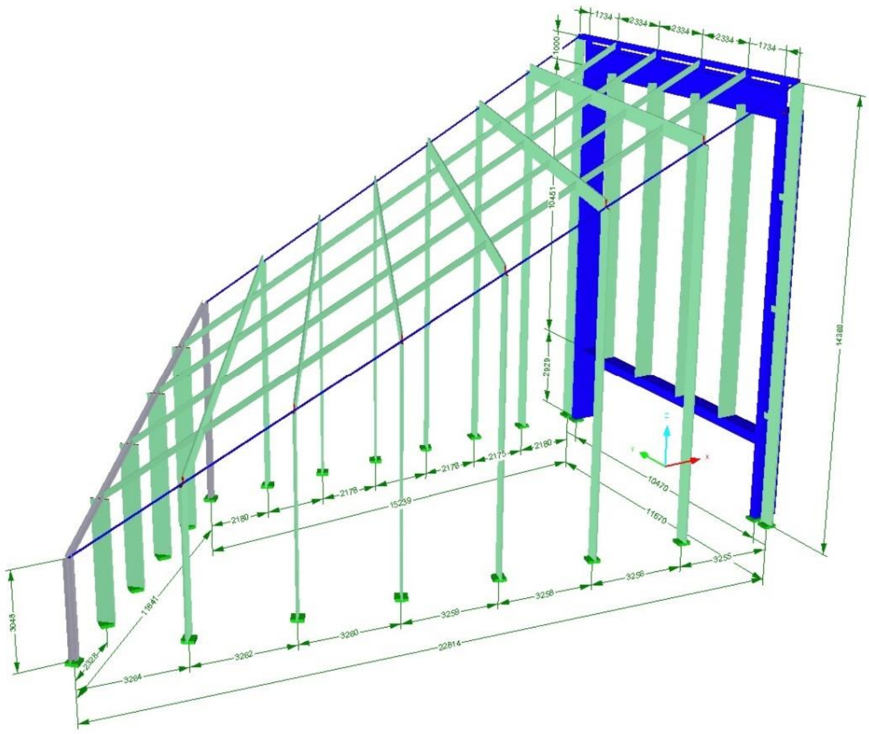

Figure 2: South entrance building – main structure

As can be seen in Figure 2, each structure is subdivided into an irregular grid that coincides with the axes of the loadbearing members. Also immediately evident are the distinctive entrance walls with their enormous portals.

2.2 Structural principle

The structural principle behind the two entrance structures is based on various systems. The portal wall at the entrance forms the basis for the entrance doors at the bottom and the transparent wall above, which with dimensions of 10.5 x 10.5m could be called a "big window". Oversize panes of glass plus vertical glass beams constitute the sole structural elements of this wall.

However, the portal wall also forms a frame on the first grid-line. Fabricated in steel with a certain constructional depth, this frame also represents the first primary loadbearing and bracing element. Glass frames have been positioned on the other grid-lines of this structure, contributing to the lateral stability through fixity effects. The connections, in what is not a true frame in the structural sense, were modelled as hinges so that the connection details only have to handle shear and axial forces. Transverse glass beams on the grid and steel sections along the verges hold and stabilized the glass frames. The steel sections are in turn fixed back to the substantial portal frame. The end walls include glass fins to carry the loads. The fins are positioned on the grid-lines of the secondary beams and also carry the vertical loads from those beams.

Global stability is therefore achieved by the "frame elements" described above and also, and not insignificantly, by the global plate effect of the actual façade glazing. The special glazing connection details have a certain shear stiffness and hence ensure the plate effect.

2.3 The design in detail

Portal frame

The steel portal frame is an L-shaped hollow cross-section made up of welded plates whose sturdy design is easily able to form the primary structure.

For the legs of the frame, one leg of the cross-section is a glass element in order to achieve a degree of transparency. The fixing at the base is by way of anchors cast into the reinforced concrete to tie down the structure.

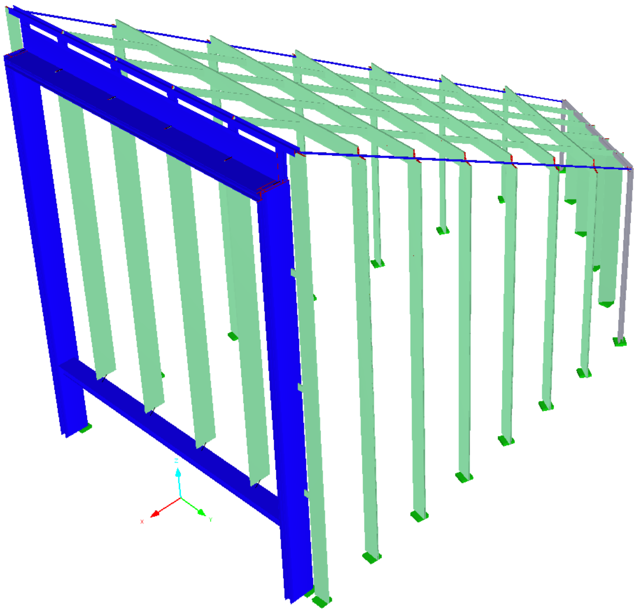

Figure 3: South entrance building – entrance portal frame and all-glass frames

Glass wall in portal frame

The glass wall in the opening of the portal frame has been designed for maximum transparency. Consequently, extra-long panes of glass with stiffening glass fins measuring approx. 10m x 700mm have been designed as laminated glass beams. The connections (see figure 4) were minimized with directly structural bonded glass elements to the glass fins.

The glass wall at the rear is similarly stiffened with glass fins, although in this case the fins also carry the loads from the end bay of the glass roof.

Glass frames

The construction of the glass frames is based on a frame leg that is designed to be fixed at the base. The "frame beam" is therefore a two-pin system.

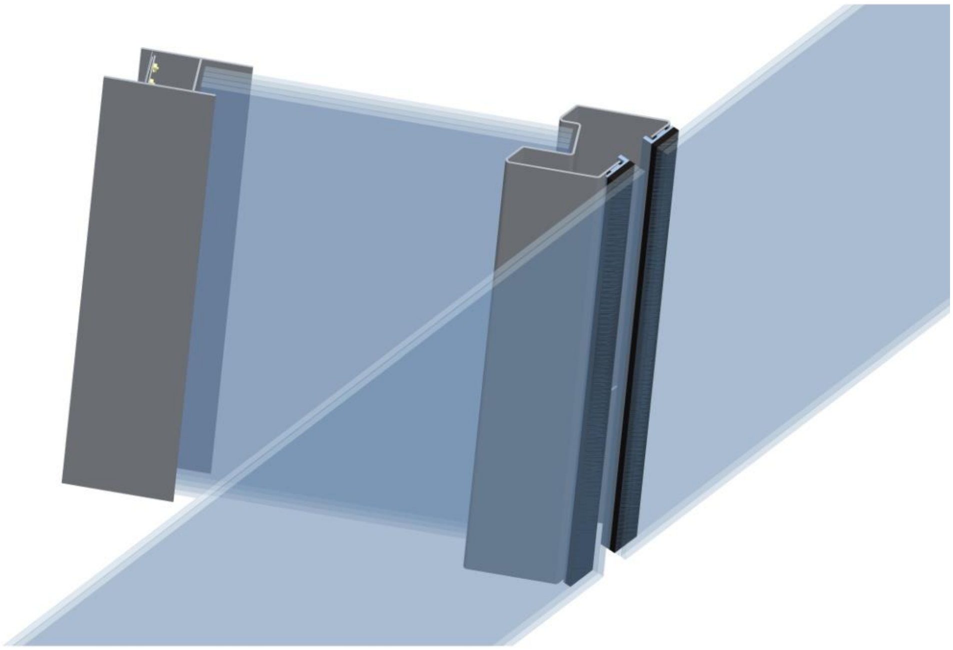

Figure 4: Cross section all-glass

The cross-section is in the form of a four-ply laminated safety glass element with special stainless steel sections top and bottom to cope with the various requirements. The structural cross-section carrying the loads is formed by glass beams with a depth that varies depending on the height and length of the frame. Residual stability is taken into account by the type of glass selected. The two special sections bonded with SG adhesive form channel cross-sections that accommodate cables and lighting. These also contribute significantly to the secondary/residual loadbearing function of the entire element. The loads from the glazing on the façades/roof are also transferred via these special sections.

The imposing maximum dimensions of these semi-glass components with a continuous length of up to 14m represent a major challenge in all senses, e.g. production, transport, erection, etc. Another challenge is the minimized glass connections that make use of items laminated into the panes of laminated glass.

Infill glazing to façades and roof

As already mentioned, the individual panes of glass also contribute to the overall stability of the structure. This is achieved by aluminum rails factory-fitted with SG adhesive and their specific shear-resistant bolting to the special stainless steel components on the glass frames. This therefore results in an "elastic" stiffening of the panes of glass, allowing them to accommodate expansion and contraction as temperatures fluctuate.

For many elements, applying the structural silicone adhesive had to be done in the factory. However, a small number of joints must be carried out and supervised on site under controlled conditions.

2.4 Tolerances and precision

A tolerance specification appropriate to this form of construction once again reveals the degree of complexity of such designs. For the fabrication and assembly of the components due to the tolerance specifications for the connecting components, the deviations are less than 1 mm. To reach such complex and accurate components we using special developed gauging tolls and a very detailed quality check of each part.

2.5 Structural analysis and Testing

The analysis of the entire structure and the connections is based on several concepts. The global loadbearing and stability concept were analysed using non-linear FE numerical models. Individual modelling for the separate analyses enabled numerical models to be derived from the overall models, which shed light on the details. As a final safeguard, a series of component tests will be carried out and then compared with the results of the calculations. We can therefore speak of rigorous analyses at both global and local level. Similar methods and approaches are also valid for failure/breakage/fragility scenarios.

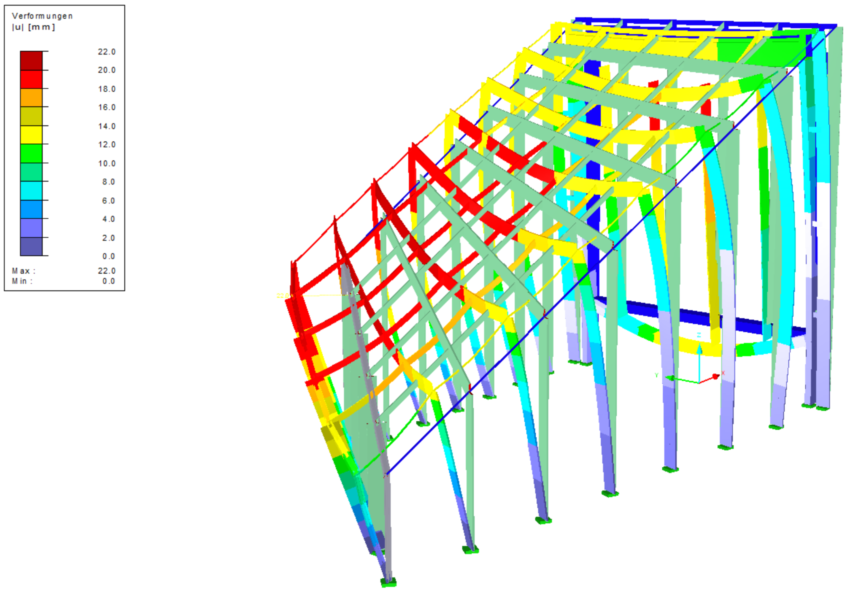

Figure 5: South entrance building – deflection under wind-load

To verify the calculations, a set of tests will be carried out:

Tests on small specimens, e.g. structural adhesive connections
For example the integrated connection bracket - figure 6a

Large-scale tests for example the bottom connection point of the glass frame - figure 6b

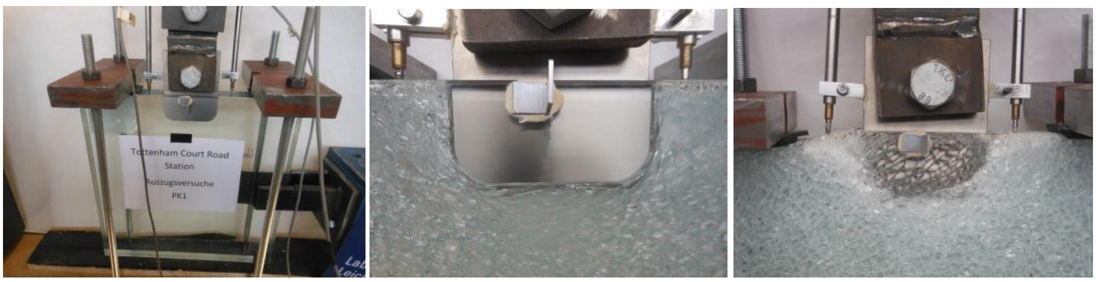

Figure 6a

Connection insert under tension forces - Test setup after breakage of inner glass pane max load 150 kN > 90 kN (= 3 x30 kN relevant and existing load) - increase load up to 215 kN – complete breakage

Figure 6b: Testing connection points in the glass fin

Test connection point glass fin - max achieved load capacity Q= 215 kN > existing Load 45 kN , pre destroyed glass fin - outer Layer

The residual stability in the case of the breakage of different elements – so essential in all-glass structures – was considered as follows:

Glass built up – performance:
The use of certain combinations of glass-types in the laminated glass product can be regarded as the first component in the safety concept because in the event of one (or more) single layers of glass breaking, the remaining elements satisfy specific loadbearing requirements.
(Mixture between annealed glass – tempered glass – HS glass and PVB /SGP interlayers)

Neighbouring elements carrying the load
A couple of accidental/fragility scenarios are incorporated in the structural analyses for the case of complete failure of whole structural elements of the building and the construction is arranged in such a way that loads are transferred to neighboring components. Consequently, under certain actions, even whole elements can fail in theory without this resulting in the entire structure collapsing.

Preventing direct actions by way of constructional protective measures

Specific measures, e.g. concrete up-stands, protective foils, protection to the edges of the glass, can be employed over the entire structure to prevent actions occurring that might damage certain components.

2.5 Special glass specification

The specification of the client, London Underground, called for the façades and roofs to be carried out in self-cleaning glass, which allows water to collect in individual droplets and is dirt-repellent. In addition, façade surfaces up to a height of about 3m above ground level must be provided with an anti-graffiti coating.

2.6 Closing remarks/Summary

The type of construction selected for this project is an impressive demonstration of the performance of structural glass components plus their contribution to the transparency of building envelopes. Innovative connection technologies and structural engineering approaches have allowed the design team to choose constructional solutions that emphasize the "crystalline" character of this structure. The engineering strategies employed have resulted in a structure that complies with all the necessary safety standards while still achieving a minimalistic form of construction. Yet another significant iconic highlight in the vast tapestry of urban architecture within the heart of London.

Figure 7: Artist impression of the lighting strategy of glazed plaza entrances

3 Acknowledgements

The author would like to acknowledge the Tottenham Court Road Station Upgrade project for the selection of such an iconic structure to form the center of the new station works in this central London location. Additional acknowledgement must go the Stanton Williams for their competition winning entry, selected by Transport for London (TfL).

4 References

[1] IB Schuler - Structural Calculation –global and detail.
[2] Stanton Williams – Stage D-Report
[3] Taylor Woodrow – BAM Nutgall JV – Documentation
[4] se-austria GmbH & Co KG – Documentation
[5] Hochschule München LSL – Test Report

Proceedings of the International Conference on Building Envelope Design and Technology, Graz
Advanced Building Skins 2015

Post-tensioned Structural Glass Beams – Comparative Experimental Study

Jagoda Cupać, M.Sc.
ICOM Steel Structures Laboratory, EPFL École Polytechnique Fédérale de Lausanne, Switzerland, jagoda.cupac@epfl.ch

Christian Louter, Dr. ir.
ICOM Steel Structures Laboratory, EPFL École Polytechnique Fédérale de Lausanne, Switzerland, christian.louter@epfl.ch

Summary

This paper presents a study of a system of post-tensioned structural glass beams. In order to increase the initial fracture strength of glass beams and provide residual load-carrying capacity in the event of glass failure, annealed laminated glass beams are reinforced with flat stainless steel tendons, which are pre-tensioned and bonded to the lower edge of the beam. When the adhesive has cured, the pre-tension is released, inducing a compressive pre-stress and an upwards bending moment on the beam. The behaviour of these post-tensioned beams is compared to reinforced beams (without post-tensioning) and reference beams (without reinforcement) through series of four-point bending tests. The results show a highly improved performance of the beams, both before and after initial glass fracture.

Keywords: Structural glass, Beam, Post-tensioning, Redundancy, Experimental study

1 Introduction

The application of glass in structural beam elements, given its brittle failure behaviour, requires special design considerations. Possible glass fracture might directly influence the overall integrity of the structure. The concept of post-tensioning a glass beam through ductile reinforcement aims to enhance the structural performance of glass in such applications by increasing the initial fracture strength of glass beams and by providing a significant residual load-carrying capacity in the event of glass failure. This concept has been explored in several projects which have proved its potential in structural glass applications, but are still largely in the domain of research [1]–[7].

This paper explores the structural performance of post-tensioned glass beams with adhesively bonded steel tendons in comparison with reinforced glass beams (without post-tensioning) and common glass beams (without reinforcement). Glass beams, consisting of three layers of annealed glass laminated with SentryGlas® interlayer, are post-tensioned through flat stainless steel tendons which are first pre-tensioned and then bonded to the lower edge of the glass beam. Once the adhesive has cured, the pre-tension is released into the beam through the adhesive bond, thus inflicting a compressive pre-stress and an upwards bending moment on the beam. As a result, the bending strength is enhanced. In the event of glass failure, the steel tendon generates a post-fracture load-carrying mechanism by taking over the tensile forces that the cracked glass section is no longer able to carry. This provides a highly redundant ductile structural response, reducing the consequences of brittle glass failure. Such mechanism has been explored in various preceding projects on reinforced glass beams [8]–[12]. Four-point bending tests have been performed on 1.5 m long glass beams with a varying level of pre-tension, as well as reinforced beams without pre-tension in order to investigate the contribution of active tendons in a post-tensioned glass beam system. A series of reference beams without reinforcement has been tested to determine the bending strength of the glass cross-section applied in the reinforced series and determine the basic structural response of simple laminated glass beams.

The following section gives a detailed description of the test specimens. It explains the post-tensioning method applied in the preparation of post-tensioned glass beams as well as the four-point bending test procedure. The results of the tests are subsequently presented and discussed, with conclusions of the study outlined at the end of the paper.

5 Materials and Methods

2.1 Test Specimens

The specimens consist of three layers of annealed float glass (6.10.6x122 mm) laminated with a SentryGlas® interlayer (1.52 mm). Reinforced and post-tensioned beam series incorporate a stainless steel section (25x3 mm, grade 1.4301) bonded to the lower edge of the glass beam by means of a two-component methacrylate adhesive Araldite® 2047-1. All glass edges have been polished after the lamination in order to ensure a perfectly aligned surface for bonding the reinforcement. The beams are 1.5 m long. The cross-sections of the specimens are shown in Figure 1.

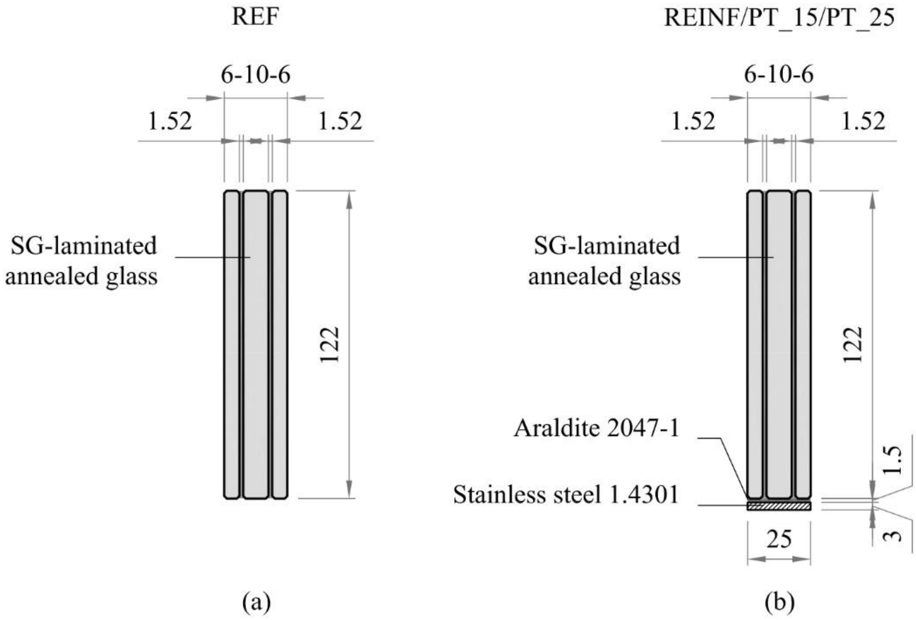

Figure 1: Cross-sections of beam specimens; (a) reference glass beam; (b) reinforced/post-tensioned glass beam; all dimensions are given in [mm].

The selection of an appropriate adhesive has been based on the following requirements:

- suitability for glass-steel bonding;
- high shear strength;
- durability (UV, humidity, cleaning agents);
- reduced tendency to creep;
- service temperature from -20°C to +80°C [13]
- shock resistance;
- suitable viscosity and curing time for the manufacturing of bonded beam specimens.

Araldite® 2047-1 has been chosen based on previous research by others [14], [15] and consultations with adhesive manufacturers. According to the manufacturer’s datasheet [16], it can achieve lap-shear strength of more than 15 MPa. Easy application and relatively short curing time (25 minutes at room temperature) facilitate fast manufacturing process.

2.2 Post-tensioning Method

The external post-tensioning of the beams is performed in a custom-made steel rig, shown in Figure 2. The steel tendon is fixed at each end to a threaded bar on which a torque is applied, thus extending the tendon. The applied tensile force is measured by means of load cells on either side of the rig. Subsequently, the adhesive is applied on a cleaned surface of the steel and the glass beam is positioned on top. Spacers are placed between steel and glass to ensure a uniform thickness of 1.5 mm. After the adhesive has cured (at least 72 hours), the force of pre-tension is released from the rig into the glass beam through the adhesive bond. During the release, the strain on the top of the glass beam is recorded by a strain gauge at the mid-span of the beam.

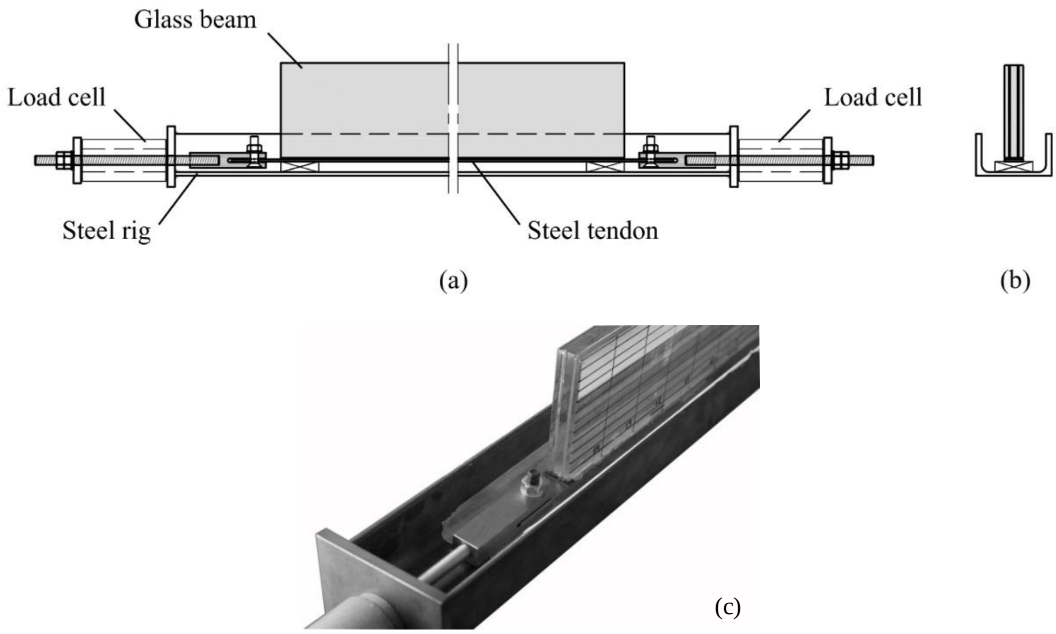

Figure 2: Post-tensioning method; (a) longitudinal and (b) cross-section of the post-tensioning rig; (c) glass beam bonded to the pre-tensioned reinforcement.

Two levels of pre-tension have been applied to the steel tendons, 15 kN and 25 kN. Considering a full composite action between steel and glass, calculated glass stress in the mid-span of the beam induced by a 15 kN pre-tension equals about -17 MPa (compression) at the lower glass edge, and 9 MPa (tension) at the top. The pre-tension level of 25 kN yields a stress of about -29 MPa at the lower edge, and 15 MPa at the top. Measurements obtained with the strain gauge on the top of the glass beam closely correspond to the calculated values, which demonstrates high shear stiffness of the adhesive bond and nearly no (instant) loss of pre-tension.

2.3 Test Setup

The beams have been tested in four-point bending. The setup consists of a custom support frame mounted in a universal compression-tension machine (Zwick 500 kN). The total span is 1400 mm, the span between load points being equal to 400 mm. The beams are laterally supported at a 200 mm from the vertical support. The tests are displacement controlled, at a fixed displacement rate of 1mm/min until initial glass failure. Subsequently, the displacement rate is increased to 2mm/min and 5mm/min to shorten the duration of the test.

The following series of tests have been performed, with three specimens tested in each series:

- REF – reference beams without reinforcement;
- REINF – reinforced beams without pre-tension;
- PT_15 – post-tensioned beams with 15 kN pre-tension in the reinforcement;
- PT_25 – post-tensioned beams with 25 kN pre-tension in the reinforcement.

6 Results

The results of the four-point bending tests are given in Table 1 and Figures 3-7. Table lists the tested specimens, indicating the pre-load applied through the reinforcement, fracture load at which the first crack in the glass appeared, maximum post-fracture load and a post-fracture reserve which presents the maximum post-fracture load as a percentage of the initial fracture load. The last column describes the failure mode, which was either a failure of the steel tendon (steel), glass failure (glass) or adhesion failure (adhesion) on the glass surface. The latter resulted in a premature failure of the beams due to de-bonding of the reinforcement.

Table 1: Results of four-point bending tests.

Specimen	Pre-load [kN]	Fracture load [kN]	Max. post-fracture load [kN]	Post-fracture reserve [%]	Ultimate failure mode
REF#1	-	8.3	2.8	33	glass
REF#2	-	9.5	2.4	25	glass
REF#3	-	8.2	2.7	33	glass
Mean (COV)		*8.6 (7%)*	*2.6 (6%)*	*31 (13%)*	
REINF#1	-	13.3	36.9	276	steel
REINF#2	-	10.7	36.7	343	steel
REINF#3	-	12.4	36.5	295	steel
Mean (COV)		*12.1 (9%)*	*36.7 (0.3%)*	*305 (9%)*	
PT_15#1	15.3	16.0	37.7	235	steel
PT_15#2	15.2	16.5	36.3	220	steel
PT_15#3	15.5	18.2	37.1	203	steel
Mean (COV)		*16.9 (6%)*	*37.0 (2%)*	*220 (6%)*	
PT_25#1	25.9	23.6	36.6	155	steel
PT_25#2	25.5	16.1	34.8	216	adhesion
PT_25#3	25.5	22.7	28.6	126	adhesion
Mean (COV)		*20.8 (16%)*	*33.3 (10%)*	*166 (23%)*	

Figures 3-6 present the load-displacement diagrams from four-point bending tests. Figure 7 shows a comparison of the typical diagrams of all series. All beams show linear-elastic response until initial glass fracture, after which the steel in the post-tensioned and reinforced specimens facilitates the continuation of loading above the initial fracture load. Finally, the yielding of the reinforcement provides a long ductile trajectory until the ultimate failure of the beam. Reference beams, on the other hand, show very low residual strength and fail soon after initial glass fracture.

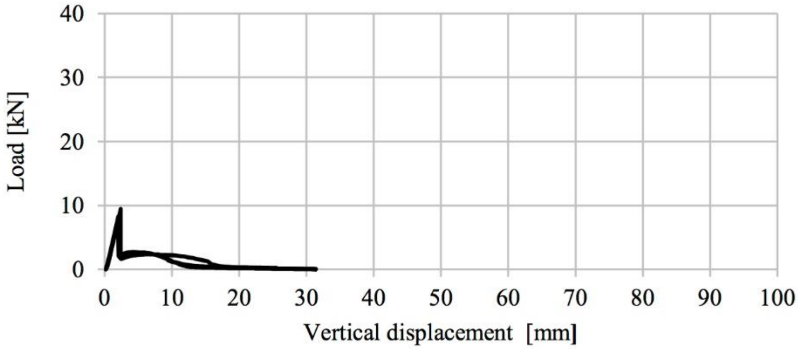

Figure 3: Load-displacement diagrams of series REF - reference beams without reinforcement.

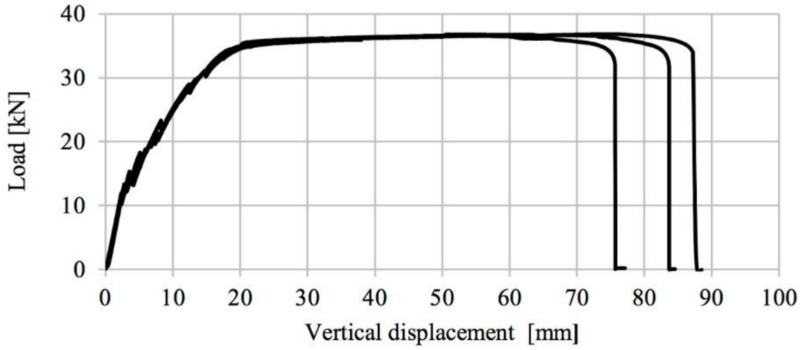

Figure 4: Load-displacement diagrams of series REINF - reinforced beams without pre-load.

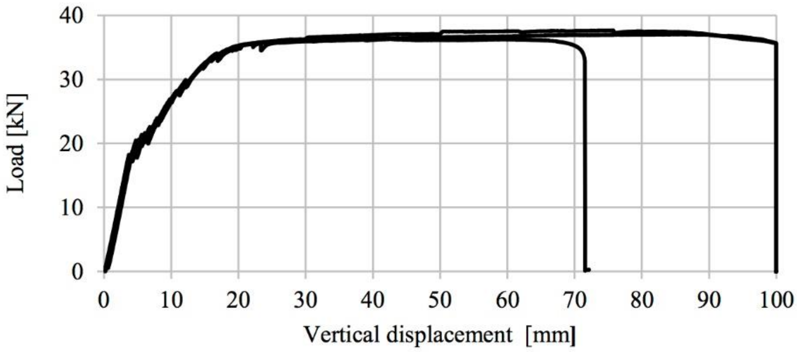

Figure 5: Load-displacement diagrams of series PT_15 - post-tensioned beams with a 15 kN pre-load.

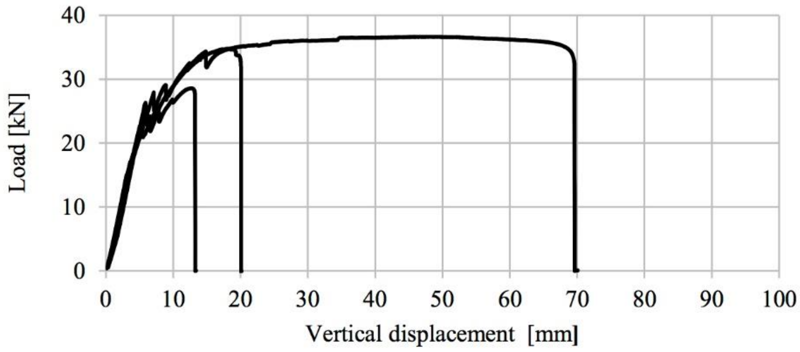

Figure 6: Load-displacement diagrams of series PT_25 - post-tensioned beams with a 25 kN pre-load.

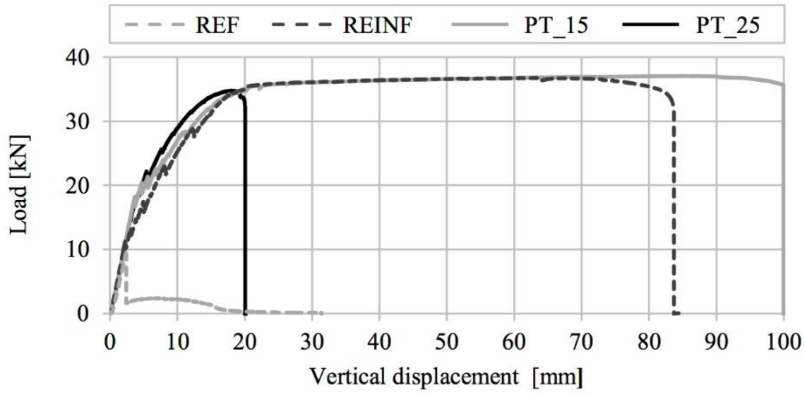

Figure 7: Comparison of the typical load-displacement diagrams of all series.

7 Discussion

Compared to the structural response of reference glass beams, both reinforced and post-tensioned glass beams demonstrate increased initial fracture strength and significantly improved post-fracture behaviour.

In the case of *reinforced beams*, enhanced initial fracture strength is a result of increased moment of inertia and a shift of the neutral axis towards the lower glass-edge, due to the composite action between the bonded steel profile and the glass section. While the average initial fracture load of reference beams amounts to 8.6 kN, reinforced beams reach 12.1 kN, which is a 40% increase. Further increase of fracture strength observed for the *post-tensioned beams* can be attributed to the applied pre-load; the compressive pre-stress generated at the lower edge of the glass annuls the tensile stress induced by four-point bending, and thus increases the initial fracture load. Beams post-tensioned with a 15 kN pre-load reached an average initial fracture load of 16.1 kN, 39% higher than the reinforced beam series, and an overall increase of 96% compared to the reference beams. In the second series of post-tensioned beams, 25 kN pre-load contributed to a 20.8 kN initial fracture load, improving the result of the reinforced beam series by 71%. Compared to the reference beams, this equals a 141% increase.

Following the procedure presented in [4], the average tensile stress calculated at the lower glass edge at initial fracture, taking into account a full composite action between steel and glass, equals 41.5 MPa for the reinforced beam series, and 40.7 MPa and 41.4 MPa for the two series of post-tensioned beams. These values correspond well with the tensile bending strength of the reference beams, which amounts to 39.9 MPa, confirming that the increase in fracture load can be fully attributed to the increase in inertia and the applied pre-stress, rather than a difference in basic glass strength.

Regarding the post-fracture behaviour, reinforced and post-tensioned beams exhibit a highly redundant performance, reaching loads significantly above the initial fracture load. The steel tendon facilitates a ductile response accompanied with progressive cracking of the glass, leading to the ultimate failure. In the series REINF and PT_15, all beams failed explosively due to the ultimate failure of the steel tendon. The shock caused a full rupture of the laminated glass section, resulting in beams splitting in half (Figure 8, left). Since the failure occurred at considerably high loads, the structural response can still be considered safe. In the series PT_25, different failure modes can be observed. Two beam specimens failed due to adhesion failure on the glass-side of the joint (Figure 8, right). The tendon de-bonded before a ductile response could be fully developed. Increased level of pre-tension, which had induced a high shear stress in the adhesive, reduced the capacity of the joint to carry increasing loads in the four-point bending test. Nevertheless, the initial fracture load was still exceeded, with one specimen reaching the ultimate capacity of the steel tendon. Reference beams, on the other hand, showed very low level of redundancy, failing soon after the first crack in the glass occurred. The average maximum post-fracture load reached only 31% of the initial fracture load.

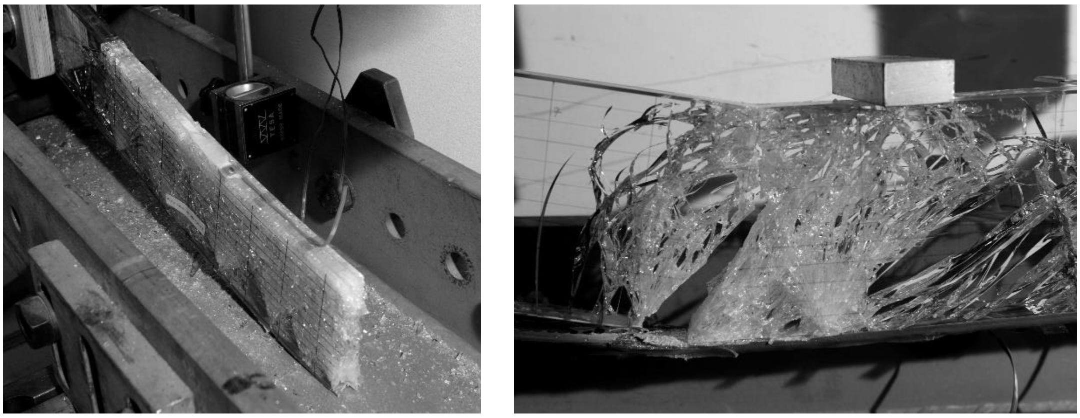

Figure 8: Beams after ultimate failure; steel failure (left); adhesion failure (right).

8 Conclusions

From the results of the experimental study which has compared the behaviour of post-tensioned, reinforced and common glass beams through series of four-point bending tests, it can be concluded that post-tensioning a glass beam through ductile reinforcement presents a feasible concept which results in increased fracture strength and enhanced post-fracture behaviour. The initial fracture strength of post-tensioned beams is enhanced by the application of compressive pre-stress through adhesively bonded pre-tensioned reinforcement. Furthermore, the steel reinforcement facilitates a ductile and highly redundant post-fracture behaviour of both reinforced and post-tensioned beams, reducing the consequences of brittle glass failure.
However, it should be noted that this study has only investigated the short-term behaviour of post-tensioned glass beams with adhesively bonded reinforcement. Permanent stressing of the adhesive may cause creep and loss of pre-stress in the glass beam. Further research will focus on exploring this phenomenon in more detail. Furthermore, alternative concepts will be studied, including a combination of mechanical and adhesive introduction of pre-stress by anchoring the reinforcement at beam-ends. In this way, the negative effect of creep might be avoided, while maintaining the favourable effect of the adhesive bond on the post-fracture response of the beam.

9 Acknowledgements

The present research is funded by the Swiss National Science Foundation through SNF Grant 200021_143267.

10 References

[1] Belis, J., Louter, C., Verfaille, K., van Impe, R., Callewaert, D.: *The effect of post-tensioning on the buckling behaviour of a glass T-beam*, ISAAG - International Symposium on the Application of Architectural Glass, Munich, Germany, 2006.

[2] Bos, F., Veer, F., Hobbelman, G., Louter, C.: *Stainless steel reinforced and post-tensioned glass beams*, ICEM12- 12th International Conference on Experimental Mechanics, Bari, Italy, 2004.

[3] Jordão, S., Pinho, M., Martins, J. P., Santiago, A., Neves, L. C.: *Behaviour of laminated glass beams reinforced with pre-stressed cables,* in: Steel Construction 7 (2014) issue 3, pp. 204–207.

[4] Louter, C., Cupać, J., Lebet, J.-P.: *Exploratory experimental investigation on post-tenisoned structural glass beams*, in: Journal of Facade Design and Engineering (to be published in the upcoming volume, available at www.iospress.nl/journal/journal-of-facade-design-and-engineering/)

[5] Louter, C., Nielsen, J. H., Belis, J.: *Exploratory experimental investigations on post-tensioned structural glass beams*, ICSA - The 2nd International Conference on Structures and Architecture, Guimarães, Portugal, 2013.

[6] Schober, H., Gerber, H., Schneider, J.: *Ein Glashaus für die Therme in Badenweiler*, in: Stahlbau 73 (2004) issue 11, pp. 886-892.

[7] Weller, B., Engelmann, M.: *Deformation of Spannglass beams during post-tensioning,* Challenging Glass 4 & COST Action TU0905 Final Conference, Lausanne, Switzerland, 2014.

[8] Louter, C., Belis, J., Veer, F., Lebet, J.-P.: *Structural response of SG-laminated reinforced glass beams; experimental investigations on the effects of glass type, reinforcement percentage and beam size*, in: Engineering Structures 36 (2012), pp. 292–301.

[09] Ølgaard, A. B., Nielsen, J. H., Olesen, J. F.: *Design of mechanically reinforced glass beams: modelling and experiments*, in: Structural Engineering International 19 (2009) issue 2, pp. 130–136.

[10] Palumbo, D., Palumbo, M., Mazzucchelli, M.: *A new roof for the XIIIth century 'Loggia de Vicari' (Arquà Petrarca - PD - Italy) based on structural glass trusses: a case study*, Glass Processing Days, Tampere, Finland, 2005.

[11] Speranzini, E., Agnetti, S.: *Strengthening of glass beams with steel reinforced polymer (SRP)*, in: Composites Part B: Engineering 67 (2014), pp. 280–289.

[12] Weller, B., Meier, A., Weimar, T.: *Glass-steel beams as structural members of façades*, Challenging Glass 2, Delft, Netherlands, 2010.

[13] ETAG 002 - Guideline for European technical approval for structural sealant glazing systems (SSGS) - Part 1: Supported and unsupported systems, EOTA - European Organisation for Technical Approvals, Brussels, Belgium, 2001.

[14] Belis, J., Van Hulle, A., Out, B., Bos, F., Callewaert, D., Poulis, H.: *Broad screening of adhesives for glass- metal bonds,* Glass Performance Days, Tampere, Finland, 2011.

[15] Nhamoinesu, S., Overend, M.: *The Mechanical Performance of Adhesives for a Steel-Glass Composite Façade System*, Challenging glass 3, Delft, Netherlands, 2012.

[16] Technical data sheet, Araldite® 2047-1, Structural Adhesives, Huntsman Corporation, 2013.

refurbishment

Proceedings of the International Conference on Building Envelope Design and Technology, Graz
Advanced Building Skins 2015

Mid-Century Modern Refurbishing Curtain Walls in the Former GDR

Bernhard Weller, Prof. Dr.-Ing.
Technische Universität Dresden, Germany, bernhard.weller@tu-dresden.de

Marc-Steffen Fahrion, Dipl.-Ing.
Technische Universität Dresden, Germany, marc-steffen.fahrion@tu-dresden.de

Sebastian Horn, Dipl.-Ing.
Technische Universität Dresden, Germany, sebastian.horn@tu-dresden.de

Summary

This article shows the construction details of an industrialized standard building called “Mehrzweckgeschossbau Typ Leipzig”, which was developed during the late 1960s in the former German Democratic Republic (GDR). One main challenge of the 21st century is the adaptation of the built environment to climate change. Therefore, the industrialized standard building is investigated concerning the consequences of elevated summer temperatures due to climate change. The climate data used to deal with climate change between 1950 and 2100 are presented. Despite of climate change heating demand remains the main challenge in preserving buildings of the 1960s and 1970s, although the cooling demand rises significantly. We present several strategies for the refurbishment of this industrialized standard building. If the emission of well mixed greenhouse gases meets the upper bounds of the Special Report on Emission Scenarios (SRES) it will be almost impossible to meet the actual German requirements for the protection against summer overheating.

Keywords: Monument Protection, Climate Change, Climate Adaptation, Summer Overheating, Building Automation

1 Introduction

Buildings of the 1960s and 1970s come into focus of the cultural heritage preservation. After more than 40 years of use, the pressure for refurbishment procedures is elevated. Among experts it becomes accepted, that unique buildings of the mid-century modern should be protected. In contrast the question if industrialized standard buildings should be preserved is under debate. Thereby such buildings particularly in the context of an architectural ensemble give a glimpse of the former ideal conception of urban development and the social ideas that are reflected by them. The permanent use of a building is a basic requirement for a persistent preservation. Therefore it is essential that buildings meet the current comfort demands of the users without having an elevated energy demand. After a basic refurbishment the new building components partially reach lifetimes of 50 years. Hence todays’ decisions have consequences until the second half of the 21st century. Therefore the projected climate change and the related changes of the environmental impacts on the built environment have to be considered. A sustainable solution has to take the future developments and the aspects of lifecycle assessment into account. Otherwise the changed boundary conditions make it necessary to replace the refurbished building components before they have reached the end of their lifetime. The consequence is a loss of grey energy. Consequently it is necessary to deal with the effects of climate change on the built environment during the planning of refurbishment procedures.

2 Mehrzweckgeschossbau Typ Leipzig

2.1 Development

The building under investigation is an industrialized standard building called "Mehrzweckgeschossbau Typ Leipzig". Mehrzweckgeschossbau means multistorey multipurpose building. It was developed during the late 1960s and the early 1970s by the Metalleichtbaukombinat (MLK) of the former German Democratic Republic (GDR) under the leadership of Rolf Engelhard, Rolf Schaufel and Siegfrid Rahm as a lightweight steel construction. It has been built several times in the GDR and Poland [1,2,3]. The development of standardized buildings in the GDR was forced by the political establishment. During the standardization conference of the national planning commission on the 11th and 12th February 1959 in Leipzig it was decided to standardize more building elements and to accelerate the development of standard buildings. The aim was the so called radical standardization. During the 1960s the focus was on concrete constructions but the Council of Ministers of the GDR concluded on the 5th October 1967 to develop preferably lightweight steel constructions. Therefore the nationally owned Metalleichtbaukombinat was founded on the 16th January 1968 in the city of Halle [4]. The research institute of the Metalleichtbaukombinat, which was situated in Leipzig developed during the year 1969 the presented building type. The first building of this type was finished in October 1971 in Siegfriedstraße in Berlin-Lichtenberg. The façade elements had a weather shell made of colored enameled steel sheets [5]. In later years weather shells of single-pane safety glass were preferred.

2.2 Building construction

The envelope of the Mehrzweckgeschossbau Type Leipzig is made of a curtain wall façade which was developed by the Metalleichtbaukombinat and which is called MLK-Vorhangwand. It is an unitized façade which has not only been used for the type Leipzig but also for other standard buildings. Unitized façades are prefabricated façade elements which span from floor to ceiling. They are delivered to the building site readily for installation (Figure 3). Because of the complete prefabrication a high manufacturing quality and a fast building progress are guaranteed. The load bearing construction of each façade element consists of U-profiles which form a steel frame that spans from floor to ceiling. The frame is divided into three sections by two further horizontal U-profiles, one between the balustrade and the window and the other one between the window and the lintel area.

The layer composition of the opaque areas of the façade is explained in brief from the inner to the outer surface. There are two different versions for the construction of the inner shell (see Figure 5, no. 9). The first version consists of a Sokalit-panel and a Gölzathen-foil. The former is a loosely bound asbestos product [6], which is used for fire protection and forms the inner surface of the building element. The latter is a vapor barrier made of polyethylene. In the second version an asbestos cement panel of 8 mm thickness fulfills both tasks, fire protection and moisture protection. The asbestos cement panel reaches a much lower water vapor diffusion equivalent air layer thickness (s_d) than the Gölzathen-foil. Using the physical values from the 1970s [7] condensation can occur in the building element. As the outer layers of the building element have a high vapor permeability the condensate is

Figure 1: Type Leipzig, curtain wall façade, weather shell made of enameled steel sheets, Berlin Siegfriedstraße.

Figure 2: Type Leipzig, weather shell made of enameled single-pane safety glass, Radebeul Wasastraße.

Figure 3: Installation of the unitized façade.

Figure 4: Prefabricated composite-steel deck floors.

able to dry out during the evaporation period. The following thermal insulation (Figure 5, no. 10) is made of 80 mm mineral wool. The outer surface, that is not fully exposed to weathering, is formed by another asbestos cement panel (no. 11). A rear-ventilated weather shell, which is optionally made of an enameled or coated steel sheet or an enameled single-pane safety glass, gives the façade its colorful appearance (no. 13). Depending on the design the ventilation gap is 62 mm or 134,5 mm wide (no. 12).

The primary structure of the multistorey building is a steel skeleton. Only the foundations, the base plate and the outer walls of the basement are made of concrete. The steel skeleton is made of two-span storey frames which span in transverse direction of the building. In longitudinal direction of the building the frames are connected by stringers. The stringers also serve as support for the prefabricated composite-steel deck floors (see Figure 4 and Figure 5, no. 2). The bottom chords of the composite-

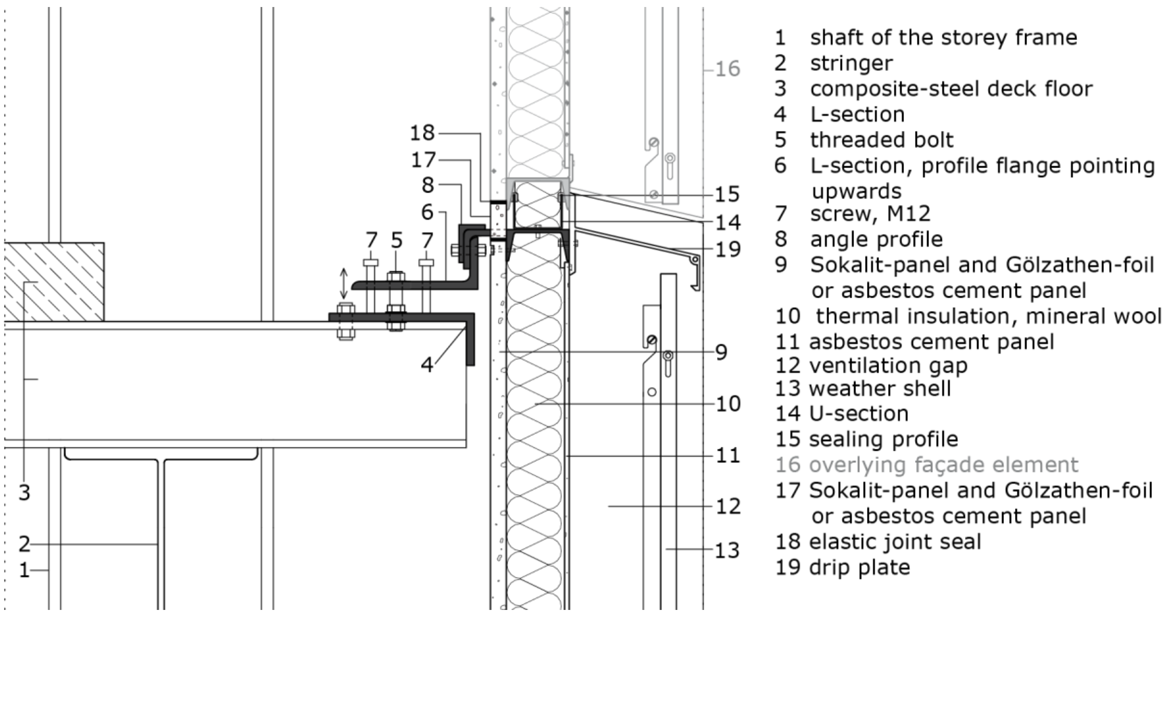

Figure 5: Vertical section through the support of the façade and the façade panels.

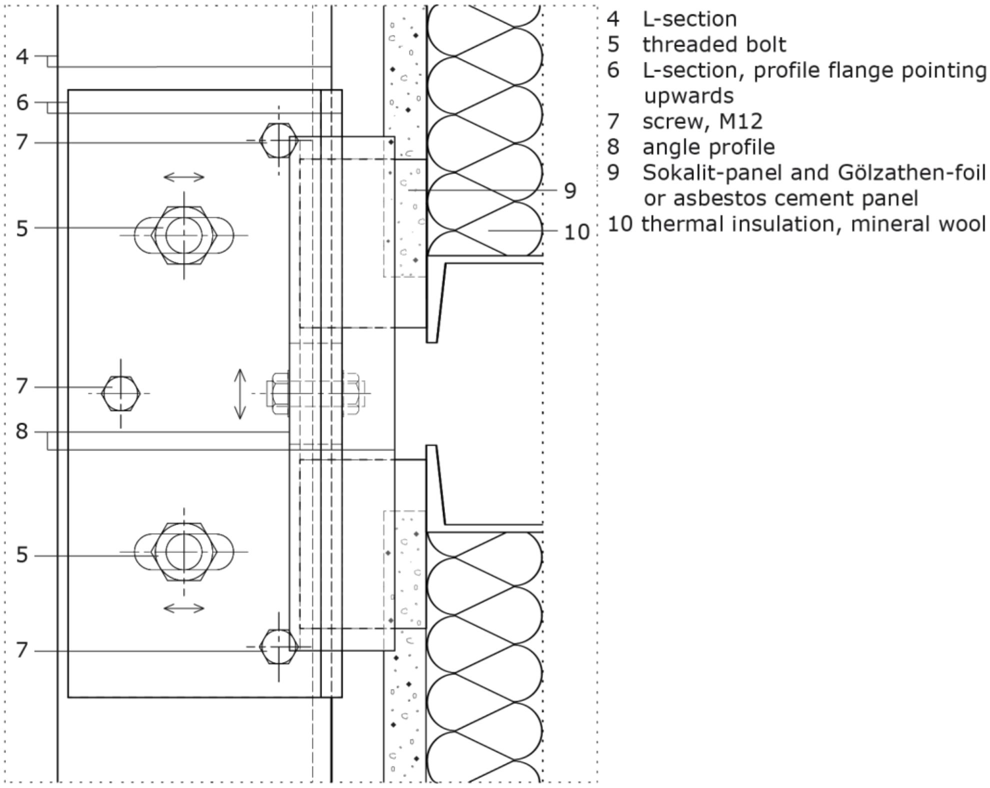

Figure 6: Top view on the support of the façade.

steel deck floors project beyond the concrete top chord. By welding, the bottom chords are connected with the stringers. The protruding steel bottom chords of the floors are used as bearing points for the curtain wall (Figure 5, no. 3).

The façade elements were delivered by trucks on transport racks (Figure 3). Afterwards they were mounted infront of the load bearing structure. The construction of the façade support and the installation of the unitized façade are explained by using Figures 5 and 6. In Figure 5 the shaft of the storey frame (no. 1) and the composite-steel deck floor (no. 3) which lies on the stringer (no. 2) that connects the different frames can be seen. The stringer is made of an I-section. The bottom chord of the composite-steel deck floor is formed by a I-section as well and projects beyond the stringers. The protruding bottom chords are connected by L-sections (no. 4) which span in longitudinal direction of the façade. They are fixed by screws. On top of the L-sections the support of the façade is installed. During the installation two threaded bolts were fixed at the L-section by screw nuts (Figure 5 and 6, no. 5). Another L-section was put on the threaded bolts, the profile flange pointing upwards (no. 6). The L-section with the upward pointing profile flange has three tapped holes with screws in them (no. 7). By screwing in and out, the support of the façade was adjusted in the height. Elongated holes in the L-section made the adjustment perpendicular to the façade plane possible (Figure 6). Afterwards the prefabricated façade elements were mounted. By shifting the façade elements on the upward pointing flange of the L-section (perpendicular to the drawing layer of Figure 5) an adjustment parallel to the façade was reached. The façade element was finally fixed by an angle profile (no. 8) that is screwed against the upward pointing flange of the L-section.

On the top side of every façade element is a U-section with the legs facing upwards (no. 14). The U-profile secures the position of the overlying façade element and plays an important role in the joint design of the horizontal intersection. Sealing profiles were put on top of the U-section legs (no. 15). A thermal insulation strip was pressed between the legs of the U-profile and the overlying façade element was mounted. The joint was closed depending on the version of the inner surface of the façade by a strip of an asbestos cement panel or a vapor barrier and a Sokalit-strip. From the outside a drip plate (no. 19), which covers the joint, was fixed.

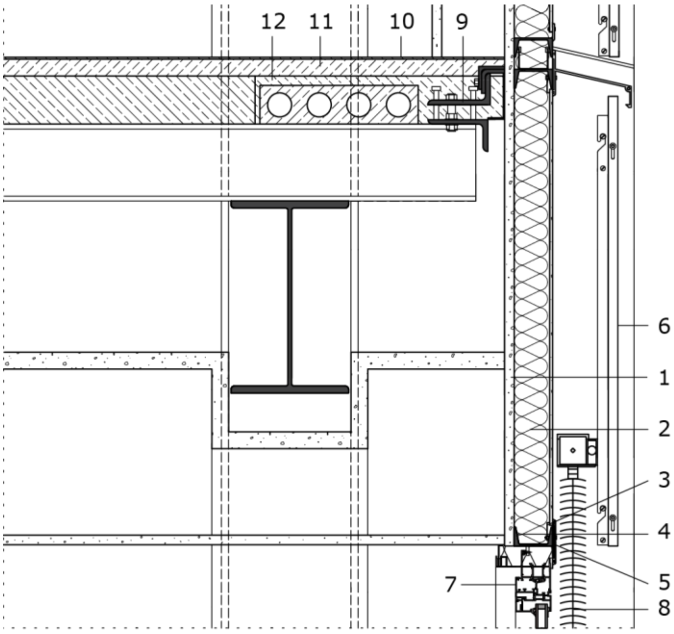

Figure 7: Vertical section through the façade of the investigated building after first refurbishment (1996).

The following investigations were made for a representatively chosen building of the type Leipzig. The original double-glazed windows were replaced by windows with thermal insulation glazing during a first refurbishment in 1996. Furthermore a second suspended ceiling was installed. A vertical section through the façade of the investigated type Leipzig in the actual state is shown in Figure 7.

3 Climate Change

The anthropogenic emission of greenhouse gases is the main reason for the observed climate change [8]. According to measurements on Antarctic ice cores todays' atmospheric greenhouse gas concentrations are with very high confidence the highest of the last 800,000 years [9]. Since the beginning of the 20th century the annual global mean surface temperature has increased by 0.89 °C [10]. Observations and climate change projections for Germany show important changes in the environmental impacts on buildings. Problems and damages caused by summer heat, flooding, torrential rain, windstorms and hail have increased and will further increase due to climate change. The building industry has to react on these changing impacts.

Climate projections for central Europe and Germany show the most pronounced and most consistent changes for the environmental impact summer heat. Heatwaves will get more intense and more frequent during the course of the 21st century [11]. While the endangering of buildings through the other mentioned environmental impacts is dependent on the location of a building, all buildings in Germany will suffer under the projected increase in summer temperature [12]. Therefore this paper focuses on the question how to cope with the increasing problems of summer overheating.

For the investigation of the effects of the observed and projected rise in summer temperatures thermal building simulations are used. Currently this is the most precise method to cope with the protection against summer overheating. For running thermal building simulations hourly datasets of several climatic elements like global radiation, diffuse radiation, air temperature, etc. are required. Test Reference Years (TRY) are climate data sets which are especially generated for the use in building simulation software. They contain the requested climatic elements in hourly resolution. For Germany there are three Test Reference Years that are based on observational data from different time periods. These are the Test Reference Years 1986 [13], 2004 [14] and 2010 [15], that are based on observational data of the periods 1951-1976, 1961-1990, 1988-2007 respectively. In contrast the Test Reference Year 2035 was developed using climate projections for the period 2021-2050 under the boundary conditions of the SRES-emission scenario A1B. With the existing Test Reference Years the observed and the projected climate change from the middle of the 20th century to the middle of the 21st century can be depicted. Numerous climate projections suggest a pronounced temperature increase during the end of the 21st century [16]. To deal with this the recorded data of the hot and outstanding summer in the year 2003 at the weather station Mannheim is used. According to different studies the recorded data in the center of the heat wave 2003 can be used as an analog of future summers for the period 2071-2100, if the future greenhouse gas emissions will follow the scenario A2 of the Special Report on Emission Scenarios (SRES) [17, 18]. All the following investigations are made for the hot summer regions in Germany according to the specifications of DIN 4108-2:2013-02.

4 Heating and Cooling demand

Using the introduced climate data the evolution of the heating and cooling demand of the investigated industrialized standard building type Leipzig under changing climate conditions is illustrated (Figure 8). The observational data of the year 2003 is not suitable to depict a characteristic winter period at the end of the 21st century. The temperatures in the winter months January, February and December in the year 2003 were below the average of the period 1961-1990 [19]. Hence an extrapolated exponential trend is used to approximate the heating demand at the end of the 21st century coarsely (black line in Figure 8). Due to climate change there is a marked decrease of the heating demand while the cooling demand rises. Nevertheless for the building under investigation the heating demand stays above the cooling demand. Several other buildings which were investigated and that are protected as historic monuments show the same behavior. For such buildings the total energy demand, this means the sum of heating and cooling demand, decreases with ongoing climate change. Consequently these buildings benefit from climate change. Buildings with higher standards of thermal insulation show a different behavior. There the absolute cooling demand can exceed the heating demand with ongoing climate change [20].

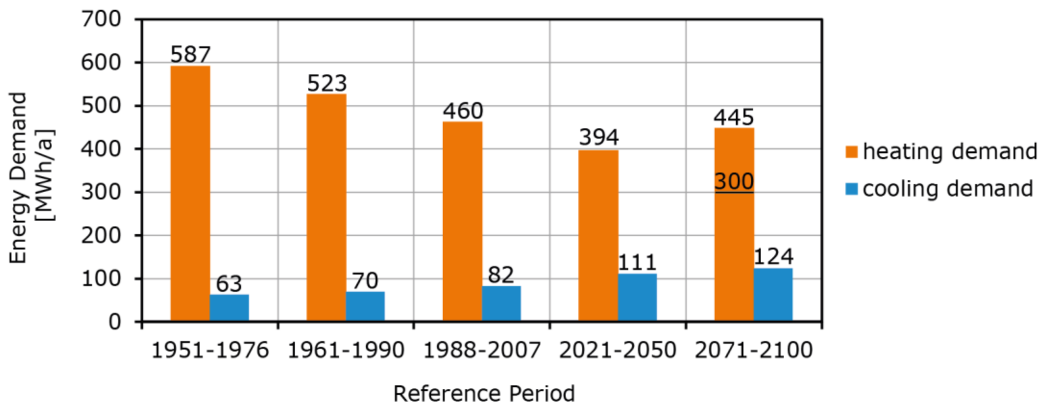

Figure 8: Evolution of heating and cooling demand under changing climatic conditions.

5 Protection against summer overheating

The thermal quality in the interior for a prolonged period of time in the hot summer regions of Germany can be assessed according to DIN 4108-2:2013-02 by using degree hours above the threshold of 27 °C. Degree hours do not only account for the duration of a temperature exceedance but also for the height of the exceedance. Degree hours are only calculated during the period of use. That means for non-residential buildings from Monday to Friday from 7 am to 6 pm. The maximum value of degree hours for non-residential buildings to satisfy the requirements of DIN 4108-2:2013-02 is 500 Kh/a (Figure 10, red line).

5.1 Assessment of the actual state

The Mehrzweckgeschossbau Typ Leipzig is a lightweight steel construction with a curtain wall façade, suspended ceilings and plasterboard drywalls. Therefore the typical rooms have a very low heat storage capacity of only 10 Wh/(Km^2). In addition the building type has large window strips and therefore high solar energy inputs. The long sides of the investigated building are oriented to the north-northeast and south-southwest. Most of the windows oriented to the south-southwest have manually controlled external venetian blinds while all the others have no sun protection (Figure 9). Due to the combination of the mentioned parameters the critical rooms of the building considerably exceed the maximum permitted value of degree hours even under actual climatic conditions (Figure 10, red line). The degree hours are calculated for three different threshold temperatures, while 27 °C is the value that has to be used for the proof according to DIN 4108-2:2013-02. The extreme increase of degree hours with ongoing climate change is striking. Therefore the focus of refurbishing procedures needs to be broaden upon the protection against summer overheating.

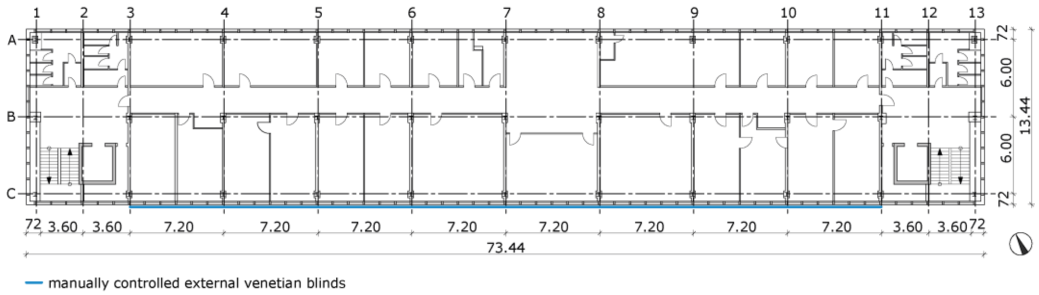

Figure 9: Floor plan of the investigated type Leipzig and sun protection measures in the actual state.

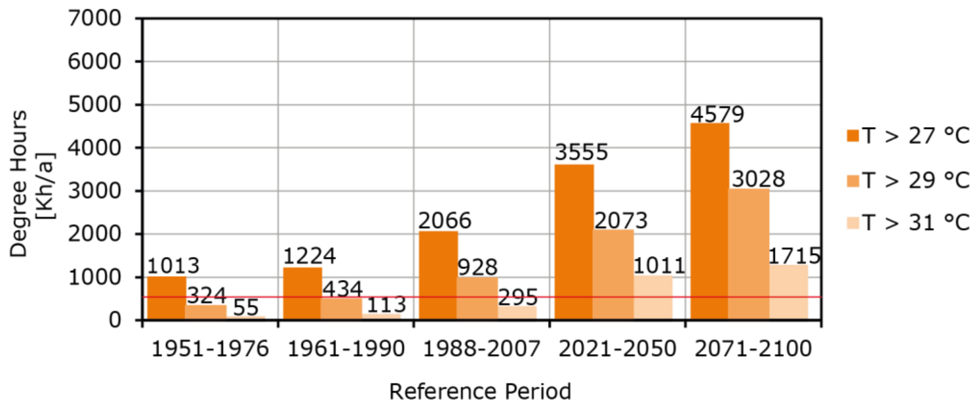

Figure 10: Degree hours for the critical room in the actual state of the building under different climate conditions.

5.2 Refurbishment

In the following different possibilities for improving the protection against summer overheating of the standard building type Leipzig are presented. In a first step the heat inputs into the building should be reduced. In a second step the remaining excess heat should be dissipated by using natural heat sinks. As long as the better part of the energy demand is satisfied by fossil fuels, refurbishment measures should avoid the use of mechanical cooling systems with high energy demand. Otherwise this is a kind of maladaptation as the energy demand and therefore the emissions of greenhouse gases would increase. To reduce the solar radiation input venetian blinds should be installed in front of the windows on the narrow sides of the building. Furthermore all venetian blinds should be automatized using radiation and wind sensors. Thus the venetian blinds are even activated outside office hours, in unoccupied rooms or in public areas of the building like staircases or tea kitchens. The lowest global irradiance value for the activation of sun protection systems that has been realized in practice is 180 W/m^2 [21]. For the thermal building simulation of the climate adaptation measures the threshold of 180 W/m^2 has been used. If the threshold is reached the venetian blinds at the corresponding façade are closed at an angle of

45°. The angle of 45° should guarantee a direct visual link to the outside, which is favorable for the comfort of the occupants. The glass façades in the staircases and the windows to the north-northeast should get a solar control glazing with a total solar energy transmittance of g = 0.33. Simulations and in-situ measurements have shown that during the summer season considerable heat gains are caused by the diffuse radiation through the windows oriented to the north-northeast. In contrast during winter the solar heat gains through the north oriented windows are negligible and have a minor effect on the heating demand.

To subsequently increase the heat storage capacity of the rooms the use of phase change materials (PCM) is favorable. Typically these are paraffins or salt hydrates. Their high enthalpy of fusion during the phase change from solid to liquid is used to store heat energy. For breaking down the bond energy of the molecules during the phase change, heat energy has to be supplied to the system. The temperature of the material does not change only the phase. With very low additional weight a large increase of the heat storage capacity can be reached. On the market there are phase change materials made of salt hydrates available that need the same amount of heat energy to be heated from 21 °C to 34 °C as a concrete element with the twelvefold mass. For a multiple use of the heat storage capacity of phase changes materials the stored heat energy should be dissipated ideally by the use of natural heat sinks like for example the cool night air.

One suggested version for the refurbishment is presented in Figure 11. First of all the two existing suspended ceilings are removed. The upper one, that is a fire protection ceiling, contains asbestos. The infill of the lintel area is asbestos contaminated and is removed as well. The infill of the lintel area is changed against louvre windows. The balustrade is not touched. The louvre windows are made of colored enameled single-pane safety glass and designed as structural glazing, therefore the colorful appearance of the lintel area can be preserved and the visible parts of the frame are reduced to a minimum.

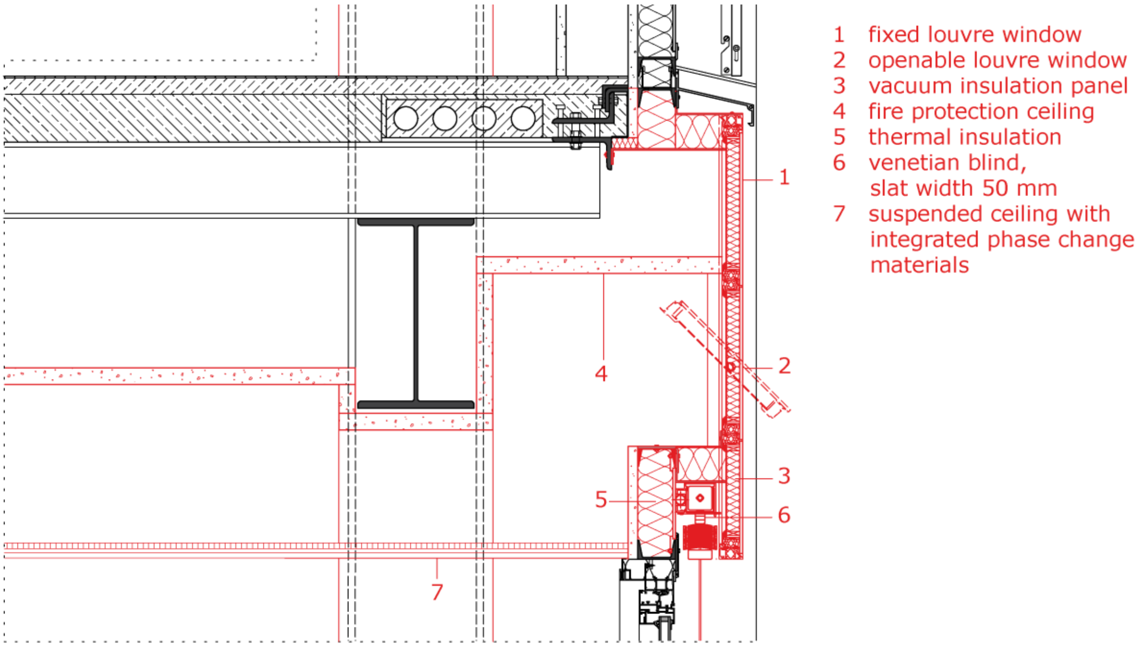

Figure 11: Refurbishment with natural ventilation and intervention in the external façade view.

To reduce the weight of the louvre windows the layer composition is as follows (from the interior to the exterior): metal sheet, vacuum insulation panel, enameled single-pane safety glass. A new fire protection ceiling and a second suspended ceiling, which contains phase change materials, are installed (Figure 11). The fire protection ceiling and the suspended ceiling with integrated PCM enclose an air gap that covers the whole building width. By opening the louvre windows the outside air can flow through the air gap and removes the heat energy stored in the phase change materials. The louvre windows should be automated during summer by a temperature sensor, so that they are opened if the temperature in the air gap is above 21.5 °C and the outside air temperature is below the temperature in the air gap. By separating the ventilation sector from the occupied zone the ventilation can be extended to the office hours without adverse effects on the comfort of the occupants. As a result the degree hours could be reduced considerably (Figure 12).

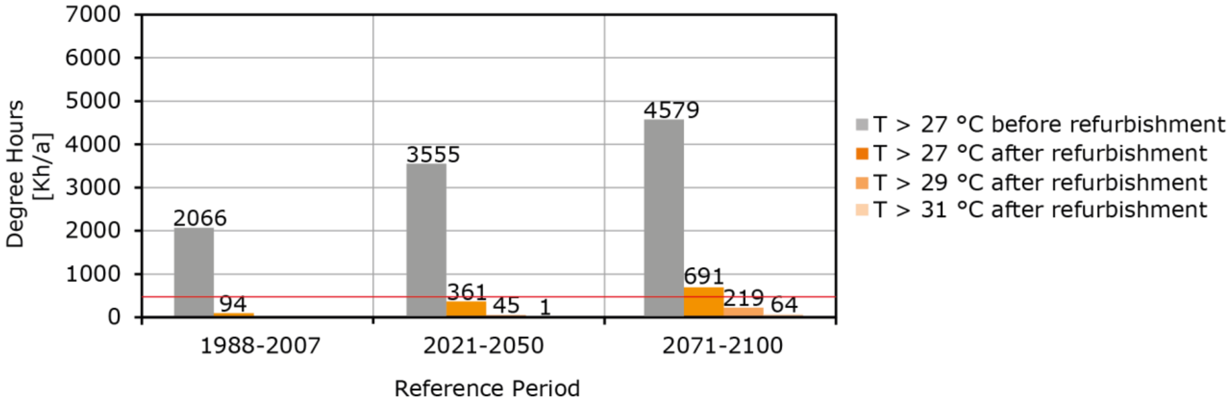

Figure 12: Degree hours after refurbishment.

Another version, which preserves the external view of the façade completely, is explained in the following. Instead of a natural ventilation of the air gap between the fire protection ceiling and the suspended ceiling with integrated phase change materials an exhaust air plant is installed. The infill of the lintel area has to be removed anyway because of the asbestos contamination. In the new lintel area controllable, insulated air inlets are integrated. The exhaust air plant creates a negative pressure and the cool night air flows through the air inlets to the interior. A ventilation of the air gap is only possible if the venetian blinds are not activated (Figure 13). The exhaust air plant is solely operated in summer to remove the latently stored heat. On the flat roof a new roofing membrane with integrated photovoltaics is installed, for delivering the energy needed by the exhaust air plant.

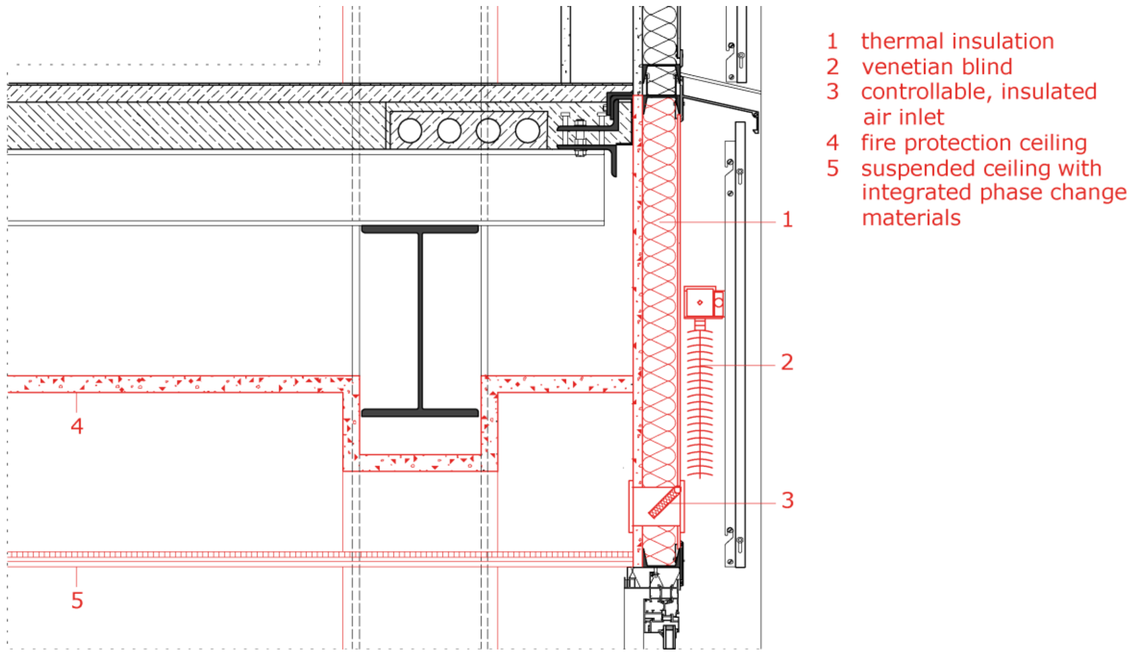

6 References

[1] Buttlar, A. von, Wittmann-Englert, K., Dolff-Bonekämper, G. (Hrsg.): *Baukunst der Nachkriegsmoderne – Architekturführer Berlin 1949-1979*, Reimer, Berlin, 2013.

[2] Hillmann, R.: *Piękno profilu metalowego. Budynki „typu Lipsk" w NRD i w Polsce / Die Schönheit des Metallprofils. Der „Typ Leipzig" in der DDR und Polen*, in: Muzeum Śląskie w Katowicach (Hrsg.): Sztuka i Przemysł / Kunst und Industrie, Katowice, 2013, pp. 251-259.

[3] Vereinigung der Landesdenkmalpfleger in der Bundesrepublik Deutschland (Hrsg.): *Zwischen Scheibe und Wabe – Verwaltungsbauten der Sechzigerjahre als Denkmale*, Imhof, Petersberg, 2012.

[4] Pisternik, W., Raeschler, H., Rebetzky, G., Bauakademie der DDR (Hrsg.): *Chronik Bauwesen Deutsche Demokratische Republik 1945-1971*, Bauinformation, Berlin, 1974.

[5] Pisternik, W., Raeschler, H., Ertel, G., Weixelbraun, A., Bauakademie der DDR (Hrsg.): *Chronik Bauwesen Deutsche Demokratische Republik 1971-1976*, Bauinformation, Berlin, 1979.

[6] Bayerisches Landesamt für Umwelt: *Schadstoffratgeber – Gebäuderückbau.* http://www.lfu.bayern.de/altlasten/schadstoffratgeber_gebaeuderueckbau/suchregister/doc/402.pdf (Stand März 2004)

[7] Kleber, K.: *Praktische Bauphysik*. VEB Verlag für Bauwesen, Berlin, 1972.

[8] Myhre, G., Shindell, D., Bréon, F.-M., Collins, W., Fuglestvedt, J., Huang, J., Koch, D., Lamarque, J.-F., Lee, D., Mendoza, B., Nakajima, T., Robock, A., Stephens, G., Takemura, T., Zhang, H.: *Anthropogenic and Natural Radiative Forcing*, in: Stocker, T. F., Qin, D., Plattner, G.-K., Tignor, M., Allen, S. K., Boschung, J., Nauels, A., Xia, Y., Bex, V., Midgley, P. M. (Hrsg.): Climate Change 2013 – The Physical Science Basis. Contribution of Working Group I to the Fifth Assessment Report of the Intergovernmental Panel on Climate Change, Cambridge University Press, Cambridge, 2013, pp. 659-740.

[9] Masson-Delmotte, V., Schulz, M., Abe-Ouchi, A., Beer, J., Ganopolski, A., González Rouco, J. F., Jansen, E., Lambeck, K., Luterbacher, J., Naish, T., Osborn, T., Otte-Bliesner, B., Quinn, T., Ramesh, R., Rojas, M., Shao, X., Timmermann, A.: *Information from Paleoclimate Archives*, in: Stocker, T. F., Qin, D., Plattner, G.-K., Tignor, M., Allen, S. K., Boschung, J., Nauels, A., Xia, Y., Bex, V., Midgley, P. M. (Hrsg.): Climate Change 2013 – The Physical Science Basis. Contribution of Working Group I to the Fifth Assessment Report of the Intergovernmental Panel on Climate Change, Cambridge University Press, Cambridge, 2013, pp. 383-464.

[10] Hartmann, D. L., Klein Tank, A. M. G., Rusticucci, M., Alexander, L. V., Brönnimann, S., Charabi, Y. A.-R., Dentener, F. J., Dlugokencky, E. J., Easterling, D. R, Kaplan, A., Soden, B. J., Thorne, P. W., Wild, M., Zhai, P.: *Observations – Atmosphere and Surface*. in: Stocker, T. F., Qin, D., Plattner, G.-K., Tignor, M., Allen, S. K., Boschung, J., Nauels, A., Xia, Y., Bex, V., Midgley, P. M. (Hrsg.): Climate Change 2013 – The Physical Science Basis. Contribution of Working Group I to the Fifth Assessment Report of the Intergovernmental Panel on Climate Change, Cambridge University Press, Cambridge, 2013, pp. 159-254.

[11] Fischer, E. M., Schär, C.: *Consistent geographical patterns of changes in high-impact European heatwaves*. in: Nature Geoscience 3 (2010) issue 6, pp. 398-403.

[12] Fahrion, M.-S., Nikolowski, J., Zimm, J., Naumann, T.: *Relevante Einwirkungen auf Gebäude*, in: Weller, B., Naumann, T., Jakubetz, S. (Hrsg.): Gebäude unter den Einwirkungen des Klimawandels, Rhombos, Berlin, 2012, pp. 1-66.

[13] Blümel, K., Hollan, E., Kähler, M., Peter, R.: *Entwicklung von Testreferenzjahren (TRY) für Klimaregionen der Bundesrepublik Deutschland* / Institut für Geophysikalische Wissenschaften – Fachrichtung Theoretische Meteorologie – der Freien Universität Berlin, Dr.-Ing. Axel Jahn Beratender Ingenieur Düsseldorf. Berlin: Institut für Geophysikalische Wissenschaften, 1986.– Bundesministerium für Forschung und Technologie Forschungsbericht T 86-051. Technologische Forschung und Entwicklung – Nichtnukleare Energietechnik.

[14] Christoffer, J., Deutschländer, T., Webs, M.: *Testreferenzjahre von Deutschland für mittlere und extreme Witterungsverhältnisse TRY*, Selbstverlag des Deutschen Wetterdienstes, Offenbach, 2004.

[15] Deutscher Wetterdienst (Hrsg.): *Aktualisierte und erweiterte Testreferenzjahre von Deutschland für mittlere, extreme und zukünftige Witterungsverhältnisse*, Deutscher Wetterdienst, Offenbach, 2011. – Forschungsbericht. Climate & Environment Consulting Potsdam GmbH, Deutscher Wetterdienst im Auftrag des Bundesamtes für Bauwesen und Raumordnung (BBR).

[16] Meehl, G. A., Stocker, T. F., Collins W. D., Friedlingstein, P., Gaye, A. T., Gregory, J. M.; Kitoh, A., Knutti, R., Murphy, J. M., Noda, A., Raper, S. C. B., Watterson, I. G., Weaver, A. J., Zhao, Z.-C.: *Global Climate Projections*, in: Solomon, S., Qin, D., Manning, M., Chen, Z., Marquis, M., Averyt, K., Tignor, M. M. B., Miller, H. L. (Hrsg.): Climate Change 2007 – The Physical Science Basis. Contribution of Working Group I to the Fourth Assessment Report of the Intergovernmental Panel on Climate Change, Cambridge University Press, Cambridge, 2007, pp. 747-845.

[17] Schär, C., Vidale, P. L., Lüthi, D., Frei, C., Häberli, C., Liniger, M. A., Appenzeller, C.: *The role of increasing temperature variability in European summer heatwaves*, in: Nature 427 (2004) issue 6972, pp. 332-336.

[18] Beniston, M.: *The 2003 heat wave in Europe: A shape of things to come? An analysis based on Swiss climatological data and model simulations*, in: Geophysical Research Letters 31 (2004), L02202, doi:10.1029/2003GL018857.
[19] Müller-Westermeier, G., Riecke, W.: *Die Witterung in Deutschland*. in: Deutscher Wetterdienst (Hrsg.): Klimastatusbericht 2003. Offenbach, 2004, pp. 71–78.
[20] Weller, B., Fahrion, M.-S., Horn, S., Pfuhl, A.-M.: *Doppelfassaden im Zeichen des Klimawandels*, in: Bauphysik 36 (2014) issue 2, pp. 68-73.
[21] Lichtmeß, M.: *Aktivierung von Blend- und Sonnenschutzsystemen*. Bergische Universität Wuppertal, Fachbereich D, Abteilung Architektur, Lehrgebiet Bauphysik und Technische Gebäudeausrüstung b+tga, 2008. – Forschungsbericht. Im Auftrag des Bundesministeriums für Wirtschaft und Technologie.

Proceedings of the International Conference on Building Envelope Design and Technology, Graz
Advanced Building Skins 2015

Experience-based guidelines for Architectural Industrialized Multifunctional Envelope Systems (AIM-ES)

Samuel Dubois, Dr. Ir.
Belgian Building Research Institute (BBRI), Belgium, sdu@bbri.be

Michael De Bouw, Prof. Dr. Ir.-Arch.
Belgian Building Research Institute (BBRI), Belgium, mdb@bbri.be
University of Antwerp, Department of Design Sciences, Belgium

Summary

The project *AIM-ES* revolves around the major theme of reducing the energy consumption of existing dwellings, and improving the comfort and living cost of its occupants. The main focus is put on the rehabilitation of ensembles of buildings by means of an industrialized approach, where large-sized prefabricated façade modules are applied to the existing envelope. This brings advantages in terms of performance, speed of retrofitting and disturbance reduction for the surroundings and users.

This paper outlines the final outcome of the project, i.e. a set of guidelines for this technique, aimed towards key stakeholders (owners/users, architects, producers and contractors) and based on experience feedback from realized retrofitting cases. Also, the opportunities and the barriers for the application of some of the investigated systems for the Brussels Capital Region are explored.

Keywords: Retrofit, prefabricated envelope systems, experienced-based guidelines, case studies

1 Introduction

Reducing the energy consumption of existing dwellings is a central aspect to achieve European goals in terms of carbon dioxide emissions [1]. Moreover, it is intrinsically linked to improvements in terms of comfort and living costs for its occupants. In most European cities, the existing building stock is characterized by aging materials and assemblies, outdated envelope conception with limited or no insulation, and technologies that have reached their end-of-life. A real challenge exists for these buildings to match modern criteria of performance [2], as demolition and re-construction is not always environmentally nor economically justified.

The evolution of industrial processes offers innovative techniques for the retrofitting of building envelopes. Prefabricated envelope modules can be assembled off-site and attached in a following stage on the existing structure, providing an accelerated on-site phase with enhanced quality assurance and many possibilities in terms of volume expansion [3]. Under certain conditions, the old building is easily ‘wrapped’ with a new skin on top of the existing walls, avoiding therefore large disturbance for the neighborhood and for occupants who might keep using most of their living accommodation.

Prefabricated envelope modules can be designed in many ways; three keys parameters being their size, level of prefabrication and level of technicality. The last parameter is linked to the possibility of integrating various technologies inside the new envelope [4]. Generally, due to the cost implied by a heavier conception phase compared to traditional refurbishment methods, such industrialized envelope systems are more suited for the rehabilitation of large buildings or ensemble of buildings showing a (semi-)repetitive architecture, as is for instance often the case with social housing or garden cities.

During the last decades, innovative EU demonstration projects have shown that these prefabricated systems can be used for high quality envelope retrofitting, while allowing inhabitants to retain the use of their homes during the works, usually only lasting a few days (e.g. *IEA Annex 50*, *TES EnergyFaçade*, *E2ReBuild*) [5–7]. Such systems, however, have been well-deployed neither on the Belgian nor Brussels market, notwithstanding their suitable building stock. Most importantly, no experience-based feedback has been collected concerning various demonstration systems/cases, nor do experience-based guidelines exist to support potential stakeholders in their decision process.

The present paper is elaborated on the project *AIM-ES – Architectural Industrialized Multifunctional Envelope Systems* for building refurbishments in Brussels – which tried to remedy these shortcomings in order to assure the uptake of these promising techniques by the Belgian building industry. The paper will emphasize successively on the origins of the project (see 2), the identified European systems (see 3), and the analysis of the identified realized European cases (see 4). Finally, it concludes with the outline of the elaborated guideline (see 5).

2 Project initiation and outline

It was in the light of the abovementioned pioneering European projects that the Brussels project *AIM-ES* was carried out by the *Belgian Building Research Institute* (*BBRI*) during the period 2013-2014 [8]. The project proposed to bring together and analyse the existing experience across the EU with regard to the topic of large-scale industrialized envelope systems for retrofitting of housings. A detailed comparative analysis, including site visits and interviews with the stakeholders that intervened in different European case implementations, served as a main input to explore the opportunities, benefits and possibilities, but also the barriers for the application of selected systems in the Brussels Capital Region. The goal of this approach being the mobilisation of several Brussels stakeholders (industry, government, social housing companies) in order to prepare demonstration cases in Brussels in the near future and elaborate Belgian technical guidelines.

The project evolved around four main tasks. The first one produced a detailed inventory of existing multifunctional system envelopes and demonstration projects across Europe, including context and specific conditions. Based on this inventory, the second phase emphasized on the evaluation of the cases and systems that were most relevant for the Brussels context. The objective of the third part was to identify the crucial process parameters of this type of renovation technique. The fourth and final phase tailed the project idea by elaborating technical guidelines for each stakeholder (owners/tenants, contractors, architects, producers) and each phase of the retrofitting project. Some typical questions that were addressed are for example:

- how to analyse the present state of a building and record necessary information, including techniques to determine the geometry for the prefabrication, pathologies, current indoor environment quality, present energy use, constraints for the interventions, etc.;
- what are the possible envelope systems and which are the technologies to be integrated, in function of building typology, orientation, architectural characteristics, present state, etc.;
- how to avoid/foresee on-site installation/timing problems.

The *AIM-ES* project originally came to an end in December 2014 and this paper presents the main findings of the project up to that date. However, the Brussels Institute for Innovation and Research (*InnovIRIS*) granted a third year to the project under the name '*AIM-ES performs!*' in order to (a) get the guideline fine-tuned and validated by the Belgian building industry, (b) initiate some Brussels demonstration cases, and (c) perform research on some open questions on stability and recording issues that are associated to the typical Belgian way of building.

3 Industrialized and multifunctional envelope systems

As mentioned before, a large freedom exists when designing prefabricated façade elements for retrofitting applications. The design parameters are numerous: the type of structural material, the size of individual modules, the level of prefabrication, the types of building services directly incorporated, etc. Several suchlike systems were developed in Europe and are well documented in literature. One important part of the *AIM-ES* project was to study this diversity and to identify the typologies of prefabricated solutions most suited for implementation in Brussels. The *AIM-ES* project revealed that six major typologies can be identified at the moment (Table 1).

Table 1: Overview of the six identified major industrialized envelope systems.

	'Swiss' system	**GAP³ system**	**'Portuguese' system**	**RECOLCI system**	**MeeFS system**	**TES systems**
Structure	Wood	Wood	Steel	Steel	Composite materials	Wood
Size	Mid-scale	Large-scale	Small-scale	Large-scale	Small-scale	Large-scale
Technicality	+++	++	+	+	++++	+ → +++
Related research project(s)	*Annex 50*	*Annex 50 & E2Rebuild*	*Annex 50*	*Annex 50*	*MeeFS*	*TES EnergyFaçade & E2Rebuild*

The first system was developed in Switzerland and is extensively described in *Annex 50* documentation [9]. Mid-scale wood-based modules are designed around the window and door openings, and stacked on top of each other per story (Figure 1). The empty horizontal area between the modules is filled by means of traditional techniques for exterior insulation. The main characteristic of this approach is its high technicality: ducts for ventilation, water, heating canals, etc. are integrated within the structure and modules are chained through elaborated junctions. This causes particular challenges during the module production phase, as non-standardized accessories are needed for ducts integration, and during the execution phase, for alignment and connection of elements. One should note that only a version of this system based on large-scale elements (so without the more traditional infill) has been tested on real-scale demo cases.

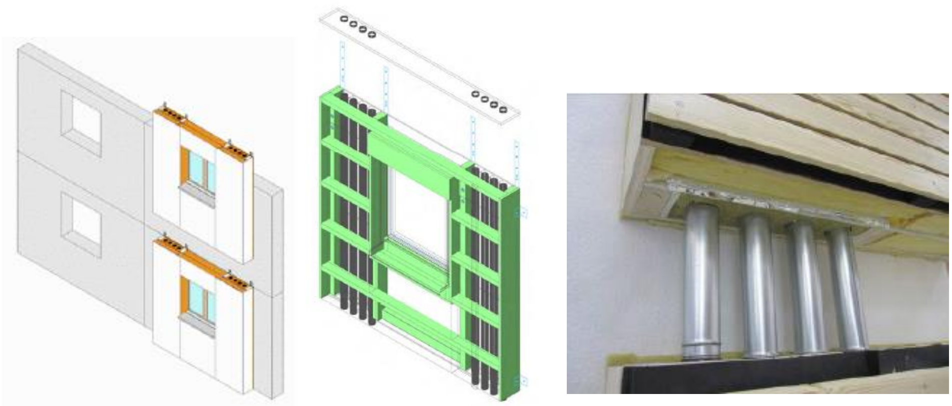

Figure 1. 'Swiss' system. [9]

The *GAP³* system, also described in *Annex 50*, is based on a large-scale timber-based structure on top of which a solar façade system is attached. The latter is made of glazing, behind which are a ventilated air gap and a specific alveolar structure of cellulose that captures sunlight to create a buffer zone whose temperature is higher than the outside air. The temperature gradient across the wall being substantially reduced, the heat losses by transmission through the wall are diminished. The operation of the system depends on the season. In summer, very oblique sunrays hardly penetrate the alveolar structure. The system therefore absorbs little energy and the ventilated cavity helps prevent overheating, fresh air is sucked by the movement of warm air up the facade. In winter, the rather horizontal sunlight penetrates the alveolar structure, thereby heating the air in its hollow zones and the mass of the underlying material.

Figure 9. *GAP* system. [9]

The ‘Portuguese’ and *RECOLCI* systems are the two last systems being analyzed in *Annex 50*, both based on metal structures. The first one is composed of small modules (about 1x1m) made of polystyrene, agglomerated cork and an aluminum finishing, the manageability serving as guiding principle. These modules are mounted on two lateral steel studs, with a system of pins and holes (Figure 10). Despite advantages in terms of handling and interchangeability, the system requires lots of on-site efforts and presents risks in terms of thermal bridges, support corrosion and vandalism. The *RECOLCI* system consists of large-scale modules made from 20 cm thick cold-laminated profiles. The maximum unit height is two stories and modules/vertical profiles can be horizontally spaced with a maximum distance of 60cm – the empty are being filled with insulation. The thermal bridges linked to the metallic structure and its relative complexity are the main disadvantages of this technique. However, the chosen self-standing structure allows the implementation of an extra story during the retrofitting, which is not possible with the Portuguese system.

Figure 10. ‘Portuguese’ (left) and *RECOLCI* (right) systems. [9]

A fifth system that was identified is the multifunctional *MeeFS* system [10] (Multifunctional energy efficient Façade System). The key concept here is its modularity. A structure made of a composite material (fibre-reinforced polymer) can host a variety of square-shaped technological units, including insulation, green façade, ventilated façade, solar protection and absorption (by means of PCMs) and photovoltaic systems. The management of these technologies in an autonomous control perspective is planned through the use of various sensors and actuators. As this system is still in (very) early research phase and a first proof of feasibility has still to be provided, it is only mentioned in the *AIM-ES* research, but not incorporated for further evaluation at the moment.

Figure 4. MeeFS façade system. [11]

The sixth typology includes the more traditional timber-based systems. During 2008-2010 a research project entitled *Timber-based element systems for improving the energy efficiency of the building envelope* (*TES EnergyFaçade*) was led by researchers from Finland, Germany and Norway. Its main objective was to propose a façade retrofitting method (TES method) based on prefabricated large-scale elements for improving the energy efficiency of existing buildings throughout Europe. The TES modules are based on a self-supporting wood structure with insulation infill and sheathing board(s) (Figure). In fact, the 'TES' designation covers a wide range of design possibilities, in terms of module conception, module mounting configuration, and service systems integration. It's a very broad definition, and in fact, the *GAP³* system could also be considered as a TES design, with a solar façade component. In a similar manner, the 'Swiss' system used in a continuous large-scale configuration (not centered on windows) is somewhat a high-tech form of standard TES designs.

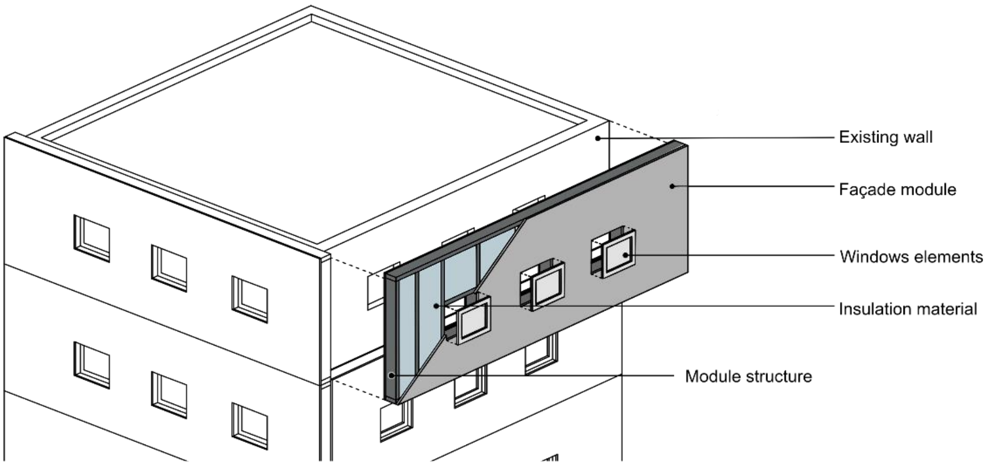

Figure 5. Principle of large-scale TES system (horizontal layout illustrated)

Research rapidly indicated that these large-scale wood-based modules are the most suitable or Brussels capital city. Indeed, in addition to ensuring a low thermal-bridge in comparison to a metallic structure, the traditional 'know-how' associated with timber construction ensures a rapid adoption of this method by the industry. Many projects were achieved in Europe during the last years and proved the efficiency and adaptability of the method. Within *AIM-ES*, three particular 'types' of TES-based façade modules were ultimately retained for further analyses, namely the *closed* type, *closed with solar façade* type, and *the open* type (see Figure).

The first type is widely described in *TES-Energy Façade* project manual [12]. The wood structure is closed on both of its sides with sheathing boards and the main insulation layer of the module is almost always implemented off-site. An 'adaptation layer' is necessary to fill the void space between the new envelope and the existing wall. Solar façade panels can be implemented on the exterior face of closed modules. The *GAP³* system is one example of such configuration, but others exist such as *Lucido* [13].
The open TES is very similar with on major variation: there is no sheathing board on the rear side of the module. A compression ribbon - acting as leveling layer - is applied on the back side of the structural wood studs and will directly lie against the existing façade. After the fixation of such 'empty' panels on the existing walls, the insulation is injected via holes, which are pre-drilled off-site. The main resulting advantages are a simplified levelling process and a reduced weight of modules.

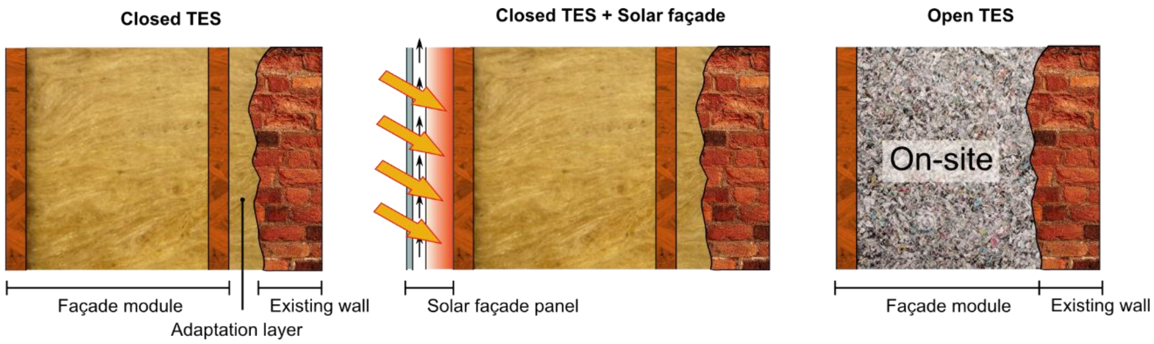

Figure 6. Chosen modules types for the Brussels context: principle diagrams

4 Case studies

The guidelines are referring to some 'exemplary cases' in order to provide real-life examples and propose adequate technical solutions in the light of the building properties. In that respect, an inventory of European projects retrofitted with industrialized enveloped systems was fulfilled in the early stages of the research (Figure). Among the inventoried cases, the ones with sufficient documentation (from literature, visits and interviews) were compared on the basis of relevant parameters distributed in three topics of analysis: the general information concerning the building (type and size of the building, dates of construction and renovation, type of walls, weak points, etc.), the renovation process (energy consumption after renovation, construction time, space extension, measures for envelope, measures for HVAC, etc.), and façade module design (orientation, dimensions, load-bearing system, etc.). In an ultimate step, about fifteen buildings were selected upon three criteria to support the guidelines recommendations. First, the final sample of cases had to reflect the diversity of buildings which are concerned by prefabricated envelope elements. Secondly, the technique used for the façade module construction had to correspond to one of the three types retained earlier in the project (see 3). Finally, the technical information had to be plentiful and cover a large range of domains (detailed plans, HVAC services, types of infrastructure used during modules fixing, etc.).

Figure 7. Indication of inventoried projects and analysed case studies (in red)

Figure 8. Some exemplary cases used to illustrate the guidelines; (left) terraced houses retrofitted with closed TES modules (Roosendaal, NL), (middle) terraced houses retrofitted with a solar façade system (Graz, AUT) and (right) an apartment block retrofitted with open TES modules (Berlin, GE)

5 Experienced-based guidelines

Much information related to prefabricated envelope systems is already available in literature, in the form of project reports, scientific papers or technical documentation. However, the survey of Belgian professionals performed within *AIM-ES* revealed that such knowledge is not well disseminated in Belgium. Scientific results and real-life cases already proved that several wood-based modules systems have a great potential (fast on-site execution, high quality construction, cost-effective, reliable, etc.), yet these findings are not widespread, nor well-known. *AIM-ES* wants to resolve this problem by providing technical guidelines addressing the actors of the retrofitting sector so that pilot projects can be encouraged in Belgium. In that context, the proposed document had to summarize without too much redundancy the available information, with a focus on critical design and decisions parameters, and adapted to the Belgian context and legislations.

The guidelines are organized around the typical different phases of a retrofitting project (Figure 9), in accordance with the 'Guidelines to Preliminaries/Survey' developed in E2Rebuild project [14]:

- The *pre-project phase* extends from the project initiation, with the definition of objectives meeting the wishes of the building operator, to the planning of the project organizing the subsequent phases. A feasibility study will determine whether the use of industrialized façade module is relevant, based on a basic building survey.
- The *pre-construction phase* is separated in an investigation and a design stage. These two stages are indivisible as an in-depth building study is crucial to determine the design constraints and optimize the execution process.
- The *construction phase* is separated into an off-site and an on-site stage. The off-site operations cover the prefabrication of the façade modules based on a production model. The on-site execution stage groups all of the actions and interactions during the preparation of the site and building and during the mounting of the modules.
- The *post-construction phase* assembles the tasks that follow the actual interventions on the building and ensures that the building meets the planned performances. Another critical aspect covered by this phase is the formation of occupants.

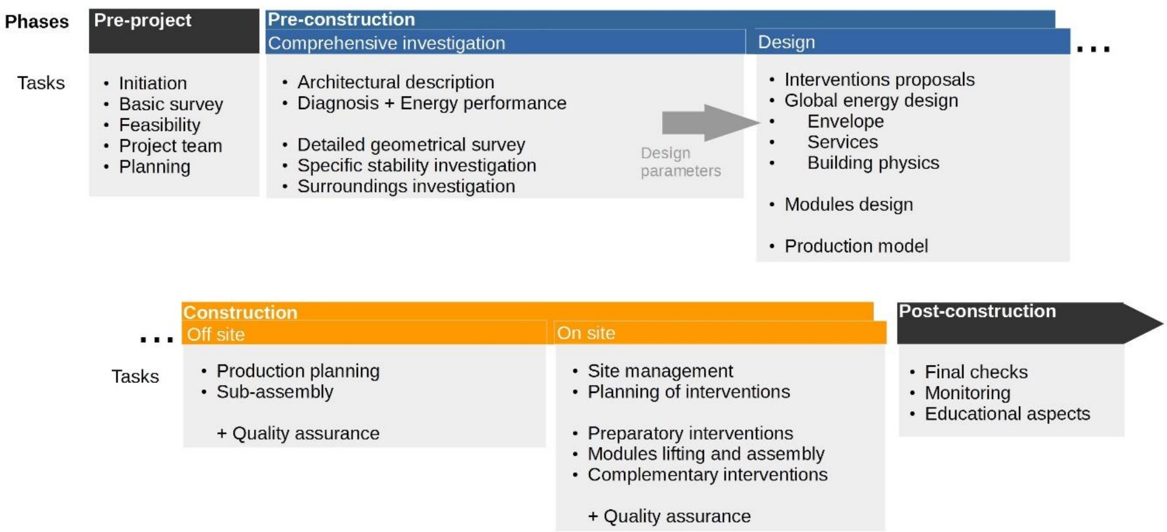

Figure 9. Phases of a retrofitting project involving the use of multifunctional envelope modules

For each task linked to a particular phase of the project, the professionals who are concerned primarily are mentioned in a summary box (Figure 0). The latter also provides relevant questions to be investigated when performing this task as well as indications concerning expected inputs and outputs. Of course, the reality can (and will) be much more complex as several roles can be endorsed by the same actor (the modules designer can also be in charge with their production) or several actors can intervene in the same tasks. In addition, the project team always needs to be scaled to suit the complexity and size of the project. In a similar way, all tasks and concomitant questions are not systematically relevant considering the specificity of each building (previous refurbishments, constraints of interventions, etc.).

Actor(s) concerned:
- *Architect*
- *Stability engineer*

Relevant question:
- *What is the ability of the existing building to carry the additional load caused by the prefabricated modules with possible volume extensions?*
- *What is the load reserve of foundations?*
- *What is the accessibility of structural elements?*
- *How can the stability of façade elements be characterized?*
  - *Is a specific study for cavity walls necessary?*
- *...*

Information needed:
- *D. BUILDING DESCRIPTION REPORT (Position, span and dimension of all load bearing parts)*
- *Historical standards of the existing construction (stability design)*
- *(Original structural calculations)*

Output information:
- *F. STABILITY SURVEY*

Figure 10. 'Summary box' which can be found all along the developed technical guidelines for the different tasks (illustrated here: the stability survey during the investigation phase)

Some key project phases and tasks focused a particular attention inside the *AIM-ES* guidelines (Figure), with adaptation to the context of Brussels, while others were more briefly addressed since a lot of well-structured information can already be found in literature. In this respect, the building investigation phase was extensively studied with a clear highlighting of the connections it has with the façade module design. Prefabrication results in a faster speed of on-site execution compared to traditional insulation solutions for retrofit (e.g. ETICS), in exchange for a lower assembly tolerance. It explains why the building should be known precisely from both its original design and current state standpoint. As it is seen on Figure , the various surveys constituting the building investigation phase define some preconditions that will preferentially orient the designer to specific technical solutions. A typical example is the choice of the adaptation layer that lies between the new façade modules and the existing walls. Several types of levelling layer exist, with different 'tolerance gaps' that can be filled. The choice of levelling technique will depend on the geometrical survey – which is generally a 3D model – that determines the unevenness of the existing façade. It is also intrinsically linked to the load-bearing configuration and support elements, which themselves depend on the building stability survey. The 'catalog' of technical solution is thus analysed in the document in the light of the investigation phase with practical experience feedback.

Besides, the façade module design clearly orients the on-site interventions as well as the site management. For example, the choices in terms of façade module equipment (e.g. decentralized ventilation units) can cause additional on-site interventions (e.g. holes for ducts in the existing walls). In the section dedicated to the on-site phase, the document presents all possible interventions with the connections to all aspects of module design. Again, the chosen European cases support the guidelines by providing the necessary feedback and delivering examples of practical implementation choices.

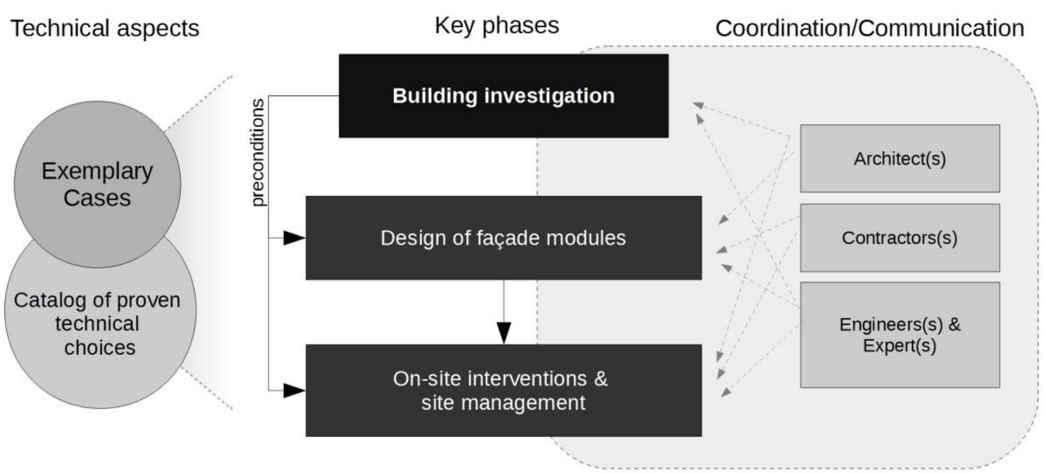

Figure 11. Key attention points in the AIM-ES guidelines document

6 Conclusion

This document presents the results of the project *AIM-ES*, which was carried out in Brussels to sensitize Belgian industry towards retrofitting buildings by means of multifunctional industrialized envelope systems. Such systems present great perspectives for improving the refurbishment process for buildings showing a certain repeatability by bringing advantages in terms of performance, speed of execution, disturbance reduction for the surroundings and users, and indoor volume extension. The final outcome of the project is an experience-based set of guidelines for these industrialized façade renovation systems, aiming at different levels in the chain of stakeholders (owners/users, architects, producers and contractors). These recommendations should guide these stakeholders throughout the entire rehabilitation process: from the very start with a thorough analysis of the existing building, the selection of the most suitable façade system, towards the practical aspects of design, logistics, transport and the mounting of the façade elements.

The paper briefly presented the context of the research project and the existing prefabricated envelope systems, including the ones retained for potential application in Brussels. The exemplary cases selected as feedback purpose were then introduced before illustrating the content of the final guidelines and the way they are organized.

To conclude it can be mentioned that the original setup of the *AIM-ES* project – viz. to assure the uptake of these promising techniques by the Belgian building industry and triggering the application of these techniques in Brussels and Belgium – succeeded. The project formed the basis of the initiation of three further projects that started by the end of 2014 / start of 2015 (*AIM-ES performs!* in Brussels, and *Mutatie+* and *EcoRen* in Flanders), all of them focussing on the application of the investigated techniques by means of living labs for social housing districts.

7 Acknowledgements

The project AIM-ES is subsidized by the Brussels Institute for Scientific Research "*InnovIRIS*" as part of the multidisciplinary platform "Brussels Retrofit XL" [15], which brings together eleven Brussels research projects on different aspects related to the retrofitting of the Brussels housing market.

8 References

[1] Dall, G., Galante, A., Pasetti, G.: *A methodology for evaluating the potential energy savings of retrofitting residential building stocks*, in: Sustainable Cities and Society 4 (2012), pp. 12–21.
[2] Hens, H., Verbeeck, G., Verdonck, B.: *Impact of energy efficiency measures on the CO2 emissions in the residential sector, a large scale analysis*, in: Energy and Buildings 33 (2001) issue 3, pp. 275–281.
[3] Cronhjort, Y., Riikonen, V., Kolehmainen, M., Nordberg, K., Huss, W.: *smartTES - Book 2: TES Extension*, 2014. [Online] Available: http://www.tesenergyfacade.com/downloads/smarttes_b2_Extensions.pdf [Accessed: 14-Jan-2015].
[4] Ott, S., Loebus, S., Time, B., Homb, A., Botsch, R.: *smartTES - Book 3: Multifunctional TES*, 2014. [Online] Available: http://www.tesenergyfacade.com/downloads/smarttes_b3_Multifunctional [Accessed: 26-Jan-2015].
[5] *IEA ECBCS Annex 50 – Prefabricated systems for low energy renovation of residential buildings, IEA ECBCS.* [Online] http://www.ecbcs.org/annexes/annex50.htm [Accessed: 26-Jan-2015]
[6] *TES Energy Façade – Multifunctional timberbased element system for improving energy efficiency of the building envelope.* [Online] http://www.tesenergyfacade.com/ [Accessed: 26-Jan-2015]
[7] *E2ReBuild – Industrialised energy efficient retrofitting of resident building in cold climate*. [Online] http://www.e2rebuild.eu. [Accessed: 14-Jan-2015].
[8] *BrusselsRetrofitXL – Experience-based guidelines for Architectural Industrialized Multifunctional Envelope Systems (AIM-ES).* [Online] http://www.brusselsretrofitxl.be/projects/aim-es/ [Accessed: 14-Jan-2015].
[9] Kobler, R., Binz, A., Steinke, G., Höfler, K., Geier, S., Aschauer, J., Cousin, S., Delouche, P., Radelet, F., Ruot, B., Reynier, L., Gobin, P., Duforestel, T., Senior, G., Silva, P., Almeida, M.: *IEA ECBCS Annex 50: Retrofit module design guide*, IEA ECBCS, Duebendorf, 2011.

[10] *MEEFS – Multifunctional energy efficient façade system.* [Online] http://www.meefs-retrofitting.eu/ [Accessed: 26-Jan-2015]

[11] Rosanska, M.: *MEEFS Retrofitting – first year progress report*, 2013. [Online] Available: http://www.meefs-retrofitting.eu/images/meefs%20publishable%20summarry_2013-08%20web.pdf [Accessed: 26-Jan-2015].

[12] Heikkinen, P., Kaufmann, H., Winter, S., Larsen, K.E.: *TES EnergyFaçade manual – prefabricated timber based building system for improving the energy efficiency of the building envelope*, München, 2011. [Online] Available: http://tesenergyfacade.com/downloads/TES_Manual-ebookFINAL.pdf [Accessed: 14-Jan-2015]

[13] *Lucido®* construction system. [Online] http://www.lucido-solar.com/lucido/lucido/ [Accessed: 26-Jan-2015]

[14] Ott, S., Hernandez-Maetschel, S., Lattke, F.: *E2Rebuild – Guidelines to Preliminaries/Survey*, 2011. [Online] Available: http://www.e2rebuild.eu/en/links/deliverables/Documents/E2ReBuild_D4.1_GuidelinesPreliminariesSurvey.pdf [Accessed: 26-Jan-2015].

[15] *BrusselsRetrofitXL - Research platform with focus on the renovation of the Brussels housing market*. [Online] http://www.brusselsretrofitxl.be [Accessed: 14-Jan-2015].

Proceedings of the International Conference on Building Envelope Design and Technology, Graz
Advanced Building Skins 2015

A Façade Refurbishment Toolbox Supporting Energy Upgrade of Residential Building Skin

Thaleia Konstantinou, Post-doc researcher
Delft University of Technology, The Netherlands,
t.konstantinou@tudelft.nl

Summary

Over the next decade investments in buildings energy saving need to increase, together with the rate and depth of renovations, to achieve the required reduction in buildings related CO2 emissions. Although the need to improve residential buildings has been identified, guidelines come as general suggestion that fail to address the diversity of each project and give specific answers on how these requirements can be implemented in the design. During early design phases, architects are in search for a design direction to make informed decisions, particularly with regard to the building envelope, which mostly regulated energy demand.

To result into a sustainable existing residential stock, this paper proposes a methodology to support refurbishment strategies design. The result or the proposed methodology enables designers to make informed decisions that generated energy and sustainability conscious designs, without dictating an optimal solution, from the energy point of view alone. Its applicability is validated through interviews with refurbishment stakeholders.

Keywords: Refurbishment, residential energy upgrade, design process

1 Introduction

The motivation to improve existing buildings lays in society's efforts for sustainable development. The required reduction in buildings related CO2 emissions reaches up to 90% by 2050, indicating the building sector's importance and the urgency for measures uptake. Over the next decade investments in buildings energy saving need to increase, together with the rate and depth of renovations [1]. The domestic sector can potentially make a significant contribution to reducing energy consumption [2]. Additional studies have shown that households have larger energy saving potential and benefit than other sectors, along with the necessary higher investment [3]. Moreover, residential buildings account for 2/3 of building floor area, while the condition and efficiency of a large part of the residential stock still needs attention.

Since the need to reduce the energy demand of the residential building sector is urgent, the efforts must focus on the existing buildings. While new constructions add annually 1% or less to the existing stock [4-6], the other 99% of buildings are already built and produce about 24% [7] of the energy-use induced carbon emissions. Residential buildings account for 70% of building floor area [8], while the condition and efficiency of a large part of the residential stock still needs attention. On the other hand, demolition is not the solution. Regarding materials and waste, studies show that the environmental impact of life cycle extension of a building is definitely less than demolition and new construction [9]. However, buildings suffer from a variety of physical problems. Taking into account that the expectation for the structural life of a building often exceeds 60 years, while the envelope shows signs of obsolescence after only in 20 or 30 years [10, 11], it is understandable that the residential stock is in need of refurbishment.

Although the need to improve existing residential buildings has been identified, guidelines come as general suggestion that fail to address the diversity of each project and give specific answers on how these requirements can be implemented in the design. The integration of all design aspects during the early design phases is complex. At this stage, the architects are in a constant search for a design direction to make informed decisions [12], particularly with regards the building envelope, which is the most influential to energy consumption. The energy need for heating and cooling of buildings is directly related to heat losses through building envelope components, such as external wall, windows, roof and ground floor, ventilation and air infiltration and inversely related to heat gains in the building through solar radiation.

To result into a sustainable existing residential stock, this paper proposes a methodology to support refurbishment strategies design. In the first part, refurbishment design process is analysed and a methodology to integrate the energy saving potential into the design is proposed. The methodology called "façade refurbishment toolbox approach" is based on compiling and quantifying retrofitting measures that can be also seen as "tools" used to upgrade the building's energy performance. Subsequently, the effect of each measure is quantified. The building performance is assessed in terms of energy efficiency. The result or the proposed methodology enables designers to make informed decisions that generated energy and sustainability conscious designs, without dictating an optimal solution, from the energy point of view alone. Its applicability is finally validated through interviews with refurbishment stakeholders.

2 The Design Process

Achieving energy savings in buildings is a complex process. Reducing the energy demand requires the deployment of effective solutions which in turn makes it necessary to understand what affects people's decision-making processes [1]. In order to systematize the decision-making process, researchers have identified different phases in the design and execution of refurbishment strategies. Ma et al. [13] reviewed the main phases of a sustainable refurbishment program and identified five steps, starting from the project setup and pre-refurbishment survey and ending with validation and verification of the refurbished building. Similarly, Ferreira et al. [14] define five steps that include definition of refurbishment scope, diagnosis real building's conditions, identification of alternative scenarios according to client's choices, technician's experience etc., assessment of the scenarios and optimization. These stages are present not only in the case of refurbishment, but the construction process in general. Cooper et al. [15] set up a process protocol model that breaks down the design and construction process into 10 phases that can be grouped into four broad stages; pre-project, which includes determining the need for the project solution, pre-construction, when an appropriate design solution is developed, construction, which produces the project solution and finally post-construction, which aims at monitoring and maintenance of the project.

Based on literature and experience with refurbishment stakeholders, refurbishment design and construction process have been divided in the five phases, shown in Figure 1**Fehler! Verweisquelle konnte nicht gefunden werden.**. The phases described are typically encountered, but variations are possible. There are cases where a more interdisciplinary process was followed. The design team consists of different experts from the early phase, which blurs the boundaries of which decisions and evaluations were made in each phases. Nevertheless, the phases are considered indicative both in interdisciplinary design teams or more traditional team composition.

Refurbishment project starts with the pre-design, which is Phase 1. This is when the requirements that the refurbished building need to fulfil are defined. It begins with identifying the need to intervene, which then initiates the refurbishment project. The building owner typically makes the decision, according to regular refurbishment cycles, as well as reported problems and users' dissatisfaction. Subsequently, the specific requirements of the project are set. Requirements are formed by the building owner, typically a house corporation or individual homeowners, often with the involvement and advice of architects or other experts.

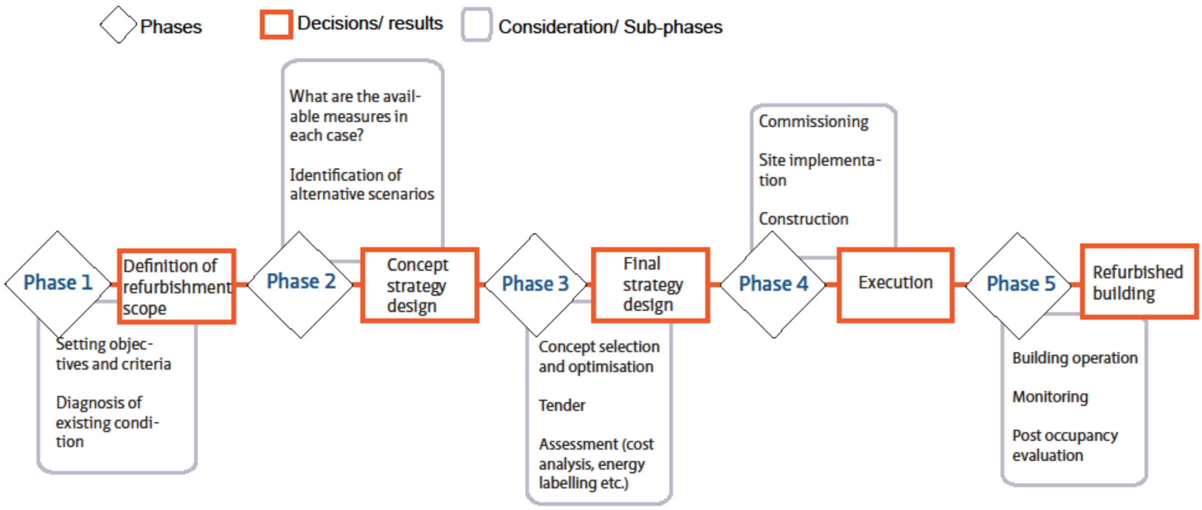

Figure 1: Scheme of the design process phases

After the requirements for the refurbished building have been established, the design stage begins. More than 80% of the building performance, both in terms of energy savings, generation, and cost, is set during this stage [16]. The design can be divided in two phases: the concept and the final design. During the concept design (Phase 2), the team looks at the possible measures to implement and identify possible scenarios, which are evaluated in order to select the scenario to be further developed in the final design phase. The scenarios and the decision that shape the strategy are typically developed by an architect, who has to take in to account the parameters defined on the previous phase such building programme, architectural qualities, and depth of refurbishment. At this stage, the architects search for information to support the design direction [12]. An evaluation is needed to support the decision-making, when various scenarios are discussed. The evaluation concerns the performance in general, such as energy, comfort, spatial and aesthetical benefits, together with investment aspects. The final design begins after the design team has chosen the strategy concept (Phase 3). It includes the optimisation and assessment of the selected concept. The assessment of energy use, often in the form of energy certificates, occurs at this stage.

When the design has been finalised and the assessment has resulted in the desired performance, the execution phase comes. It refers to the realisation of the designed intervention, which is the construction on the building site, including demolition of components to be replaced, fixing of damages, acquisition and installation of new components and material etc. Finally, the execution (Phase 4) results into the refurbished building and the last phase of the project, which is the operation by the users (Phase 5).

The interest of the present thesis lies on the first three phases, as they are more influential for the building energy upgrade. Requirements for energy performance are normally already set in Phase 1, the pre-design phase. The assessment, however, often happens in Phase 3, when the different options have been investigated and the design is being finalized. To determine the energy performance of a building, architects typically rely on the input of outside experts, which can slows down the design process [17].

Estimating the refurbished building performance is essential during the decision-making for refurbishment and there are already methodologies developed to make this estimation. Building Performance Simulation (BPS) computer software provides this opportunity. However only 1% of these tools is targeting architects during the early design phases, while architects consider these tools non-user-friendly and are reluctant to integrate them into the early design phase of high performing buildings. Decisions taken during this stage can determine the success or failure of the design [12]. Analysis of some tools has identify as problem the level of performance feedback in relation to a specific design phase [17], as they are often used for post-design evaluation [18]. There is a need for decision support tools that integrate energy simulation into early design in the architectural practice.

3 The toolbox approach

Information to support refurbishment decision-making often come in the form of general suggestion, which are not always easy for the designer to incorporate in the decisions. Moreover, some of the information target the occupants, owners and public authorities, who are parties that influence or even determine the decisions made, but do not actively participate in the actual designing of the strategy. To improve these aspects, our approach focuses on the architect of refurbishment strategy that makes decision on the design quality. The developed approach is also referred as a "toolbox approach", because the different retrofitting measures can be conceived as the "tools" that constitute the refurbishment strategy. In this sense, the organisation of the different measures compiles a "Façade Refurbishment Toolbox" (FRT), from which the refurbishment design selects the tools to use to upgrade the building envelope. In this paper, the compilation and quantification of the FRT, as well as its applicability, are presented.

3.1 Compilation of retrofitting measures

In order to be able to assess the energy performance of the refurbished building in the early stages of the design phase, refurbishment options have to be systematically organised. The options compiled aim at giving design solutions to upgrade the thermal envelope and translate the general design principles and performance benchmarks into specific retrofitting measures. After identifying the key components for an integrated refurbishment strategy, solutions are given for each one. The measures are state-of-the art refurbishment solutions being used in refurbishment. Different measures are proposed for each component, based on refurbishment practice and experience, as well as literature review of research projects on refurbishment, such as EPIQR [19], TABULA [20], SUSREF [21], IFORE [22], and other [23].

The compilation of the options of resulted in the Façade Refurbishment Toolbox. This toolbox is essentially a database of possible measures that can be implemented in refurbishment projects. The information is organised in a matrix, according to the key components of the building envelope, as presented in Table 1. The measures can be combined depending on the specific requirements of every project and design, resulting in the integrated refurbishment strategy. Addressing solutions for all the above composes integrated refurbishment strategies. The measures are scaled according to effort and level of intervention. In this way, each project can be located on the top, middle or bottom of the table according to requirements. Moreover, it is possible to combine various levels, for example apply a more complex solution for the wall and a simpler one for the rest of the components. Moreover, the toolbox matrix is organised according to the efficiency of the measure and the level of intervention, based on preliminary calculation [24]. This helps to easily identify the possible options depending on the projects ambitions and, thus, facilitate the selection.

3.2 Quantification

The toolbox approach aims at providing an assessment of refurbishment options impact on the energy performance of residential building. The goal of an integrated refurbishment is improving all components of the building envelope where heat losses occur; hence, the different retrofitting measures are presented according to the component they address. Apart from catalogue the retrofitting measures, information to evaluate and compare them is needed. To this end, the measures are quantified, according to the energy saving, in comparison with the existing building energy demand, prior to the measure application. To quantify this effect, dynamic simulation is used. The software used for the thermal simulation is DesignBuilder [25]. There is a wide variety of software for building energy analysis [26]. DesignBuilder was chosen as appropriate for the purpose of this study, because it can generate a range of environmental performance and it provides a modelling interface, integrated with EnergyPlus, which is the U.S. DOE building energy simulation program for modelling building heating, cooling, lighting, ventilating and other energy flows.

Table 1: The toolbox matrix

	Building envelope					Building Systems	
	Exterior wall	Window	Balcony	Roof	Ground floor	Ventilation	Heat source
Existing construction	Masonry/ cavity wall no insulation	Single glazing	Continuous slab, no insulation	Pitched roof, timber rafters no insulation/ occupied loft	Slab on ground, no insulation	Natural ventilation	Gas stove
	Lightweight concrete/hollo w brick, no insulation	Early, double-glazing	Separate slab no/little insulation	Pitched roof, timber rafters no insulation/ unheated loft	Basement unheated. Concrete slab, no insulation		Fossil fuel boiler in each dwelling
	Little/outdated insulation			Concrete slab, no/little/outdat ed insulation	little/outdated insulation	Trickle ventilation	Fossil fuel boiler per block
Retrofitting measures	Cavity insulation	Upgrade windows	Insulate balcony slab	Pitched roof, no insulation/ unheated loft	Insulation on top of ground/first floor slab	Natural inlet/ mechanical exhaust	Replace existing boiler in each dwelling, high efficiency
	Internal insulation	Secondary glazing single	Cut off balcony	Pitch roof insulation	Insulation under existing floor	Mechanical inlet/ natural exhaust	Replace existing boiler per block, high efficiency
	Exterior Insulation and Finishing Systems (EIFS)	Secondary glazing double	Balcony cladding - Single glazing	Insulation of top floor slab		Mechanical ventilation	CHP installation
	Ventilated façade		Balcony cladding - Double glazing	Flat roof		Ventilation system with heat recovery (HR)	Heat pump
	Timber-frame wall	Replace windows (Double pane)		Green roof			
	Second Façade/ Single glazing	Replace windows (Triple pane)					
	Second Façade/ Double glazing	Shading adjustable					Biomass boiler
	BIPV's			Photovoltaic			Solar collectors
	Added space/ Second façade integrated	Shading fixed	Integrated balcony				Geothermy
	Lift addition	Enlarged windows	New balcony	Additional floor/ occupied loft	Additional floor/occupied basement		District/ community heating

The assumptions used as input in the calculations were based on European standards, such as EN15251 [27]. They were regarding ventilation, heating and cooling user thermal comfort criteria, as well as values for internal gains and occupancy. Based on the inputs, the building thermal performance was simulated on an hourly basis, throughout the year and gave results on the energy demand of the modelled building and the internal temperature. The toolbox quantification aimed at results that can be comparable, the simulation settings were kept as much as possible fixed when simulating different measures. This means that the performance of each measure can be further optimised, if a high resolution simulation, to predict more detailed performance, was required. This was, however, beyond the scope of the approach.

The measures are quantified in terms of heating energy demand, which represents more than half of the final energy consumption of residential buildings in the EU is used for space heating, reaching up to 70% in some countries [1, 8]. This is the energy needed to balance the heat losses in order to maintain the required temperature. As a large part of heat losses are through the building envelope components, the retrofitting measures reduce these losses and, hence, the energy demand. Replacing the existing system with one of higher efficiency will result in additional savings in delivered and primary energy demand than the savings in heating energy demand already suggested by the toolbox calculation. To estimate the savings in primary energy, however, it is necessary to consider the fuel type or the energy mix, with the respective primary energy factor (PEF), as well as the system efficiency. This information is site-specific and cannot be generalised in the toolbox data.

To evaluate and compare refurbishment measures, each option needs to be quantified separately. Since this quantification is expressed as reduction in current energy demand, the method used to isolate the impact of each option has two distinct steps. First the existing building's condition was simulated, to determine the current energy demand and, subsequently, the building after the refurbishment measure application, to evaluate the impact on energy demand. The toolbox options calculations generated specific figures on energy demand reduction related to each retrofitting measure. The following figure presents an overview of the potential savings as an effect of the retrofitting measures application. However, these percentages can vary in buildings that differ in the characteristics such as construction, window-to-wall ration (WWR) and orientation Based on the specific building characteristics, the FRT approach has available data that provides an indication of the measure effect, expressed in percentage of heating energy demand reduction compared to the current demand [28].

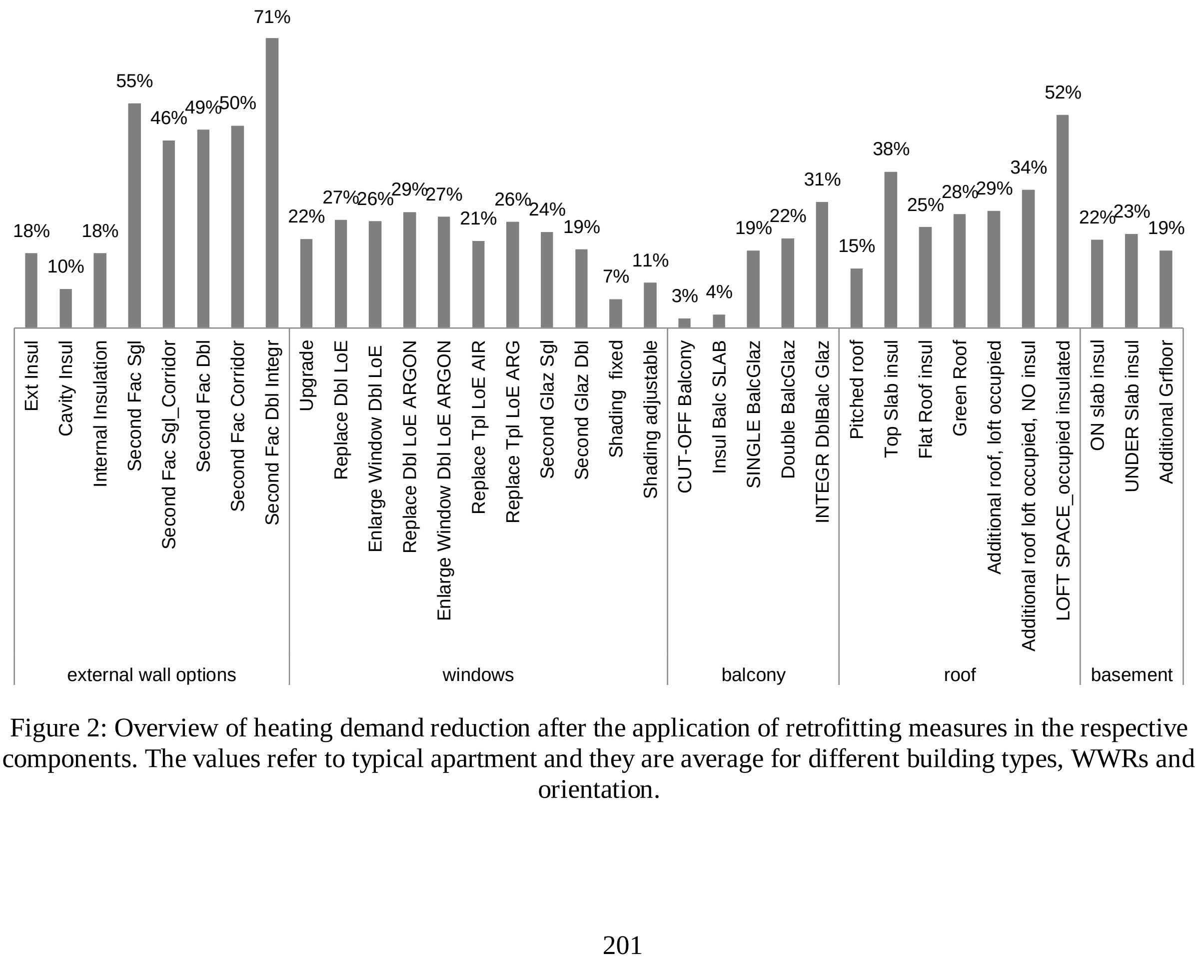

Figure 2: Overview of heating demand reduction after the application of retrofitting measures in the respective components. The values refer to typical apartment and they are average for different building types, WWRs and orientation.

3.3 Applicability

The toolbox calculation results can be used in refurbishment project, based on the existing building characteristics. The quantification of the measures is based on simulation of different building types before and after the application of a measure. The result is the percentage of reduction on the energy demand. In future projects, the building to be refurbishment must be associated with the pre-calculated models according to each component construction, providing an indication of energy saving potential of different retrofitting measures without new simulations, to be support the early stages of the design.

Based on the pre-calculated models, the approach can provide percentages of energy demand reduction after the various measures application regarding each specific building. The steps to follow to obtain those data are shown in Figure 3. First, the existing construction, together with WWR and the façades orientation need to be identified. According to this information, the building can be associated with the pre-calculated model. Moreover, it needs to be determined whether it is relevant to look at the typical apartment or the whole building. In most cases, particularly in apartment building, the savings of the typical apartment are a better indication to consider in the decision-making, as the effect of the measure is greater than in other types. Nevertheless, depending on the building type and the objectives of the design team, the whole building consumption may be also relevant. Finally, the percentage of potential energy demand reduction for each component retrofitting measure can be obtained be referring to the simulation results of the respective building types [28], composing the measures overview graph, as the one shown in Figure 2.

The usability of the approach and particularly the energy saving potential overview were validated by building industry professionals, who are expected to use it in the refurbishment strategy decision-making. The information sought was of qualitative nature, as they refer to the design process and the usability of the approach. Therefore, semi-structured interviews were used as a mean of qualitative data collection. The first part of the interview got the respondents acquainted with the approach, while in the second phase, they were asked on their opinion regarding refurbishment design process and the impact of the toolbox information.

The main categories of respondents are designers and stakeholders, divided in different groups. Since the approach focuses on the design phase, architects were an important respondent group to provide feedback. Additionally architectural students working on refurbishment projects were part of the designers' category. Aside from designers, refurbishment decisions are influenced by other building industry parties, referred as stakeholders. The respondents were selected on the basis of their experience on refurbishment decision-making. They include housing companies that are often the refurbishment initiator and shape the specification, together with maintenance and renovation constructors and climate consultant.

The interviews resulted that energy upgrade is typically part of the project requirements. However in most cases it does not influence the concept development and comes as an additional parameter to be incorporated in the final design. Efforts toward reversing this process are taking place, particularly from the stakeholders' point of view. Multi-disciplinary teams, often, but not always, with the participation of architects, aim at making refurbishment decisions based on the solution performance. Stakeholders appear to be more aware compared to architects of the need to integrate the energy performance in their decisions. The reason is the direct relation of energy savings and cost, which is the most decisive factor for stakeholders. Housing companies and refurbishment consultants are already using tools to get early indicators of performance, while architects mostly rely on their experience and general knowledge. In this context, the approach focus on architects is justified.
In general, the participants believed that the toolbox information is useful to provide an overview of possibilities and arguments within the design team. Even if the decision is not on the measure with the higher energy savings, it is beneficial that it triggers the discussion on why an efficient measure is not selected. On the other hand, it can direct the design towards high-saving options. Most importantly, the information can be valuable when negotiating possible options with clients.

The investment cost came up several times during the interviews, as the main factor to determine the decisions taken by the client. Even though the approach does not provide specific numbers for the cost of a measure, it addresses its importance as a parameter in the matrix organisation. Measures that are more intervening and are, hence, expected to be more expensive are placed after the less intervening measures. Calculating the expense of a measure it is not possible within the scope of the approach as it depends on the specific project, in terms of scale, location, detailing of the solution etc. Nevertheless, when a specific project is considered and the expenses are known, the toolbox information can easily give an indicative payback time, based on the calculated energy savings.

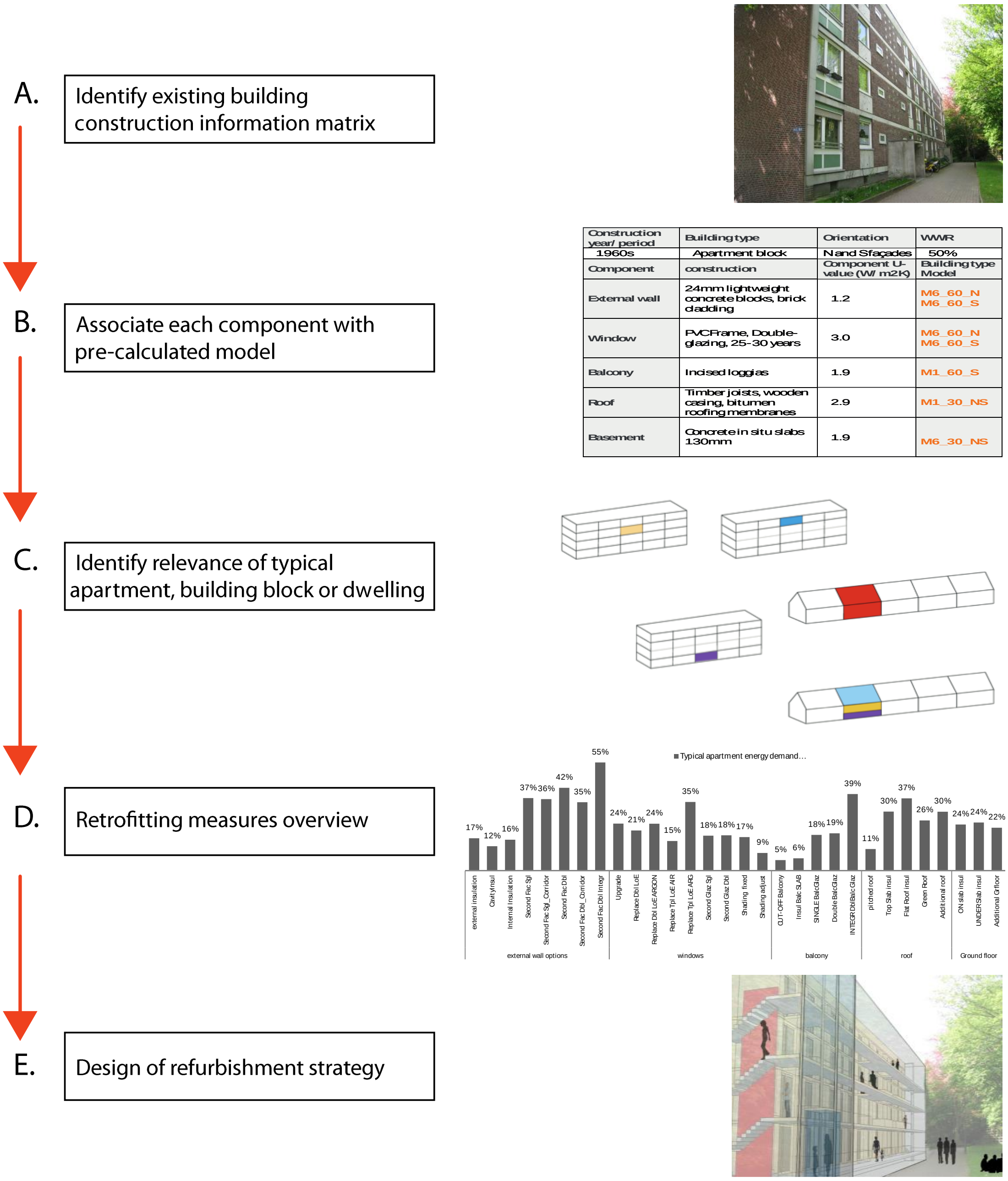

Construction year/ period	Building type	Orientation	WWR
1960s	Apartment block	N and S façades	50%
Component	construction	Component U-value (W/ m2K)	Building type Model
External wall	24mm lightweight concrete blocks, brick cladding	1.2	M6_60_N M6_60_S
Window	PVC Frame, Double-glazing, 25-30 years	3.0	M6_60_N M6_60_S
Balcony	Incised loggias	1.9	M1_60_S
Roof	Timber joists, wooden casing, bitumen roofing membranes	2.9	M1_30_NS
Basement	Concrete in situ slabs 130mm	1.9	M6_30_NS

Figure 3: Steps to associate an existing building with the Façade Refurbishment Toolbox (FRT) approach pre-calculated models. In this way, an indication of energy saving potential of different retrofitting measures is available without new simulations.

4 Conclusion

The Façade Refurbishment Toolbox (FRT) approach provides information that can support the decision-making of residential façade refurbishment strategies. Firstly, the building envelope components that need to be addressed in an integrated refurbishment strategy are identified and different retrofitting measures for each one are proposed, composing the façade refurbishment toolbox. Secondly, the measures are quantified in terms of energy upgrade potential, expressed by the simulated energy demand reduction after the measure application.

As a result, the toolbox calculations provide an indication of the potential energy demand reduction at the early stages of the design and give the possibility to compare different measures when decisions need to be taken. Additionally the toolbox matrix helps in organising the available options and highlight key considerations during the process that the toolbox information can have an impact on. All the information can support the decision-making within the refurbishment strategy design team. The approach primarily targets the architect, that has to make the design development, but the information can also be used by users, owners and other stakeholders.

To validate the approached further applicability, building industry experts, designers and stakeholders were interviewed to give feedback on the qualitative assessment of the approach usability. The respondents were selected on the basis of their experience on refurbishment decision-making. Apart from designers, who are the main target of the approach, housing corporation and renovation constructors were included as validating parties.

Both designers and stakeholders have found the energy saving potential and the level of information provided by the approach useful information, not only during their own decision-making, but also in their argumentation within the project team and the client. The approach provided a general, but clear idea for the effect of different measure, by quantifying measure impact on energy demand. If more specific data on energy consumption are needed, simulating the performance of the final strategy is required. Nevertheless, this does not conflict with the objective of the FRT, which aims at providing an indication at the early stages of the design. The integration of measures' cost was recommended as further development of the toolbox. Additional consideration that influence the decisions, particularly form the architects perspective, included the improvement of building's function and appearance, the flexibility of the solution to be adjustable to occupants needs and the preservation of building existing value. The toolbox information can support the decision, integrating the energy savings to the project specifications, leading to the design of energy conscious refurbishment strategies for the residential buildings' façades.

5 Acknowledgements

The research presented in this paper is part of the PhD research conducted in Faculty of Architecture and the Built Environment, The Delft University of Technology. The author would like to thank the promotors of the PhD, Prof.Dr.-Ing. U. Knaack and Prof.dr.ir. A. van Timmeren, as well as Dr.-Ing. Tilllmann Klein, leader of the Façade Research Group, for their support and contribution during the development of the research.

6 References

[1] BPIE, *Europe's buildings under the microscope*. Building Performance institute Europe. Brussels, 2011.

[2] Gaterell, M.R. and M.E. McEvoy, *The impact of climate change uncertainties on the performance of energy efficiency measures applied to dwellings.* Energy and Buildings 37 (2005) issue 9 pp. 982-995.

[3] Rademaekers, K., et al., *The Energy Efficiency Investment Potential for the Building Environment:Two approaches*. Ecorys for DG ENER: Rotterdam, 2012.

[4] Power, A., *Does demolition or refurbishment of old and inefficient homes help to increase our environmental, social and economic viability?* Energy Policy 36 (2008) issue 12 pp. 4487-4501.

[5] Poel, B., G. van Cruchten, and C.A. Balaras, *Energy performance assessment of existing dwellings.* Energy and Buildings 39 (2007) issue 4 pp. 393-403.

[6] Thomsen, A., *Paradigm shift or choke? The future of the Western European housing stock.*, in *Housing: the next 20 years - CCHPR Conference* Cambridge, 2010.

[7] Eurostat, *Environment and Energy*, in *Europe in figures: Eurostat yearbook 2010*, Office for Official Publications of the European Communities: Luxembourg. 2010.

[8] Itard, L. and F. Meijer, *Towards a sustainable Northern European housing stock*. Sustainable urban areas. Vol. 22, IOS. Amsterdam, 2008.

[9] Thomsen, A.F. and C.L. van der Flier, *Replacement or reuse? The choice between demolition and life cycle extension from a sustainable viewpoin*, in *Shrinking Cities, Sprawling Suburbs, Changing Countrysides*, Centre for Housing Research, UCD. 2008.

[10] Brand, S., *How buildings learn : what happens after they're built*. Viking. New York, NY, 1994.

[11] Chandler, I., *Repair and renovation of modern buildings*. McGraw-Hill. New York, 1991.

[12] Attia, S., et al., *Simulation-based decision support tool for early stages of zero-energy building design.* Energy and Buildings 49 (2012) issue 0 pp. 2-15.

[13] Ma, Z., et al., *Existing building retrofits: Methodology and state-of-the-art.* Energy and Buildings 55 (2012) issue 0 pp. 889-902.

[14] Ferreira, J., M.D. Pinheiro, and J.d. Brito, *Refurbishment decision support tools: A review from a Portuguese user's perspective.* Construction and Building Materials 49 (2013) issue 0 pp. 425-447.

[15] Cooper, R., et al., *Process Management in Design and Construction*. Wiley, 2008.

[16] Ad-Hoc, I.A., *Energy-efficient Buildings PPP beyond 2013: Research & Innovation Roadmap*, in *Energy Efficient buildings*. Energy Efficient Buildings Association: Brussels, 2012.

[17] Riether, G. and T. Butler, *Simulation Space*, in *eCAADe 2008: architecture "in computro", Integrating Methods and Techniques Education and Research in Computer Aided Architectural Design in Europe*. The Higher Institute of Architectural Science: Antwerp. p. 133-142, 2008.

[18] Attia, S., *A Tool for Design Decision Making Zero Energy Residential Buildings in Hot Humid Climates*, in *Faculté d'architecture, d'ingénierie architecturale, d'urbanisme, LOCI*. Université catholique de Louvain: Louvain, 2012.

[19] Flourentzou, F., J.-L. Genre, and C.-A. Roulet, *EPIQR-TOBUS: a new generation of refurbishment decision aid methods*, in *Towards Sustainable Building*, N. Maiellaro, Editor, Springer Netherlands. p. 161-169. 2001.

[20] TABULA. *Typology Approach for Building Stock Energy Assessment*. 2012 [cited 2013 30-07].

[21] Häkkinen, T., *Systematic method for the sustainability analysis of refurbishment concepts of exterior walls.* Construction and Building Materials 37 (2012) issue 0 pp. 783-790.

[22] Sdei, A., et al., *Dynamic Thermal Modeling of Retrofitted Social Housing in England and France*, in *CLIMA 2013 - 11th REHVA World Congress and the 8th International Conference on Indoor Air Quality, Ventilation and Energy Conservation in Buildings*, M.U. Karel Kabele, Karel Suchý, Miloš Lain, Editor., Society of Environmental Engineering (STP): Prague. p. 6882, 2013.

[23] Nemry, F., et al., *Options to reduce the environmental impacts of residential buildings in the European Union--Potential and costs.* Energy and Buildings 42 (2010) issue 7 pp. 976-984.

[24] Konstantinou, T. and U. Knaack, *An approach to integrate energy efficiency upgrade into refurbishment design process, applied in two case-study buildings in Northern European climate.* Energy and Buildings 59 (2013) issue 0 pp. 301-309.

[25] DesignBuilder, *DesignBuilder*. DesignBuilder Software Ltd: Stroud, 2012.

[26] DOE. *Building Energy Software Tools Directory*. U.S. Department of Energy 2012 [cited 2013 11-03]; Available from: http://apps1.eere.energy.gov/buildings/tools_directory/subjects.cfm/pagename=subjects/pagename_menu=whole_building_analysis/pagename_submenu=energy_simulation.

[27] EN15251, *Indoor environmental input parameters for design and assessment of energy performance of buildings addressing indoor air quality, thermal environment, lighting and acoustics*. European Commitee for Standardization (CEN): Brussels, 2007.

[28] Konstantinou, T., *Facade Refurbishment Toolbox. Supporting the Design of Residential Energy Upgrades*, in *A+BE | Architecture and the Built Environment; No 9 (2014): Facade Refurbishment Toolbox*. Delft University of Technology. p. 420, 2014.

Proceedings of the International Conference on Building Envelope Design and Technology, Graz
Advanced Building Skins 2015

Renovation and upgrading of a residential building from the 1960s to an energy-plus building

Werner Nussmüller, DI Arch.
Nussmüller Architekten ZT GmbH

Summary

Prefabricated wooden elements which form the façade and also contain all the building services are the key to the Johann Böhm renovation. The building-height elements are prefabricated complete with windows and doors. Prefabrication in the factory building, which is unaffected by the weather, enables all components, such as windows, doors, building services, and active elements, such as PV and solar modules, to be fitted with extreme precision. As a result, the construction time is accurately estimated and costs are reduced. Of course, there is a significant price advantage over single-unit production due to the possibility of series production.

Keywords: Renovation, prefabricated façade modules, post-war buildings, energy efficiency, prefabricated component

1 Introduction

There are a large number of existing buildings from the post-war period in Styria and throughout Austria which require much too much energy due to their type of construction. In many cases, it would be possible to use smart measures to turn the existing buildings into zero-energy buildings. Building renovation represents a good starting point at a time when attempts are being made to reduce energy consumption and therefore to make a contribution to environmental protection. The greatest potential for energy conservation lies in the renovation of existing buildings from the post-war period.
This principle was implemented in an exemplary manner during the renovation of a residential building from the 1960s in Kapfenberg, Austria.

2 Project aim

The aim was to use the latest technologies to dramatically reduce energy consumption. 80% saving on annual heat requirement, 80% saving on CO_2, 80% use of renewable energies. However, the aim of renovation was not merely to reduce costs but also to upgrade the living quality in general. Taking all the factors into account, the following project aims were achieved: improvement of the residential environment and the layouts, optimal lighting, use of sunlight and cross-ventilation of the living areas, expansion by means of balconies and terraces, adaptation to new living standards and achievement of the energy targets mentioned above.

3 Project partners

The development and implementation involved an interdisciplinary team of architects, technical designers, companies and university research departments.
The research project was carried out under the scientific lead of AEE INTEC, with the architectural design of Nussmüller Architects and with Gem. Wohn.- und Siedlungsgenossenschaft Ennstal, the innovative building owner, and the town of Kapfenberg. Additional project partners were Geberit and Gap Solutions.

Conversion of the apartment block is a demonstration project from the “Haus der Zukunft Plus” *[Energy-Plus House of the Future]* program line sponsored by the Austrian Federal Ministry for Transport, Innovation and Technology. The project was handled with the support of the Austrian Research Promotion Agency FFG. Other project partners were Kulmer Bau GesmbH und CO KG, Technisches Büro Ing. Bernhard Hammer GmbH, Geberit and Gap Solution.

4 Implementation

4.1 Architecture

The four-storey structure oriented east to west is 62.0 m long and 10.5 m deep and originally accommodated 48 apartments. The structure was divided by a partition wall into two identical blocks with several units (accessed by the same stairway) on each storey. The infrastructure provision was via two internal stairways on the east side. The apartments were between 20 m^2 and 65 m^2 in size and no longer met the current requirements of the housing market.
As a result of the existing infrastructure in the centre of the building, only the corner apartments could support an apartment floor plan extending front to back on the east and west side which made renting the apartments difficult.
Thanks to the new floor plan design for the apartments and an external balcony arranged on the east side for access to the infrastructure, it was possible to create apartments that met the standard of a new building. In addition, all the apartments were designed to be accessible and to meet the needs of the disabled. Elisa and Rainer Rosegger looked after the residents sociologically during the conversion and resettlement.
It was generally possible to fulfil the users’ requirements for convenience as well as comfort by improving the indoor climate. This was achieved by, among other things, high-quality ecological building materials which minimised the pollutant load in the inner rooms.
The existing roof was removed and replaced with a “solar wing”. This is reminiscent in its appearance of a butterfly which, while looking for a place to rest after flying, alights and soaks up energy again from the sun.

Figure 1: Annual heat requirement before and after the renovation

4.2 Energy design concept

The base heat supply is provided via thermal solar collectors on the south side ("solar sail" approx. 144 m^2, equates to approx. 39,500 kWh/a) which enable partially solar space heating and hot water production. The residual heat cover is provided by the existing piped district heating system of Kapfenberg's municipal utility company; this is made up mainly of waste heat from the Böhler plants (steel production of VOEST). The ventilation system with heat recovery significantly reduces ventilation losses. In the 2nd construction phase, the rooms are ventilated with window vents, a used air extraction system and a heat pump. The renewable energies generated feed an energy accumulator (7,500 l) installed in the new plant room. The power for heating and hot water is distributed by means of a two-wire supply system and an apartment boiler in every apartment.
A photovoltaic system measuring approx. 630 m^2/ca. 70,000 kWh was provided on the roof of the building (solar wing on the flat roof instead of the existing pitched roof). The electricity generated is fed into the grid and purchased back from the grid.
The reduction in electricity required in respect of domestic and auxiliary power due to energy-saving equipment and appliances and awareness raising is an essential requirement for implementing an energy-plus building. A fully furnished show apartment was used to demonstrate to the residents how much electricity can be saved with new equipment and appliances that are better. This and other measures to raise awareness are also intended to reduce energy consumption.
The measures described make it possible to design an energy-plus building, that balances the books based on the primary energy in the renovation.

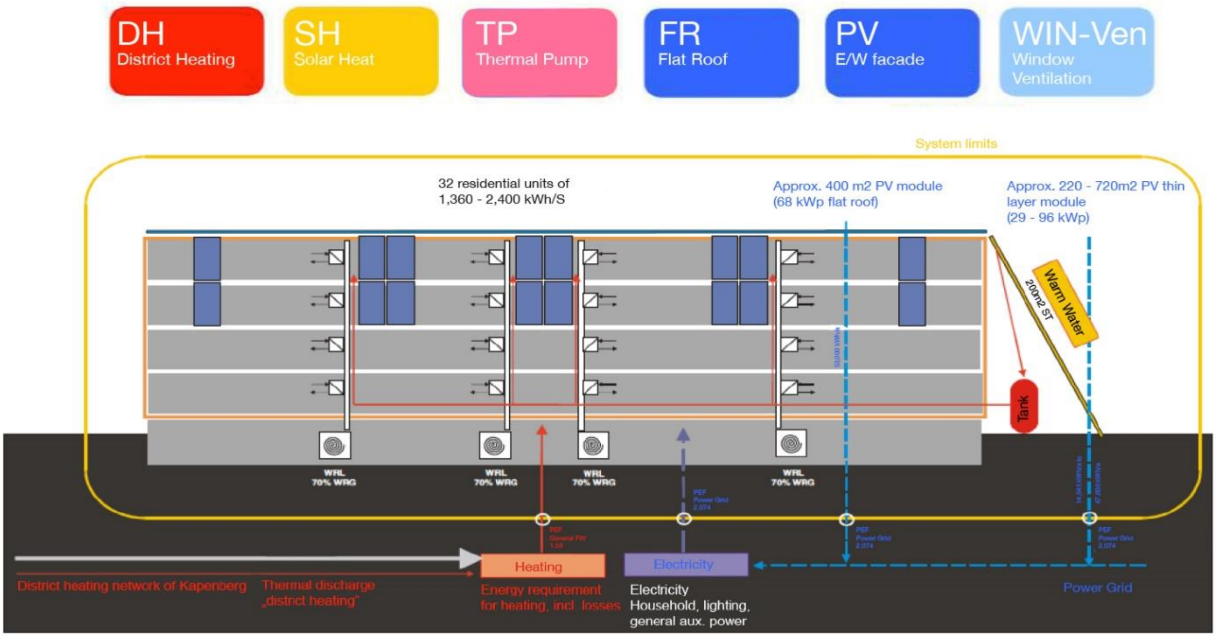

Figure 2: Building services design concept

4.3 Façade and building services modules

The prefabricated wooden modules used are large-sized timber frame or slab elements. The building-height elements (12 m x 3 m) can be prefabricated complete with windows, doors and external installation shafts. A high level of precision in the execution is achieved thanks to prefabrication in the factory.
The prefabricated wooden façade elements also mean that the building costs can be defined accurately, construction times on site can be shortened and façades can be realised in high technical quality. Prefabrication in the factory building, which is unaffected by the weather, enables all components, such as windows, doors, building services shafts and solar modules, to be fitted with extreme precision. The joint and connection details of the completely prefabricated elements are designed so that all the required building physics functions, such as thermal insulation and fire protection, air-tightness and sound insulation, are guaranteed.

The use of façade and building services modules represents a significant improvement in the thermal quality (reduction of transmission heat losses, elimination of thermal bridges) which is applicable to similar building types. The façade modules include traditional ventilated structures (various possible surfaces) and energy-generating active elements ("plus" energy generators), such as solar collectors, solar honeycombs and PV systems. It is therefore possible to match and optimise the number and configuration to the given situation (zero-energy or plus-energy).

Figure 3: Attachment of the façade modules

Renovation and upgrading of the building services was achieved using prefabricated building services shafts which were relocated from inside the building to the new building envelope.

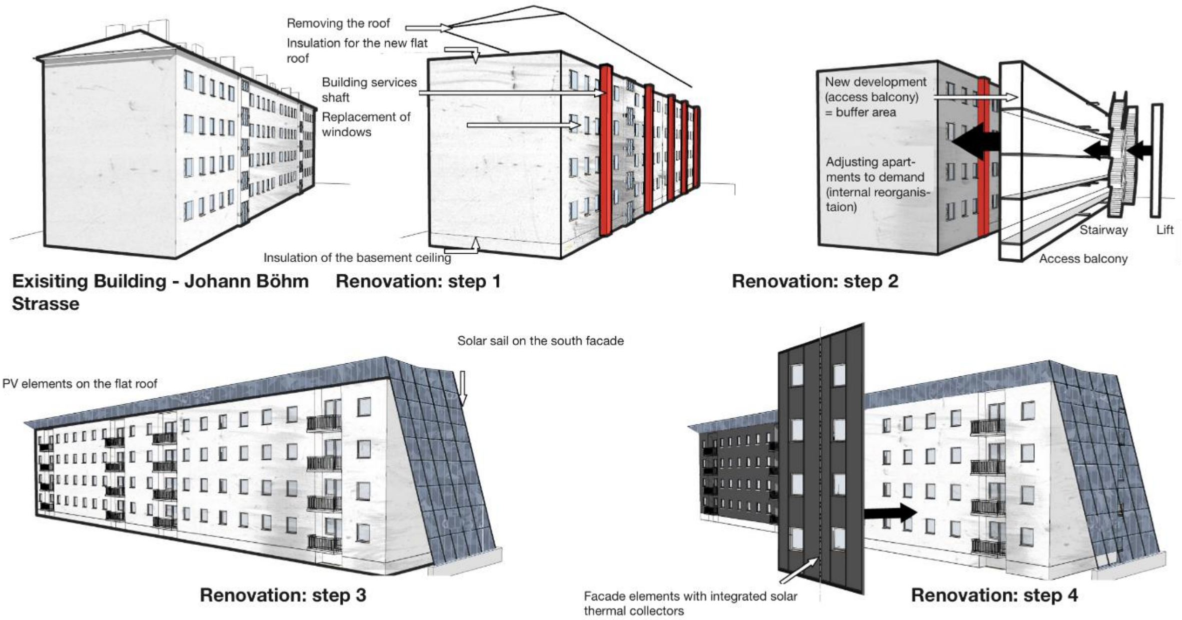

Figure 4: Renovation steps

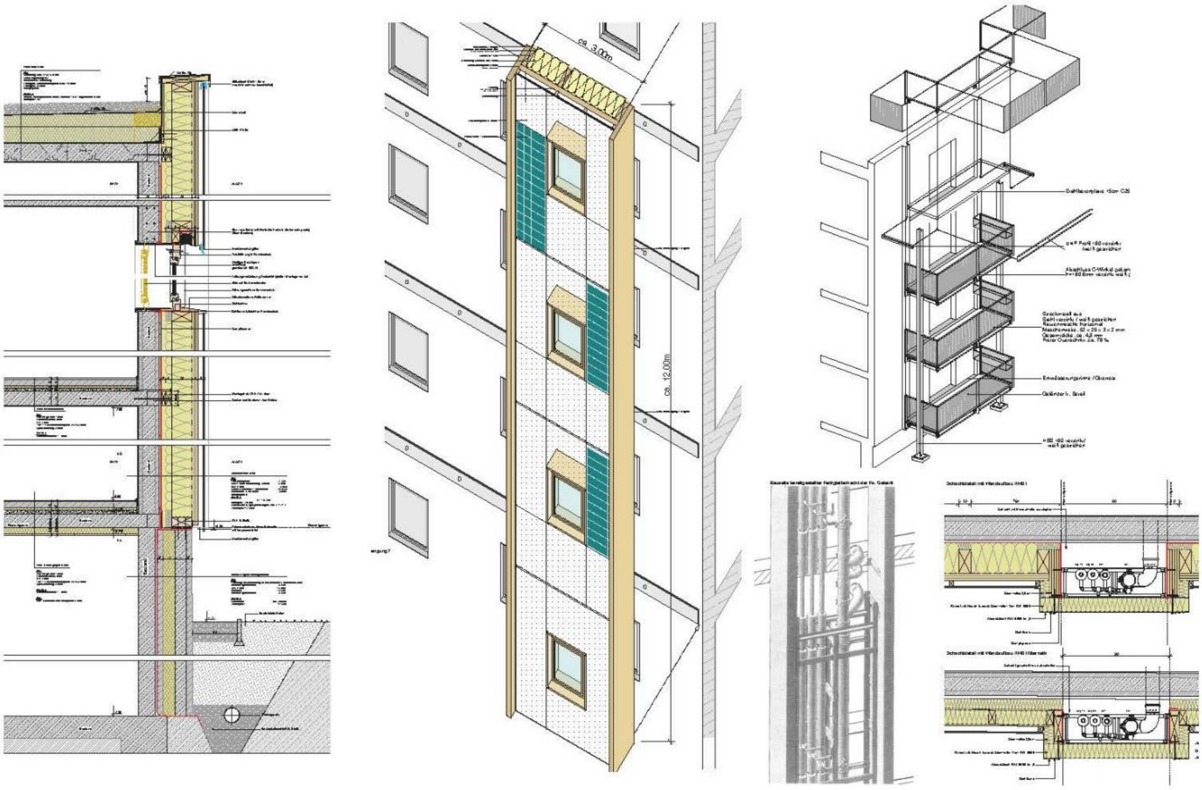

Figure 5: Façade details

5 Current status

Project development was launched in 2012, implementation took place in 2013 and the building was handed over in 2014.

Figure 6: Renovation of the Johann Böhm apartment block after completion

6 Evaluation

Reducing the electricity consumption within the household of the individual residential units is a development process that is mainly organisational. Raising awareness takes place constantly during routine operation. Conclusion: to achieve the objectives of an energy-plus standard, it is absolutely imperative for all the innovative components to be optimally matched. A trend-setting innovative upgrading method can only be implemented in the overall system. The project will be supervised scientifically for 2 years. Other successful examples for the renovation of post-war buildings are Markartstrasse in Linz, a building located on Dieselweg in Graz, Stahlstrasse in Leoben, a building in Liebenauer Hauptstrasse in Graz and Alingsas in Sweden. Here too, it was possible to demonstrate ways in which to create energy-plus buildings from energy guzzlers using prefabricated façade modules.

7 Prizes

The Johann Böhm renovation was awarded a gold certificate by klima:aktiv as it achieved a score of 943 out of a possible 1000.
The bm:vit and Haus der Zukunft *[House of the Future]*, headed by Minister Doris Bures, awarded the status “First Energy-Plus Renovation of a Residential Building in Austria” in June 2014. The records state, “By renovating the “Johann Böhm Strasse 34/36” residential complex in Kapfenberg dating from the 1960s, it will be the first multiple family building in Austria to be renovated and upgraded to become an energy-plus building using a specially designed, prefabricated façade system in addition to an innovative building services and energy system.
The Johann Böhm renovation was also nominated for the Climate Protection Prize 2014 and for the Styrian Timber Construction Prize 2013.

8 Outlook

An enormous social benefit is to be anticipated from series production of the façade and building services modules.
The energy and building services design concepts and the large-sized prefabricated passive and active façade modules can be transferred to many buildings of the post-war period and the 1960s.
The pilot project e80^3 is trend-setting for energy conservation in all post-war buildings. In interdisciplinary collaboration, the project engineers have already won several prizes and awards in the area of structural timber construction and energy-efficient renovation and revitalisation and they can tap into a wealth of in-depth specialist knowledge.

9 Additional Facts

Building:
Usable area: 2,240 m^2
Heated usable area: 2,240 m^2
Façade area: 1,622 m^2
Building costs: EUR 3.4 million
Users: 32 residential units
Year of construction: 1959, renovation 2012-2013
New construction/renovation: 2013 renovation and upgrading to energy-plus building

Architecture:
U-values W/m^2K: Exterior wall 0.12; roof 0.10; windows 0.85
Air tightness: n50 less than or equal to 1.5 l/h

Costs and financing:
Costs of renewable energy: approx. EUR 420,000 for solar thermal and photovoltaic including technical equipment room
Total costs: EUR 1,520/m^2

Monitoring:
Energy monitoring: Extensive monitoring is planned for 2 years, the first data will not be available until mid-2014.

Design/draft
Target: 80% saving on annual heat requirement, 80% saving on CO_2, 80% use of renewable energies. Motivation: Annual heat requirement to approx. 15 kWh/m^2a, zero-energy primary energy balance

Key energy indicators:
Primary energy requirement: 220,000 kWh/a, 80 kWh/m^2a
Final energy requirement: 118,200 kWh/a, 43 kWh/m^2a
Energy efficiency class: A+ (OIB 2007)

Photovoltaics:
Installed output: 92 kWp
Annual yield: 70,000 kWh (target)
Collector area: 630 m^2

Solar heat:
Installed output: 100.8 kW
Annual yield: 39,500 kWh/a (target)
Collector area: 144 m^2

Wood Based Curtain Wall for Building Retrofit – Development and Performance

Jan Tywoniak, Prof. CSc., Antonín Lupíšek, PhD., Michal Bureš, Martin Volf
Czech Technical University in Prague, Czech Republic, tywoniak@fsv.cvut.cz

Summary

This paper describes an own development of a curtain wall panel system. The leading idea of the project was to prepare an alternative solution for replacement of old metallic curtain walls during the refurbishment of nonresidential buildings from the 1960ies – 1970ies. Presented solution use wood and wood based materials (laminated veneer lumbers) for construction of panels, with clear preference to non-oil based materials for thermal insulation. System allows for different type of external cladding (cement based boards, wooden claddings, integrated PV, support for greenery). Integration of other technical components, like venetian blinds, decentralized ventilation units, is possible. Thermal performance of this new envelope suitable for nearly-zero energy buildings together with environmental oriented assessments is discussed.

Keywords: Curtain wall, refurbishment, thermal performance, wood based construction

1 Introduction

Since 1960´s, a significant share of facades on non-residential buildings has used lightweight curtain walls (CW) [1], then perceived as a highly advanced building technology. However, these solutions have caused various issues. They were characterized by a high energy-demand in terms of space heating. Moreover, the curtain walls with their large glazed areas and low thermal inertia have contributed to overheating the buildings [2] and/or led to a significant cooling energy demand. Significant thermal bridges were usually present. In the Czech Republic, the presence of asbestos fibers in the boards used in curtain walls was recognized as another key-problem to be solved during the building retrofit [3].

Many of the curtain walls from 1960´s have already been replaced. However, many of them remain more or less in their original state, including more than 290 school buildings solely in the Czech Republic. Other countries in Central Europe appear to be in a similar situation.

Several technologies for refurbishment of such buildings can be identified in practice: a) complete replacement of the existing curtain wall with a new one, b) partial replacement: principal frame remains, new structural elements are added together with the filling, cladding and windows, c) complete replacement by a traditional aerated concrete wall accompanied with an external thermal insulation composite system (ETICS) and windows. The choice of technology is influenced by the overall architectural solution, total size of the building, accessibility of the site, the time available for the building retrofit and other reasons (tradition, skills of the contractor, etc.). Generally, an advanced, industrialized way of assembly shall be preferred as it enables new and more efficient construction of building envelopes.

2 Inspiration

The replacement of the original curtain wall from 1971 by new one at one of the campus buildings of Czech Technical University in Prague [4] (Fig.1) generated a principal question about the possibility to find a modern and applicable solution for curtain walls with higher respect the environment. New facade (Fig.1 at right) with very low thermal transmittance, integrated motor controlled venetian blinds, indoor shading blinds, etc. is increase the comfort significantly and is suitable for low-energy and passive buildings but the embodied energy is relatively high [5]. Having such search for overall optimum solution in mind a first study was performed how to reduce the embodied energy and other negative impacts by using of wood and wood based materials instead of aluminum and oil based materials.

As a result, a new panel system was developed (Fig.2). It consists of a frame made of laminated veneer lumber, insulation from mineral or wood fibers. All other components for the panel are selected with the preference to materials with low embodied energy and other negative impacts as well.

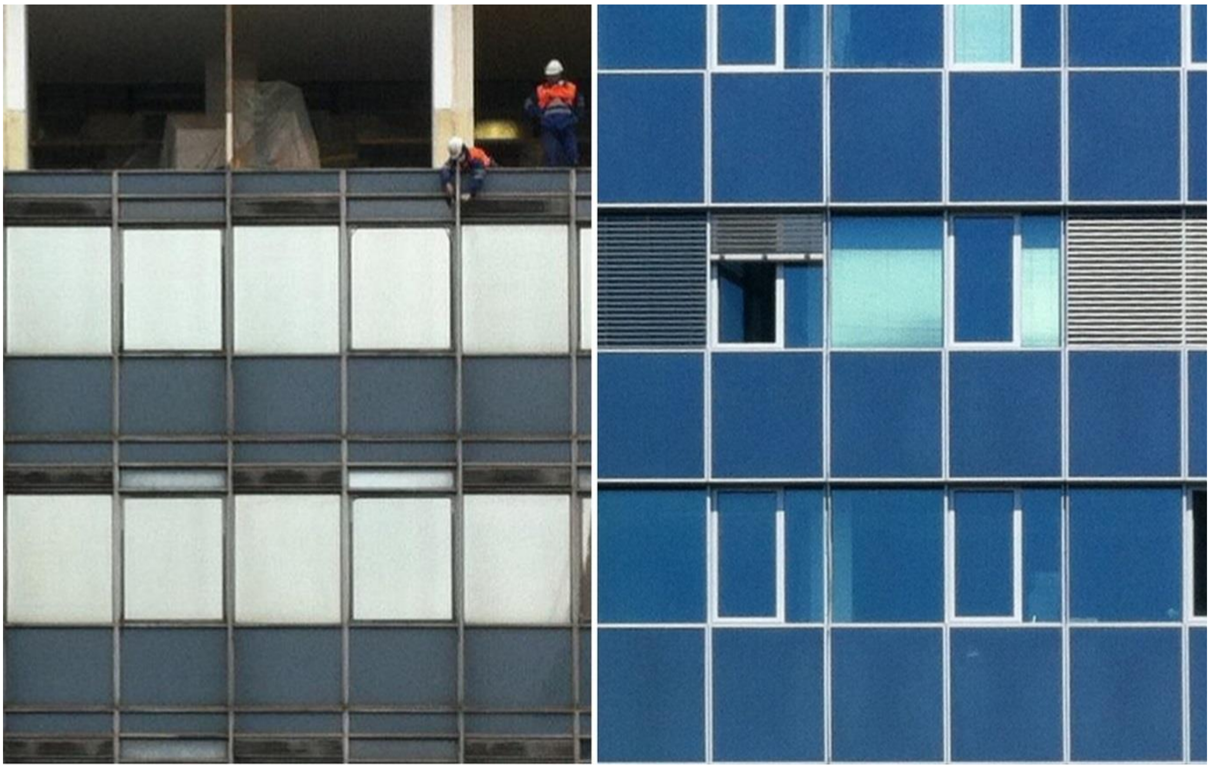

Figure 1: Retrofit of the campus building (2013). Left: dismounting of original curtain wall from 1971 (overall U-value approx. 3.0 W/(m^{2}K). Right: New curtain wall, triple glazing, venetian blinds motor controlled, overall U-value 0.7 W/m^{2}K) by 60% glazed area

3 Technical solution a performance

3.1 Materials and construction

Main structural materials (panel supporting frame, exterior and interior design boards) and supplementary materials (thermal insulation and façade cladding, window frames and sash) of the proposed wall system are made of wood-based materials. The system is executed with attention to detail. Where possible, the elements are prefabricated using precise CNC machines; main elements are made of advanced renewable materials. The anchors with fine rectification and joints connecting the panels enable installation without any extra work from the outside (no need of scaffolding on-site) and thanks to flexible seals expansion movements are possible. Anchoring into the load-bearing ceiling plate is situated at the bottom part of the windowsill.

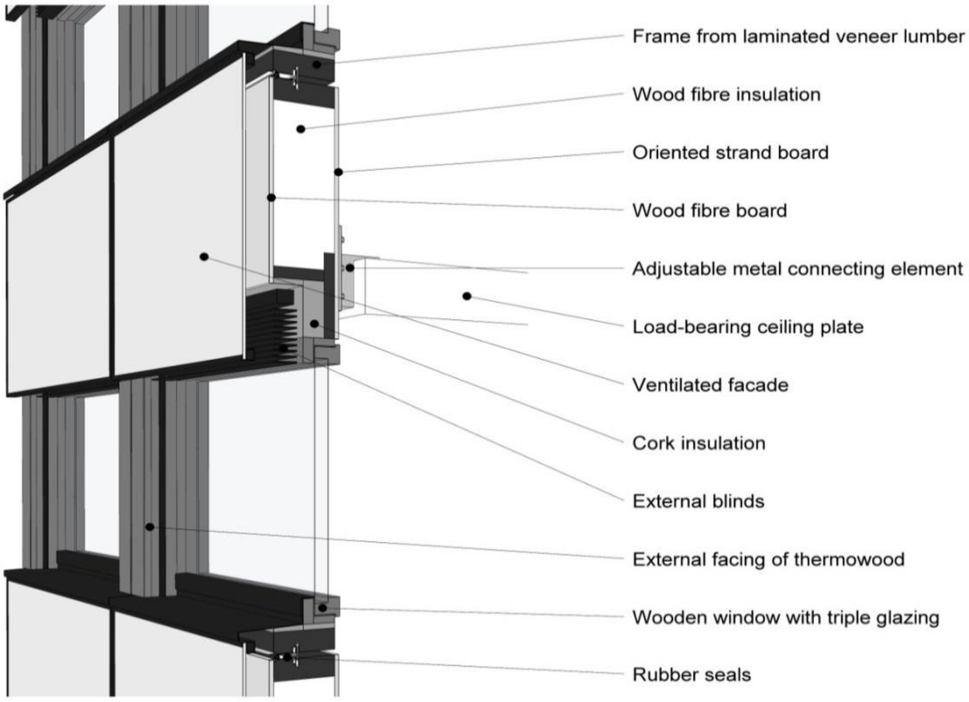

Figure 2: Scheme of a curtain wall made of a wood-based panel

Typical composition of the building envelope:

Indoor drywall lining, thickness 50-100 mm
Oriented strand board, thickness 15 mm
Wood fiber insulation, thickness 240 mm
DHF Fiberboard, thickness 15 mm
Ventilated façade

Two levels of rubber seals from exterior side and EPDM based membrane from interior side is used to ensure the water- and air-tightness at joints.

The panel is designed so that it can be used with various additional components. An opaque part can have a form of a ventilated façade equipped with active renewable energy components (photovoltaics, solar heat collectors), supporting grid for greenery purposes or traditional cladding materials (glass, wood, fiber-cement, etc.). Units for de-centralized mechanical ventilation with heat recovery, motor controlled external blinds and other devices can be used as well to improve the overall energy balance of the building. The curtain wall installation is completed by common gypsum board wall from the interior side. The piping (electrical wiring, weak current systems, heating distribution) can be installed in the cavity. Furthermore, it can contain control elements of the blinds, heating, cooling and ventilation.

3.2 Thermal properties

The total thickness of the panel in the basic version is 270 mm; flexible thermal insulation made of natural wood fibers has a thickness of 240 mm. The quality of the thermal insulation can be improved by using new generation materials, for example vacuum insulation panels (VIP). These can be placed into the protected position already in the factory without the risk damage during the construction process on-site. Depending on the type of the thermal insulation material, the construction reaches thermal transmittance values ranging from 0.16 to 0.09 W/(m^2.K) (Tab. 1).

Table 1 Basic thermal properties of opaque part of the panel

	Thermal transmittance [W/(m2K)] without considering thermal bridges
Basic solution with wood-fiber thermal insulation	0.16
Thermal insulation using quality mineral wool	0.14
Thermal insulation using mineral wool and 20 mm VIP	0.11
Thermal insulation using phenolic foam	0.09

The panels are equipped with wooden windows suitable for passive buildings (U_w 0.8 W/(m^2.K), triple glazed. Motor controlled external aluminum blinds are used to limit summer solar heat gains. The blinds are placed in an imbedded lintel box. A vacuum insulation panel or aerogel thermal insulation is used there to limit a thermal bridge. Linear thermal transmittance was calculated for all construction details [5]. It expresses the influence of additional heat flows through thermal bridges and thermal joints. Final thermal transmittance of a panel with the size of 1.5 m x 3.3 m and 60% glazed area is below 0.6 W/(m^2K). Fully opaque panel of the same size has thermal transmittance by 0.27 W/(m^2K). In both cases usual wood fiber insulation was considered. Such properties help decrease the thermal loss through the building envelope by 70 % in comparison to the old type of the curtain wall. Annual energy demand for heating and related costs of heating can be reduced by more than 50 % by changing solely the building envelope.

Environmental oriented assessments of opaque panels showed [5] that the proposed solution could reduce the embodied energy to 58 % (compared to metallic curtain wall) and to 83 % (compared to alternative with aerated concrete + thermal insulation (ETICS)). Results concerning global warming potential (GWP) are even more promising: Reduction to level of 4 % compared to metallic curtain wall.

4 First installations

First full scale installation was performed in the climatic room at the research facility UCEEB [7] (Fig.4). 4 facade elements equipped with temperature and humidity sensors are placed together in one opening (3.0 m x 3.2 m), which represents the real application: the interior temperature and relative humidity can be adjusted to typical indoor conditions, external climatic conditions are real (west oriented). Long-time observation is scheduled here.

Figure 3: Prototyping - Left: Model for development studies (Thermowood, cement based boards, venetian blinds integrated). Right: Placing of vacuum insulation boards into full scale prototype

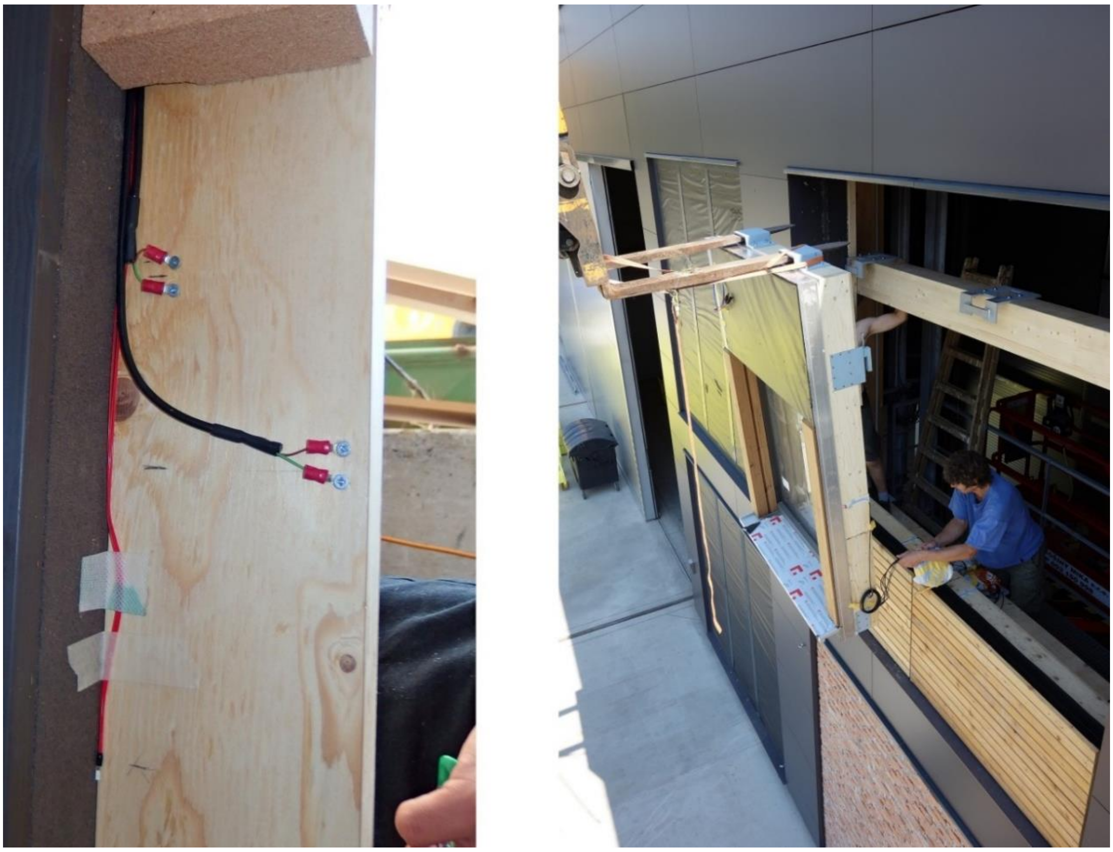

Figure 4: Panels equipped with sensors placed in one of 6 openings in climatic room for long-time observation under conditions close to reality

At the same time a larger installation is under preparation covering overall area of 48 m^2. Panels shall differ in width: 1.2, 1.5, 1.8 and 3.0 m having unified height of 3.3 m. Again, different type of insulation materials will be used: combination of vacuum plates and traditional mineral wool, wood fibers or hemp insulation. From the exterior side the panels will be equipped with different, PV-panels, wooden support for greenery. Several types of high performing glazing should be used here as well. The observation and measurements are planned for at least two years.

5 Concluding remarks

Long-time testing together with pilot installation is still in process. Use in construction practice is expected from July 2015. Lessons learned from this project can be used in a slightly modified version in similar very important task: industrialized retrofitting of residential buildings. Key requirements for advanced solutions here are the minimized negative impact on building occupants, increasing the indoor comfort and keeping or upgrade the architectural diversity of future facades. Wood based panels with similar construction can be used here as an additive system to existing wall (mainly brickwork or concrete panel). Complex solutions with focus on proper installations of technical services components are subject of the European project MORE CONNECT [8] with the participation of our team.

6 Acknowledgements

This work has been supported by the European Union, OP RDI project No. CZ.1.05/2.1.00/03.0091 – University Centre for Energy Efficient Buildings and by the H2020 project MORE CONNECT, grant agreement No. 633477.

7 References

[1] EN ISO 13830:2003 *Curtain walling – Product standard*
[2] Hegger, M., Fuchs, M., Stark, T. and Zeumer, M. *Energie Atlas. Nachhaltige Architektur.* Birkhäuser Verlag, Basel, 2008
[3] Werner, L.: *Curtain walls containing asbestos are at least in 293 school buildings,* in Czech, available from http://zpravy.idnes.cz/boleticke-panely-s-azbestem-jsou-nejmene-v-293-skolach-f9w-/domaci.aspx?c=A111202_145209_domaci_wlk *[accessed 2014-07-29]*
[4] Skanska LOP-Unit. *Replacement of curtain wall of building A, Faculty of Civil Engineering, Czech Technical University in Prague,* (Detailed design documentation for execution), Prague 2012
[5] Tywoniak, J., Bureš, M., Volf, M., Lupíšek, A.: *Curtain Walls for Building Retrofit Purposes*. Proceedings of 8th International Conference Improving Energy Efficiency in Commercial Buildings (IEECB14)
[6] EN 13947 *Thermal performance of curtain walling - Calculation of thermal transmittance*
[7] www.uceeb.cz
[8] Project MORE CONNECT – H2020 Framework Programme for Research and Innovation. EU 2014

Achieving Nearly Zero Energy Buildings - A Lifecycle Assessment Approach to Retrofitting Buildings

Paul Moran, PhD Researcher
National University of Ireland, Galway, Ireland, p.moran3@nuigalway.ie

Magdalena Hajdukiewicz, Dr
National University of Ireland, Galway, Ireland, magdalena.hajdukiewicz@nuigalway.ie

Jamie Goggins, Dr
National University of Ireland, Galway, Ireland, jamie.goggins@nuigalway.ie

Summary

It is now widely recognised in the academic and business worlds that energy efficiency in buildings provides significant environmental and economic opportunities, but also challenges. The building sector offers considerable opportunities to reduce Europe's energy consumption and carbon emissions. With the percentage of new buildings representing 1% of the total building stock and the low efficiency levels of the older building stock, retrofitting is recognised as the most immediate, pressing, and cost effective mechanism to reduce energy consumption and carbon emissions in the building and construction sector. It is necessary to double or triple the current retrofitting rate to reach EU short and long term energy reduction goals. However, given the age, diversity, size of the Irish and EU building stock, and the economic variables associated, retrofitting to meet sustainability targets on time represents a big challenge. This paper focuses on the current findings on the most effective energy measures for building retrofitting, and the limitations in research on the retrofitting of buildings. Moreover, the paper discusses how the currently on-going research project nZEB-RETROFIT in the National University of Ireland, Galway can address these issues.

Keywords: Retrofit, Materials Technology, Lifecycle Assessment, Sustainability, Nearly Zero Energy Buildings

1 Introduction

1.1 Background

People spend approximately 90% of their lives indoors [1]. Thus, it is very important to maintain safe, healthy and comfortable living conditions in buildings. However, it is now widely acknowledged that a substantial proportion of energy is required to maintain these conditions in buildings. About 40% of the world's energy consumption and approximately a third of greenhouse gas (GHG) emissions are associated with buildings [2].

In the European Union (EU), the improvement of building sector's energy efficiency is among the main priorities of the Energy Performance of Buildings Directive (EPBD) introduced through the legislation in 2002 [3] and 2010 (recast) [4]. This legislation tightens the energy performance standard requirements of the European building stock with the aim of reducing the gap between the practices in the EU Member States. The recast directive [4] requires that all new buildings and existing buildings that receive significant renovations are nearly zero energy buildings (NZEB) by end of 2020. All public buildings are required to be NZEB by the end of 2018. The recast directive [4] defined an NZEB building as a building that has a very high energy performance. The nearly zero or low amount of energy required should be covered to a very significant extent by energy from renewable resources, including those produced on site or nearby.

Further improvements in the energy efficiency of the European building sector include the 2007 EU '20-20-20' [5] initiative. This initiative requires Member States to cut their emissions, source their power requirements from renewables and improve energy efficiency by 20% from 1990 levels by 2020. Thus, EU legislation stipulates a significant amount of work to be done on the building stock in order to meet these targets. The EU is committed to reducing greenhouse gas emissions to 80 - 95% below 1990 levels by 2050 [6]. As the percentage of new buildings relative to existing buildings is increasing at a rate of only 1% per year [7] and a significant proportion of the old buildings stock will still be standing in the future, retrofitting is recognised as the most immediate, pressing and cost effective mechanism to reduce energy consumption and carbon emissions in the building and construction sector [8]. It is necessary to double or triple the current retrofitting rate of 1.2 - 1.4% per annum in order to reach the EU short and long term goals for energy and carbon reductions [9].

1.2 Overview of Irish housing stock and construction sector

The total number of dwellings in Ireland in the most recent 2011 Census was 1,994,845 [10]. The Irish housing stock has been ranked the youngest of all of the EU Member States [11]. However, over a third of the Irish dwellings were built before 1980 (Figure 1).

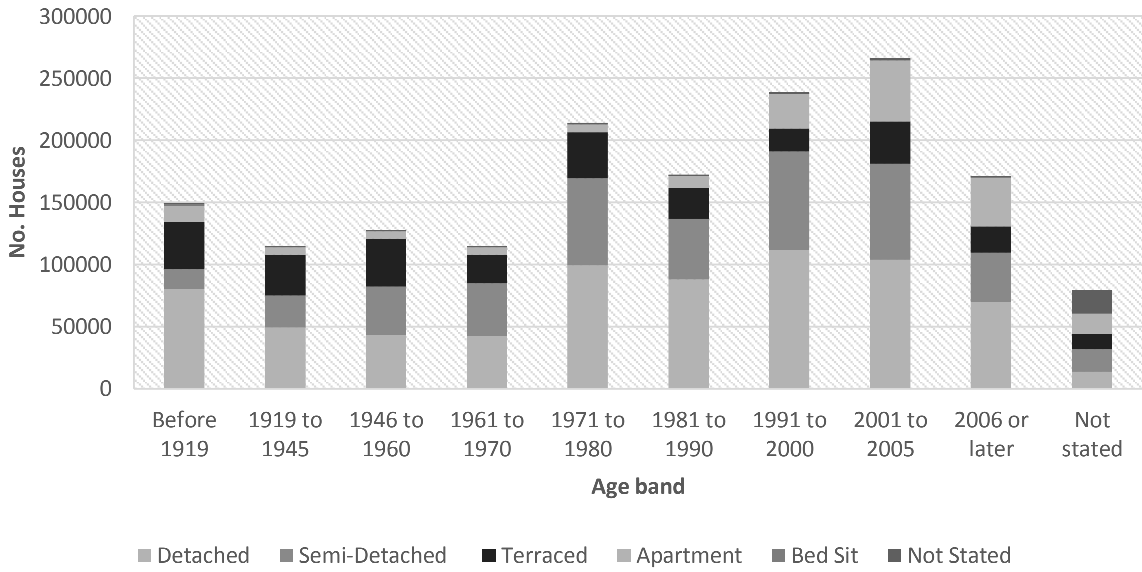

Figure 1: Age bands of Irish housing stock [10]

The type of dwelling (e.g. apartment, detached, semi-detached, terraced, etc.) is an important factor in terms of its energy consumption. Apartments are generally smaller consumers of energy compared to detached houses, but only represent 11% of the Irish housing stock. This is among the lowest in Europe [7], but the growth rate of apartments in Ireland is increasing (Figure 1). Detached houses are the most common type of dwelling in Ireland (Figure 1 and 2) and represent 42% of the Irish housing stock. These are primarily located in rural areas (72%) and are larger than the average European house. The houses located in rural areas use solid fuels or oil based heating systems as their scattering means they are not connected to the national gas grid [11].

The Building Energy Rating (BER) assessment system was set up due to the requirements of EPBD 2002 [3]. A BER is an energy label which rates the energy performance of buildings on a simple scale of A to G. It is based on the characteristics of the building and is not dependent on the behaviour of the occupants [12]. An A rated dwelling equates to the most operational energy efficient building. The primary energy consumption in a building of A1 and G ratings are 25kWh/m^2/yr and 450kWh/m^2/yr, respectively. Thus, the primary energy consumption of an A1 is approximately 5% of that of a G rated building. One in eight homes in Ireland is rated at F/G with only 0.1% of A-rated buildings.

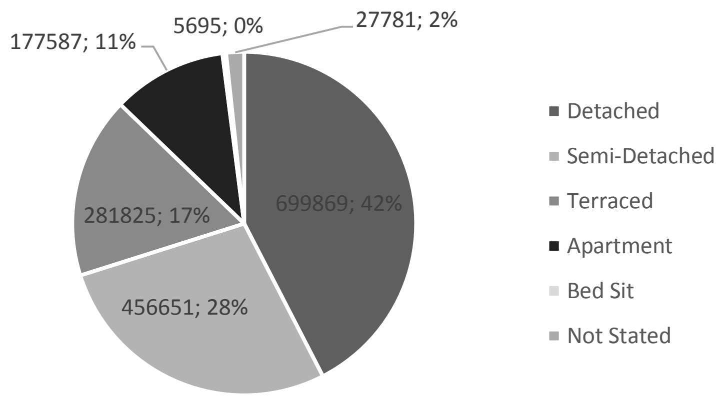

Figure 2: Residential housing stock by dwelling type

Thus, given the above and the fact that thermal performance standards were not introduced until the Building Regulations of 1979 [13], it can be seen why the Irish housing stock is among the poorest in Europe in terms of energy efficiency [10]. Therefore, the residential sector is a key area where Ireland can significantly reduce its energy consumption and carbon emissions in order to meet the mandate set out by the EU [5], [6]. The Irish residential sector accounts for 27% of the country's energy use, emits 10.5 million tonnes of CO_2 annually and is expected to contribute 35% of the energy savings required by the EU [11].

Compared to year 2006, when the Irish construction sector reached its peak levels, the number of people working in this sector had fallen by just over 56,000 in 2011 [14]. Given Ireland's recent austerity budgets, unemployment rates and emigration figures, a recovery is yet to have materialised. In order for the Irish construction sector to have a successful recovery, innovation is required. Areas of innovation in construction include prefabrication and modularisation, Building Information Modelling (BIM), materials innovation and smart infrastructure. Those are essential for the sustainable development of the Irish construction sector and should play a key role in the retrofitting of the Irish housing stock.

However, given the age, diversity, size of the Irish and EU building stock, and the economic variables associated, retrofitting to meet sustainability targets on time represents a big challenge. This paper highlights the findings on the most effective energy measures for building retrofitting, the limitations in research on the retrofitting of buildings and discusses how the currently on-going research project nZEB-RETROFIT [15] in the National University of Ireland, Galway can address these issues through a multi layered approach.

2 Overview of current research

Given the high variability of the characteristics of the Irish and EU building stock, there are many possible strategies to retrofitting a building to a higher energy standard. Thus, in order to achieve a NZEB, the most effective energy saving measures are needed. There are several published studies on the retrofitting of buildings. These studies focused on the evaluation of retrofit measures for buildings in terms of their energy savings, economic cost, lifecycle energy, carbon and cost as well as their influence on the occupant's thermal comfort.

2.1 Operational energy, carbon and cost analysis

The reviewed literature for the evaluation of energy, carbon and economic savings through the retrofitting of buildings have a common methodology. This involved the identification of common buildings and characteristics that best represent the housing stock of their respective countries using single [16], [17], [18], [19], [20] and multiple [21], [22], [23] case studies. Software tools were used to evaluate the effect that proposed multiple retrofit actions had on the energy consumption of buildings. These retrofit actions were then ranked in terms of either their energy, carbon or cost savings.

Wang & Holmberg [21] found the use of heat recovery ventilation, external and attic insulation to commonly yield the greater energy savings for residential buildings. Whereas, the upgrading to sensor controlled high efficiency lighting and improving the air tightness were the most common cost effective measures. The difference of energy savings in light (measures with high energy saving impacts) and advanced (measures with high and low energy saving impacts) retrofitting of the buildings was found to be between 36-54%. However, advanced retrofitting did not always yield long term economic profits for some archetypes. Furthermore, the findings of a comprehensive investigation into the retrofitting of eleven multi-family found that the highest energy savings were achieved with the upgrading of the building envelope and ventilation systems. The use of plant (PV, solar thermal panel) and adjusting the temperature set points were considered to be the substantially profitable retrofit measures [22].

Capeluto & Ochoa [16] identified the improvement of either the glazing or ventilation to be the optimal single retrofit option for an apartment in northern and central European climate zones. A combination of either shading and glazing or ventilation and glazing were the most effective combination of retrofit actions in terms of energy savings. A study into the retrofitting of a Danish apartment built in 1896 using varying combinations of insulation, window and HVAC retrofit options showed that a NZEB cannot be achieved without the use of renewables in the retrofit [17]. Eight of the simulated retrofit measures were installed in the apartment. Despite this, only the theoretical operational energy post retrofit was provided.

Morelli et al. [24] followed up on this with a method for determining an economic optimal combination of energy saving measures based on a cost of conserved energy (CCE) method. However, the methodology considered each of the retrofit options as individual components and did not account for the influence each of the components had on the other in terms of energy savings. The use of insulation was the most cost effective measure on an apartment building but it was found that predicting the price of future energy costs had a significant effect on the results. A study involving five residential buildings in Belgium [23] indicated that it was better to invest in the thermal envelope of the building first, then the heating system and then renewable technology.

A study of a residential building in a central region of Portugal found that there existed a threshold up to which energy savings might be obtained with a small retrofit and any further improvement required a substantial investment cost [18]. Building upon the research, the authors found that achieving higher energy savings or lower costs with a combination of retrofitting options did not necessarily lead to better thermal comfort for the residents [19]. Tronchin et al. concluded it was more expensive to invest in insulation than in heating plant, as retrofit measures [20].

2.2 Lifecycle energy, carbon and cost analysis

The previously discussed studies focused on the operational energy and cost savings that retrofitting measures would achieve. They did not evaluate the energy investment required to upgrade the buildings to a lower energy standard and if the operational savings were offset to a different stage of a buildings lifecycle. Lifecycle studies on building retrofits have been conducted previously, e.g. [25], [26], [27], [28]. These studies generally used one of two methods. The first involved defining the life cycle boundary limits from when the building was originally constructed and the calculation of the embodied energy (EE), embodied carbon (EC), operational energy (OE) and operational carbon (OC). The OE was simulated using building energy simulation software, e.g. EnergyPlus. The investment of EE in retrofit measures to reduce the OE/OC was used to determine a new life cycle energy and carbon for the building and to see if the reduction in OE/OC was not offset in EE/EC to a different stage of the lifecycle [25], [27]. The second method used in the lifecycle studies was similar to the first one with the only difference in relation to the life cycle boundary limits. The life cycle of the building was taken to start before the retrofit measures were applied to the building, meaning the EE related to the original construction of the building was not quantified [26], [28].

A cradle-to-grave life cycle analysis by Beccali.et al [25] of a house retrofit in Italy showed that an increase in embodied energy investment led to a reduction in the OE of the building. The retrofit of a residential building in Canada showed that the environmental upfront cost of retrofit was paid back within two years of the retrofit

[27]. Despite the retrofit measures being installed, there were no residents inhabiting the house; thus, the measurements of the energy consumption were only simulated and not physically measured.

Various retrofit options were applied to seven different public building typologies in seven different locations across Europe in one particular study [26]. Each building had a different combination of retrofit actions applied to it, which made the comparisons difficult. However, based on the energy savings and avoided Global Warming Potential (GWP), the most significant effects were related to the improvement of the thermal envelope. The OE before and after retrofit was monitored. However, the study did not discuss whether simulations of each of the buildings were carried out to determine the theoretical energy savings of the retrofitting measures.

Lower life cycle energy and GWP could be achieved through new builds according to a study of Canadian residential houses [28]. However, only basement, attic insulation and air leakages (or a combination of these) were the considered retrofit options with the basement insulation providing the greatest energy savings. On the other hand, retrofitting the existing building in this study was the best option instead of constructing a new building in terms of having the lowest EE and lifecycle economic costs.

3 Methodology

The common conclusion emerging from the literature review to date for retrofitting buildings in terms of energy efficiency was that it is best to first improve the thermal envelope, then the heating system and then invest in renewables. However, some studies ranked these energy savings measures in different orders. There are many factors to consider for the reasoning behind this. One is that no two buildings are the exact same. Factors such as the buildings age, location, orientation, human behaviour, type of retrofit measure can have a bearing on the results of the energy efficiency assessment.

Thus, the work presented in this paper uses a systematic method which takes into account climatic conditions of the region where the case studies were located in order to make appropriate comparisons to see if the findings are applicable to the housing stock in Ireland (Table 1). In this method, the type of climate zone is based on the amount of hot degree days and cold degree days [29]. Taking 18°C as the base temperature for all climate types, the limits of each zone are shown in Table 1. Heating degree days (HDD) and cooling degree days (CDD) are a measure of how much (°Celsius) and for how long (days) outside air temperature was lower and higher than the base temperature. Using information gathered from an online degree day database [30], climate zones were assigned to each of the case study locations.

Out of 13 studies reviewed (Table 2), it can be seen that Zone D and E were the most common climate zones studied in the reviewed literature. As the Irish climate falls within Zone E, it is expected that a similar trend would follow for retrofitting Irish housing stock, where it is best to focus on the improvement of the thermal envelope first, then on the heating system and finally invest in renewable technologies in order to achieve a NZEB. This would particularly apply to the older Irish housing stock built before 1979 given its poor insulated properties, large floor areas and solid/oil fuel based heating systems.

However, out of 13 studies reviewed (Table 2), only four of the studies had calibrated their computational models against billed or measured data. Moreover, it was found that none of the reviewed case studies had monitored the impact installed retrofit measures had on the energy consumptions of the buildings and if they agreed with predicted computational results. Even though this paper does not imply that such published literature does not exist, it infers that there is a lack of research that involves validating predicted energy savings through installation of proposed retrofit actions and monitoring their influence on buildings' energy consumption. Studies have shown significant differences between simulated and actual building energy usage [31], [32]. This weakens the confidence and increases uncertainty in the accuracy of the theoretical energy savings presented by some published studies.

Table 1: Climate zone criteria [29]

Zone	Description	Requirements
A	CDD ≥ 500 and HDD < 1500	High cooling needs, low heating needs
B	CDD ≥ 500 and 1500 ≤ HDD < 3000	High cooling needs, medium heating needs
C	CDD < 500 and HDD < 1500	Low cooling needs, low heating needs
D	CDD < 500 and 1500 ≤ HDD < 3000	Low cooling needs, medium heating needs
E	CDD < 500 and HDD ≥ 1500	Low cooling needs, high heating needs

Table 2: Overview of building retrofit case studies (with more than one retrofit measure adopted)

Ref.	Objective Functions	Retrofit Measure	Software/	Calibrated	Building type	Location/Climate Zone
[21]	Lifecycle cost, cost effectiveness, energy demand	Insulation, window, ventilation, thermal bridging, electricity source	IDA ICE, EnergyPlus	✓	4 residential buildings	Stockholm: E
[16]	Energy efficiency and thermal comfort	Climate, colour, glazing, insulation, shading, ventilation, single vs combination	EnergyPlus	X	Apartment building	Stockholm: E, Helsinki: E, Kaunas: E, Warsaw: E, Berlin: E, Vienna: E, Prague: E, London: E, Paris: D, Porto: C, Madrid: B, Rome: B, Athens: A
[22]	Lifecycle cost, primary energy use, CO2 emissions	Attic, external, floor and basement insulation, windows, doors, heat exchange and recovery ventilation system, water heat recovery, adjust indoor temperature, solar water panel, PV, energy efficient lighting and presence control	BV2 2010, IDA ICE	✓	11 multi-residential buildings.	11 towns located in the Gavel Bourg region, Sweden: E
[17]	Energy savings	Insulation, windows, HVAC system, roof	BE10-one zone model	✓	Apartment building	Copenhagen, Denmark: E
[33]	Heating Load	Insulation thickness, core and perimeter temperatures,	EnergyPlus	X	Residential building	Toronto, Canada: D
[20]	Cost optimal retrofit option	Wall, floor, roof insulations, windows, heating technology and energy carrier	UNI/TS 11300	X	Residential building	Ravenna, Italy: B
[19]	Retrofit cost, energy savings, thermal comfort	External wall insulation, roof insulation, window types, solar collector installation	Trnsys, GENOpt, MATLAB	X	Residential building	Central Portugal: B
[18]	Retrofit cost, energy savings	External wall insulation, roof insulation, window types, solar collector installation	RCCTE, MATLAB	X	Residential building	Central Portugal: B

[23]	Retrofit cost	Wall, roof , floor insulation thickness, glazing type, space heating system, solar and PV panels	EPR	X	5 residential buildings	Belgium: D
[25]	Lifecycle Energy, CED[a], GWP[b], ODP[c], AP[d], EP[e], POCP[f]	Insulation, Condensation boiler, PV	Trnsys	✓	Residential building	Palermo, Italy: A
[26]	Lifecycle energy, carbon and savings of building retrofit actions	Wall, roof and floor insulation, windows, lighting, boiler, heat pump, heat recovery, CHP, PV, solar thermal, wind turbines, ventilation	N/A		7 public buildings	Stuttgart: E, Hol: E, Plymouth: D, Vilnius: E, Brno: E, Provehallen: E, Borgen: E
[27]	Lifecycle energy, carbon and energy footprint	Insulation, windows, envelope panels, flooring, wall studs, communication and electrical wiring, duct work, heat pump, solar thermal	Hot 2000	X	Residential building	Kitchener, Canada: B
[28]	Lifecycle energy, environmental and economic	Attic insulation, basement insulation, air leakage	Athena-EE, Hot2000 – OE	X	Residential building	Toronto, Canada: D

a=Cumulative Energy Demand, b=Global Warming Potential, c=Ozone Depletion Potential, d=Acidification Potential, e=Eutrophication Potential, f=Photochemical Ozone Creation Potential

Stakeholders (government agencies, property management companies, local authorities, householders etc.) need to be able to accurately quantify the potential energy, carbon, cost savings, payback time and risk involved in retrofitting strategies of building stock in order to achieve NZEB requirements. This is especially true for the retrofitting of the Irish housing stock given its high proportion of one-off houses and the amount of different energy saving measures currently available on the market. However, the timeframe for the development of innovative technologies and business models to meet the EU's 2050 targets has narrowed to less than ten years [34]. The nZEB RETROFIT project aims to tackle these retrofitting issues through a multi-layered approach.

3.1 nZEB-RETROFIT

The work presented here is part of the nZEB-RETROFIT project: Achieving nearly zero-energy buildings – A lifecycle assessment approach to retrofitting existing buildings. nZEB-RETROFIT is an ongoing research project in the National University of Ireland, Galway, Ireland which aims at tackling the issues relating to the retrofitting of the building stock. The overall goal of the project is to examine the effectiveness of innovative building structural elements and systems, regarding their structural, environmental and energy performance in retrofitting of existing buildings.

The goals of the project will be achieved through laboratory scale research, on site full scale research based on real-time data, numerical modelling and desktop research using a multi layered approach (Figure 3).

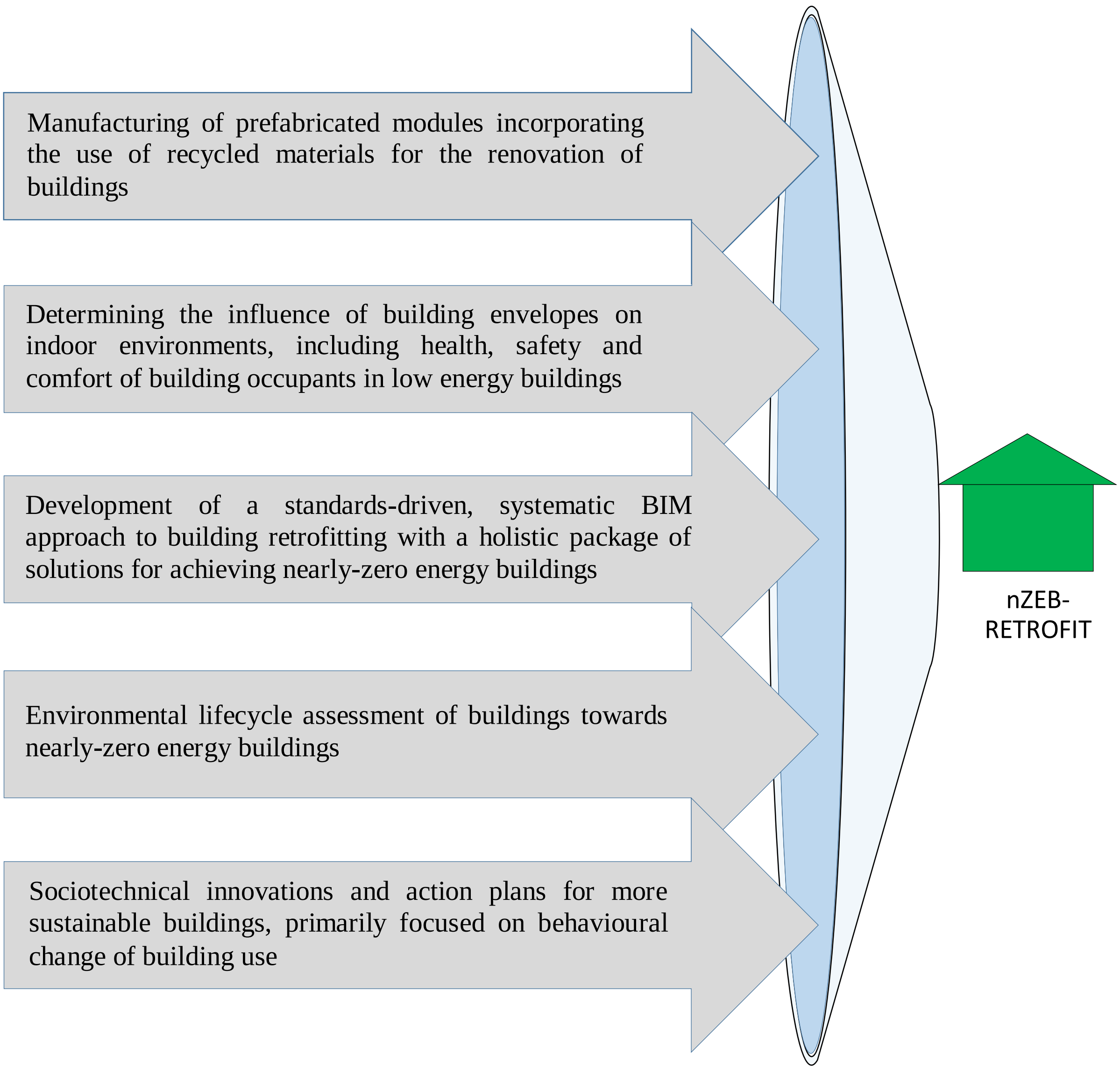

Figure 3: Multi-layered approach of the nZEB-RETROFIT project

4 Conclusion

Retrofitting is recognised as the most immediate, pressing and cost effective mechanism to reduce energy consumption and carbon emissions in the building sector for Europe to reach its short and long term goals. However, given the age, diversity, size of the Irish and EU building stock, and the economic variables associated, retrofitting to meet sustainability targets on time represents a big challenge.

Research into the most effective retrofit measures revealed that for climates where buildings require low cooling and high heating demands the best practice is to first improve the thermal envelope, then the heating system and then increase the use of renewable technologies in order to achieve a NZEB. However, only few studies calibrated their building energy simulation results with the physical data in order to reassure the quality of computational results. Moreover, it was found that none of the reviewed case studies had monitored the impact installed retrofit measures had on the energy consumptions of the buildings and if they agreed with predicted computational results. Thus, there is lack of knowledge and tools available for decision makers in the retrofit stakeholder value chain to make crucial decisions in regards to the renovation of buildings to low-energy standards.

With the ambitious targets set out by the EU for each of its Member States to reach, the rate of building retrofits is required to double or triple in order to reach these goals. It is therefore vital not to repeat the mistakes of the past. Proper planning is required to produce high quality solutions and construction practices within the industry to achieve the NZEB requirements set out by the EU. In order to do this, key decision makers in the stakeholder value chain require the knowledge, tools and confidence in order to develop high quality solutions to renovate buildings to the required NZEB standards.

The nZEB RETROFIT research project aims at tackling some of these challenges through its previously discussed multi-layered approach. The expected impacts of this research include strengthening the economy by introducing innovative products and tools for retrofitting buildings, creating high value jobs in the stagnant construction sector, and enhancing health and quality of life of the building occupants.

5 Acknowledgements

The authors thank Science Foundation Ireland (SFI) for the financial support of this research (Grant No. RSF1295). The authors would also like to thank the National University of Ireland Galway and particularly the Department of Civil Engineering in the College of Engineering and Informatics for the help with the project.

6 References

[1] U.S. EPA & U.S. CPC, "The Inside Story : A Guide to Indoor Air Quality," Office of Radiation and Indoor Air (6604J), United States Environmental Protection Agency and the United States Consumer Product Safety Commission, 1995.

[2] UNEB SBCI, "Buildings and Climate Change Summary for Decision Makers," United Nations Environment Programme Sustainable Buildings & Climte Initative, 2009.

[3] European Commission, "Directive 2002/91/EC of the European Parliament and of the Council of 16 December 2002 on the energy performance of buildings," *Off. J. Eur. Communities*, pp. 65–71, 2002.

[4] European Commission, “Directive 20/31/EC of the European Parliament and of the Council of 19 May 2010 on the energy performance of buildings (recast),” *Off. J. Eur. Communities*, pp. 13–35, 2010.

[5] Commission of European Communities, “Communication from the Commission to the Council, the European Parliament, the European Economic and Social Committee and the Committee of the Regions Limiting Global Climate Change to 2 degrees Celsius The way ahead for 2020 and beyond,” Brussels, 2007.

[6] European Commission, “Energy Roadmap 2050 Impact assessment and scenario analysis,” Brussels, 2011.

[7] Buildings Performance Institute Europe, “Europe’s Buildings Under the Microscope A Country-by Country Review of the Energy Performance of Buildings,” 2011.

[8] E2APT, “The Fundamental Importance of Buildings in Future EU Energy Saving Policies,” Energy Efficiency Action Plan Taskforce of the Construction Sector, 2010.

[9] European Commission, “Stock Taking Document Towards a new Energy Strategy for Europe 2011-2020,” 2010.

[10] CSO, “This is Ireland Highlights from Census 2011, Part 1,” Central Statistics Office, Dublin, 2012.

[11] Irish Government, “Better Buildings A National Renovation Strategy for Ireland,” Department of Communications, Energy and Natural Resources, 2014.

[12] SEAI, “A Guide to Building Energy Rating for Homeowners,” Sustainable Energy Authority of Ireland, 2014.

[13] SEI, “Retrofitted Passive Homes Guidelins for Upgrading Existing Dwellings in Ireland to the Passivhaus Standard,” Sustainable Energy Ireland, 2009.

[14] FORFÁS, “Ireland’s Construction Sector: Outlook and Strategic Plan to 2015,” Department of Enterprise, Trade and Employment, 2013.

[15] IRUSE, “nZEB-RETROFIT.” [Online]. Available: http://www.nuigalway.ie/iruse/nzeb_retrofit.html. [Accessed: 13-Feb-2015].

[16] I. G. Capeluto and C. E. Ochoa, “Simulation-based method to determine climatic energy strategies of an adaptable building retrofit façade system,” *Energy*, vol. 76, pp. 375–384, Nov. 2014.

[17] M. Morelli, L. Rønby, S. E. Mikkelsen, M. G. Minzari, T. Kildemoes, and H. M. Tommerup, “Energy retrofitting of a typical old Danish multi-family building to a ‘nearly-zero’ energy building based on experiences from a test apartment,” *Energy Build.*, vol. 54, no. 2012, pp. 395–406, Nov. 2012.

[18] E. Asadi, M. G. da Silva, C. H. Antunes, and L. Dias, “Multi-objective optimization for building retrofit strategies: A model and an application,” *Energy Build.*, vol. 44, pp. 81–87, Jan. 2012.

[19] E. Asadi, M. G. da Silva, C. H. Antunes, and L. Dias, “A multi-objective optimization model for building retrofit strategies using TRNSYS simulations, GenOpt and MATLAB,” *Build. Environ.*, vol. 56, pp. 370–378, Oct. 2012.

[20] L. Tronchin, K. Fabbri, and M. C. Tommasino, “On the cost-optimal levels of energy-performance requirements for buildings : A case study with economic evaluation in Italy,” *Int. J. Sustain. Energy Plan. Manag.*, vol. 03, pp. 49–62, 2014.

[21] Q. Wang and S. Holmberg, “A methodology to assess energy-demand savings and cost effectiveness of retrofitting in existing Swedish residential buildings,” *Sustain. Cities Soc.*, vol. 14, pp. 254–266, Feb. 2015.

[22] L. Liu, B. Moshfegh, J. Akander, and M. Cehlin, “Comprehensive investigation on energy retrofits in eleven multi-family buildings in Sweden,” *Energy Build.*, vol. 84, pp. 704–715, 2014.

[23] G. Verbeeck and H. Hens, "Energy savings in retrofitted dwellings: economically viable?," *Energy Build.*, vol. 37, no. 7, pp. 747–754, Jul. 2005.

[24] M. Morelli, M. Harrestrup, and S. Svendsen, "Method for a component-based economic optimisation in design of whole building renovation versus demolishing and rebuilding," *Energy Policy*, vol. 65, pp. 305–314, Feb. 2014.

[25] M. Beccali, M. Cellura, M. Fontana, S. Longo, and M. Mistretta, "Energy retrofit of a single-family house : Life cycle net energy saving and environmental bene fi ts," vol. 27, pp. 283–293, 2013.

[26] F. Ardente, M. Beccali, M. Cellura, and M. Mistretta, "Energy and environmental benefits in public buildings as a result of retrofit actions," *Renew. Sustain. Energy Rev.*, vol. 15, no. 1, pp. 460–470, Jan. 2011.

[27] G. Bin and P. Parker, "Measuring buildings for sustainability: Comparing the initial and retrofit ecological footprint of a century home – The REEP House," *Appl. Energy*, vol. 93, pp. 24–32, May 2012.

[28] B. Dong, C. Kennedy, and K. Pressnail, "Comparing life cycle implications of building retrofit and replacement options," *Can. J. Civ. Eng.*, vol. 32, no. 6, pp. 1051–1063, Dec. 2005.

[29] K. Tsikaloudaki, K. Laskos, and D. Bikas, "On the Establishment of Climatic Zones in Europe with Regard to the Energy Performance of Buildings," pp. 32–44, 2012.

[30] B. S. Limted, "Degree Days.net-Custom Degree Day Data," 2014. [Online]. Available: http://www.degreedays.net. [Accessed: 26-Nov-1BC].

[31] M. Persson, "Measured and predicted energy demand of a low energy building : important aspects when using Building Energy Simulation," vol. 3, pp. 223–235, 2007.

[32] J. H. Scofield, "Do LEED-certified buildings save energy ? Not really . . .," vol. 41, pp. 1386–1390, 2009.

[33] E. Dixon, R. Richman, and K. Pressnail, "Nested Thermal Envelope Design construction : Achieving significant reductions in heating energy use," *Energy Build.*, vol. 54, pp. 215–224, 2012.

[34] E2BA, "Energy Efficient Buildings European Initiative," Energy Efficient Buildings European Initiative, 2011.

Design concept for lightweight timber-glass module to be applied for energy-efficient refurbishment of existing buildings

Tina Špegelj, BSc
Rihter d.o.o, Slovenia, tina.spegelj@rihter.si

Vesna Žegarac Leskovar, Assist. Prof. Dipl.-Ing. Dr.techn.
Faculty of Civil Engineering, University of Maribor, Slovenia,
vesna.zegarac@um.si, http://www.fg.um.si/osebje/vesna.zegarac/Strani/default.aspx

Miroslav Premrov, Prof. Dipl.-Ing. Dr.eng.scie.
Faculty of Civil Engineering, University of Maribor, Slovenia,
miroslav.premrov@um.si, http://www.fg.um.si/osebje/miroslav.premrov/Strani/default.aspx

Summary

The current study presents the design concept for the timber-glass upgrade module with the optimal glazing size in the south-oriented façade for the purpose of energy-efficient refurbishment of the existing energy-inefficient buildings. The optimal design of the upgrade module resulting in minimal annual energy demand for heating and cooling is defined through a parametric numerical analysis including variations of the module's aspect ratio (*a/b*), thermal transmittance of its envelope (*U*) and glazing size in its south-oriented façade (*AGAW*). The developed functional dependence between the energy consumption and the module's design parameters permits a selection of the optimal module design with respect to baseline characteristics of the existing building and allows for a more systematic process of energy-efficient renovation.

Keywords: Energy-efficient upgrade, Module shape, Glazing size, Timber-glass structures

1 Introduction

The domain of energy policy in buildings is witnessing a worldwide trend whose aim is to reduce primary energy consumption and energy induced greenhouse gas emissions. In Europe, the existing stock exceeds the number of new construction 'Konstantinou et al. [1]'. While newly built buildings add annually 1% or less to the existing stock 'Poel et al. [2]', the rest of the buildings which account for 99% are already built and produce about 24% [3] of carbon emissions. In order to satisfy sustainability requirements, we need to start refurbishing the existing energy-inefficient buildings and reduce their heating demands 'Poel et al. [2]'. 'Kohler [4]' even suggests putting a stop to constructing new buildings in view of the above mentioned fact.

The activities related to energy efficient building renovation are in practice predominantly carried out through a set of fragmental renovation processes such as thermal improvement of the building components, installation of efficient technical systems, etc., which may be referred to as "basic renovation tools". As these are most frequently carried out with no support of a complex renovation project planned by experts in the domain, the energy saving potential fails to be fully exploited. The efficient and complex renovation requires searching for multiple renovation tools along with envisaging the possibilities of their adjustment to each individual case.

Energy-efficient renovation of the existing housing stock in the sense of finding optimal complex solutions and procedures has not yet been widely discussed in scientific writing. The results of a Serbian project on energy efficiency are given in the study by 'Bećirović et al. [5]' whose research involves 62 public buildings situated around the country. The listed buildings were subject to the following energy-efficiency oriented procedures:

window and door replacement, installing new thermal façade and roof insulation, in addition to the heating system renewal. Due to rather strict cost-efficient refurbishment plans the project resulted in a mere 47% reduction of the annual energy demand. 'Konstantinou et al. [1]' present various approaches to renovation of multi-family buildings and the subsequent impact on their energy efficiency. The authors point out the importance of a planned design process of renovation which takes into account the specifics of individual buildings. An interesting renovation tool seen in the case of a three-storey residential building involved a complete replacement of the existing pitched roof followed by installing, onto specific roof parts, an additional lightweight-construction residential unit. Similar renovating projects including light construction upgrade modules have already been carried out in practice, such as the revitalisation of the Zanklhof II residential estate in Graz-Austria [6], or that of Ford-Siedlung in Köln-Germany [7]. However, they are generally not based on systematic analyses which would allow for the choice of the optimal design of the added volume and the subsequent achievement of optimal energy savings.

Determination of the optimal design for the upgrade module plays an important role in the saving potential of the renovation process. The most vital findings to lean on are those by 'Žegarac Leskovar et al. [8]' who developed an analytical functional dependence between the optimal size of the triple glazing in the south-oriented façade (AGAW) and the thermal transmittance of the external timber wall element for the case study of single family timber house. A selection of their extensive analyses based on new timber houses will be applied to energy-efficient refurbishment cases.

Studies on the optimal proportion of glazing mainly focus on optimizing the glazing size in the new housing stock, with a purpose of achieving energy efficiency and examining potential refurbishment of the existing energy-inefficient buildings. A novelty approach of the present study goes to developing the optimal upgrade module with the optimal shape and glazing size in the south-oriented façade, a module ensuring simple installation onto the existing energy-inefficient buildings and resulting into a decrease in the energy demand per m2 of usable area within the refurbished building.

2 Timber-glass upgrade module

The current study treats the design parameters of lightweight timber-glass upgrade module to be applied as one within the set of available tools forming a complex process of renovation of the existing energy-inefficient buildings. A difference between previously carried out researches on the optimal glazing size in the south-oriented façade of new residential buildings '[8]' and the energy-efficient refurbishment lies in the change of energy flows as the "bottom plate" of the upgrade module becomes a building element between two heated rooms having the same indoor temperature (Figure 1).

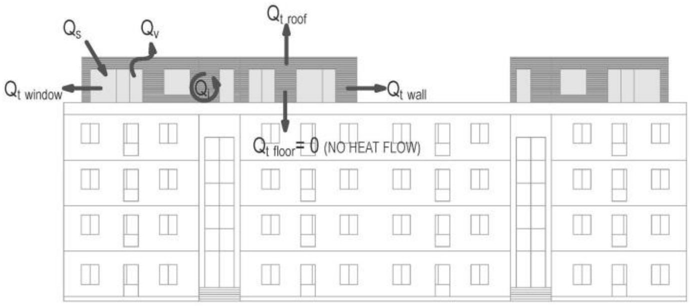

Figure 1: Energy flow in existing building with the upgrade module.

The previous study [8] analysed individual building whose bottom plate was in direct contact with the ground beneath. The change affects the annual energy demand for heating and cooling as well as the optimal glazing size in the south-oriented façade. The optimal upgrade module design is defined by the sum total of the annual energy demands for heating and cooling and depends on three variable parameters: the module shape, the proportion of glazing in the south-oriented façade, in addition to the thermal transmittance of the external walls and the roof.

3 Parametric numerical study on the optimal design of the upgrade module

The scope of the present research is limited solely to the upgrade module which is seen as one of the options within energy renovation of the existing energy-inefficient buildings. The research is based on a monthly energy efficiency calculation method set by EN ISO 13790 standard [9] and takes the heating (Qh) and cooling demands (Qc) into consideration. Energy performance of the upgrade module is computed by using the Passive House Planning Package (PHPP) [10].

3.1 The aim of the study and its basic limitations

The parametric numerical study analyses the timber-glass upgrade module to be applied as one within the set of available tools forming a complex process of renovation of the existing energy-inefficient buildings. The basic goal of the present research is to define the optimal shape of the upgrade module with the proportion of glazing AGAW1-2 = 35 %, 45 % in the south-oriented facade, which allows its installation on the existing buildings with various shapes of floor plans. The analysis of the existing energy-inefficient building along with the possibilities of its energy renovation is subject of further research. The present research is a follow-up stage of a previously carried out research work on the influence of glazing on the energy-efficiency of the energy-efficient timber single-family house of 'Žegarac Leskovar et al. [8]'. As discussed in Chapter 2, a difference between the present research and '[8]'lies in the fact that the bottom plate of the upgrade module becomes a building element between two heated rooms having the same indoor temperature, which means negligible, i.e. zero (in computation) transmission losses through the module's bottom plate.

3.2 Characteristics of the module

Climate data
The module is based in the Slovenian town of Velenje which belongs to the Cfb climate zone according to Köppen – Geiger climate map 'Kottek et al. [11]' and 'Peel et al. [12]'. The town, situated at an altitude of 390 m records the average annual temperature of 9.1 °C, in addition to the average daily summer temperature range of ± 10.5 K and the horizontal solar radiation being 1224 kWh/m2 'Meteonorm 7 [13]'.

Construction of the module
External walls of the module are made of macro-panel construction system wall elements. In addition to the benefits of good insulation achieved even at lower thickness, the system offers a further advantage – that of lower mass which enables its installation onto the existing buildings. The thermal transmittance of the external walls and the roof is U1 = 0.100 W/m2K.

Windows
The glazing used has a thermal transmittance coefficient of Ug = 0.51 W/m2K with the permeability coefficient of the total solar energy being g = 52 %. A PVC spacer between the glass panes has the value of Ψ = 0.033 W/mK.

Shading
Summer time shading is provided by using external shading devices, which is the most effective means of protection against solar radiation. The calculation is based on the shading factor of z = 50 %.

Internal sources
The influence of body heat and household appliances heat emission in the module are considered as the average constant value of 2.1 W/m2.

Active technical systems

Heating and ventilation are ensured by using a compact device within which the heat recovery ventilation unit attains the efficiency value of η = 80%.

Orientation
Side a of the module – where the glazing is installed –faces south, as shown in Figure 2.

3.3 Variable parameters

Module shape
The chosen module's floor plan is rectangular, with the length of the sides being a and b which are subject to variation (Figure 5). Variations of the module shape (the sides a to b aspect ratio) are a prerequisite for achieving the applicability of the module since different floor plans of the existing buildings demand a variety of upgrade module shapes. In our analysis, side a always faces south, side b is perpendicular to side a. Altering the shape of the module means changing the sides a to b aspect ratio. The lengths of the sides a and b vary parametrically within a range of ratios from 0.18 to 8.0. The net heated floor area A = 200 m2 and the heated volume of the module V = 500 m3 remain constant, which is a significant limitation of the analysis while the surface of the thermal envelope and subsequently the shape factor f0 = S/V change, as do the energy demands of the building.

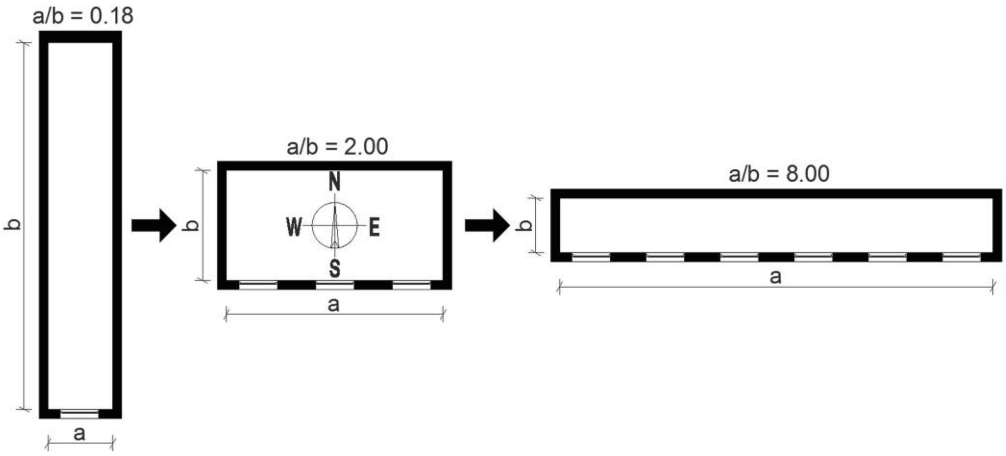

Figure 2: Shape of the upgrade module and its variations.

Glazing ratio
The glazing area in the south-oriented facade changes according to the length of the module's side a and in relation to the proportion of glazing in the south-oriented facade. A specific module's shape (the sides a to b aspect ratio) undergoes calculations at two different glazing proportions: AGAW1-2 = 35 %, 45 %.

3.4 Analysis and the results

Figure 3 shows the heating (Q_h) and cooling (Q_c) demands of the upgrade module depending on the module shape at the glazing size of *AGAW = 35%* and the thermal transmittance of the external walls (*TF-1*) $U_1 = 0.100$ W/m^2K. Functional dependence at other analysed glazing sizes *AGAW* and that of TF-2 wall modules with the thermal transmittance of $U_2=0.165 W/m^2K$ is similar to the above and therefore not presented as a separate result. Another datum seen in Figure 3 is the glazing size in the south façade (A_{glass}) depending on the upgrade module shape; the glazing size increases in a parabolic curve following the higher *a/b* ratio and consequently proportionally results in higher solar gains of the module.

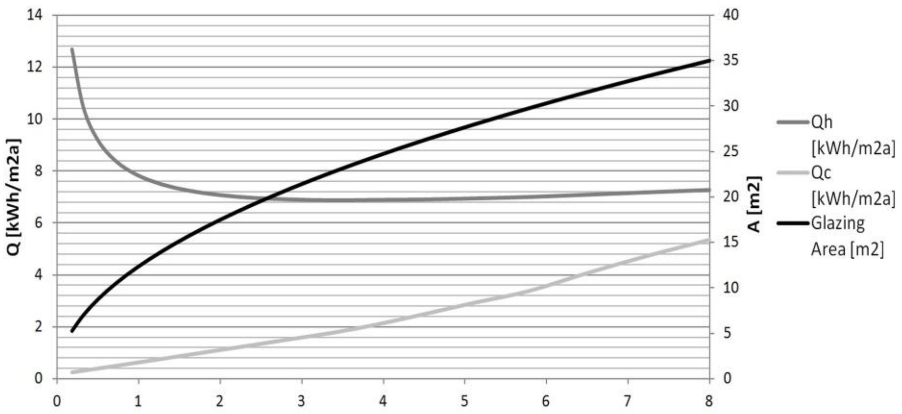

Figure 3: Annual energy demand (Qh + Q_c) and the glazing size A_{glass} at A = 200 m^2, AGAW = 35%, U_1 = 0.100 W/m^{2}K.

As seen in the figure above, the energy demand for heating demonstrates a steep decrease until reaching the value of the sides aspect ratio *a/b = 0.98*, from which point the curve slopes more gently. From the value of *a/b = 1.62* onwards, the Q_h proves to be nearly constant, i.e. independent of the module shape. The module's annual energy demand for cooling (Q_c) exhibits a constant linear increase, following the variations of the upgrade module shape. The annual energy demand for heating (Q_h) of the module in the chosen climate zone is considerably higher than the demand for cooling (Q_c).

The sum total of the heating and cooling energy demands ($Q_h + Q_c$) of the module with the thermal transmittance of the external walls (*TF-1*) and the roof $U_1 = 0.100\ W/m^2K$ is seen in Figure 4. The optimum functional value at the glazing sizes of AGAW = 35% and 45% is defined at the points where each of the ($Q_h + Q_c$) functions attains its minimum with the relevant *a/b* value on the x-axis being the optimal module shape.

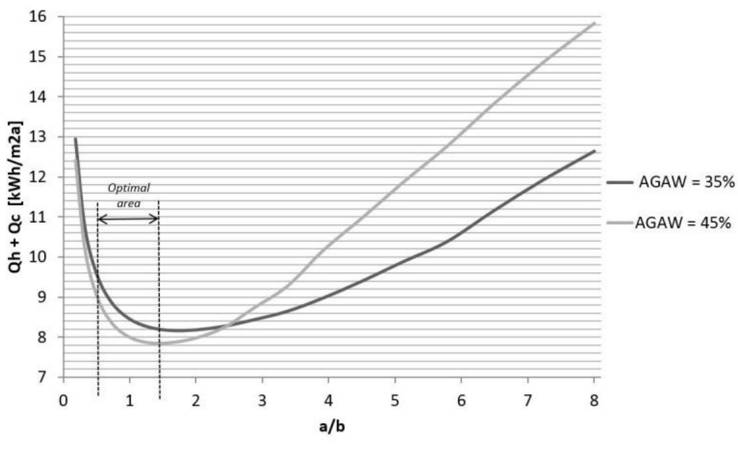

Figure 4: Annual energy demand ($Q_h + Q_c$) at A = 200 m^2, AGAW = 35% and 45% at U_1 = 0.100 W/m^{2}K with marked "optimal area" for AGAW 35% and "neutral area" for both treated AGAW values.

As demonstrated above, the annual energy demand for heating and cooling of the module changes along with variations of the shape (*a/b*) and specific glazing proportions (*AGAW*). The highest $Q_h + Q_c$ value at the two selected glazing sizes is reached with the shape of the module *a/b = 8.00*. It is interesting to observe that the annual energy demand for heating and cooling ($Q_h + Q_c$) at the glazing sizes of AGAW = 35% and 45% exhibits minimal change with certain module shapes, i.e. the shape of the module defined by the *a/b* ratio exerts minimal influence on the energy requirement ($Q_h + Q_c$) within the given range. The range within which the individual function curve does not exceed 5% deviation from the optimal (minimal) $Q_h + Q_c$ value is referred to as the »optimal area«, as seen in Figure 4, showing the above mentioned area for the glazing size of AGAW = 35%.

Almost any shape of the module at a given glazing size *AGAW* (from *AGAW 35% to 45%*) can be selected within the so-called »optimal area« range owing to a minimal change in the annual energy demand ($Q_h + Q_c$).

The existing energy-inefficient buildings have various shapes. Their floor pans will thus not always allow for installation of the so-called optimal upgrade module shape, defined and seen in Figure 4. An additional analysis will therefore be carried out in order to determine the optimal glazing size in the south-oriented façade of the upgrade module ($AGAW_{opt}$) according to the value of *a/b* with a purpose of its potential application in the case of an existing energy-inefficient building with an unfitting floor plan. The results of the numerical analysis

of the previously analysed thermal transmittance value of the U_1 and U_2 wall elements are shown in Figure 5.

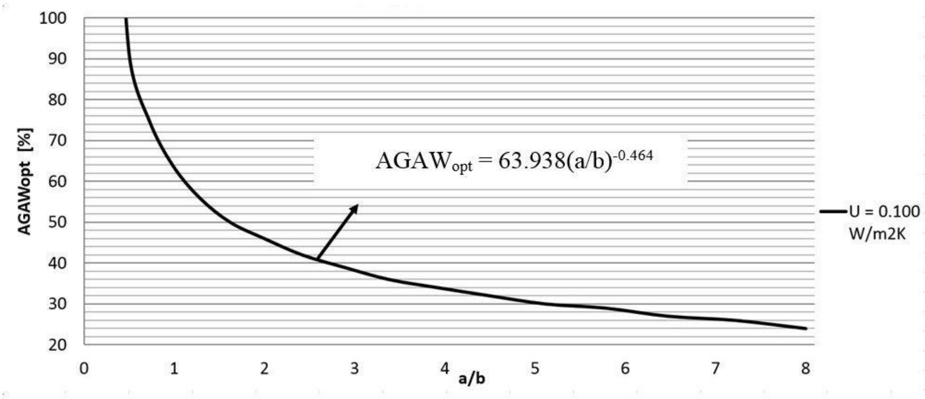

Figure 5: $AGAW_{opt}$ in relation to the module shape at U_1 = 0.100 W/m^{2}K.

The optimal glazing size in the south façade of the module whose envelope thermal transmittance values equals $U_1 = 0.100\ W/m^2K$ and whose shape ranges from *a/b = 0.18* to *a/b = 0.32* exceeds 100%, which means that the optimum is not attained. The reason is a small glazing size along with the consequently low solar gains and low energy demand for cooling. The prevailing energy demand is that for heating which decreases proportionally with a larger glazing size. Variations of the module shape in the range form *a/b = 0.50* to *a/b = 8.00* result in a gradual decrease of the $AGAW_{opt}$ value, which is a consequence of extending the length of the south wall with the subsequent enlargement of the glazing size in the south façade. As expected with reference to previous studies [8], the optimal glazing size in the south-oriented façade with the thermal transmittance of the wall and the roof $U_1 = 0.100\ W/m^2K$ case can be determined for any selected form a/b thus. Increasing the glazing size means higher solar gains and better passive heating of the module. The function of $AGAW_{opt}$, resulting from the presented numerical parametric analysis can be written in the analytical form as:

$$U_1 = 0.100\ \mathrm{W/m^2K}:\ AGAW_{opt} = 63.938\,(a/b)^{-0.464} \qquad (1)$$

4 Conclusion

A well-designed upgrade construction module consisting of a combination of classical prefabricated timber wall elements and prefabricated wall elements with insulating glazing is developed and analysed with the aim to be used for the purpose of renovation and the consequent reduction of the energy demands of the existing building. In order to achieve the latter, the module needs to have an appropriate design following the guidelines for the optimal floor plan and the glazing size. With the aim of defining the above mentioned optimum, we developed functional dependence between the annual energy demand for heating and cooling of the building and the module's floor plan for different glazing sizes in the south-oriented façade for the module with the overall envelope thermal transmittance factor $U_1 = 0.100\ W/m^2K$. The optimal area (Figure 4) defined related to aspect ratio for modules with AGAW=35% can be found between 0.98 ≤ a/b ≤ 2.88 and the optimal area for the modules with AGAW=45% varies between 0.72 ≤ a/b ≤ 2.42. The glazing size in the south façade thus proves to have a substantial impact on the energy efficiency of the module, which means that defining the optimal glazing size ($AGAW_{opt}$) depending on the module shape (Figure 5) is most sensible in the cases where the optimal values from Figure 4 cannot be adopted, owing to the shape or the orientation of the existing building.

The results of the present research study will serve civil engineers and architects in their selection of the suitable upgrade module for the given floor shape of the existing building and the given thermal transmittance of the module's envelope. Their planning will be assisted by data on the approximately optimal glazing size in the south-oriented façade along with an estimation of the annual energy demand for heating and cooling of the chosen module at different proportions of glazing in the south façade (*AGAW*). Architects and civil engineers will thus be in position to make a fairly reliable prediction of the energy performance of the building to be refurbished.

The present analysis treats the upgrade module as an individual structure, separately from the existing building which is subject to approximation based refurbishment preventing energy losses between both structures. Our further research work will therefore focus also on the energy analysis of the existing energy-inefficient buildings to undergo refurbishment by means of installing the upgrade module, in which case they both function as a single unit. Nevertheless, one needs to be aware of the unique features of every building, of its existing energy performance and other parameters that will strongly influence the results.

5 Acknowledgements

»Operation part is financed by the European Union, European Social Fund. Operation is implemented in the framework of the Operational Programme for Human Resources Development for the Period 2007 - 2013, Priority axis 1: Promoting entrepreneurship and adaptability, Main type of activity 1.1.: Experts and researchers for competitive enterprises.«

6 References

[1] Konstantinou, T., Knaack, U.: An approach to integrate energy efficiency upgrade into refurbishment design process, applied in two case-study buildings in Northern European climate, in: Energy and Buildings 59 (2013) pp. 301-309.
[2] Poel, B., van Cruchten, G., Balaras, C.A.: Energy performance assessment of existing dwellings, in: Energy and Buildings 39 (2007) issue 4, pp. 393–403.
[3] Eurostat: Environment and energy, in: Energy performance assessment of existing dwellings, Europe in figures: Eurostat yearbook 2010, Office for Official Publications of the European Communities, Luxembourg, 2010.
[4] Kohler, N.: The relevance of the green building challenge: an observer's perspective, in: Building Research and Information 27 (1999) pp. 309–320.
[5] Bećirović, P. S., Vasić, M.: Methodology and results of Serbian Energy-Efficiency Refurbishment Project, in: Energy and Buildings 62 (2013) p.p. 258–267.
[6] A & N Planungs. Verwaltungs GmbH & Co KG: Zanklhof II, Revitalisierung – Umbau – Ausbau, 2009.
[7] Rösener, M., Leuters B.: Gesamtsanierung und Aufstockung – Fordsiedlung LEG Köln, Forum Holz Bau Energie, Köln, 2008.
[8] Žegarac Leskovar, V., Premrov, M.: An approach in architectural design of energy-efficient timber buildings with a focus on the optimal glazing size in the south - oriented facade. in: Energy and Buildings 43 (2011) pp. 3410–3418.
[9] EN ISO 13790:2008, Energy performance of buildings - Calculation of energy use for space heating and cooling, 2008.
[10] Feist, V.: Passiv House Planning Package, Energy balance and Passive House design tool for quality approved Passive Houses and EnerPHit retrofits, Darmstadt, 2012.
[11] Kottek, M., Grieser, J., Back, C., Rudolf, B., Rubel, F.: World Map of the Köppen-Geiger climate classification updated, in: Meteorologische Zeitschrift, 3 (2006) pp. 259-263.
[12] Peel, M. C., Finlayson, B. L., McMahon, T. A.: Updated world map of the Köppen-Geiger climate classification, in: Hydrology and Earth System Sciences, 11 (2007) pp. 1633 – 1644.
[13] Meteonorm 7.0, Global Meteorological Database for Engineers, Planners and Education, http://www.meteonorm.com (retrieved January 2014).

geometry

Parametric Workflows for Complex Enclosure Structures

Jeffrey C. Vaglio, PE, AIA, LEED AP [BD+C]
Director, Enclos Advanced Technology Studio, USA
Ph.D. Candidate, University of Southern California, USA

Tyler J. Tucker, Designer
Enclos Advanced Technology Studio, USA

Summary

This research identifies common tasks that benefit from a parametric approach in the delivery of complex facade structures from the facade contractor's perspective based on recent project application experience. One case study is reviewed in-depth to exemplify the role of the parametric model throughout its life with the facade contracting team. Starting with pre-sale estimating tasks, a complex geometry is reduced to a core set of control information; most often a set of work point coordinates or control surfaces. This minimal foundation is the central link to all subsequent tasks and models: estimating, structural analysis models, drawing and data sheet development, fabrication drawings and installation studies. Knowing that design iterations are inevitable, the parametric workflow logic implemented by the facade contractor during a design-assist period requires adaptability and interoperability.

Keywords: Parametric, complex geometry, workflow logics, design-assist

1 Introduction

Architectural designs are articulating increasingly complex forms, challenging the a/e/c community to overcome classic paradigms of form, structure, collaboration and project delivery. The rampant integration of parametric tools and digital workflows is well documented [1, 2]. Often these views highlight the architectural development, environmental analysis, optimization studies, geometric rationalization exercises and supporting analysis during design development. Additionally, the turnaround associated with consultants' engineering analysis to drive architects' decision making continues to accelerate, thus shortening the feedback loop [3]. What is often missing in this dialogue is the role of parametric processes in the delivery of scope by the contractors who fabricate and install the elements that make-up the architecture. This paper seeks to describe how parametric workflows support the design and delivery of complex enclosures from the perspective of a facade contractor.

Projects with increased geometric complexity present the facade contractor with an opportunity for early involvement to understand the architectural concept, influence the enclosure design, bring key constructability drivers to the forefront and integrate parametric tools early in the design development. This support role is intended to aid the design towards a rationalized solution within project constraints: material, fabrication and shipping limitations; project budget and schedule; and system performance requirements. The parametric tools are used to provide expedited information and design responses during an iterative development process. This dynamic process requires a structured approach to interdisciplinary communication, three-dimensional model exchanges and a familiarity of the parametric tools used by the architect. This process is increasingly carried out in a 'design-assist' project delivery where an intermediate phase is established for the contractor to collaborate with the design team, working towards a buildable solution within target performance and budgetary metrics.

1.1 Philosophy

One key advantage about parametric modeling is that it anticipates change throughout design development. It can avoid the burden of drastic overhauls and minimize repeating time consuming documentation steps. A parametric approach aims to build a model up, logically, with a firm understanding of geometry and the relationships between it and the subsequently designed items that make up a building enclosure.

1.2 Design-Assist Delivery

The design-assist process has proven to be effective in mitigating the risk posed by unique and complex design requirements, and the use of emergent materials and specialized technology. The process involves the following steps:

1. development of a clear scope of work, budget, schedule, aesthetic and performance goals,
2. qualification and selection of a design-assist contractor,
3. collaborative research and development of project specifications and documents with the design-assist contractor performing most of the work with direction from the architect,
4. confirmation of scope, budget and schedule by the contractor for the developed design,
5. contracting of build services with the design-assist contractor.

2 Integrating Parametric Workflow

Establishing a simple central core of control information that serves as a basis to build upon is vital. This core is generally rooted in a set of control coordinates or a control surface established by the architect. Identifying this overarching control platform early – during pre-sale activities – is essential to successful post-sale maturation of the parametric model and information. Grasshopper – a visual algorithmic software linked to a 3D modeler – is an effective tool at linking this core.

2.3 Pre-Sale Estimating

Integrating Grasshopper with cost estimating and material take-off efforts makes efficient use of the data-centric side of parametric programs. While Grasshopper has powerful tools used for form creation, manipulation, and rationalization, it also stores information about each operation being conducted and can easily produce quantities, sizes and relevant geometric information. This information can be visually displayed on drawings or diagrams for clarification, or just as easily exported as raw data into spreadsheets. Specific routines can be created within Grasshopper to find very detailed pieces of information, including panel size and cut dimensions for pattern cut lites, number of atypical units, and number of unique panels. Furthermore, if continuous estimation is to be conducted with a developing design, the initial investment of building a parametric model can drastically reduce time and resources required for pricing updates at design checkpoints. As changes are made to the project, take-offs are automatically updated, reflecting price and quantity changes at the same speed as design.

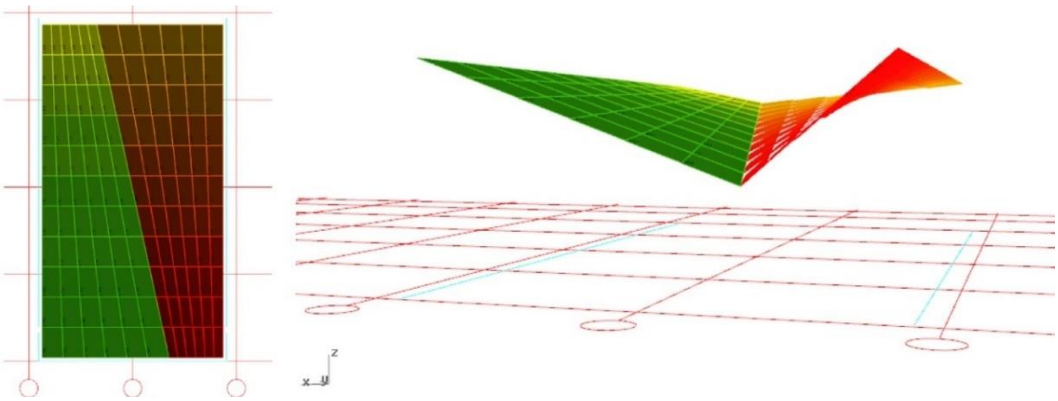

Figure 1: Warpage analysis of panels on a hyperbolic control surface.

2.4 Design Iterations

When the facade contractor is introduced during a design-assist initial phase, it is anticipated that the design development will go through a number of iterations. It is the contractor's opportunity to bring constructability constraints as well as material or vendor limitations to the table. Parametrics have proved useful in performing the following analysis throughout design and pricing iterations inherent to a design-assist phase:

- *Panelization*: optimizing surface subdivision through alternate approaches,
- *Warpage Analysis*: assessing the warped magnitude of panels in a hyperbolic surface,
- *Size Constraint*: reviewing panels to see if they adhere to min./max. size requirements,
- *Reducing Variability*: develop alternate subdivisions to increase repetition,
- *Automating Model Steps*: generating repeating details throughout a 3D model space.

The figure below is an example of a *panelization* study that uses a Grasshopper routine to extract information about the initial subdivision pattern of double-curved glass lites as well as provide an alternate approach aimed at *reducing variability*. As much as parametric tools are thought of as an intelligent design tool, they are also a critical data extraction device.

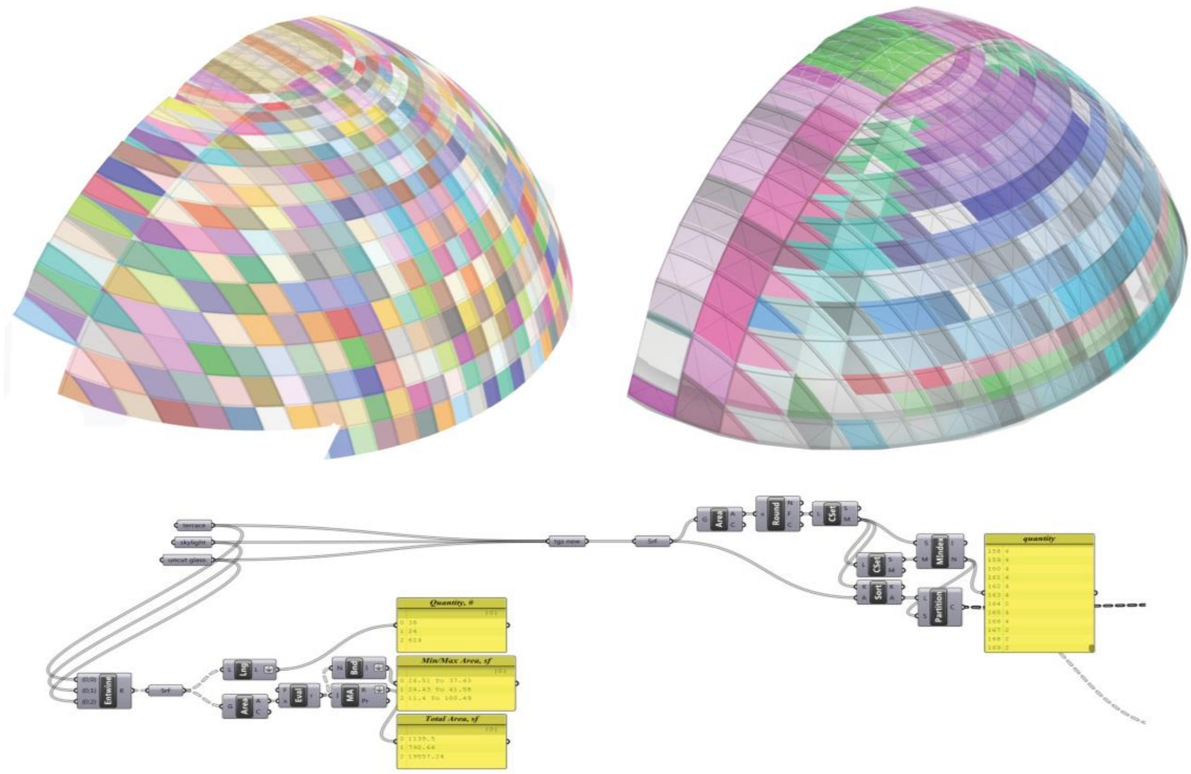

Figure 2: Subdivision study that shows spherical subdivisions that 1) refine an initial subdivision to get all glass lites to be within manufacturable dimensions (left), and 2) an alternate subdivision that decreases variability through subtle modification to the subdivision logic (right).

2.5 Engineering

Parametrics have proved useful in performing and supporting structural engineering tasks during design development, including:

- *Analytical Model*: assist the rapid generation of simplified, segmented, single-line and surface (where applicable) models for import into structural analysis software,
- *Iteration Comparisons*: rapid processing and overlays of multiple design iterations,

- *Visualizing Analytical Output*: visualizing structural model output data within parametric 3D model for heightened manipulation of data legibility and context.

2.6 Fabrication

Automating the generation of details that may use repeating parts or common logic, but occur at a variety of conditions (e.g., many angular instances on a complex surface that have intersecting nodes) accelerate documentation tasks that previously were labor intensive. Related to the facade, this could include anything from glass pattern cut sheets, minimum block sizes for glass fabrication, variant anchorage conditions, structural nodes in a gridshell and more.

2.7 Construction

The parametric model serves as a tool to educate field installation crews prior to arrival on site as well support on-site activities. These include:

- *Virtual Construction*: model geometry from very detailed parametric models can be used as the basis for 3D animation sequences that outline the installation approach for a job; a crucial hurdle on every project, but even more so when dealing with a complex geometry, unusual structure, tight field constraints or unconventional installation methods,
- *Mapping Survey Data*: receiving extensive coordinate data on a non-rectilinear structure from on-site laser surveys (e.g., as-built anchor locations) can be an even more daunting task that can be eased by a parametric workflow's ability to integrate survey coordinates for comparison against theoretical design locations so field adjustments may be made.

3 Case Study

3.1 Overview

The San Francisco Museum of Modern Art's expansion's feature wall consisted of a composite assembly of an opaque fiberglass reinforced plastic (FRP) rain-screen panel in front of an insulated unitized backup system. The project was being designed under a design-assist contract with the architect, meaning the design would undergo many changes and would need periodic updates to cost estimates and material take-offs to validate targets were being met. The architect provided standard architectural drawings and a development BIM model to start with. The information given was based off the beginning of design development and would knowingly change multiple times throughout the design lifespan of the project. The design team worked collaboratively to narrow in on a design solution that achieved architectural desire within budgetary constraints and material limitations.

The make-up of the enclosure was a juxtaposition of two key layers: 1) an outer rippled surface made of contoured fiberglass reinforced polymer (FRP), and 2) an insulated opaque performance barrier with interlocking curtainwall technology and 115 mm of insulation. The outer ripple surface required each panel to be a unique geometry, thus requiring intensive CNC milling technology of unique molds for each of the 700+ panels out of polystyrene blocks. The inner performance curtainwall maximized off-site, shop-controlled assembly to maximize quality control of key features. Following fabrication of the FRP panels, they were transported to the curtainwall assembly shop where the two systems were mated prior to delivery to site. Both shops were within 80 km of the project site.

3.2 Base Surface Development

The initial starting point was to define the interior surface of the outer skin. The location of this surface was driven inwards out due to programmatic requirements and defined slab edges. Factoring an offset between back-of-system and the slab edge, a set of interior control surfaces were established. The control surfaces utilized several large triangulated regions (highlighted in Figure 3) to create planar regions – in lieu of warped surfaces – between floors with significant inward/outward steps between respective slab edges. With control surfaces in place, the next step was to introduce joints. Maintaining a constant relationship between top of slab and stack joints was desired, so the horizontal datums were established first. The maximum floor-to-floor unit height is 7.9 m tall. With the surface and horizontal joints established, the next step was to integrate the control surfaces into Grasshopper and introduce vertical joints and iterate the unit warpage.

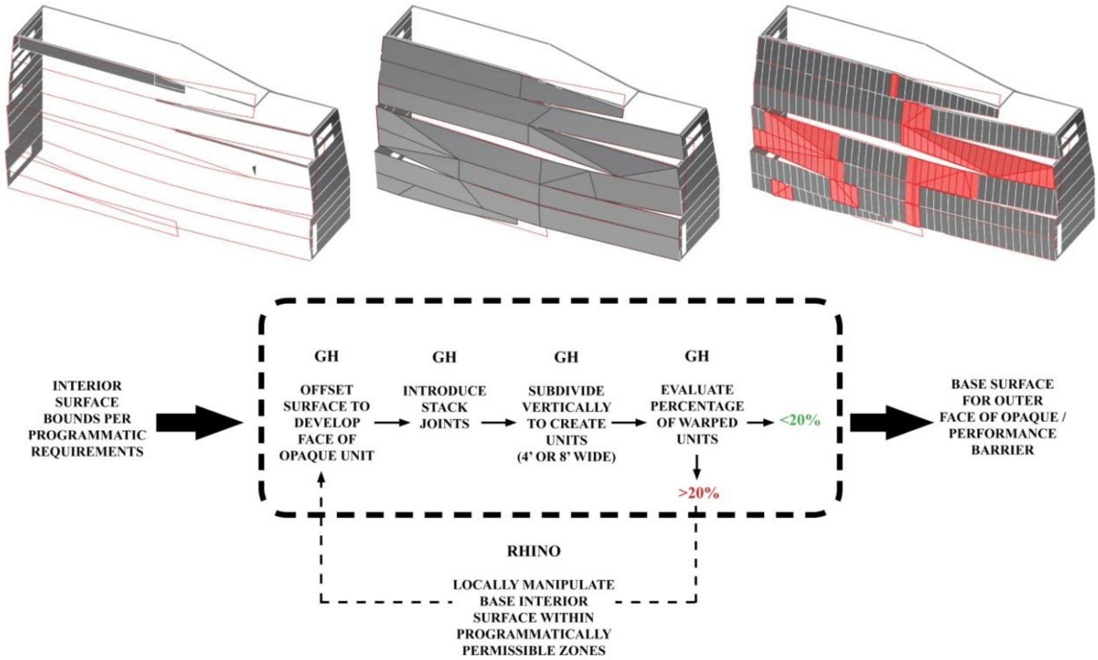

Figure 3: Development of back of system control surface.

3.3 Opaque Unit Check

The initial rationalization of the opaque surfaces planned to cold-warp units into position. Various panel widths (between 1.2 m and 2.4 m wide) were analyzed in Grasshopper (Figure 4) to determine the spectrum of warpage that would result from the respective subdivisions. A goal of <20% warped units was the project target during design-assist.

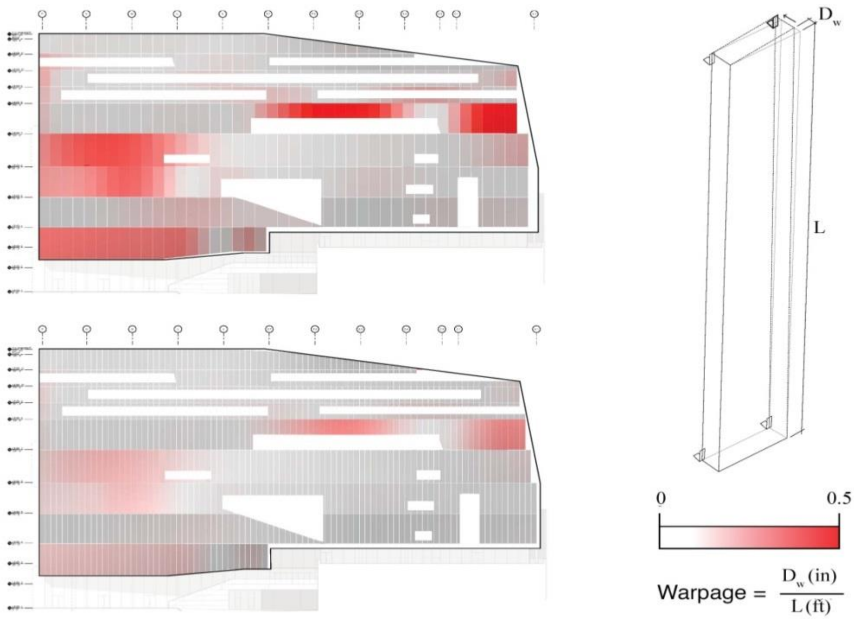

Figure 4: Warpage analysis of backup unit at 2.4 m (top) and 1.2 m (bottom) wide modules.

As would be expected, the wider unit module resulted in a greater absolute warpage as well as a greater relative warpage with respect to the unit's height. The initial panel subdivision considered (2.4 m wide) resulted in an excessive number of warped units. An objective of the design-assist process was to reduce the extent of warped units. The alternate considered at that time was a 1.2 m wide unit module that essentially doubled the total number of units while drastically reducing the quantity of excessively warped units. However, the quantity of warped – or non-planar – units still exceeded the targeted threshold of less than 20%.

In the end, after many subdivision iterations, what was learned was that the target threshold was met by a combination of planar units in mild runs with exaggerated transition zones. These are represented in Figure 5 as grey for the *opaque base geometry* (or planar units) and gold for the *transition units*. The initial iteration of this approach maintained a 2.4 m wide module and required 25% of the units to be *transitions* that have a faceted assembly folded across the diagonal. The second iteration of this approach implemented a 1.2 m wide module and required only 6% of the units to be *transitions.* This approach however had disadvantages of a greater extent of FRP material used in the returns, more aluminum in the opaque system's mullions, more anchorage locations to be coordinated with primary structure and greater labor associated with the installation means and methods. The final solution struck a balance between material/install optimization and limiting the extent of *transition units*. The final panel widths ranged from approximately 1.5 m to 1.7 m resulting in over 700 unique units, of which, approximately 9% are *transitions*. The extensive use of a common base surface as the driver in a series of parametric iterations was key in evaluating the ramifications of unit subdivision schemes.

3.4 FRP Ripple Surface Generation

As the system was developed, means and methods drove the system to a more unitized system that did not require extensive cold-warping. To trace the initial ripple surface with planar units, the FRP panels were utilized to make up the double-curved surface within the first 500 mm off the face of the planar units. Where the curvature exceeded the bounds of the FRP, faceted transition units (seen in gold in Figure 5) were utilized to re-align the next set of planar surfaces with the architect's control surface. Grasshopper was utilized to link the base control surface geometry to a series of routines that 1) subdivided the planar surface regions with equally spaced modules to create zones with common-length mullion pieces, 2) automated the generation of each unit's control geometry, 3) offset the control surface to create constraint volumes where the outside face of the FRP ripple surface was to occupy, and 4) minimize the number of faceted transition units. The planar units were permitted to have FRP occurring within a 500 mm offset volume while the faceted panel of a *transition unit* encroached within this depth and thus reduced the permissible FRP offset volume to 300 mm in these zones. These limits were implemented to minimize atypical details, FRP material required for returns at joints and supplemental support structure.

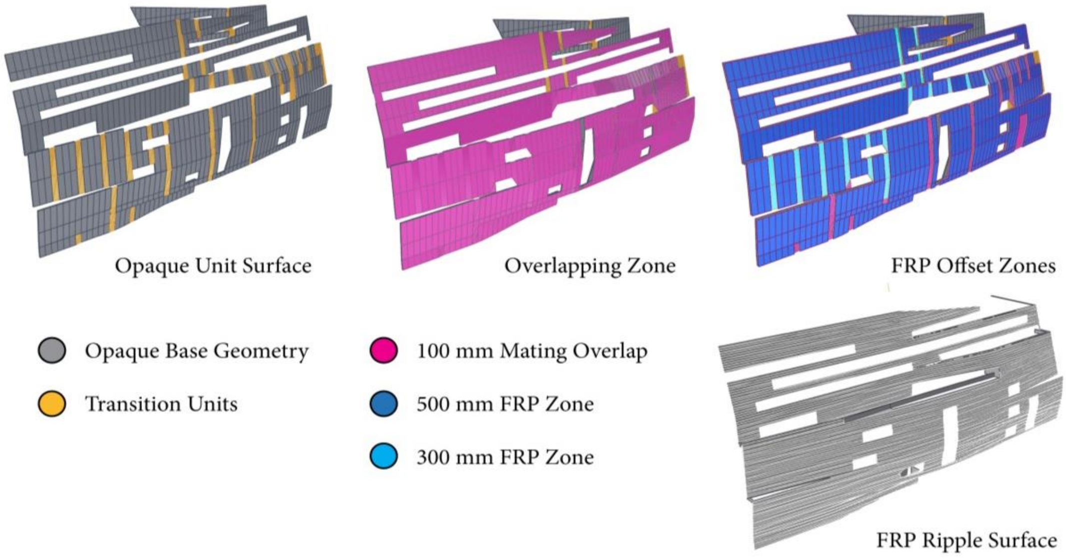

Figure 5: Development of opaque outer surface, overlapping zone, FRP offset zones and final ripple surface.

These zones of opportunity were generated for the architect to create the contoured FRP ripple surface within. Using Grasshopper to develop a logic routine aided the facade contractor in rapidly reviewing the architectural FRP ripple surface during rounds of design development and quality control. The iterative process was a refinement of the initial *opaque unit surface* informing the subsequent *FRP ripple surface* until a balance was struck where all constraints were met by both the *opaque* and *ripple surfaces*. The final byproduct of the design-assist phase is a master geometry control Rhino model that is acceptable to the architect and thoroughly vetted by the facade and FRP contractors.

3.5 Production Engineering

At the conclusion of the design-assist phase, control of the enclosure modelling is wholly transitioned to the facade contractor with the design development Rhino model serving as the basis for a production model maintained in Revit to assist in coordination and clash detection with other trades. The Revit model developed by the enclosure team served as the hosts for the geometry coordinate wireframe that was fed into Inventor for the development of individual unit assemblies and part drawings for fabrication. The level of detail in the Inventor unit models has all information regarding parts and preparations for fabrication and assembly, but far exceeds that required for coordination with the broader project team and other trades.

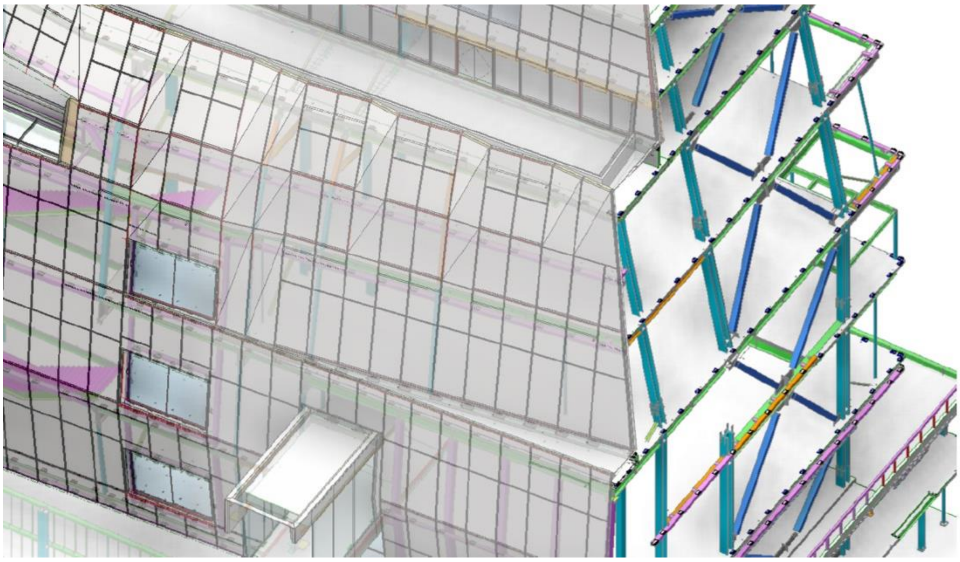

Figure 6: Overlay of curtainwall system coordinated with anchor locations on primary structural concrete and steel (Revit model with integrated IFC from steel fabricator).

3.6 Construction

The FRP and insulated curtainwall unit assemblies arrived on-site as single entities that were 1.5 to 1.7 m wide and up to 7.9 m tall. The articulated ripple contours travel across the vertical and horizontal joints of the unit subdivisions (Figure 7), so it was essential that field installation occurred at the highest level of precision. Tight tolerances across large unit dimensions were demanding, but the result is a facade that embodies a timely sense of digital technology and craftsmanship.

Figure 7: Photos from the enclosure installation at the project site: detail of contours and joints (left), unit size during rigging (middle) and continuity of ripples across units at lowest level (right).

4 Conclusions

The processes aided by parametric concepts for the San Francisco Museum of Modern Art's enclosure included but were not limited to: warpage analysis of the control surface iterations, panelization of the base surface into units, estimating material takeoff for different panelization schemes, automation of offset volumes for the FRP ripple surface to occupy and quality control when reviewing the contoured surface for size constraint and offset compliance. Utilizing Grasshopper to establish routines for each of these steps eased the demand and expedited the effort to process and review over 700 unique panel geometries.

Dealing with a complex form and the goals of automating processes, such as part drawing generation, can be challenging. Developing parametric tools tends to rely on intense up-front efforts to test and trouble-shoot definitions and routines, but are extremely adaptable to unforeseen changes or applications. Moving forward on future design-assist delivery projects, parametric-infused estimation and material take-off can inform the design process more readily.

Within this case study, a design solution for panelization, warpage, and many other constraints were reached not by the initial subdivision and sizing ideas (2.4 m subdivision) or the next alternative (1.2 m), but rather discovered through an understanding of the early results and attempting more iterations – taking the best pieces of many ideas to combine into one optimal solution. At the root of this process – design iterations fueled by parametric software – is the ability to rapidly increase the size of the solution space, finding the very best design solutions; some that may not have been initially thought of at all.

Overall, parametric software enables cost estimation, material take-off, design development studies, engineering tasks and review of survey data to be completed quicker and more accurately. On some complex projects, the geometry would otherwise be difficult to extract information from. The rapid accessibility to data and efficiency of digital models ensures that time can be spent refining designs rather than manually documenting.

5 Acknowledgements

The San Francisco Museum of Modern Art Expansion project team included but was not limited to: Snøhetta (architect), EHDD (architect), Webcor (general contractor), Arup (consultant), MKA (structural engineer), Enclos (facade contractor) and Kreysler Associates (fiber-reinforced polymer panel fabricator).

6 References

[1] Marble, S. (ed.): *Digital Workflows in Architecture: Designing Design -- Designing Assembly -- Designing Industry*, Birkhäuser, Basel, 2012.

[2] Gerber, D.J.: *The Parametric Affect: Computation, Innovation and Models for Design Exploration in Contemporary Architectural Practice*, Harvard Design School, Cambridge, MA, 2009.

[3] Holzer, D., Downing, S.: *Optioneering: A New Basis for Engagement Between Architects and Their Collaborators* in: Architectural Design, volume 80 (2010) issue 4, pp. 60-63.

Proceedings of the International Conference on Building Envelope Design and Technology, Graz
Advanced Building Skins 2015

Performance-based material selection and design for freeform building envelopes

Isabelle-Denise Paparo and Mauro Overend
University of Cambridge, UK, idjp2@cam.ac.uk, mo318@cam.ac.uk

Fabio Micoli
Newtecnic, UK, fmicoli@newtecnic.com

Summary

A leading architectural trend for building envelopes incorporates complex geometries and freeform facades. This paper addresses the concept system design for the glazed facade system for the Abdullah Financial District (KAFD) Metro Station in Riyadh, currently at scheme design stage, which makes full use of freeform facades. Through a state of the art review and by developing design concepts for the KAFD façade system, the fundamental design principles of current technologies used to construct complex envelopes are evaluated. The paper shows that existing technologies present key limitations in achieving the complexity required for the project. The paper outlines the benefits of using emerging technologies, such as fibre reinforced composite materials, largely adopted in the aerospace and marine industries and presents a better performing design solution based on these principles. The performance of this novel approach is assessed at conceptual design level.

Keywords: freeform, FRP-Panel, complex geometry

3 Introduction

A distinctive strand of modern architecture is the use of geometrical complexity in building envelopes. This approach calls into question the validity of conventional design solutions for building envelopes, which typically address each individual performance requirement in turn. This design approach typically leads to a succession of layers in the build-up of the envelope, where each layer addresses a particular performance requirement. The resulting building envelope systems often meet the required environmental and structural performance, but in a complex and costly manner. Digital and parametric analysis tools, recently introduced into the design process, enable the analysis of thermal and structural systems of higher complexity than was previously possible in the timescale of projects. The ability to accurately design more complex systems unlocks new design solutions, especially in the use of less conventional and higher performing materials.
These challenges and opportunities in free-form building envelopes are explored and discussed in context of a live project: the King Abdullah Financial District (KAFD) Metro Station in Riyadh.
The first part of this paper focuses on the façade design approach for the KAFD project, based on existing technologies used to achieve complex building forms. Four main technologies have been identified, together with representative built precedents. A final assessment on the merits of each technology is provided, which aims to identify the effectiveness of each design approach. The second part presents an innovative design approach using fibre-reinforced polymers (FRP) in order to overcome the limitations identified in existing technologies.

4 Design Approach of integrated facade concept for King Abdullah Financial District (KAFD) Metro Station

4.1 Description of façade systems concept and requirements

The planned King Abdullah Financial District (KAFD) Metro Station [Figure 11] is a live project within the Riyadh Transportation Strategy Plan. The design for the external envelope exhibits a complex geometry, combining different facade systems: Opaque areas clad in open jointed doubly curved panels (rainscreen on steel structure)

(i) Glazed areas with external complex solar shading elements
(ii) Glazed areas at ground level with external extruded aluminium shading louvers

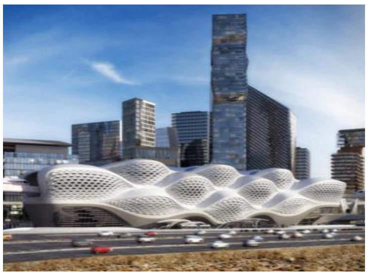

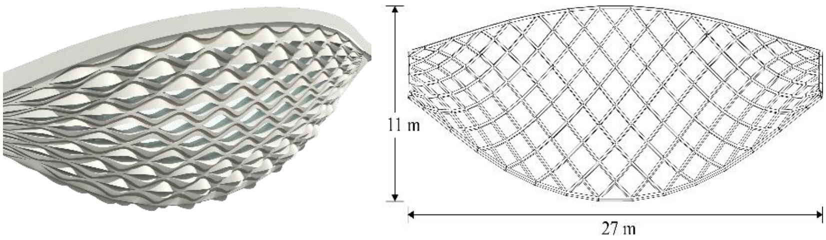

(a) (b)

Figure 11: External 3D view. Figure 12: Close up: (a) one entire glazed "eye" (b) Steel diagrid

This paper focuses on the design of one glazed "eye" formed by the glazed area and the external solar shading elements [Figure 12 (a)]. Existing technologies and representative case studies have been evaluated [Table 1 to Table3] in order to develop a suitable design approach for this system based on the following requirements:

- The façade has to follow a complex structural shape and provide a waterproofed and thermally insulated envelope around a structure, which is not driven by a structural primitive, which seeks to provide structural efficiency. The form is driven by the requirements to enclose the space with the minimum amount of internally air-conditioned volume. Consequently, the zones for the depth of the façade and its supporting structure are required to be minimised to contribute to this concept.
- The speed of installation of the façade systems, given the programme requirements of constructing a rapid transportation system,
- The durability of the façade materials given the extreme environmental conditions to which the building will be exposed.

4.2 Design development based on current technologies

Structural shells

The first approach considered is to achieve the complex geometry of each "eye" directly through the shape of the primary structure. The material used typically for this purpose is reinforced concrete. The main benefit of using concrete is that it can be cast into large-scale monolithic forms of any shape without joints in the material. Concrete can be either poured directly into formwork, or sprayed onto pre-mounted reinforcement, or delivered as pre-cast elements on site. For complex geometries, in-situ concrete is not efficient in terms of time and cost due to the preparation of the complex shaped formwork. Consequently, sprayed concrete is increasingly used for complex shapes, despite the fact that its inherent disadvantages of reduced durability and stiffness which results in a thicker cover and increased overall depth of the cast element.
The thermal insulation is set either within the concrete during pouring or alternatively is point-fixed on the internal or external face of the concrete. The waterproofing, normally liquid polymers or resin, is applied externally and can be coloured or transparent. The facade can be either left with a fair-faced concrete appearance or finished with decorative elements [1].

Another trend for opaque complex geometries is the use of a skeletal steel substructure onto which a façade a façade build-up is applied, comprising insulation, waterproofing and gypsum panels internally and cladding panels externally.

For the KAFD glazed system the major limitation of this opaque shell technology is the required number of perforations needed to meet the natural daylighting requirements, which would have led to a highly complex formwork if a concrete solution had been preferred Moreover, given the restriction of a steel primary structure [Figure 12], a concrete wall would exceed considerably the allowed superimposed dead load from the envelope. Consequently a façade solution using a supporting steel structure was developed.

*Table **1**: Structural shell: list of precedents.*

Precedent	*Location*	*Key features*
The Selfridges Building	Birmingham (2003)	Free-form sprayed concrete envelope coated with liquid plastic (waterproofing guaranteed for 35 years), covered with decorative elements.
Museo Soumaya	Mexico City (2011)	Primary steel structure provides support for the opaque façade mesh. Decorative aluminium cladding finishes the outer skin of the façade construction
Restaurant Los Manantiales	Xochimilco (1958)	Doubly-curved thin shell exposed concrete; thermal performance not a design parameter at that time of construction.

Site-assembled modules

The facade system of the KAFD project has opaque and glazed areas, protected by shading elements [Figure 13]. A site-assembled approach lends itself to the combination of two existing technologies: the stick system and the rain screen system. The thermal insulation and waterproofing of the building are realised on site, whilst rain screen technology is used for the complex shading devices that define the external complex form of the façade. The first design approach draws from stick glazing technology. Stick systems are assembled on site by fixing infill panels to a loadbearing steel or aluminium sub-frame, which follows the complex geometry of the building. Individual opaque or glazed elements are set into place and attached to the carrier structure, including thermal breaks while assembling. This technology is adapted for rectilinear glazed curtain walls as well as for non-modular constructions and allows a high degree of freedom in its installation sequence. Methods of fixing are either toggle type, pressure plate or point fixing, sometimes with decorative caps [1]. The integrated, flexible silicone seal between the different panels can accommodate structural movement. This site-assembled construction approach leads to a layered construction addressing in turn each environmental and structural requirement. The site-assembled option would require the following build-up: marine grade plywood (or similar composite board substrate), vapour barrier, thermal insulation and waterproofing membrane on top, integrated into an aluminium sub-frame, which is fixed back to the diagrid steel structure [Figure 13]. Glazed elements are framed and also set into the aluminium sub-frame [1]. The fixing points of the external solar shading elements and internal GRG cladding panels penetrate the waterproofing and thermal line and need a special wet seal performed on site [Figure 13(b)]. A wet seal applied on site is also required to waterproof the interface between glazing panels and the aluminium sub-frame. A stick system is usually drained and ventilated at the outer surface. A ventilated zone behind the rubber based wet seal creates a pressure equalised chamber between outside and inside the system avoiding water to being drawn into the system. This chamber is also internally drained, providing a second layer of protection against moisture penetration. Due to its double level of protection, this technology can be used for overhead applications, where the action of gravity increases the risk of leaks and water can therefore be collected and drained in the internal chamber. The thermal insulation of stick systems is secured by providing a full thermal break through the structural profiles. Evaluating the KAFD façade, the complexity of the alternating glazing and opaque pattern results into a considerable number of interfaces, which require most components to be cut and assembled on site. This requires a continuous waterproofing membrane in order to ensure a continuous weatherproofing line and avoid risk of moisture penetration through the many interfaces. The use of continuous waterproofing membrane does not allow a clear strategy for accommodation of movements of the complex supporting structure at defined movement joints. This increases the risk of the membrane tearing at highly stressed locations during the service life of the building, leading to moisture penetration, which is both difficult to trace and to repair. This design approach relies on precise overlapping of waterproofing membranes and on-site wet sealing at several interfaces, presuming excellent workmanship to achieve the same quality that can be achieved with factory-assembled systems. Site-assembled systems are also likely to require scaffolding, which would inevitably slow down installation which is not compatible with the construction programme and the subsequent need to perform different operations in parallel on-site.

In order to overcome these obstacles, the use of pre-fabricated panels has been considered. Prefabricated panels can combine opaque and transparent elements. Each panel consists of a supporting aluminium frame, which provides the required structural stiffness for the infill panel, a substrate of marine plywood to support the thermal insulation (open or closed-cell) and a double-glazed unit already sealed to the supporting frame. The pre-fabricated panels are clamped together and fixed back independently to the primary structure [Figure 14]. The use of a continuous waterproofing membrane on top or wet-sealing of the interfaces (in case the individual panels are waterproofed already) is required to ensure a continuous waterproofing line of the build-up.
Both the application of wet-seals and the installation of a continuous waterproofing membrane would require high-level of workmanship on site and possibly scaffolding.
The waterproofing layer requires additional protection against UV radiation. This extra layer needs to accommodate the complex outer geometry, to provide the required shading and must be easily replaceable. The solution considered to meet these requirements is the application of the rainscreen principle. Rainscreens are cladding elements that are mechanically fixed to the primary structure. A rainscreen protects the waterproofing membrane, reducing the combined effect of wind and rain by creating an air-barrier between the facade surface and the waterproofing layer. Providing an air gap between façade structure and the water-repellent line allows the circulation of air on the moisture barrier and reduces the risk of trapping water and humidity within the facade system [1]. Complex fixing brackets can be used to provide adjustability in three directions and accommodate complex geometries, such as doubly curved surfaces, independently from the supporting substructure whilst simultaneously accommodating structural movements. The architectural intent and environmental conditions of the KAFD project demand a material that can be moulded into complex shapes and exhibits a high durability of the material, in terms of resistance against corrosion, UV radiation and fire. Composite materials are suitable to meet these requirements.

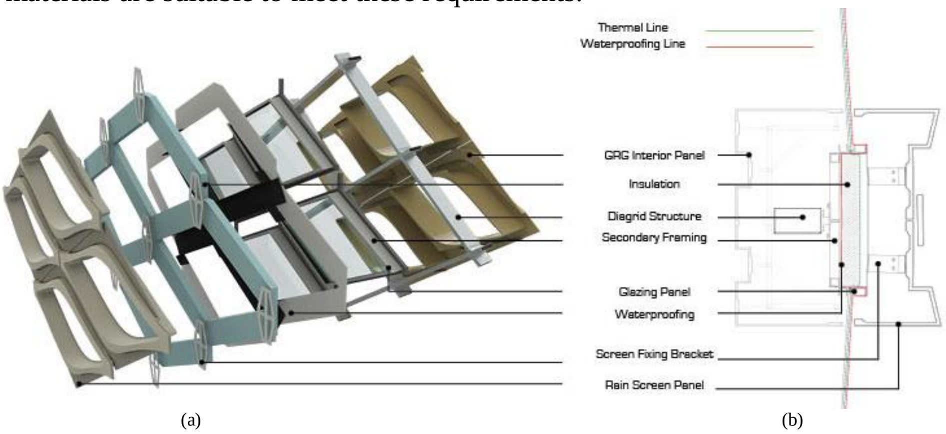

Figure 13: 1st design approach: on-site stick elements & rain screen (a) exploded view (b) cross-section detail.

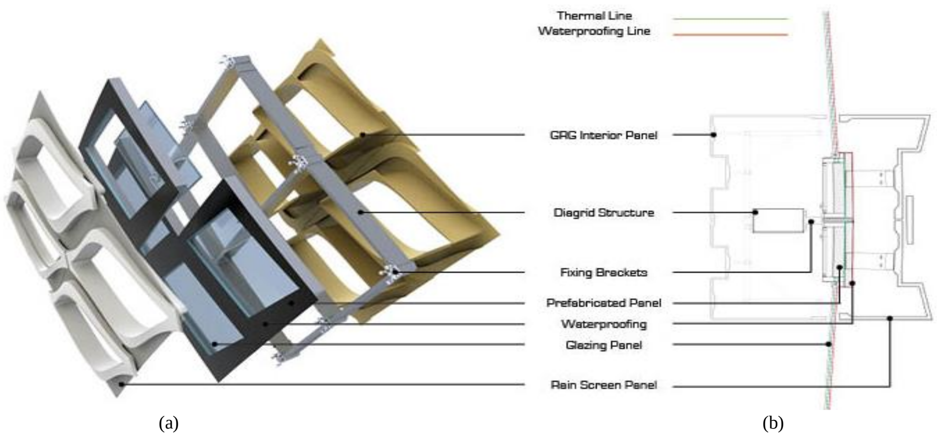

Figure 14: 2nd design approach: on-site stick pre-fabricated elements & rainscreen (a) exploded view (b) cross-section detail.

For both site-assembled and the pre-fabricated systems the shading elements are installed after the waterproofing is applied and therefore require additional workmanship on site. This requirement can be resolved with the use of a unitised technology.

Table 2: Side assembled modules & rain screen: list of precedents.

Precedent	*Location*	*Key features*
Site assembled modules		
British museum	London (2000)	On-site welded steel substructure (process results in minimal tolerances), acting as support for framed, triangulated glazing, which differs in size in order to take up the geometry
Terminal 3, Bao'an International Airport	Shenzhen (2013)	Double-skin facade using three different layers of supporting steel frame; fulfilment of requirements & assembling with consecutive layers
Myzeil Shopping Centre	Frankfurt (2009)	The stick shells geometry was made with grids of pre-fabricated six-beam nodes with edge-clamped glazing and beams welded on-site.
Dali museum	St. Petersburg (2011)	Double-node technology solves free form geometric issues of beam twist with aluminium edge-clamped glazing.
The Canopy at the Smithsonian Institution's Kogod courtyard	Washington D.C. (2008)	Aluminium framed, flat glass elements fixed to U-profiles attached to steel sub-frame. Dome-shaped glazed roof allows drainage through U-profiles and final drainage through pillars
Dalian International Conference Centre	Dalian (2013)	Stick glazing with aluminium outer rain screen or metal louvers on top is supported by a structural steel mesh.
Prada Aoyama	Tokyo (2003)	Toggle-fixed, silicone sealed glazing elements with partly double curved glass; attached back to a diagrid-shaped steel frame.
CET Budapest by ONL	Budapest (2010)	Complex curved shaped achieved with alternating toggle-fixed glazing and opaque facade elements fixed to the structural steel.
Park House	London (2012)	Semi-unitised System: prefabricated fixing frame, acting as mullion with toggle fixed glazing and opaque elements
King Abdulaziz Centre	Dhahran (expected 2015)	Semi-unitised System: the stick glazing provides the waterproofing and thermal line; external shading consists of pre-fabricated stainless steel tubes, attached to adjustable brackets.
Rainscreen		
Georges-Frêches School	Montpellier (2012)	Cast in-place and free-form sprayed concrete envelope with complex-shape aluminium rain screen.
Guggenheim Museum	Bilbao (1997)	Titanium rain screen combined with stone cladding and glazed areas; self-healing membrane as waterproofing line.

Unitised technology

The use of pre-fabricated components leads to the development of the system into a fully unitised system based on the principle of fixing each panel independently to the primary structure by rapid installation on site. This approach accommodates the movements of the panels and the structure in the joints between panels, specially designed to provide a watertight interface. The possibility of fixing the panels directly with the shading elements incorporated without requiring any additional waterproofing applied on site allows the installation to be accelerated and provides a high level of quality control during manufacturing. The system can also be structurally designed to a higher degree of precision to accommodate engineered seals between panels. Typically, glazed unitised panels are set side by side, floor by floor, restrained on one end and fixed on the other. Panels are secured by brackets fixed to a steel frame, which is then is attached to the primary structure [1]. The movements are accommodated in the joints between panels. The frame of each unitised panel is usually aluminium. The gaps between each panel are sealed with synthetic rubber gaskets. The waterproofing is generally fixed to the panel before installation and works when panels are slotted into place. The outer line of defence is provided by rubber-based baffles set on each panel so that they press together to form a seal. An aluminium drip can be added to the outside as a first wind barrier, but allowing water to drip out again behind this profile. Any rainwater penetrating the profile is stopped in a pressure-equalised chamber that prevents water getting any further and is drained out again. The main advantages of unitised systems in construction are the speed of installation and the level of quality control possible within controlled workshop conditions. Unitised panels are particularly popular in vertical façades of high-rise buildings. Non-vertical applications are possible, but they require significant adjustments to accommodate the new waterproofing conditions.

Given the system requirements for the KAFD Metro, particularly the need for fast installation, the application of unitised technology is particularly appealing. Figure 15 shows the assembly sequence of four unitised panels fixed onto the supporting diagrid structure. Each panel consists of a steel frame with a glazed unit and sizes approx. 2 x 2 m. Panels are fixed independently to the steel diagrid. The main limitations of this unitised approach is the waterproofing of the system on the inclined doubly-curved surface. The draining technology is based on water being able to drain within the framing elements; for this reason the conventional system is ill-suited to overhead and inclined applications. Only minimal inclinations (usually up to 10°-15°) are allowed to avoid risk of leakage. Thermal breaks set into the frame reduce thermal bridging through the frame. Overall, the solution presented [Figure 15] cannot respond to the geometry requirements without modification.

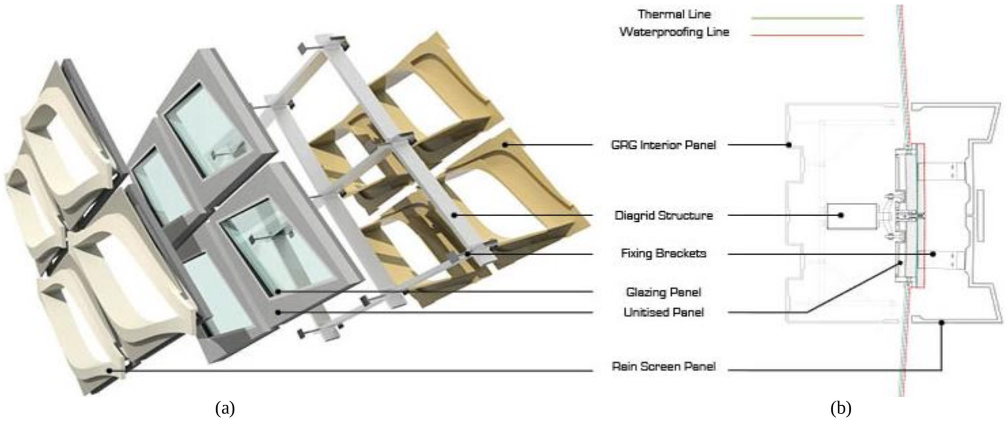

Figure 15: 3th Design Approach: assembly of unitised system; (a) exploited view (b) cross-section detail.

Table 3: Unitised technology: list of precedents.

Precedent	*Location*	*Key features*
62 Buckingham Gate	London (2013)	Unitised curtain wall divided into 11 facets, each exhibiting a different inward and outward inclined angle (between -5° to 10°) for the glazing.
30 St Mary Axe - Gherkin	London (2004)	Unitised system for small inclinations combined with stick system for large inclinations located at the top of the building

5 Comparison of precedents

The Table4 shows the comparison of the selected representative precedents for each technology against the same parameters in order to gain a general overview about the performance achieved by each technology when applied to real projects. The main benefits and drawbacks of each design approach are evaluated in terms of the ease of the construction sequence, the integration of facade layers, the general facade design time and post-construction durability issues.

Table 4: Comparison of complex shaped precedents using current technologies.

	Type	Geometric Complexity	Ease of installation	Integration of facade layers	Facade design time	Post-construction durability issues
The Selfridges	1	I	0	+	-	✓ long lasting exposed waterproofing
Museo Soumaya	1	II	-	+	+	
British museum	3	II	0	0	+	
Terminal 3, Bao'an International Airport	3	II	-	-	+	✗ Initial leakage
Myzeil Shopping Centre	3	II+V	0	0	0	
Dali museum	1+3	II+V	0	0	0	✗ Leakage after 4 months
Canopy at Smithsonian Institution's courtyard	3+4	II	0	0	+	
Dalian Int. Conf. Centre	3	I	-	-	0	
Prada Aoyama	3	V*	0	0	-	
CET Budapest by ONL	3	II	0	0	0	✗ Initial leaking
Park House	3	I+V	0	0	0	
King Abdulaziz Centre	1	I	-	-	+	
Georges-Frêches School	1	I	-	-	-	
Guggenheim Museum	2+3	I	-	-	0	
62 Buckingham Gate	4	V	+	0	+	
30 St Mary Axe Gherkin	3+4	II	+	0	+	

Type	1	Structural shell, opaque	Complexity of geometry	I	Doubly curved envelope; curved elements	Evaluation notation	-	Low
	2	Rainscreen		II	Doubly curved envelope; flat elements		0	Medium
	3	Site assembled envelope		III	Singly curved envelope; curved elements		+	High
	4	Unitised technology		IV	Singly curved envelope; flat elements			
				V	Flat envelope; variable inclination possible			

* integrates flat and doubly curved elements

From the evaluation of the initial design proposals and the corresponding precedents, it can be observed that current technologies, originally conceived for more straightforward buildings, are often used in the construction of geometrically complex buildings. However, none of these technologies was specifically developed for complex geometries. From the above review and comparison of precedents, the following remarks can be made:

- Using site-assembled modules for complex opaque and glazing pattern difficulties in defining a clear structural strategy to accommodate structural movement. At the same time it relies on high quality of workmanship on site, which leads to a high risk of leakage post construction. Installation often requires the use of scaffolding and is time-intensive.
- Prefabricated modules increase the level of manufacturing and control of quality within the workshop and ensure faster installation. Panels are clamped on site, require an additional waterproofing finish, either using a waterproofing membrane or wet-sealing the interfaces. The shading panels are installed after the waterproofing. This still relies on a skilled workmanship on site and potential use of scaffolding. Given the limitations in panel size due to its self-weight, the large number of joints or interfaces presents an elevated risk of leakage.
- Unitised panels offer substantial advantages in terms of installation speed and movement accommodation, but cannot respond easily to complex geometries, given the high risk of leakage on inclined surfaces.

6 Composite materials

The use of emerging technologies and materials allows a re-think of the design strategy for the KAFD Metro, starting from a more radical approach that aims to achieve a complex envelope on a light-weight supporting structure.

The key parameters for this design approach are as follows:

- Maximise span of the modules to reduce number of joints
- Minimise weight of modules in order to minimise loads and resulting movements on the light-weight supporting structure. This also facilitates maintenance and replacement of components.
- Predicable behaviour of the system in terms of accommodation of structural movements.
- Reduce on-site operations to maximise speed of installation, whilst avoiding scaffolding around complex shapes.

The limiting factor in achieving larger spans is the use of infill panels set into spanning framing elements. More efficient structural materials would allow the use of panels as load bearing, self-spanning shell structures. This is commonly achieved by composites in transportation and other industries, but these are still novel materials in the construction industry, where the design is not only driven by structural efficiency but is largely restricted by the need for longer term durability. The main advantage of composites is their ability to provide an integrated and light-weight structural solution for complex shapes. Furthermore, composites can be engineered to be highly durable to achieve high design life requirements and the recent development of fire retardant epoxy resins ensures an appropriate fire rating.

FRP Sandwich elements

Fibre-reinforced polymers (FRP) are able to meet a full range of structural, environmental and geometrical facade performance requirements integrated within one layer [2]. It is a lightweight composite material, exhibiting a high tensile strength. FRP consists of liquid resin containing fibres such as glass, carbon or aramid, all exceeding the ultimate tensile strength of steel in several orders of magnitude. The thermal expansion is a function of the fibre content and is higher than the values for concrete, glass and steel, but similar to aluminium and wood [3]. FRP can achieve excellent fire- and corrosion resistant and weather-tightness properties, which allow a long-term external use of the material [2]. Stiffening of the material is either obtained with a thicker and therefore costly lay-up or by a structural composition of different elements and/or shapes [3]. In the construction industry FRP Sandwich panels with foam core have a wide application range, because the integrated thermal insulation cuts down significantly the workmanship on site. A panel consists of two FRP outer skins and a structural foam core, which incorporates a higher shear resistance as well as the insulation layer. The final resin coating protects the fibre and polyester lay-up from moisture. The structural advantages of a sandwich panel are the high stiffness-to-weight ratio allowing spans and the good fatigue strength. Additionally, a very good thermal insulation and acoustical absorption can be achieved [2]. As it is a moulded material any shape can be manufactured using prefabricated moulds. The recently developed vacuum assisted infusion moulding method allows the creation of high performance units with the potential to meet load-bearing application. As the KAFD façade requires large, lightweight panels in order to reduce the amount of panel connections, a lightweight and extremely stiff fibre material, such as carbon, is chosen.

*Table **5**: FRP composites: list of precedents.*

Precedent	*Location*	*Key features*
PCT Prototype RAK Gateway	*(in process)*	FRP façade panel integrates outer skin requirements
The Eyecatcher building	Basel (1997)	Primary structure and façade elements consist of GFRP
Enexis Building	Zwolle (2013)	Facade panels made out of FRP (13x3 m)

4.1 Conceptual design evaluation

The final design approach is based on a CFRP sandwich panel, acting as a structural element, which incorporates different components, such as insulation, water proofed skin, structurally bonded glazing elements and cast-in anchors used as fixing points for the inner and outer cladding panels; without creating thermal bridges or major conflicts with the waterproofing membrane. Carbon fibres provide the stiffest panels and are therefore preferred to aramid or glass fibres. The set-up of the CFRP panel enables the combination of 4 panels into one; the potential size of 4 m x 4 m is shown in Figure 16. CFRP is a high performance material, which easily can withstand point loads, e.g. via bolts. Cast-in threaded inserts allow the CFRP panel to be fixed back to the primary structure using a simple bolt connection. Spider brackets as connecting point to the primary structure enable the simple adjustment of structural differences and reduce bending on the supporting structure by acting on the structural nodes of the diagrid to transfer façade loads. Each panel can be independently fixed to control movements at the joints. Due to its high stiffness-to-weight ratio spans of up to 10 m can be achieved. The initial panel size of approx. 2 m by 2 m is no longer a restriction; shape and size of the panels are only limited by transportation constraints. The larger spans of CFRP panels also allows a further simplification of the inner structural metal-grid and leads to considerable steel savings. The integrated insulation and the high performance fibres made of carbon fibre enable an overall component thickness of only 120 mm, exhibiting a high strength [Figure 16].

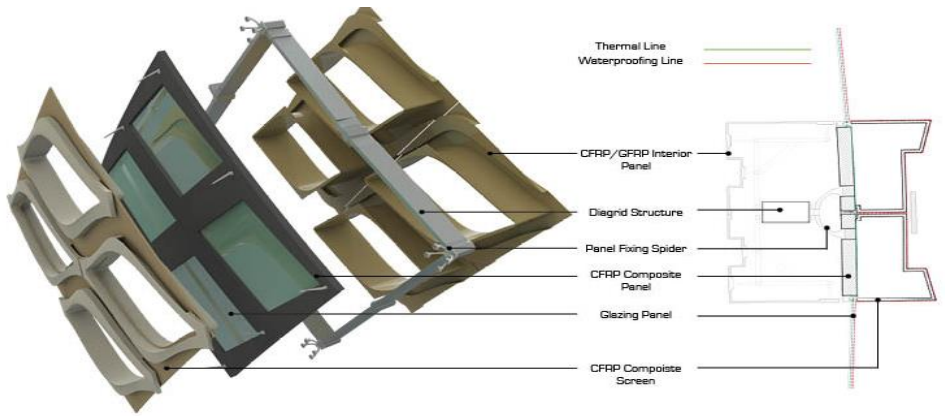

(a) *(b)*

Figure 16: Build-up optimized design approach using CFRP; (a) exploited view (b) cross-section detail.

CFRP panels can be connected in various ways. The conventional method consists of clamped fixing using pressure plates, which simplifies the connection complexity. The panels are clamped together on-site and the clamps allow for internal drainage and therefore their use for inclined applications.
Gluing is also being explored as a technical solution for the joints. This would allow structural continuity to be achieved between panels, potentially even further savings on the supporting diagrid structure and faster installation [Figure 17].

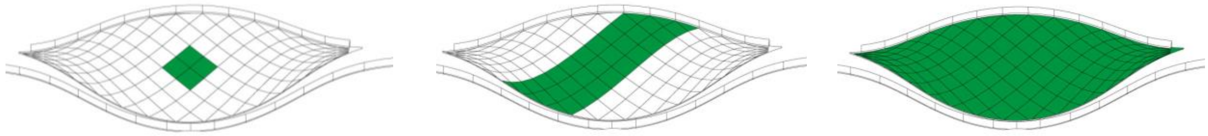

Figure 17: possible panel sizes for glued connection

The main benefits of adapting the CFRP option are the significant reduction in self-weight of the façade and simpler waterproofing.
Nevertheless designing with CFRP is complex as it is not a conventional material in the construction industry and the design process needs to be assisted by analytical and experimental validations. For the preliminary structural and thermal analysis a panel of the size 4 m by 4 m is evaluated. This panel represents the merging of four 2 m by 2 m elements used in the original design [Figure 18].

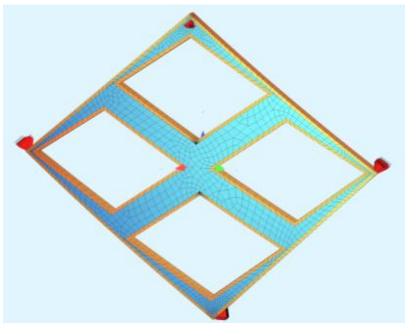

Loads	[kN/m²]
Wind suction w_s	-4
Wind pressure w_p	1.5
Self weight	0.55

Figure 18: CFRP Panel FE model and Loads.

Table 65: Build- up and material properties [i].

Ply #	Fibre orientation	Thickness [mm]	Young's Modulus [MPa]	ε_{ten} [%]	Shear strength [MPa]
	0°/90°	0.86	47 050	1	
	0°	0.72	92620	1.2	
Carbon	0°	0.72	92620	1.2	
	±45°	0.57	10510	1.2	
PVC-80 [kg/m²]	-	120	63		1.2
	±45°	0.57	10510	1.2	
	0°	0.72	92620	1.2	
Carbon	0°	0.72	92620	1.2	
	0°/90°	0.86	47 050	1	

The numerical model of the FRP panel has been developed with Sofstik 2014 [Figure 18]. QUAD elements are used; the model is defined as a shell, where the material properties are assigned to the surfaces. The build-up and the material properties chosen are shown in Table 6. The boundary conditions comply with a statically determinate system. The analysis was carried out for SLS and ULS respectively. The maximum principal stresses are 48.8 MPa on the top site and -46.7 MPa on the bottom site of the panel [Figure 9]. The panel thickness of 125.7 mm reaches a maximum deflection of 11 mm over a span of 4 m [Figure 10]; the deflection is within the critical limitation of 20 mm given by the span over 200. The stress distribution across the thickness was also determined. It was found that the limiting parameter is the deflection, as the stresses throughout the different layers range several orders of magnitude below the equivalent resistance strength ($\sigma_{max,2^{nd}layer} = 94\,MPa \le 1111\,MPa = \sigma_{r,2^{nd}layer}$). The preliminary conservative evaluation of the shear stresses shows, that the foam core is able the resist the maximum shear forces ($\tau_{max,foam} = 0.8\,MPa \le 1.2\,MPa = \tau_{r,foam}$) without taking the outer carbon fibre sheets into account. The stress contour and deflection plots are not shown here for brevity.

The preliminarily thermal analysis was undertaken with the software flixo pro 7.0. The thermal analysis has been performed according the BS Eurocode [5]. In accordance with the standard BS EN ISO 10077:2012 the external temperature is 0 °C and internal temperature 20 °C. In order to evaluate the improvement in thermal performance the design approach based on the FRP Panel is compared with the semi-unitised approach using prefabricated panels and on site assembling. The same cross-section is considered. It represents the worst-case scenario including the fixing elements for the external and the internal cladding. The system using carbon fibres presents higher thermal performance. An overall reduction in the heat flux [W/m] of 25 % is achieved as well higher surface temperatures, reducing the risk of superficial condensation [Figure 19].

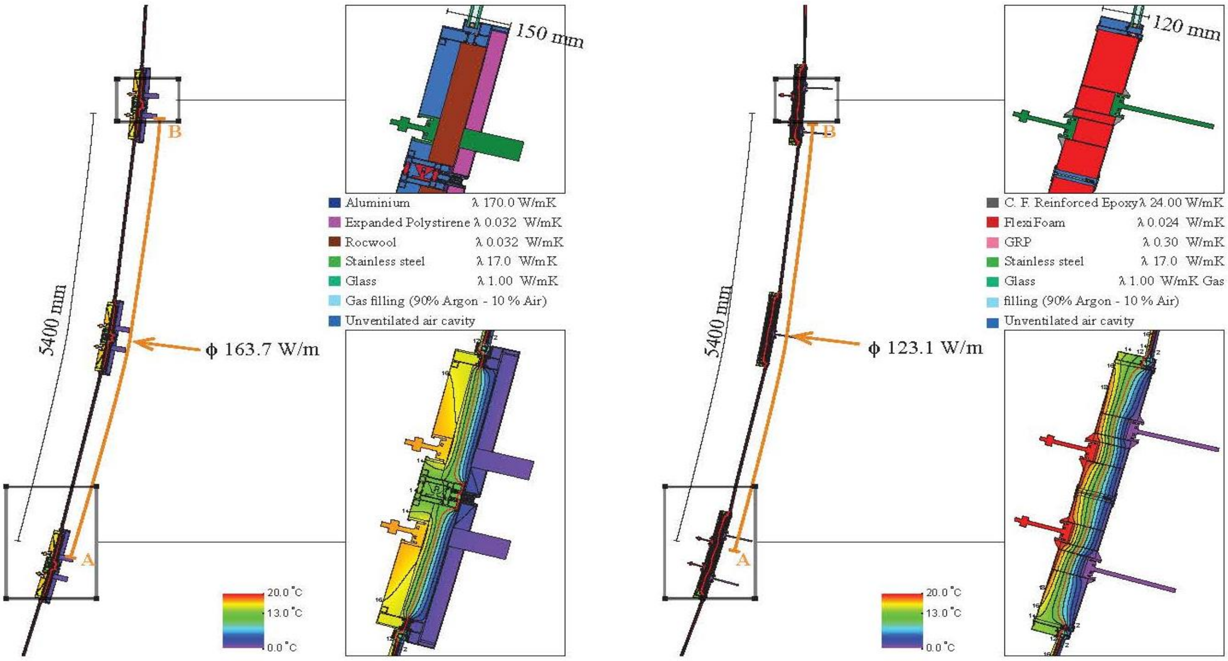

Figure 19: thermal analysis of prefabricated panel (left) and FRP Sandwich element (right).

4.2 Future work

To verify the mechanical properties of the CFRP panels it must be subjected to (destructive) tests in order to evaluate [6]:

- Delamination strength of the laminate/ bonding strength between core and laminate
- Tensile and bending strength (4PB test) of the laminate/ shear strength of the core
- The connection methods used between CFRP panels and between CFRP panels and the primary structure need to be developed and require experimental validation.

Furthermore, the fibre content across the panel can be optimized to suit the stress distribution and deflection. Possible combinations of integrating the rainscreen as structural element of the façade panel will be explored.

5 Acknowledgements

The elaboration of the design concepts and the technical development was undertaken with the engineering design team at Newtecnic. Information about composites and technical support was provided by CarboNovus S.r.l.. Technical evaluation and comparative assessments of the design concepts developed were undertaken with the systems of Seele, Josef Gartner and Novum.

6 References

[1] Watts, A: *Modern Construction Envelopes*, Ambra│V, 2nd Edition, Vienna, 2014.
[2] Reis, E.M., Rizkalla, S.h.: *Material characteristics of 3-D FRP sandwich panels*, Elsevier, Amsterdam, 2007.
[3] Brookes, A.J., Meijs, M.: *Cladding of buildings*, Taylor&Francis, 4th edition, 2008.

[4] Technical data provided by Carbonovus S.r.l
[5] Standards and Codes: BS EN ISO 10456:2007, BS EN ISO 6946:2007, BS EN ISO 10211:2007, BS EN ISO 14683:2007, BS EN ISO 12631:2012.
[6] Gullberg, O.: *Design and Construction of GRP Sandwich Ship Hulls*, The Royal Institute of Technology, Dept. of Aeronautical Structures and Materials, Stockholm, 1990.

building physics

Energy performance assessment of adaptive transparent building envelope through test cells and in-field monitoring

Lorenza Bianco, Arch.
TEBE research group, Department of Energy, Politecnico of Torino, Italy,
lorenza.bianco@polito.it

Valentina Serra, Prof.
TEBE research group, Department of Energy, Politecnico of Torino, Italy,
valentina.serra@polito.it

Marco Perino, Prof.
TEBE research group, Department of Energy, Politecnico of Torino, Italy,
marco.perino@polito.it

Summary

Adaptive building envelope will probably constitute the future for new building belonging to the Nearly Zero Energy Buildings typology. These innovative façade concepts are almost "self-sufficient" building skins that show a dynamic behavior and incorporate different technologies, requiring different approaches for what concern their energy performance assessment. In this paper the attention is posed on adaptive transparent building envelope. Some case studies are described and the methodology to evaluate the energy behavior is discussed. Furthermore a review of the testing facilities and of the main potential and criticism in the measurement process, is reported.

Keywords: Adaptive envelope, Transparent building skins, Experimental activity, Facility, Infield measurement, Test cell, performance parameters.

1 Introduction

The new generation of building envelope needs to offer higher and higher performance in terms of energy efficiency and indoor environmental quality provided. Technologies are now largely available on the market to overcome the negative effects typically related to conventional building components, as the winter thermal discomfort or the high energy losses. Furthermore, adaptive façades are being developed to modify their energy behaviour and/or thermal and optical properties according to the different boundary conditions, in order to optimise the energy gain and loss and fulfilling the objectives of nZEBs.
Unfortunately, due to their complex behaviour it is quite hard to describe their energy performance through conventional synthetic indexes and starting from few technical data provided by manufacturers.
In the common architectural practice many simplifications are used in order to quantify the façade effect in heat transfer [1], but a correct and complete overview of the building envelope thermal properties is the pillar of a correct design process [2]. A recent study faced the problem related to the opaque envelope, highlighting that the values of thermal conductivity for highly insulating layers are generally well established, thanks to laboratory measurement while other materials such as not homogeneous bricks and tiles are not as well characterized [2]. For what concern the in-field measurement the well-known method presented by standard ISO 9869 [3] describes how to measure in situ thermal transmittance of opaque envelope, but this method is not suitable to characterize the thermal behaviour of a component characterised by a dynamic behaviour and most of all, the method is not suitable for transparent building envelope.

Transparency makes the measurement task quite difficult, due to the component of the solar radiation directly transmitted, that can influence the sensor itself. Highly dynamic and adaptive transparent building envelopes need measuring campaign along different seasons and under different boundary conditions. Test cell campaigns allow measuring the technology behavior under real condition and, above all, when exposed to solar radiation. On the contrary in the laboratory the solar radiation is hardly reproduced and the cost of the facility rises considerably up.

In the last 10 years the authors carried out a number of monitoring campaigns on advanced adaptive façades (i.e. on active mechanically ventilated and hybrid façades, on thermotropic and photocromic glazing, on PCMs filled glazing) and a suitable methodology has been defined. In this paper the prototypes studied are briefly described and the main monitoring campaigns are reported, focusing on the facility used and the results that this kind of experimental activity allows to obtain in terms of energy balance and indoor comfort. Furthermore the main criticisms which can raise during measurements are pointed out.

2 Adaptive transparent building envelope

Adaptive or responsive building envelopes will probably constitute the future for new building belonging to Nearly Zero Energy Building category. Regarding transparent building envelope, the research is mainly concentrated on the challenging topic of adaptive thermal and optical technologies; smart glass or smart window components and active façades. The passive resistance of transparent building envelope reached very high value thanks to the integration of TIM (Transparent Insulation Material) such as aerogel or the new technology of evacuated window, and different commercial products are already available, though still expensive [4,5]. Smart glass or smart window technologies are able to dynamically control the solar energy and light transmission coefficient by changing the optical features of the glass pane such as electrochromic, thermochromic, photochromic layers, liquid crystal panes and suspended particle devices [6]. Some products are already available on the market but the research is keeping investigating in order to increase the building integration level. Another field of research is the enhancement of thermal inertia of glazing component through the incorporation of PCMs in the cavity [7,8,9]. Moving from the component to the system scale, Active Integrated Façades (AIFs), i.e. climate façades and double skin façades, constitute a well-known technology but the research on this topic is still alive. The high complexity of AIFs requires a deep knowledge of the system working according to different configurations, under different boundary conditions and with different level of integration with HVAC systems.

New emerging technology are fluid façades that integrate water or other fluids in the façade [10,11] and in some case transforming the façade in a bio-reactive façade with microalgae [12]. Furthermore, some studies have been performed on multifunctional façades able to store and produce energy through the integration of thermoelectric heat pumps [13].

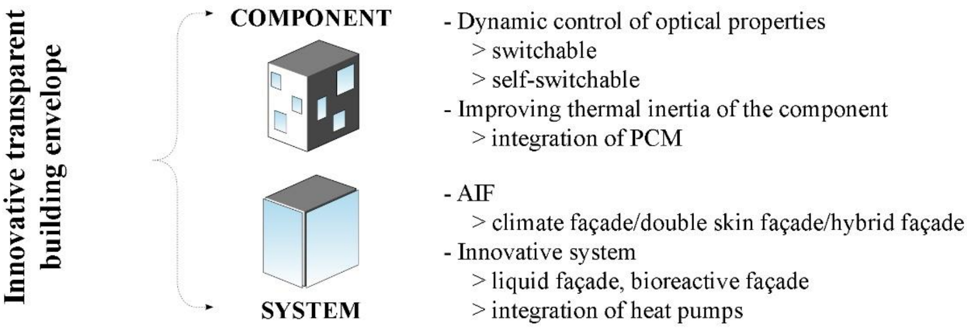

Figure 1: Adaptive transparent building envelope.

3 Experimental assessment of the energy performance

3.1 Aims of the experimental campaign

The characterization of the energy performance of an adaptive transparent technology is not a trivial task. The peculiarity of these technologies is the ability to modify their properties at the varying of the external condition. Indeed to assess their energy behavior is usually set up an experimental campaign under real boundary conditions in order to collect enough data to give a representative picture of the different behaviors occurring. Synthetic performance parameters traditionally settled for windows and glazing, such as thermal transmittance (U-value) and solar factor (g/TSET value), are no more able to describe the behavior of these technologies [14,15]. Regarding IEQ, acoustic, thermal and lighting aspects should be contemporarily analyzed so to completely characterize the adaptive building envelope performance. The analysis has therefore carried out moving to a larger scale: from the scale of the component/façade interface to the scale of the indoor environment. This paper, for the sake of brevity, it is focused just to the interface envelope level.

3.2 Facility potential and criticism

The assessment of the energy performance of adaptive transparent building envelopes can be mainly carried out through:

- In-field measurement of the full scale tested façade, on a real building, under real operating conditions
- Outdoor Test cell or mock up measurement, with real solar radiation impinging on the façade
- Indoor Lab Facilities to measure thermal and optical properties at the material/component scale

The main feature of these façades is their responsive behaviour which needs to be studied under different boundary conditions and it makes necessary an assessment covering different configurations. An experimental campaign performed in test cells, full-scale test facility or in mock up [16], presents the advantage that the tested component or system is exposed to real boundary conditions covering different seasons. The main disadvantage of this facility is that the measurement should last for months. Experimental campaign in controlled test cells can be either set up to improve a façade component. In this case, different configuration of the technology can be tested and then compared. Experimental campaign on adaptive façades can also be conducted in real functioning building, through in-field measurement and for commissioning purpose; in this case the presence of real users can reveal to be useful to get information on users' behaviour and interactions with the façade dynamics but, on the other hand it could influence and interfered with the monitored data [17]. The collected data can be analysed comparatively or quantifying specific indexes [16]. The first method was applied in TWINS a Test WINdow System available on the rooftop of the dept. of Energy (figure 2). This experimental apparatus was specifically developed to study advanced building envelope components. The facility is composed by two identical test cells, built following the specifications of IEA -SHC TASK 27 measuring 1.6 m x 3.6 m and height 2.6 m. Test cell A is normally used for testing the transparent building envelope, while in test cell B is mounted a reference technology in order to make possible to comparatively study the test technology. The two test cells do not present any obstruction and they can rotate and easily change their exposition. The indoor air in the test cell can be continuously maintained at the desired set point, with an accuracy of ±1◦C, by means of an all air system. The thermal measurement are carried out by means of thermocouples, heat flux meters, pyranometers previously tested and verified in the laboratory. The sensors are connected to a data logger that continuously registers data every time series. In figure 5 a schematic portion of a transparent building envelope shows the position of the sensors used. In case of a tall façade, the same scheme should be repeated along the façade to evaluate the stratification of the temperature at different height. Besides measuring the thermal performance of the component, boundary conditions were as well monitored. Through this measurement it is possible to define the amount of energy crossing the envelope, considering both the solar quota and the heat fluxes exchanged through the envelope. Different synthetic indexes reported in paragraph 3.3 have been assessed to describe the monitored façade performance. Starting from these data it is either possible to carry out thermal comfort evaluation , analysing the surface temperature registered. For what concern acoustic measurement a sound intensity probe with two-microphone for measuring sound intensity can be used to evaluate the intensity of sound transmitted through the envelope. This kind of sensor is particularly suitable to evaluate different technology applied in test room, being the measure punctual and not influenced by joints and connections (usually not acoustically solved in test cells). For the lighting aspect, the amount of light transmitted can be evaluated through a portable luxmeter and further evaluation regarding the visual comfort aspects related to glare and color rendering index, can be carried out through measurements with a videoluminance meter and portable spectrophotometer.

Figure 2: TWINS facility.

In general, both for opaque and transparent building envelope, the measurement of heat fluxes and temperature presents a certain error due to the presence of the sensor itself, that produce a local modification of the thermal field. The transparency of the building envelope constitutes a critical point for in-field measurement. Actually, the sensors applied during the campaign need to be shielded to the solar radiation impinging on the instruments to avoid measurement errors due to different solar absorption coefficient of the sensors. A reflective tape and a shading plastic semi cylindrical element can be used to protect the sensor as shown in figure 3a and 3b. Attention has to be paid to the fact that the shading devices introduce a further error, because the measured area is shaded and it will present a lower temperature than the rest of the sample. During the experimental campaign on PCMs, the presence of shading device introduced a modification in the components performance leading, if not correctly solved, to a noticeable under or over estimation of the heat and solar fluxes crossing the façade. As it is shown in figure 3b the Phase Change Material behind the reflective tape do not melt as the rest of the material because is shaded. A similar problem was registered during the experimental campaign on the glazing with switchable technologies, where the shading effect of the sensor and of the tape on the technology created an area of the film with different optical properties. Regarding the experimental test rig on active transparent systems the same attention was paid and furthermore a micro-fan to ventilate thermocouples was applied to register the air temperature in the cavity (figure 3c).

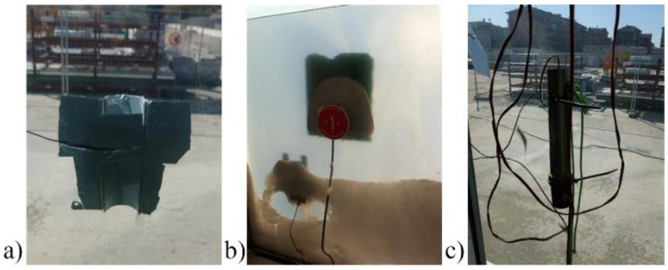

Figure 3: a) and b) Shielded sensors, c) Micro-fan for ventilated thermocouple.

In order to evaluate the thermal behaviour of the test elements in shorter time, test cell exposed to artificial exterior climate could be used. A climatic chamber called “BET cell” has been set up in the Dept. of Energy, consisting in a double room with a separation frame that host the sample walls.

The external environment is recreated in the sub module “A”, which is equipped with an HVAC systems that allows to simulate both steady state and transient dynamic boundary conditions. The sub module can be continuously maintained at the desired set point temperature, with an accuracy of ±0.5 °C, by means of an all air system working on temperature range of 12/40°C. The internal boundary condition was recreated in the sub module “B” equipped with a radiant heating systems and the sub module was continuously maintained at the desired set point temperature. This kind of equipment presents the disadvantage that the solar radiation cannot be appropriately reproduced, so it is adoptable when the aim is the assessment of the dynamics due to temperature variations (excluding the effects related to directly transmitted solar irradiance)
Complementary to in-field and test cells measurement, other laboratory measurements can be performed to characterise the thermal and optical properties of the subcomponents of the façade system. For what concern the steady-state and transient-state heat transfer through the sample, a heat flow meter or a guarded hot plate can be used (such as Lasercomp FOX600 available in the Dept. of Energy of the Politecnico of Torino) [18] Regarding spectrophotometric measurement, an integrating sphere can be adopted in order to assess spectral and angular properties of the tested elements (especially when showing a diffuse behaviour). In case of switchable technology the activation of the technology needs to be driven in order to conduct the measurement when the material is activated and not [19].

a) b)

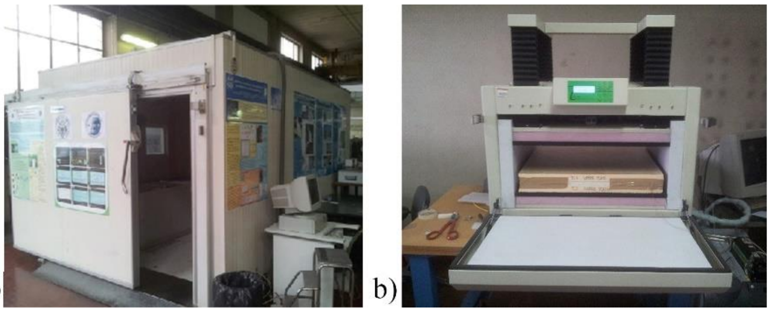

Figure 4: a) Climatic chamber BET and b) Hot box apparatus.

3.3 Performance Metrics

As far as transparent building envelope is concerned, the energy performance can be assessed through synthetic index such as conventional parameters as thermal transmittance or thermal conductance and total solar energy transmitted, but measured under different conditions and representing some representative key behaviour under specific conditions. In general, the position of the sensors to assess the energy performance is presented in figure 5.

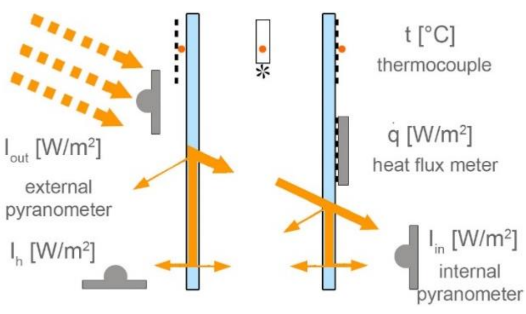

Figure 5: Schematic position of sensors and shading tape.

The *thermal transmittance* or *conductance* can be evaluated by means of the linear best-fit of the measured specific heat fluxes ($\dot{q}$, figure 5) at the indoor surfaces of the component plotted versus the measured temperature difference between the indoor and outdoor facing surfaces. The slope of the best-fit line represents the thermal conductance of the glazing. To evaluate the parameter only winter data limited to early morning hours have been used, to avoid the influence of the solar radiation. This method is suitable for technologies with

a low dynamic behaviour. In case of systems with ventilated cavities night values with low ventilation rate in the cavity, have to be chosen.
Experimental measurement in test cell or on real buildings do not allow to evaluate directly the *solar factor* of a transparent system. During the experimental campaign the solar radiation transmitted through the technology was measured by means of an internal pyranometer (I_{in}, figure 5) while the heat flux was monitored with a heat flux meter $\dot{q}$, (figure 5). which is equal to the quota of the energy flux per unit area that overall leaves the indoor facing surface of the inner glass pane. Its value includes both the contribution due to the temperature difference and that due to the long-wave radiative heat exchange [17]. Indeed, it is not possible to measure the quota of heat flux absorbed by the glazing and released in the indoor environment to evaluate directly the g-value. For this reason an indirect evaluation was proposed, calculating the daily total energy crossing (E_{24TOT}, in Wh/m^2) the element and subtracting the long-wave energy crossing the component (E_{24}, in Wh/m^2). E_{24} is calculated as the product of the temperature difference and the equivalent thermal transmittance.

$$TSET* = \frac{E_{24TOT} - E_{24}}{E_{24}in}$$

In order to characterize the thermal performance of the different tested technologies it seems more useful to analyse the *surface heat fluxes*, assuming that a negative heat flux corresponds to a heat loss, under different representative conditions. In the analysis carried out by the authors it was selected a representative day for the different seasons under analysis, presenting peak boundary condition. The hourly value monitored by heat flux meter was plotted to analyse the dynamic of the façade ($\dot{q}$ in W/m^2). The same analysis was conducted for the solar radiation transmitted by the technologies (I_{in} in W/m^2). The algebraic sum of the two quantities represents the total heat fluxes crossing the transparent building envelope (in W/m^2). The integral of the heat fluxes over the day will correspond to the daily energy value. Energy are usually analysed evaluating positive heat fluxes and negative heat fluxes separately, in this way cooling energy and heating energy are assessed.
To evaluate the energy performance of adaptive façade system characterized by a ventilated cavity different synthetic indicator have been proposed: for the heating season (η and $b*tr$) and for the cooling season (ε). The pre-heating efficiency (η) assesses the capability of the façade to pre-heat the ventilation air flow rate during the cold season (heating periods) [17,20]. It is defined as:

$$\eta = \frac{t_{exh} - t_{inlet}}{t_{in} - t_e} \qquad (2)$$

A new metric for heating period was also developed. This metric is derived from a parameter (correction factor for an unconditioned adjacent space) used in the International Standard ISO 13790:2008. This metric allows estimating, during the winter period, the reduction of the transmission loss through an active façade [23].

$$b^*_{tr} = \frac{t_{out} - t_{cav}}{t_{cav} - t_{in}} \qquad (3)$$

The dynamic insulation efficiency was calculated during summer season and it assesses the capability of the air in the cavity to remove the solar heat gain [17,20].

$$\varepsilon = \frac{\dot{Q}_r}{\dot{Q}_{inc}} = \frac{\dot{m} \cdot c_p \cdot (t_{exh} - t_{inlet})}{\dot{m} \cdot c_p \cdot (t_{exh} - t_{inlet}) + \dot{q} \cdot A + \dot{q}_s \cdot A} \qquad (4)$$

4 Selected case studies

The cases studies discussed in this paper related only to transparent building envelope, belong to two different categories: components and systems. The distinction is a matter of scale: the transparent components constitute an element of the vertical façade while the transparent system constitute the entire façade and usually it presents a higher integration with the building systems. In this paragraph different case studies of components and system are presented. Only some results regarding the technologies tested are discussed in order to analyze the different performance indicators. Detailed energy performances of the technologies are reported in [7, 8, 14, 15, 17, 21, 22].

4.1 Active transparent façades

Active transparent systems have been studied since 2000 when the experimental apparatus TWINS was built on the roof top of the Politecnico of Torino Dept. of Energy. The technologies analyzed presented two transparent skins with an air ventilated cavity (belonging to climate façades and double skin typology). The transparent systems presented in this paper were characterized by different strategy of ventilation and different layers. The first transparent systems tested in TWINS were a climate façade and a hybrid-ventilated façade (CSa) [21]. One transparent system was tested at the time and it was compared to a reference façade mounted on the other test cell. The second case study is a real building under actual operating condition (CSb) [21]. This building presented a climate façade that was continuously monitored along two consequently years. The analysis were conducted comparing the thermal performance of the transparent system to a traditional continuous façade with a double glazing and a reflective façade. Lastly a mock-up of a tall building façade in construction in Torino was monitored in a real scale mock-up during the construction site (CSc). In this case the monitoring activity was aimed at evaluating two different solutions of transparent system façade mounted on the same mock up [22].

Figure 5: Monitored active transparent façades

The energy performance of an active transparent façade can be assessed through the evaluation of the heat fluxes during representative days and periods corresponding to different configurations of the façade, i.e. shading on and off or different ventilation rate in the cavity. The same evaluation can be also conducted for estimating an energy value representative of a seasonal value. The energy performance evaluated for CSa and CSb was then compared to a reference traditional reflective continuous façade, while for CSc the experimental activity was aimed at evaluating two different configurations of the same active façade. As it was described in paragraph 3.3 the method to evaluate the equivalent thermal transmittance is suitable for technologies characterized by scarcely dynamic behavior. As shown in figure 6 it is possible to see that the linear correlation is able to describe the traditional technology (R-CSb, figure 6 left graph), but for highly dynamic component, (CS2, figure 6 right), the coefficient of determination (R^2) is not satisfactory and the data are dispersed in the graph without following a linear correlation [14,15]. As discussed in [14, 15] conventional synthetic metrics are not fully able to replicate the thermo-physical behavior of the technologies. Two main limits can be outlined: firstly, these conventional parameters are evaluated with boundary conditions as close as possible to the stationary regime, so only night data are used neglecting the high dynamicity presented by the technology investigated; secondly one single parameter is not sufficient to represent the complex performance of these façades.

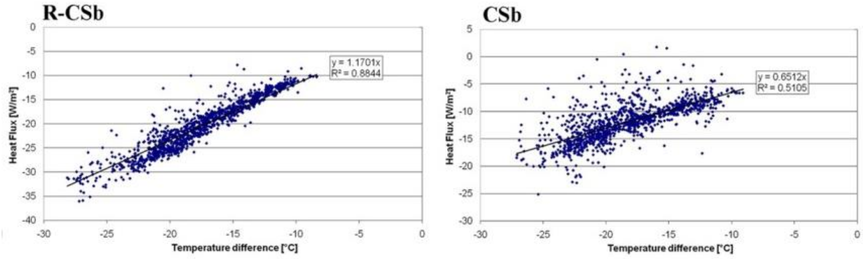

Figure 6: Equivalent thermal conductance of CSb (on the right) and of the reference technology (on the left)

The equivalent solar factor evaluated with equation 1 is a daily value and it varies as a consequence of the solar radiation and the ventilation rate in the cavity of the façade. The average value over the different seasons corresponds to an equivalent *TSET** value of the system façade. Discussing the equivalent solar factor evaluated with equation 1, firstly it is important to point out that the indicator is calculated with an equivalent *U-value* obtained with night data. Secondly the *TSET** parameter is evaluated assuming an equivalent *U-value* for the selected season, that do not consider the dynamic of the system. Despite the criticisms, the equation (1) is the only method to evaluate *TSET** through experimental data in test cell. Otherwise, it is possible to use a calorimeter apparatus for a more precise measurement with a higher cost and a limited dimension of the sample, which could influence the ventilation in the cavity. Synthetic parameter, as defined in equation 2, 3, 4, are able to assess the energy performance of the façade both in cooling and heating seasons. These parameters assess an efficiency of the system and they are mainly suitable to compare different façade configurations. In the graph in figure 11 are reported the results of two of the synthetic parameters. It is possible to notice that the value of the parameters is strictly influenced by the position of the shading. For each technology investigated two different lines define the performance according to shading position. These synthetic indicators are not able to fully describe the energy performance of the system [20]: actually comparing the value of the pre-heating efficiency η and of the b^*_{tr} metric a not relevant differences is shown between technologies that are characterized by different thermal resistance [20].

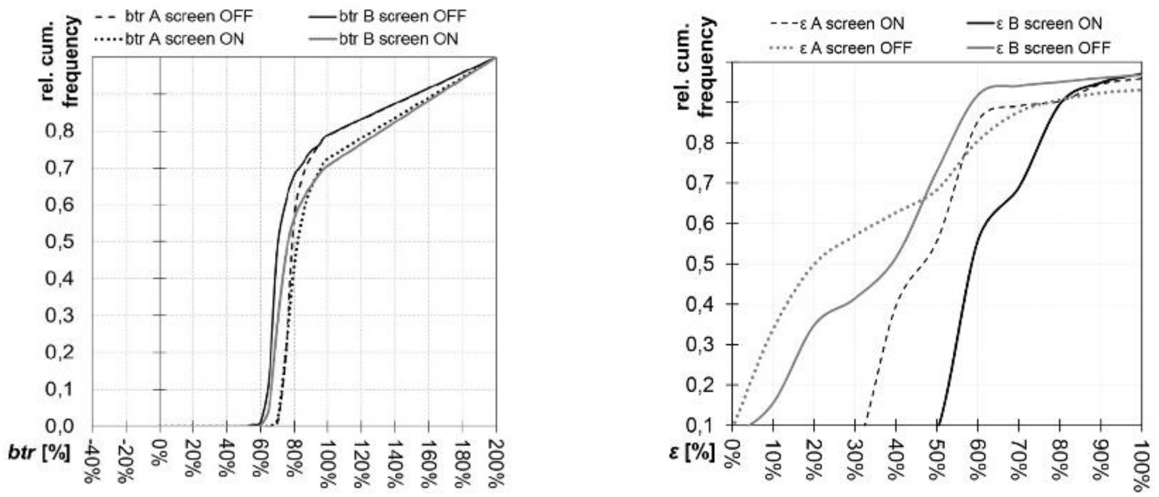

Figure 11: Synthetic indicators for CSc façades, left b*tr (left), ε (right).

4.2 Dynamic glazing

The research on this topic started in 2008, focusing on the novel opportunity to integrate PCM in the cavity of a double glazing unit. The main objective of the research was to develop an innovative smart window with a higher thermal inertia than a traditional transparent component and showing a dynamic behaviour able to control the visual and thermal comfort [8]. The new component with PCMs was in fact able to regulate the short-wave and the long-wave fluxes crossing the window thanks to the melting/solidification process of the PCM in the cavity. The PCM was a paraffin based material and it was selected with a melting temperature of 35°C. At the melting point the material changed its phase passing from solid and translucent to liquid and transparent. At the same time, also the visual transmittance of the component, besides changing as a function of the incident angle, varied during the day according to the state of the phase change material [7]. The first experimental activity was carried out on a prototype of double glazing containing liquid paraffin wax (CS0). Starting from the weak points of this first prototype a further case study was developed integrating a different typology of phase change material, microencapsulated (CS1). A more responsive new prototype was then developed integrating the PCMs in a triple glazing unit combined with a thermotropic layer (CS2) [8]. In this prototype it was experimented the possibility to regulate the amount of solar radiation impinging on the PCMs using the thermotropic glazing. The concept was to maintain the PCM in the transition phase as long as possible since previous monitoring campaigns outlined the drawbacks due to overheating phenomena occurring when the melting process was completed. The thermotropic glazing (TT) acted as a self-switching shading, modifying its optical properties according to its temperature, and reducing its transmittance when the temperature increased due to the back-scattering effect. Another aspect investigated on the prototype CS2 was the influence of the position of the

PCMs in the cavity. As the prototype was a triple glazing unit it was investigated the insertion of the material in the outer and inner cavity.
Lastly a new prototype was developed combining a triple glazing unit integrating PCMs with a photocromic layer (CS3). The concept was to develop a transparent smart component able to reduce the internal glare discomfort through the activation of the photocromic layer [23].

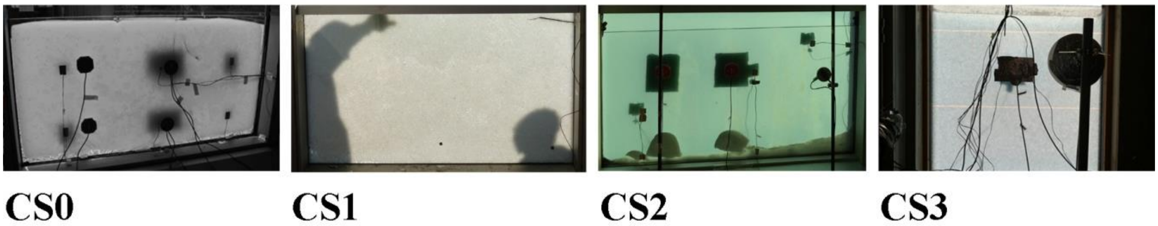

Figure 6: PCMs based adaptive glazing .

The energy performance of the proposed dynamic glazing was assessed comparatively with a traditional double or triple glazing unit. Thermal equivalent conductance evaluated for dynamic glazing was affected by the same criticisms indicated for active transparent façades. It was observed that the dynamic glazing with PCM presented a low coefficient of determination with a position of the points along the line jeopardized. In this case, the measurement in laboratory presented some limits: the convective and radiative heat transfer coefficients do not correspond to the reality and most of all the measurement had to be conducted simulating different state of the PCMs.
For this technology surface heat fluxes and energy were analyzed in three different days characterized by a low, average and high level of irradiance. It is interesting underline the different performance observed at the varying of the boundary conditions. The choice of the days to analyze was done considering two different aspects: the selected days should represent an average weather and had to be representative of the typical season conditions and at the same time, peak conditions had to be identified so to verify the energy behavior of the tested technology under limit conditions. The measured heat fluxes was integrated over the time (daily, weekly or seasonally) resulting as energy in Wh/m^2. Furthermore energy for cooling and heating was assessed separately considering respectively only the positive heat fluxes and the negative ones and a normalized energy value over the DD (Degree Day) was defined in order to compare different configurations measured during different periods. The evaluation of the optical and thermal properties of the dynamic glazing was then assessed in the laboratory through complementary measurement [19].

5 Conclusion

In this paper the methodology adopted by the authors to experimentally assess the energy behavior of adaptive transparent building envelope is described. Some key points are outlined concerning the experimental apparatus to be used and the attention to be paid to avoid not negligible errors due to transparency and dynamicity of the samples tested. Furthermore the main performance parameters to assess the energy behavior of active transparent façade and dynamic glazing is investigated presenting some case studies carried out by the authors. The standard analysis of heat flux and energy is briefly presented, giving some indications on the selection of the analysis periods. New performance metrics are presented and limits related to the use of conventional parameters such as *U-value* and *g-value* is underlined. Results showed that further research and experimental analysis on this topic should be conducted and that the complex behavior of adaptive technologies can hardly be defined by a single parameter as for traditional glazing.

6 Acknowledgements

The results of different research project are presented in this review: the Polight pProject SMARTGlass and three commercial contracts with manufacturers SOMEC, Teleya and Coopsette. The results presented have been collected over 10 years by the Research Group TEBE, Building Envelope Technologies R.U, Politecnico di Torino. The achievements presented in the paper have been reached thanks to the work of professors, researchers, students and technicians.

7 References

[1] Guillen, I., Gómez-Lozano, V., Fran, J.M., López-Jiménez, P.A.: *Thermal behavior analysis of different multilayer façade: Numerical model versus experimental prototype*, in: Energy and Buildings 79 (2014), pp. 184-190.

[2] Asdrubali, F., D'Alessandro, F., Baldinelli, G., Bianchi, F.: *Evaluating in situ thermal transmittance of green buildings masonries—A case study*, in: Case Studies in Construction Materials 1 (2014), pp. 53–59.

[3] ISO 9869 (1994) Thermal insulation - Building elements - In-situ measurement of thermal resistance and thermal transmittance.

[4] OKALUX, www.okalux.de

[5] Spacia Pilkinton, www.pilkington.com

[6] Baetens, R., Jelle, B.P., Gustavsen, A.: *Properties, requirements and possibilities of smart windows for dynamic daylight and solar energy control in buildings: a state-of-the-art review*, in:Solar Energy Materials & Solar Cells 94 (2010), pp. 87–105.

[7] Goia, F., Perino, M., Serra., V.: *Experimental analysis of the energy performance of a full-scale PCM glazing prototype*, in: Solar Energy 100 (2014), pp.217-233.

[8] Goia, F., Bianco, L., Cascone, Y., Perino, M., Serra, V.: *Experimental Analysis of an Advanced Dynamic Glazing Prototype Integrating PCM and Thermotropic Layer*, in: Energy Procedia 48 (2014), pp. 1272-1281.

[9] GLASSX, www.glassx.ch.

[10] Ritter, V.: *Fluidglass, an adaptive glazing,* in Façade 2014 – Conference on Building Envelopes, Adaptive Building Envelopes, Symposium, 28th November 2014, pp. 76-83.

[11] Gil-Lopez T., Gimenez-Molina C.: *Environmental, economic and energy analysis of double glazing with a circulating water chamber in residential buildings*, in: Applied Energy 101 (2013), pp. 572–81.

[12] International Building Exhibition (IBA) in Hamburg, 2013, ARUP, www.arup.com.

[13] Xu X., Dessel S Van: *Evaluation of an Active Building Envelope window-system*, in: Building and Environment 43 (2008), pp.1785–91.

[14] Bianco, L., Goia, F., Serra, V.*: Energy performance assessment of advanced glazed façades in office buildings*, in: CLIMA 2013 11th REHVA World Congress and the 8th International Conference on IAQVEC, Prague, Czech Republic, 16/06-19/06/2013. pp. 4680-4690.

[15] Goia F., Bianco L., Serra V., Perino M.: *Energy Performance Assessment of Advanced Integrated Façades by Means of Synthetic Metrics,* in: Lecture notes in electrical engineering 263 (2013) pp. 21-28.

[16] Janssens, A., Roels, S., Vandaele, L.: *Full scale test facilities for evaluation of energy and hygrothermal performances,* (2011), BFG, UGent, Belgium.

[17] Corgnati, S. P., Perino, M., Serra, V.: *Experimental assessment of the performance of an active transparent façade during actual operating conditions,* in Solar Energy 81 (2007), pp. 993-1013.

[18] Bianco, L., Serra, V., Fantucci, S., Massolino, M., Dutto, M.:*Thermal insulating plaster as a solution for refurbishing historic building envelopes: First experimental results,* in: Energy and Buildings, article in press, available on line.

[19] Goia, F., Zinzi, M., Carnielo, E., Serra, V., *Spectral and angular solar properties of a PCM-filled double glazing unit,* in: Energy and Building 87 (2015) pp. 302–312.

[20] Goia, F., Bianco, L., Perino, M., Serra, V., *Energy performance assessment of and advanced integrated façade through experimental data analysis,* in: Energy Procedia 48, (2014) pp. 1262-1271.

[21] Serra, V., Zanghirella, F., Perino, M.: *Experimental evaluation of a climate façade: Energy efficiency and thermal comfort performance,* in: Energy and Building 42 (2010) pp.50-62.

[22] Bianco, L., Goia F., Lo Verso V.R.M., Serra V.: *Light and energy performance of an active transparent façade: an experimental study in a full scale office room mock-up,* In: CISBAT 2013, CleanTech for Smart Cities and Buildings-From Nano to Urban Scale, Lausanne, Switzerland, September 4-6, 2013. pp. 133-138.

[23] Simion, N., *Involucro Dinamico e Adattivo Integrato,* Master thesis in Architecture, 2014, Politecnico di Torino, tutors: V. Serra, F. Peron, L. Bianco.

Building Envelope Test CELL: development of an indoor test cell for advanced façade systems thermal performance assessment

Fabio Favoino, PhD fellow
Department of Engineering, University of Cambridge, UK, ff279@cam.ac.uk

Stefano Fantucci, PhD fellow
Department of Energy, Politecnico di Torino, Italy, stefano.fantucci@polito.it

Valentina Serra, Associate Professor
Department of Energy, Politecnico di Torino, Italy, valentina.serra@polito.it

Marco Perino, Full Professor
Department of Energy, Politecnico di Torino, Italy, marco.perino@polito.it

Summary

This paper describes the development of a new facility for testing building envelope systems called Building Envelope Test cell (BETcell), implemented at Politecnico di Torino. The test facility is aimed at characterizing the thermal performance of building envelope components and systems in realistic boundary conditions (real world climatic conditions), but yet controllable. This becomes particularly important when the thermal performance of the building envelope system depends on the boundary conditions (i.e. responsive building envelope elements and multifunctional facades) and when the characterization of the whole façade system is required, in order to reduce the resources needed for outdoor testing. The integration with an outdoor test facility and a guarded hot plate enable a complete thermal characterization of building envelope systems, components and/or materials. The aim of the BETcell is to provide the building industry with an instrument that will enhance the development of innovative and low-energy building envelopes.

Keywords: Building envelope testing, test cell, thermal properties measurement, energetic characterization, façade performance.

1 Introduction and aims

The performance of the building envelope, both opaque and transparent, and the interface between these two parts and between the building envelope and the building structure itself, play a fundamental role in achieving high performing buildings in terms of both energy consumption and indoor environmental quality. The experimental assessment of the environmental performance of building envelope technologies is a fundamental but non-trivial task. This is particularly important for integrated façade systems which present more innovative characteristics as more complex geometries, multi-functionality, responsiveness and adaptive behavior. Nevertheless it is widely recognized for traditional façade systems, as well as for more innovative ones, that the environmental performance is not just the sum of the single components or layers performances, and that the overall performance in actual operating conditions could be different than the one measured in laboratory or calculated analytically. Moreover some aspects of thermal performance (mainly as far as adaptive façade materials and systems are concerned) depends on boundary conditions. For these reasons full scale testing in dynamic realistic boundary conditions is often required.
Testing in outdoor climate for the thermal characterization of full scale façade systems and components is on one hand very reliable in order to determine the actual thermal behavior of building envelope systems, but on

the other hand present some limitations: long monitoring period, results influenced by the specific climatic context of the experiment, uncontrollable and unstable boundary conditions.
Therefore parallel to center of panel steady state measurement of building envelope thermal characteristics by means of hot box apparatus [1-2], and of steady state thermal bridge effect measurements by means of hot box apparatus [3], some example of climatic chambers were used in order to test some specific performance of building envelope component in dynamic controllable boundary conditions (single [4] and double [5] environment chamber). Nevertheless the few existing apparatus in which dynamic boundary conditions can be superimposed are either not able to integrate steady-state and dynamic measurements or cannot house full scale façade systems.
This paper presents a newly developed Test Cell for Building Envelope technologies called BETcell. This facility aims to characterize the overall environmental performance of traditional and innovative façade systems in real dynamic environmental conditions, but yet controllable. The test cell is built in the laboratories of the Department of Energy of the Politecnico di Torino in Italy, having two controllable environments (one with dynamic conditions simulating the external climate) separated by an adaptable frame used to house the façade components to test. The test cell is part of a bigger test rig aimed at characterizing the complete overall thermal performance of building envelope systems, components and materials. The aim of the BETcell is to provide the building industry and the building envelope research community with an instrument that will enhance the development of innovative and low-energy building envelope solutions.
The second section of the paper contains the description and the calibration of the experimental apparatus. The third section presents the kind of experimental characterizations that could be performed, together with the façade components and systems that could be tested. Finally some results from different tests are presented in the forth section with the purpose of showing some first measurements performed, together with presenting some possible upgrades for additional potential tests that could be done with this test facility.

2 The building envelope test cell

2.1 BETcell description

The test facility called “BETcell”, acronym for Building Envelope Test Cell, is a climatic chamber aimed at characterizing the thermo-energetic performance of building envelope component and systems in both steady-state and dynamic boundary conditions, in a controllable laboratory environment.
To this end the climatic chamber is built as two separate environments separated by a frame that can house the specimens to be tested. The general layout and a photo of the BET cell are shown in Fig 1.
The overall sizes of the BETcell are 2.74 m width, 4.84 m length and 2.34 m height, and it is located in a laboratory environment of steady daily temperatures. The size of the frame can be easily adjusted in order to host building envelope elements of different frontal dimensions (width x height), maximum sizes 240 cm height and 275 cm width, and different thicknesses with a maximum thickness of 50 cm. A frame with such sizes can easily house most of the building envelope elements/construction. Although the frame dimensions (mainly height) is lower than a typical floor-to-floor height, the thermo-energetic performance of a higher element can be easily and accurately scaled from measurements of smaller specimens. Moreover more than one building envelope component could be tested at the time, if the overall dimensions of the specimens together do not exceed the hosting capacity of the frame, in order to reduce testing time and to measure the physical quantities of interest in the exact same boundary conditions.
The two environments on both side of the specimen frame can reproduce the boundary conditions of a typical outdoor environment (sub-module “A”), and of a typical indoor environment (sub-module "B"). The sub-module A can be accessed through a door from the outer laboratory environment while the sub-module B can be inspected through a door between the two sub-modules. The two sub-modules present sizes of 240 cm height and 275 cm width while the depth is respectively 300 cm (A) and 165 cm (B).
In order to reproduce typical outdoor and indoor boundary conditions the two sub-modules are equipped with an HVAC system (including fans and PID controller) able to control air temperature, humidity and speed, with a relatively uniform temporal and spatial distribution. In order to ensure such a uniformity, as far as air speed is concerned, a transparent curtain was placed in each environment, parallel to the frame and with an adjustable distance from it to suit measurement requirements. In the sub-module A the air temperature and humidity can

be controlled with both a steady (±0.5 °C) and a dynamic profile (12/40°C, sinusoidal variation with a controllable period). In the sub-module B a steady set point temperature can be maintained, with an accuracy of ±0.3 °C, between 20 and 50 °C. The temperature difference between the two environments could be up to 40 °C, if a specimen with a high thermal resistance is placed between the two environments.
The BET cell is integrated into a bigger test facility (called ABEEC test facility, Advanced Building Envelope Energy Characterization test facility), aimed at characterizing the complete thermo-energetic performance of building envelope materials, components and systems. This facility integrates the BETcell with a guarded heat flow meter (GHFM), and with an outdoor test facility called TWINS, presenting two twins outdoor test cells that could house building envelope mock-ups of variable dimensions up to 175cm width and 350 cm height [6]. A picture of the other two integrated testing facilities is shown in Figure 2.

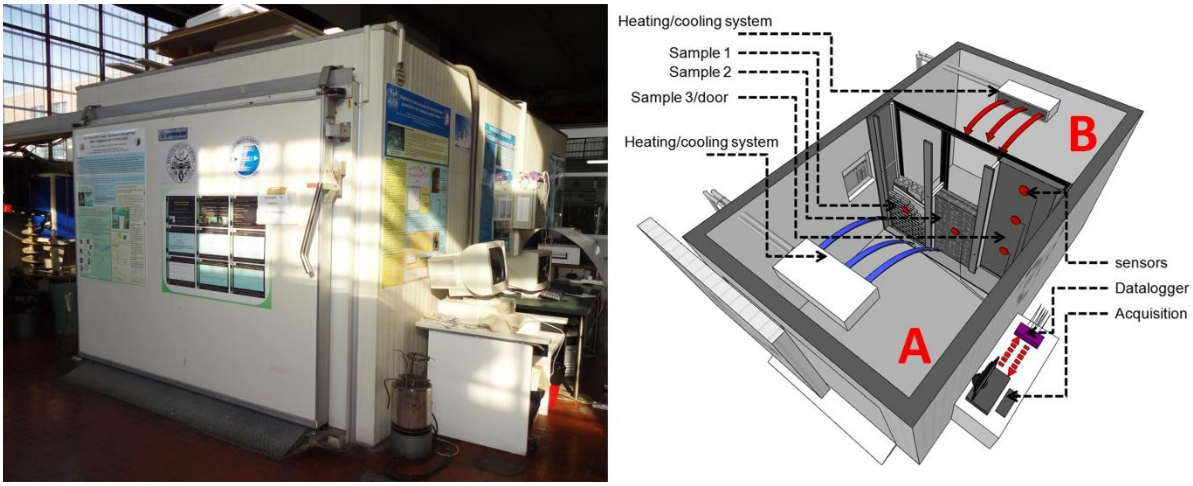

Figure 1: BET cell picture and schematic representation.

Figure 2: (a) Guarded heat flow meter (GHFM), (b) TWINS outdoor testing facility.

The BET cell is equipped with a monitoring apparatus consisting of two PCs (one to control the BET cell and one to control the measurement apparatus), two expandable data loggers (16 analog channels each) and the measurement apparatus consisting in all the sensors that can be employed in the BET cell. The basic sensor equipment installed in the BET cell consists of:

- Air and surface temperature: 36 (type T) thermocouples;
- Surface temperature: infrared camera (Testo 875);
- Heat flow: 12 heat flow meter plates, of which 4 smaller ones can be employed when higher resolution heat flow measurements are required, such as in the case of transparent component thermal bridges.

This can be further expanded with the following equipment to suit experimental requirements:

- Data logger expansions (additional 20 analog channels);
- Surface temperature: additional infrared camera (NEC ThermoTracer TH9100MV/WV);
- Air velocity and flow rate: pressure tap, gas tracer equipment (Bruel and Kyaer gas monitor 1302), hotwire anemometers and ultrasonic anemometer;

When the infrared camera is used on reflective surfaces a black tape is employed on the surface in order to avoid the so-called "narcissus" effect (reflection of the operator/equipment on the surface of interest).

2.2 BETcell measurement apparatus calibration

The accuracy of all the basic equipment sensors employed in the BET Cell is provided in Table 1 corresponding to a Confidence Interval of 95% (CI 95%).

Table 6 - Accuracies of the measurements apparatus

T	ε	T_{IR}	T_{IR}	T_{IR}	HF		IR pixel	T_{PR}	T_{REFL}
Max	TIR - T avg (space and time)	ε n/a	ε from spot measure	ε from avg measure	Type 1	Type 2	iFOV	T	All (ε=1)
[°C]	[-]	[°C]	[°C]	[°C]	[%]	[%]	[m]	[°C]	[°C]
0.18	0.02	2	0.6	0.22	5.0%	10.0%	0.009	0.3	0.9

To calibrate the thermocouples within their operating range (-20°C to 80°C), their measurements were compared against a reference platinum thermo-resistance PT-100 at three different temperatures (0°C, 30°C and 60°C). The emissivity of the specimen surfaces is characterized by comparison of the infrared camera measured temperature (T_{IR}) with the spatial and temporal average of the temperature measured by means of thermocouples. This is an "apparent" emissivity, that is compensating for different sources of error of the IR camera measurement [2], meaningful only for the specific test set-up. Therefore T_{IR} can be measured with different accuracies, according to an unknown emissivity, a calculated one by means of a spot comparison with the thermocouple and an averaged one compared to a time series of thermocouple measurements. The planar radiant temperature referred to a certain surface can be measured by means of surface temperature measurements and view factor calculations (T_{PR}) or by means of IR camera measurement (with unitary emissivity) of a wrinkly aluminum tape placed on the surface of interest (T_{REFL}). The spatial and temporal uniformity of air temperature in both environments is shown in Figure 3. The air temperature is measured by three thermocouples in each environment (cold, A, hot, B) at three different heights form the floor (50,100,150 cm). Figure shows the trend of the air temperature measured in both environments (steady state and stabilized periodic temperature control are showed for sub-module A). The grey areas represent periods in which the doors of both environments are opened, a relatively low thermal inertia is associated with both environment, so that steady state conditions can be reached in a short amount of time.

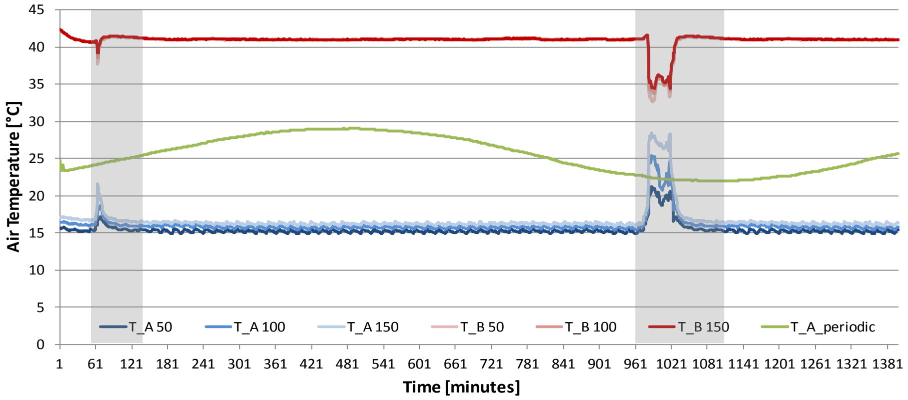

Figure 3 - Trend of the air temperature at different heights and in different boundary conditions.

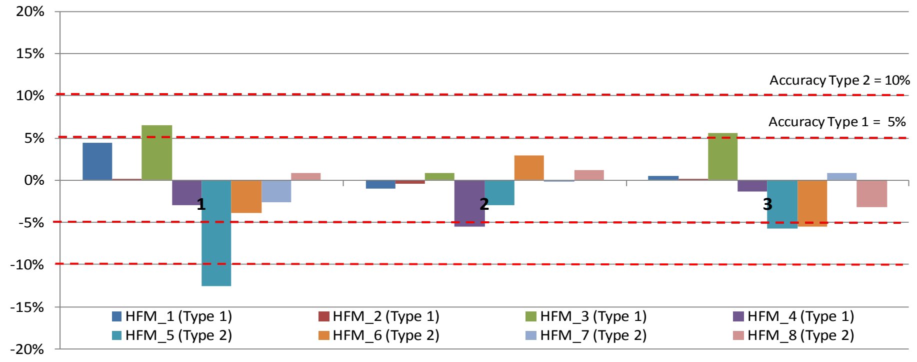

Figure 4 - Deviation of the λ measured by means of each HFM from the λ values measured with the hot plate

In order to calibrate the heat flow sensors, a series of tests was performed on an opaque panel comparing the thermal conductivity of the construction measured by means of the BET cell apparatus with the one measured by means of the GHFM according to EN ISO 12667 [13]. Eight heat flow sensors were placed on the same side of the panel while three thermocouples per side were used to detect the surface temperatures. Different tests were performed placing the heat flow sensors on the cold side or on the hot side of the panel. The deviation for each test and for each heat flow sensor from the guarded hot plate measured thermal conductivity is shown in Fig. 4. Given that the accuracy of HFM type 1 is 5%, and that one of the HFM type 2 is 10% (C.I. 95%), as shown by the dashed red line in Figure 4, there is no need or any compensation of the heat flow measurements. More information about the accuracy of specific measurements is given in section 4.

3 Overview of BET cell measurements

The BETcell test facility described in section 2 can be used to experimentally evaluate the thermo-energetic performance of both transparent and opaque building envelopes. In particular the following performance metrics can be measured:

- steady state thermal parameters: thermal transmittance *U* and thermal resistance *R* [14];
- thermal bridging effect: linear thermal transmittance ψ[17];
- dynamic thermal parameters: periodic thermal transmittance $|Y_{mn}|$, time lag Δt and decrement factor *f* [16];
- dynamic insulation parameters: dynamic insulation efficiency ε , heat recovery efficiency $\eta_{recovery}$ and pre-heating efficiency $\eta_{pre\text{-}heat}$ [6, 7];

The BETcell apparatus can be used to characterize the above performance metrics for different kind of building envelope materials, components and systems:

- Single and multilayer walls;
- Frame wall construction and structural joint in ETICS (External Thermal Insulation Composite. Systems) [8,9];
- Dynamic insulated wall (parietodynamic) [10,11];
- Glazing materials and transparent façade;
- Multifunctional and double skin façade [6, 7, 12].

Table 2 shows a complete picture of the possible experimental tests using BETcell apparatus, while some example of tested envelope systems are reported in figure 6 and 7. In the results section some preliminary performance characterizations are showed for different metrics and building envelope components, which are shown in bold characters (**X**) in Table 2. For the sake of brevity this results are not detailed and only explanatory of some basic tests that could be performed with the BETcell. All the other possible tests were either not performed yet, or presented in dedicated publications (i.e. dynamic insulation parameters [11]).

Table 2: Overview of the possible test

Typology	Figure	Component classification	Steady state metrics	Dynamic thermal metrics	Thermal bridge metrics	Dynamic insulation metrics
Single layer wall	Figure 5a	opaque	X	**X**	-	-
Multilayer wall	-	Opaque	**X**	X	X	-
Frame construction and ETICS	Figure 6a	opaque	X	-	X	-
Parietodynamic	Figure 5b	opaque	X	X	X	X
Glazing	Figure 6b	transparent	**X**	-	X	-
Whole Façade System	Figure 6b	transparent/opaque	X	X	**X**	-
Multifunctional / adaptive façade	-	transparent/opaque	X	X	X	X

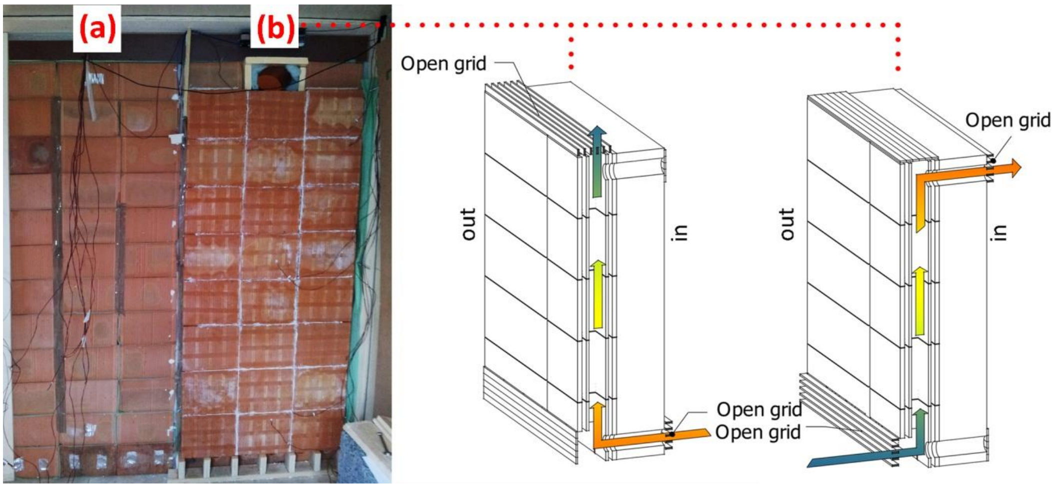

Figure 5: (a) Bricks solid wall, (b) parietodynamic wall.

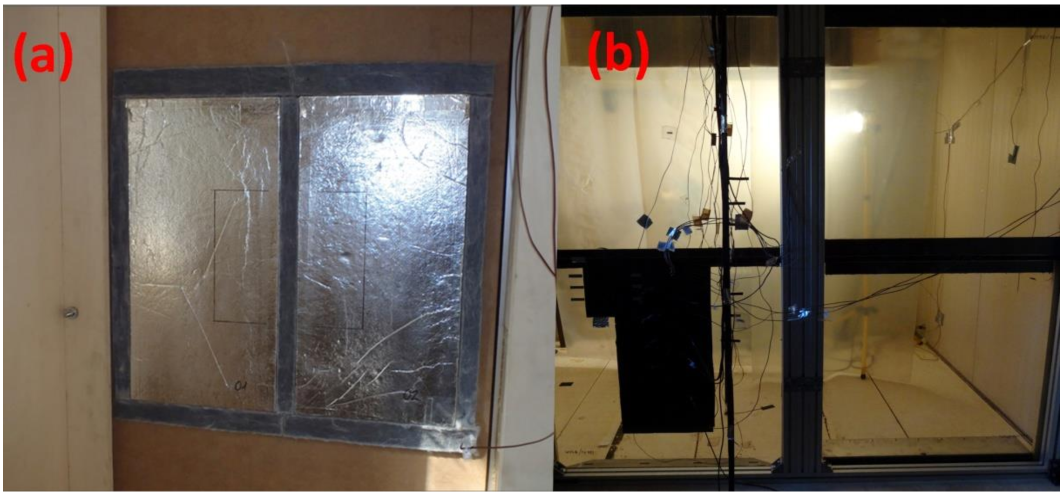

Figure 6: Thermal bridging measurement of : (a)Vacuum insulated panels for ETICS, (b) Glazing façade frames.

4 Overview of possible measurements

4.1 Steady state R-value measurements

The steady state R-value of 2 specimens was evaluated, using two different methodologies: EN ISO 9869 [15] by means of the BET cell test facility and the more accurate EN ISO 12667 [13]. The latter is done by means of either the guarded heat flow meter available in the integrated ABEEC test facility, or what is declared by the component manufacturer (test done by a Hot Box apparatus), respectively. The second methodology is used as a term of reference for the measurement done by means of the BET cell. The two specimen evaluated were a multilayered wall panel (6 mm MDF and 21 mm of XPS) and a double glazed unit (6-10-6 mm with argon filled cavity and low-e coating, U-value = 1.60 W/m^{2}K). The R-value does not include the indoor and outdoor surface heat transfer coefficients. The boundary conditions for the two tests were:

- For the heat flux measurement in the BET cell, the temperature of the two sides of the specimens were maintained constant with a difference of 25.00 ±0.2 °C;
- For the second methodology, for either guarded heat flow measurements (GHFM) and BET cell measurement a temperature difference of 20°C between the two plates was used;

The measured heat flux density and the thermal resistance *R* determined using 2 different typology of heat flux plates, HF-Type 1 and HF-Type 2, and the average of all heat flow sensors in the BETcell were compared to the reference values for the opaque component (Table 3) and the transparent one (Table 4).

Table 3: Experimental results for the opaque component

Method	Sensor	Q_{avg} [W/m^2]	R [m^{2}k/W]	ΔR [%]
GHFM (EN ISO 12667)	-	-	0.682	-
BET cell	HF- Type 1	27.01	0.650	-4.9
BET cell	HF- Type 2	26.10	0.672	-1.4
BET cell	HF_{avg}	25.75	0.674	-1.2

Table 4: Experimental results for the transparent component

Method	Sensor	Q_{avg} [W/m^2]	R [m^{2}k/W]	ΔR [%]
Manufacturer	-	-	2.197	-
BET cell	HF- Type 1	37.63	2.209	+0.5
BET cell	HF- Type 2	37.77	2.217	+0.9
BET cell	HF_{avg}	37.28	2.188	-0.4

As expected the results shows a little divergence *ΔR* between the BETcell and the guarded heat flow meter measurement for each sensor, anyway below ±5% and ±10% (typical accuracy of the heat flow sensors of different types used). Very small differences with the reference values are measured when the heat flow meter measurements are averaged.

4.2 Measurement of the façade dynamic thermal performance

The dynamic thermal performance of an hollow clay bricks wall (Figure 7) was experimentally evaluated using the BETcell apparatus, during the test the side B of the chamber was maintained at the constant temperature of 40°C while the side B temperature was swing controlled at 23.5 ±5°C with a period of 24h.

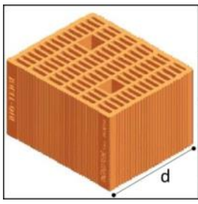

R [m²K/W]	0.964
ρ [kg/m³]	950
c [J/kgK]	830
d [cm]	24.2

Figure 7: thermal properties of the hollow clay brick used in order to calculated the specific performance metrics.

Figure 8 shows the graphic results of external surface temperature T_{se} (boundary condition on side A) and the heat flow density measured on the internal side q_{si} (response on side B), the approximated values of T_{se} and q_{si} required to calculate the dynamic thermal performance metrics are reported in dashed line, while the dotted lines represent the measured signal of thermocouples TT and heat flow meter of Type 1.

The time lag Δt was determined as the time difference in the peak of the lower surface temperature on side A ($T_{se,min}$) and the maximum heat loss density measured on side B $q_{si,max}$, moreover the periodic thermal transmittance module $|Y_{mn}|$ was determined using equation (1) according to [16], the experimental and the calculated results are reported in table 5.

$$|Y_{mn}| = \frac{|Q_{si,\max} - Q_{si,avg}|}{|T_{se,\min} - T_{se,avg}|} \quad (1)$$

where $T_{se,avg}$ is the average surface temperature of side A while $Q_{si,avg}$ represent the average heat flux density measured on side B. The periodic thermal transmittance $|Y_{mn}|$ was calculated in a stabilized period cycle (sub-module B temperatures are controlled with a periodic trend for a multiple of the 24 hour period, only the last cycle is then considered for the measurements).

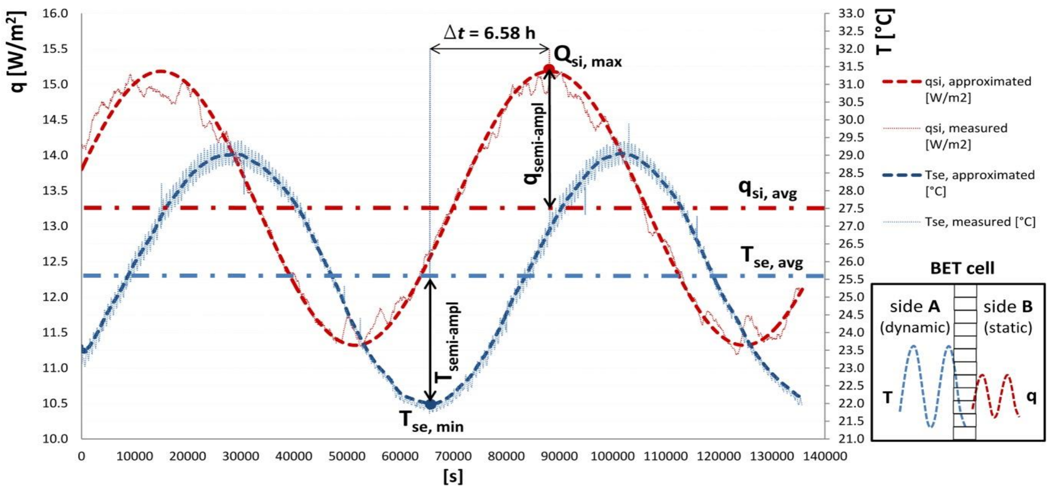

Figure 8: Dynamic test: experimental results.

Table 5: Comparison between experimental and calculated results [x].

Δt [h]		Δt (divergence) [%]	$|Y_{mn}|$ [W/m²K]		$|Y_{mn}|$ (divergence) [%]
Exp	Calc [16]		*Exp*	Calc [16]	
6.58	6.92	4.9%	0.547	0.567	3.6%

The time shift experimentally measured shows a deviation of the order of magnitude of ≈20 minutes (around 5%) compared to the calculated one using the admittance calculation method according to EN ISO 13786 standard, while the module of the periodic thermal transmittance $|Y_{mn}|$ shows a divergence around 3.6% compared to the calculated value.

4.3 Measurement of the thermal bridging effect

The quantitative evaluation of the thermal bridge effect in building envelope systems can be performed by means of the BET cell facility using two different methods, both of them based on thermo-metric measurements of physical quantities in both the undisturbed area and in the disturbed area. The undisturbed area is that area not influenced by the thermal bridge, where one dimensional heat transfer is present (l_{1D}), while the disturbed one is the area affected by the thermal bridge, where two or three dimensional heat transfer occurs (l_{TB}). The first method relies on the measurement of the heat flow density and surface temperatures in different points along a line perpendicular to the thermal bridge in the disturbed area, where an higher spatial resolution depending on the sizes of the thermal bridge is required in order to capture the trend of the heat flow density and of the surface temperatures. The second method relies on the measurements of surface temperatures only, this can be done by the only help of an IR camera, and it is based on the hypothesis of uniform surface heat transfer coefficients in both the disturbed and undisturbed area [2].
The sensors used and the area of the measurements for both methods are shown in Fig. 9 (right), for the case of a transparent unitized façade system. The black area corresponds to the black tape used on the glass surface in order to avoid the "narcissus" effect with the IR camera. Moreover Fig. 9 (left) shows a set of results from a typical test on a transparent façade system mock-up, highlighting the trend of surface temperatures measured by means of thermocouples (on both sides of the mock-ups) and IR camera, together with the trend of the heat flow density.
The thermal bridge effect is characterized with both methods by means of the ψ-value [W/mK] according to EN ISO 14683 [17]. A comparison between the ψ-value calculated by means of the heat flow meter measurements (ψ-value $_{HFM}$) and by means of the IR camera (ψ-value $_{IR}$) is shown in Table 6.

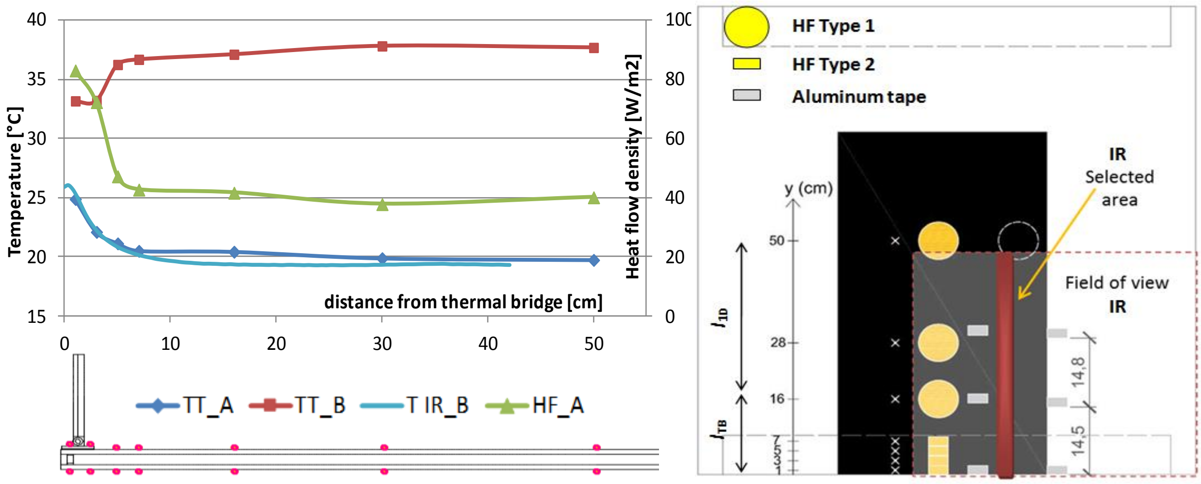

Figure 9: Measurement of thermal bridge effect and sensors placement.

Table 6: Experimental results

Element	Method	ψ-value [W/mK]	Δψ-value [%]
Transparent	HFM - Test 1	0.0733	-
Transparent	HFM - Test 2	0.0698	-
Transparent	IR	0.0816	-

5 Discussion and conclusion

This paper describes the development of a new facility for testing building envelope systems called Building Envelope Test cell (BETcell) at Politecnico di Torino. The test facility is aimed at characterizing the thermal performance of building envelope components and systems in realistic boundary conditions (real world climatic conditions), but yet controllable. The integration with an outdoor test facility and a guarded hot plate enable a complete thermal characterization of building envelope systems, components and/or materials.

The thermal performance of different possible building envelope components and systems could be tested by means of BET cell test facility, in which different performance metrics can be characterized. These includes steady states and dynamic performance metrics, that could be referred to the center of panel only or to a whole facade system. Some first preliminary results demonstrated the testing capability of the BETcell and the integration with the bigger testing rig.

Possible upgrades of the test facility are currently being explored. These upgrades will have the aim to perform a more comprehensive thermo-energetic performance characterization of façade components and systems. Among the other options the possibility of upgrading the test facility with a solar lamp (increasing the cooling capacity of the sub-module A as well) could have the biggest return in terms of possible performance metrics that could be measured: from durability and structural integrity due to high temperatures, to dynamic metrics as dynamic insulation and pre-heating efficiency for dynamic facades, to g-values and T-vis of transparent systems. Moreover a full calibration of the heat gains/losses (conductive and by means of ventilation) of the entire test cell and metering of the HVAC loads could be possible for calorimetric purposes.

6 References

[1] Asdrubali, F., Baldinelli, G.: *Thermal transmittance measurements with the hot box method: Calibration, experimental procedures, and uncertainty analyses*, in: Energy and Buildings 43 (2011), pp. 1618–1626.

[2] Asdrubali, F., Baldinelli, G., Bianchi, F.: *A quantitative methodology to evaluate thermal bridges in buildings*, in: Applied Energy 97 (2012), pp. 365–373.

[3] Martin, K., Campos Celador, A., Escudero, C., Gómez, I., Sala, J.M.: *Analysis of a thermal bridge in a guarded hot box testing facility,* in: Energy and Buildings 50 (2012), pp. 139–149.

[4] Ferrari, S., Zanotto, V.: *The thermal performance of walls under actual service conditions: Evaluating the results of climatic chamber test*, in: Construction and Building Materials 43 (2013), pp. 309–316.

[5] Ulgen, k.: *Experimental and theoretical investigation of effects of wall's thermophysical properties on time lag and decrement factor*, in: Energy and Buildings 34 (2002), pp. 273-278.

[6] Corgnati, S.P., Perino, M., Serra, V.: *Experimental assessment of the performance of an active transparent facade during actual operating conditions*, in: Solar Energy 81 - 8 (2007), pp. 993‑1013.

[7] Serra, V., Zanghirella, F., Perino, M.: *Experimental evaluation of a climate facade: energy efficiency and thermal comfort performance*; Energy and buildings 42; 2010; pp. 50-62.

[8] Lorenzati, A., Fantucci, S., Capozzoli, A., Perino, M.: *The Effect of Different Materials Joint in Vacuum Insulation Panels,* in: Energy Procedia 62 (2014), pp. 374–381.

[9] Fantucci, S., Favoino, F., Capozzoli, A., Perino, M.: *Experimental Analysis on Advanced Insulation System*, Proceding of CLIMA 2013 - 11th REHVA World Congress and the 8th International Conference on Indoor Air Quality, Ventilation and Energy Conservation in Buildings, Prague (2013).

[10] Imbabi, M.S.: *A passive-active dynamic insulation system for all climates*; International journal of sustainable built environment 1 (2012), pp. 247-258.

[11] Fantucci, S., Serra, V., Perino, M.: *Experimental assessment of the energy performance of an advanced ventilated clay bricks façade,* (in preparation).

[12] Favoino, F., Goia, F., Perino, M., Serra, V.: *Experimental assessment of the energy performance of an advanced responsive multifunctional façade module,* in: Energy and Buildings 68-B (2014), pp. 647-659.

[13] EN ISO 12667:2002 Thermal performance of building materials and products - Determination of thermal resistance by means of guarded hot plate and heat flow meter methods - Products of high and medium thermal resistance.

[14] EN ISO 6946:2008 Building Components and Building Elements. Thermal Resistance and Thermal Transmittance. Calculation Method.

[15] EN ISO 9869:2014 Thermal insulation - Building elements - In-situ measurement of thermal resistance and thermal transmittance.

[16] EN ISO 13786:2007 Thermal performance of building components - Dynamic thermal characteristics - Calculation methods.

[17] EN ISO 14683:2008 Thermal bridges in building construction, Linear thermal transmittance, Simplified methods and default values.

[18] EN ISO 12567-1:2000 Thermal performance of windows and door. Determination of thermal transmittance by hot box method–Complete windows and doors.

A new façade generation – iconic skin SCF

Heiko Mertel, Senior Project Manager
iconic skin GmbH, Germany, heiko.mertel@seele.com, www.iconic-skin.com

Summary

The iconic skin is a new integral double skin façade concept. Its main advantage is a wide range of combination possibility of the transparent and opaque façade parts within one unit, while a minimum amount of visible joints between the elements are necessary. The façade has a homogeneous appearance. The shading device could be incorporated in the transparent part of the cavity of the double skin façade. A pressure equalization of the façade cavity is realized by the new developed system of self conditioning façade (SCF). The SCF concept is a passive, self-sufficient system, which allows designing large façade cavities without condensation.

Keywords: multi-layered façade, pressure equalization, SCF, condensation risk, self conditioning facade, …

1 Introduction

Double-skin façade units have a long tradition and are not an invention of these days. So-called box-type windows have been installed to increase thermal properties. Inherent problems like condensation and pollution within the cavity were well-known and have been encountered by operable parts in the interior skin to allow maintenance. The French approach of "respiring IGUs" (vitrage respirant) also asks for removable inner skins to react on system's failures. Thus, motivation for improvement is driven by the approach of a multi-layered façade element with enlarged cavity to integrate solar shading devices combined with fixed glazing without necessary access to cavity for cleaning or maintenance purpose. The approach is governed by a closed cavity design where disadvantageous load cases due to pressure differences require reduction of pressure situation within cavity. Here, the basic "respiring" idea serves to equalize the pressure difference and to allow the interaction between cavity and outside conditions. Condensation within the cavity is prevented by correctly designed filters leading to balanced vapour compensation within the cavity with respect to outside conditions: a self conditioning cavity without additional M&E requirements.

2 SCF concept

The seele Self Conditiononig Façade concept is based on a multi-layered façade element with increased cavity between inner and outer skin to integrate sunscreen shading devices. The self conditioning cavity allows pressure equalization without condensation and, thus, avoids disadvantageous load cases due to pressure differences. The self conditioning is based on the consideration and utilization of thermo-physical interrelations within the cavity. The conditioning of the cavity results from a self-regulating, coordinated interaction of thermal properties of the façade with fluid-mechanical effects during vapour compensation. The conditioning occurs without the exchange of important air flow from the cavity, thus not affecting the thermal properties of the façade unit. The self conditioning happens totally self-sustaining without external intervention. No external energy supply or control units are necessary. The cavity is protected against pollution and therefore has not to be opened for cleaning or maintenance. This conditioning concept ensures a long-term and low maintenance functionality of the façade without the use of energy driven system engineering.

2.1 Self conditioning cavity

The cavity is connected to the external conditions by a special system of vapour pressure compensation and filtering. This compensation concept allows nearly unobstructed interaction of cavity humidity with external climate while avoiding impurities or pollution to infiltrate into the cavity.
Basically, this approach has been introduced with the “vitrage respirant” concept [1] in France during the 1980s. This “respiring IGU” technique was successfully applied by seele for the first time for the realization of the curved isolating glazing units at Hôtel Wagram, Paris in 2009 [2].

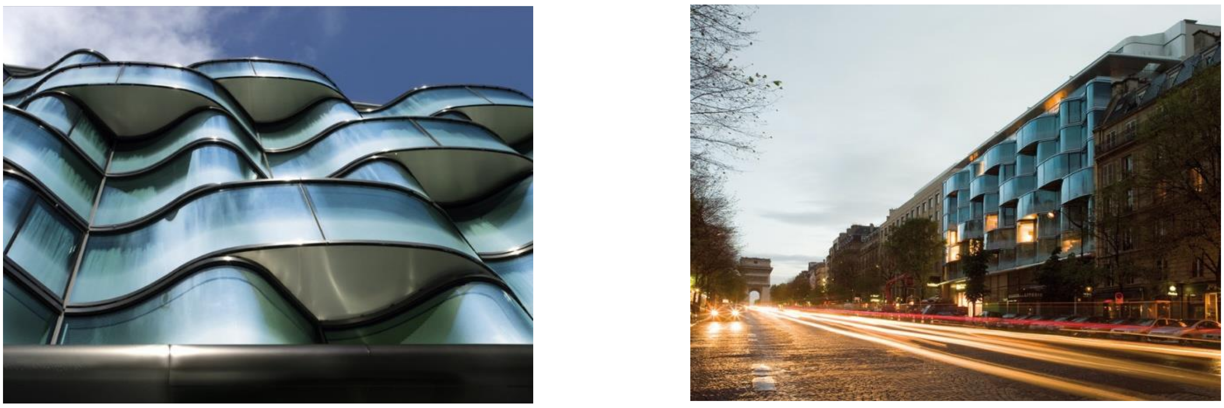

Figure 20: Curved IGU facade, Hôtel Wagram Paris.

Further development of this respiring technique to a self conditioning cavity with increased volume allowed applying this approach to double-skin façade elements.
The enlarged air volume of double-skin facades results in important pressure differentials between cavity and ambient atmosphere. Thus, pressure equalization of the cavity is required. This pressure compensation is realized by interaction of the cavity with external atmosphere. Condensation within the cavity is avoided by the subsequent factors:
Direct and unobstructed connection of the cavity with external conditions (short distance, adequate exchange area) enables conditioning of cavity vapour pressure.
Surface temperatures within cavity are increased by outer IGU, thus leading to a higher safety margin with respect to dew point temperature of cavity air.
These two main factors can be described as the fundamental driving forces of the self conditioning concept. Interaction between cavity and external conditions result in similar vapour pressures, adequate thermal design with increased surface and air temperatures within the cavity lead to reduced relative humidity values and, thus, assure a stable prevention of condensation.
The diagram in Fig.2 shows the time history of the vapour pressure outside (DD_ext) and within the cavity (DD_int): The vapour pressure “DD_int” easily adjusts to the outside vapour pressure “DD_ext” by the compensation technique and proves the direct interaction between cavity and external conditions.

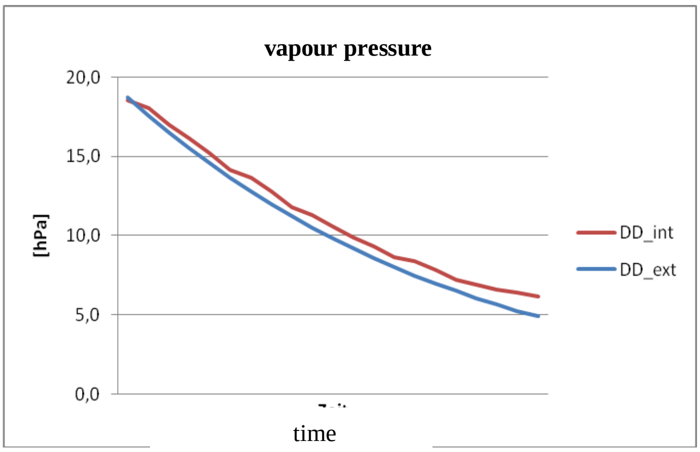

vapour pressure @ cavity
outside vapour pressure

Figure 2: Interaction between cavity and external atmosphere / vapour pressure compensation

Dew point temperature “T_sc” within the cavity is governed by air temperature “T_cav” and relative humidity “RH_cav” within the cavity. Surface temperatures “T_s” within the cavity are influenced by the thermal properties of the glazing and the façade design. Surface temperatures “T_s” are balanced above critical dew point temperature “T_sc” by the optimized heat transfer characteristics of the design.

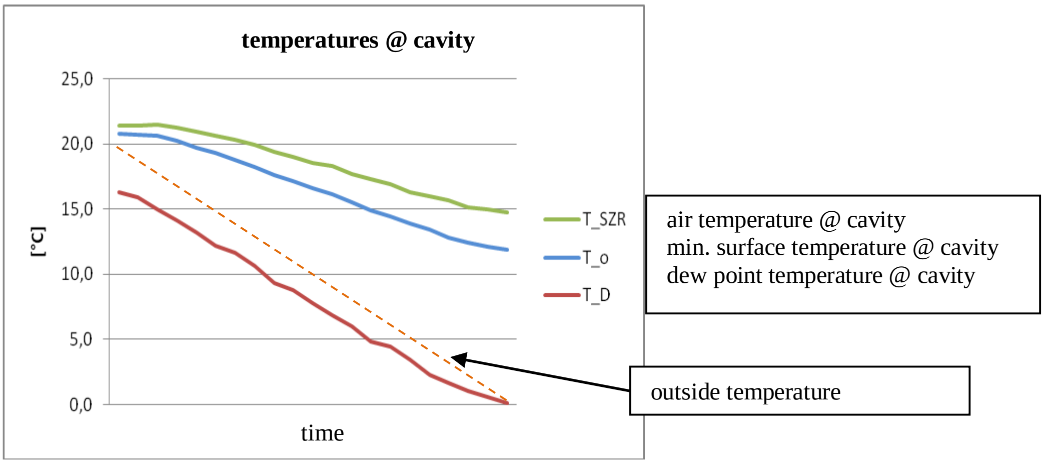

Figure 3: Cavity temperatures compared to dew point temperature during external temperature drop

2.2 SCF design

The principal design of a SCF unit is illustrated below indicating the basic driving forces of the self conditioning concept:
The double-skin façade unit with its air cavity interacting with the external atmosphere; thus, pressure differentials are equalized and vapour pressure is conditioned. Thermal properties are designed to create higher air and surface temperatures within the cavity to avoid condensation.

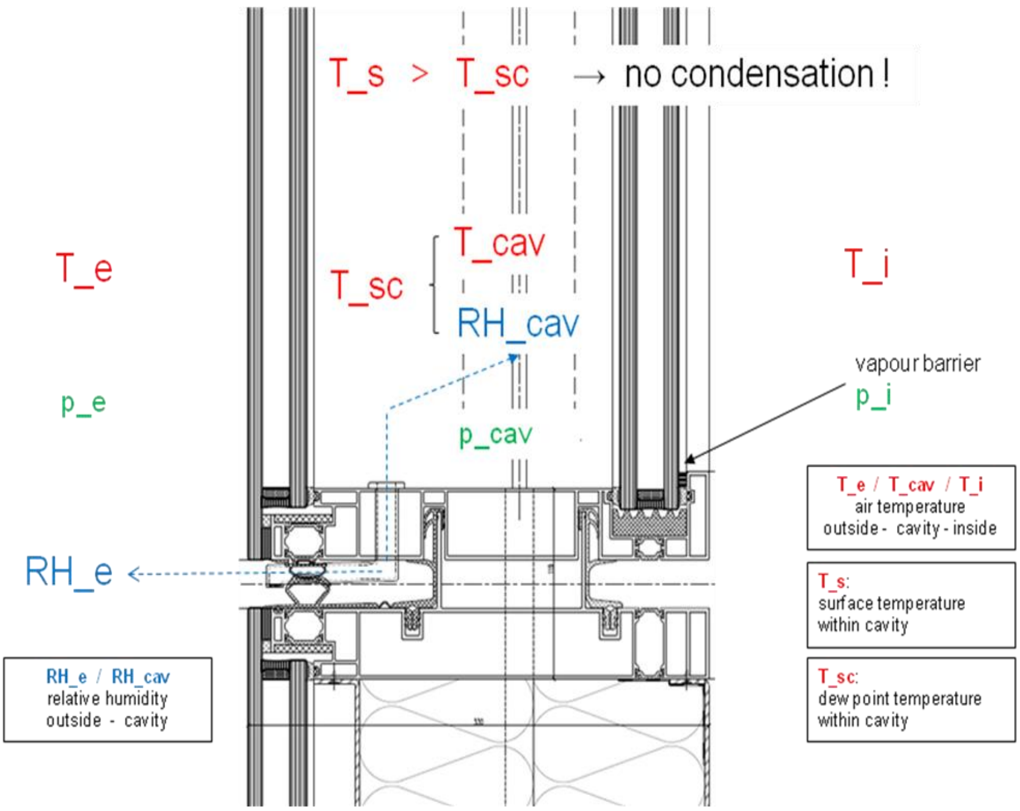

Figure 4: Prevention of surface condensation due to vapour pressure equalization of the cavity to outside conditions combined with thermal properties

3 Thermal calculations

The thermal properties and the corresponding performance of the unit have been detected to be one of the essential driving forces for a self-sustaining cavity climate. The relations between external conditions and temperature situation within the cavity can be illustrated by thermal finite element calculations.
Comparing minimum surface temperature values with dew point temperature levels in the cavity shows sufficient safety margins to prevent condensation within the cavity.

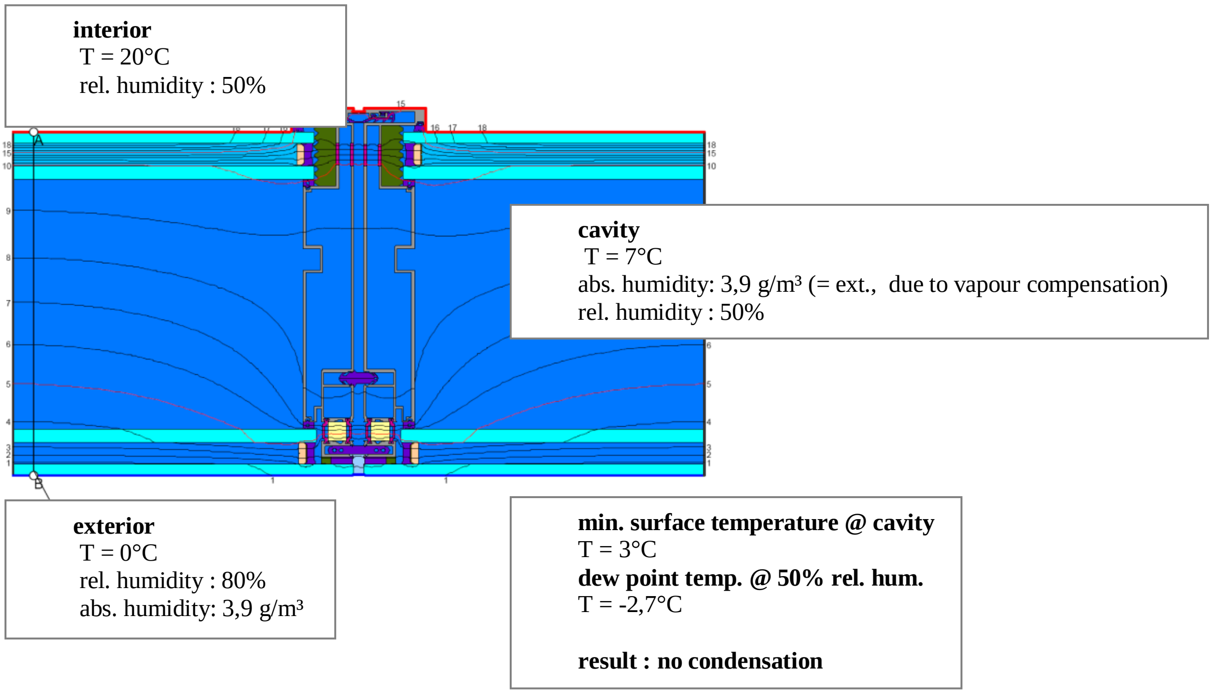

Figure 5: Thermal calculations showing temperatures and humidity values within the cavity illustrating the absence of condensation risk.

4 Long-term measurements

4.1 Fraunhofer Institute for Building Physics

To analyze and determine characteristics of modern façade concepts the Fraunhofer Institute for Building Physics offers the possibility to install façade units in a laboratory test building (VERU) in Holzkirchen, Germany. This enables to conduct long-term observations and measurements of the building envelope with respect to realistic climate conditions.
Within the development of the SCF concept long-term measurements have been performed on a SCF sample unit to monitor climate situation within the cavity: air/surface temperatures and humidity levels were analyzed to evaluate condensation risk, air volume exchange rate was measured to allow pollution risk assessments, etc.

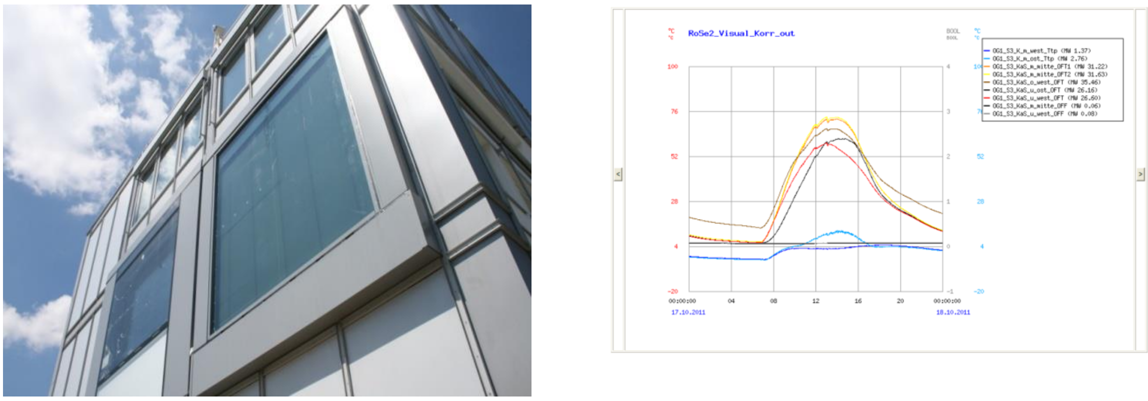

Figure 6: SCF sample unit installed in VERU test building with correpsonding mesurement data

The long-term measurements clearly proved the functionality of the self conditioning cavity concept and confirms the theoretical ideas and thermal relations described above.

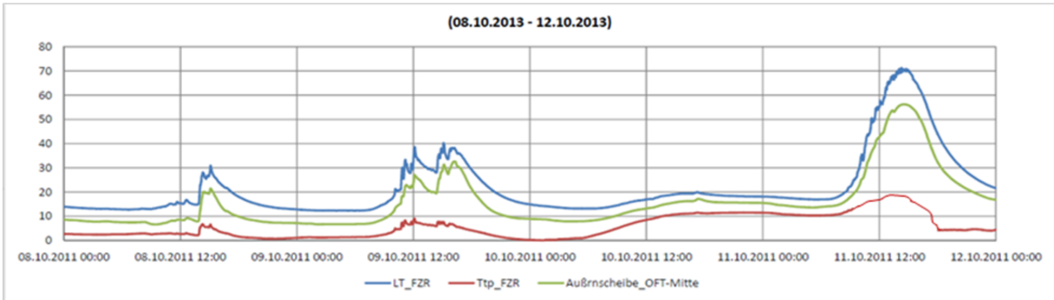

Figure 7: long-term monitoring of climate data within cavity to analyse condensation risk

5 seele iconic skin

5.1 Concept

The many years of experience with façades and the expertise gained from that has enabled **seele** to develop a completely new all-glass façade element which has been given the name **seele** iconic skin. Unprecedented architectural and design options are possible with this façade element, coupled with technical and economic benefits. The results of the intensive development activities, which began in the middle of 2012, have come together in the test building. Fundamental idea of this approach is a double-skin "wall type" unit with complete new aesthetic appearance: homogeneous surfaces, flush transitions between opaque and transparent areas and integrated, non-visible structural elements result in a very reduced, clear design.

Architects have a huge choice of design options for these elements. The internal and external glass surfaces, which can be digitally printed with patterns and colours, present almost infinite possibilities for individual designs. Virtually any number of transparent areas can be included in practically any shape or size. The maximum format of the iconic skin elements is 3.20m wide x 15m high. Opening elements, sunshades and glare protection can be integrated into the façade as required. Further advantages are the excellent thermal and sound insulation values plus the quick and clean erection on site. The integral, double-skin facade unit combines important features of an innovative, trendsetting building envelope: high performing interface between interior and exterior, structure, architectural benchmark, economic criteria.

A high level of industrialization in the fabrication of the facade elements does also allow individualisation at reasonable cost. It was the principle of the self-conditioning façade (SCF), developed and patented by **seele**, that first made this form of construction possible.

Figure 8: **seele** iconic skin

5.2 Prototype building

The **seele** iconic skin facade concept was successfully realized in a first prototype building in Gersthofen, Germany. There, the results of the very intense research and development activities are concentrated and successfully realized: maximum unit dimensions of 3,20m width and 13m height are combined with integrated shading devices, operable parts and a diversity of design options.

Permanent monitoring of climate data within the cavity is installed to observe vapour compensation processes and control condensation risk. Surface temperatures readings allow the evaluation of solar heat gain effects.

Figure 9: prototype building with different types of seele iconic skin options (left and top right), temperature and humidity sensors within cavity (bottom right)

5.3 seele iconic skin product presentation

The new façade generation iconic skin SCF was presented to the market for the first time at the Bau exposition from January 19th to 24th 2015 in Munich.

6 References

[10] Thomas M., Fleury G.: *Principe et fonctionnement des vitrages isolants respirants*. Cahier du CSTB n°1964, 1984.

[11] Hoffmann S., Trommer E.: *Gebogene Isolierglaseinheiten: Bauphysikalische Herausforderungen in einer gekrümmten Fassade*. In: Fassadentechnik 15(2009) Nr.5, S.16-19.

Proceedings of the International Conference on Building Envelope Design and Technology, Graz
Advanced Building Skins 2015

Experimental assessment of the energy performance of an advanced ventilated clay bricks façade

Stefano Fantucci, PhD fellow
Department of Energy, Politecnico di Torino, Italy, stefano.fantucci@polito.it

Valentina Serra, Associate Professor
Department of Energy, Politecnico di Torino, Italy, valentina.serra@polito.it

Marco Perino, Full Professor
Department of Energy, Politecnico di Torino, Italy, marco.perino@polito.it

Summary

This paper shows the results of an extensive experimental campaign on a ventilated opaque double skin façade based on hollow clay bricks. Summer and winter thermal performance has been investigated on three different façade configurations both through an in-field monitoring campaign and through a series of laboratory tests in a double climatic chamber apparatus. The Dynamic insulated façade (DIF) configuration was assessed in laboratory test representing the typical winter working condition, whilst the natural ventilated façade (NVF) configuration was analysed through an extensive in-field monitoring campaign in real operating summer conditions.

Keywords: Ventilated façade, dynamic insulation, double skin façade, climatic chamber.

1 Introduction

In Italy the use of clay bricks is largely diffused in the building sector, due to the high thermal mass and good thermal resistance provided, particularly suitable in temperate climates. Unfortunately according to the latest energy legislation, focused mainly on the reduction of the U-value, its thermal performance results to be not sufficient to fulfill the energy requirements unless the clay brick system is coupled with high thickness insulation layers. In order to allow an extensive use of this construction system both in new buildings and retrofit interventions, maintaining standard wall thicknesses, new concepts have to be developed.
In this direction the integration of ventilation strategies in the clay brick systems seems to offer an interesting opportunity to be investigated.
Dynamic insulated façade (DIF) and naturally ventilated façade (NVF) have thus been developed in the last few years focusing on the reduction of energy need respectively for heating and cooling.
Within a Research Project aimed at developing a new clay bricks system, a ventilated façade working under different operating conditions has been specifically developed in Politecnico di Torino and an extensive experimental campaign has been carried out in order to assess its energy performance The purpose of the research was to explore the possibility to combine different ventilation strategies, generating an adaptive ventilated double skin façade for both new buildings and energy retrofit of existing buildings, improving the performance along the whole year.
In particular an extensive in-field monitoring campaign was carried out during the summer period in Turin (Lat 45.67N, Lon 7.65E), on a NVF installed on an existing building , with the aim of assessing the potentials of the naturally ventilated clay brick façade on lowering the entering heat fluxes.
Moreover a further experimental campaign in a double climatic chamber was carried out on the same ventilated façade but working under different ventilation strategy in order to estimate the heat loss reduction in representative winter conditions.

The climatic chamber test was carried out on two different DIF configurations where the façade was highly integrated with a mechanical ventilation system:

- The Exhaust air façade (EAF) using the façade as an indoor exhaust air heat recovery;
- The Supply air façade (SAF) using the façade as a supply air pre-heater.

1.1 The opaque ventilated façades OVF

In Advanced Integrated Façade (AIF), the most common classification considers the ventilation strategy, the flow path and the system configuration as major items [1].
In particular, three different strategies can be considered: natural ventilation (NV), mechanical ventilation (MV) and hybrid ventilation (HV) that utilizes both natural and mechanical ventilation as driving forces.
The possible façade arrangements are schematically represented and classified according to the air flow path and the ventilation typology, as shown in figure 1, where: (EA) is the exhaust air configuration, (SA) is the supply air configuration, (OAC) and (IAC) represent respectively the outdoor air curtain and indoor air curtain configurations.

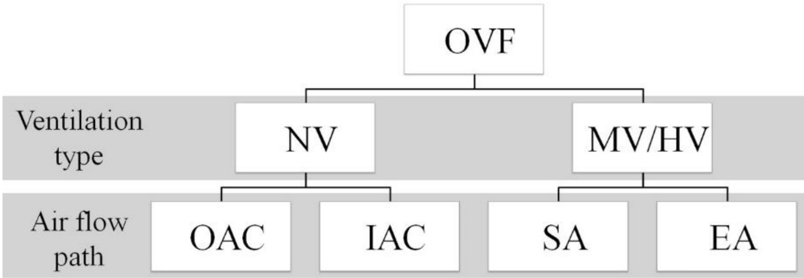

Figure 1: Façade classification scheme.

SA and EA configurations were commonly considered as dynamic insulation systems [1] and differ from OAC for the air flow origin and destination.
These solutions are still not widely adopted, despite their great potential, mainly because there is a lack of case studies and experimental results about their actual performance in building applications.
Nevertheless, in recent years some researchers tried to fill the gap, focusing their attention on the performance of this kind of technology. The most studied DIF configurations proposed in literature were principally divided in permeodynamic breathing wall, analyzed in [2] and [3], and parietodynamic walls, studied in [4].
OAC façades were also investigated, in particular [5] proposed experimental results of a long term experimental campaign. The evaluation of ventilated wall with an external clay cladding was proposed in [6], some other authors have suggested analytical model to assess the thermal performance of ventilated façade [7] while in [8] and [9] a numerical model for ventilated façade were experimentally validated.

2 Wall systems configuration

The different façade configurations used for the experimental tests here presented are reported in figure 2 and also summarized in table 1.

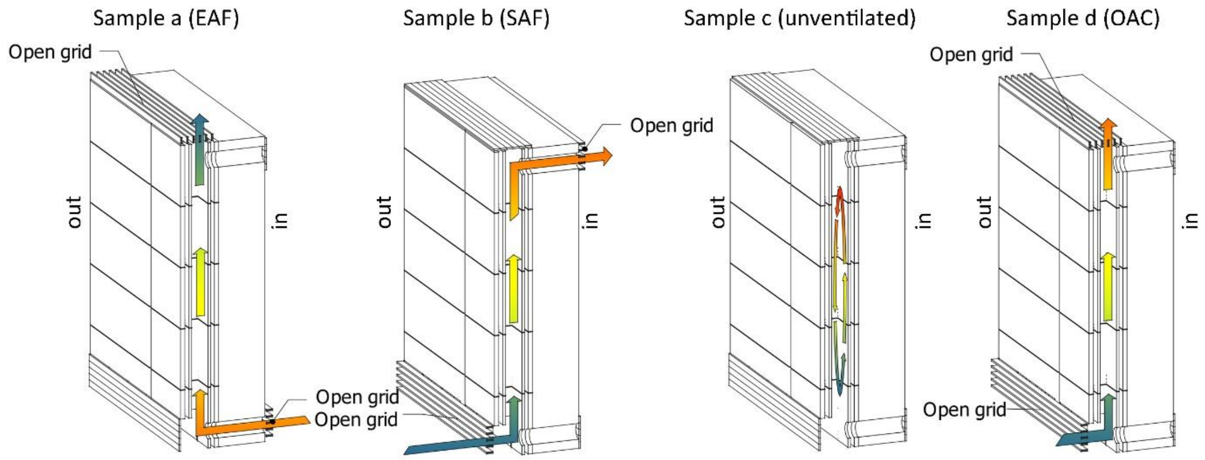

Figure 2: Tested façades, (a) Exhaust air façade EAF, (b) Supply air façade SAF, (c) Reference unventilated façade RUF, (d) Outdoor air curtain OAC

Table 1: Overview of the tested façade configurations.

Test Sample	Ventilation Type	Air Flow Path	Experimental Condition	Performance Investigated	Air Flow Origin	Air Flow Destination
a	MV	EA	laboratory	winter	interior	exterior
b	MV	SA	laboratory	winter	exterior	interior
c	unventilated	-	in field/laboratory	summer/winter	-	-
d	NV	OAC	in field	summer	exterior	exterior

2.1 The mechanically ventilated EA-SA façade

Tests specimens (a) and (b) (figure 3) consists in brick ventilated façades (height 230 cm and width 76 cm). The wall assembly is summarized in table 2.
Samples (a) and (b) are mainly divided in two parts:

- the ventilated façade (layer 1,2,3,4,5);
- the structural wall (layer 6).

The reference structural brick wall was constituted only by layer 6 and it was realized with the aim of comparing the thermal performance of the dynamic insulated façade and assess the performance improvement of the dynamic insulated façade (a) and (b).
Sample (a) consists in an exhaust air façade configuration (EA) while sample (b) is a supply air (SA) façade configuration, as represented in figure 2. The two façades differs for the direction of the air flow and also for the air flow origin and destination.

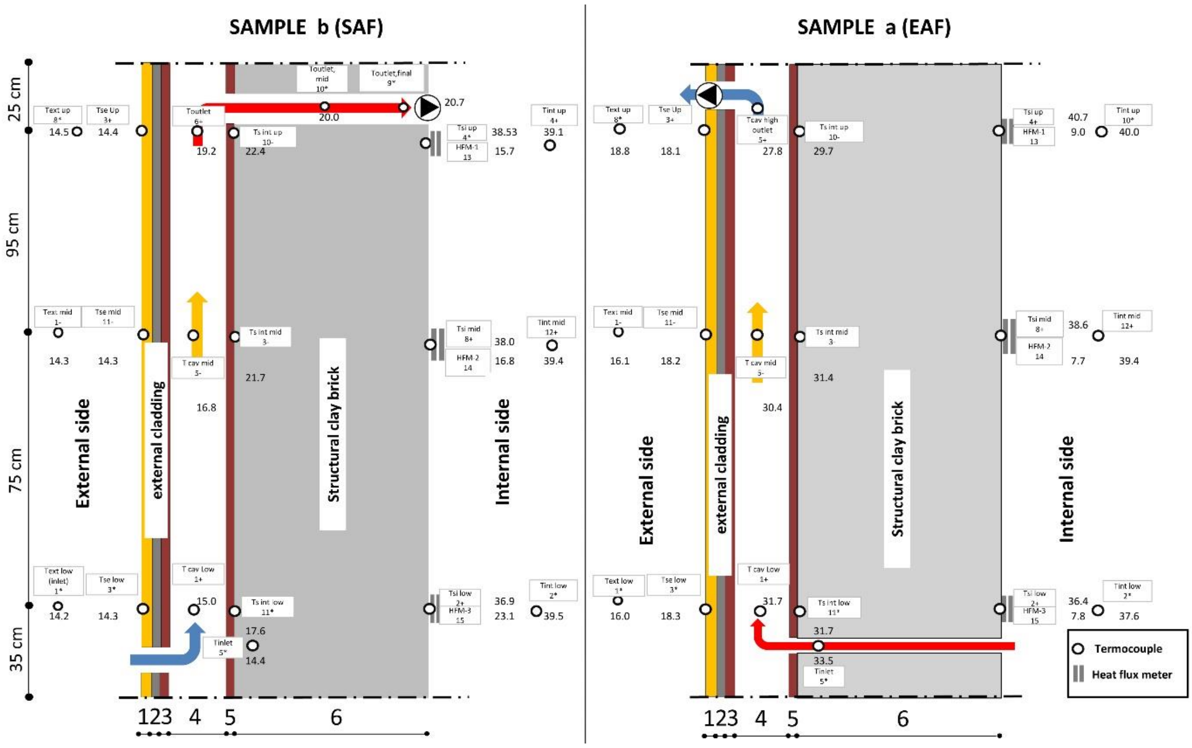

Figure 3: Samples schemes, (b-left), (a-right).

Table 2: Sample assembly from inside to outside

number	name	Thickness [mm]	Thermal Conductivity [W/mK]	Thermal Resistance [m^2K/W]
1	EPS	20	0.035	0.571
2	MDF	12	0.103	0.117
3	External brick layer	10	0.401	0.025
4	Ventilated air cavity	50	-	-
5	Internal brick layer	10	0.401	0.025
6	Structural brick	250	-	1.05

2.2 The naturally ventilated OAC façade

The external air curtain façade (OAC) was built on a South-West façade of a laboratory building (LATEC) in Politecnico di Torino.

The ventilated brick façade was build adherent to the existing lightweight insulated precast façade. At the same time a reference non ventilated façade (made of the same materials) was built in order to compare and quantify the ventilation effect on reducing the heat load in summer conditions.

The wall assembly is represented in figure 4 and summarized in table 3.

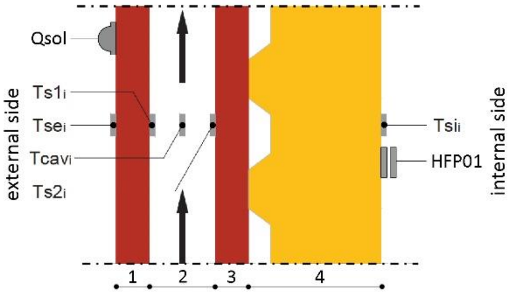

Figure 4: Specimen (d) stratigraphy.

Table 3: Assembly from inside to outside

number	name	Thickness [mm]	Thermal Conductivity [W/mK]	Thermal Resistance [m^2K/W]
1	Hollow brick cladding	10	0.401	0.025
2	Ventilated air cavity	50	-	-
3	Hollow brick cladding	10	0.401	0.025
4	Existing wall (mineral wool)	100	-	2.700

3 The experimental campaign

3.1 In field test methodology

The in-field tests were carried out on sample (c) and (d), during summer 2014.
For the continuous monitoring of the façades summer performance, a series of sensors and devices were adopted. Air and surfaces temperatures were measured using thermocouples type-T, the heat flux crossing the walls was measured using heat flux meter plates HFP01, while a hot wire anemometer was used for a spot measuring of air velocity inside the external air channels; finally, in order to measure the solar irradiance on the same vertical plane of the façade, a pyranometer was used.
The in-field test was carried out for different façade configurations (figure 5), varying the air cannel height, the ventilation grills opening and the joint typology. In this paper, for the sake of brevity, only the results of the configuration described in section 2.2 were reported.

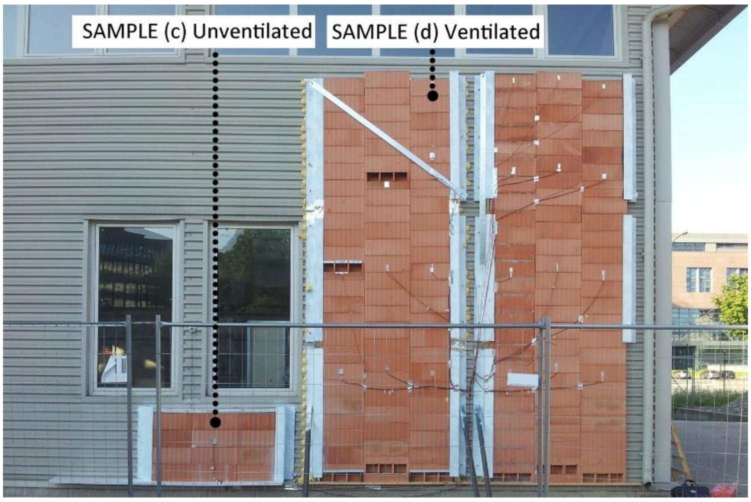

Figure 5: (OAC) samples installed on the south-west façade of the laboratory.

3.2 Laboratory measurement

For the steady state experimental characterization (samples a and b) a climatic chamber (Building Envelope Test Cell “BET cell”) was adopted (figure 6). Moreover for the experimental evaluation of the thermal resistance of the materials that constitute the samples walls, a guarded heat flux meter LASERCOMP FOX600 was used, according to the international standard EN ISO 12667:2002 [12].

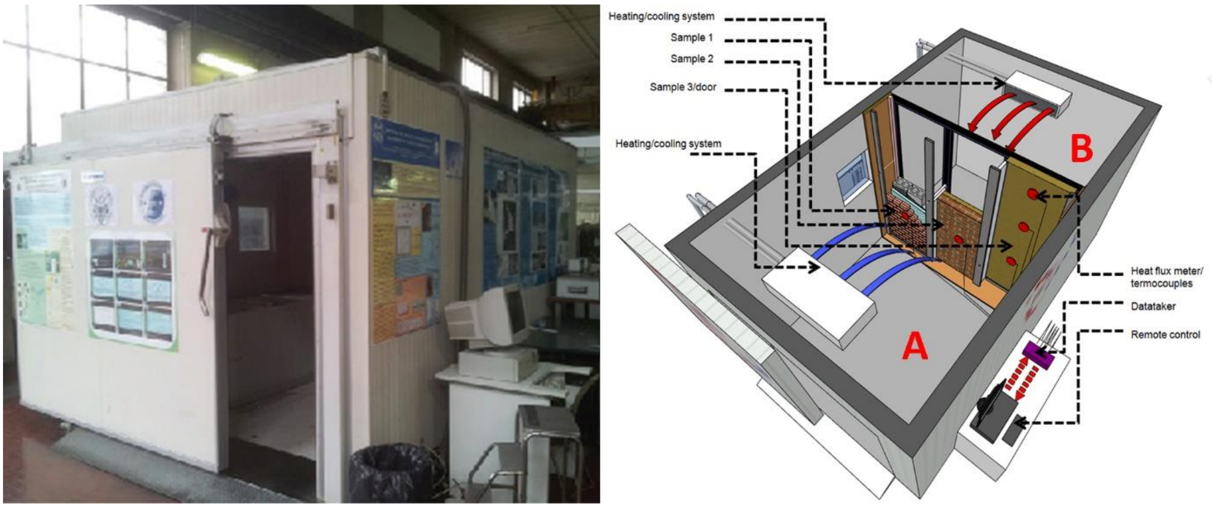

Figure 6: BET cell schematic representation.

The climatic chamber called “BET cell” has been specifically implemented to test advanced building envelope component and consists in a double room with a separation frame that can host the sample walls.
The test-cell rooms dimensions for both the sub-module “A” (outdoor condition) and sub-module “B” (indoor condition) are 240 cm height and 275 cm width, while the depth is respectively 300 cm (A) and 165 cm (B).
The external environment is recreated in the sub module “A”, which is equipped with an HVAC systems that allows to simulate both steady state and transient dynamic boundary conditions. The sub-module can be continuously maintained at the desired set point temperature, with an accuracy of ±0.5 °C, by means of an all air system working on temperature range of 12/40°C.
The internal boundary condition was recreated in the sub module “B” equipped with a radiant heating system. The sub module can be continuously maintained at the desired set point temperature, with an accuracy of ±0.3 °C, the maximum and minimum temperature range depends on the temperature difference between the two modules and the thermal transmittance of the samples.

The testing apparatus is equipped with a monitoring system for the measurement of thermal resistance and thermal transmittance, according to EN ISO 9869:2014, consisting into 4 heat flux meters (HFP01) and 36 (TT) thermocouples, connected to a datataker. [13].

4 Experimental results

4.1 Summer thermal performance of external ventilated façade configuration (NVF)

The summer thermal performance of the external ventilated façade configuration was investigated with a heat flux metering campaign.
The façade systems were constituted by a ventilated cavity brick (d) and a reference configuration unventilated (c), as presented in figure 4.
Equation (1) and (2) were used for the summer thermal performance evaluation. The *ΔTL* parameter introduced in [5] represents the daily thermal load energy reduction obtained by using a fixed unventilated façade configuration (sample - c) compared to the ventilated façade configuration (sample - d).

$$\Delta TL = 1 - \frac{E_{(c)}}{E_{(d)}} = 1 - \left(\frac{C\Delta t \int_{\tau}^{\tau'} [T_{s2}(\tau) - T_{si}(\tau)]_{(c)} d\tau}{C\Delta t \int_{\tau}^{\tau'} [T_{se}(\tau) - T_{si}(\tau)]_{(d)} d\tau} \right) \quad (1)$$

and hence:

$$\Delta TL = 1 - \frac{\int_{\tau}^{\tau'} [T_{s2}(\tau) - T_{si}(\tau)]_{(c)} d\tau}{\int_{\tau}^{\tau'} [T_{se}(\tau) - T_{si}(\tau)]_{(d)} d\tau} \quad (2)$$

where:

- T_{s2} is the temperature of the inside cavity surface (interface 2-3, figure 4);
- *E(c)* represents the daily thermal energy load crossing the unventilated façade (c);
- *E(d)* represents the daily thermal energy load crossing the ventilated façade (d);
- T_{si} is the internal surface temperature;
- T_{se} is the external surface temperature;

The integer interval is between the hour of day in which the temperature difference becomes >0, indicated with τ, and the hour of day in which the temperature difference becomes <0 indicated with τ'. Figure 7 reports the daily trends of temperature and solar irradiance of a typical sunny day while the results of the whole monitoring period are reported in figure 8. The *ΔTL* value ranges between 34% and 80% (triangle points) depending on the daily average outdoor temperature, represented by circle points. Moreover a 42.4% reduction of average thermal load energy (ΔTL_{avg}) were calculated for the whole monitoring period, and reported in dash-dotted line in figure 8.

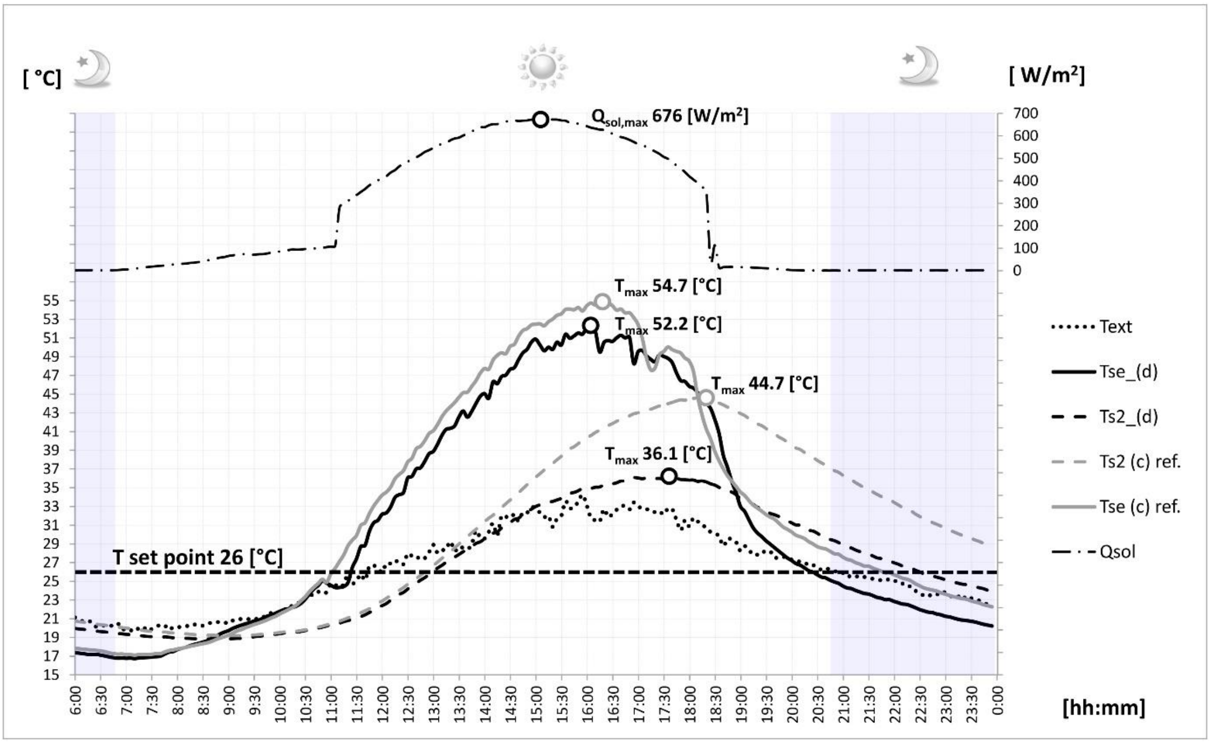

Figure 7: Solar radiation and surface temperature daily profile for reference unventilated façade RUF (c) and OAF (d).

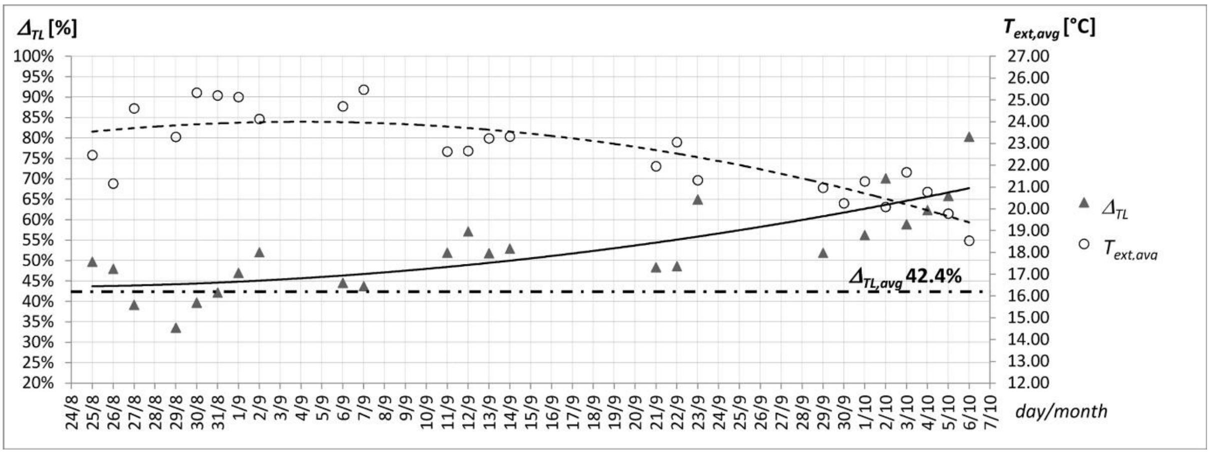

Figure 8: Average daily temperature $T_{ext,avg}$ and ΔTL for each monitoring day.

4.2 Winter thermal performance of supply air façade configuration (SAF)

The winter thermal performance of the supply air façade configuration was investigated with a heat flux metering experimental campaign using the double climatic chamber facility described in section 3.2.
The experimental samples consist in two different wall assemblies. First of all the thermal resistance of a simple brick wall (reference wall) without the adoption of any ventilation strategies was assessed through heat flux meter measurements, according to EN ISO 9869:2014 [13]. After that the experiments with ventilated walls were performed using different electrical fans and the air flow rate for the entire wall cavity was measured through the tracer gas method.
The thermal performance of the supply air configuration, as shown in figure 9, was evaluated trough the pre-heating efficiency $\eta_{pre\text{-}heat}$ parameter[10], calculated using equation (3)

$$\eta_{pre-heat} = \frac{(T_{inlet} - T_{out})}{(T_{in} - T_{out})} \qquad (3)$$

Where:
T_{inlet} is the supply air temperature measured at the top of the façade air cavity;
T_{out} is the outside air temperature, maintained at 39°C (cold side A);
T_{in} is the inside air temperature, maintained at 14°C (hot side B).

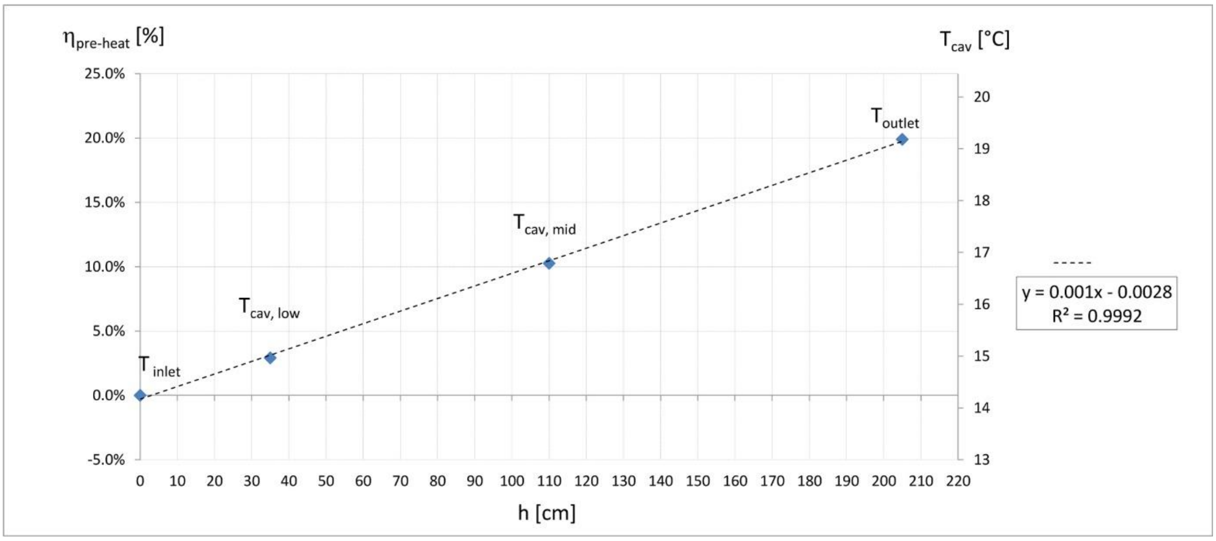

Figure 9: Air cavity temperature T_{cav} and $\eta_{pre-heat}$ at different façade heights.

In figure 9 are reported the results of the air cavity temperature T_{cav} and the pre-heating efficiency $\eta_{pre-heat}$ at different façade heights (between 0 cm - T_{inlet} and 205 cm - T_{outlet}). In this height ranges the results present a linear behavior increasing by around 2°C for each meter height. At 205 cm height the air results pre-heated from 14.2 °C to 19.2 °C, corresponding to a 20% of pre-heating efficiency.

4.3 Winter thermal performance of exhaust air façade configuration (EAF)

The experimental performance evaluation of the exhaust air façade configuration was carried out following the same methodology proposed in section 4.2, through a comparison with the reference wall (without the ventilated façade).
The heat loss reduction Δq of the exhaust air façade compared to the reference wall was calculated using eq. (4)

$$\Delta q = 1 - \frac{q_{(b)}}{q_{(ref)}} \qquad (4)$$

Where:
$q_{(b)}$ is the average heat flux measured in the sample wall (b);
$q_{(ref)}$ is the heat flux measured in the center of the reference wall (ref).

As shown in figure 10, the heat flux reduction Δq goes with the increase of the air flow rate Q (between 46% and 68%).
The graph shows an asymptotic behavior for air flow rates higher than 35 m^3/h for a 76 cm façade width, which means that any additional increase of the air flow rate have a low impact on the façade thermal performance.

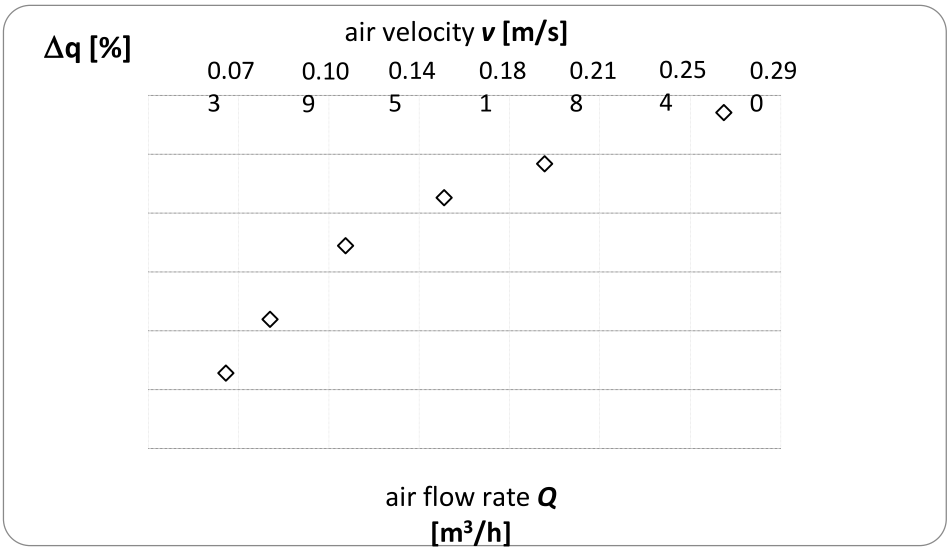

Figure 10: Heat flux reduction for different air flow rates *Q* and air velocity *v*.

5 Conclusions

An extensive experimental campaign was carried out on different ventilated façade configuration. Main results can be synthetized as:

- For OAF, a daily thermal load energy reduction around 42% can be obtained considering the whole monitoring period;
- For SAF, the air pre-heating efficiency can reach 20% for a 205 cm height façade;
- For EAF, the heat loss can be reduced by 46% ÷ 68% depending on the air flow rate.

Results obtained for the OAF façade are in good agreement with the few results reported in literature [5], [6] and [7].

EAF configuration shows important improvements of the performance (more than 46%) for air flow rate higher than 9 m^3/h for a 76 cm width façade.

SAF façade does not present noticeable thermal advantages, but it should be noticed that the steady state experimental campaign did not take into account the influence of the dynamic external boundary conditions and in particular neglected the effect of the solar radiation, that could play a key role in pre-heating the supply air.

It is important to underline that the experimental results presented in this paper are related to the single season performance of each façade configuration. Nevertheless in order to optimize the façade thermal efficiency and the adaptive behavior in every season, the three different façade configurations should be combined and integrated with the HVAC systems.

In particular the coupling of SAF and HVAC systems could significantly increase the coefficient of performance COP due to the minimization of the temperature difference [11].

This work represents a first step of a wider research activity on these kinds of façades. Results are encouraging and underline the great potential of this technology, demonstrating how the alternative use of the tree configurations EAF, SAF and OAF integrated with adaptive and dynamic controls, can lead to a noticeable energy demand reduction along the whole year.

6 Acknowledgements

The research was developed in the framework of the POLIGHT project “BLOCK-PLASTER –funded by Regione Piemonte. The project was developed in cooperation with DAD_Politecnico di Torino, VIMARK s.r.l., VINCENZO PILONE s.p.a. and NovaRes s.r.l.

7 References

[1] Perino, M., – Annex 44-State of the art review. Vol. 2A. *Responsive building elements*, Oyvind Aschehoug: Norwegian of science and technology (NTNU), Trondheim, Norway, Marco Perino, Politecnico di Torino, Dipartimento di Energia (Torino), 2010.

[2] Taylor, B.J., Imbabi, M.S., *The application of dynamic insulation in buildings*, Renewable Energy 15 (1998) 377-382.

[3] Taylor, B. J., Webster, R., Imbabi, M. S., *The building envelope as an air filter*, Building and Environment 34 (1999) 353-361.

[4] Imbabi, M.S., *A passive-active dynamic insulation system for all climates*; International journal of sustainable built environment 1 (2012) 247-258.

[5] Marinosci, C., Semprini, G., Morini, G.L., *Experimental analysis of the summer thermal performances of a naturally ventilated rainscreen façade building*, Energy Build. 72 (2014) 280-287.

[6] Stazi, F., Tomassoni, F., Vegliò, A., Di Perna, C., *Experimental evaluation of ventilated walls with an external clay cladding*, Renewable Energy 36 (2011) 3373-3385.

[7] Balocco, C., A simple model to study ventilated façades energy performance, Energy Build. 34 (2002) 469–475.

[8] Marinosci, C., Strachan, P.A., Semprini, G., Morini, G.L., *Empirical validation and modelling of a naturally ventilated rainscreen façade buildings*, Energy Build. 43(2011) 853–863.

[9] Seferis, P., Strachan, P., Dimoudi, A., Androutsopoulos, A., *Investigation of the performance of a ventilated wall*, Energy Build. 43 (2011) 2167–2178

[10] Serra, V., Zanghirella, F., Perino, M., *Experimental evaluation of a climate facade: energy efficiency and thermal comfort performance*; Energy and buildings 42; 2010; pp. 50-62.

[11] Cianfrini, C., Corcione, M., Habib, E., Quintino, A., *Energy performance of a lightweight opaque ventilated façade integrated with the HVAC system using saturated exhaust indoor air*, Energy and Buildings 50 (2012) 26–34.

[12] EN ISO 12667:2002 Thermal performance of building materials and products - Determination of thermal resistance by means of guarded hot plate and heat flow meter methods - Products of high and medium thermal resistance.

[13] EN ISO 9869:2014 Thermal insulation - Building elements - In-situ measurement of thermal resistance and thermal transmittance.

Proceedings of the International Conference on Building Envelope Design and Technology, Graz
Advanced Building Skins 2015

Simulation-Based Determination of Pressure Coefficients for Multi-Story Double-Skin Facades

Jeffrey C. Vaglio, PE, AIA, LEED AP [BD+C]
Director, Enclos Advanced Technology Studio, USA
Ph.D. Candidate, University of Southern California, USA

Summary

This research investigates how various airflow configurations affect the pressure coefficient distribution on multi-story double-skin facades. Multi-story double-skin configurations are the focus due to their prevalence in the United States, as learned following a review of 30 existing projects of which 21 had a multi-story cavity partitioning. For this study, a prototypical geometry is developed and computational fluid dynamic simulations are run for four configurations of airflow inlet and outlet combinations. The simulation method is first calibrated and reviewed against existing wind tunnel studies. The interior skin's coefficient of pressure profile varies considerably depending on the varying inlet configuration.

Keywords: Double-skin facade, multi-story, pressure coefficients, CFD

1 Double-Skin Facades in the United States

Double-skin facade (DSF) technology evolved significantly during the mid-1990's and through the first decade of the 2000's. The initial concentration of double-skin facades were implemented in Northern European climates and primarily on office buildings. The primary motivations for implementing double-skin facades in Europe included improved thermal insulation during both hot and cold seasons, reduced solar heat gains, access to natural light, protection for shading devices, natural ventilation, and adaptability for reductions in energy consumption. The application of modern double-skin facades in the United States began with a multi-story solution on the Occidental Chemical Center (or Hooker Building) in Niagara Falls, New York over three decades ago in 1980. Nearly twenty years passed before additional projects integrated DSF solutions in the United States. Beginning in the early 2000s, however, more than two dozen such projects have been realized. As the sample size grows, the differences in motives and justifications for double-skin facades in the United States as compared to Europe continue to reveal themselves.

1.1 Review of Built Double-Skin Facades in the United States

Within this research, a search was conducted to identify existing applications of double-skin facades in the United States to understand the typological distribution used in existing and future buildings. The search was performed by reviewing 1) existing literature in the form of books, conference proceedings and journal articles, 2) attending technical conferences where facades were the topical focus, 3) inquiries with architects, 4) interfacing with United States based facade contractors familiar with forthcoming projects, and 5) internet articles. Thirty examples of built and documented buildings utilizing a double-skin facade concept were identified in the United States. Projects without documentation were excluded. One such example is the Prudential Life Insurance Company in Princeton, New Jersey that was designed by Skidmore Owings and Merrill in collaboration with Princeton University in the late 1980s [1]. This three-story building featured a double exterior glass wall with a cavity depth of approximately 46 cm that was used to harness solar heat gain and redistribute to building zones that require heating [2]. In addition to these 30 built examples, six forthcoming examples that had substantial information were documented to demonstrate the fact that double-skin facades in the United States are continuing to be explored through application in the present and near future. These six forthcoming projects were excluded from any data analysis presented in this section, though they are shown in Table 1 to present the double-skin facades' characteristics.

The projects were reviewed and summarized in a manner similar to Perino's evaluation of 215 DSF/AIF projects across the globe in *State of the Art Review Vol. 2A: Responsive Building Elements* [3] with a focus on typological factors: cavity partitioning, ventilation type and ventilation mode ('flow path' per Perino). The review was used to identify the most common DSF configurations to inform the development of an analytical prototype.

Table 1: Summary of Double-Skin Facades in the United States

		Location			Typological Characteristics			
Project Name	**Year**	**City**	**State**	**Architect**	**Cavity Partition**	**Vent. Type**	**Vent. Mode**	
Warren Petroleum Executive HQs	1957	Tulsa	OK	SOM, Bruce Graham	SH-C	n/a	B	
Occidental Chemical Center	1980	Niagara Falls	NY	Cannon Design Inc.	MS	N	OAC	
Yazaki North American	1999	Canton	MI	Plantec	MS	N	OAC	
Levine Hall - Pennsylvania School of Engineering	2001	Philadelphia	PA	Kieran Timberlake Associates	BW	M	IAC	
Seattle Justice Center	2002	Seattle	WA	NBBJ, Kerry Hegedus	MS	H	OAC	
Manulife US Headquarters	2003	Boston	MA	SOM, Permasteelisa	SH-JM	M	IAC	
Genzyme Headquarters	2003	Boston	MA	Behnisch, Behnisch and Partner	SH-C	N	OAC	
Foundry Square	2003	San Francisco	CA	Studios Architects	MS	N	OAC	
UMass Medical School	2006	Worcester	MA	Payette Associates	MS	N	OAC	
Loblolly House	2006	Taylors Island	MD	Kieran Timberlake Associates	SH-JM	N	OAC	
Univ. of Michigan Biomedical Science Research Bldg	2006	Ann Arbor	MI	Polshek Partnership Architects	MS	N	OAC	
Museum of Contemporary Art	2007	Denver	CO	David Adjaye w/ Davis Partnership	MS	M	AE	
Comcast Tower	2008	Philadelphia	PA	Robert A.M. Stern	MS	M	AE	
Riverhouse - One River Terrace	2008	New York	NY	Polshek Partnership Architects	BW	N	OAC	
Loyola Information Commons	2008	Chicago	IL	Scolomon Cordwell Buenz	MS	H	OAC	EXISTING
Walter Cronkite School of Journalism	2008	Phoenix	AZ	Ehrlich Architects	MS	N	OAC	
Whatcom Museum	2009	Bellingham	WA	Olson Kundig Architects	MS	N	OAC	
Art Institute of Chicago - Modern Wing	2009	Chicago	IL	Renzo Piano Building Workshop	MS	N	OAC, B	
Cleveland Museum of Art - East Wing	2009	Cleveland	OH	Rafael Viñoly Architects	SB	M	B	
Cambridge Public Library	2009	Cambridge	MA	William Wrawn Associates	MS	N	OAC	
100 Park Avenue	2009	New York	NY	Moed de Armas & Shannon Architects	BW	N	B	
USC Eli and Edythe Broad CIRM Center	2010	Los Angeles	CA	Zimmer Gunsul Frasca	MS	N	OAC	
New York Presbyterian Hospital	2010	New York	NY	Pei Cobb Freed	MS	M	AE	
University of Oregon Jaqua Center	2010	Eugene	OR	Zimmer Gunsul Frasca	MS	N	OAC	
New World Center	2011	Miami	FL	Gehry Partners	MS	M	B	
University of Baltimore Angelos Law School	2013	Baltimore	MD	Behnisch Architekten	B	N	OAC	
Harvard Business School - Tata Hall	2013	Boston	MA	William Wrawn Associates	MS	N	OAC	
Cedars-Sinai Advanced Health Sciences Pavilion	2014	Los Angeles	CA	HOK	MS	N	OAC	
Weill Cornell Medical College - Belfer Research Bldg	2014	New York	NY	Ennead Architects	MS	N	OAC	
Univ. of Kansas School of Architecture - The Forum	2014	Lawrence	KS	Studio 804	MS	N	OAC, B	
Northwestern University Recital Hall	2015	Evanston	IL	Goettsch Partners	MS	M	IAC	
Rodino Federal Office Building	2015	Newark	NJ	Dattner Architects	MS	N	OAC	
A.J. Celebreeze Federal Building	2015	Cleveland	OH	Interactive Design Eight Architects	SH-C	N	B	FUTURE
PNC Plaza Tower	2015	Pittsburgh	PA	Gensler	SH-JM, BW	N	AS, B	
Columbia University Jerome Greene Science Center	2015	New York	NY	Renzo Piano Building Workshop	MS	M	AE	
New Stanford Hospital	2018	Palo Alto	CA	Rafael Viñoly Architects	BW	M	B	

Notes:

Cavity Partitioning
- B Baffle
- BW Box-Window
- AF Alternating Façade
- SB Shaft-Box
- SH-C Story-Height Corridor
- SH-JM Story-Height Juxtaposed Modules
- MS Multi-Story
- MS-S Multi-Story Shingled
- MS-L Multi-Story Controllable (Louvers)

Ventilation Type
- N Natural
- H Hybrid
- M Mechanical

Ventilation Mode
- OAC Outdoor Air Curtain
- IAC Indoor Air Curtain
- AS Air Supply
- AE Air Exhaust
- B Buffer Zone

1.2 Identifying the Most Common Configuration

This section summarizes the 30 existing projects presented in Table 1 and compares the findings to Perino's findings from a review of 215 DSF/AIF projects across the globe [3].

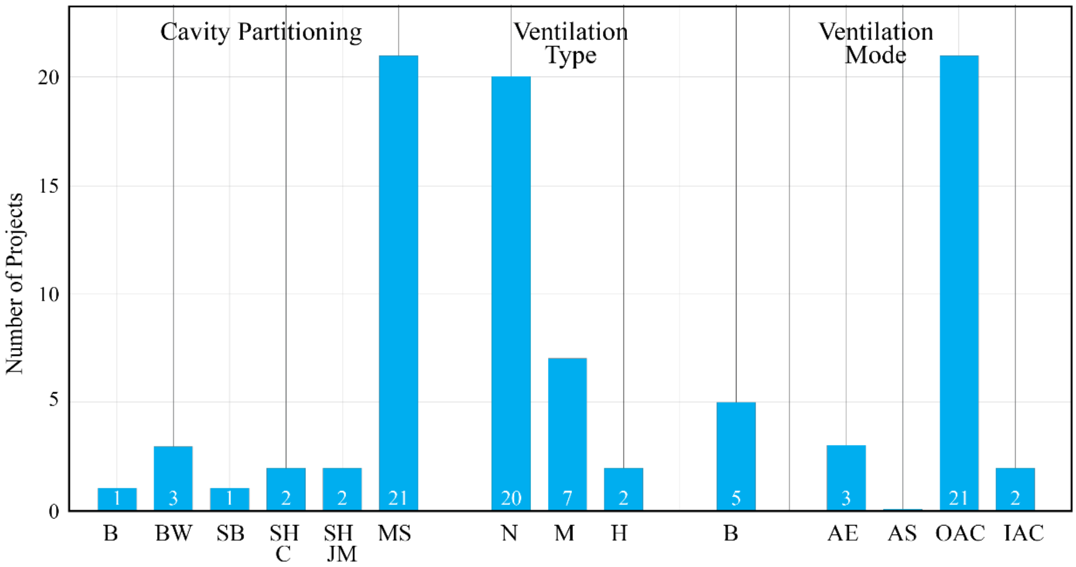

Figure 1: Typological summary of identified buildings with DSF's in the United States.

Cavity Partitioning: The cavity partitioning configuration that is most common in the United States is the multi-story (70.0%) followed by the box-window (10.0%). In Perino's evaluation, the multi-story represented 47.0% of the global projects surveyed [3].

Ventilation Type: The ventilation type that is most common in the United States is natural (69.0%) followed by mechanical (24.1%). In Perino's evaluation, natural ventilation represented 58.1% of the global projects surveyed [3].

Ventilation Mode: The ventilation mode that is most common in the United States is the outdoor air curtain (70.0%). In Perino's evaluation, the outdoor air curtain represented 49.1% of the projects surveyed [3]. It must be noted that many double-skin facades feature an ability to switch between modes. The primary mode of operation is identified for the purposes of this analysis.

2 Development of a Multi-Story Prototype

2.1 Dimensional Trends of Multi-Story Double-Skin Facades in the United States

Having identified the multi-story as the predominant cavity partitioning of double-skin facades in the United States in the previous section, 21 projects were then isolated and evaluated for trends within this subset. The dimensional characteristics are summarized below. It should be noted that many of the projects include multiple instances of double-skin facades (e.g. Yazaki North American contains ten unique 20.5 m wide by 15 m tall instances, and the Art Institute of Chicago has three instances on the north, three on the south and others on the east or west elevation). When a project contains multiple instances (usually a repeating dimension across occurrences), only the largest was included. Dimensional data was gathered from projects drawings, technical presentations, journal publications and periodical articles.

Height: The multi-story cavities range in height from 5.5 m to 69.0 m with an average of $\bar{h}$ = 21.1 m.

Width: The multi-story cavities range in width from 5.5 m to 112.8 m with an average of $\bar{a}$ = 46.8 m.

Cavity Depth: The multi-story cavities range in depth from 0.23 to 3.0 m with an average of $\bar{s}$ =1.01 m.
Aspect Ratios: The multi-story cavities range in height-to-depth aspect ratio from 6.0 to 101.8 with an average of $\overline{h/s}$ = 27.8. The average cavity height-to-width is $\overline{h/a}$ = 0.672 meaning the cavities are more frequently wider than they are tall. The average cavity depth-to-width is $\overline{s/a}$ = 0.031.

2.2 Multi-Story Double-Skin Facades Prototype

The outdoor air curtain ventilation mode has been utilized on 17 of the 21 multi-story double-skin facades (81.0%), an increased rate than the 30 project sample of all cavity partitioning configurations. A multi-story double-skin facade with an outdoor air curtain, double-skin height of h_{top}= 21 m, building height of h = 20 m, width of a = 45 m and cavity depth of s = 1.0 m was deemed the prototype configuration for analysis. In this research the airflow opening and exhaust configurations are treated as variables; all exhaust configurations are *forward* in this paper.

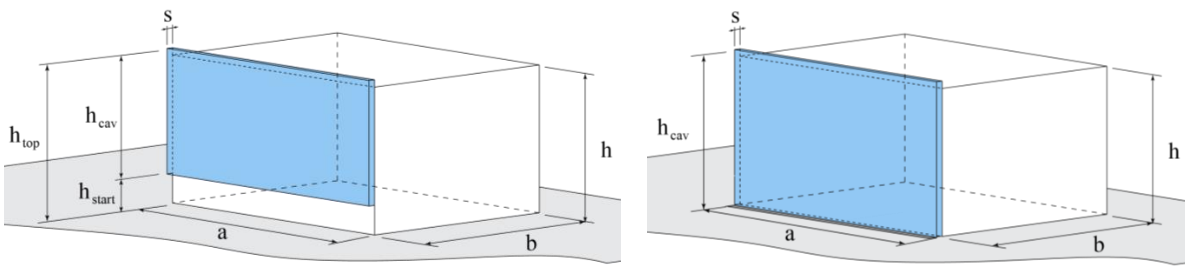

Figure 2: Multi-story double-skin facade prototype variations: *raised* inlet (left) and *trench* inlet (right).

2.3 Airflow Inlet Configurations

Airflow into the double-skin facade cavity may occur through the five generalized opening configurations below. The sealed intake configuration is also shown; this is the mode of many multi-story double-skin facade systems when the operable mechanisms or louvers are closed.

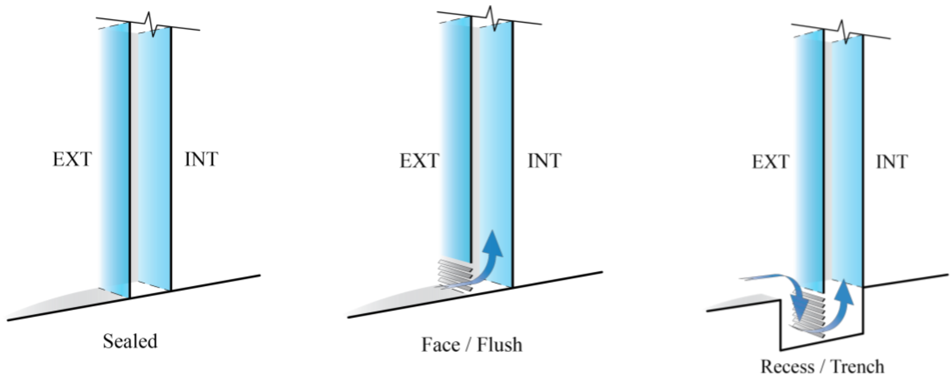

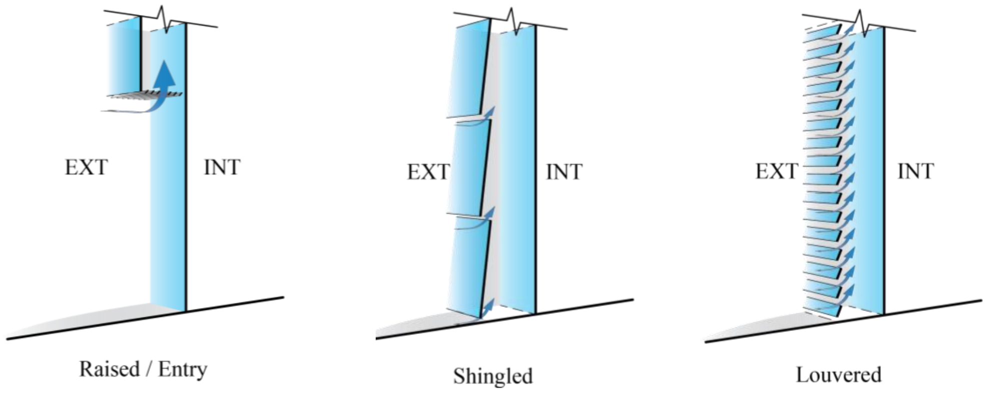

Figure 3: Multi-story DSF airflow inlet configurations.

2.4 Airflow Exhaust Configurations

Airflow out of the double-skin facade cavity may occur through the three generalized exhaust, or outlet, opening configurations below. The three exhaust opening configurations all occur at the top of the cavity, or on the adjacent vertical planes, taking advantage of the stack effect. The *forward* configuration exhausts air over the building's roof through the inner vertical plane while the *return* condition thrusts the air back into the impinging direction via the outer vertical plane.

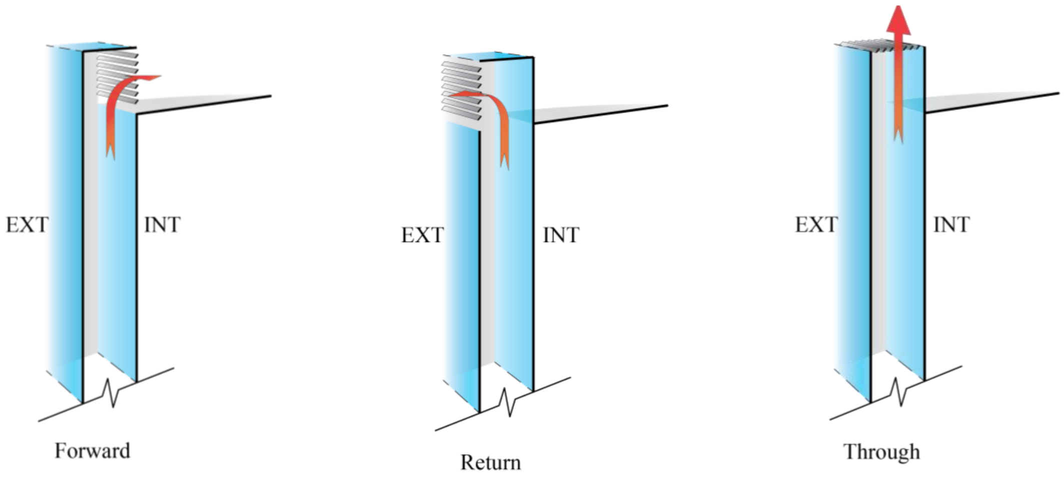

Figure 4: Multi-story DSF airflow exhaust (outlet) configurations.

3 Simulation-Based Determination of Pressure Coefficients for Multi-Story Double-Skin Facades

The use of simulation for this research requires special attention be given to tuning the modeling process in an effort to preserve the relevancy of the results. Researchers have identified the potential of CFD modeling, when used in conjunction with wind tunnel studies, to tackle challenging design situations. Once standard modeling procedures are established, wind tunnel tests are used to calibrate CFD modeling and predict accurate pressure distributions on facade structures [4]. To evaluate a computational fluid dynamics workflow for determining pressure coefficients for multi-story double-skin facades, this research aimed to simulate reduced scaled wind-tunnel studies within the simulation domain. The first step in refining an analytical model was to calibrate the method to existing sources of wind tunnel data.

3.1 Calibration Studies

The initial calibration step is replicating simulations of existing wind tunnel data for multi-story, single-skin and double-skin facade configurations. Two wind-tunnel studies were conducted to calibrate the CFD modeling in COMSOL Multiphysics. The first calibration exercise was that of a simplified isolated cube in an atmospheric boundary layer wind-tunnel. This experiment was carried out by 12 separate institutions with wind tunnels, results were compared [5], then carried out separately – and more recently – at full-scale measurements and reduced scale wind-tunnel experiments [6]**. Both of these research efforts were summarized in** *Overview of Pressure Coefficient Data in Building Energy Simulation and Airflow Network [7]. The second* calibration, presented herein, adopted the most similar physical testing to date: Marques da Silva and Gomes' tests of *Gap inner pressures in multi-story double-skin facades* [8, 9]. An *Unsheltered* and *Sheltered Tower* were simulated at a model scale of λ = 1/40 in an open-circuit wind tunnel with a 9 m x 3 m x 2 m test section. In this paper's research, the *Unsheltered* and *Sheltered Towers* were simulated and compared to the aforementioned wind-tunnel results, maintaining the original studies parameters: λ = 1/40, U =10.5 m/s, α = 0.18, and scaled building configurations dimensions; a = 32.5 cm, b = 20 cm and h = 70 cm, per Marques da Silva and Gomes [8]. The calibrations maintained all parameters mentioned, but varied the inlet's initial turbulence intensity (I_T) and floor surface roughness length (z_0) to identify the combination that generated the most comparable net pressure coefficients across the double-skin facade layouts, thus suggesting the most similar simulated turbulent flow environment.

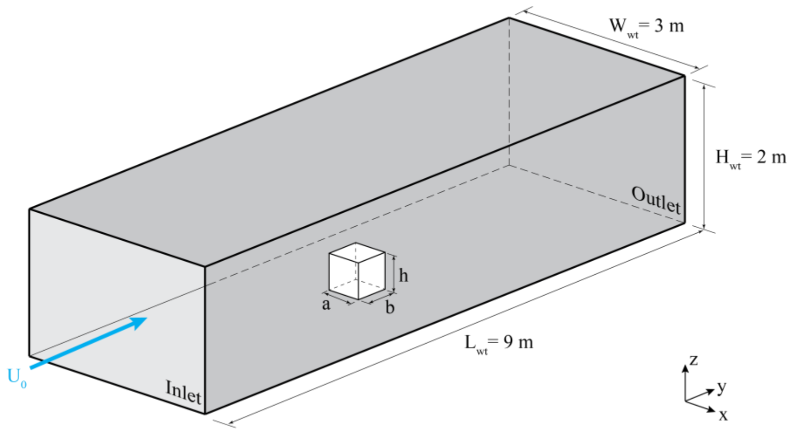

Figure 5: Simulated atmospheric boundary layer wind tunnel configuration.

For the simulated models, the three-dimensional solution domain places the study model — or building — at the center along the L_{wt} length and W_{wt} width, as well as placed with its base at z = 0.

Inlet: The vertical boundary plane at y = 0, the upstream inlet, has an initial velocity of U_0, defined below. The resulting pressure distribution between the inlet and outlet is variable. The initial turbulence intensity (I_T) and turbulent length scale (L_T) are also defined at the inlet.

Outlet: The vertical boundary plane at y = 9, or the downstream outlet, is specified as a zero gauge pressure (p_0 = 0) with no viscous stress.

Floor: The floor is defined as a wall function with applied roughness. The surface roughness length (z_0) varies based on terrain exposure and is modeled by the equivalent sand roughness ($k_{S,ABL}$).

Velocity Profile: The velocity profile varies as a function of the reference velocity (U_{ref}), height (z) and the power law exponent (α):

$$U_0 = U_{ref} * \left(\frac{z}{z_{ref}}\right)^{\alpha} \tag{1}$$

Sheltered Towers. Two sheltered tower configurations were used for comparison between the wind-tunnel studies and these simulations. The first, *Layout A*, is best described as a sheltered tower on the front and one lateral (left) side where both second skins have a raised/portal inlet, a through outlet/exhaust and unsealed laterally. The second, *Layout D*, is similar to *Layout A*, with the one difference being that the vertical edges of the cavity are closed, making this layout laterally sealed.

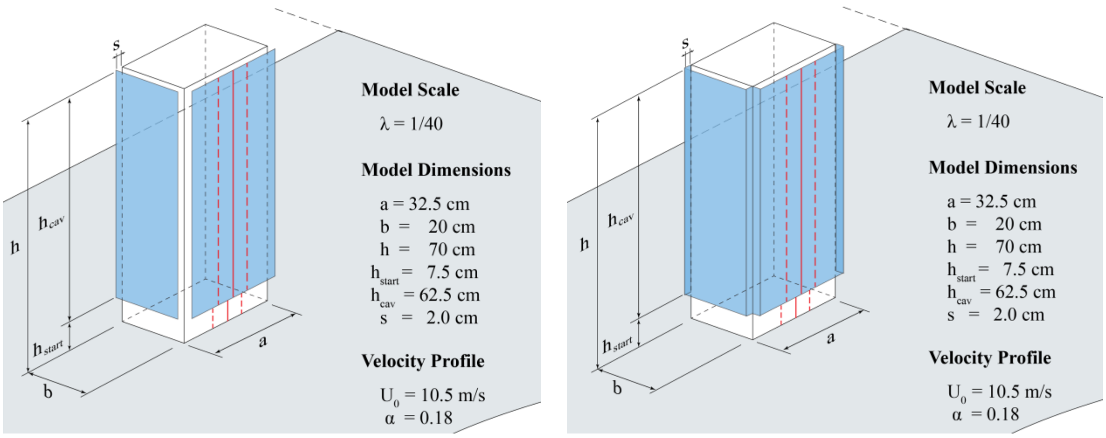

Figure 6: Sheltered Tower calibration model configurations: Layout A (left) and Layout D (right).

The overarching parameters that consistently yielded agreeable (or near-agreeable) results for the multiple layouts considered were an inlet turbulence intensity of $I_{T,inlet}$ = 0.15 and a roughness length of z_0 = 2.0 m. The $C_{p,net}$ profiles at *x/a* = 0.35 and 0.67 for Layout A and Layout D of Marques da Silva and Gomes [9] are shown in Figure 7. **The graph shows that for both Layout A and D, the selected set of input parameters yield** $C_{p,net}$ profiles that are near-matches for the peak pressures just above the air inlet, 0.1 < *z/h* < 0.2. For 0.2 < *z/h* < 0.4, the simulations for both Layout A and D have a greater magnitude than the wind-tunnel results. For *z/h* > 0.4, the Layout A simulation follows a near match profile shape through the center of the building height with slight over magnifications at times while Layout D maintains a constant over-magnification for the remaining height of the building.

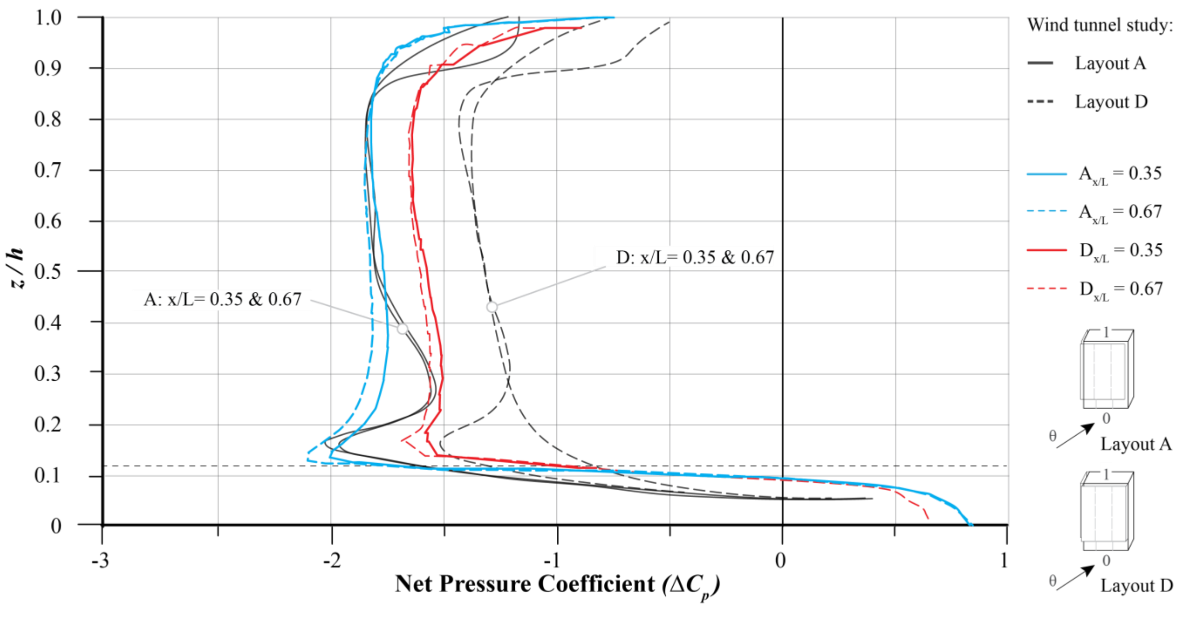

Figure 7: $C_{p,net}$ profiles at *x/L* = *x/a* = 0.35 and 0.67 for simulations ($C_{p,net}$ = $C_{p,int}$ - $C_{p,ext}$) compared to wind-tunnel studies ($C_{p,net}$ = $C_{p,DSF\ int}$ - $C_{p,unsht}$) [9], with U = 10.5 m/s, I_T = 0.15, α = 0.18, z_0 : 2.0 m, s = 0.8 m.

3.2 Description of Multi-Story Steady-State Simulation

The steady-state simulations utilized a three-dimensional simulation domain representative of the wind-tunnel test section, as shown in Figure 5. The turbulent flow simulations incorporate a Reynolds Averaged Navier Stokes (RANS) turbulence model type with a k-ε turbulence model with incompressible flow. The simulations maintain the parameters: U = 10.5 m/s, I_T = 0.15, α = 0.18, z_0 = 2.0 m. The building geometry is the same as the multi-story prototype outlined in Section 2.2: height of h_{top}= 21 m, width of a = 45 m and cavity depth of s = 1.0 m at a model scale of λ = 1/40.

In this research the airflow opening and exhaust configurations are treated as variables: all outlet configurations are *forward*, exhausting the cavity airflow at roof level in the same direction as the impinging load. The inlet and exhaust openings are of equal dimension, maintaining a total area of each at $s * a$. The analysis used four DSF configurations, varying the inlet configuration while maintaining a *forward* exhaust:

Face-Forward (FF): The *face* inlet occurs within the vertical plane of the outer skin immediately adjacent to the ground or plaza level.

Trench-Forward (TF): The *trench* inlet permits airflow into the cavity space through a recessed volume that is equal depth and inlet height as the cavity depth.

Raised-Forward (RF): The *raised* air inlet is lifted one story, beginning at *z/h* = 0.25 and occurs in the horizontal plane, or underside, of the cavity volume.

Shingled-Forward (SF): The *shingled* inlet permits airflow into the cavity through four opening bands, each 0.25**s* tall, that occur at ground level and hypothetical floor levels at quarter points up the facade.

3.3 Results

The interior and exterior pressure coefficients for each model are extracted; the pressure coefficient contour elevations for the *raised-forward* model are shown in Figure 8 with a line of symmetry (shown at the left of each elevation) at mid-width (*x/a* = 0.5).

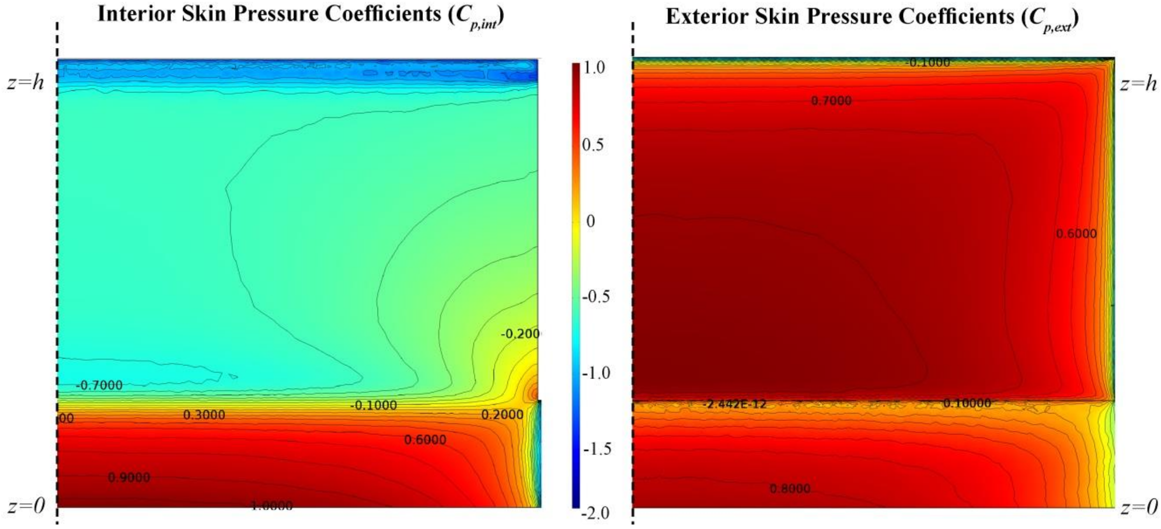

Figure 8: C_p contoured elevations for the *raised-forward* model's interior (left) and exterior (right) skins.

Each simulation model's pressure coefficient profiles at the center (*x/a* = 0.5) along both the interior ($C_{p,int}$) and exterior ($C_{p,ext}$) skins are reported in Figure 9. The $C_{p,ext}$ profiles possess a similar positive magnitude, $C_{p,ext} \approx$ 0.9, amongst all four configurations with the *shingled* inlet creating multiple declining profiles at each inlet band and the *raised* configuration halting at *z/h* = 0.25 since it is not full height. Both the *trench* and *face* inlet configurations follow a similar profile for both the inner and outer skins with slight shifts for near-ground peaks due to the vertical location of the openings. The interior skin profiles vary significantly depending on inlet configuration. The $C_{p,int(RF)}$ profile for the *raised* configuration is considerably (approximately 40%) less than the $C_{p,int(FF)}$ or $C_{p,int(TF)}$ profiles for the *face* and *trench* inlets. Furthermore, the *shingled* interior skin $C_{p,int(SF)}$ increases in magnitude in a step-like manner as it rises up the building towards roof level. At the roof level where the interior skin has the *forward* exhaust, all four inner skins' $C_{p,int}$ profiles converge around -1.0 to -1.2.

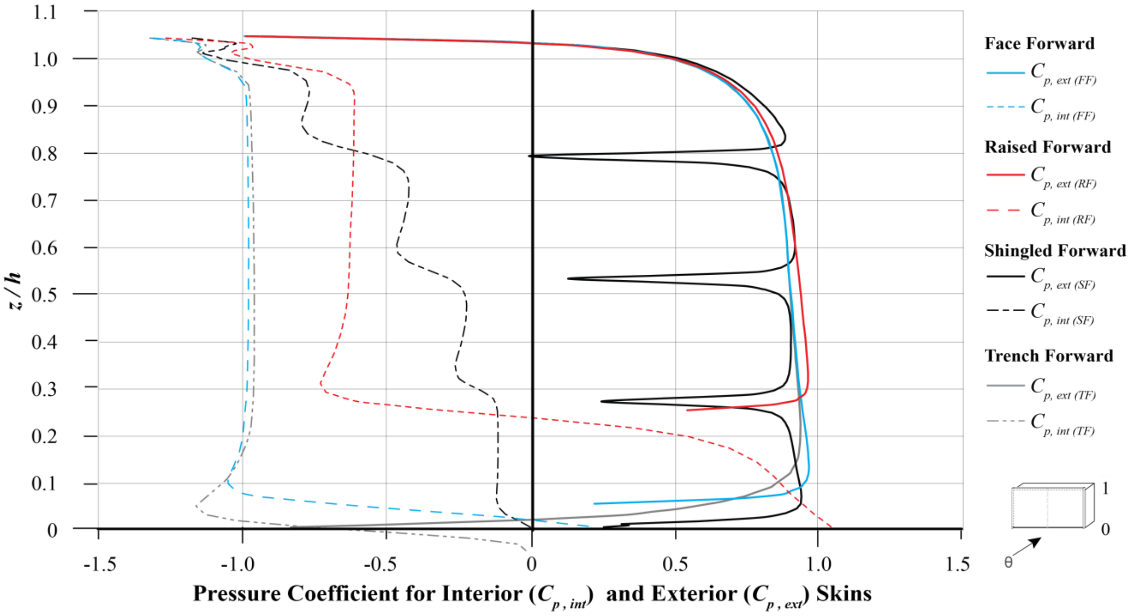

Figure 9: C_p values at x/a = 0.50 for interior and exterior skins.

The net pressure coefficient, $C_{p,net}$ (or $\Delta C_p = C_{p,ext} - C_{p,int}$), is calculated across the outer skin for each of the four models at x/a = {0.50, 0.67, 0.90} in Figure 10. The outer most profiles at x/a = 0.90 for all four configurations has the smallest magnitude (as compared to x/a = 0.50 and 0.67) for z/h < 0.95. Above that (z/h > 0.95), the x/a = 0.90 profiles increase to be the greatest magnitude, indicative of increased loads in the upper corners. The overall greatest $C_{p,net}$ values occur just above ground level for the *trench*- and *face-forward* configurations, nearing 2.0.

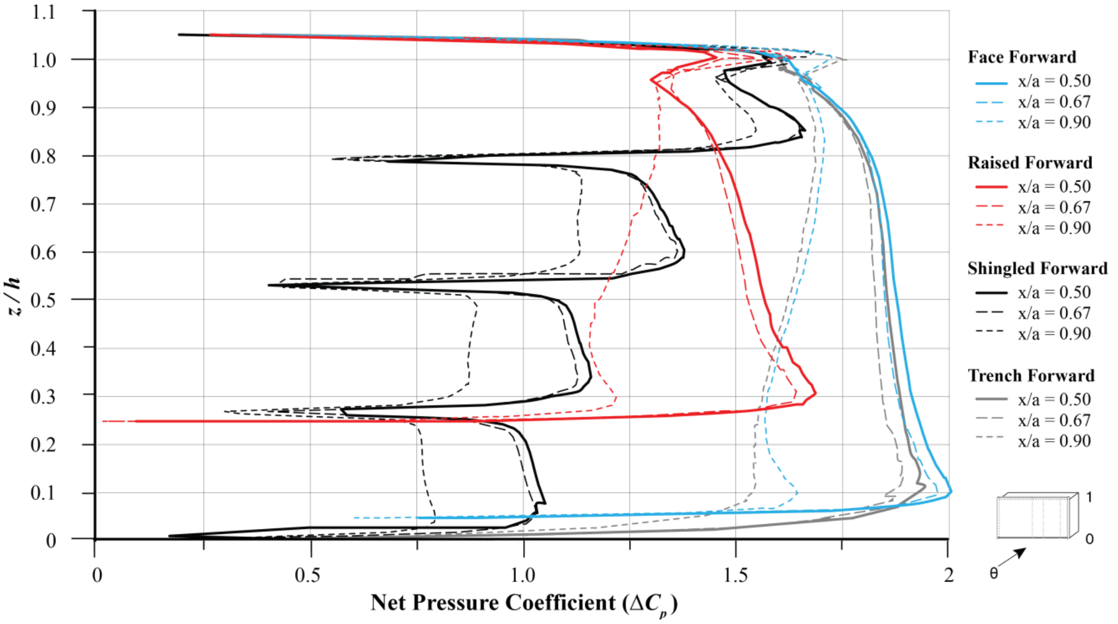

Figure 10: $C_{p,net}$ profiles at x/a = {0.50, 0.67, 0.90} for four simulations, all with *forward* exhaust condition.

A comparison of the outer skin's $C_{p,ext}$ (or $C_{p,DSF\ Outer}$)is compared to the equivalent for a sealed, single-skin facade, $C_{p,Single}$. The ratio is calculated for each of the four models at x/a = {0.50, 0.67, 0.90} in Figure 11. For the center portion of the building, 0.1 < z/h < 0.85, the outer skin receives an increase of 10 to 20% when compared to the single-skin facade. There are a few areas of a decrease in pressure, generally associated with the vicinity of inlet opening features. In the lower half, several spikes occur for the *face* and *raised* conditions at x/*a* = 0.90, indicating an increase in outer-skin loads near the building's lateral edges. In the upper region (*z/h* > 0.85) and near-roof edge, the ratio dramatically increases, peaking anywhere from 2.0 to 5.8 times that of a single skin (beyond the extents of the graph's x-axis) for the 12 different profiles.

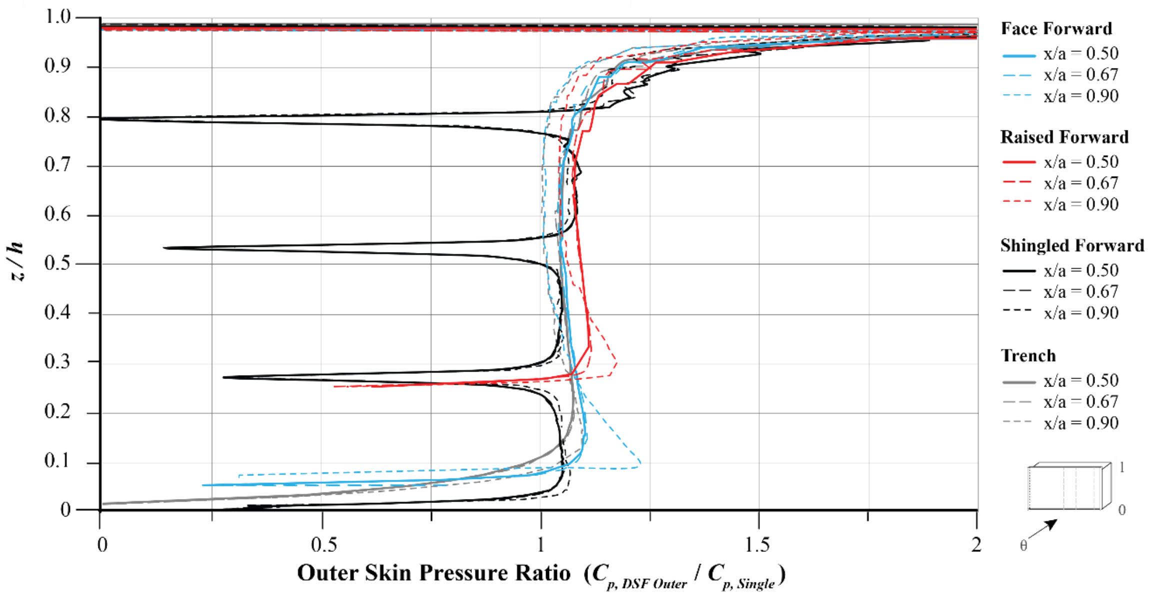

Figure 11: Outer skin pressure ratio profiles at x/a = {0.50, 0.67, 0.90}.

3.4 Future Work

This research will continue to explore the same set of inlet configurations but in combination with the *return* and *through* exhaust configurations. Special considerations unique to each inlet-outlet combination will be identified and summarized.

4 Conclusions

Previous wind tunnel studies of multi-story double-skin facade configurations [8, 9] were simulated in a CFD domain and showed reasonable agreement of net pressure coefficient differences for two layouts. These were predecessor studies to a series of multi-story DSF configurations for a prototypical building geometry deduced from a review of built multi-story double-skin facades in the United States. The analytical models varied the airflow inlet configuration while maintaining a *forward* exhaust.

The airflow inlet configuration has a noticeable impact on the pressure coefficients of multi-story double-skin facades, particularly the negative pressure on the inner skin within the cavity space. Inlet configurations that elevate (*raised)* or distribute the opening across the vertical height (*shingled*) exhibit a reduced magnitude of negative pressure in the cavity space through the lower and center portions of the elevation. The simulations highlight the dynamic pressure behavior that occurs at a building's edges and airflow openings that must be considered for each multi-story double-skin facades unique configuration.

5 Acknowledgements

The author would like to thank the following for their support of this research endeavor: the University of Southern California, Graduate School, Oakley Fellowship; the Advanced Technology Studio of Enclos; and Design Tectonics.

6 References

[1] Boake, T.M.: *Structure and Its Enclosure*, ACSA Technology Conference, Portland, Oregon, ACSA, 2002, pp. 64-73.
[2] Horsley, C.B.: *Prudential Project Includes 'Ice Pond'*, in: The New York Times, May 17, 1981.
[3] Perino, M. (ed.): *State of the Art Review Vol. 2A: Responsive Building Elements*, in: Annex 44: Integrating Environmentally Responsive Elements in Buildings, Aalborg University, International Energy Agency, 2007.
[4] Zammit, K., Overend, M. and Hargreaves, D.: *Improved computational methods for determining wind pressures and glass thickness in facades*, in: Challenging Glass 2, Delft University of Technology, 2010.
[5] Holscher, N., and Niemann, H.J.: *Towards quality assurance for wind tunnel tests: A comparative testing program of the Windtechnologische Gesellschaft*, in: Journal of Wind Engineering and Industrial Aerodynamics 74 (1998), pp. 599-608.
[6] Richards, P.J., Hoxey, R.P., Connell, B.D. and Lander, D.P.: *Wind-tunnel modelling of the Silsoe Cube*, in: Journal of Wind Engineering and Industrial Aerodynamics 95 (2007), pp. 1384-1399.
[7] Costola, D., Blocken, B. and Hensen, J.L.M.: *Overview of pressure coefficient data in building energy simulation and airflow network programs*, in: Building and Environment 44, no. 10 (October 2009), pp. 2027-2036.
[8] Marques da Silva, F. and Gomes, M.G.: *Gap inner pressures in multi-storey double skin facades*, in: Energy and Buildings 40 (2008), pp. 1553-1559.
[9] Marques da Silva, F. and Gomes, M.G.: *Effects of different multi-storey double skin facade configurations on surface pressures*, CISBAT 2005, Lausnne, Switzerland, 2005.

Changing Internal Pressure to Achieve Variable Thermal Conductivity in Thermal Insulation

Axel Berge, PhD student, MSc. Eng.
Chalmers University of Technology, Sweden, axel.berge@chalmers.se

Carl-Eric Hagentoft, Full Prof., PhD
Chalmers University of Technology, Sweden

Paula Wahlgren, PhD
Chalmers University of Technology, Sweden

Bijan Adl-Zarrabi, PhD
Chalmers University of Technology, Sweden

Summary

Cold climates might have a variable need for thermal insulation. When there are large heat loads a low U-value is preferable, and opposite when heat loads are low and it is cold outdoors. One way to adjust the U-value is to change the gas pressure within the insulation. This would be especially effective in nano-porous materials where the relation between pressure and thermal conductivity is stronger. Measurements have been conducted on an aerogel blanket and a fumed silica material. The results show an almost linear dependence in thermal conductivity at pressures between 1 kPa and 100 kPA for both materials. In the measurements, the thermal conductivity increase by a factor between 1.5 and 2.6 (highest conductivity divided by lowest conductivity).

Keywords: Adaptive façade, varied pressure insulation, thermal insulation, thermal conductivity, nano-porous insulation

1 Introduction

For buildings with high heat loads, placed in a cold climate, the optimal U-value of the walls varies. As long as the outdoor temperature is lower than the indoor temperature, a high U-value helps cooling the building when cooling is needed, while a low U-value reduce the need for additional heating when the heat load is not high enough to cover the heat losses. Thereby, adaptive walls with variable U-values could replace the heating system to regulate the temperature [1].

There are a lot of different solutions for facades which can adapt to the climate. Loonen have collected a lot examples in a comprehensive review [2]. The major parts of the adaptive facades are glazing systems and systems to utilize or avoid heat from the sun. Opaque facades can commonly achieve lower U-values why there is an interest in adjusting these as well.

One way to vary the thermal conductance through the walls would be to vary the gas pressure in the walls. One solution, where a wall partitioned in cells Is evacuated by a vacuum pump is patented [3]. The problem with this solution is that a really low pressure is needed, which would need a very tight structure. Also, the solution would transfer a large amount of heat through radiation. One solution to the problem with the pump is the so called Switchable insulation where a metal hydride releases hydrogen when heated and reabsorbs it when cooled down [4,5]. One downside with these is that the release of hydrogen demands a high temperature in the metal hydride which is why the papers recommend uses such as solar collection walls and automobiles. Also, the thermal conductivity of hydrogen and other gasses are approximately constant around atmospheric pressure, which is why the pressure in the panels has to be constantly low.

Today some new types of insulation materials have been introduced to the building sector, such as fumed silica and aerogels, with a pore size in the nanometer range. In this size range, the thermal conductivity changes and become close to linearly dependent on pressure. This leads to a concept of a vacuum pumped wall containing nano-porous insulation.

1.1 Scope

This paper covers measurements on nano-porous materials at varying pressures. Two materials have been tested: an aerogel blanket and fumed silica. One sample of each material have been tested with the aim to investigate the materials behavior when the pore gas pressure change. Both steady state properties and transient responses have been measured and compared to numerical simulations.

1.2 Method

The samples have been measured in a heat flow meter. Each sample was put in an air tight bag which could be evacuated so that the gas pressure within the samples varies. The results have been analyzed in comparison to one dimensional transient finite volume simulations.

2 Thermal conduction through nano-porous materials

The thermal conductivity through a porous material can approximately be separated into three parts according to Equation (1):

$$\lambda_{tot} = \lambda_{solid} + \lambda_{radiation} + \lambda_{gas} \qquad (1)$$

where λ_{tot} is the apparent thermal conductivity of the porous insulation material, λ_{solid} is the conductivity of the solid structure of the material, $\lambda_{radiation}$ is the thermal conductivity by radiation through the pores and λ_{gas} is the thermal conductivity through the pore gas. This is a somewhat simplified description due to some heat transfer effects occurring in the interface between gas and solid but it can help to describe the principles..

Conventional insulation materials consist of porous materials where the function of the solid structure is to keep the gas still. The apparent thermal conductivity of the material will thus never be less than the conductivity through the pore gas. For a material with an average pore size in the nanometer range, this changes. In smaller volumes, the probability of collision between molecules decreases in favor of collisions between the molecules and the solid walls enclosing the volume. The collision between gas and solid commonly transfer less energy than a collision between two gas molecules which lead to a decrease in thermal transport through the gas. This is called the Knudsen effect [6].

The thermal conductivity through a gas is in large volumes independent of the pressure. In nano-porous materials, a lower pressure would mean even less collisions between molecules, reducing the thermal conductivity in the gas even further. Theoretical values for the thermal conductivity through air are shown in Figure 21. The characteristic size corresponds to a theoretical distance between two parallel plates.

Figure 21 shows that for pore sizes above 10 µm the effect can be neglected for all but very low pressures. For smaller pore sizes, the effect will increase in influence and the thermal conductivity also becomes more linearly dependent on pressure.

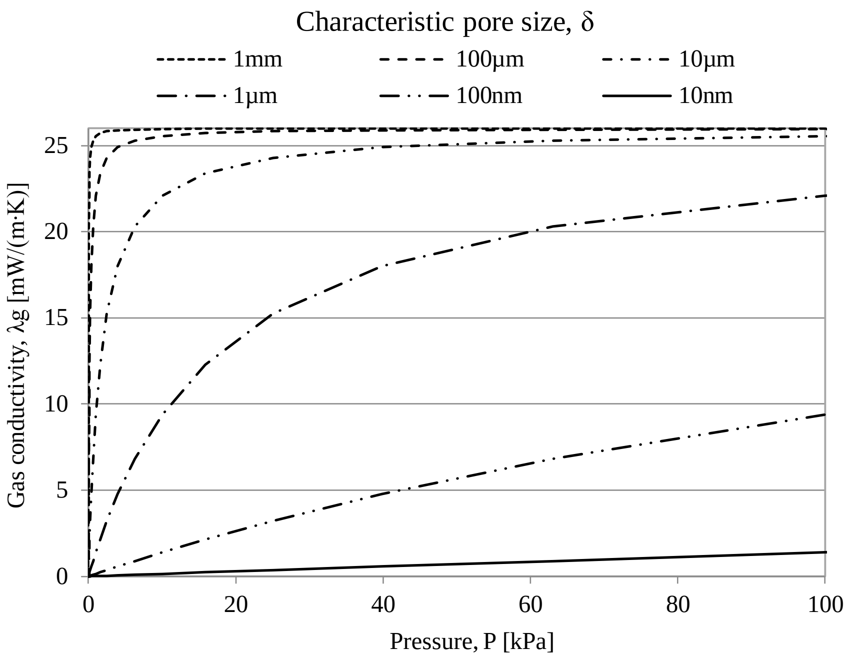

Figure 21: Theoretical relation between thermal conduction in a gas, gas pressure and characteristic pore size.

3 Measurements and simulations

Heat transfer measurements were made for two nano-porous sample materials: an aerogel blanket and fumed silica harvested from a vacuum panel. The heat flow through a sample was measured with a guarded heat flow apparatus with a square measurement area of 0.1x0.1 m^2 positioned on the cold side of the sample. The measurement area is surrounded by 0.1 m wide guard areas with the same regulated temperatures as for the measurement area. The guards create a one directional heat flow through the measured part of the sample.

In order to test the sample at various pressures, it was set-up according to Figure 22. The sample was put in an air tight bag. When the bag was evacuated, the bag itself closed tight and hindered the air from evacuating the sample, why perforated tubing was added around the sample. The evacuated air passed through a polyurethane filter to protect the vacuum pump and the manometer from dust particles leaving the sample material. A valve was added to regulate the pressure. Both the evacuation and the refilling took close to 30 s.

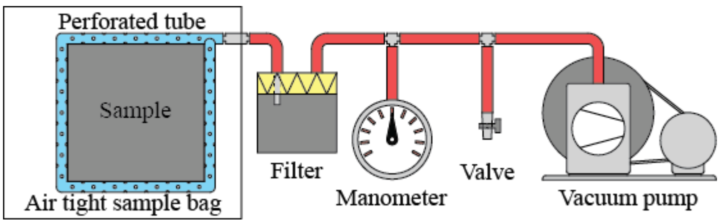

Figure 22: Set-up heat flow meter samples.

The evacuation of air changes the thickness of the samples during the measurement. But, in this study, the variation in heat flow through the sample was the main interest rather than the actual thermal conductivity. Therefor, the thickness measured before the first measurements have been used for all thermal conductivity calculations. The aerogel blanket was 20 mm thick and the fumed silica sample was 22 mm thick.

The results at various pressures are shown in Figure 23 together with the linear trend for each curve. Both materials' thermal conductivity shows a linear dependency on the pressure all the way up to atmospheric pressure, which makes the conductivity easy to regulate. For both materials the conductivity seems to make a drop from the linear trend at low pressures, giving an even better performance. Though, the reason for this drop have not been investigated within this study.

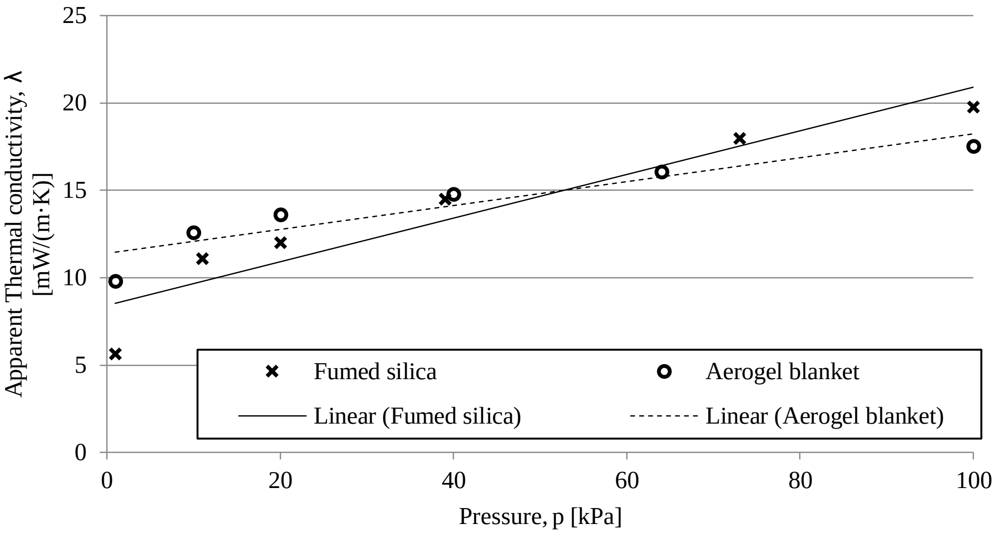

Figure 23: Apparent thermal conductivity for aerogel blankets and fumed silica at various pressures between 1 kPa and 100 kPa (atmospheric pressure).

The linear trend of the aerogel blanket results in a thermal conductivity between 12 mW/(m·K) and 18 mW/(m·K) at 1 kPa and 100 kPa respectively. This gives a variation factor of 1.5 defined in Equation (2):

$$VF = \frac{\lambda_{pmax}}{\lambda_{pmin}}, \qquad (2)$$

where *VF* is the variation factor and λ_{pmax} and λ_{pmin} are the thermal conductivities at the maximum and the minimum pressure respectively. The highest obtainable U-value with the aerogel blanket would be variation factor times the lowest U-value. This does not account for the structural elements in the wall system which will lower the variation factor even further.

The linear trend of the fumed silica shows a thermal conductivity between 8 mW/(m·K) and 21 mW/(m·K) at 1 kPa and 100 kPa respectively. This gives a variation factor of 2.6. If the lowest and the highest measured values, at 5.6 and 19.8 mW/(m·K) respectively, are used instead of the linear function the variation factor would be 3.5.

The time scale of the regulation of walls with varying pressure was tested by cycling the samples between a high and a low pressure while measuring the heat flow output continuously. The cycle length was adjusted until the sample reached close to a steady state in every cycle. The results are shown in Figure 24 where the fumed silica had a cycling time of 40 min while the aerogel blanket had a cycling time of 20 min.

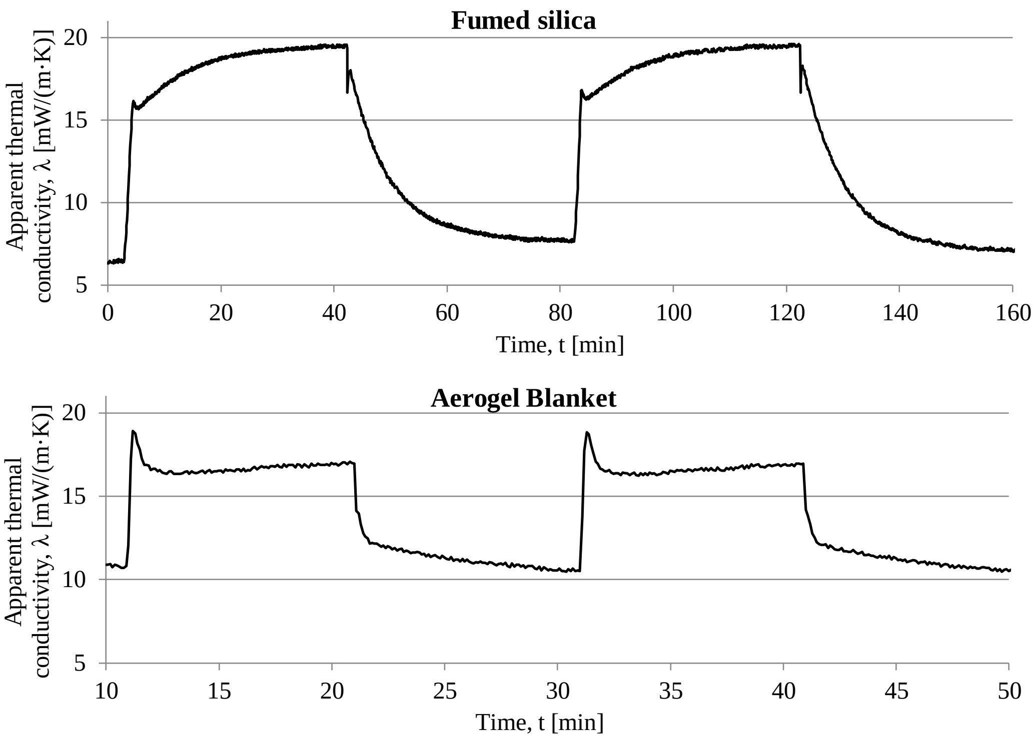

Figure 24: Time dependent behavior of the apparent thermal conductivity of samples for a pressure cycling between 2 kPa and 100 kPa . A fume silica sample on top and an aerogel blanket sample at the bottom.

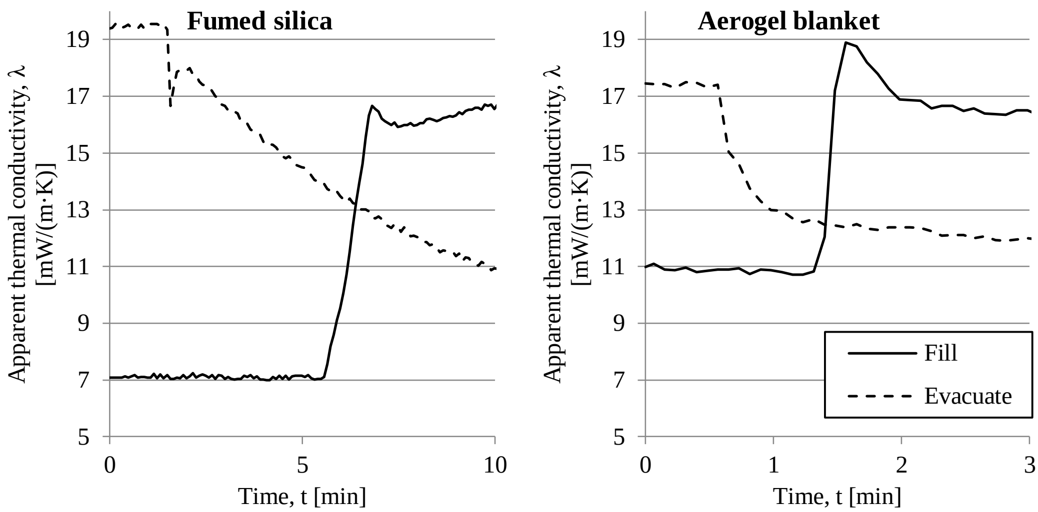

Figure 25: Detail of the time dependent measurements showing the initial phase of both the filling and the evacuation. The results from the fumed silica are shown to the left and the results for an aerogel blanket is shown to the right.

Aside from the delay to reach a new steady state, some fluctuations appear the first minutes after the pressure is changed. The fluctuations are shown in more detail in Figure 25. For both materials there is a peak in the thermal conductivity when the sample is filled and for the fumed silica there is a valley when the material starts to be evacuated. Four mechanisms that could influence the behavior have been investigated:

- Internal diffusion of gas in nano-porous material delaying the change in pressure and thereby delaying the improvement in thermal conductivity.
- Thermodynamic influence on temperature when pressure is changed. An increased pressure heightens the temperature while a decrease in pressure lowers the temperature.
- When the pressure is increased, the sample is filled with air from the laboratory. The temperature of the air will influence the measurement.
- In the used heat flow meter there is thermal resistance between the cold temperature and the sample. This resistance will influence the steady state temperature distribution and thus make the sample to readjust to steady state.

The four mechanisms where tested by one dimensional finite volume simulation. At the moment of evacuation or filling the room, air temperature change was applied to the simulation according to Equation (3) and the thermodynamic temperature change was applied according to Equation (4).

$$T_{t+1}(x) = T_{room} \cdot \frac{C_a}{C_a + C_m} + T_t(x) \cdot \frac{C_m}{C_a + C_m} \tag{3}$$

$$T_{t+1}(x) = T_t(x) + \Delta T_{therm} \tag{4}$$

where T_{t+1} and T_t are the temperatures before and after the change, T_{room} is the room temperature, C_a and C_m are the volumetric heat capacity of the air and the solid material respectively and ΔT_{therm} is the temperature difference created by a pressure change in the gas. The temperatures T_{room} and ΔT_{therm} were 24.2°C and 0.5°C respectively and were obtained by temperature measurements with thermocouples positioned in the room air and in the center of the sample during measurement,.

The diffusion of gas into the material was assumed to be governed by Equation (5);

$$P_{t+1} = P_t + D \cdot (P_t - P_{out}) \cdot \Delta t \tag{5}$$

where P_{t+1} and P_t is the pressure before and after the time step, P_{out} is the imposed pressure cycling between a maximum and a minimum, D is a diffusion term and Δt is the time step length. The thermal conductivity of the sample was then defined as linearly dependent on the pressure, varying between a maximum thermal conductivity and a minimum thermal conductivity at the maximum and minimum pressures respectively.

Table 17: Material data for aerogel and fumed silica for use in the simulations.

Property	Aerogel	Fumed silica	unit
Specific heat capacity, C_p	950[1]	850[2]	J/(kg· K)
Density, ρ	114[1]	175[2]	kg/m^3
Porosity, P	93[1]	93[2]	%
Max pressure conductivity, λ_{High}	18[3]	20[3]	mW/(m·K)
Min pressure conductivity, λ_{Low}	11[3]	7[3]	mW/(m·K)

[1] [7], [2] [8], [3]Measurements

The resistance in the heat flow meter was treated as an additional constant resistance on the cold boundary in the model. The material data used in the simulations are shown in Table 1.

The results from the simulations are shown in Figure 26. The thin dashed lines show the cases where one of the mechanisms have been active, while the thick solid line show the case with all the mechanisms. Figure 26 can be compared to Figure 24. The figure shows the fluctuations shown in measurements in the beginning of the filling and in the evacuation. Although, the effect look sharp compared to the measured case. This might be due to that the effects from temperature change were modeled as instant rather than a process over time.

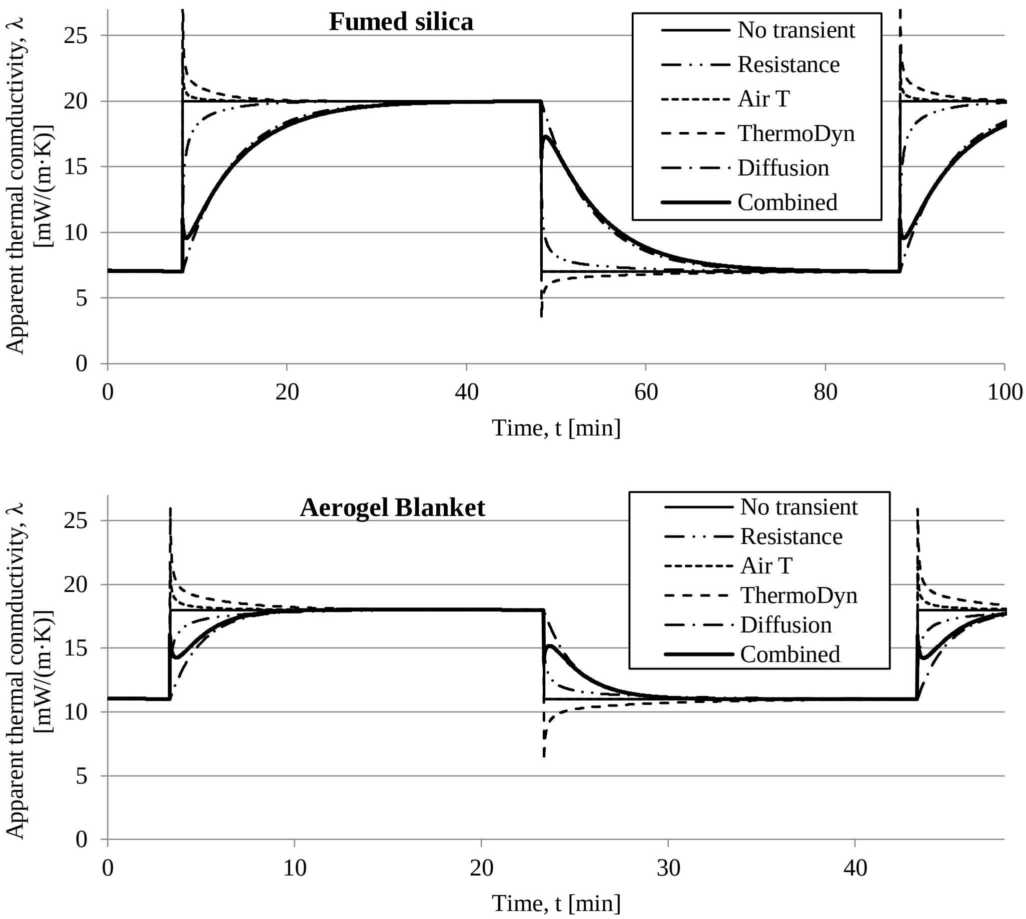

Figure 26: Simulation results

4 Conclusions

Both aerogel blankets and fumed silica could be used as insulation material in a varying pressure wall. Both materials show a close to linear relation between thermal conductivity and pressure. The variation factor, defined as the maximum thermal conductivity divided by the minimum thermal conductivity was somewhat better for the fumed silica (2.6 compared to 1.5 for the aerogel blanket). This is the upper theoretical limit of how much the U-value could change in a wall assembly. It should be mentioned that none of the materials have been optimized for this kind of application.

For both materials it takes some time before the thermal conductivity changes when the pressure is changed. The pressure change seems to be delayed by some effect connected to the spread of air into the nano-porous material. The timescale of the materials in this experimental set-up was around 10 min for the aerogel and around 40 min for the fumed silica.

There are also other effects influencing the heat flow from the sample. Both the warm ambient air inserted into the sample when it is air filled, and the thermodynamic effect from expansion or evacuation of air seems to have a significant effect on the outflow from the sample for a small time period.

5 Future research

This study will continue with whole building simulations of buildings with variable U-values. The simulations will use the variation factors from these measurements.

The energy flows during filling and evacuation will be studied even more thoroughly. The aim is to analyze how energy is stored and released in the material when the pressure changes and if it is beneficial or not.

This is a first overview of the possibilities to use nano-porous materials in variable pressure vacuum insulation. Before it could be used in a real product there are a lot of practical issues which have to be solved. Some examples are:

- How the vacuum pipes should be drawn through a building.
- How much energy the vacuum pump would need.
- Choice of materials and sealing techniques to use for the panel envelopes.
- Possibility to create a better material for the panel cores.
- How a complete and fast enough evacuation can be guaranteed for larger panels or panel systems.
- How the panel airtightness could be protected.

6 References

[1] Hagentoft C-E. *Potential impact on innovative and active building envelope components and materials.* Proc. 5th IBPC, Kyoto, Japan: 2012, p. 309–15.

[2] Loonen R. *Climate Adaptive Building Shells. Master of science thesis.* TU Eindhoven, 2010.

[3] Xenophou T. *System of using vacuum for controlling heat transfer in building structures, motor vehicles and the like* US patent No. 3,968,831. 1976.

[4] Meister M, Horn R, Hetfleisch J, Caps R, Fricke J. *Switchable Thermal Insulation for Solar Heating.* Therm. Conduct. 24THermal Expans. 12, Lancaster, USA: Technomic Publishing Company Inc.; 1997, p. 417–27.

[5] Benson DK, Potter TF, Tracy CE. *Design of a variable-conductance vacuum insulation.* SAE Technical Paper; 1994.

[6] Baetens R, Jelle BP, Gustavsen A. *Aerogel insulation for building applications: A state-of-the-art review.* Energy Build 2010;43:761–9.

[7] Aspen Aerogel. *Spaceloft insulation Technical Guide*. 2009.

[8] Simmler H, Brunner S, Heinemann U, Schwab H, Kumaran K, Quénard D, et al. *Study on VIP-components and Panels for Service Life Prediction of VIP in Building Applications (Subtask A)*. IEA/ECBCS Annex 39; 2005.

functional glass

A Movable Canopy

Jürgen Neugebauer, FH-Prof. DI. Dr.
University of Applied Sciences, Graz, Austria, juergen.neugebauer@fh-joanneum.at

Summary

Flexible structures in which the glass must pursue all deformations means a completely new and exciting way of constructing with the building material glass. This visionary idea has been realized in the company SFL Technologies GmbH headquartered in Austria. The special feature of this foldable roof is its flexibility. The roof can be opened and closed. The need for flexibility is achieved by usage of very thin glass “Gorilla Glass” from Corning Incorporated based in USA with a thickness of d=0.7mm. To comply all safety aspects for overhead glazing two thin glass plies were laminated to a laminated safety glass. This laminated safety glass can be described with a base weight of less than 5kg/m² as ultra-light. The flat produced LSG is forced while open the canopy into conical geometry. Hence a statically stable form is achieved.

Keywords: thin glass, canopy, chemical strengthening, thermal treatment

1 Introduction

The tendency in the last couple of years goes to more transparency in the façade. With this tendency the fact of larger glass elements is connected. With larger dimensions of the glass the upcoming problem of too much weight arises. This problem of the weight has consequences for the substructure and therefore it is currently a pursuit of reduction of the weight.

Everybody knows thin glass in the application as a screen for laptop, tablet or handy. The application of such a glass in building is new and an interesting topic for the future. Glass with a thickness of 0.55 up to 2.0 mm can be defined as a thin glass or even as ultra-light. On the market there are several suppliers which offer such a thin glass. On the one hand there are e.g. the “GORILLA GLASS” [1] of Corning Incorporated or the “LEOFLEX” of AGC [2] which are pre-stress by chemical treatment and on the other hand there normal soda lime silicate glass which is pre-stress by thermal or chemical treatment.

The design with thin glass causes a totally new kind of thinking. This thin glass is very weak against local bending stresses and has a large capacity against membrane stresses. For this reason structures with less part of local bending stresses and large part of membrane stresses had to be found. Such structures are more or less curved structures. For example cylindrically or conically shaped geometries of glass a favorable for such transfer mainly by membrane forces.

The visionary idea of a movable canopy by APG International had been realized by the company SFL Technologies GmbH headquartered in Austria. The special feature of this foldable roof is its flexibility. The roof can be opened and closed.

2 Thin glass

For the production of such thin glass beside normal float glass facilities two additional process are available. The so call “Dawn draw process” and the “Overflow fusing process” are described in the following sub-chapters.

2.1 Dawn draw process

The molten glass flows through a small gap in the bottom of the melting tank down and is down cooled by annealing furnaces, as shown in figure 1. After this controlled down cooling the glass is cut into certain sizes

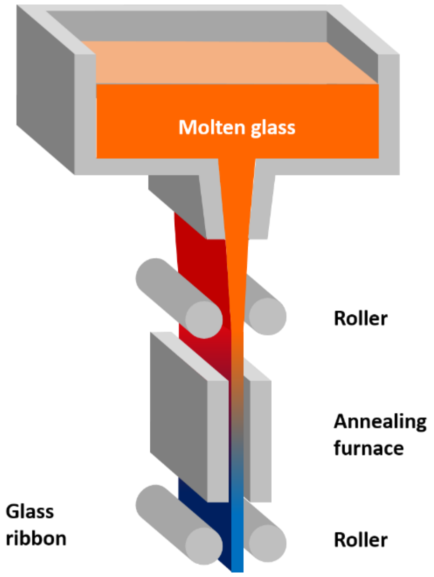

Figure 1: Dawn draw process.

2.2 Overflow fusing process

The molten glass is poured into a spill-way. From this spill-way the molten glass flows, as shown in figure 2, on both sides down and fuses at the junction together. After a down cooling phase the glass is cut into panels with certain sizes.

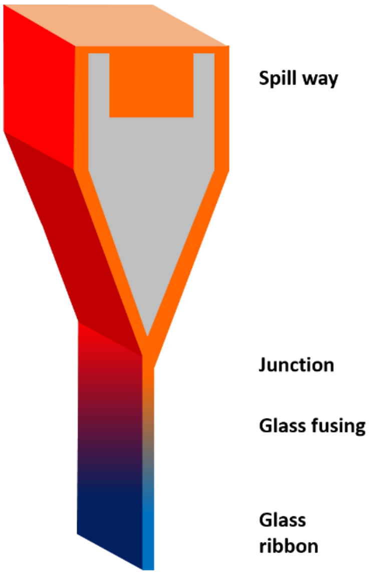

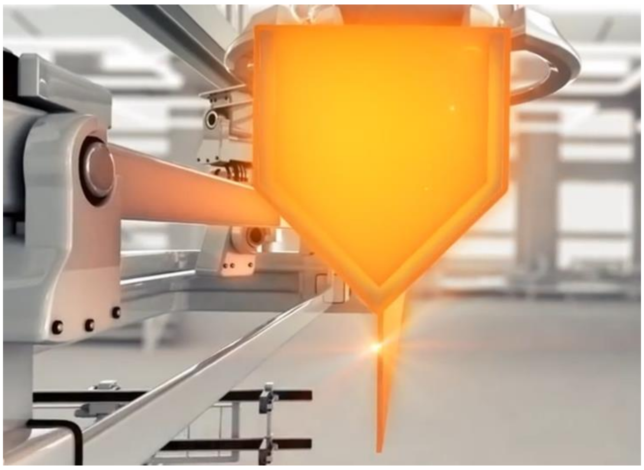

Figure 2: Over flow fusing process. [1]

3 Pre-stressing of glass

To increase the ultimate bending strength, the glass is pre-stressed. With a thermal or chemical treatment are two different possibilities available for the pre-stressing of the glass.

3.1 Thermal treatment

In figure 3 below two different possibilities for a thermal treatment are shown. The right sketch illustrates the typical process in which the glass is moved on rolls forwards into the heating zone and is heated up above the transition point. After this heating process the glass is blown up with air. During this down cooling process the glass is permanently moved forwards and backwards. The thinner the glass the more so called roller waves occurs.

For this reason the Austrian company LISEC has investigated a new process in which the glass is transported on air cushions, as shown in figure 3 left. With this technique it is possible to pre-stress a thinner glass by thermal treatment without roller waves.

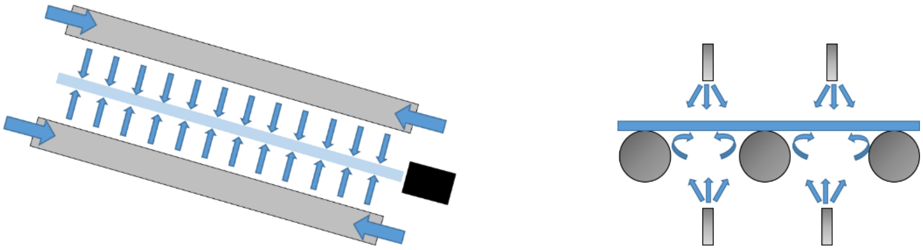

Figure 3: Thermal treatment.

3.2 Chemical treatment - Ionic Exchange

Another possibility to pre-stress the glass is the chemical treatment. The glass is immerged into potassium nitrate. At a temperature of approx. 370 °C the effect of ionic exchange takes place. The smaller sodium ions diffuse from the glass into the liquid potassium nitrate and the larger potassium ions penetrate into the glass matrix, shown in figure 4. Due to the larger ionic diameter the compressive strength in the close up range of the surface results. The thickness of the compressive zone is around 200 µm.

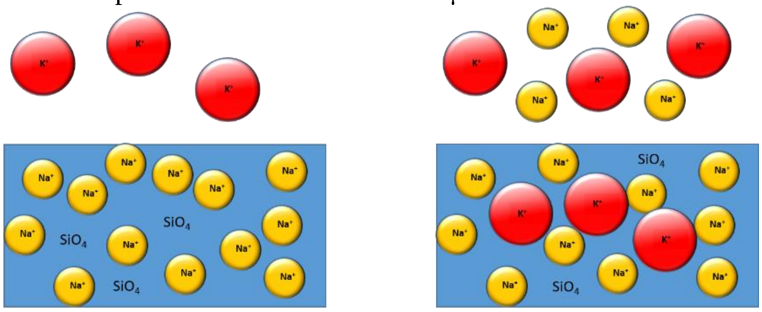

Figure 4: Chemical treatment – Ionic Exchange.

The compressive strength is given by the different suppliers. Corning Incorporated shows in their data sheet for the "GORILLA GLASS" a compressive strength (pre-stress) of 600 MPa [1] and AGC for the "LEOFLEX" a compressive strength 800 MPa [2]. The values for ultimate bending strength, which are important for a structural design, are still missing in the data sheets.

4 Movable canopy

A wonderful application of the thin glass technology is the movable canopy which is described in the following sub-chapters. Not only became a canopy realized, this canopy can be opened and closed. For the realization of canopy a couple of difficulties problems had to be solved. One of these were the description of the movement of all parts of the canopy.

4.1 Concept of movement

The basic idea comes from a paper lantern which can be find at the most birthday celebrations for children. One can buy such lantern as a flat folded paper and it can be opened. In the open position the flat paper is forced to a conical geometry. The same principle was use for the canopy, but instead of paper glass was used. In addition not a whole circle only the half of a circle was designed. With this a static system of an arch had been achieved. The flat glass was forced into a conical geometry which is a stable structure.

Figure 5 below shows the opened and the closed canopy. The front view illustrates the movement of the glass which is in the opened position a half circle (blue). If the top of the cone, marked with S, moves from the position S´ (opened) to the position S (closed), the glass becomes flat and the arch radius increases (red). The connecting line between S and S´ is not straight it is a curved line, as shown in the side view. In sum the glass makes a movement between a flat and a conical geometry of the glass.

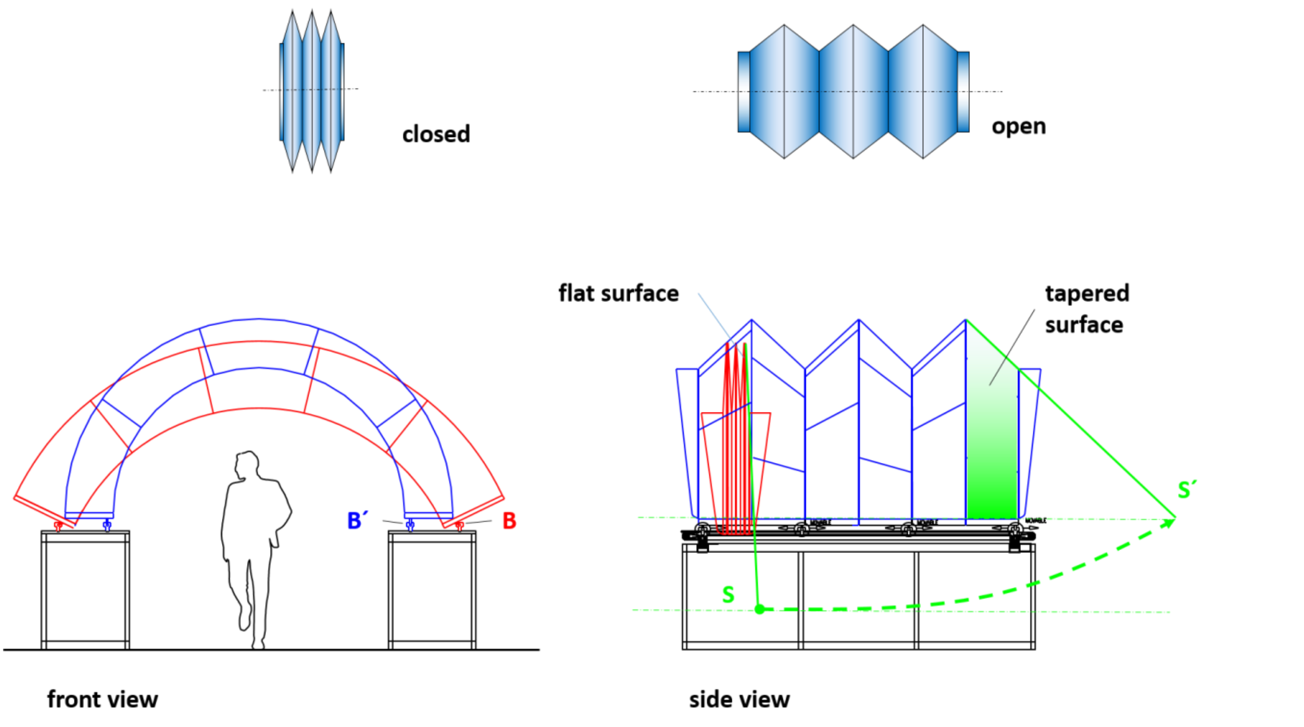

Figure 5: Concept of movement

Beside the movement of the top of the cone the lines of movement of the basis points are important. As shown in in the diagram in figure 6 below, the line of movement also not linear. The blue line indicates movement of first, the red line the second and the green line the third the pair of basis point. Due to the same geometry of the three arches the longitudinal movement of the second pair of basis points is the double of the first pair of basis points and the movement of the third pair basis points is the threefold. Inward and outward all the basis point have the same movement.

This investigation was for the design of the motor devices very important. The movement inward and outward is not uncoupled from the movement longitudinal. In the case of this realized canopy a system of rails longitudinal was arranged for the process of opening and closing. A system of rails perpendicular to the axis of the canopy handles the movement of the basis point inwards and outwards. The longitudinal rails were driven by an electrical motor to force the basis points inward and outward. This leads to the effect that the canopy opens and closes.

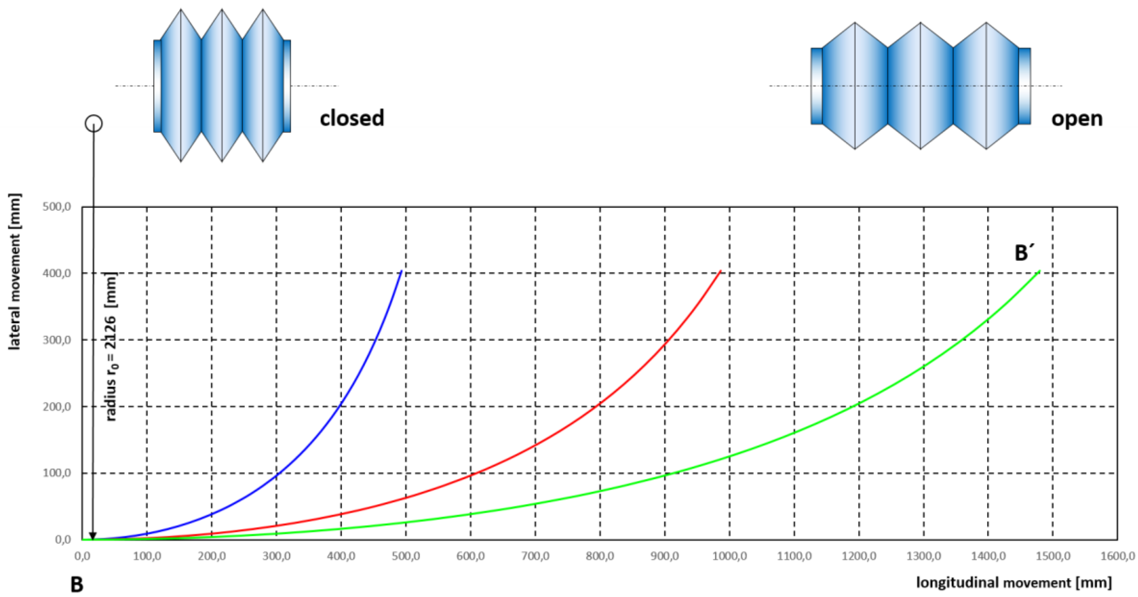

Figure 6: Movement of base points B to B´

This can only be possible with extreme flexibility of the used glass. Figure 7 shows in three pictures out of an animation three steps of the process of opening and closing the canopy.

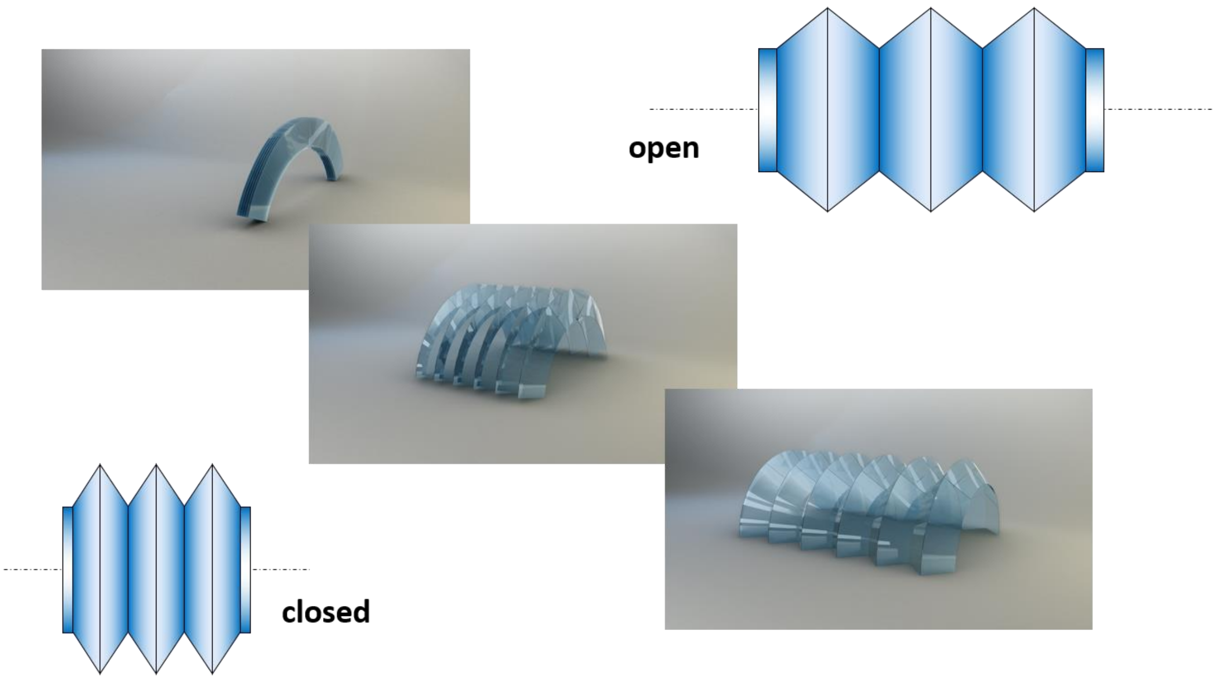

Figure 7: Visualization of the concept [3]

Here the body text continues.

4.2 Realized movable canopy

The realized canopy consist of 3 arches and each arch consists of two sides. The side of the arch is built with 5 glass elements on the one side and 4 glass elements and two halves of an element on the other side. For safety demands each element is a laminated safety glass consists of two plies “Gorilla Glass” with a thickness of 0.7 mm. A PVB-interlayer with a thickness of 0.38 mm was used. One element has an arch length of approx. 1200 mm at the outer radius and a height of approx. 700 mm. All these laminated glass units were glued to a stainless steel strip on both sides. This strips have the task to distribute the local effects to a larger area.

All side were connected with hinges to a steel rod which continuously reaches from one basis point to the opposite basis point. The steel rod at the top and in the valley has the function of a back bone.

At both ends of the canopy so call end caps were mounted. These end caps guarantee the stability of the arches, especially in the closed position.

Figure 8: Picture of the canopy - front view

Figure 9: Picture of the canopy - side view

Figure 10: Picture of the canopy - back view

5 Acknowledgements

Many thanks to the owner of SFL Technologies Mr. Hans Höllwart who financed this wonderful movable canopy.

6 References

[1] CORNING Incorporated; Corning® Gorilla® Glass 3 Product Information Sheet
[2] AGC Electronics America; Leoflex Architectural Glass
[3] APG International; Rederings

A new dawn rising - Energy efficient building skins with Vacuum Glass

Helmut Hohenstein, Dr
Dr.Hohenstein Consultancy

Summary

Glass Companies compare too often VG price today with triple insulating glass with 2 coatings considering similar windows and facades production only. But with VG the door is wide open for complete new solutions and advantages in window, façade and wall constructions minimizing these considerable costs. Architects, who come more from a holistic approach and the performance side, balance costs for investment against utilization and operational costs.

If one considers the frame development for windows, it is easy to be seen that there is a lack of new solutions for energy saving and it was more a development of steady growth of the cross section. Frames have taken more and more surface area on a window. We can use with VG the former space of IG especially for triple IG as an excellent opportunity to build, for example, a new box-type or counter-sash windows replacing the triple IG, but with the option to integrate other functions on a smallest version. We are only at the beginning. Very few experts and companies have shared their thoughts on these aspects. But we do need less independent actions; we need more integrated vertical oriented teams to find holistic solutions.

Energy Plus Houses with VG - the future of building: There is so much to do and so much to achieve. This industry should have a general concept to utilize VG in order to satisfy the present architectural requirements and future expectations.

1 Introduction

In the past twenty years a series of technical difficulties need to be conquered in order to mass produce high-quality vacuum glazing. High-quality means high performance and long-life, the two are inter-related. A mass production line must be able to achieve these two requirements if it is to produce VG products that can be accepted by the building society. Gradually this has to be improved and developed by continuous reduction of cost and maximization of production capacity.

It is a pity that the leading glass companies were not willing to invest in a real production scale, they remained on the research level compared to Professor Tang's strategy, and lose still time. Professor Tang succeeded with his first projects and sales whilst at the same time learned a lot from actual practise. This led to the eventual break-through today.

His developing company - owned by a governmental real estate holding in Beijing - trusted the long term success and had been producing a small automated line of Vacuum Glass for some time and sold VIG to Chinese governmental projects from 2004 onwards as shown below. Importantly from 2004 to the present day these buildings can confirm almost no failures – providing proof that Professor Tang's innovative solutions are working well.

1.1 What is Vacuum Glass?

The top surface of the vacuum glass will remain at near room temperature all the time. This is the magical thermal insulation and preservation properties of VG. It uses the principle of vacuum thermos flasks, where a narrow vacuum space (about 0.2mm) between two sheets of glass is maintained in order to prevent thermal and sound conductance via air.

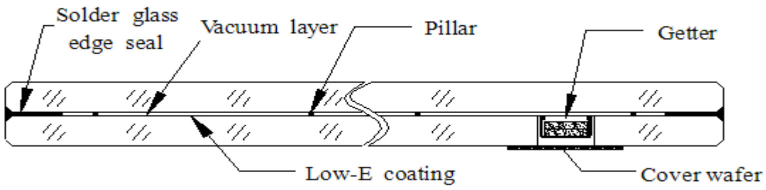

Figure 1: Vacuum Glass Structure

Considering security, one can use hybrid IG+VG = VIG. If the security requirement is higher, EVA-lamination on VG, which is thinner, can be taken, PVB can only be applied in a rubber bag process.

1.2 The advantages and disadvantages of VG applied in Green Buildings

Apart from energy performance, shading, sound insulation, safety and other properties are also better than for standard insulating glass. Plus, it has relatively thin thickness, lightweight, and Low-E coating is better protected. Thus VG offers an overall advantage compared to insulating glass.

- Thermal insulation property of VG superior than for IG, much thinner
- Excellent sound insulation 37 dB, compound VG is up to 44 dB, whereas Ig has only 29 dB
- Superior anti-frost and anti-condensation performance
- No breaking or crack problem of VG, used in areas with low air pressure (like Tibet). It can be transported from low altitude to high altitude area because the vacuum layer could avoid cavity expanding, lacking any convection and gas expansion by atmospheric conditions
- U-value invariable - when used horizontally or inclined, VG has due to the lack of convection no loss of insulation (regular IG up to 50 %). Thus, VG is especially effective for skylights, overhead solutions and roof windows.
- VG has high strength under wind pressure. That is because the two panes of VG are connected rigidly by soldered glass - > 5000 Pa
- Designed life time 50 years due to patented getter solution. VG is sealed with inorganic material, in this case with a glass frit
- Pillar - appropriate strength, fully gas extracted, little visible effect, low thermal conductivity
- Heat strengthened and tempered VG

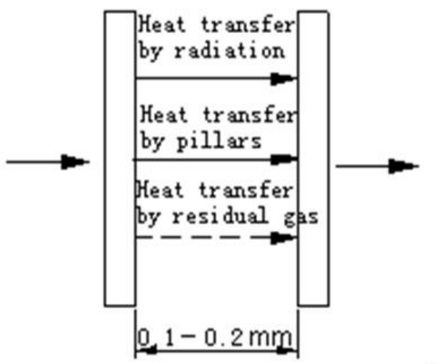

- With Low E and $\varepsilon < 0{,}03$ contribution is low < 0,15 W/m²K
- Most important contribution with pillar distance of 40 mm ~ 0,27 W/m²K
- When $P \leq 0.01$Pa, $C_{gas} \leq 0.004$ W/m²K, C_{gas} can be ignored

Figure 2: Thermal energy flux transfer mechanism in VG

- Enormous weight reduction for glass, windows and facades possible
- New window profiles and façade construction technologies required and possible
- Increased visible area per window possible; Better window/wall ratios

- Two combined VG`s (wall) with Low E of best Emissivity reach U-values of < 0,2 W/m²K
-

Combining the upper opportunities, VG is perfect for refrigerators and train and bus glazing. VG basically offers a new approach for automotive insulation glass systems, too.

Pillar array distance (mm)	25	30	35	40	45	50
Thermal conductance of pillar ($Wm^{-2}K^{-1}$) potentials	0.707	0.491	0.361	0.276	0.218	0.177

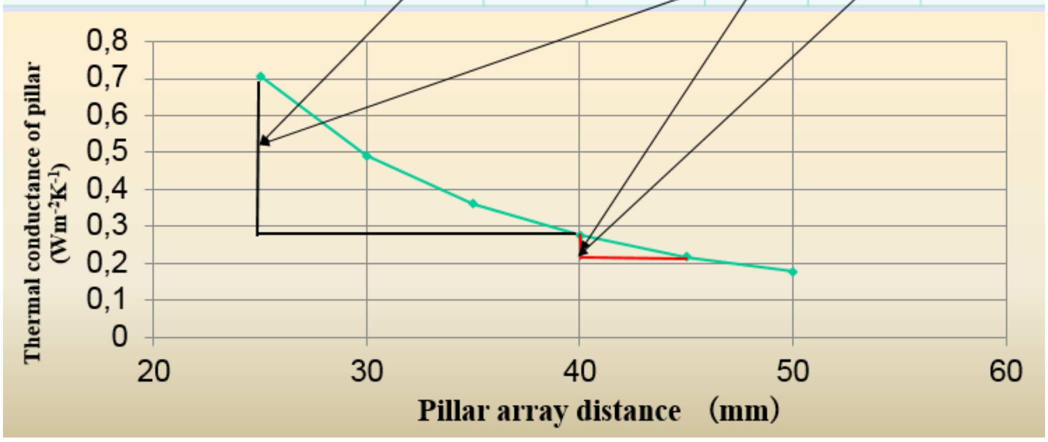

Figure 3: Variation of thermal conductance of ring-shaped pillar with different pillar array distance

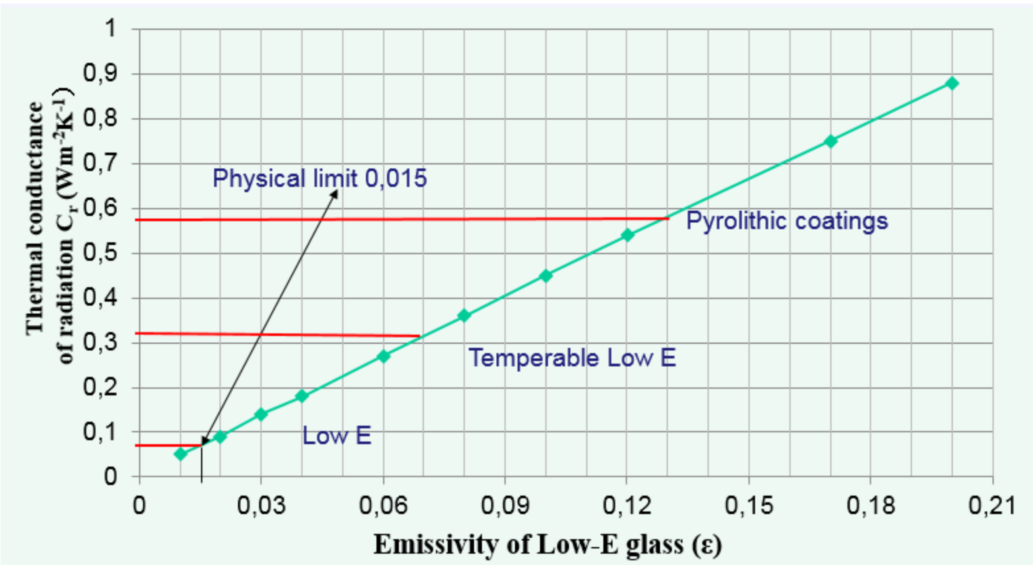

Figure 4: Variation of thermal conductance of radiation (C_r) of single Low-E vacuum glazing with emissivity of *Low-E glass (ε).*

2 Fully automatic VG production

2.1 Key factors for VG production within Beijing Synergy Vacuum Glazing Technology Co., Ltd.

Using the intellectual properties and experiences they gained over the past twenty years, they started building an industrialization base of vacuum glass production in 2012. This factory close to Beijing has the first automatic vacuum glazing production line in the world. As of today, the factory is completed, also the old production line is still running and the new automatic production line is in the final stage of debugging.

In December 2007, with the support of China Building Materials Academy CBMA and China Architectural Glass Standardization Technical Committee the first VG industry standard was created, and received approval by the National Development and Reform Commission NDRC.

Items	$C_{radiation}$ W/m²K / C_{pillar} W/m²K	ε=0.01, Cr=0.05	ε=0.02, Cr=0.09	ε=0.03, C_r=0.14	ε=0.07, C_r=0.32	ε=0.08, C_r=0.36	ε=0.11, C_r=0.49	ε=0.17, C_r=0.75
U value W/m²K	Pillar array distance=30 mm, C_{pillar}=0.491	0.50	0.54	0.57	0.71	0.74	0.84	1.02
	Pillar array distance=40 mm, C_{pillar}=0.276	0.31	0.36	0.42	0.57	0.57	0.68	0.87
	Pillar array distance=45 mm, C_{pillar}=0.218	0.26	0.30	0.35	0.50	0.53	0.63	0.83

Note: 1. The data are calculated by Window 7 software. Use boundary conditions according to JGJ151-2008 Standard.
2. The pillar in vacuum glazing is ring-shaped from Synergy. The pillar array distance is 40 mm.

Figure 5: The relationship of thermal conductance of radiation and pillar with different distance and U-value *of single Low-E VG*

- High vacuum guaranteed for a minimum of 20 years. First ensure the products achieve the vacuum degree during production, and second retain vacuum for a long time – optimization of process and getter system
- Hermetic sealing system available, to ensure high vacuum and easy handling as well
- Virtually invisible micro spacers (=pillars), put in place with less than 1 % surface and not harmful to the Low E coating
- Excellent equipment to temper glass with perfect flatness to fulfill alignment requirements. There are very few machine suppliers, who can provide feasible equipment, but it is the operator finally who brings the quality to the glass.

As the VG is more sensitive to production process and to handling, the manufacturing equipment has to be high quality to ensure the required results. Here is room for further achievements by skilled partners.
Synergy invested 50 million € to build a new continuous automatic production facility. The automatic production line will be completed in April/May and the production capacity will be 600,000 ㎡ (single sheet 2.8 x1.8 m²). It can produce heat-strengthened, tempered and laminated VG, plus Vacuum Insulating Glass VIG with U value lowest of 0.37 W/m²K.

The entire line has automatic machines and devices

- frit dispensing,
- assembly,
- pillar placing
- etc.

Average speed for each m² VG is 50 seconds.

Figure 6: New Factory for fully automatic Vacuum Glass Production in Beijing with VIG-facade

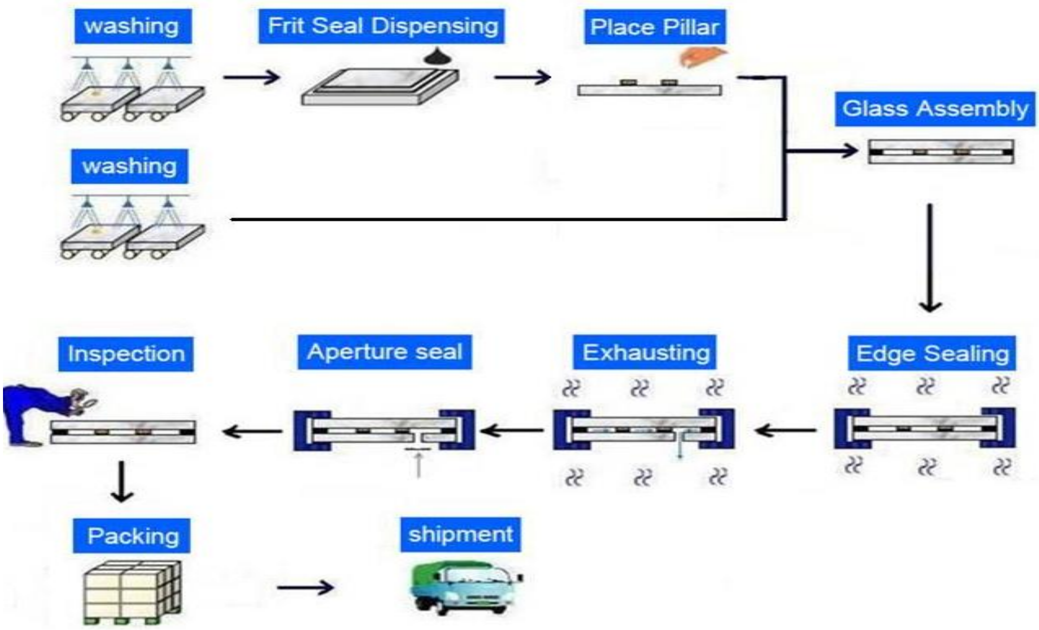

Figure 7: Technological Process of Vacuum Glass Production

Cost is always an issue, VG has a much better performance compared with triple IG, but also higher price and investment is higher. The price of VG will decline by improving yield and capacity as well as using new materials and technology, but probably never to the same level. Besides this one has to consider the costs of windows and facades, which includes glass, frame, hardware and metal joint connectors. Vacuum Glazing is light and thin, the frame could also be light and thin andmetal joint connectors also could be less expensive, even more façade construction saving. additional weight. There are more cost advantages considering the whole benefit for new designed houses with VG.

- Material costs of VG might be lower than triple IG, but process costs has a potential for further improvement

- Machines are mainly developed under quality aspects and considered less cost aspects
- Cost reduction opportunities for the next development phase
    - Window frames and/or facade construction
    - Much less or zero HVAC equipment, natural ventilation
    - Much less or zero Shading Devices
    - More space in rooms for sale
    - Reduced total building costs
- Savings
    - Heat and cooling energy
    - Lowest CO_2 emissions

Drying oven

Edge sealing oven

Vacuum oven

Robot for pillar setting

Figure 8: Pictures of the fully automatic production line

3 Applications in Practice - more than 30 completed VG projects

Application is the best way to test a certain product in practice. VG/VIG of Beijing Synergy has been used since 2005 in many buildings. Some of them are the “firsts” of domestic, even international market. For example, Beijing Sky Plaza is the first project of which all the glass units are VIG. And also it is the first time that large area glass curtain wall of VG is used in actual project. By now, Beijing Synergy has provided the most Vacuum Glazing units and actual projects all over the world. The main applications of Vacuum Glazing of Beijing Synergy are listed in Table 1. There were other companies offering VG in China and South Korea, but on a lower performance level without heat-strengthened VG. Maybe this was the reason the development was not taken seriously globally and may have perpetrated the negative belief about the quality of Asian VG.

In the early years it was difficult to get good quality Low E in China. The emissivity was mostly around 0.10 and later not lower as 0.06, having influence on the final U-value tested in China and abroad and which was 0.6 - 0,8 W/m²K for VIG at that time. Only recently one can get even triple Ag Low E with an emissivity of about 0,03.

Further it shows that we can adjust total solar energy transmittance and selectivity by selecting different Low-E glasses. Usually, the visible light transmittance, selectivity, total solar energy transmittance need to be adjusted according to the region and towards especially in China with vast territory.

Table 1: Vacuum Glass application projects

o.	Project Names	Glass area m^2	Glass type	Application type	Time
	Domestic projects				
	Water front building of Qinhuangdao in Hebei	830	heat strengthened VG	Glass wall	2013
	Great glory century building in Shandong	3000	heat strengthened VG	Window	2013
	Exhibition Centre Zhongguancun, Beijing	1200	VG; heat strengthened VG	Glass wall; Sunny roof	2012
	Zhengzhou library	10000	VG; heat strengthened VG	Glass wall	2011
	Culture park of Changsha in Hunan	12700	VG; heat strengthened VG	Glass wall	2011
	Hebei province land and resources office building	3000	Vacuum Glazing	Window (reform)	2010
	Science and Technology Bureau of Hebei	4000	Vacuum Glazing	Window (reform)	2010
	Tiantaitongbai library	1500	Vacuum Glazing	Glass wall	2009
	Construction service center, Hebei prov.	3000	Vacuum Glazing	Window	2009
0	Meilinqingcheng residential house	10000	Vacuum Glazing	Window	2009
1	Micro Energy Consumption Kindergarten, Beijing	Sunny roof 500, Window 1000	Vacuum Glazing	Window; Sunny roof	2008
2	The college of life science	Glass wall 600 Sunny roof 600	Vacuum Glazing	Glass wall; Sunny roof	2006
3	Long river high-grade residential house	1000	Vacuum Glazing	Window	2006
4	Sky plaza building in Beijing	10000	Vacuum Glazing	Glass wall; Window	2005
5	Ultra-low power demonstration bldg., Tsinghua University	1000	Vacuum Glazing	Glass wall	2004
	International projects				
6	Switzerland	28	heat strengthened Vacuum Glazing	Window (reform)	2012
7	Qatar	13	heat strengthened Vacuum Glazing	Window (reform)	2012
8	Germany (Frankfort)	73	Vacuum Glazing	Window (reform)	2011
9	Germany (Stuttgart)	63	heat strengthened Vacuum Glazing	Glass wall (active building)	2014

Sky Plaza building

Low energy consumption building, Tsinghua Univ.

Tiantaitongbai Library

Construction service center of Hebei Province

Culture park of Changsha, Hunan

Micro energy consumption Kindergarten of Beijing

Figure 9: Beijing Synergy Vacuum Glass Projects

4 Outlook and perspectives

4.1 Missing innovation of window frames

If one considers the frame development for windows, it is easy to see that there is a lack of new solutions for energy saving and it was more a development of steady growth of the cross section. Frames have taken more and more surface area on a window. Years ago this was only around 10 % and now more than 30 %. For smaller sizes it can be even 50%. Many people do not like the big thick frames demanded by energy efficiency. It is time now to re-consider that. With the high efficiency of VG, it should be possible to cut down this surface effect to a minimum thus having a better U-value for the whole window. Of course other important points like tensile stress and condensation have to be considered carefully.

Also we have to consider that glass as part of the window costs with triple IG glass has a share of 10-15 % only. Space enough for an overall cost optimization. Today VG with an U-value of 0,4 W/m²K made with a Low E coating and emissivity of minimum 0,03 opens up many new options. The distance between the 2 panes is only 0.2 mm. Thus VG can be seen like a single pane of 6, 8 or 10 mm. Can anyone imagine the market size, if we provide soon a solution to exchange globally the glass of single glazed windows against VG? The demand would be unprecedented, the challenge is high. Glazing techniques are demanded here too.

One can use the former space of IG especially for triple IG as an excellent opportunity to build, for example, a new box-type or counter-sash window replacing the triple IG, but with the option to integrate other functions for sun shading like lamella systems or additional switchable glazings on the outside. Many other combinations with PV integration are possible. Just these solutions have a new pace and will decrease energy costs of a house. Thus we can generate solutions which mean very low heating and cooling loads and need much less technical equipment or in the most advanced solutions, almost no equipment.

There is a need for a new definition of the different parts in such houses. Please consider that the combination of 2 VG's can have a U-value of 0,2 W/m²K, needing a thickness of less than 20 mm. Completely new challenges for planning houses, as there is no building mass for energy storage but with a lot more space to sell. Of course climate concepts for such houses have to be made first. And not to forget there are excellent options for sound proofing and fire proofing solutions.

We are only at the beginning. Very few experts and companies have shared their thoughts on these aspects. But we do not need independent action; we need integrated vertical teams to find new ways. This has to be combined also with new power and energy storage systems. First research projects are started.

We hope that the governmental bodies and the relevant authorities give more support on VG industrialization worldwide, as it contributes dramatically to energy saving in hot and cold climates and also to environmental savings of carbon emissions and last but not least offers many advantages for comfort and building options.

VG could be used further in building and cold chain industry because of its excellent thermal insulation property.

In spite of a better U value, VG is much thinner and lighter than IG. This means that less frame material and hardware is required for windows and facades and less bearing load for construction must be considered. It also allows VG to be used as one piece of glass. The thinnest version is 3 mm/0.2mm/3 mm and thus with only 6mm thickness and a possible U-value of 0.3 W/m²K. VG can be integrated in IG as VIG or combined with laminated glass or many other glass products to create e. g. photovoltaic VG and high end solar control solutions with integrated switchable coatings, lamella systems or other innovative solutions. First time there is an option to solve hot and cold climate requirements within one glazing element. Even when such glasses are more expensive the total system will lead to lower costs due to lighter construction elements and better performance. Cooling and heating loads can rapidly be diminished.

At the beginning, VG will be used as an alternative to insulating glass for the high-end market or for a market that has higher demand and requirements for energy saving. However, as regulatory requirements on building energy conservation become more and more tight, and the limits of insulating glass become so obvious, it is easy to imagine that VG will be the ultimate choice to replace single glasses in listed heritage buildings, but even more in the refurbishment sector and in new buildings, too.

Structure Outside Inside	Thickness (mm)	Visible light transmittance τ_{vis} (%)	Glazing selectivity coefficient S	Solar heat gain coefficient g	Emissivity of Low-E	Heat transfer coefficient U ($Wm^{-2}K^{-1}$)	Sound insulation (dB)
Laminated+ IG+VG T5+0.76P+TL5+9A +TL5+V+T5	29	61.13	1.6	0.382	0.17 0.059	0.463	39

Figure 10: Active Plus House in Weissenhof-settlement, Stuttgart, by Professor Sobek with VIG

Figure 11: Project VISIONEUM ENERGIE+ Professor Sahner Univ. Augsburg

With VG the door is wide open for complete new solutions and advantages in window, façade and wall construction. Architects, who come more from a holistic approach and the performance side, balance costs for investment against utilization and operational costs. Initial discussions with leading engineering groups and architects showed a potential for prices even above 130 €/m².

4.2 Energy Plus houses with vacuum glass - the future of building

We are generally faced with a very powerful development of so-called Energy or Active Plus Houses like recently presented by a serious of leading engineering offices and architects under the support of the German Ministry BMVBS and BMWi. Among others these experts are Professor Gerhard Hausladen, University Munich, known for his pioneering Climate Engineering concepts, Professor Manfred Hegger, from Darmstadt University, who has won the Solar Decathlon, Professor Norbert Fisch in University Braunschweig and Professor Werner Sobek from University Stuttgart, who have all built first Energy Plus Houses, where the house can gain energy and power over the whole year. The glass industry needs such promoters. First projects are done as shown in figure 10 and planned (figure 11).

membranes

Impact of material properties on the structural analysis of coated woven fabrics

Elke Sachsenmaier, Dipl.-Ing.
Institute of Building Construction, Graz University of Technology, Austria
elke.sachsenmaier@tlorenz.at

Manfred Zellinger, Dipl.-Ing. Dr.techn.
Institute of Building Construction, Graz University of Technology, Austria
manfred.zellinger@tugraz.at

Oliver Englhardt, Univ.-Prof. Dipl.-Ing. Dr.nat.techn.
Institute of Building Construction, Graz University of Technology, Austria englhardt@tugraz.at

Summary

Recently, the design of tensile membrane structures is not codified but is based on experience and know-how drawn from completed projects. Modern tensile fabrics are composites with a non-linear, anisotropic and non-elastic behaviour that cannot be compared with conventional building materials. One of the biggest challenges in structural analysis of tensile membrane structures is the description of the complex material behaviour using an eligible material model. The commonly used material models employ experimentally determined elastic constants. The absence of design codes for tensile membrane structures leads to a large amount of testing methods for elastic constants of membrane materials. Depending on the combination of testing methods and examination methods, there can be different results for the elastic constants of the one and the same membrane product. In the course of a Master Thesis [10] at Graz University of Technology at the Institute of Building Construction, some parametric studies were undertaken using the example of a hyperbolic paraboloid with varying material, geometrical and loading parameters to estimate the impact of material stiffness spectrum according to the different testing method on the statically analysis of tensile membrane structures. The results should highlight the need for harmonized engineering standards on tensile membrane structures.

Keywords: tensile membrane structures, coated woven fabrics, material behaviour, material properties, testing methods, parametric study

1 Introduction

In addition to the common building materials like steel, concrete, timber and glass, modern tensile fabrics are increasingly used in recent architecture. Modern tensile fabrics are composites consisting of woven yarns. The commonly used natural and synthetic fibres for yarns are listed in Figure 1. In comparison to synthetic fibres, the length of natural fibres like cotton is restricted. The length of yarn out of natural fibres can be extended by the use of spinning methods. To obtain the woven fabric, the plain or the 2-2 basket weaving method is applied to the yarns. By definition, the longitudinal direction of the fabric is called warp and the orthogonal direction fill. Due to the weaving process, the yarns in warp and fill direction have a characteristic crimp. The crimp of the fill yarn is related to the production bigger. After the weaving process, the coating is applied to protect the fabric. Frequently used coating materials are PVC, PTFE and silicon. Both the weaving and the coating process have significant influence on the material properties of the final product. The commonly used materials for tensile membrane structures are PVC-coated PES fabrics and PTFE-coated glass fibre fabric [6, 7, 11, 12].

natural fibres				
animal fibres	**vegetable fibres**		**anorganic**	
goat hair	hemp		asbestos	
sheep wool	cotton			
silk				
synthetic fibers				
natural polymer	**synthetic polymer**		**anorganic**	
viscose	polyester	PES	glass fibre	GF
	polyamide	PA	carbon fibre	CF
	aramid	AR	metall fibre	MTF
	polyethylene	PE		
	polyethylene high-tensile	PE		
	Fluorpolymere	PTFE		

Figure 1: Fibre materials.

2 Material behaviour and modelling methods for coated woven fabrics

For the structural analysis of tensile membrane structures, the material behaviour according to load, time and temperature is very important. Modern tensile fabrics are composites, whose mechanical behaviour is not equal to the sum of its components. Their material behaviour cannot be compared with conventional building materials. Coated woven fabrics as they have been used for tensile membrane structures have a non-linear, anisotropic and non-elastic material behaviour that additionally has multi-attribute dependences [2].
First of all, the material behaviour of coated woven fabric depends on the yarn properties, the coating stiffness and the fabric structure. The higher crimp of the fill yarn leads to a lower stiffness of the woven fabric in this direction. Furthermore, there is an interaction of both yarn directions (Figure 2). A tension load in warp direction causes strain of the warp yarns and their yarn geometry becomes straighten. However, at the same time the crimp of the fill yarns raises, which changes the tension stiffness of the fabric in this direction. The straighter the yarn geometry becomes, the higher the tension stiffness of the fabric in this direction. The resistance against the warp yarn extension gets higher if there is also tension in the fill direction. The intension of the yarn interaction depends significantly to load level and load rate between warp and fill. Due to the permanent elongation after each loading-unloading-cycle, the yarn geometry becomes straighter and the tension stiffness of the fabric raises with each reloading (Figure 3). The elastic module is therefore not constant but load-dependent. However, after at most ten loading-unloading-cycles, the tension stiffness of the fabric does not change significantly. In addition, the tension stiffness decreases if the load direction is not parallel to the yarn directions of the fabric (Figure 3) [2, 6, 9, 11, 13, 14].

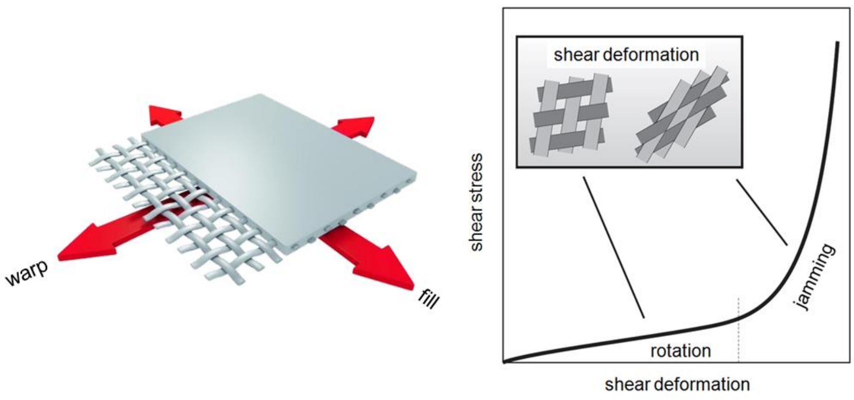

Figure 2: Yarn interaction (left), Jamming Condition (right) [15, 1].

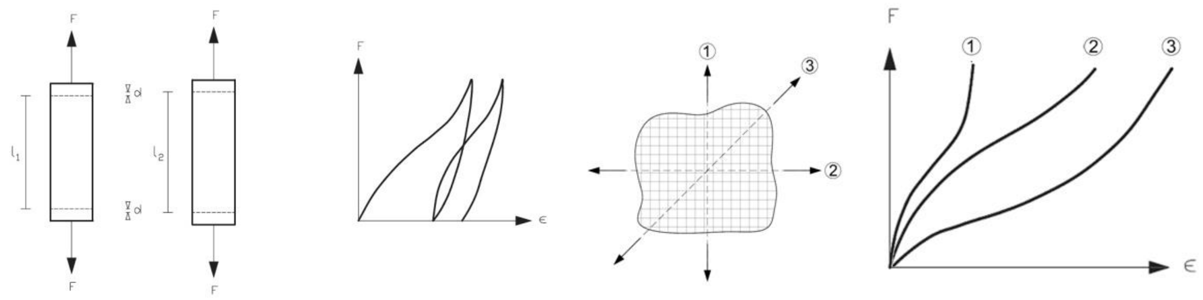

Figure 3: Dependencies of material behaviour: loading-unloading-cycles (left), fabric orientation (right) [11].

The shear stiffness is in comparison to the tension stiffness of the fabric comparatively small. At the beginning, the fabric permits shear deformation by what the shear stress stays little. Particularly when loaded not in parallel to the yarn, the fabric yarns twist against each other. The shear stiffness is low and is only generated by the coating as long as this twisting is not impeded (Figure 2). Once the shear deformation becomes too large, the yarns get jammed and the shear stiffness raises suddenly (Jamming Condition) [3, 4, 11].

The real material behaviour of coated woven fabric cannot be described exactly at the moment. The definition of an eligible material model that can enable a good approximation of the real behaviour is one of the challenges in structural analysis of tensile membrane structures. The methods for material behaviour simulation can be separated into phenomenal or structural material models. Structural models use models of the microstructure to represent the real material behaviour of the fabric. Therefore, the yarn geometry and the yarn properties are required. Presently, phenomenal material models are preferred due to the less demands on computing capacity. In this case, the microstructure is not considered and the composite is simplified to a homogeneous continuum. In literature, three different approaches for phenomenal material models can be found: linear-elastic, multi-linear-elastic and non-linear. In current structural analyses of tensile membrane structures, the linear-elastic approach is most commonly used. The difference between the measured and the calculated graph demonstrates the simplification of this approach (Figure 4) [13].

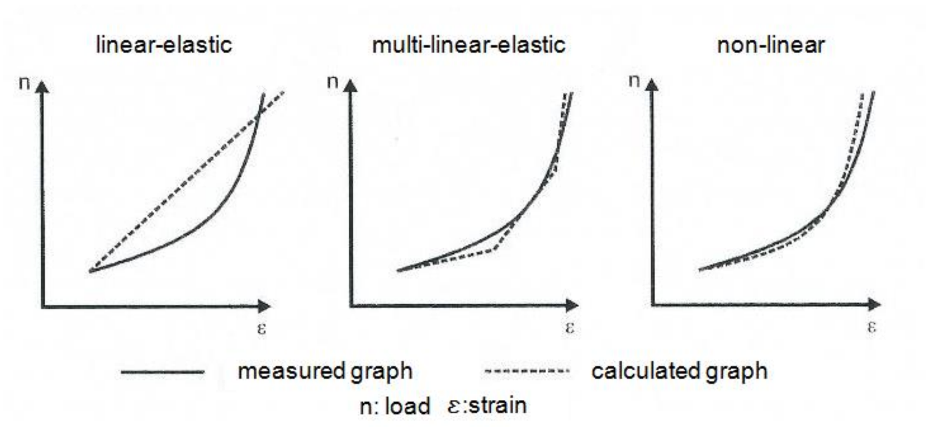

Figure 4: Different approaches for phenomenal material models [13].

The linear-elastic material model uses a system of equations to describe stress and strain of surface elements in consideration of a symmetry condition equation (1) and (2). The unknown elastic constants (tensile stiffness and shear stiffness) can be determined experimentally. The absence of design codes for tensile membrane structures leads to a huge amount of testing methods and examination methods for elastic constants of membrane materials. The testing methods are classified into uniaxial and biaxial tensile tests where the yarns are aligned with the loading direction as well as shear tests where the load is applied at 45° with respect to the yarn direction [3, 5, 8, 13].

$$\begin{bmatrix} \varepsilon_w \\ \varepsilon_f \\ \gamma_{fw} \end{bmatrix} = \begin{bmatrix} \frac{1}{E_w t} & -\frac{\mu_{wf}}{E_f t} & 0 \\ -\frac{\mu_{fw}}{E_w t} & \frac{1}{E_f t} & 0 \\ 0 & 0 & \frac{1}{Gt} \end{bmatrix} \begin{bmatrix} n_w \\ n_f \\ n_{fw} \end{bmatrix} \tag{1}$$

$$E_w t = \frac{\mu_{fw}}{\mu_{wf}} E_f t \tag{2}$$

3 Material properties

In contrast, the material properties of coated woven fabric vary much more due to following factors:

- dependency of the material behaviour on yarn properties, fabric structure, coating stiffness, fabric-load-orientation, yarn interaction, load type and load period (Chapter 2)
- producer and production methods
- joining techniques
- temperature and time effects (creeping and relaxation)
- testing method and examination method

The material properties for the same fabric type can differ between different producers due to their in-house production methods. Small changes in process chain can also lead to varying material properties between product charges. Furthermore, local changes in stiffness are to be expected at welded joins where the material thickness becomes doubled. Furthermore leads the huge amount of testing methods and examination methods to variation of material properties. Depending on the combination of the testing method and the examination method, and due to the multiple dependences of the material behaviour, there can be different results for the elastic constants of one and the same membrane product. To get a dimension for the spectrum of elastic constants of coated woven fabrics according to the different testing methods and examination methods, literature research was done and stiffness data was gathered from architectural and engineering offices, material producers and testing laboratories [6, 14].

4 Parametric studies

To estimate the impact of material stiffness spectrum according to the different testing method and examination method on the structural analysis of tensile membrane structures, some parametric studies were executed using the example of a hyperbolic paraboloid. Therefore, two different investigations were executed:

- investigations with variation of tension stiffness (E_{warp} and E_{fill}), constant shear stiffness and fabric orientation parallel to the principal curvature and
- investigations with variation of shear stiffness, constant tension stiffness and variable fabric orientation

Additionally, the geometry (boundary conditions, base and height) and the prestress level were varied. Furthermore, a neglect of the shear stiffness was analysed. Two load cases with different load directions were considered. The first load case represents snow and wind pressure and the second one represents wind suction. The load assumptions were determined realistically and target a selected stress utilization of the fabric of approximately 75 % for design-relevant load case. The investigations consider PVC/PES type I to VI and PTFE/Glass type II to IV. For the stiffness spectra that were used in parametric studies, the gathered stiffness data from architecture and engineering offices, material producer and testing laboratories was analysed and selected (Table 1).

Table 1: selected stiffness spectra for different woven fabrics.

fabric	$E_{w,min}$ [kN/m]	$E_{w,max}$ [kN/m]	$E_{f,min}$ [kN/m]	$E_{f,max}$ [kN/m]	G_{min} [kN/m]	G_{max} [kN/m]	$E_{w,average}$ [kN/m]	$E_{f,average}$ [kN/m]	$G_{average}$ [kN/m]
PVC/PES type I	650	800	500	650	7	14	720	590	10
PVC/PES type II	900	1200	600	1050	10	17	990	810	13
PVC/PES type III	900	1500	550	1150	13	16	1220	810	14,5
PVC/PES type IV	1450	1750	1000	1300	14	17	1570	1160	15
PTFE/GLASS type II	1050	1500	800	1250	20	40	1220	1000	30
PTFE/GLASS type III	1800	2400	1100	1600	40	60	2130	1310	45
PTFE/GLASS type IV	1900	2100	1250	1850	60	80	2000	1520	70

Figure 5 and 6 give a detailed overview about the workflows of the parametric studies and the varied parameters.

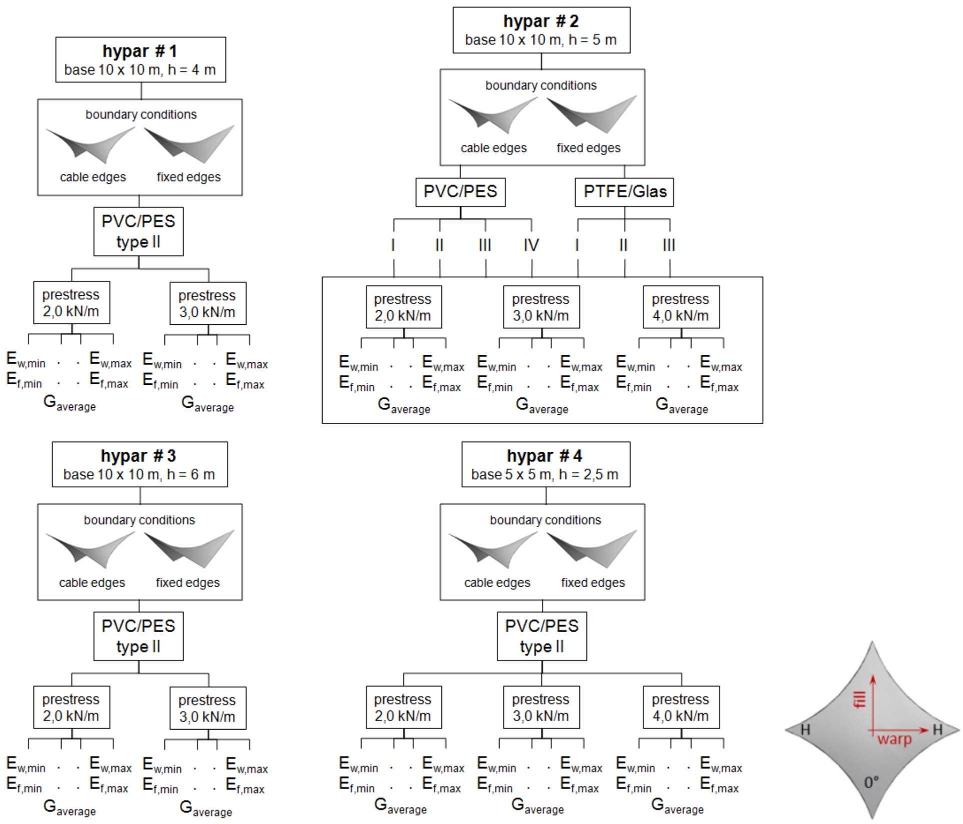

Figure 5: Workflow of investigations with variation of tensile stiffness.

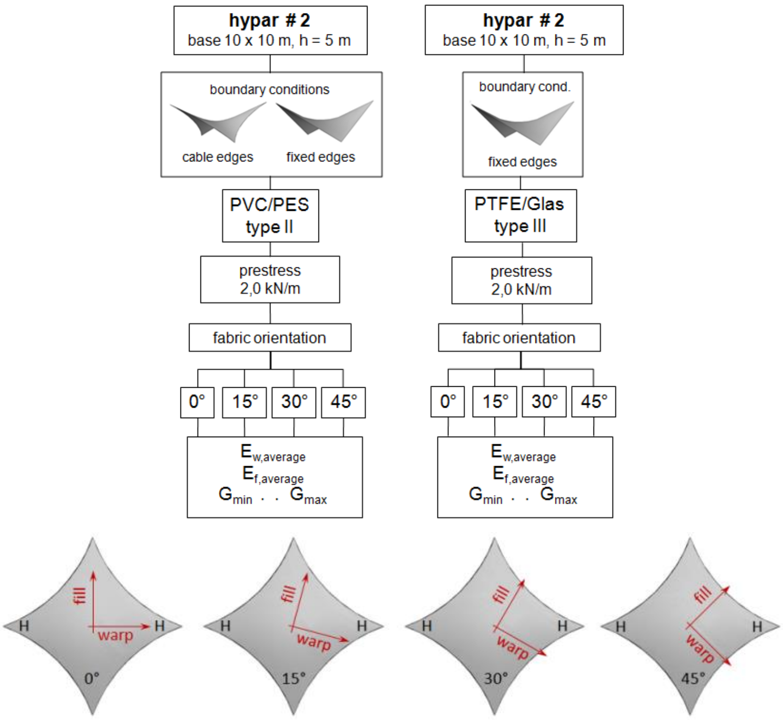

Figure 6: Workflow of investigations with variation of shear stiffness.

The investigations with variations of the tension stiffness and constant shear stiffness showed that the result deviation can be up to 9 % for fabric tension stress, and up to 93 % for deformation.
The results of the investigations with variations of the shear stiffness and constant tension stiffness show that if the fabric is orientated parallel to the principal curvature, the result deviation is only 3 % for fabric tension stress and deformation. The result deviation of fabric shear stress is not significant. However, once the fabric orientation is not parallel to the principal curvature, the shear stresses rise significantly and reach their maximum value at 45°. The result deviation amounts up to 11 % for fabric tension stress, 15 % for deformation and 60 % for fabric shear stress.
There are differences in the results of investigations with neglected shear stiffness and considered shear stiffness. The result deviations are up to 4 % for fabric tension stress and 12 % for deformation if the fabric orientation is parallel to the principal curvature. If the fabric orientation is not parallel to the principal curvature, the result deviations rise up to 28 % for fabric tension stress and 32 % for deformation. Additionally, the investigations showed that if shear stiffness is considered and fabric orientation is not parallel to the principal curvature, the values of fabric shear stress can be up to 26 % of the maximal fabric tension stress and therefore can be significant for structural analysis.

5 Conclusion

The results of the parametric studies showed that the variation of material properties has significant impact on the results of structural analysis of tensile membrane structures. It should be an aim in the future to reduce the spectrum of material properties and the implicated result deviations in structural analysis by working on harmonized design codes for tensile membrane structures and testing methods for elastic constants of membrane materials. The non-linear material behaviour of membrane materials and its multi-attribute dependences (load, yarn interaction, fabric structure, etc.) should be considered by developing such harmonized design codes. Another aim should be the formulation of a design concept for membrane materials similar to already existing concepts. An additional approach could be the implementation of other material models in recent calculation software as well as the development of structural models. It is common practice to determine only the tension stiffness experimentally and leave the shear stiffness undefined. In the future, the experiments for tension stiffness and shear stiffness should be linked so that, in the literature, also values for shear stiffness are available. Furthermore, the results showed if the fabric orientation is not parallel to the principal curvature the fabric shear stress can reach values which should not be neglected for structural analysis. Therefore, shear stiffness should be considered once the fabric orientation is not corresponding to the principal curvature. This requires further experimental investigations since neither literature nor material producers specified any design values for shear stresses. The results of the investigations showed the significance of material properties in the structural analysis of tensile membrane structures and highlight the need for harmonized engineering standards. Prospectively, a lot of work will need to been done until the completion of the Eurocode for Tensile Membrane Structures.

6 Acknowledgements

The authors would like to thank all architecture and engineering offices, material producers and testing laboratories supporting us during the material properties research. Furthermore, we express our gratitude to the Thomas Lorenz ZT GmbH to have participated in drafting this paper.

7 References

[1] Ballhause, D.: *Diskrete Modellierung des Verformungs- und Versagensverhaltens von Gewebemembranen*, Dissertation an der Universität Stuttgart, 2007.
[2] Blum, R.: *Zeltbaumaterialien*, in: Leicht und weit - Zur Konstruktion weitgespannter Flächentragwerke, SFB 64, VCH Verlagsgesellschaft, 1990.
[3] Forster, B., Mollaert, M.: *European Design Guide for Tensile Surface Structures,* Tensinet, 2004.
[4] Frei, O., et al.: *Lufthallenhandbuch*, Karl Krämer Verlag, Stuttgart, 1983.
[5] Galliot, C., Luchsinger, R.H.: *The shear ramp: A new testing method for the investigation of coated woven fabric shear behaviour - Part 1: Theory*, in: Composites A 41 (2010) , pp. 1743-1749.
[6] Hoppe, D.S.: *Freigespannte textile Membrankonstruktionen*, Böhlau Verlag , 2007.
[7] Moritz, K.: *Membranwerkstoffe im Hochbau*, in: Detail 6 (2000) , pp. 643-651.
[8] Münsch, R., Reinhardt, H.-W.: *Zur Berechnung von Membrantragwerken aus beschichteten Geweben mit Hilfe genäherter elastischer Materialparameter*, in: Bauingenieur 70 (1995) , pp. 271-275.
[9] Reinhardt, H.W.: *Ein- und zweiachsige Verformungs- und Festigkeitsuntersuchungen an einem beschichteten Gittergewebe*, Universität Stuttgart Mitteilungen 31, 1975.
[10] Sachsenmaier, E.: *Einfluss der Materialkennwerte auf die Spannungs- und Verformungsberechnung beschichteter Gewebemembranen*, Master Thesis - Graz University of Technology, Graz, 2014.
[11] Seidel, M.: *Textile Hüllen - Bauen mit biegeweichen Tragelementen*, Ernst & Sohn Verlag, Berlin, 2008
[12] Sobek, W., Speth, M.: *Von der Faser zum Gewebe*, in: DBZ 9 (1993), pp. 74-81.
[13] Stranghöner, N., Uhlemann, J.: *Möglichkeiten und Grenzen bei der Erfassung des Materialverhaltens von Gewebemembranen in der Tragwerksplanung,* in: Essener Membranbau Symposium, Shaker Verlag, Aachen, 2012.
[14] Uhlemann, J., Stranghöner, N.: *Einfluss fiktiver elastischer Konstanten von textilen Gewebemembranen in der Tragwerksanalyse von Membranstrukturen,* in: Stahlbau 82 (2013) issue 9, pp. 643-651.
[15] *http://de.sergeferrari.com/corporate-de/die-patentrechtlich-geschutzte-technologie-precontraintserge-ferrari/*, 18.10.2014.

Proceedings of the International Conference on Building Envelope Design and Technology, Graz
Advanced Building Skins 2015

Transformable Tensile Façade: Performance assessment on energy, solar and daylighting

Simon K. Chiu, Partner
Tensile Evolution North America, USA, Simon@TensileEvolution.com
Ph.D. Candidate, *University of Southern California, School of Architecture*

Eve S. Lin, Ph.D., Research & Development Associate
Tensile Evolution North America, USA, Eve@TensileEvolution.com

Summary

Tensile membrane façades have been deemed a potential means of improving building performance due to their lightweight and flexible nature. However, their performance improvement has hardly been accurately gauged or demonstrated due to compounding issues of complexity in both geometric and physical properties. To address this issue, this research first focuses on understanding the impact of performance simulations with the inclusion of a membrane's optical properties. Followed by two case-based experiments, the limitations of current tools and processes can be revealed. In performing said experiments, the benefits of the tensile membrane façade can be further confirmed through comparative studies of differing geometric variations.

Keywords: Tensile Membrane Façade, Optical Properties, Energy Simulation, Daylighting Analysis, Responsive System

1 Introduction

Building façade plays an important role in an overall building design. Its distinctive appearance represents the unique DNA that the designer encodes for each building. Moreover, it significantly impacts energy consumption and other performance aspects of the building throughout its lifecycle [1]. With a growing concern for sustainable design and a rising demand for higher performing buildings, exploring methods and materials that effectively reduce energy consumption and improve daylighting and thermal comfort have become an industry priority. The focus of various research has been in adopting effective façade configurations, shading strategies and control systems to improve building performance [2-6]. However, when designing a building that occupies a constantly changing environment, a dynamic responsive system is an opportunity to push the current boundaries of building performance. Although several attempts have demonstrated the potential of using a dynamic shading or façade system [7,8], the rigidity and complexity of such systems have reduced their economic feasibility and raised longevity issues. This research recognizes the potential of using tensile membrane façade systems to address these problems.

Tensile membrane structures are lightweight and flexible in form, thereby enabling a wide range of dynamically unique design forms. These unique characteristics also enable tensile membrane structures to potentially be more responsive towards improving building performance than more rigid building systems. With the advancement of tensile membrane material, the performance of the tensile membrane façade is considered more environmentally friendly in terms of thermal and lighting performance when compared to a conventional glass façade [9-11]. In addition, some tensile membrane façade can be fully recycled, thereby increasing their contribution to a sustainable design solution. It can also withstand wind, sun and fire [12,13]. However, due to the physical properties and geometrical complexities of the tensile membrane system, several associated obstacles arise and impede designers from incorporating tensile membrane structures. Consequently, the potential of using responsive and transformable tensile membrane systems to improve building performance has been neither accurately gauged nor demonstrated. In response to these observed gaps in current conditions, this research intends to explore how designers can gauge the impact of utilizing tensile membrane façade systems, which significantly increase the complexity of both the geometric and physical properties of their design. Compounding the issue is the inclusion of determining the performance impact of a dynamic and responsive control system. To address this fundamental conflict, this paper presents two case-based experiments, devised to understand the impact of performance simulations when adopting membrane's optical properties. In addition, the benefit of the tensile membrane shade and the inclusion of geometric variation can be initially observed through comparative studies of the experiment's results. Furthermore, the limitations of current tools and processes can be revealed and discussed.

2 Research Method

In order to incorporate textile membrane façades and gauge their performance potential during the design process, designers need to rely on computer simulation tools to assess and predict their design. However, existing research that compares textile membrane shade with other shading strategies rarely considers the angular optical properties of the textile membrane [6,14,15] despite their relevance to the analysis results [16-19]. Within the current architectural design field it is still not the norm to incorporate the physical characteristics of the textile membrane during the simulation process. Therefore, it is necessary to investigate a way for designers to simulate the physical characteristics of complex textile membrane glazing systems in their renderings. Furthermore, it is also important to understand whether the physical property input of the textile membrane is significant enough to impact the simulation results. To address these issues, this research explores two case-based experiments to understand the performance potential in tensile membrane façade as well as its impact on the design analysis process. The first case-based experiment is designed to incorporate a membrane's angular optical properties into the solar and energy simulation process to better understand its impact on the simulation results. The impact of different shading design strategies and how they perform in various climates is also explored. The second case-based experiment explores a transformable membrane façade system in order to support the potential of introducing geometric variation to membrane layers. While the end goal is to bring extensive performance aspects into consideration, daylighting is selected as the initial attempt as a proof of concept. By measuring the daylighting performance for each variation of a transformable membrane façade at different times of day and year, the performance of each façade configuration can be revealed and compared. In doing so, the potential of the performance improvement from the interchangeable façade can be observed. The design of each case-based experiment is further detailed in the following sections.

3 Case-Based Experiment I: External Textile Shade

The objectives of this case-based experiment is to understand the impact of a textile membrane's optical properties on the solar and energy simulation results, as well as the potential benefit of the textile membrane shade. There are a total of six shading scenarios tested in three different climate zones. One of the scenario incorporates the test sample's optical properties extrapolated from the photo-goniometric measurement conducted in Lawrence Berkeley National Laboratory (LBNL) [20,21]. IES <VE> [22] is selected as the simulation tool due to its ability to conduct both whole building energy analysis and solar heat gain analysis [23]. In addition, it allows the user to specify and incorporate the different angular transmission (Ts) properties into the simulation. The selected textile membrane shade for this experiment is Serge Ferrari's Stamisol® FT 381-3109, which is a high-quality PVC-coated polyester open fabric that is pre-tensioned during coating [24]. The technical specification from the manufacture is summarized in Table 8. The listed transmission and reflection data are measurements from normal-incidence without other angular considerations. The observation focus of this experiment can be listed as following:

- The performance difference due to the physical property input of the fabric;
- The performance difference due to the different shading strategies;
- The performance difference due to the building site for the same strategies.

The two observed performances are:

- The solar gain of the East, South and West façade on the fifth floor of the tested building, measured in MJ.
- Monthly and annual consumption of total building system energy consumption and its breakdown (i.e. chiller, boiler and auxiliary energy) measured in MJ/month and MJ/yr.

While the shading strategies can impact the electrical lighting energy consumption if dimming sensor control is considered in the simulation process, it should be noted that this research excludes the electrical lighting control as part of the simulation to better understand the impact of total system energy consumption alone.

Table 8: Technical specification of Stamisol® FT 381-3109 [24,25].

Property Name	Property value
Color 3109:	light grey /silver
Material:	PVC coated polyester
Use:	Exterior / interior
Yarn:	1100 Dtex PET HT
Weight:	600 g/m²
Thickness:	1.1 mm
Tensile Strength (wrap/weft):	330/330 daN/5cm
Tear resistance (wrap/weft):	65/65 daN/5cm
Water penetration resistance:	-
Temperature resistance:	-30°C a + 70°C
Flame retardancy:	ASTM E84, NFPA 701, M1/NFP 92-507, B1/DIN, 4102-1, BS 7837, VKF 5.3
Euroclass:	B-s2,do/EN 13501-1
Transmission (Ts):	29 (Is the % of solar radiation which goes through the fabric).
Reflexion (Rs):	36 (Is the % of solar radiation which reflects on the fabric).
Absorption (As):	35 (Is the % of solar radiation that the fabric absorbs).
Visible transmission (Tv):	29 (Is the % of visible light which goes through the fabric screen).

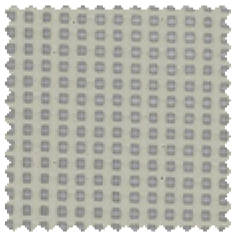

3.1 Photo-Goniometer Lab Testing

In order to simulate the impact of building openings on the building's lighting and thermal performance, it is necessary to predict the light entering and exiting the building envelope. For typical glazing, the method to obtain these spectral data, i.e. transmission and reflection, is straightforward and can be calculated from accepted equations [26]. However, when there are textile membrane shades involved, the angular properties of the light coming through an opening can no longer be obtained via a simple formula due to the fabric's light redirecting and/or diffusing characteristics. While these characteristics of textile membranes are where the potential for textile shades to improve lighting and thermal performance derive from, they complicate the predictions of lighting behavior as it requires additional angular behavior measurement beyond the necessary spectral transmittance and reflectance [16]. As a result, before the research can utilize a simulation tool to predict the impact of textile shades, the angular properties of the textile need to be obtained first. Unfortunately, there are no angular properties immediately available in fabric product specifications in the current marketplace. Therefore, the first step of the research is to obtain the angular properties of the selected textile via a photo-goniometer lab testing.

Typically, the angular properties of a complex system, such as fabrics, can be described by a Bi-directional Scattering Distribution Function (BSDF) [16]. A material's BSDF is defined by using reflection and transmittance properties for both sides. Hence, a BSDF is a combination of 2 Bi-directional Transmittance Distributions Functions (BTDFs) and 2 Bi-directional Reflectance Distribution Functions (BRDFs). These directions can be measured by a photo-goniometer through a discrete hemisphere that is composed of a number of patches. For this research, the photo-goniometer testing was conducted at the Windows Group Complex

Glazing Lab of the Lawrence Berkeley National Laboratory (LBNL) with a total measuring duration of approximately 4.5 hours excluding the post data processing. The detailed lab testing report can be found in Chiu [21].

While the full angular optical properties of the tested textile was obtained, no currently available energy simulation tools are capable of utilizing the full BSDF. This can be considered as a limitation of currently available energy simulation tools. However, a more relevant question is whether the resolution of the full BSDF properties is considered too high to be practically adopted during the simulation process, especially if the simulation is intended to assist design decision making during the design process. Nonetheless, this is a research question that worth future exploration. In order to incorporate the measured angular properties, the research needed to extrapolate the measured results based on the simulation tool's acceptable angular data resolution. The selected simulation program, IES <VE>, is only able to consider seven sun angle transmission factors in 15° increments from perpendicular. As a result, the extrapolated input for later simulation is listed in Table 92. Though there is the concern that the resolution of the energy simulation input cannot represent the entire BSDF measurement, the impact on the simulation results can still be observed. However, due to the unavailability of this detailed information, any disparities caused by the input resolution that might occur during the simulation are not considered. This concern, however, is outside of the current research scope and will be included for future work.

Table 9: Extrapolated transmission input for energy simulation.

Incidence Angle	0°	15°	30°	45°	60°	75°	90°
Transmission factor	0.24	0.23	0.21	0.18	0.14	0.09	0.01

3.2 External Textile Shade: Experiment Design

The experimental project for this case-based experiment is a six-floor office building as summarized in Figure . To fulfill the research objectives, there are a total for six simulation scenarios run for the test building in three different climate zones: Los Angeles, Chicago and Abu Dhabi.

- SC01: No shade - this simulation scenario serves as the benchmark scenario and does not include any shading strategies.
- SC02: 0.6m Horiz. - This simulation scenario applies 0.6m exterior horizontal shades for the top 4 levels of the building. The rigid shades are placed at 3m height for East, South, and West exterior perimeter façades, and on the East, North, and West courtyard-facing façades. The North exterior perimeter wall is left unshaded.
- SC03: NS 0.6m Horiz. + EW 0.6m Fin - Similar to the SC02, this simulation scenario applies exterior rigid shades for the top 4 levels of the building. However, for this scenario, the horizontal shades are only placed on the South façade and North side of the courtyard. For the East and West perimeters and courtyard, 0.6m fins are placed on every other vertical mullion.
- SC04: Oper. fixed Ts Stamisol® FT381 ctrl.@500: This simulation scenario places Stamisol® FT381 on the East, South, and West exterior perimeter glazing, and on the East, North, and West courtyard-facing glazing for the top 4 levels. The shading control mechanism is to control the operable shade at the threshold of 500 W/m². When the solar energy reaches to the assigned threshold value, shades are deployed as "full-down" position. When the solar energy is below the threshold, shades are designated as "full-up" condition. Regarding the transmission value (Ts) in this scenario, the fixed Ts value is used as provided by the manufacture without considering the fabric's angular optical properties.
- SC05: Oper. fixed Ts Stamisol® FT381 ctrl.@250: This simulation scenario is identical to SC04 with the only difference being that the operable threshold is set to 250 W/m².
- SC06: Oper. LBNL Ts Stamisol® FT381 ctrl.@500: This simulation scenario is identical to SC04 except that the Ts value in this scenario is replaced with the value extrapolated from the photo-goniometer lab testing.

Table3 provides the simulation matrix of the experiment with each run's associated observation focuses and performance measurements.

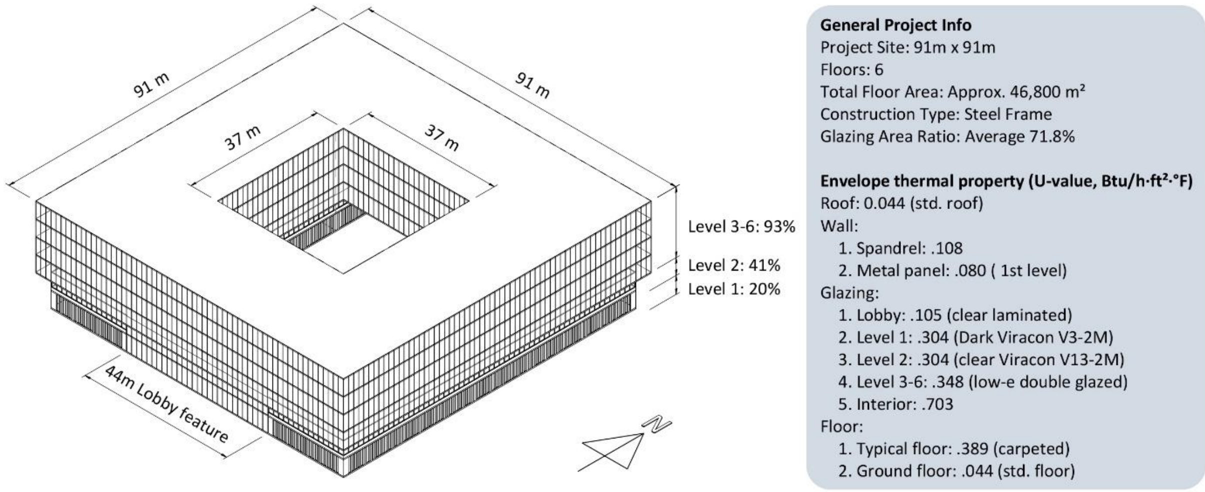

Figure 1: Experimental project illustration and project construction summary.

Table 3: Simulation run matrix of the research.

		Observation Focus			Measured Performance		Tested Climate Zone		
ID	Simulation Scenario	Obj1: Ts input	Obj2: Shading strategies	Obj3: different climate zone	Solar Gain MJ)	Building Energy Consumption(MJ)	Los Angeles	Chicago	Abu Dhabi
SC01	No shade		○	○	○	○	○	○	○
SC02	0.6m Horiz.		○	○	○	○	○	○	○
SC03	NS 0.6m Horiz. + EW 0.6m Fin		○	○	○	○	○	○	○
SC04	Oper. fixed Ts Stamisol®FT381 ctrl.@500	○	○	○	○	○	○	○	○
SC05	Oper. fixed Ts Stamisol® FT381 ctrl.@250		○	○		○	○	○	○
SC06	Oper. LBNL Ts Stamisol® FT381 ctrl@500	○		○		○	○	○	○

3.3 External Textile Shade: Simulation Results & Interpretations

The impact on the Ts value is the first area to consider in relation to the research objective. This impact can be observed through the comparison of the results for SC04 and SC06. Both scenarios have the same settings and control threshold, but SC06 uses the extrapolated value from LBNL lab testing and SC04 uses the value provided by the manufacturer. Although the resulting annual total system energy consumption have some differences, the variation is not considered very significant (as shown in Figure). For Los Angeles and Abu Dhabi, SC06 is slightly better than SC04, but SC04 is better than SC06 in Chicago. It can be assumed that SC06 represents a more accurate result since it takes angular properties into account. However, whether the difference this made is significant enough to be considered relevant is still unclear and requires further study. The second observation focus of the experiment is to understand the impact of different shading strategies and can be observed by comparing the overall scenario runs as illustrated in Figure 272 and Figure 3. In general, the textile shade strategies with control settings perform better than the rigid shade strategies. In addition, the impact of the control strategy can be observed through the comparison of SC04 and SC05's results since both scenarios are textile shade with different control thresholds. It is apparent that SC05's control threshold is more effective than SC04 and almost doubles the performance in all three climate zones. Furthermore, it can be observed in Chicago's result that the optimal shading strategy is varied through seasonal variation. This observation confirms the findings of prior research and highlights the need for dynamic and responsive systems to pursue higher performing results. The last observation focus of the research is to understand the impact of different climate zones. As described previously, the results are in agreement with prior research, which establishes that textile shade is more effective in warm climates as it will increase the heating load for cold climate buildings. However, it might still worth investigating whether the use of dynamic shading strategies can further improve the energy performance in both warm and cold climate.

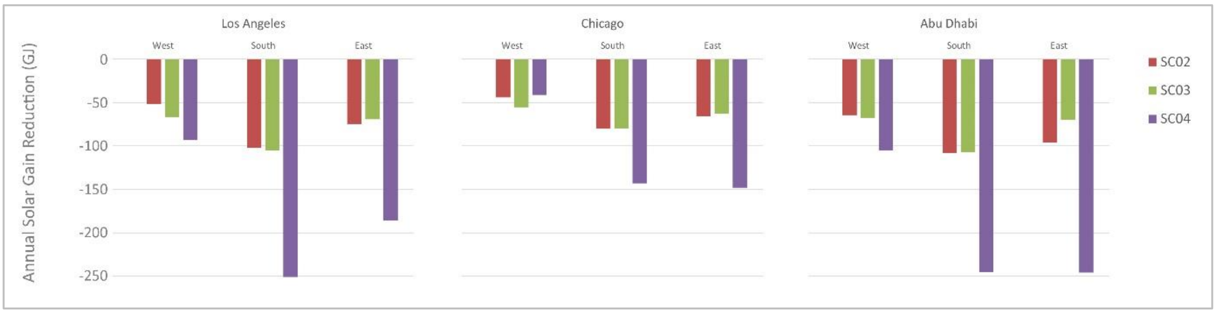

Figure 27: Different shading strategies' annual solar gain reduction compared to the benchmark scenario.

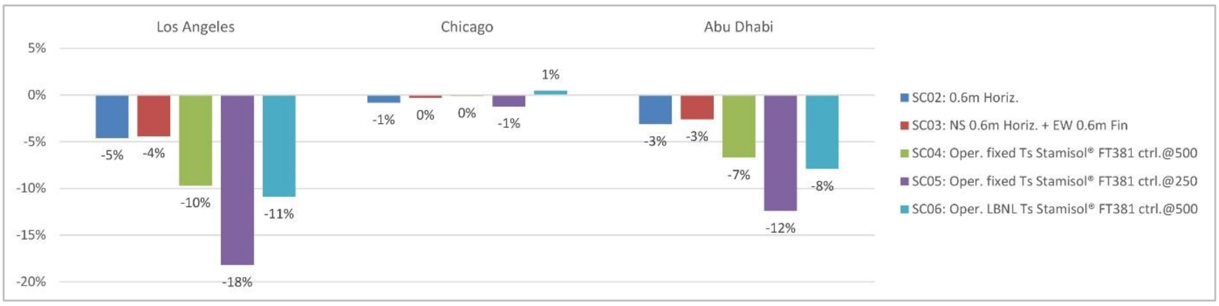

Figure 3: Annual energy saving percentage for different shading strategies compared with the benchmark case.

4 Case Based Experiment II: Transformable Membrane Façade

The objective of this experiment is to explore and validate the concept that using a transformable membrane façade system will improve building performance and encourage inspirational design synchronously. In order to achieve this objective, a shoebox model is utilized with a series of interchangeable membrane façade configurations to observe their relative daylighting performance during various time periods. By contrasting the results of a single configuration with multiple configurations, the potential for transformable façade to achieve higher performance can be revealed.

4.1 Transformable Membrane Façade: Experiment Design

A three-story parallelepiped model with Southeast oriented ETFE membrane façade as the outer skin is used for this case-based experiment, as illustrated in Figure 28. The hypothetical site of this experiment is located at the Orly Airport, Paris, France (48.73° N, 2.4° E) using the weather data obtained from the U.S. Department of Energy [27]. Desktop Radiance [28] is utilized as daylighting analysis engine through the user interface of Autodesk® Ecotect® Analysis 2011 (Ecotect) [29]. The daylighting performance is measured and observed through the illuminance levels. There are a total of five different façade variations (M0-M4) tested in this study, where M1-M4 are designed with the intent that their membrane geometries are interchangeable through the movement of structure frame, as illustrated in Figure 29. In order to isolate and compare the impact of different membrane's geometric configurations, the reflectance (R) and visible transmittance (Tv) values are assigned consistently throughout the tested scenarios. For this experiment, the Tv value of the ETFE layer adopts the test result from Gibbs et al. (2009) where the Tv value of a single layer ETFE is 0.85. To set up the transformable membrane façade system, M1, M2 and M3 are designed as the scenarios composed of two layers of ETFE which can be inflated to form M4's pillow shape if the control strategies applied in the future. As a result, the simulated

ETFE Ts value for M1~M3 is two layers of ETFE Tv value, 0.85 x 0.85 = 0.7225. The illuminance analysis is done through a 2D analysis grid placed on the working plane of the 2nd level, which is 0.76m above the floor plane. The grid size is 30.48 cm x 30.48 cm encompassing all the interior area and the area covered by the outer layer membrane. For each scenario, an illuminance analysis is conducted respectively at 9am, 11am, 1pm, 3pm and 5pm for summer solstice, fall equinox, and winter solstice (June 21st, September 21st, and December 21st). This resulted in a total of 75 simulation runs for this experiment. Daylighting performance is evaluated by LEED BC+D v4 through the demonstration of illuminance levels between 300 and 3,000 lux for 9 a.m. and 3 p.m., both on a clear-sky day at the equinox, for 75% or 90% or regularly occupied floor area [30]. Based on this standard, it is determined by this research that the optimal illuminance performance is to demonstrate more than 75% of the area can have illuminance levels over 300 lux. In addition, in order to eliminate the excessive heat and glare introduced by daylight, when two scenarios are both designated as optimal, the scenario with less illuminance (>1,200 lux) is preferred.

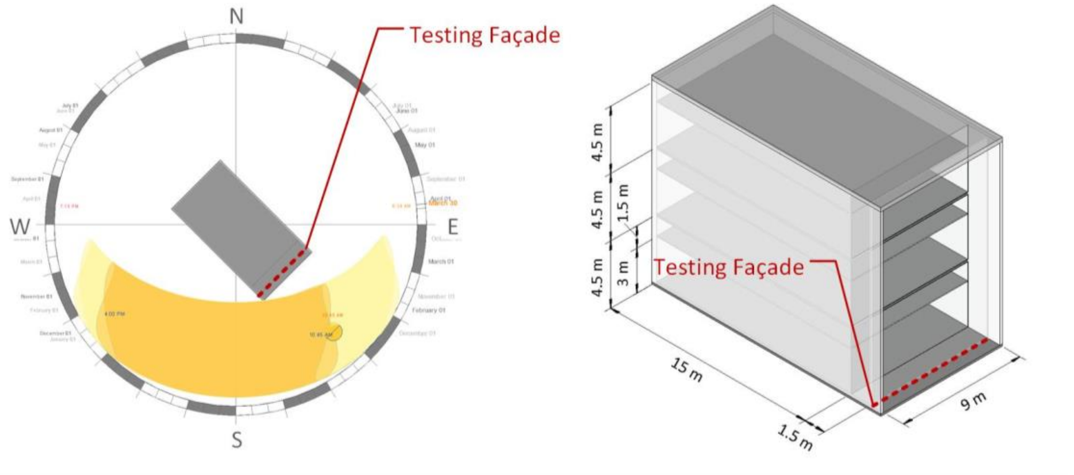

Figure 28: The parallelepiped model for Case-based Experiment II.

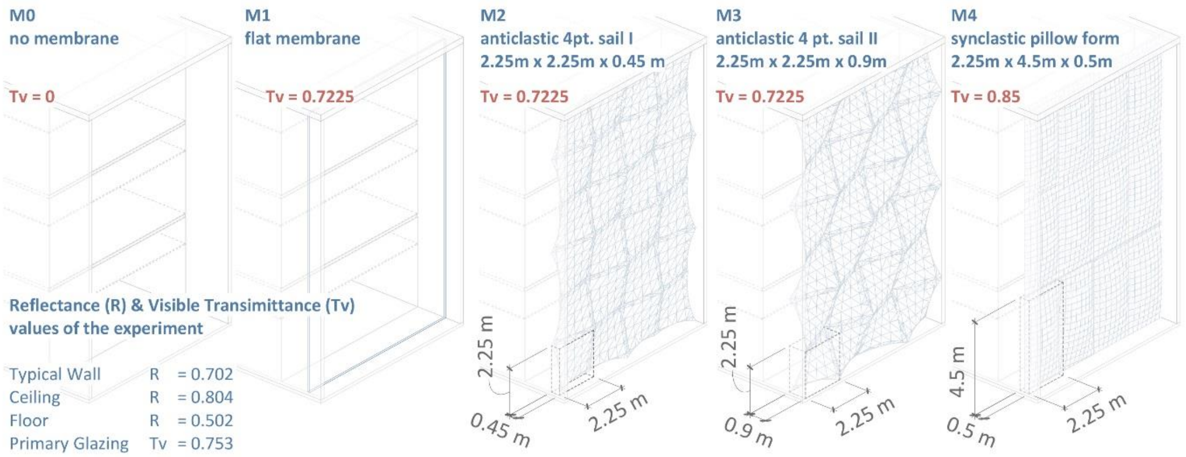

Figure 29: Summary of the scenario designs of Case-based Experiment II.

4.2 Transformable Membrane Façade: Simulation Results & Interpretations

The collected data for each simulation include a batch of Radiance's output files along with a color-coded image (*.bmp) to illustrate the illuminance distribution of each analysis. A consistent coloring scale, ranging from 0 lux (blue) to 1200 lux (yellow), is applied to every analysis to ensure the comparability of each result. Based on the definition of this research, the optimal condition is a resulting image with a color ranging from burgundy (240 lux) to yellow (1200+ lux), larger than 75% of the floor area. When multiple optimal conditions exits, the image with less yellow and orange color is preferred. In order to observe the optimal membrane configuration for different times and dates, this research divides 75 illuminance distribution images into three groups based on the simulation dates: June 21st, September 21st, and December 21st. Each group has 25 simulation runs, composed of the results from five different times making for five different scenarios on the same date. For comparison purposes, each group of the results are arranged on a matrix (Figure 6) so that each column represents a specific time, from 9am to 5pm, and each run represents a specific scenario, from M1 to M4. Additionally, the best illuminance performance (as defined by the research) is also determined and highlighted. It can be observed that the illuminance levels for different configurations has noticeable variance during different times and dates, and vice versa. For summer solstice, M3 provides the best illuminance distribution in the morning while the flat membrane, M1, is preferred in the afternoon. During fall equinox, the membrane configuration of M4 is considered more suitable to accommodate the morning low sun angle since it provides adequate illuminance levels for work while minimizing the illuminance contrast throughout the space. On the other hand, M2 presents better performance during the winter morning. No scenario provides illumination levels that meet the criteria during the winter afternoon. Therefore, M1 is chosen for being the highest performing during winter afternoon. This experiment demonstrates how the use of geometric-adjustable membrane façade system can provide nearly consistent high-performing illuminance levels despite the constantly changing exterior environment.

While this study only applies a basic model, it shows that the adaptive membrane façade system is able to accommodate needs for different occupancy zones during different times, dates and orientations. Additionally, the use of the adaptive membrane façade enables appearance variation with assorted possible configurations. This can broaden designers' design space with inspirational yet high performing components. Imagining how the adaptive membrane façade system can be integrated with a geometrically-complex architectural skin, opportunities emerge for designers to expand their design spectrum with sexier, more aesthetically appealing elements that simultaneously improve performance.

5 Conclusion and Future Work

In order to pursue and promote the use of tensile membrane façade system to enable responsive, higher performing buildings, a goniometric lab test was first conducted to obtain the optical properties of the test sample followed by two case-based experiments to understand the impact of input optical properties, different shading strategies, and the impact of membrane's geometric variations. For the first case based experiment, there were a total of six shading scenarios tested in three different climate zones. Based on current simulation results, although the performance variation can be observed, the impact of the Ts value might not be significant enough to affect the design decision making process. However, this research only tested flat fabric shading surfaces and excluded the potential of electrical lighting energy reduction; the actual impact of using optical properties cannot be accurately gauged based on the current results. When comparing different shading strategies, textile shades are more effective than other tested scenarios in a warm climate condition in terms of solar heat gain and the total system energy reduction. The results also demonstrate that the control mechanism of the textile shade has a significant impact on the performance.

To further support the conclusion drawn from the previous experiment, the second case-based experiment focused on observing the potential introduced by a transformable membrane façade system. A parallelepiped model with four tensile membrane façade configurations was explored and compared based on each configuration's daylighting illuminance levels. It is evident that each configuration provides varying performance throughout different times and dates. However, none of the configurations singularly met the designated criteria throughout the testing period. On the other hand, if transformability is allowed, the façade system is able to provide nearly consistent daylighting performance based on user-defined criteria regardless the time and date. This result begins to support and validate the research hypothesis that a transformable membrane façade system can provide higher building performance. Furthermore, it expands the design space and encourages designers to rethink façade design. Currently, the research only explored a relatively simple system with the focus on limited performance aspects, i.e. energy, solar heat gain and daylighting performance. There are several unknowns and questions that need to be explored further. However, it is evident that the transformable membrane façade system with kinetic and responsive control has potential and can be expected to be explored further. With the advancement of the design and control technologies, this research believes that the use of transformable membrane façade system is the most promising and economically feasible means to overcome growing performance demands and meet the increasing design complexity synchronously.

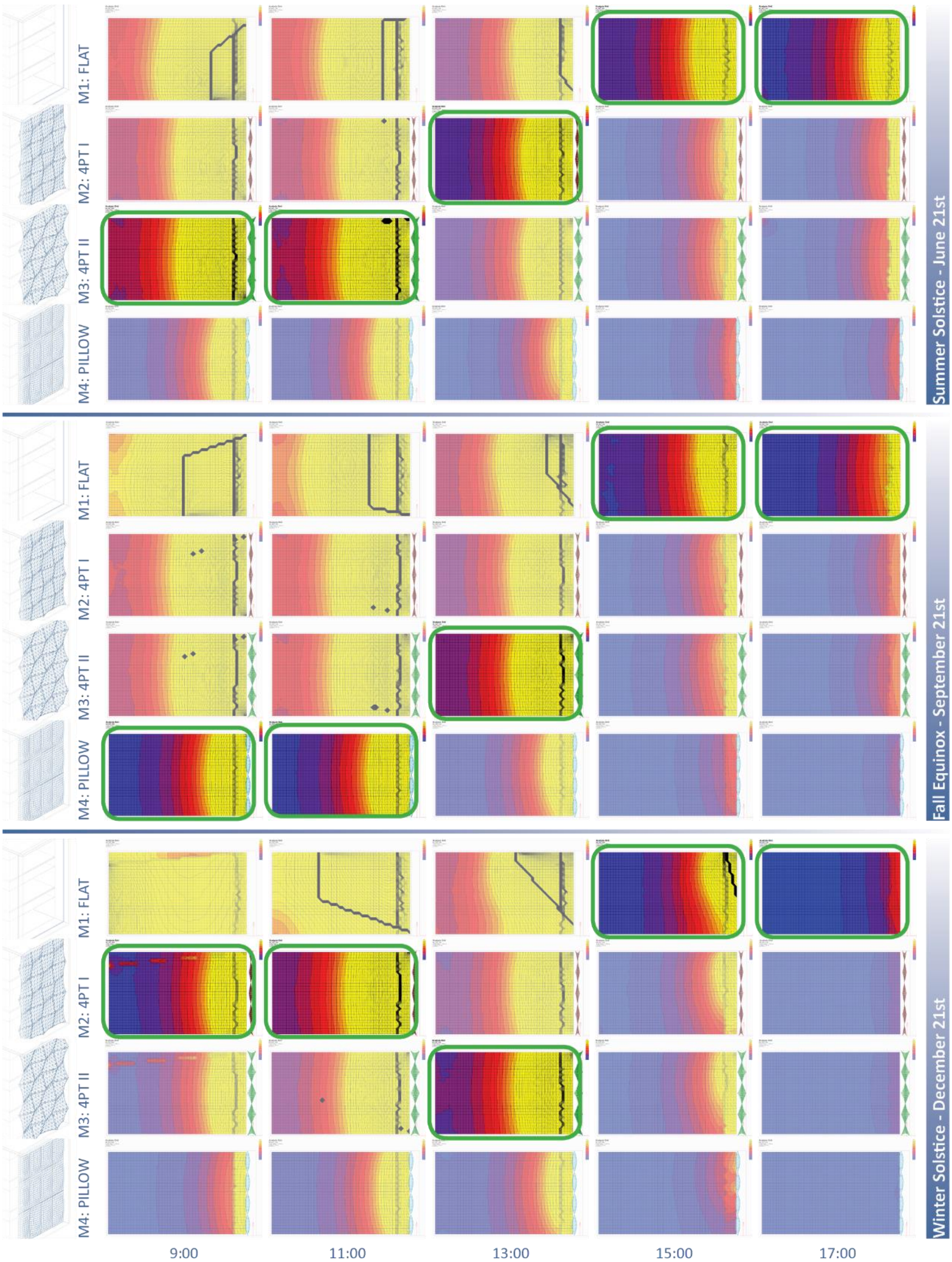

Figure 6: Illustration of the optimal façade variation for summer solstice, fall equinox and winter solstice.

6 Acknowledgements

First we would like to acknowledge Steve Fredrickson, Jim Driggs, and Robert McGilvray of Serge Ferrari whom provided the instigation, support, and considerable enthusiasm for this research. We would also like to acknowledge the efforts of Dr. Jacob C. Jonsson of the Lawrence Berkeley National Laboratory (LBNL), and the guidance of USC Professor Kyle Konis and Aarhus University Professor Steffen Petersen in this laboratory testing. In addition, we would like to thank John Adams of Gensler Los Angeles for facilitating the digital building model for simulation use, and Joseph Lewis and Alper Erten who provided energy modeling advice.

7 References

[1] Cardoso, D., Michaud, D., Sass, L.: *Soft façade: Steps into the definition of a responsive ETFE façade for high-rise buildings*, 25th eCAADe Conference: Predicting the Future, Frankfurt am Main, Germany, 2007.
[2] Atzeri, A.M., Pernigotto, G., Cappelletti, F., Gasparella, A., Tzempelikos, A.: *Energy performance of shading devices for thermal and lighting comfort in offices*, BSA2013, Bozen-Bolzano, Italy, 2008.
[3] Eskin, N., Türkmen, H.: *Analysis of annual heating and cooling energy requirements for office buildings in different climates in Turkey*, in: Energy and Buildings, 40 (2008) issue 5, pp.763-773.
[4] Wienold, J., Frontini, F., Herkel, S., Mende, S.: *Climate based simulation of different shading device systems for comfort and energy demand*, Building Simulation 2011, Sydney, Australia, 2011.
[5] O'Neill, B.: *Model-based control of venetian blinds* Department of Building, Civil and Environmental Engineering, Concordia University, 2008.
[6] Wankanapon, P.: *The impact of translucent fabric shades and control strategies on energy savings and visual quality*, Doctor of Philosophy in Architectural Engineering, The Graduate School, College of Engineering, Pennsylvannia State University, 2009.
[7] Winstanley, T.: *AD Classics: Institut du Monde Arabe / Jean Nouvel* ArchDaily, 2011.
[8] Baraona Pohl, E.: *Phare Tower / Morphosis Architects*, ArchDaily, 2009.
[9] Gibbs, R.J., Pollock, K.M., Jennings-Temple, M.A.: *Evaluation of light transmission properties under an Ethylterafluoroethylene (ETFE) structure*, in: International Turfgrass Society Research Journal, 11 (2009) issue, pp.351-364.
[10] Robinson, L.A.: *Structural opportunities of ETFE (ethylene tetra fluoro ethylene)*, Thesis, Massachusetts Institute of Technology, 2005.
[11] Architen Landrell: *Materials - Few materials match the dama and interest of lighweight tensile fabrics*. (2014). http://www.architen.com/materials/. Accessed on 5 August 2014.
[12] Richards, C.: *Tensile fabric structures and performance*. (2010). http://www.architen.com/articles/tensile-fabric-structures-and-performance/. Accessed on 11th June 2014.
[13] Zhao, X., Long, E.S., Huang, L.H.: *Design measures of low carbon buildings with exterior envelope made of ETFE air pillows*, in: Advanced Materials Research, 168-170 (2010) issue, pp.2524-2528.
[14] Wankanapon, P., Mistrick, R.G.: *Roller shades and automatic lighting control with solar radiation control strategies*, in: International Journal of Building, Urban, Interior and Landscape Technology, 1 (2011) issue 1, pp.35-42.
[15] Yao, J.: *An investigation into the impact of movable solar shades on energy, indoor thermal and visual comfort improvements*, in: Building and Environment, 71 (2014) issue, pp.24-32.
[16] Kohler, C.: *Simulation of complex glazing products; from optical data measurements to model based predictive controls*, BEST 3 Conference, Atlanta, GA, 2012.
[17] Grobe, L.O., Wittkopf, S., Apian-Bennewitz, P., Jonsson, J.C., Rubin, M.: *Experimental validation of bidirectional reflection and transmission distribution measurements of specular and scattering materials*, Photonics for Solar Energy Systems III, Brussels, Belgium, 2010.
[18] Jonsson, J.C., Lee, E.S., Rubin, M.D.: *Light-scattering properties of a woven shade-screen material used for daylighting and solar heat-gain control*, SPIE Optics+Photonics, San Diego, CA, 2008.
[19] Ward, G., Mistrick, R., Lee, E.S., McNeil, A., Jonsson, J.: *Simulating the daylight performance of complex fenestration systems using bidirectional scattering distribution functions within radiance*, in: Journal of Illuminating Engineering Society of North America, 7 (2011) issue 4.
[20] LBNL: *Photo-goniometer*. (2009). http://windowoptics.lbl.gov/facilities/big-gonio-spectrometer/pgii-data-post-processing-for-use-in-window-6-and-other-software. Accessed on 17 July 2014.
[21] Chiu, S.K.: *Transformable Tensile Facade: Performance Assessment on Energy Solar and Daylighting*, Master Thesis, Membrane Lightweight Structure, 2014.
[22] IES: *Integrated Environmental Solutions*. (2014). http://www.iesve.com/. Accessed on 5 August 2014.

[23] Bambardekar, S., Poerschke, U.: *The architect as performer of energy simulation the early design stage*, Building Simulation 2009, Glasgow, Scotland, 2009.
[24] Industrias BEC, S.A.: *Stamisol FT 381*. (2014). http://www.bec.es/en/fabrics-for-curtains-blinds-screens-and-textil-architecture/textile-meshes/stamisol-ft-381/. Accessed on 15 July 2014.
[25] Ferrari: *Stamisol® FT 381 Stamisol® Color* www.ferrari-architecture.com.
[26] Karlsson, J., Roos, A.: *Modelling the angular behaviour of the total solar energy transmittance of windows*, in: Solar Energy, 69 (2000) issue 4, pp.321-329.
[27] U.S. Department of Energy: *EnergyPlus Energy Simulation Software - Weather Data*. (2013). http://apps1.eere.energy.gov/buildings/energyplus/weatherdata_about.cfm. Accessed on 12 September.
[28] LBNL: *Desktop Radiance*. (2000). http://floyd.lbl.gov/deskrad/dradHOME.html. Accessed on 11 September 2014.
[29] Autodesk: *Autodesk Ecotect Analysis*. (2014). http://usa.autodesk.com/ecotect-analysis/. Accessed on 10 September 2014.
[30] U.S. Green Building Council: *LEED BD+C: New Construction | v4 - LEED v4: Daylight*. (2014). http://www.usgbc.org/node/2614118?return=/credits. Accessed on 15 September.

Proceedings of the International Conference on Building Envelope Design and Technology, Graz
Advanced Building Skins 2015

Innovative Daylighting and Shading Concept - The Energy Efficiency Center

Michaela Reim, Dr.
ZAE Bayern, Germany, michaela.reim@zae-bayern.de, www.zae-bayern.de

Werner Körner, Dr.
ZAE Bayern, Germany, werner.koerner@zae-bayern.de

Summary

This work describes the daylighting and shading concept of the recently constructed "Energy Efficiency Center". There, an efficient utilization of natural lighting in the offices, corridors, function room and technical center was realized by use of a translucent membrane roof with subjacent translucent aerogel modules. Selectively coated solar blinds guide the visual spectrum of the sunlight into the rooms while blocking the infrared parts. Roller blinds for glare protection with special low-e-coatings improve thermal comfort in the office rooms. A high-level building automation system controls the different systems. The goal was to minimize the energy consumption for artificial lighting and at the same time to minimize the solar energy input into the rooms in summer while providing a good thermal and visual comfort to the users. The design of the sun protection and daylighting systems was geared towards the summer case. The performance of the systems was measured and optimized in the summer period of 2014. In this work additional results for the winter period 2014/2015 are shown.

Keywords: membrane; daylighting; artificial lighting; aerogel glazing; luminescence

1 The Energy Efficiency Center

The Energy Efficiency Center (EEC) is a combined office (1st floor) and laboratory (ground floor) building with a function room attached to the north side. It is located in Würzburg, Germany and was finished in June 2013. The overall aim of the project is to create a reference building which implements innovative techniques, serves demonstrational purposes, and sets new standards. The roof of the main building consists of translucent PTFE-glass-membranes and partially of transparent ETFE films. The membrane acts as a climate interlayer above the thermal insulation level, the ceiling of the 1st floor. Parts of the ceiling of the 1st floor are transparent or translucent. The ceiling of the corridor consists of triple glazing. Parts of the ceiling of the office rooms away from the façade consist of translucent multiple skin sheets filled with Lumira-aerogel. The roof of the function room to the north consists of translucent, double-layered, air filled PVC-membrane cushions.

The sun protection system on the south facade consists of an outside sun protection system with spectrally selective lamellae. The lamellae position is controlled in order to avoid glare.

Additionally, all rooms are equipped with an inside glare protection system, a roller blind with a low-emissivity coating on the inner surface. The luminaries are dimmed automatically when necessary to achieve an illumination level of 500 lx. Depending on the heating or cooling demand of the room, the solar energy input through the facade can be varied by using either the outside (low solar energy input) or inside (high solar energy input) shading device. The operation of the lighting and sun protection systems were tested for summer conditions, meaning high altitude of the sun and a control strategy for the sun protection system with the goal to minimize solar energy input through the façade [Reim et al. 2015]. Similar tests for intermediate and winter conditions will be presented in this paper. When the correct operation of the control systems is verified the interaction of the users with the control system will be investigated by monitoring the user interventions with the building control system.

2 Lighting and shading concept

The goal of the lighting and shading concept is to minimize the energy consumption of the artificial lighting system by maximizing the daylight input into the rooms while at the same time reducing the heating/cooling loads by maximizing/minimizing the solar energy input into the rooms as applicable. Figure 1 shows the main building viewed from south-east. The main axis of the building runs east-west.

Figure 1: Energy Efficiency Center viewed from south-east. Clearly visible is the textile roof with translucent PTFE-glass membranes and partially transparent ETFE films.

Figure 2: The textile roof with translucent PTFE-glass membranes and partially transparent ETFE films.

Most of the office rooms are located on the south side on the 1st floor. In the north side there are staircases and lift, the library and two conference rooms as well as some office rooms. The basement mainly contains laboratories. To the north an additional single-story part contains a function room and a technical center.

The roof of the main building consists of translucent PTFE-glass-membranes and partially of transparent ETFE films, see figure 2. The membrane acts as a climate interlayer above the thermal insulation level, the ceiling of the 1st floor, which itself is partly transparent or translucent. The ceiling of the corridor in the 1st floor is glazed, so it is naturally illuminated through the translucent and transparent membrane roof, see Figure 3.

Figure 3: Corridor in the 1st floor in east-to-west direction illuminated by daylight (left); Translucent aerogel glazing in the stairways (right).

Part of the ceiling of the corridor and stairways is glazed with an aerogel glazing [Okalux, 2013]. The ceilings of most of the office rooms contain a translucent double-skin-sheet filled with Lumira-aerogel [Cabot, 2013] with a width of about 1 m located in the back of the room, thus enabling an additional illumination of the room depth through the translucent roof (see Figure 3).

The roof of the single-story function room and technical center at the north consists partially of translucent, double-layered, air filled PVC-membrane cushions with a glass fiber interlayer.

The sun protection system on the south façade consists of outside blinds with spectrally selective lamellae. The solar reflectance of the lamellae in the visible spectral range is significantly higher than the reflectance in the solar spectral range [Warema, 2008]. The result is a total solar energy transmittance which is lower than that of non-selective lamellae with the same visual transmittance. Figure 5 shows the geometry and the cut-off-angle of these lamellae. The cut-off-angle is the angle to which the lamellae have to be closed in order to prevent direct radiation to pass through the sun protection system depending on the solar height.

On the east and west façade triple glazing with integrated lamellae was used for architectural reasons. On the north façade no sun protection system is used. In order to limit the solar energy input through the north façade a glazing with lower total solar energy transmittance was used there. Additionally, all rooms are equipped with an inside glare protection system, a roller blind with a low-emissivity coating on the inner surface to improve thermal comfort of the inhabitants.

Figure 4: the outside sun protection system and the protruding membrane roof.

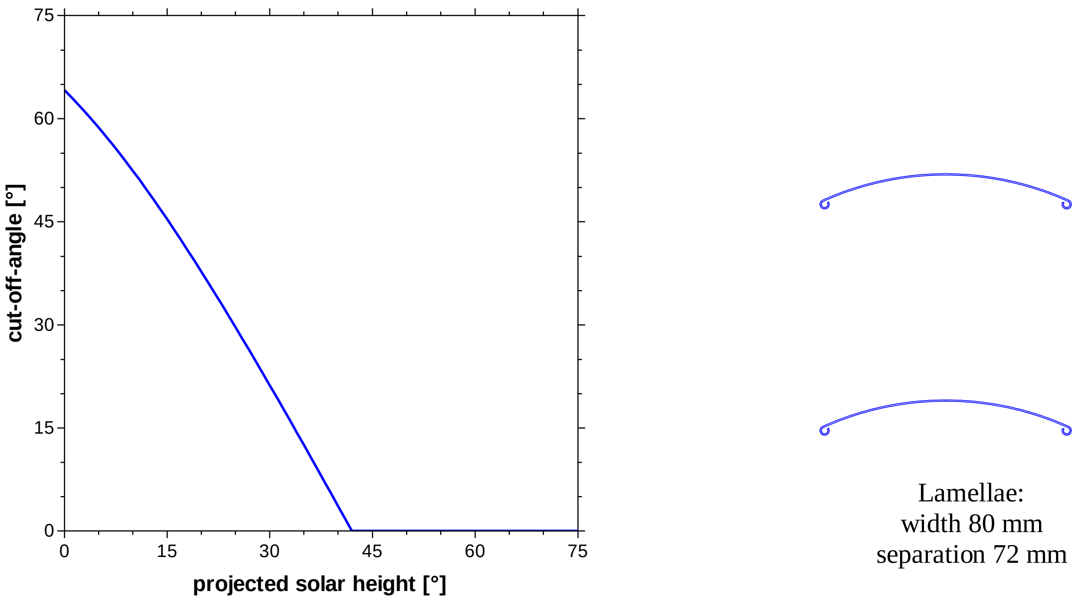

Figure 5: Geometry of the lamellae of the outside sun protection system (right). Cut-off-angle depending on the projected angle of incidence on the façade (left).

The luminaries are switched and dimmed automatically based on combined occupancy and illuminance sensors in each room.

Figure 6 summarizes the different parts of the daylighting concept, Table 1 shows the thermal and optical properties of the glazing and the translucent parts of the façade. As the roof acts as a climate interlayer the solar and visual optical properties of the materials are important. The translucent part of the roof consists of a PTFE-glass-membrane Type Sheerfill II with Everclean-Coating [Saint-Gobain, 2014]. The transparent part consists of an ETFE-Film with a thickness of 250 µm printed with a hexagonal pattern with a pattern size of 9 mm and a print coverage ratio of 89%. Figure 7 shows transmittance and reflectance of both materials in the solar spectral range. The visual transmittances of the ETFE film and glass-PTFE membrane are 57% and 11%, respectively.

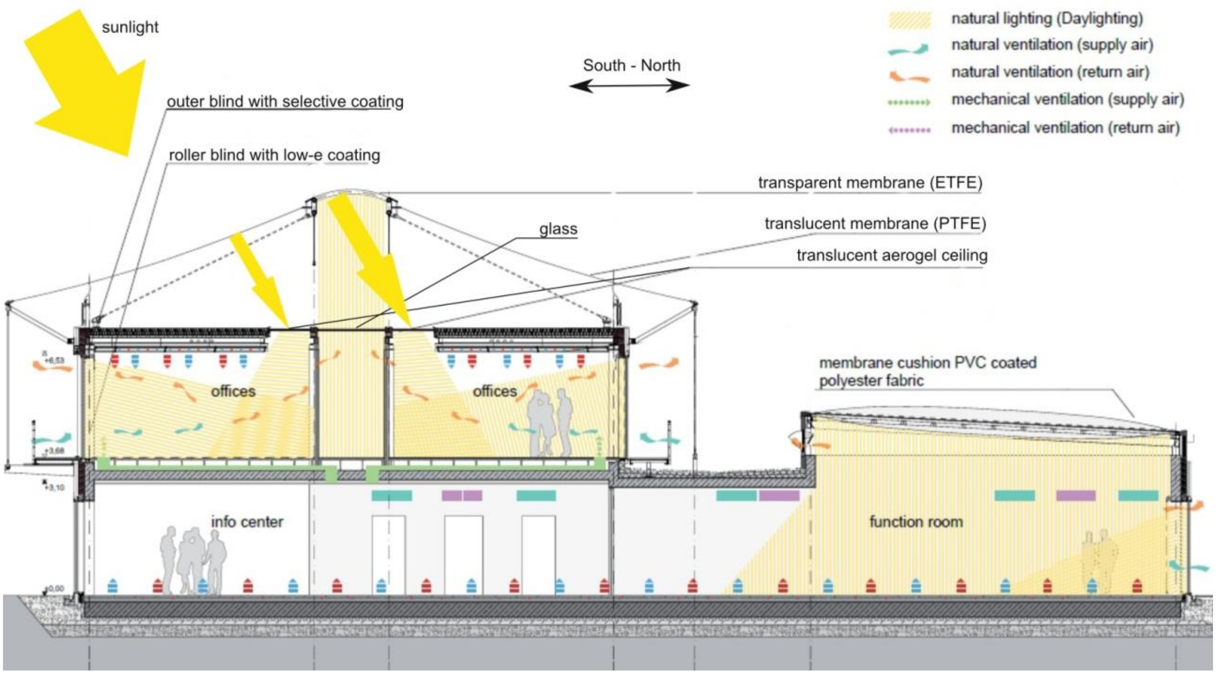

Figure 6: Daylighting concept of the Energy Efficiency Center (EEC).

Table 1: U-value (center of glass U_g and window U_w), total solar energy transmittance (g-value) and visual transmittance of glazing and transparent roof and ceiling elements.

description	U_g [W/(m2K)]	U_w [W/(m2K)]	g	τ_v
glazing (south façade)	0.6	0.9	0.47	0.72
glazing (east and west façade)	0.7	0.9	0.35	0.55
glazing (north façade)	0.7	0.9	0.27	0.55
aerogel double skin sheets(office ceiling)	0.7	0.8	0.39	0.20
aerogel glazing (corridor ceiling)	0.6	0.9	0.25	0.25
glazing (corridor ceiling)	0.6	0.9	0.27	0.55
PVC-membrane cushion (function room)	0.9	1.0	0.05	0.03

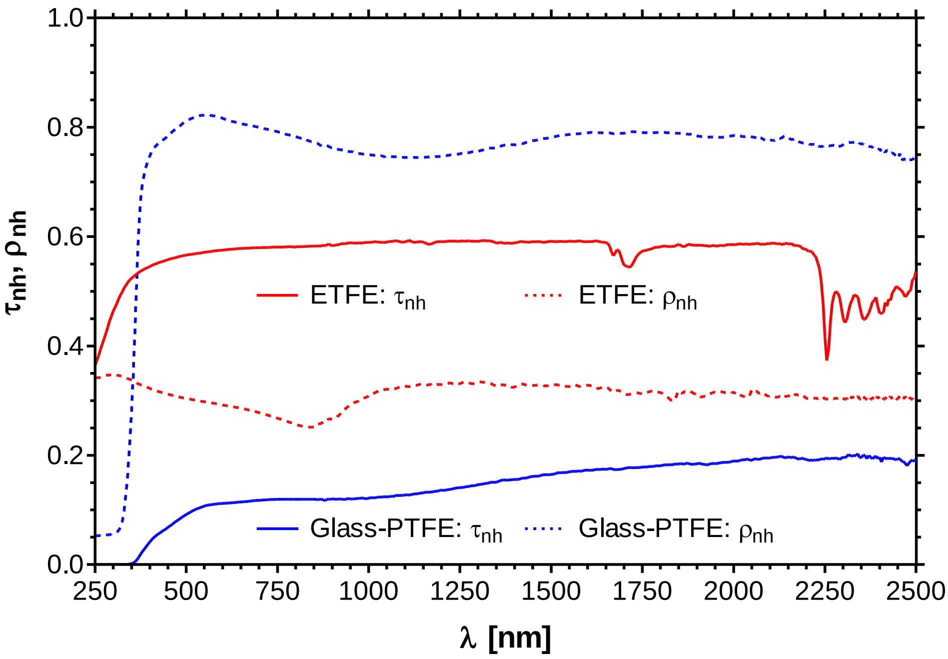

Figure 7: Spectral normal-hemispherical transmittance and reflectance of both parts of the roof: Printed ETFE film and glass-PTFE membrane.

3 Control of lighting and sun protection system

Each room is equipped with a ceiling-mounted combined occupancy and illuminance sensor. The occupancy sensor selects a low-power mode for the room when nobody is present. This includes switching off the light and opening or closing the external sun protection system depending on whether there is heating or cooling demand for the room. The sun protection system is opened when heating is necessary and nearly fully closed when cooling is necessary.

When occupied, a default illuminance level of 500 lx ([EN 12464-1, 2011] for office rooms) at the work places is maintained using artificial lighting. The position of the shading system depends on the outside illuminance on the respective façade:

- It is closed when an outside illuminance higher than 45 klx is reached for more than 30 seconds. The lamellae angle is set depending on the position of the sun and the heating or cooling demand of the room. When heating demand is present the lamellae are closed a few degrees more than the cut-off-angle, which ensures that no direct irradiation passes the sun protection system. When cooling is needed the lamellae angle is set to about 10° higher than the cut-off-angle or a minimum of about 20°, further reducing the solar energy input to the room.
- It is opened when the outside illuminance is lower than 20 klx for more than 20 minutes.
- When the outside illuminance is higher than 30 klx for more than 5 minutes the sun protection system is closed with a lamellae angle of 0°. The same state is reached when the system is closed and the outside illuminance is lower than 30 klx for more than 5 minutes.

The automatic settings for lighting and outside sun protection system can be overruled by the user, the system is reset to automatic mode after 30 minutes without occupancy in the room. The roller blinds used as inside glare protection are controlled manually.

4 Monitoring

Two office rooms at the south and north façade were equipped with some additional illuminance sensors at the working surfaces and below the translucent part of the ceiling.

5 Results

Figure 8 shows the illuminance below the translucent part of the ceiling in the south and north offices depending on the global solar irradiance for a period in summer 2014 and winter 2014/2015.
In summer this illuminance is approximately proportional to the global irradiance and peaks at about 2000 lx for the south room. The corresponding illuminance for the north room is significantly higher and peaks at above 8000 lx. This is caused by direct irradiation through the ETFE films above the corridor, which hits the translucent panels at the north side. As the visual transmittance of the ETFE films is significantly higher than the transmittance of the glass-PTFE-membrane this yields higher light input through the translucent panels for the north rooms compared to the south rooms. When comparing the illuminance E_v below the translucent part of the ceiling for overcast sky (direct solar irradiance near zero) the values for the north- and south-oriented rooms are identical.
Due to the lower elevation of the sun in winter, no direct radiation hits the translucent panels on the north side. Therefore, the illuminance below the translucent parts of the ceiling is nearly identical for the north- and south-oriented office rooms.

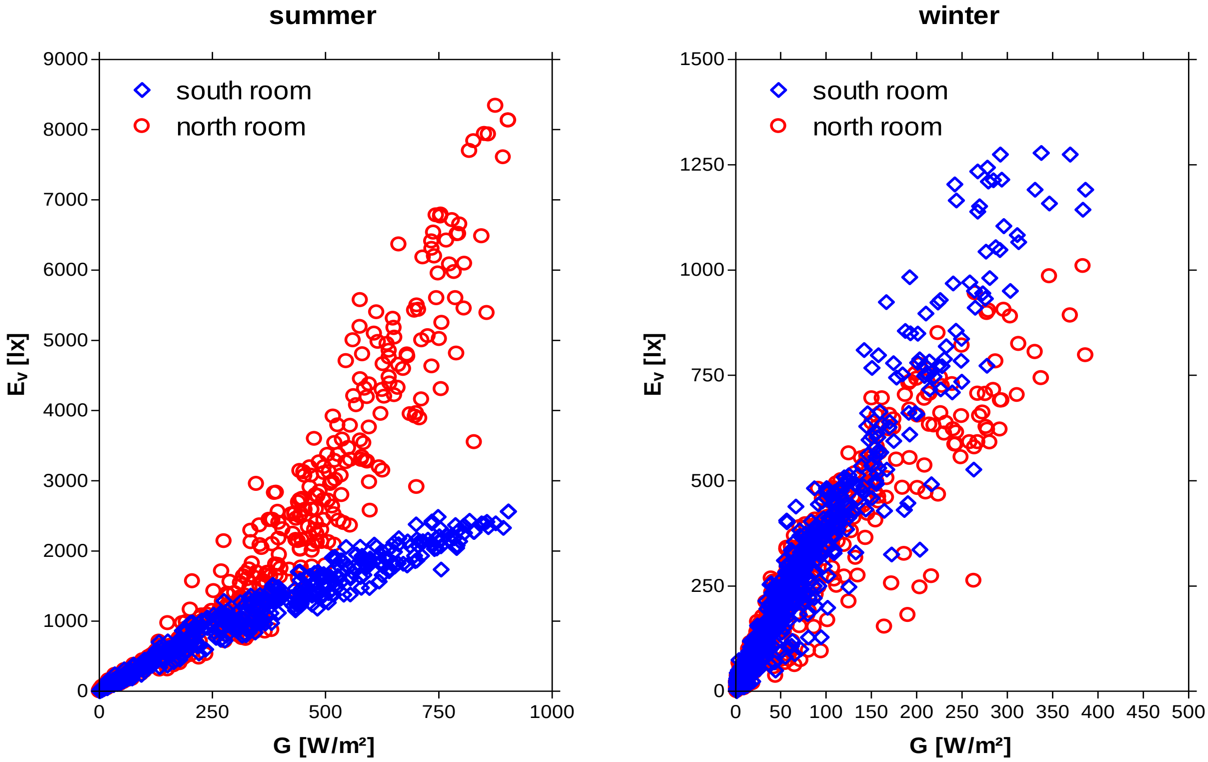

Figure 9: Illuminance E_v below the translucent part of the ceiling depending on the global irradiance G for summer 2014 (left) and winter 2014/2015 (right).

Figure 10 shows the global irradiance and the illuminance below the translucent ceiling element and in the room (measured by the ceiling-mounted sensor) for the north- and south-oriented room on a sunny day in January 2015. The artificial lighting was not used in this period and the shading systems were open (at a temperature below 8°C, the heating mode is maintained for the whole building and as a consequence of this, the sun protection system remains open). The illuminance directly below the aerogel ceiling element is nearly the same for both rooms, but the illuminance of the south-oriented room is much higher than the illuminance in the north-oriented room. In the north-oriented rooms artificial lighting is needed in winter even at sunny days in order to reach an illuminance level of 500 lx. About half of the daylight enters the room through the translucent ceiling element for the weather conditions shown in Figure 10.

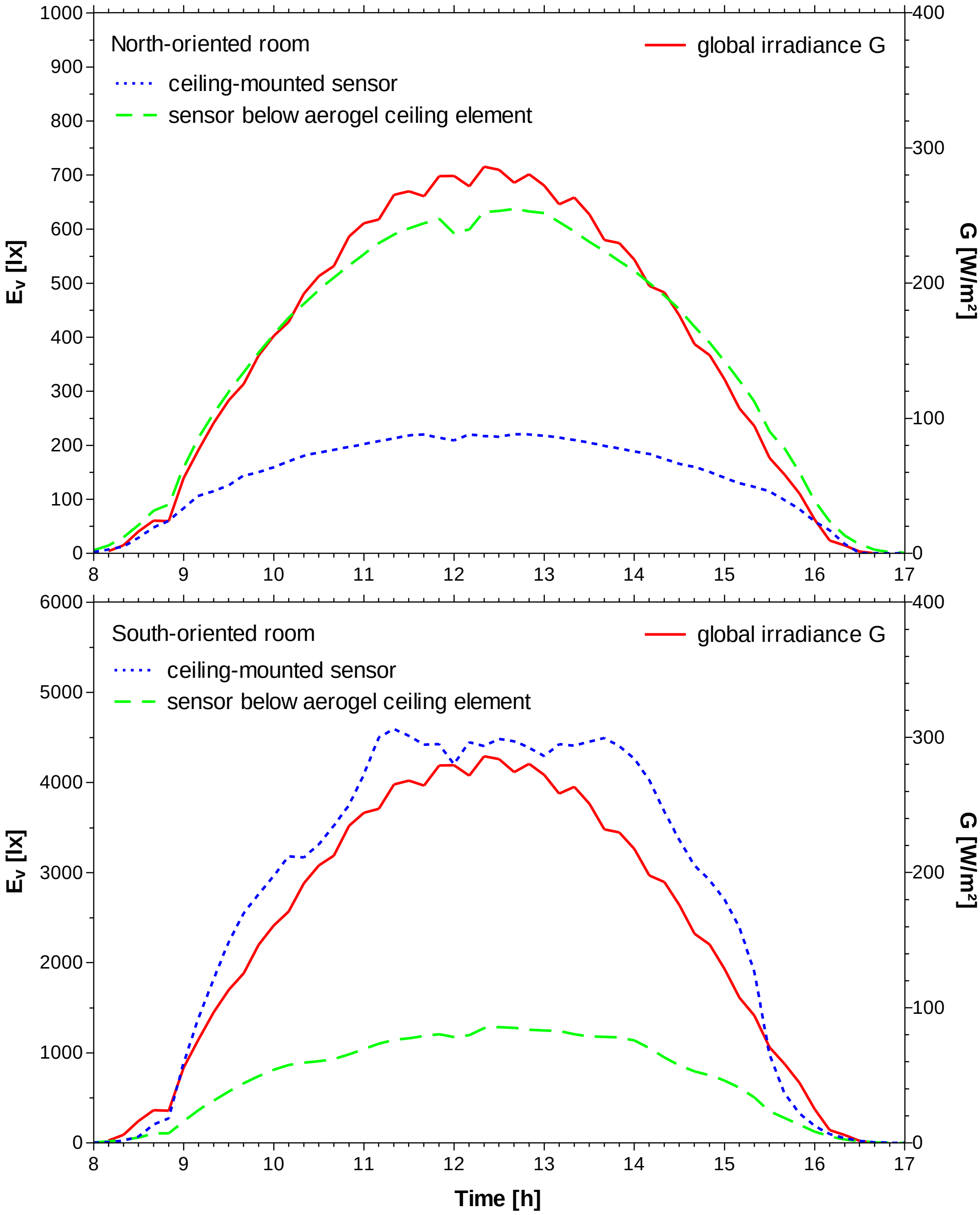

Figure 10: Illuminance E_v below the translucent part of the ceiling and measured by the ceiling mounted sensor and global irradiance G for a sunny day in January 2015.

Figure 11 shows the same data for an overcast day in January 2015. The illuminance directly below the aerogel ceiling element is still the same for both rooms, but for overcast sky the illuminance of the ceiling mounted sensor in the south-oriented and the north-oriented room are also nearly the same. In this case the artificial lighting would complete the missing illuminance up to 500 lx, if there are users inside.

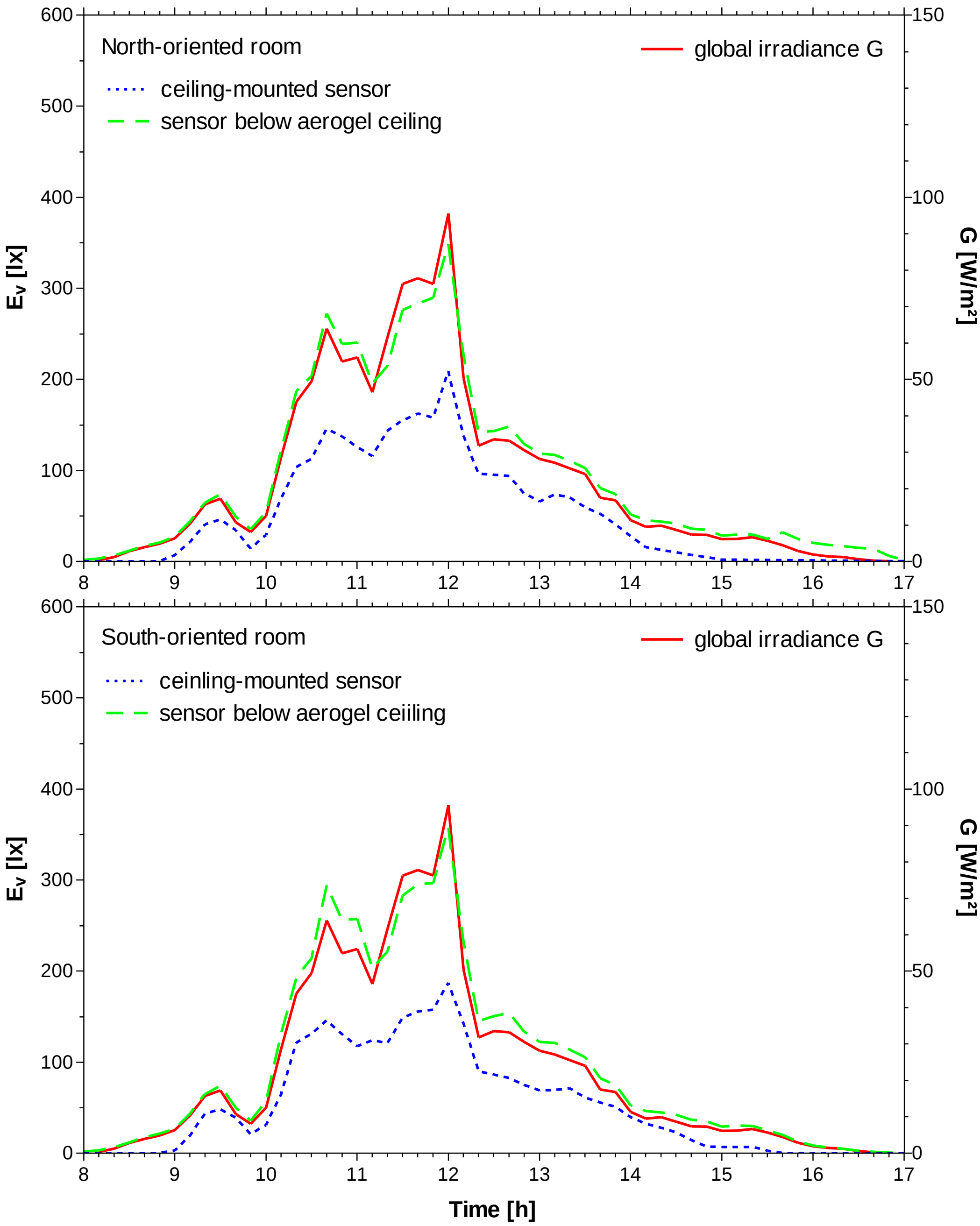

Figure 11: Illuminance E_v below the translucent part of the ceiling and measured by the ceiling mounted sensor and global irradiance G for an overcast day in January 2015.

These results show, that the translucent aerogel ceiling has an significant effect on the room illumination, especially when regarding the illumination in the room depth. Even on overcast days, the aerogel ceiling contributes significantly to the room illumination in both south- and north-facing rooms.

6 Acknowledgements

The Energy Efficiency Center is funded by the German Federal Ministry of Economics and Technology because of a decision of the German Bundestag, the Federal state of Bavaria and the Bürgerstiftung Würzburg und Umgebung.

We thank our sponsors and partners for their support:

Assmann Büromöbel GmbH & Co. KG, BSH Bosch und Siemens Hausgeräte GmbH, Bürgerstiftung Würzburg und Umgebung, Cabot Aerogel, Doerken GmbH & Co. KG, DuPont de Nemours, EEV GmbH, Ehrenfels Isoliertüren GmbH, Energy Glas GmbH, Hightex, Knauf Gips KG, Lindner AG, Maincor AG, Okalux GmbH, Porextherm Dämmstoffe GmbH, Roto Frank Bauelemente GmbH, Rubitherm Technologies GmbH, Saint Gobain PPL Cologne GmbH, SGL Carbon SE, Siemens Schweiz AG, Siemens AG Building Technologies Division, Siteco Beleuchtungstechnik GmbH, , Team Weber GmbH, Uhlmann & Zacher GmbH, uponor GmbH, va-q-tec AG, Versaidag-Indutex GmbH, Walter Stickling GmbH, Waldner Holding GmbH & Co. KG, Warema Renkhoff SE.
More information is available at http://www.energy-efficiency-center.de/en/Home/.

7 References

[1] Cabot, 2013. *Data Sheet - Lumira aerogel particles*, http://www.cabot-corp.com/wcm/download/en-us/ae/Translucent_1000_2000_DS_2013_v6_final lo res.pdf, downloaded Aug. 14, 2014.
[2] DIN 5034-1, 2011. *Daylight in interiors - Part 1: General requirements, German version* DIN 5034-1:2011-07
[3] EN 12464-1, 2011. *Light and lighting - Lighting of work places - Part 1: Indoor work places; German version* EN 12464-1:2011
[4] OKALUX, 2013. *OKAGEL light-diffusing high-performance insulating glass*, http://www.okalux.de/fileadmin/Downloads/Downloads_englisch/Infotexte/i_okagel_e.pdf, downloaded Aug. 14, 2014.
[5] Saint-Gobain, 2014. *Data sheet "SHEERFILL® II EverClean® Architectural Membrane",* http://www.sheerfill.com/uploadedFiles/SGsheerfill/Documents/Sheerfill-II-EverClean-Architectural-DIN.pdf, downloaded Aug. 14, 2014.
[6] Warema-Renkhoff SE, 2008. *"Raffstoren mit selektiver Beschichtung" (in german)*, Dok.-Nr. 114300.02.2008, Art.-Nr. 869248.

materials

Proceedings of the International Conference on Building Envelope Design and Technology, Graz
Advanced Building Skins 2015

Resource-efficient Multi-story Timber-Glass Façades

Alireza Fadai, Assistant Professor Dipl.-Ing. Dr.
Department of Structural Design and Timber Engineering, Vienna University of Technology, Austria, fadai@iti.tuwien.ac.at

Matthias Rinnhofer, Dipl.-Ing.
Department of Structural Design and Timber Engineering, Vienna University of Technology, Austria, m.rinnhofer@iti.tuwien.ac.at

Wolfgang Winter, Professor DDI
Department of Structural Design and Timber Engineering, Vienna University of Technology, Austria, winter@iti.tuwien.ac.at

Summary

The objective of several research projects of the Department of Structural Design and Timber Engineering (ITI) was to develop stiffening glass fronts, which replace wind bracings with optical prejudice and expensive frameworks. Therefore, the ITI combined the advantages of glass and the rapid-assembly of timber constructions with ductile metal fasteners, which improves the structural performance after failure and expands the scope of applications beyond the initial limits. With the purpose to meet the environmental compatibility and highest standards of cost effectiveness, the possible applications of timber-glass composites (TGC) as alternative stiffening constructions for multi-story façades were investigated. The short- and long-term load-bearing capacity of the TGC structures was studied. This paper illustrates these developments and the application of TGC multi-story façades.

Keywords: Timber, Glass, Composites, Adhesives, Stiffening, Multi-story Façade

1 Introduction

In March 2007 the European Council developed an energy strategy, aimed at a low-carbon and sustainable competitive community by the year 2020. Climate change and sustainable energy is one of five EU main issues of this strategy, which is memorable known as 20-20-20 targets. Until the year 2020, 20 % of the greenhouse gas emissions (or even 30 %, if the conditions are right) should be reduced, while the share of renewable energy in the energy mix and energy efficiency should increase up to 20 %, compared to the year 1990. Due to the long investment periods of the energy industry, the European Commission is already working on a package for the year 2050. This provides for a reduction in greenhouse gas emissions by 80-95 % compared to 1990 (cf. Europa-2020-targets [1] Fischer & Geden [2] European Commission [3]).

The ecological criteria of resource conservation and environmental impact will play a greater role in assessing the resource base of the future building than in the past. Structurally efficient combining glass with the ecological, low-energy and rapidly to assemble material timber improves the structural performance after failure and expands the scope of applications beyond the initial limits.

Up to now, the glued glass front constructions have been extensively applied. They are at the cutting edge of technology, and meet the highest standards. The objective of several research projects of the ITI at the Vienna University of Technology (VUT) was to develop stiffening glass fronts, which replace wind bracings. The possible applications of TGC structures in the existing building stock as well as in new buildings were investigated. Furthermore, the TGC elements enable a more efficient functionality of structural glass elements by allowing the use of approved timber joining techniques. The results provide a marketable component system for buildings, which optimally uses timber and glass, with advantages, concerning constructive aspects and structural behavior:

- The shear wall elements are multifunctional applicable as load-bearing, stiffening and façade elements
- Industrial prefabrication of load-bearing structure
- Near waste-free building design and recyclability of all building components after service life.

Based on the results of the previous research projects [4] [5] the ITI coordinated the follow-up international research project “Load bearing timber-glass composites (LBTGC)” within the framework WoodWisdom-Net. In consideration of long-term behavior and practical application, the objective of the research project “LBTGC” was to develop load-bearing and stiffening TGC structures. The participants were going to optimize the TGC elements for load-bearing structures, not alone in terms of their response to long-term loading but also in terms of seismic events.

With the purpose to meet the environmental compatibility and highest standards of cost effectiveness, alternative stiffening TGC constructions for multi-story façades were investigated. The load-bearing capacity of the TGC multi-story façades was developed by using linear and non-linear finite element simulations. The developed TGC multi-story façades were implemented within the framework of various pilot projects. The pilot projects enable a long-term monitoring under controlled conditions.

2 Experimental studies and structural engineering

For a reliable calculation of composite materials the question of the representation of the composite criterion (pin-shaped means of connection, bonding, mechanical composite, etc.) is relevant. With regard to load initiation, load transfer and stress as well as deformation distributions the knowledge of exact values is crucial.

In case of the TGC, the softer material reinforces the stiffer material. The composite is joined by adhesive bond lines. It is of particular interest that the ratio of the Young’s moduli of both materials corresponds roughly to the reciprocal relationship of the fracture strains.

Within the research project "LBTGC", the long-term behavior of TGC structures under permanent shear stress was investigated. Specimens were prepared in different variants. Based on the test results the modification and deformation factors for design of TGC structures were derived and a comparison to the normative specified factors according to EN 13830 [6] nor the ETAG 002 [7] was drawn. The studies on long-term behavior of TGC structures were deepened and the reliability of such structures in practical applications was proved.

With the intention to indicate the impact of compound systems, several alternatives of different construction types were compared. On the one hand the system of the Holzforschung Austria (HFA) - only shear adhesive bond-line (cf. Figure 1, left) - on the other hand the system of the ITI - shear adhesive bond line and blocking (Figure 1, right). As blocking material, the two-component epoxy adhesive Hilti HIT-RE 500-SD was chosen. The surfaces were cleaned with compressed air and primers applied as recommended by manufacturer. For all experimental studies presented here as adhesive the two-component silicone OTTOCOLL® S 660 was used. The aging of this adhesive regarding all regulations of [7] was tested in [8] and it was proven, that it fulfills all requirements. The short- and long-term load-bearing capacity of the TGC structures was studied in this project, as well as analytical calculation and sizing methods for single and coupled panes were developed.

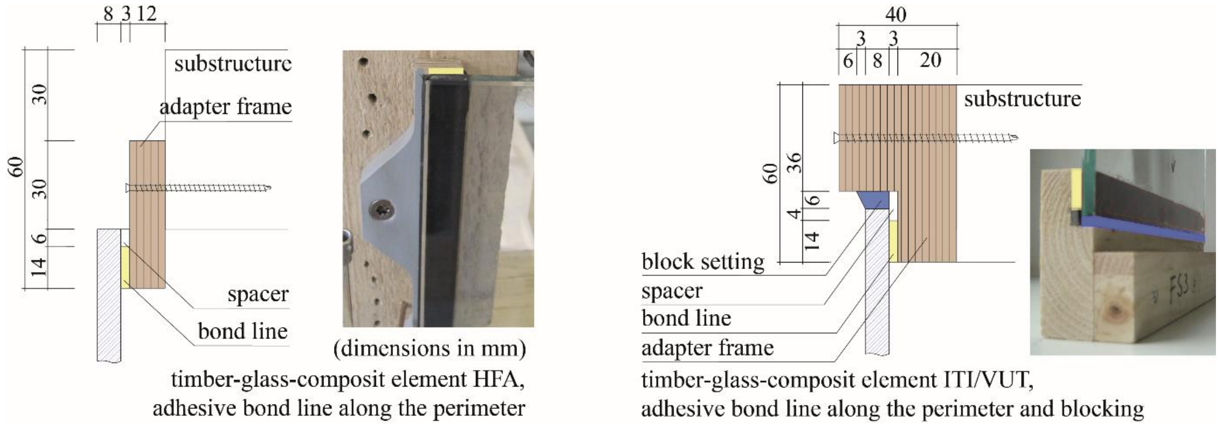

Figure 1 left: TGC element HFA, adapter frame with tooth profile; adhesive bond line along the perimeter; right: TGC element ITI, L-shaped adapter frame; adhesive bond line along the perimeter and blocking [9]

2.1 Small-sized specimens

The experimental studies on the small-sized specimens have been primarily carried out to verify the mechanical strength decrease under long-term stress and to determine the shear strength of the adhesive (cf. Figure , 3 mm x 12 mm). For this experiment, 95 specimens in total were prepared to perform different tests. 80 of these small-sized specimens were fixed in a non-conditioned room on a wall and loaded with weights (cf. Figure), which cause nominal shear stresses of 0.04 N/mm² and 0.05 N/mm². Additionally, on 15 specimens, which were loaded over twelve months, dial extensometers were mounted to check the deformation between the adapter frame and the glas. These results were compared with the previous experiment results (Figure 303 [10]).

Figure 2 left: dimensions of small-sized specimen; right: test setup [10]

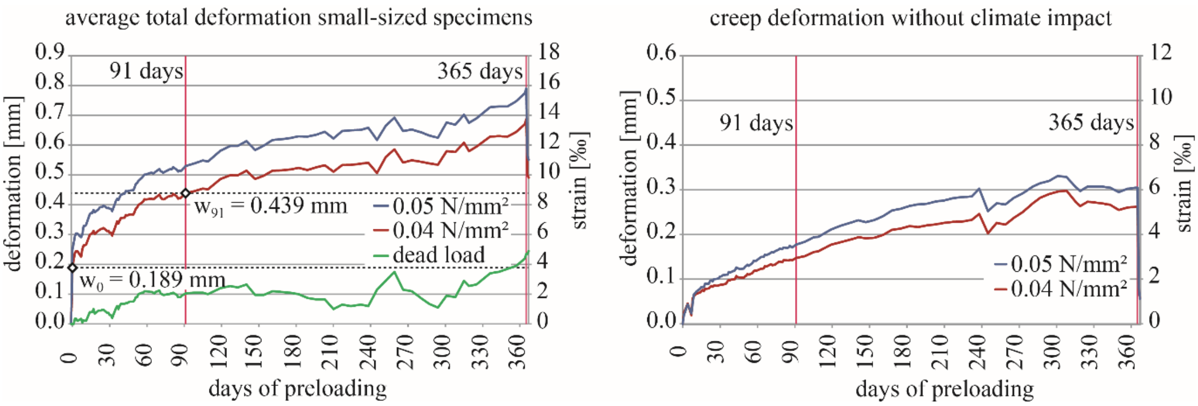

Figure 30 left: mean value of total deformation of specimen; right: creep deformation of specimen [10]

The unloaded specimens show deformations, which result from the permanent changing climatic conditions in the test room. Especially the wooden parts of the specimen shrink and swell with changing moisture, which cause certain deformations. By subtracting this climate-induced deformation from the creep curves of the loaded specimen a continuous decrease of creep can be seen. In Figure 30, right, thus only the creep deformations without climatic influence were shown. These are at the beginning more distinct than at the end of the experimental period. After about 250 days a clear irregularity can be seen, which results from a failure of the unloaded specimens.

2.2 Medium-sized specimens

The test series "medium-sized specimens" pursued the same aims as the investigations on the small-sized specimens. The geometry of the medium-sized specimens were adjusted to the small-sized specimens. A glass pane was glued on both sides with an adapter frame with tooth profile. Only the length of the bond line was extended to 1000 mm. However, the load levels were still the same. So at the end of the testing it was possible to examine whether the resisting shear strength can be increased linear with a larger adhesive surface, or whether other effects influence it. The load was generated with a gravel-filled box and applied via small blocks next to the bond line. These small blocks are marked in Figure 4 with yellow stripes. The whole experimental setup is also shown in Figure 4.

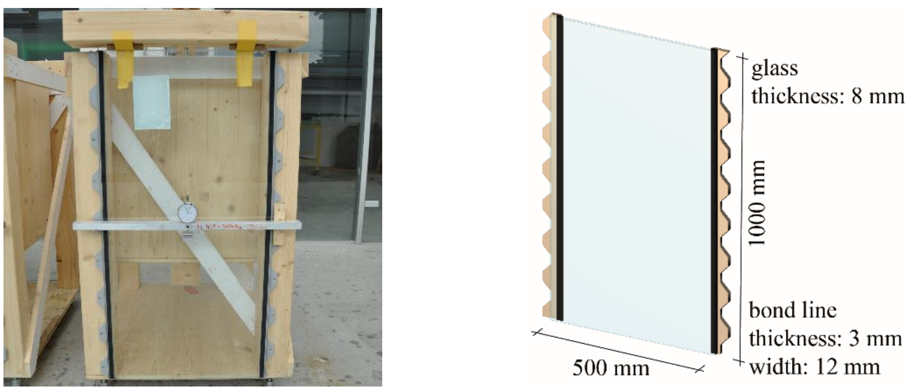

Figure 4 left: test setup; right: dimensions of medium-sized specimen [10]

The comparison of the results of the small-sized specimens with those of medium-sized specimens shows a similar creep behavior, irrespective of the length of the bond line; whereat the deformation of medium-sized specimens under a load level of 0.04 N/mm² is lower at than of small-sized specimens.
The climate difference for each start time of the experiments must be taken into account. While the small-sized specimens at the beginning of the measurements were partly exposed to hot temperatures and large differences

in relative moisture in summer, there was almost constant temperature during the first months of tests on the medium-sized specimens; however, the atmospheric moisture fluctuated.

3 Development of adapter frames for multi-story timber-glass façades

In order to allow the inclusion of a higher shear load in the bond line, it is obvious that the adhesive surface shall be increased and thus it gets lower shear stresses at the same load level. This still requires some development work and was part of the project "LBTGC" [10]. Therefore, it was considered to use an adapter frame with L-profile instead of a flat adapter frame and to implement a circular bonding (Figure 5) [11]. The special L-profile was used, to transfer the compression forces from the glass pane to the adapter frame with one block. The new development would be to use the available space between the adapter frame and glass pane and to fill this space between blocks with silicone (cf. Figure 5). With this geometry, we observed less creep under long term loading but less residual shear strength in short term tests. The results will be examined in [10].

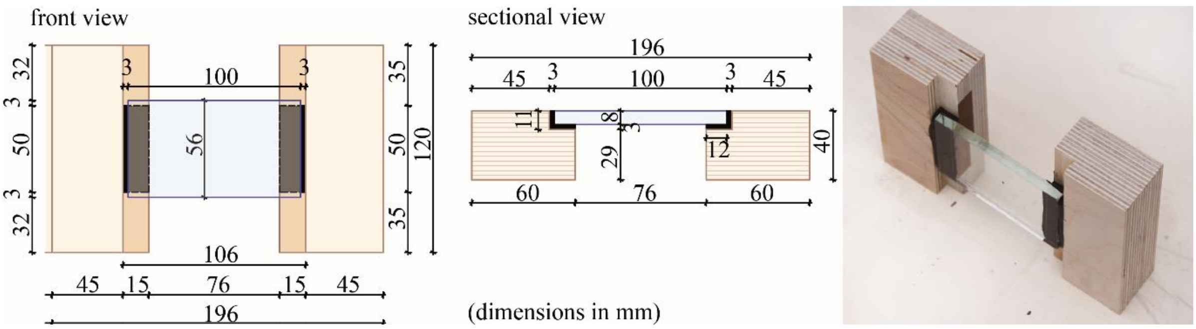

Figure 5: Developed L-profile with increased adhesive surface, small-sized specimen [10]

Since the 6 cm wide adapter frame (cf. Figure 1, right) is not suitable for coupling several single frames, a smaller adapter frame was developed (cf. Figure6; ITI [10]). As a consequence of the small dimensions of the elements, the screws cannot exclusively carry the force transmission between adapter frames and substructure. Consequently, various models of familiar connectors, e.g. brackets can be applied. Due to the brackets, mounted to the posts, the pressure forces of the compression diagonal are directly transferred into the substructure (cf. Figure6, above). In this case, the screw connection of the adapter frame can be used for installation purposes. For TGC structures able to redistribute the internal forces via connections of adequate ductility, elastic-plastic methods are used for the calculation of the internal forces in all parts of the system.

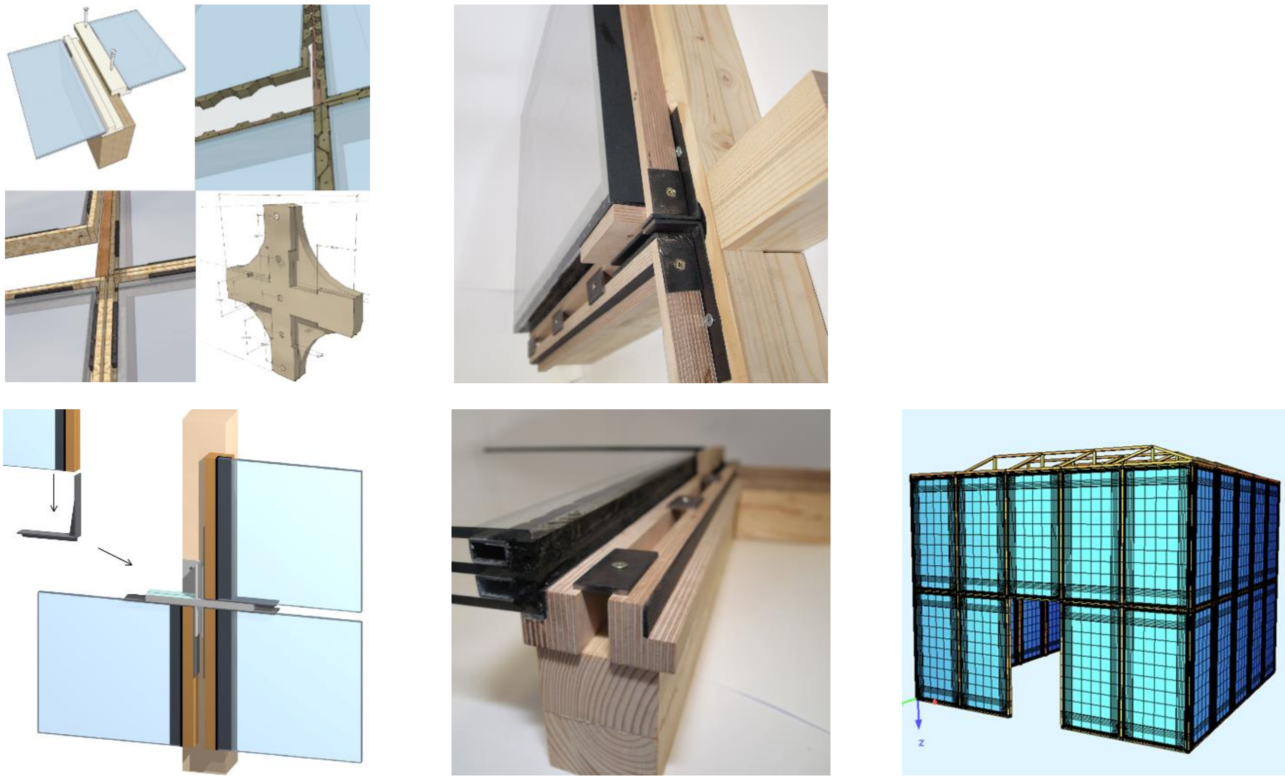

Figure 6: Details of various developed adapter frames and FEM model (ITI [10] and [11])

4 Life cycle assessment - Evaluation of environmental impacts

The construction industry is critically observed regarding the use of resources (raw materials, energy, etc.) and with respect to the induced environmental damage. The ecological criteria of resource conservation and environmental impact will play a greater role in assessing the resource base of the future building than in the past. Thus, the material component will play a more important role in the discourse of energy in building. The question of a holistic, all use and production phases including consideration of the energy flows of the materials used in construction (Life cycle assessment - LCA) will significantly change the valuation of sustainability in construction.

Comparing wood-aluminum composite constructions to conventional aluminum façade systems reveals clearly the ecological advantages of wood-based systems. According to an EU study by *Michael Bauer*, by using timber instead of aluminum profiles, the primary energy requirement (non-renewable primary energy impact values - PEI ne) is almost halved from 407 kWh/m^2 to 209 kWh/m^2 [12]. High performance building envelopes, which completely refrain from using aluminum parts present the opportunity to further, reduce negative ecological impacts.

Timber-glass components as an ecological and sustainable building material have a lot of potential to be discovered. The LCA evaluation of the developed TGC structures shows that the increase recycling rates of approximately 35 to 85 % for aluminum and from 2 to 70% for PVC does not change the environmental favorability of timber composites.

Four façade types were included in the LCA study: I) the Timber-glass composite L-profile type, II) the Timber-glass composite I-profile type, III) an aluminum profile construction and IV) a hybrid construction aluminum-timber profile (cf. Figure7, right, [13]).

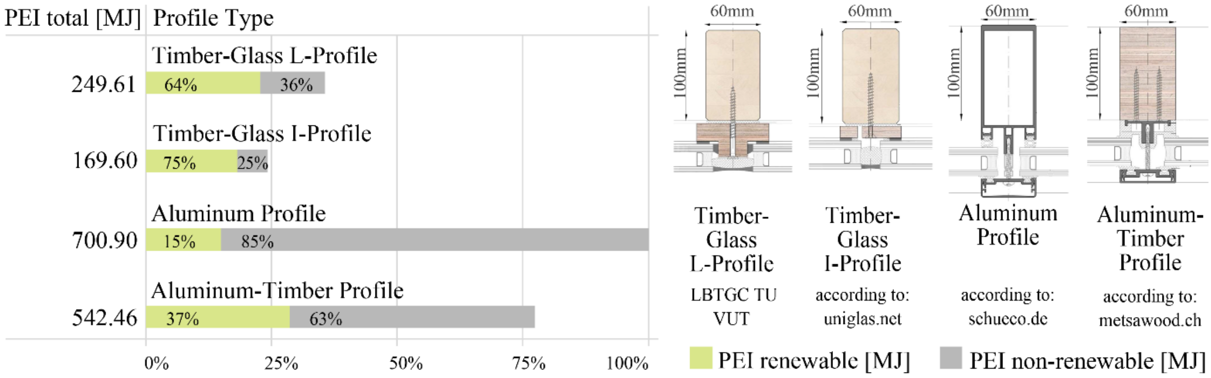

Figure 7: Evaluation of the environmental impact of different composites per 1 m^2 of a reference façades („from cradle to grave“) [13]

The use of aluminum as a basic construction material for glazed building envelopes presents up to four times higher primary energy demands then timber based composite construction (PEI total; cf. Figure, left). The estimation could be made that the use of timber instead of aluminum in building envelopes can reduce primary energy demands up to 75 % in stages of façade production (recovery potential with waste treatment). The TGC based façade systems present results of up to sixteen times less CO_2 emissions, when compared to aluminum based system. The estimation could be made that the use of timber instead of aluminum in building envelopes could reduce CO_2 emission up to 94 % in stages of façade production (recovery potential with waste treatment) [13].

Comparative evaluation of Timber-Glass L- and I-profiles had shown, that the primary driver of impacts are plywood and adhesive (e.g. silicon). The reduction of plywood and silicon use in the composite can provide a potential for optimization. The whole life cycle analysis (“cradle to grave” LCA) presents different results. The most important factors for the environmental impacts are life-span maintenance and durability of the components. Especially for timber profiles, the durability of the adapter frame material is of great importance. Woods with a low resistance (e.g. spruce, pine, etc.) have a durability of 40 years, where wood with high resistance (e.g. oak, etc.) reaches a value of 60 years [13].

The TGC-façade uses glass for static bearing and stiffening functions, consequently additional bracing elements for stiffening the building can be omitted. This added benefit on resource savings in the case of TGC shall be taken into account.

5 Conclusion and Outlook

Bonded glass front constructions have been applied for a long time and comply with the state of the art. Nonetheless, with these solutions, the glass has not a static bearing function, merely functions as an outer cover. The objective of the ITI’s research projects was to investigate alternative constructions of stiffening glass fronts, which replace wind diagonals with optical prejudice and expensive frameworks. Therefore, the ITI studied the load-bearing capacity of these construction components and developed calculation and sizing methods. TGC wall components bear vertical loads and in addition ensure the transient stability against lateral effects such as wind load and earthquake. The solutions for multi-story bracing walls were developed. They were evaluated by using linear and non-linear FEM calculation. Different types of TGC façades were compared with each other. The investigations showed that all structural systems have sufficient stiffness against horizontal displacement [4] [5] [10] [11].

The TGC façades enable a more efficient functionality of structural glass by allowing the use of approved timber joining techniques. The results provide a marketable component system for buildings, which could optimally use timber and glass. The investigations showed that all structural systems have sufficient stiffness against horizontal displacement. Timber-glass components as an ecological and sustainable building material have a lot of potential to be discovered.

The ITI sets the goal of studying additional conceivable application possibilities. The combination of timber and glass shows challenging possibilities for energy-active façade-construction. The possibilities to use bonded TGC construction as outer skin of small wooden buildings and as water protection as well as for local greenhouse effect (preheating) will be investigated (Figure 8).

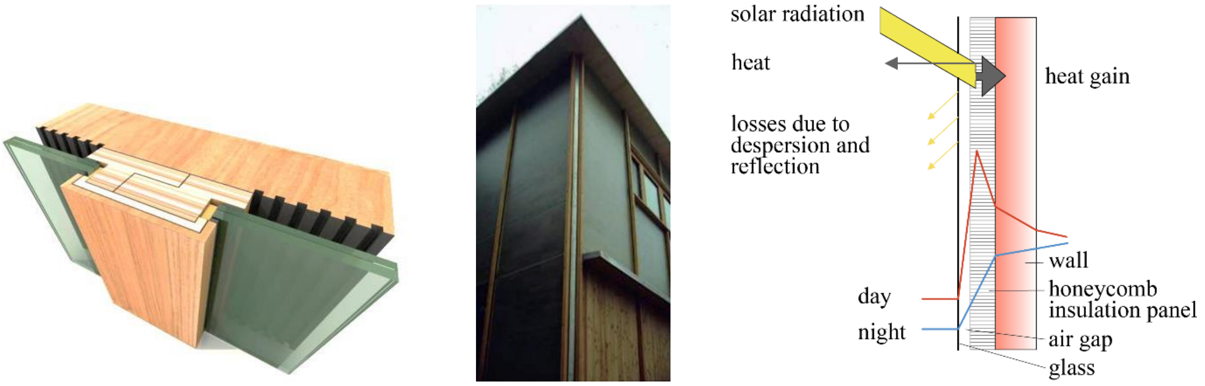

Figure 8: Examples of bonded TGC -outer skins of small wooden buildings

The advantages of using TGC structures, concerning constructive aspects and structural behavior are:

- The shear wall elements, which are multifunctional as load bearing and stiffening and as façade elements are advantageous in ecological and economical reasons,
- Industrial prefabrication of load-bearing structure,
- Near waste-free building design,
- Recyclability of all building components after service life.

The newly developed system was promoted through the initiation of pilot applications. Initiation of pilot projects could provide the possibility to acquire experiences in terms of practicality and applicability of the developed composite systems and create different design and application solutions. The developed construction is still technically unregulated since neither EN 13830 [6] nor the ETAG 002 [7] can be used directly. It is therefore necessary to seek approval from the local authorities for specific applications.

The research project results benefit several levels of the European industry. By means of the use of organic renewable resources, the innovative technology provides an alternative to the existing aluminum glass tradition. Wood-based alternatives to conventional construction also open opportunities to European countries to reduce their carbon emissions. Furthermore, the European timber construction industry will have the opportunity to export this new composite technology worldwide. Nevertheless, the unique combination of wood products with glass components will also request deeper investigations regarding the interfaces, the compatibility and the interaction of the different components and materials. The final issue consists in optimizing a composite system by using the best characteristics of each material in order to develop and advance a high competitive composite building system.

6 Acknowledgements

The authors gratefully acknowledge the financial support of the Austrian Research Promotion Agency (FFG, project number 832209) as well as the companies Petschenig Glastec, Haas Fertigbau Holzbauwerk and Otto-Chemie for funding the research project „LBTGC“.

7 References

[1] European Commission: *Europe 2020 targets*, Retrieved from http://ec.europa.eu/europe2020/europe-2020-in-a-nutshell/targets/index_en.htm, Accessed on January 21st, 2015.

[2] Fischer S. und Geden O.: *Strategiediskussion in der EU-Energie und Klimapolitik; Neue Ziele für die Zeit nach 2020*, Friedrich-Ebert-Stiftung, Berlin, 2013.

[3] European Commission: *Energiefahrplan 2050; Mitteilung der Kommission an das europäische Parlament, den Rat, den europäischen Energi Mitteilung der Kommission an das europäische Parlament, den Rat, den europäischen Wirtschaft- und Sozialausschuss und den Ausschuss der Regionen*, Europäische Kommision, Brüssel, 2011.

[4] Hochhauser W., Winter W. und Kreher K.: *Holz-Glas-Verbundkonstruktionen: State of the Art, Forschungsbericht, Studentische Arbeiten. Final report of the research project „Holz-Glas-Verbundkonstruktionen: Berechnung und Bemessungskonzept"*, Vienna University of Technology, Vienna, 2011.

[5] Hochhauser W.: *Ein Beitrag zur Berechnung und Bemessung von geklebten und geklotzten Holz-Glas-Verbundscheiben*, Doctoral thesis, Vienna University of Technology, Vienna, 2011.

[6] *OENORM EN 13830, Curtain walling - Product standard*, Austrian Standards plus GmbH, Vienna, 2000.

[7] *ETAG 002, Structural Sealant Glazing Kits (SSGK), Part 1: Supported and unsupported systems*, Guideline for European Technical Approval, Edition November 1999, 1st amendment: October 2001, 2nd amendment: November 2005, 3rd amendment: May 2012, EOTA, 2012.

[8] Holzforschung Austria: *Grundlagen zur Entwicklung einer neuen Holzfenstergeneration - Endebericht, 2. Forschungsjah*r, Vienna, 2007

[9] Fadai A. und Winter W.: *Application of timber-glass composite (TGC) structures for building construction*, Proceedings of Challenging Glass 4 Conference & COST Action TU0905 Final Conference, C. Louter et al. (Hrsg.), CRC Press/Balkema, Leiden, Niederlande, 2014, ISBN 978-1-138-00164-0, pp. 235 - 242.

[10] ITI - Department of Structural Design and Timber Engineering: *Forschungsbericht „Entwicklung und Langzeituntersuchungen von Holz-Glas-Verbundkonstruktionen mit gleichzeitiger Verklebung und Verklotzung"*, in progress.

[11] Winter W., Fadai A. und Hochhauser W.: *The potential of application of timber-glass composite structures for building construction*, engineered transparency – International Conference at glasstec, J. Schneider, B. Weller (ed.), 2012, ISBN 978-3-86780-294-9, pp. 201 – 211.

[12] *UNIGLAS-FAÇADE*, retrieved from http://www.uniglas.de/technology-fields-of-application-169.html, Accessed on January 21st, 2015.

[13] Rosliakova V., *Architectural application and Ecological Impact Studies of Timber-Glass Composite Structures*, engineered transparency – International Conference at glasstec, J. Schneider, B. Weller (ed.), 2014, ISBN 978-3-86780-402-8, pp. 345 – 352.

Freeform Precast Reinforced Brick Shells

Alexander Pick, Dipl.-Ing. Architect
TU Darmstadt, Germany, pick@kgbauko.tu-darmstadt.de
http://www.kgbauko.de

Stefan Schäfer, Prof. Dipl.-Ing. Architect
TU Darmstadt, Germany, sts@kgbauko.tu-darmstadt.de
http://www.kgbauko.de

Summary

The research aim is the development of a modular design scheme to produce prefabricated elements as well as the appropriate joints to assemble a consistent tensile reinforcement. Since the economic efficiency of the design will be largely dependent from the quantity of prefabricated parts, the number of different components can be reduced through an optimization process. First, the geometries are limited to a defined number of components in a process in order to be able to cover a range of free-form surfaces as reinforced brick shells.

Keywords: freeform geometries, reinforced brick shell, prefabrication, modular system, adaptive formwork

1 Paper Opening

1.1 Motivation

The aesthetics of Eladio Dieste's buildings impressed the authors through their simplicity and plain shapes and the contrariness to construction methods used in our region with the building material brick. The authors are fascinated what a spectrum, other than German and European standards, the use of brick and reinforcement makes possible. The aim of this paper is to develop an approach for efficient implementation of brick shells by reviewing the construction method of reinforced brick shells with the use of prefabricated parts.

1.2 Initial state

Until the 19th century brick was the most commonly used construction material in architecture. Later on brick was partly replaced by modern construction materials such as glass, steel and concrete and gradually lost its importance [1].

Eladio Dieste recognised the potential of brick at an early stage and, against the trend, developed shell structures as a composite of brick and steel that served as tensile reinforcement.
The use of this new building technique enabled him, for the first time, to incorporate wide spanning roof structures made of brick.
Dieste simplified the interior and/or exterior design of his buildings by the use of brick as exposed brickwork. Thus he achieved through his buildings in particular a broad harmony of architectural form, design and structure [2].

The beginning of his work was marked by the Casa Berlingieri in 1946, the residential building in Punta Ballena Urugua, that was executed using barrel vaults. In the following years Dieste designed several buildings for a variety of user groups that can be classified into five basic types [3].

- Arc shells
- Barrel vaults
- Double-curvature shells
- Folded structures
- Tower construction

The majority of his buildings however are out of the first three aspects mentioned above, which is why the authors also direct their focus on arc shells, barrel vaults and double-curvature shells.

In addition to the barrel vaults Dieste had carried out numerous constructions of arc shells, which resulted in double-curved shells. With the help of these arc shells Dieste was able to span distances of up to 50 m. For interior illumination Dieste solved the roof construction by arranging shed-roof like openings atypical for this material.

The combination of brick with structural steel depicts a basic design principle of tensile reinforcement. He used solid bricks or specially produced molded hollow bricks, which were laid on a flat or curved casing without bracing [2].

Bricks could be positioned on one side by the use of a nailed skirting, with the required bottom reinforcement bars directly placed in the subsequent hollow spaces on the other (see Figure 1).

Figure 1: Arrangement of bricks on formwork [5]

The help of the “molded brick” would guarantee close curvatures of brick shells without wide joints on the underside. Subsequently an approximately 3cm thick layer of mortar would be applied as an additional mat reinforcement to restrain cracks. According to the need a reinforcement diagonally to a bracing, for absorption of shearing load or so long as statically required a pretensioned reinforcement would be installed. The upper side was either simply plastered and painted white or a second layer of brick was added [2].

During his heyday, Dieste's construction method was determined by economic conditions of cheap labour, locally available material but also favourable climatic conditions.

1.3 Approach a solution method

The authors see today's aspects of higher labour costs and a dearth of abilities in skilled manual work as being critical for an economic implementation of Dieste's construction method. In a contrasting juxtaposition of construction methods such as reinforced concrete sheath construction there lies much more potential in applied "lightweight construction" of a relatively reduced material usage and a time-reduced construction period.

The basic idea of a meaningful and efficient implementation of brick shells is based on the transfer of the manner of construction to that of the prefabricated construction method and the manufacturing of individual planar, rectangular, reinforced brick elements. In the first step the aesthetic standard of Dieste's brick shells with curved homogeneous forms would be deliberately discarded in favour of a simple manufacturable solution.

The economics of precast parts will mostly be determined by the production rate of the producible number of individual elements. The production of single or double curved precast elements and the related, complex construction formwork was excluded in advance in favour of an easy-to-produce planar solution. Thereby it was assumed that the brick represented the smallest determining parameter.

For convenience, a standard format - "NF" (Normalformat) 24 * 11.5 * 7.1 cm and a thin format - "DF" (Dünnformat) 24 * 11.5 * 5.25 cm was established as a common brick format in order to review the approach to the development of a precast-principle in the production of reinforced brick shells. The advantage of using common brick formats, lies in the use of the measurement system based on 1/8 meter.

1.4 Form finding

In order to ensure the implementation of Dieste's manual construction method with planar components the single and/or double curved forms must be fabricable through flat construction elements.

First, a simple arc with dimensions of 20 * 5 m was modeled. Initially, the shape of the arc has the advantage that, ideally, if it follows the reversal of catenary curve (pressure line) it will only have to carry normal compressive forces. If you follow this approach, no reinforcement would be necessary; only the cross section of the arc will have to be adjusted with the individual loading conditions. From the viewpoint of a light and delicate design, which also follows the aesthetic appeal of Dieste's buildings, a solid arc would be excluded from consideration from the very start.

In addition to the aesthetic appeal also the range of forms should be expanded. As an initial solution the arc was modelled with a positive Gaussian curvature $k \geq 0$, (double curved) and the parameters of the support line was suppressed in the form-finding process. The newly modified frame conditions had the result that on the one hand the construction is capable of withstanding compressive, tensile and shear forces while being able to absorb bending moments on the other (cf. chapter 2.1).

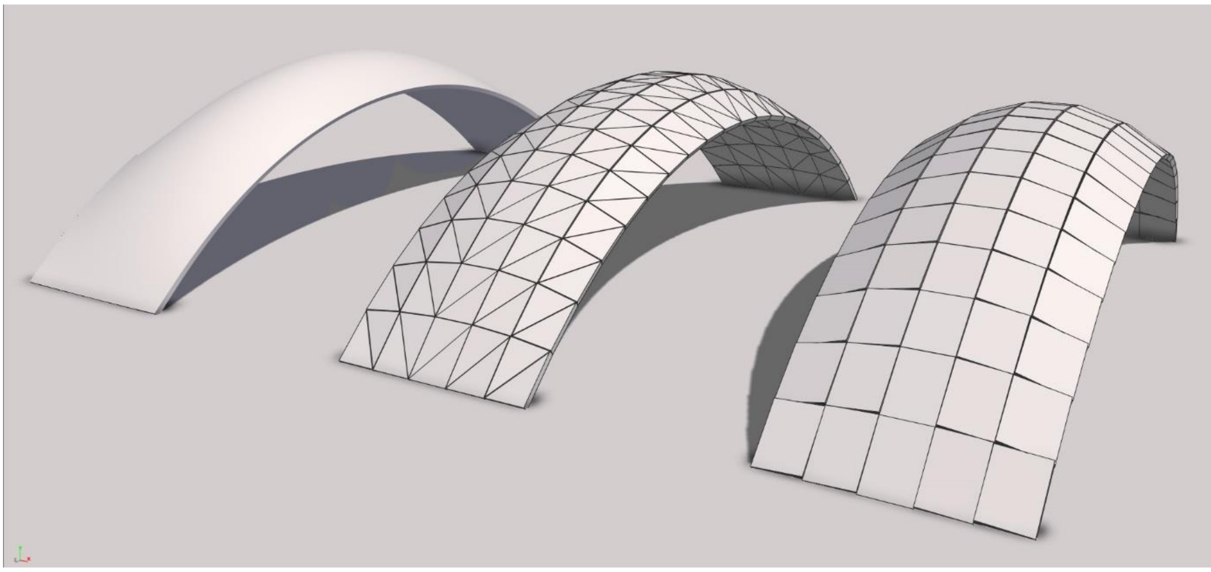

Figure 2: Development of planar components

The area was divided into planar triangles through surface triangulation in order to fragment the selected freeform surfaces into planar rectangles as a first step (Figure 2). The advantage of the process of triangulated arcs lies in the multiplicity of contiguous planar elements. Since this solution produces a number of unwanted edges and as this makes the production of the precast elements difficult or rather influence the "optical image" of the brick structure too much, the surface of the arc was further optimised and divided into planar rectangles (Figure 3).

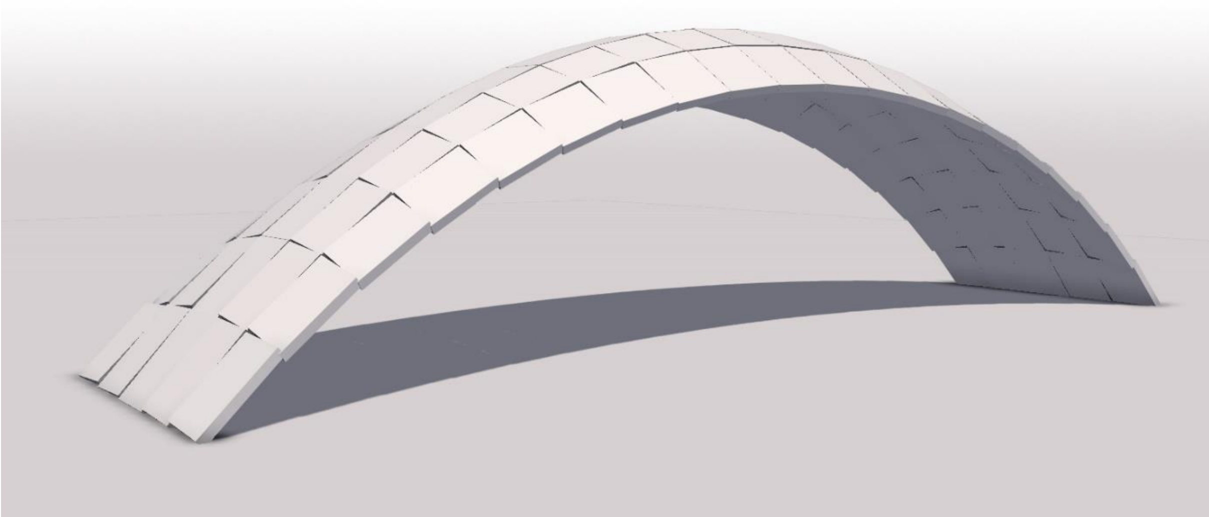

Figure 3: Arc with planar components

Firstly, a planar rectangular grid was generated using a simple algorithm. The problem with the method applied is in the resulting intersections of individual adjacent components. Diverse displacements to adjacent components resulted depending on the degree of curvature. In addition, the curvature of this method is not arbitrarily selectable, since otherwise strong axis deviations are produced, which complicate the assembly and may make it impossible (Figure 4).

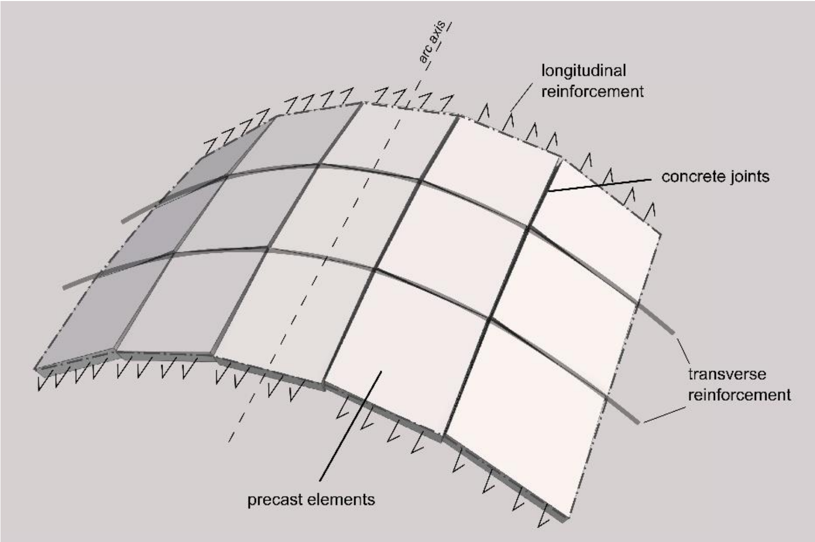

Figure 4: Structural principle

In order to counter these problems external algorithms or software solutions such as the evoluteTools are used in the latter stages for further optimisation of planar components.

2 Development of key details of precast brick shells

2.1 Finite Element Method (FEM)

In the course of the work the developed arcs were analysed using the finite element method. To estimate the internal forces and the required amount of reinforcement in the arc, a finite element analysis was carried out using an exemplary construction of reinforced concrete. As already mentioned in the beginning of this paper the aesthetic demands of Dieste's buildings served as a motivational and inspirational factor for the authors to handle the work, the chosen design should be slender and delicate. As an examination a cross-section of d = 10 cm was set over the entire arc and analysed. Even at this small cross section, the forces were relatively low. As already assumed at the beginning, the major part of the forces are transferred via compressive forces due to the form of the arcs.

In the upper reinforcement tensile forces occurred only in the vertex of the arcs. But this occurred only to a small degree so that the smallest steel mesh of the type Q188 A/B was sufficient for reinforcement in longitudinal and transverse directions.

In the area of the lower reinforcement layer the resulting forces were similarly lower than expected. On the one hand tensile forces were to be noticed above the abutment as well as on the border areas of the lower vertex. As a result, a tensile reinforcement had to be installed in the axis of the arc itself which were integrated to individual joints of the component. In addition, the structure has to bear further tensile forces in the transverse direction to the arc axis. This was done by using reinforcement bars in the joints of the connections of prefabricated parts.

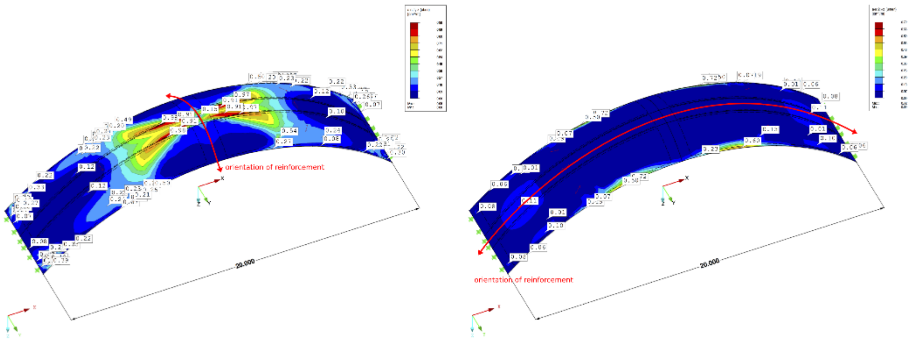

Figure 5: FEM – Required upper and lower reinforcement

The thrust occurring at the base as well as the total deformation of the arc were also negligible. The deformation was only 7 mm at the vertex and 5 mm in the area above the abutment (see Figure 6).
The gained knowledge of the arrangement of the reinforcement, which is further discussed in the later stages, could now be included in discussions on the development of prefabricated parts.

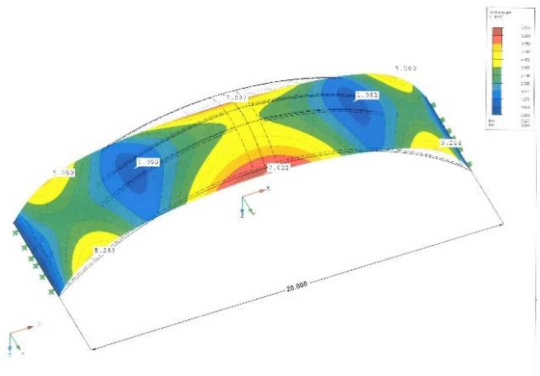

Figure 6: FEM – Deformation of the arc

2.2 Constructive specifications

Based on the assumption that the arc would be regarded as an outer component of the building, the brick side is shielded with a moisture stress and exposure class XC 3 set with a concrete cover of minimum 20 mm. For the top was calculated with an alternating wet and dry conditions, so that exposure class XC 4 was estimated at a minimum concrete cover of 40 mm [6].

This meant that the cross section in the choice of a thin format - DF - be enlarged to 14 cm, so that the required concrete cover was guaranteed. The use of a normal brick format - NF - was rejected due to the increased component cross section.

2.3 Analysis of each planar square

With the help of the algorithm, calculated rectangles were dissected from the 3D model to 2D data in order to analyse the different dimensions and angles of the rectangles. The sheet consists of a total of 95 rectangles with 30 different elements, each differing in size in x and y direction (see Figure 7).

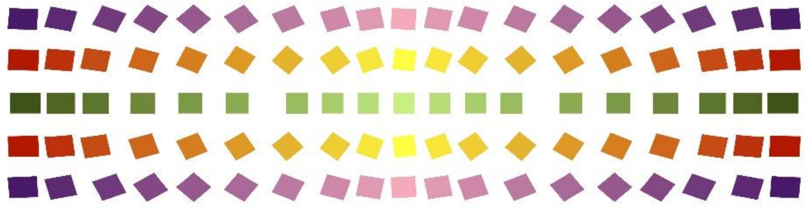

Figure 7: Projection of planar, prefabricated elements

Problems with the use of the method are posed on the one hand by the components themselves and on the other on site predominant conditions. It is imperative to develop a solution, that to a high degree allows tolerances in the addition of components which can nonetheless be integrated in the "association" of the brick.

Although no masonry association rules must be adhered to, the arrangement of the tiles within a cross joints grid is not without problems. The joint grid must be so arranged that despite the rotation the joint pattern continues and the stones follow a comprehensible picture (see Figure 8). This was ensured by the arrangement of a joint grid across all components. Solely in the port areas, the stones were cut and run into the next element. This has the advantage that the optical structure of the network is maintained and the bricks, providing no break, can be used further.

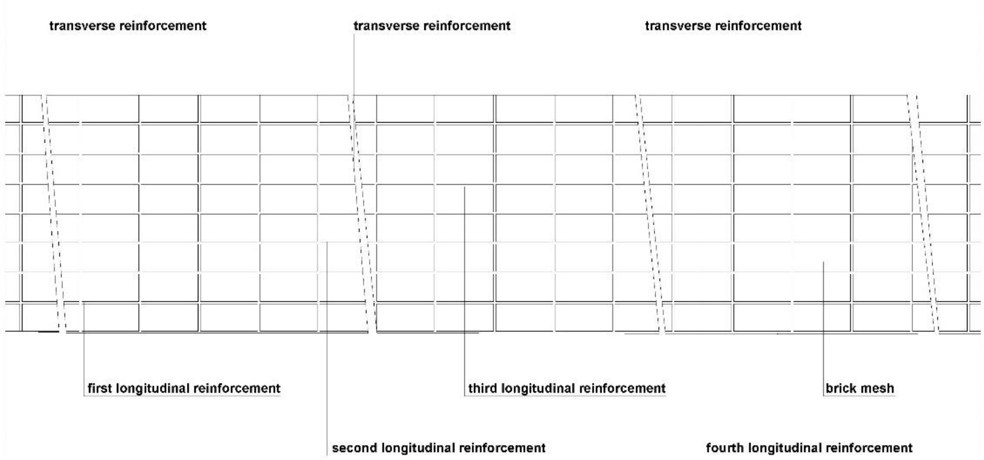

Figure 8: Joint grids of prefabricated elements

2.4 Development of the prefabricated element's connections

To create the arcs, the rectangles generated through approximation should be non-positively connected to each other at the edges of the rectangles. The thereby resulting joint grid is used to accommodate the longitudinal and transverse reinforcement and is locally sealed with high performance concrete (see Figure 9).

As butt joints threaded sleeve splices were first investigated. These connections have however the disadvantage, as did the also studied screw connections with opposing screw threads, that they are axially fixed and can accommodate virtually no tolerances.

As a solution, a sleeve-joint has been developed that can hold tolerances through the tapered ends and must be subsequently cast with a high-performance injection mortar. However, since this component has only an experimental character, a current and above all verifiable push was sought. This was found in a conventional lap joint. This solution is simple to make and at the factory can already exhibit the necessary angle for connection to neighbouring components.

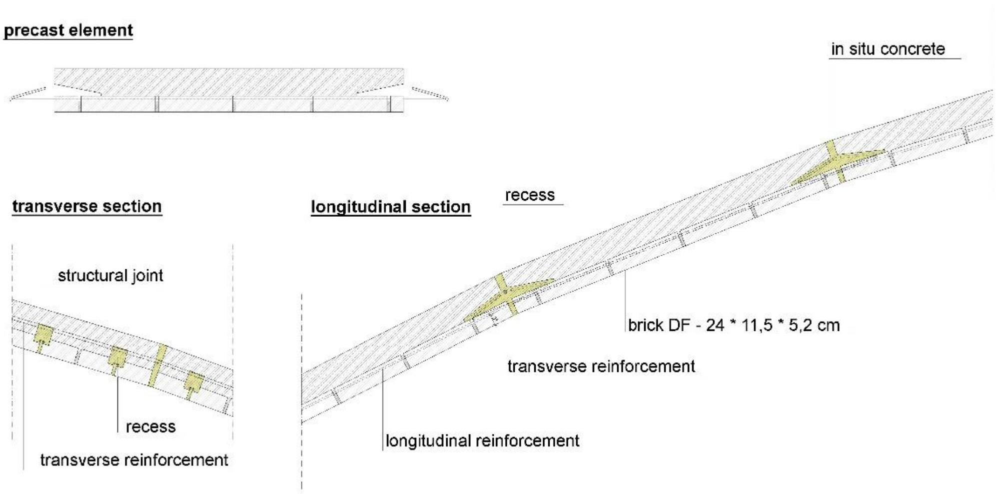

Figure 9: Prefabricated element's connection

2.5 Production of the prefabricated parts and construction of the arc

The individual bricks are placed in the prefabricated part plant on a planar formwork, arranged in the predetermined grid and cut if necessary. In the second step an additional formwork is placed on the prefabricated elements to concrete the connection points on site. The lower and upper reinforcement layers as reinforcement bars and wire mesh reinforcement as well as tensile reinforcement with overlapping joints are then incorporated before the last step of concreting.
When constructing the arc one can abstain from using large-area formwork systems by reducing the construction method to prefabricated components. With the help of centring the arc construction is achieved which defines the curvature of the arc in segments. It is only required as a backing and creates a support in the subordinate joint pattern of the prefabricated components. Except for the border areas each item supports two adjacent prefabricated components.
The individual parts must now be plugged into existing gaps in the direction of the arc in the area the reinforcement connections, so that the individual overlap connections in each prefabricated elements can be safely connected through the concreting. In this production step, the individual transverse reinforcements are used in the subordinate frame of the precast as reinforcement bar.

Afterwards the centring can then be removed and the arc squires its desired shape (cf. Figure 10).

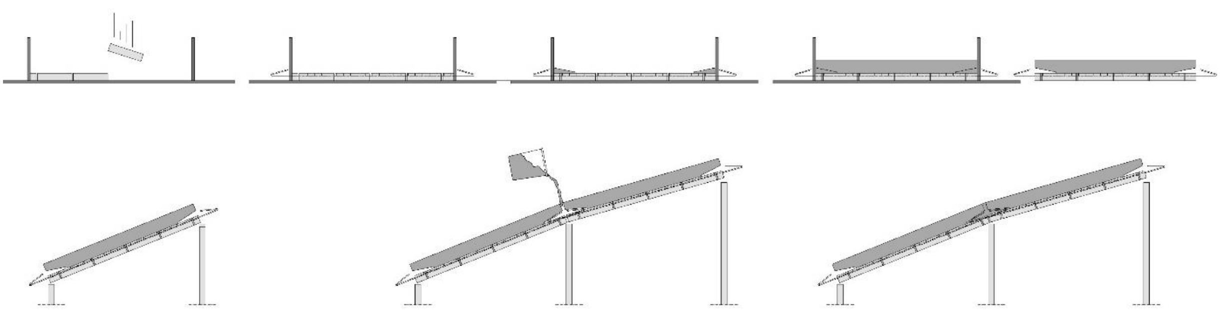

Figure 10: Production of the prefabricated parts and construction of the arc

3 Conclusion

3.1 Summary

The transferability of Dieste's design principle under the given conditions is affected by many factors in Germany and the EU. Norms and laws to respect, records to be kept and economically viable solutions to be developed. These complex mechanisms have to first be filtered and then divided into work packages. The first work package should prove that brick shells can basically be produced out of prefabricated components.

In the process, already early the first knowledge has been gained by the restriction on the choice of bricks. Solely comparing the normal format (NF) with the thin format (DF) in construction there is a loss of 20 mm., although appearing comparatively low at a first glance, it can have a major impact on the appearance of fragile components such as brick shells. By choosing a NF brick the assumed arc in this paper would have a component cross-section of 160 mm, instead of the assumed 140 mm.

Furthermore, only certain curvature radii can be illustrated by the applied algorithm. In addition, the distribution of the elements and the adopted joint pattern are critical to the dimensions of the precast components themselves. In this paper the width of the precast components (x-direction) is limited, so that the bricks can meaningfully be arranged on the formwork. The bricks are cut only in the y-direction, leading to a change of the brick and joint network. By making slight changes to the joint width, changes in x and y direction could be solved, with larger deviations this simple distribution to the individual joints would however be no more feasible.

The complexity of the relationships between bricks, joints, additions and precast components need to be solved in the future in terms of a canon.

3.2 Prospects

The proposed design is to be understood as a first approach to achieve an economical solution in the manufacture of brick shells. Among the already identified problems in the machining process, such as the optical structure of the planar elements or the climatic influences, new problems in the implementation of complex shapes or the development of moulded bricks have emerged. These issues will be dealt with in future research in the area of brick shells.

4 References

[1] Bucciarelli, P.; in: Mäckler, C.; *Werkstoff Stein*, Birkäuser-Verlag für Architektur
[2] Barthel, R.; *Eladio Dieste – Form und Konstruktion*, München, Verlag Das Beispiel GmbH, Darmstadt; 2001.
[3] http://www.tu-cottbus.de/projekte/de/great-engineers/ingenieure/dieste-eladio-1917-2000/projekte.html, (10.12.2013)
[4] DAIDALOS 43/1992; *Triumphe des Backsteins / Triumphs of Brick*, p.80.
[5] Anderson, S.; *Eladio Dieste – Innovation in Structual Art*, New York, ;Princeton Architectural Press, 1. Auflage 2004., p.199.
[6] Goris, Alfons (Hg.): *Schneider Bautabellen für Ingenieure. Mit Berechnungshinweisen und Beispielen*, Köln 20. Auflage 2012.p.5102-p.5104.

Proceedings of the International Conference on Building Envelope Design and Technology, Graz
Advanced Building Skins 2015

Freeform Shells Made Of Sheet Metal Profiles

Jakob Reising, Dipl.-Ing.
Technische Universität Darmstadt, Germany, reising@kgbauko.tu-darmstadt,de, http://www.kgbauko.de/

Stefan Schäfer, Prof. Dipl.-Ing.
Technische Universität Darmstadt, Germany, sts@kgbauko.tu-darmstadt,de, http://www.kgbauko.de/

Manuel Neuwirth, M. Sc.
Technische Universität Darmstadt, Germany, neuwirth@ptu.tu-darmstadt.de, http://www.ptu.tu-darmstadt.de/

Summary

Newly developed freeform architecture offers great potential. But it also puts strong demands on design and manufacturing technologies. New developments in the fields of CAD and CAM open new possibilities. Therefore, both new production methods and new planning tools are necessary to manufacture these architectural forms more efficiently.

The Collaborative Research Center 666 (CRC 666) explores different methods of cold forming of sheet metal. In particular, flow splitting and bend splitting both are resulting in an ultrafine grain structure of the metal and thus a material hardening. These profiles can be manufactured with defined curvature radii. In following processing steps cut-outs can be milled. These technologies are offering the possibility to use sheet metal material for structural element of free-form shells or skins.

To apply these new manufacturing technologies to highly individualized structures, the production processes need to be considered already in the early design phase of a building. Therefore, it is necessary to consider the requirements and restrictions of these production technologies.

Keywords: CAD, approximation, flow splitting, sheet metal, free-form shells

1 Introduction

Sheet metal is often used in the construction industry for example as a cladding of sandwich panels, but it is rather rare that they have a load-bearing function. In particular, the bifurcated and multiply curved profiles, as developed in the Collaborative Research Centre 666 (CRC 666) „Integral Sheet Metal Design with Higher Order Bifurcations– Development, Production, Evaluation", enable new construction systems due to their enhanced rigidity [1].
At the same time free multiply curved forms are becoming increasingly important in contemporary architecture. Progress in the field of CAD (Computer Aided Design) and CAM software (Computer Aided Manufacturing) in the last several years has already allowed the planning and execution of spectacular building designs [2]. These forms not only offer new opportunities for the design and aesthetic aspects but also allow the planning of statically very efficient shell and vault structures. However, the steps from design and detailing to manufacturing are a challenge that has still to be solved individually for each project.
Products of the roll forming industry are common practice as they can be produced fast, at a reasonable price and in large quantities. In building construction for example they are used in the form of trapezoidal sheet metal or in lightweight construction stud walls. However, they usually have a relatively simple repetitive geometry. The potentials that result from flexible roll forming machines are already seen in the cladding of complex freeforms with curved metal panels. Examples for this technology are the "Messe Halle 3" in Frankfurt [3], or

the roof of the Southern Cross Railway Station in Melbourne [4](both designed by Grimshaw Architects). But a very complex substructure of beams, paneling, insulation and finally the roof covering is still required. This structure leads to high demands on the dimensional tolerances which must be respected by the successive building companies. The flexibilization of the flow splitting and roll forming process is currently researched at the “Technische Universität Darmstadt”. This may allow the production of profile components that integrate the functions of all structural parts of a roof (load bearing, thermal insulating and sealing) in one component.

2 State of Research

The CRC 666 examines the technology of flow splitting. This Technology can produce different profile geometries from sheet metal. Sheet metal from a coil runs through several tooling systems. “The tooling system for linear flow splitting consists of driven supporting rolls which fix and transport the sheet metal. Laterally positioned splitting rolls together with the supporting rolls create a roll gap sf which leads the metal sheet to be formed into the desired cross-section” [5] (see figure 1 and 2). In addition to these remodelling processes, an ultrafine grained (UFG) structure with a corresponding material hardening occurs [6]. In the following roll forming steps the profile can be further processed and for example form a multi-chamber profile. So far this technology has only been used for linear elements.

Figure 1: Flow splitting facility

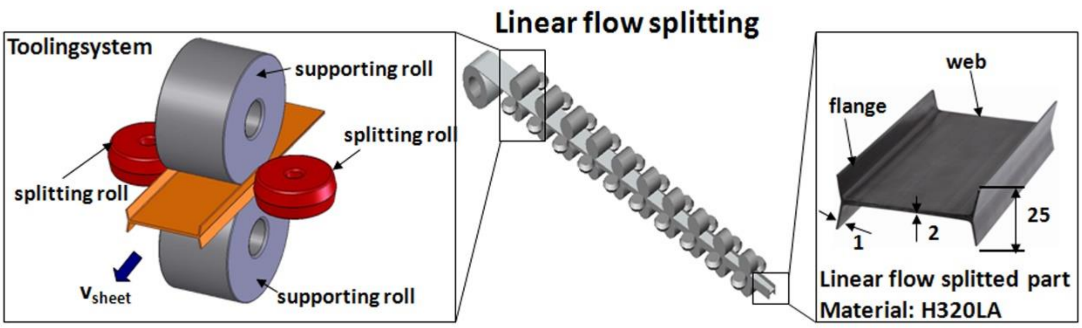

Figure 2: Liner flow splitting

New developments in the CRC 666, allow the flexibilization of this process. By using rolls with several degrees of freedom (translation and rotation) profiles with flexible cross-section become possible [5] (see figure 3). The present test facility can work only on one side of the sheet metal, but a bilateral system is already under

construction. At the moment there is only one tooling system, which is used repetitive on the same sheet metal. However the integration into a complete flow production will be possible in the future.
In addition different components can be manufactured on the same production line due to the previously mentioned degrees of freedom. This predestines this technology to produce similar modules, which differ in detail, as needed for the realization of free-form surface structures.
Examples of the use of flexible roll forming already exist. However, these are profiles with relatively simple cross section without load bearing effect. Especially the progress in the field of flexible flow splitting enables the production of profiles with a sufficiently complex cross section to provide a load bearing function [7]. To create the supporting profiles for free-form geometry roofs enormous degrees of freedom in the manufacturing process are required. In addition to the length between the folds, the angle of the folds has to be variable over the course of the profile (see figure 6).

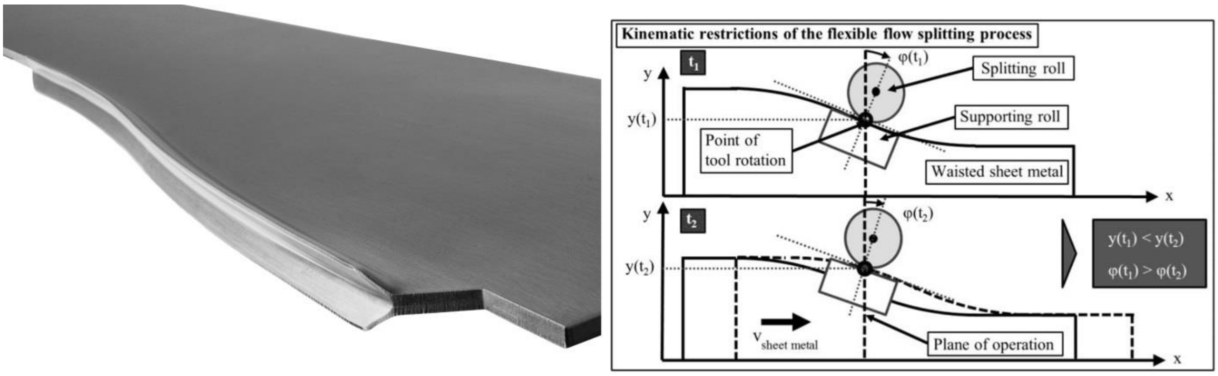

Figure 3: Flexible flow splitting (source [5])

3 Profiles building Shell structures

By adding many profile elements, wide span shell structures can be produced. By splitting the sheet edges branches, which are used to connect the individual profiles with screws, can be produced (see figure 4, 5 and 6). The improved material properties resulting from the forming processes (UFG microstructure, material hardening) can be utilized to improve the stability of these critical points. Later the screws can be covered with an additional profile. The individual profiles can be filled with foam, to achieve a thermal insulation effect and additional rigidity. Initial FEM simulations show, that with a sheet thickness of 3mm and a shell thickness of 15cm a span widths of more than 30m can be obtained.
The manufacturing steps of such a profile are described below.

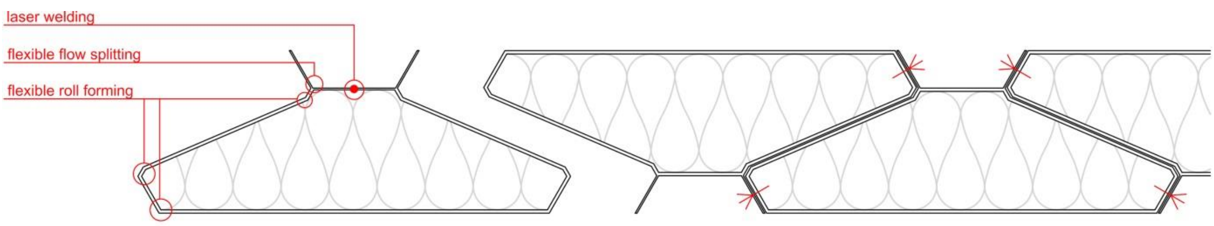

Figure 4: Possible profile geometry

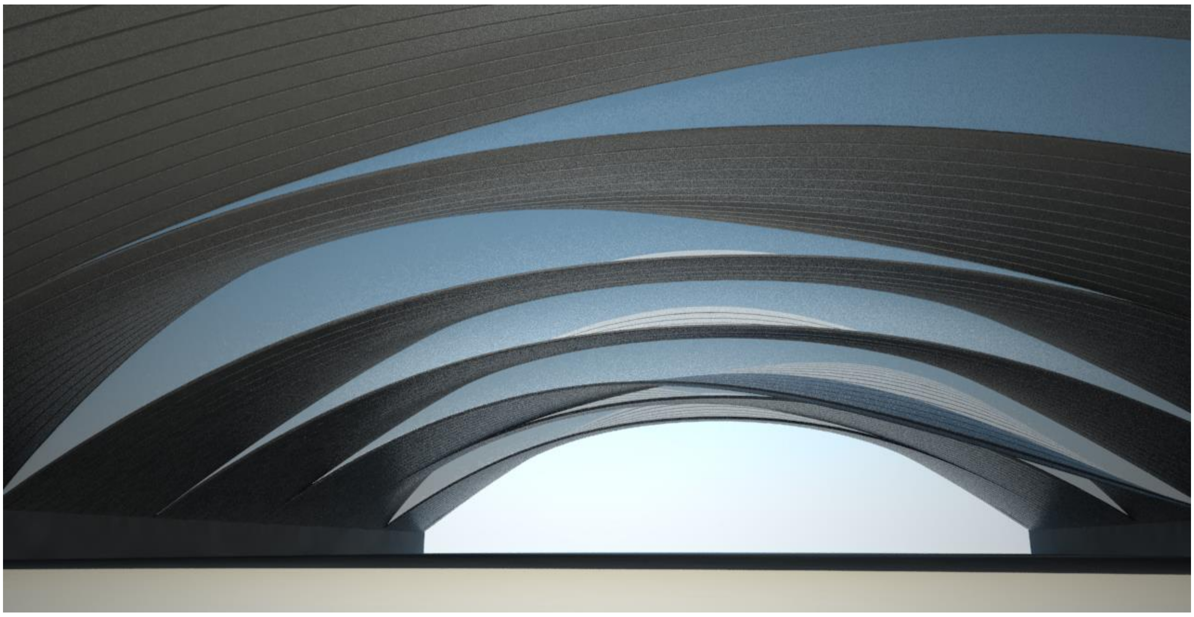

Figure 5: A roof constructed with curved profiles

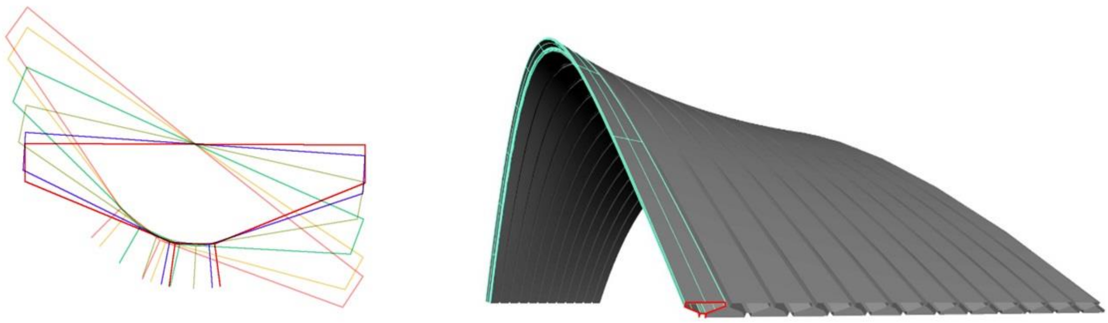

Figure 6: The cross section is variable over the course of the profile

4 Manufacturing steps

The sheet is unrolled from the coil; the curvature caused by the winding of the coil is straightened (see figure 7, step 1).
Firstly, the sheet will be cut to obtain the desired flexible cross section (see figure 7, step 2). Subsequently, the edges are split by a flexible flow splitting process (see figure 7, step 3). With flexible roll forming the defined profile cross sections can be formed in the next steps [8, 9] (see figure 7 step 4). The profile can now be closed by laser welding (see figure 7, step 5). Finally, the profile can be cut by a movable saw without interrupting the production process. These flat profiles are now bent and twisted in a subsequent process (see figure 7, step 6).
The flow production with flexible flow splitting and flexible roll forming has the enormous advantage of high speed. It will not reach the speed of linear roll forming machines (about 100m per min), but a working speed of 10m per min is quite possible to produce individual and flexible profiles.

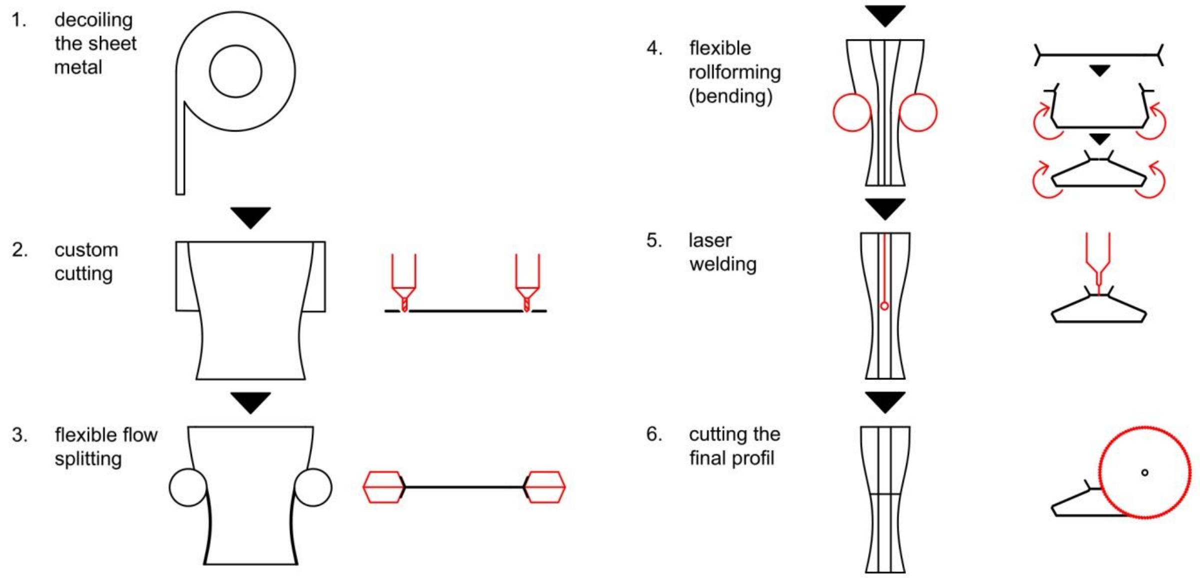

Figure 7: Manufacturing steps

5 Discussion

By the means of the proposed manufacturing technology, it could be possible to manufacture shell structures efficiently and economically.
The initial costs for developing and building the necessary machines are certainly not justified for a single building. But this method can be used to efficiently manufacture wide spanning halls. The degrees of freedom of the design are of course limited by the construction of the machine. But the shape spectrum provided is extensive, so that such a building system could lead to high marked demands.
The presented single shell design, in terms of its thermal insulation properties as well as its sound insulation (for example in the case of heavy rain), is not yet optimal. A double-shell structure could compensate these weaknesses.

6 Prospects

Using flexible flow splitting and flexible roll forming it will be possible to produce highly complex and individual structural elements in flow production. Very fast production speeds as well as small component tolerances are advantages of the flow production. Since the components can be made directly from the coil, its length is only limited by handling and transport. Utilizing these technologies large scale sheet metal shell structures can be produced very efficiently.

7 Acknowledgements

The investigations presented in this paper were carried out within the research projects D2, of the Collaborative Research Centre 666 'Integral sheet metal design with higher order bifurcations - Development, Production, Evaluation'. The authors want to thank the German Research Foundation (DFG) for founding and supporting the CRC 666.

8 References

[1] Englhardt, O., Bergmeister, K.: *First Studies on the Buckling and Post-Buckling Behavior of Glass Plates*, ASEM 04 – Advances in Structural Engineering and Mechanics, Seoul, Korea, 2004.

[2] Zellinger, M., Mandl, P.: *Die Generalsanierung des Johann Joseph Fux Konservatoriums aus der Sicht der Tragwerksplanung*, in: Beton- und Stahlbetonbau 106 (2011) issue 9, pp. 655-663.

[3] Menges, A.: *Opus 41: Nicholas Grimshaw &Partners: Halle 3, Messe Frankfurt am Main*, Edition Axel Menges, Stuttgart, 2002

[4] Sir Nicholas Grimshaw: *Grimshaw Architecture: The First Thirty Years*, Prestel Publishing, 2010

[5] Schmitt, W., Neuwirth, M., Kretz, F., Groche, P.: *On the Origin of Specimen: load-adapted integral sheet metal products*, 11th International Conference on Technology of Plasticity, ICTP 2014, 19-24 October 2014, Nagoya, Japan

[6] Kaune V., Müller C.: *Formation of UFG-surface layers on a HSLA steel by a continuous Surface-SPD-Process*, Mater. Sci. Eng. A 535, S. 1-5, (2012)

[7] Schmieder, M., Mehrtens, P.: *Cladding Freeform Surfaces With Curved Metal Panels – a Complete Digital Production Chain*, in: Hesselgren et al., Advances in Architectural Geometry 2012, SpringerWienNewYork, Wien, 2013

[8] http://www.ptu.tu-darmstadt.de/mu_forschung/mu_prozesskettenundanlagen/abgeschlossene_forschungsprojekte_pa/menu_flexibleswalzprofilieren/index.en.jsp (27.01.2015)

[9] http://www.datam.de/produkte-loesungen/flexibles-walzprofilieren/ (27.01.2015)

Proceedings of the International Conference on Building Envelope Design and Technology, Graz
Advanced Building Skins 2015

Extension of the Ars Electronica Centre Linz

Andreas Treusch, Architect Dipl.-Ing.
TREUSCH architecture ZT GmbH, Austria, office@treusch.at, www.treusch.at

Summary

The Ars Electronica Center AEC was planned and built as museum for future technology. It is the main project from the City Linz, the City was cultural main City of Europe in 2009. The main idea in the designing process was the integration of a lighting object in the landscape with the Danube as landmark and a multifunctional building for installations of art projects. The facade and the place before the building are a the main tools to set the multifunctional aspect, it has a installation grid for artists projects around the building, can be opened and closed and is able to play picture and sound like screen with big pixel.

Keywords: lighting, object, crystal, sculpture, walkable, skin, landmark, culture

1 Introduction

The existing Ars Electronica Center is connected to the new main and supply building by a steel & casted glass construction. The double glass facade, partly transparent and partly translucent, can be illuminated by LED (liquid emitting diode) technology. The LED is installed in the space between the two layers of the façade. The animation of lighting can be animated by the work of artists and musicians.
Each facade element with its own LED panel can be individually controlled with variable colour and brightness/intensity (RGBW).
This innovative lighting system, unique in Europe, presents artists with a whole new range of imaginative creativity.
The Ars Electronica Center also presents another speciality as standard illumination, the facility to display pure white light. The AEC building turns into a glowing white crystal at the touch of a button.

Figure 1: east elevation – view from the esplanade

2 Guiding principle

The main thought behind the design has been to create a sculptured building with a structure totally accessible by foot, and therefore an exciting experience within itself. The existing Ars Electronica Center and the new extension are connected to form one unit to be perceived as an ensemble. The crystal-like appearance generates a homogeneous interaction with its surroundings, at the same time becoming a distinctive landmark.
As a result of the refurbishment and expansion of Austria's largest rsearch and development center for electronic arts, the city of Linz and the venue itself have benefited from an increase in space and functions. Together with the "Brucknerhaus" and the Lentos Art Museum sitting on the opposite bank of the Danube, the Ars Electronica Center is one of the main cultural hotspots in Linz.
The aim of the design was to wrap 2,000 m² in existing buildings and 4,000 m² in new buildings with a uniform and multi purpose building envelope that forms a remarkable, shiplike-prismatic silhouette on the bank of the Danube. The cuboid section of the building set at the base of the Nibelungen Bridge and a new abutting parallel building wing symbolize the stern of the ship, while an adjacent low-rise exhibition hall emulates the main deck and a two-storey office wing the bow.

3 Urban concept

The urban concept is based on the principle of dialogue between architecture and environment with due consideration to important factors, such as preserving the view across the River Danube and protecting the surrounding historic buildings, in order to create an attractive ambience.


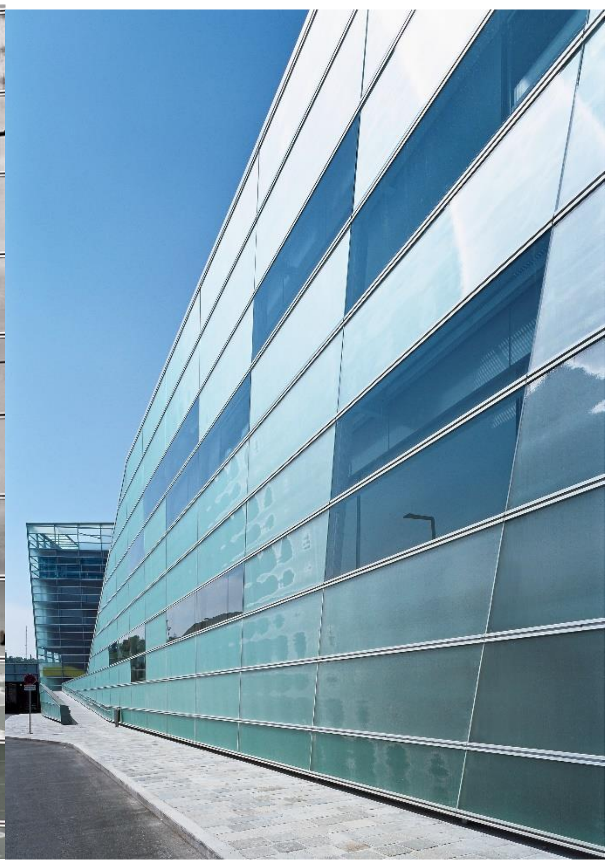

Figure 2: Façade of AEC in front of ancient architecture / Figure 3: Southeast elevation – view from the esplanade

4 The Layout of the Ars Electronica Center

- Multi-storey main and supply building adjoining the existing AEC

The new building forms a unit with the existing AEC. By designing the building in the form of a large glass cube with a double facade, an impression of homogeneity is achieved.

- Exhibition area beneath the main deck

The exhibition area is located beneath this outdoor platform – the main deck – between the main building and the future lab facilities and can be flexibly divided into larger or smaller exhibition areas.

- Future lab facilities and upper deck

The future lab facilities – for media art research – comprise laboratories and workshops in the basement with offices and recreation rooms above. The upper deck, which is also an outdoor platform two storeys higher than the main deck offers space for additional exhibition areas, presentations, events, etc.

Figure 4: Northeast elevation – view from the upper deck

5 Façade Design - Projection Surfaces

The existing Ars Electronica Center is connected to the new main and supply building by a steel & glass construction.

The double glass facade, partly transparent and partly translucent, can be illuminated by LED (liquid emitting diode) technology installed in the space between the two layers of the facade.

Each facade element with its own LED panel can be individually controlled, with colour and brightness/intensity (RGBW) infinitely variable.

This innovative lighting system – unique in Europe – presents artists with a whole new range of imaginative creativity. The Ars Electronica Center also presents another speciality as standard illumination, the facility to display pure white light. The AEC building turns into a glowing white crystal at the touch of a button.

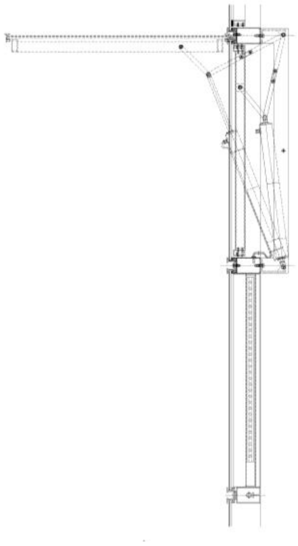

Figure 5: Detail of the opened and closed wing of the outside facade

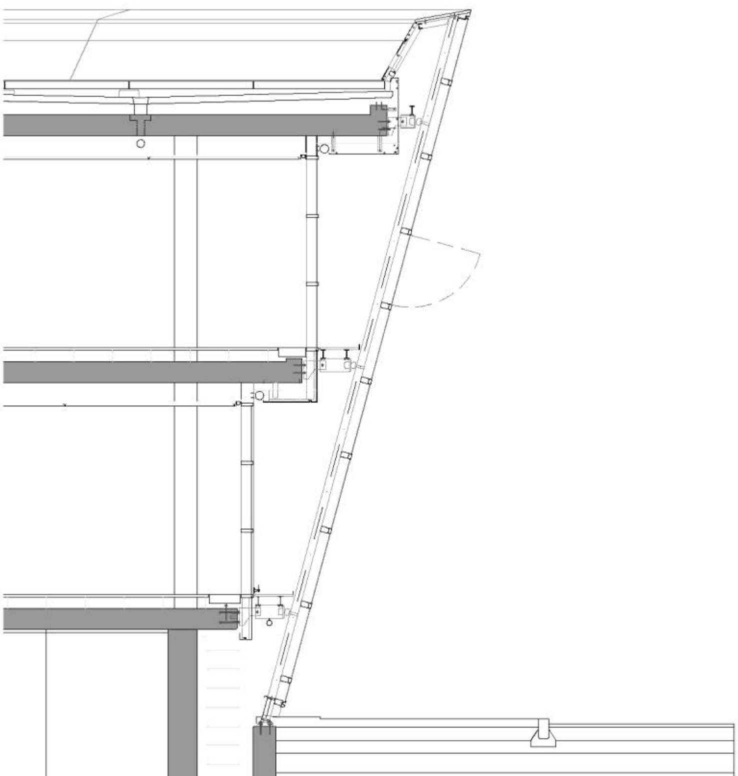

Figure 6: Section of the façade of the Future Lab

6 Site Layout

The generously-sized presentation & activity area – the main deck – is at the heart of the Center and provides open-air exhibition facilities. It nestles between the River Danube and the historic buildings on the one hand and the new Ars Electronica Center on the other.
Wide steps leading to the upper deck provide seating for open-air theatre and film presentations
For special events, the open space can also be used for cultural and artistic presentations or just simply as a meeting place for moments of leisure.

Figure 7: Area for diverse cultural activities, concerts and exhibitions, restauration


Figures 8 & 9: Restaurant and staircase to the terrace, Lobby and staircase

7 Static constructive concept

- Main- and supply building with several stories, conterminous to the existing AEC

An encasing steel-glass-construction connects the existing and new several stored main- and supply building. All new main bodies will be erected with massive construction.
At the main and supply building with 3 basements, ground floor and 5 upper floors, the solid ceilings reach from exterior wall ~12m from exterior wall to exterior wall. The exterior wall till inclusive 1 upper floor will be accomplished through massive ferro- concrete walls with minimum approx. 50% wall percentage. Beyond there is a frontage-backup- system which is absorbing the ceiling.
The encumbrances will be bleed off by raft footing into the underground. All assemblies are accomplished as waterproof Ferro concrete construction till the level of the 500 annual flooding. The lift security is given by empty weight.
The occurred horizontal encumbrances are bleed off into the underground through the north side arranged staircase core as well as the massive exterior walls in connection with the stiff ceiling disc.

- Exhibition space in the basement with a place lying upon - main deck

The one floored underground arranged exhibition building is performed as waterproof Ferro concrete construction, because it is completely situated below the level of the 500 annual flooding. The ceiling was conzipied as massive construction with 60cm thickness –on the one hand to improve the bonding with the ground/propulsion safety and on the other hand to bestride the exhibition space.
The ground plate is performed with minimum 1m thickness with additional pole traction for the warrantee of the propulsion safety.

- Future Lab with Upper Deck

The future lab is performed as waterproof ferroconcrete building till the level of the 500 annual flooding. The propulsion is resolved because of the dead wight of the building. Above the water surface the buiding is concipied with a central point and pillars in the area of the exterior frontage. Thereby the vertical- and horizontal load transfer optimal solved.

Figure 10: light performance